UNIVERSITÀ
DEGLI STUDI
DI PADOVA

Sede Amministrativa: Università degli Studi di Padova

Dipartimento di Biologia

SCUOLA DI DOTTORATO DI RICERCA IN: BIOSCIENZE E BIOTECNOLOGIE
INDIRIZZO: BIOLOGIA CELLULARE
CICLO: XXVII

PHARMACOLOGY OF NATURAL POLYPHENOLS: PRODRUGS AND BIOCHEMISTRY OF RESVERATROL AND PTEROSTILBENE

Direttore della Scuola: Ch.mo Prof. Giuseppe Zanotti
Coordinatore d'indirizzo: Ch.mo Prof. Paolo Bernardi
Supervisore: Dr. Mario Zoratti

Dottorando: Michele Azzolini

Contents:

Riassunto:

Questa tesi riguarda aspetti della farmacologia di due polifenoli: il Resveratrolo e lo Pterostilbene.

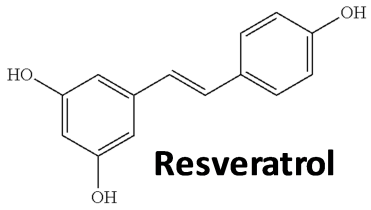

Resveratrol

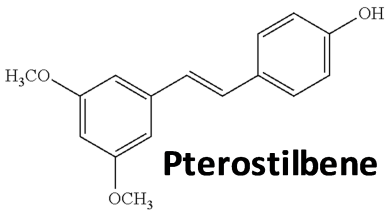

Pterostilbene

Queste molecole di origine vegetale sono oggetto di intensa ricerca alla luce dei loro effetti biologici e biomedici, d'interesse per varie e distinte patologie legate all'età, infiammazione, cancro, obesità, neurodegenerazione e diabete. Tuttavia i meccanismi alla base dell'attività del Resveratrolo ed in particolare dello Pterostilbene non sono completamente noti. Inoltre, la presenza di gruppi idrossilici liberi (caratteristica tipica dei polifenoli) rende queste molecole un buon substrato per gli enzimi del metabolismo di fase II, la cui attività ne limita fortemente la biodisponibilità e lo sfruttamento farmacologico.

Nel corso del mio dottorato mi sono occupato di entrambi questi temi. Descriverò prima il lavoro fatto per aumentare la biodisponibilità delle molecole precedentemente menzionate. In secondo luogo riassumerò le indagini sui meccanismi molecolari che sottendono l'attività dello Pterostilbene e del Resveratrolo.

La strategia adottata dal mio gruppo per aumentare la biodisponibilità di questi polifenoli, considerati alla stregua di farmaci, si basa sull'uso di pro-farmaci. I pro-farmaci sono essenzialmente versioni protette di una determinata molecola. Il Resveratrolo in particolare presenta tre siti principali che dovrebbero essere protetti dagli enzimi del metabolismo di fase II, i gruppo idrossilici. Attraverso un processo di derivatizzazione chimica (svolto dal gruppo della prof.ssa Cristina Paradisi) i gruppi idrossilici sono stati protetti con dei gruppi sostituenti. La scelta della funzionalità chimica e dei sostituenti usati per la protezione è fondamentale per ottenere un pro-farmaco utile. Noi intendiamo i pro-farmaci come molecole terapeutiche adatte per la somministrazione orale. Questa via di somministrazione presume un'elevata stabilità negli ambienti gastrici ed intestinali, seguita da una moderata instabilità in altri ambiti fisiologici (sangue, tessuti, fluidi extracellulari) così da rigenerare il polifenolo naturale, attivo. Durante il mio progetto di dottorato abbiamo ottimizzato questi componenti dei pro-farmaci, il legame ed il gruppo sostituente, lavorando con il Resveratrolo, e poi abbiamo applicato i risultati ottenuti allo Pterostilbene.

Ho iniziato lavorando su derivati acetalici del Resveratrolo. Abbiamo prodotto e testato una serie di composti "decorati" con brevi oligomeri di glicole etilenico legati agli ossigeni fenolici con dei legami di tipo acetalico. Tramite esperimenti *ex vivo* ed *in vivo* abbiamo

identificato la molecola con quattro unità di glicole etilenico ed il legame acetale propriamente detto (Resv-O-CH(CH_3)-OR) come pro-farmaco più promettente di questa serie di composti (capitolo 1: "Acetal derivatives as prodrugs of resveratrol").

La deprotezione completa per rigenerare Resveratrolo è risultata tuttavia piuttosto lenta. Abbiamo quindi deciso di testare nuovi derivati aventi un diverso legame chimico e diversi gruppi sostituenti. Il capitolo 2, "New water-soluble carbamate ester derivatives of resveratrol", presenta i risultati ottenuti con derivati del Resveratrolo recanti PEG 350 o sostituenti di tipo zuccherino incorporati come carbammato N,N-di-sostituito. Queste molecole presentano il vantaggio di essere più idrosolubili, mantenendo al contempo la stessa capacità di permeazione delle membrane cellulari. Tuttavia, l'elevata stabilità di questi composti è risultata ancora problematica.

La stabilità del legame carbammico può essere modulata variando il numero e caratteristiche dei sostituenti sull'atomo di azoto; abbiamo quindi testato il legame estere carbammato N-mono-sostituito, che ci attendevamo fosse più labile rispetto al suo equivalente di-sostituito. I capitoli 3 e 4 (rispettivamente "N-monosubstituted carbamate ester derivatives of resveratrol" and "Synthesis and evaluation of hydrophilic carbamate ester analogos of resveratrol") presentano due serie di derivati del Resveratrolo contenenti aminoacidi, brevi oligomeri di glicole etilenico o sostituenti zuccherini collegati allo "scaffold" stilbenico con questo gruppo. La versione N-mono-sostituita del legame estere carbammato presenta un'elevata stabilità in ambiente acido, una buona stabilità a pH neutro e viene idrolizzata con un'opportuna cinetica in sangue di ratto. La stabilità di questi composti dipende in parte dal gruppo sostituente legato all'azoto. Tuttavia la maggior parte di essi ha dimostrato una reattività idonea all'uso come pro-farmaci del Resveratrolo (capitolo 3).

Oltre a subire un rapido metabolismo di fase II, il Resveratrolo è anche poco solubile in acqua. La sua somministrazione è limitata a pillole o all'uso di eccipienti. Derivati del Resveratrolo solubili in acqua potrebbero quindi facilitarne la somministrazione, specialmente se cronica. Nel capitolo 4 presento derivati del Resveratrolo tri- di- e mono-derivatizzati come esteri carbammici N-monosostituiti; in queste molecole il gruppo sostituente è di tipo poliidrossilico (diidrossipropile o 6-deossigalattosio), e conferisce un'elevata solubilità in acqua. I derivati con il galattosio sono sostanzialmente confinati nell'intestino, dove si accumulano in particolare nei tratti finali, subendovi la progressiva perdita dei gruppi protettori. I derivati con il diidrossipropile vengono invece assorbiti dall'intestino. In particolare, i risultati migliori sono stati ottenuti somministrando i derivati mono-sostituiti.

Ho quindi applicato le conoscenze acquisite lavorando con il Resveratrolo allo Pterostilbene, l'analogo 3,5-dimetilato del Resveratrolo. Poiché lo Pterostilbene è ancora poco caratterizzato abbiamo innanzitutto eseguito una dettagliata analisi sulla distribuzione della molecola negli organi dopo la sua somministrazione orale (capitolo 5, "Pharmacokinetics and tissue distribution of pterostilbene in the rat"). I livelli di

Pterostilbene negli organi sono risultati molto elevati in paragone a quelli misurati nel sangue. Tuttavia, eccetto che nel cervello, il suo metabolita solfato è risultato la specie più abbondante nei tessuti esaminati. Abbiamo quindi testato una piccola libreria di pro-farmaci dello Pterostilbene basati sul legame carbammico N-monosostituito e amminoacidi naturali. Come ci attendavamo, la stabilità di questi derivati è compresa in un intervallo utile per l'uso come pro-farmaci. L'assorbimento dei derivati recanti amminoacidi apolari è fortemente incrementato (capitolo 6, "Boosting pterostilbene's effects: a prodrug approach"). Oltre ad un intenso e sostenuto assorbimento intestinale, alcuni precursori si sono distinti per i livelli di Pterostilbene rigenerati nel sangue. Uno di questi composti è stato selezionato come più promettente e la sua distribuzione negli organi dopo somministrazione orale è stata mappata seguendo gli stessi criteri adottati per lo Pterostilbene (descritti nel capitolo 5). Il derivato stesso è stato la specie più abbondante misurata negli organi esaminati, eccetto che nel cervello, mentre i livelli del metabolita solfato erano diminuiti e quelli dello Pterostilbene aumentati nella maggior parte degli organi esaminati. I pro-farmaci possono quindi essere utili strumenti per aumentare la biodisponibilità di alcuni polifenoli.

Nella seconda parte del mio dottorato ho condotto indagini, ancora in corso, su aspetti dei meccanismi cellulari con cui agiscono Resveratrolo e Pterostilbene. A tal scopo abbiamo adottato un duplice approccio, sia *in vitro* che *in vivo*, presentati in questa sede in due diversi capitoli (capitoli 7 e 8, rispettivamente "Transcription factor EB is a crucial transducer of the biomedical action of pterostilbene and resveratrol" and "Pterostilbene and cognitive performance in the aged rat model: preliminary findings").

Gli effetti pleiotropici attribuiti al Resveratrolo ed allo Pterostilbene possono essere spiegati da interazioni multiple con proteine che occupano posizioni apicali in importanti processi cellulari. L'autofagia è stata a lungo considerata come un banale processo catabolico che si svolge in sottofondo tra le varie attività cellulari. Oggi è invece considerata come uno dei processi che controllano l'omeostasi cellulare, e la sua errata regolazione è implicata in varie patologie. Oltretutto è stato recentemente scoperto un fattore di trascrizione, TFEB, che governa la maggior parte degli eventi correlati con l'autofagia lisosomiale. Abbiamo verificato se lo Pterostilbene e il Resveratrolo potessero agire anche sulla regolazione di questo fattore di trascrizione. Entrambi si sono dimostrati in grado di indurre la traslocazione di TFEB dal citoplasma, dove è normalmente confinato, al nucleo, dove può promuovere gli eventi correlati all'autofagia. Abbiamo inoltre incluso nel nostro lavoro lo studio di alcuni dei principali metaboliti del Resveratrolo e dello Pterostilbene. Mentre i solfati di entrambe le molecole sono risultati poco attivi, le forme ridotte, tipicamente prodotte dalla flora intestinale, hanno dimostrato un'efficacia simile a quella delle molecole non modificate. Ulteriore lavoro rimane per poter chiarire quale via di segnalazione sia a monte dell'attivazione di TFEB. Sia il Resveratrolo che (ed in particolare) lo Pterostilbene determinano un aumento dei livelli di AMPciclico citosolico in cellule HeLa in coltura, probabilmente inibendo

determinate classi di fosfodiesterasi. Ulteriore lavoro sarà necessario per valutare il coinvolgimento di altre vie di segnalazione (capitolo 7).

Nel capitolo 5 riporto che lo Pterostilbene presenta un elevato tropismo per il cervello. Le concentrazioni misurate in tale organo danno valore ad alcuni lavori che riportano un effetto dello Pterostilbene nel contrastare il deterioramento cognitivo legato all'età ed alle patologie neurodegenerative come l'Alzheimer e il Parkinson. I meccanismi sottostanti questi effetti dello Pterostilbene sono tuttora poco caratterizzati. Lo Pterostilbene, attraverso un incremento di AMPciclico citosolico può attivare la via di segnalazione PKA/CREB/CBP che, come illustrato dal premio Nobel Eric Kandel, può giustificare gli effetti sulla memoria e sull'apprendimento. La sola attivazione di questa via tuttavia non può spiegare gli effetti dello Pterostilbene nel trattamento del deterioramento cognitivo legato all'età. Recentemente, è stato scoperto che la proteina RbAp48 è negativamente regolata in soggetti anziani, sia topi che umani. Questa proteina è fortemente coinvolta nei processi di rimodellamento della cromatina, quindi nell'espressione genica. I processi complessi come la formazione della memoria richiedono l'espressione coordinata di molti geni. I fattori di trascrizione come CREB possono indurre l'espressione genica qualora i geni siano loro accessibili. Il rimodellamento della cromatina è quindi un processo richiesto e necessario per l'azione del CREB. Abbiamo quindi deciso di verificare se l'attività dello Pterostilbene fosse, almeno in parte, mediata dalla modulazione di RbAp48. Allo stato attuale i risultati sono ancora preliminari, ma sembra che nel giro dentato di ratti anziani TFEB, RbAp48 e Rest siano positivamente regolati dopo somministrazione cronica di Pterostilbene. Altro lavoro è però necessario per poter chiarire questi punti, inoltre il numero di animali esaminato deve essere incrementato per poter avere un dato statisticamente significativo.

Infine, nel corso del mio dottorato sono stato coinvolto in altri progetti in corso nel gruppo. Questa partecipazione ha fatto sì che io fossi incluso fra gli autori di tre pubblicazioni, che includo in questa tesi come capitoli 9, 10 ed 11.

Summary:

This thesis deals with aspects of the pharmacology of two polyphenols: Resveratrol and Pterostilbene.

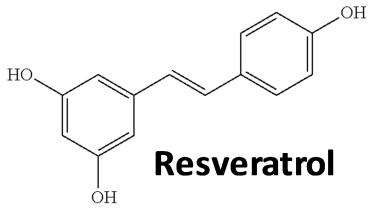

Resveratrol

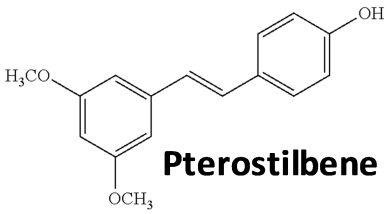

Pterostilbene

These plant-made molecules are the object of intensive research due to their biological and biomedical activities, of interest in the context of various pathologies related to age, inflammation, neurodegeneration, cancer, obesity and diabetes. However, the mechanisms underlying the activity of Resveratrol, and in particular of Pterostilbene, are not completely known. Moreover, the presence of free hydroxyl group(s) (the common feature of polyphenols) renders both molecules good substrates for enzymes of phase II metabolism, whose activity strongly limits the bioavailability and the pharmacological exploitation of polyphenols.

During my graduate studies I have worked on both these themes. I will describe first what has been done to increase the bioavailability of both molecules. Second, I will summarize my ongoing investigation of the molecular mechanisms accounting for the activity of Pterostilbene and Resveratrol.

The strategy adopted by my research group to improve the efficacy of these polyphenols, viewed more as pharmaceuticals than as nutrients, involves the use of prodrugs. Prodrugs are essentially protected versions of a given molecule. Resveratrol in particular presents three main sites that ought to be protected from phase II enzymes, the hydroxyl groups. Through chemical derivatization (performed by the group of prof. Cristina Paradisi) the hydroxyl groups were reversibly protected with pro-moieties. The choice of linker group and of the pro-moiety is of fundamental importance to construct a useful prodrug. We intend prodrugs as therapeutic molecules designed for oral administration. This route of administration demands a suitable stability in gastric and intestinal environments, and a moderate instability in other physiological matrices (e.g. blood, tissues, extracellular fluids) so as to regenerate the active polyphenol once in the latter. During my PhD project we have optimized the two key components of the prodrug, the bond and the substituent group, working with Resveratrol, and we have then applied the results to Pterostilbene.

I started my project working on acetal derivatives of Resveratrol. We produced and tested a series of derivatives bearing short ethyleneglycol oligomers (OEG) linked to the phenolic oxygens via acetal/formal/ketal bonds. Through *ex vivo* and *in vivo* tests we have identified the acetal derivative Resv-O-CH(CH_3)-OR, with R = tetrameric OEG, as the most

promising prodrug of this series (chapter 1, “Acetal derivatives as prodrugs of resveratrol”).

Complete deprotection to give Resveratrol was however rather slow. We thus decided to test new derivatives based on a different bond system, and different substituent groups. Chapter 2, “New water-soluble carbamate ester derivatives of resveratrol”, presents the results obtained with Resveratrol derivatives bearing a PEG 350 or a sugar promoiety joined to the stilbenoid core through a N,N-di-substituted carbamate ester functionality. These molecules present the advantage of an increased water solubility, while maintaining to some degree the ability to permeate membranes. However, the high stability of these molecules was again problematic.

The stability vs. hydrolysis of the carbamate bond can be modulated varying the number and characteristics of the substituents on the Nitrogen atom; we tested therefore the N-mono-substitute carbamate group, which we expected to be more labile than its di-substitued analog. Chapters 3 and 4 (respectively “N-monosubstituted carbamate ester derivatives of resveratrol” and “Synthesis and evaluation of hydrophilic carbamate ester analogos of resveratrol”) present two series of derivatives of Resveratrol comprising amino acids, short ethyleneglycol oligomers (OEG) or sugar promoities linked to the scaffold via this group. The N-mono-substituted version of the carbamate bond shows high stability in acid, a suitable stability at near-neutral pH, and it undergoes hydrolysis with opportune kinetics in rat blood. The stability of these molecules depends in part on the substituent group on Nitrogen. However most of our derivatives hydrolyzed with a time course compatible with their use as prodrugs of Resveratrol (chapter 3).

Besides its rapid phase II metabolism, Resveratrol is also poorly soluble in water. Its administration is therefore usually as pills or with excipients. Water-soluble prodrugs would facilitate Resveratrol administration, especially if given chronically. In chapter 4 I present Resveratrol derivatives in which all three, two or one hydroxyl group(s) are incorporated into N-monosubstituted carbamate ester moieties; in these molecules the pro-moiety is a polyhydroxylated group (dihydroxypropyl or 6-deoxygalactose), and confers high water solubility. Galactosyl derivatives were substantially confined to the intestine, where they accumulated especially in the lower segments, undergoing the progressive loss of the protecting groups. Dihydroxypropyl derivatives instead were partly absorbed. Notably, the best results were achieved using mono-substituted derivatives.

I have then applied the knowledge and know-how gained working with Resveratrol to Pterostilbene, the 3,5-dimethylated analogue of Resveratrol. Since Pterostilbene is still poorly characterized from a pharmacological point of view we first of all performed a detailed analysis of the distribution of the molecule and its major metabolite in the organs of rat after its oral administration (chapter 5, “Pharmacokinetics and tissue distribution of pterostilbene in the rat”). The levels of Pterostilbene in the organs were much higher than those measured in blood. Nonetheless, its sulfate was the predominant specie in all tissues examined except the brain.

We tested a small library of pro-drugs of Pterostilbene bearing amino acids linked to the phenolic oxygen via the N-monosubstitute carbamate ester group. As expected, the rates of hydrolysis of these derivatives fell in a range suitable for their use as prodrugs. Absorption of Pterostilbene derivatives bearing apolar amino acids was greatly increased (chapter 6, "Boosting pterostilbene's effects: a prodrug approach"). Apart from an intense and sustained absorption from the intestinal wall, a few precursors were notable for the levels of Pterostilbene they regenerated in blood. One of these compounds was selected as the most promising one and its distribution in rat organs was analyzed, following the same criteria adopted for Pterostilbene (described in chapter 5). The prodrug itself was the major specie measured in all organs examined, except the brain, while levels of the sulfate metabolite were decreased and those of regenerated Pterostilbene increased in most of the organs examined (in comparison with the administration of Pterostilbene itself). Prodrugs can thus be a useful tool to increase the bioavailability of some polyphenols.

In the second phase of my PhD project I conducted an investigation, still to be completed at this point, of the cellular processes set in motion by Pterostilbene and Resveratrol. For this purpose we adopted *in vitro* and *in vivo* approaches, presented here in two separate chapters (chapter 7 and chapter 8, respectively "Transcription factor EB is a crucial transducer of the biomedical action of pterostilbene and resveratrol: work in progress" and "Pterostilbene and cognitive performance in the aged rat model: preliminary findings").

The pleiotropic effects attributed to Resveratrol and Pterostilbene can be explained by multiple interactions with proteins occupying apical positions in important and interconnected signaling cascades. Autophagy has been long considered as a "banal" background catabolic process. Currently it is instead recognized to be one of the important processes that maintain cell homeostasis, and its dysregulation is implicated in various pathologies. A transcription factor, TFEB, that governs most of the events in lysosomal autophagy has recently attracted much interest. We thus verified whether Pterostilbene and Resveratrol might have an impact on the regulation of this transcription factor. Both proved capable of inducing the translocation of TFEB from the cytosol, where it is normally confined, to the nucleus, where it can promote autophagy-related events. We also included in our work the study of some of the major metabolites of Resveratrol and Pterostilbene. While sulfates of both molecules were poorly active, the reduced forms, typical products of the colonic flora, showed an efficacy comparable to that of the unmodified parent molecules. Further work is needed to clarify what signaling pathways are involved upstream of TFEB activation. Both Resveratrol and (in particular) Pterostilbene determined an increase of cytosolic cAMP concentration in cultured HeLa cells, probably by inhibiting certain classes of phosphodiesterases, but more work is needed to explore the possible involvement of other pathways, suggested by some aspects of our results (chapter 7).

In chapter 5 I have reported that Pterostilbene presents an elevated tropism for the brain. The concentrations measured in this organ strengthen the reports showing an effect of Pterostilbene in contrasting cognitive aging and neurodegenerative diseases such as Alzheimer's and Parkinson's. The mechanisms accounting for these effects are however poorly characterized. Pterostilbene, through an increase in cytosolic cAMP, can activate the PKA/CREB/CBP pathway, which, as shown by Nobel prize winner Eric Kandel, can account for the effects on memory formation and learning, boosted by this molecule. The activation of this pathway cannot however explain by itself the striking effects of Pterostilbene in the treatment of cognitive aging. Recently, the protein RbAp48 has been discovered to be downregulated in aged individuals (humans and mice). This protein is deeply involved in the chromatin remodeling, thus in the modulation of gene expression. Processes like memory formation require the coordinated expression of many genes. Transcription factors, such as CREB, can induce gene expression provided that the genes themselves are accessible. Chromatin remodeling is thus required for the action of CREB. We thus decided to investigate if Pterostilbene activity might be, at least in part, mediated by a functional interaction with RbAp48. Our results are still preliminary, but it seems that in the Dentate Gyrus of old rats the transcription factor TFEB, RbAp48 and Rest are upregulated upon chronic administration of Pterostilbene. Further work needs to be done in order to clarify these points, and the statistical set ought to be increased to achieve significance.

Finally, during my doctoral training I have also been involved in other ongoing projects in my group. This involvement has led to my presence in the author list of three publications, which I include in this thesis as chapters 9, 10 and 11.

Organization of the thesis:

After a relatively brief general introduction, the bulk of this thesis is organized in chapters corresponding to individual topics of research. This organization has been favoured over a more traditional, monograph-style layout in part because my work actually developed as a series of closely related - but distinct - activities, and mainly with the intent of facilitating reading. Some of the chapters correspond to papers already published or almost ready to be submitted, in other cases the specific parcel of work was still unfinished as the thesis was due. The corresponding section reports the available data and comments, and mentions what remains to be done. At the end I have included three papers of which I am a co-author, but which fall outside my main research project, although they are related to it. Thus, the chapters are not homogenous in length and relevance, and there are may be repetitions. I hope the benefits of such an organization outweigh this disadvantage.

Introduction:

Polyphenols are a large and diversified class of plant-derived compounds. Their precise definition has been a matter of debate. In 2011 Stephen Quideau proposed this definition: "*the term polyphenol should be used to define plant secondary metabolites derived exclusively from the shikimate-derived phenylpropanoid and/or the polyketide pathway(s), featuring more than one phenolic ring and being devoid of any nitrogen-based functional group in their basic structural expression*".[1] However more relaxed definitions of polyphenols are generally accepted. Fig 1 presents some of the most common and studied classes of polyphenols.

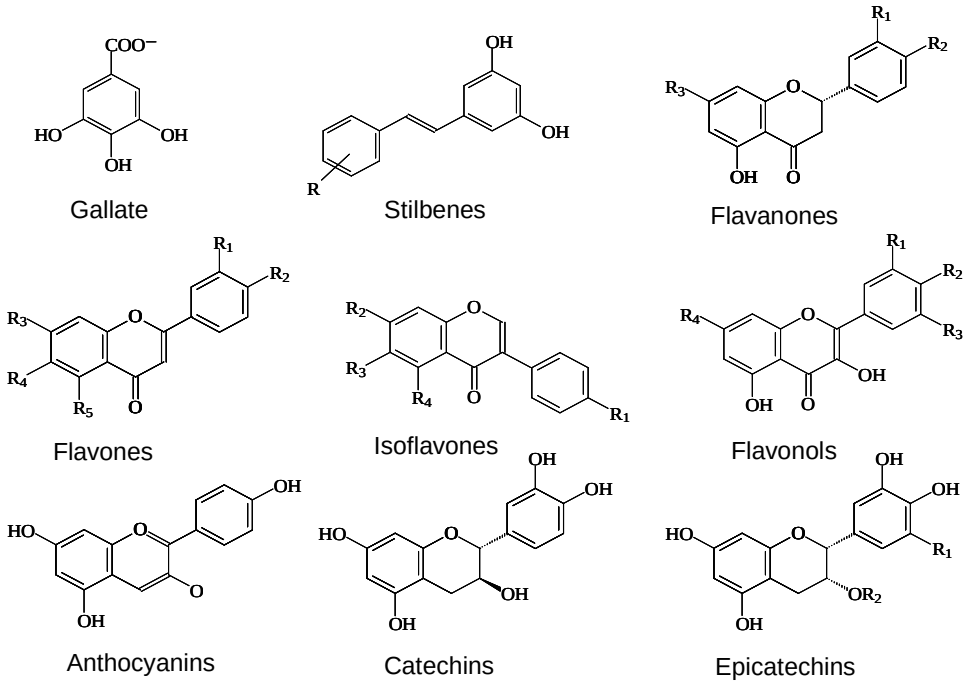

Fig. 1. Some of the most important polyphenol subfamilies.

Polyphenols are normally produced by plants in response to stressors such as pathogens [2, 3] or U.V. radiation,[3, 4] or in the regulation of physiological processes (i.e. hormone production; [5]).

Much evidence (at least in *in vitro* studies) suggests that these compounds can be potentially useful for human health care. Currently it is widely accepted that these molecules can have a role in contrasting cancer, obesity, cardiovascular diseases and disorders related to aging, such as neurodegeneration, diabetes and chronic inflammation (e.g. [3, 6-13]).

Among the thousands of known plant polyphenols (5000 - 8000 different molecules), during my PhD project I worked with Resveratrol and its analogue Pterostilbene (fig 2), which were already the major model polyphenols in use in my group when I joined it. The choice had been motivated in part by the eminence of these two compounds (especially

resveratrol) in the field, due to the evidence linking their intake to a variety of (potential) positive effects on consumers' health, and in part by their relatively simple structure and fair stability, which obviously facilitate their chemical elaboration and analysis.

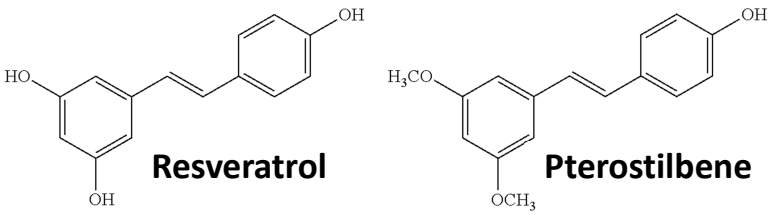

Fig 2: Molecular structure of Resveratrol and Pterostilbene.

Resveratrol (3,5,4'-trihydroxy-trans-stilbene) is one of the polyphenols that have attracted the most attention from scientists and physicians. It is a stilbene found in grapes, wine, certain roots and its celebrity can probably be traced back to the "French paradox".[14, 15] Two decades of intensive research support Resveratrol as a promising drug for the treatment or prevention of many human diseases such as type 2 diabetes, Alzheimer, Parkinson, cancer, inflammation-related pathologies, cardiovascular problems and obesity (e.g. [16-24]).

Pterostilbene (3,5-dimethoxy-4'-hydroxy-stilbene) is found primarily in blueberries and grapes. The presence of the two methyl groups renders Pterostilbene more lipophilic than Resveratrol. This property in turn leads to a higher bioavailability of the molecule since it can diffuse across membranes and tissues more easily. The effects of Pterostilbene are still little known, since research has focused mainly on Resveratrol, but it is nowadays accepted that its bioavailability makes Pterostilbene even more interesting than Resveratrol.[25-32]

The biological effects of polyphenols have been ascribed both to their redox properties and to interaction with proteins. The structure of polyphenols allows delocalization of charges and unpaired electrons, rendering them good radical scavengers (and thus antioxidants; [33, 34]). An excessive load of radical oxygen species (ROS) can cause damage at both cellular and tissue level. A model that remained popular for several years thus ascribed the beneficial activities of polyphenols to a direct anti-oxidant action. However, *in vitro* studies that demonstrate the ROS scavenging activity of polyphenols are usually performed at high concentrations (20-200 µM), which can hardly be relevant *in vivo* because of their poor bioavailability (see below) and because cells normally possess a pool of effective antioxidants, e.g. glutathione, with an overall concentration in the mM range. Furthermore, depending on factors such as their concentration, the pH, the presence of metal ions capable of maintaining a redox cycle ($Fe^{2+/3+}$, $Cu^{+/2+}$) or of oxidizing enzymes such as tyrosinases ("polyphenol oxidases"), polyphenols can act as pro-oxidants rather than anti-oxidants.[34-43]

Some evidence suggests that a mild ROS intoxication can lead to an increase in health and lifespan by inducing the production of proteins involved in the regulation of the oxidative level and of mitochondrial homeostasis (mitochondria are the main site of ROS production; [44-48]). This is the concept of hormesis, which may help explain, in particular, preventive effects.[49-56] The scheme envisions redox-sensitive transcription factors and enzymes driving a feedback loop to maintain the cell's oxidative balance (fig. 3).[55, 57-60] Potentiation of antioxidant defenses induced by mild pro-oxidants such as dietary polyphenols may help blunt a major oxidative challenge, as occurring, for example, at reperfusion after ischemia,[61, 62] and have positive effects on health and lifespan in general.

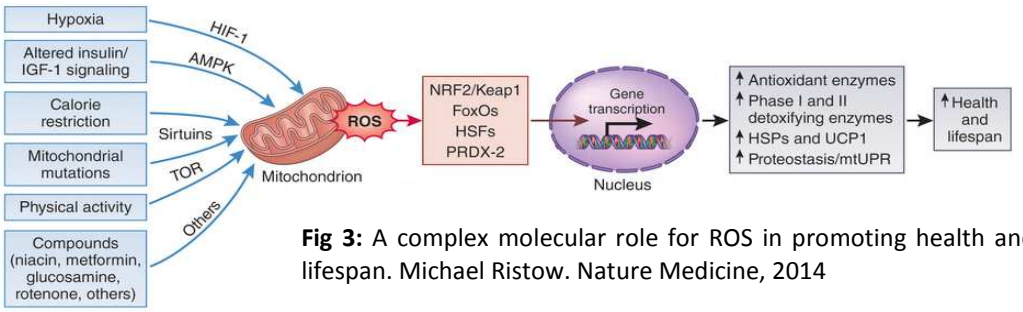

Fig 3: A complex molecular role for ROS in promoting health and lifespan. Michael Ristow. Nature Medicine, 2014

On the other hand, current opinion attributes a major role to the interaction of polyphenols with proteins, which may account for hormetic or preconditioning effects as well. Several such interactions have been documented. For example, resveratrol has been shown to interact with hemoglobin,[63] human and bovine serum albumin,[63-66] caseins,[67] β-lactoglobulin,[68, 69] glutathione sulfotransferase-π (GSTP1),[70] the mitochondrial ATPase (F1),[71] PKC-α and –β (but not -ε and -ζ),[72] integrin αVβ3,[73] estrogen receptor-β (ER-β),[70] dihydronicotinamide riboside quinone reductase 2 (NQO2),[74] cycloxygenase-1 and -2,[75] phosphodiesterases,[76, 77] peroxisome proliferator-activated receptor (PPAR) -γ and -α[78] and several other proteins.[17] In some cases interactions are known to exist, but the binding partner has not yet been identified. For example, high-affinity (10^{-8} M range) binding of stilbenoids to brain and skin receptors has been observed by Quirion and coworkers.[79-81] Whether this involves the EGCG-binding laminin receptor[82-86] or other membrane protein(s) remains to be established. In other cases functional effects suggest a direct interaction, which however remains to be proven. Examples are PKC-γ[87] and a splice variant of PKC-δ.[88] In most cases these interactions occur with relatively low affinity. Thus, e.g., COX-1 and -2 are inhibited by Resveratrol with IC50's of 2.27 and 3.40 µM respectively,[75] IKK at about 1 µM,[89] PKC isoforms α and β are half-inhibited at about 2 µM,[72] PDE's 1-4 at about 6-14 µM,[76] DNA topoisomerase II at an irrelevant 65 µM,[90] while binding to PPAR-γ occurs with an affinity of 1.4 µM,[78] to BSA of about 4 µM.[64, 66] These data highlight the importance of finding ways to increase the levels of active polyphenolic species in the organism, where concentrations in the µM range are seldom reached (see below).

These various mechanisms and multiple molecular interactions impact on many branches of the vast and interconnected signaling network in cells. An intense activity is underway in many laboratories to characterize the seemingly endless mechanistic facets of polyphenol action, and there appears to be no shortage of work in sight in this field of investigation. The cellular biochemistry engaged depends not only on the specific phytochemical under study, but also on cell type and conditions. Effects on the apical elements of signaling cascades, e.g. on PDE's, integrins or NF-kB, can impact on a plethora of enzymes and transcription factors. Modulation of gene expression via epigenetic mechanisms is also important. Resveratrol, to keep the focus on stilbenes, can influence the cellular transcriptome and proteome via the nucleosome remodeling and deacetylating (NuRD) complex[91] and, most famously, via activation of SIRT1, an enzyme with multiple activities including that of NAD-dependent lysine deacetylase. The action of resveratrol on SIRT1 has been a controversial issue, but a consensus seems to have been reached: resveratrol does activate the sirtuin, although it might do so indirectly, with the intermediacy of AMPK ([92-95] but see [96, 97]). A direct interaction and modulation has been demonstrated for SIRT3 and SIRT5, two of the three mitochondrial isoforms of the 7-membered family.[98, 99] Sirtuins are thought to modulate gene expression, metabolic control, cell survival, development, inflammation, aging, neuroprotection (e.g. [100-105]).

This multi-faceted character of polyphenol action has been identified by some authors as their key asset: according to this view the simultaneous engagement of multiple pathways and processes hampers a re-adjustment of the system to neutralize the action of the drug, as often happens with single-target medicinals.[17, 106] For diet-or herbal preparation-associated effects, cooperativity among the polyphenolic components, as well as with other ingredients of food is also considered important, precisely because multiple pathways can be activated.[107-111]

In this complex scenario the real effectiveness of polyphenols *in vivo* is still questioned.[112-114]

Despite the multitude of effects and applications proposed for Resveratrol and Pterostilbene, their low bioavailability limits their full pharmacological exploitation.[115-117] An extensive phase II metabolism affects the efficacy of these two compounds in *in vivo* studies. After oral administration in fact mainly metabolites are present in the bloodstream ([118-120]; this thesis, chapter 5 [121]), a statement that applies to all polyphenols, since their hydroxyl groups make them ideal substrates for methyl, glucuronyl- and sulpho-transferases. Hence the well-founded suspicion that metabolites, rather than the parent aglycones, may actually be responsible for the effects of polyphenols. Work is underway to explore this obviously complex matter (e.g. [122-129]). What seems clear so far is that generalizations ought not to be made: whether a metabolite is active (and at what levels) or not depends on the specific molecule and cellular process under study. The conjugation step leading to the formation of glucuronides or sulphates is reversible, so

that these metabolites may well act as a "reservoir" of aglycone, which can be gradually regenerated by the action of glucuronidases and sulfatases.[88, 130, 131]

A topic which had received insufficient attention until recently (see for example the assessment by Scalbert et al., [132, 133]), except for some cases, notably equol (revs.: [134-137]), is that of the metabolites (catabolites) formed by the intestinal flora in the lower segment of the intestine (e.g [138-142]). These seem to be more bioavailable than the parent polyphenols, accounting probably for most of the total absorption of polyphenol-derived species, and may well be responsible for a large part of the benefits provided by polyphenol consumption.[143-155]

More details on these various aspects can be found in the introductory sections of the following chapters, where more specific information is presented to provide a context for each aspect of this work.

The project:

My Ph.D. thesis work has evolved coming to address two aspects of polyphenol research. The final goals of these related projects are to increase polyphenol bioavailability, and thus, presumably, efficacy, and to gain a better understanding of mechanistic aspects of their biological action. Both lines contribute to the development of a pharmacology of these natural compounds, which are generally thought of as nutrients, but arguably deserve the status of medicinal compounds as well. As briefly mentioned above, much of the research concerning polyphenols has been rightly criticized as involving solely *in vitro* systems and unrealistically high concentrations of the compounds (e.g. [156]). To avoid this pitfall I have adopted throughout mainly an *in vivo* approach.

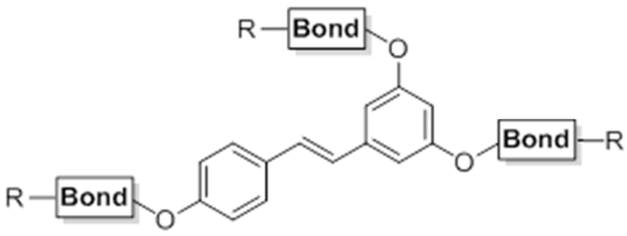

Fig 4: Schematic example of a prodrug of Resveratrol

Bioavailability:

Continuing a previously established project in my research group, I have spent the first part of my PhD period working on the bioavailability of Resveratrol and Pterostilbene (chapters 1-6). Most of the efforts to improve absorption and effectiveness of polyphenols has relied so far on the use of sophisticated formulations: a variety of colloidal preparates, nanoparticles, liposomes and other carrier systems have been deployed, in many cases using mainly *in vitro* systems to assess their efficacy (for an overview see, e.g., chapter 9 and [157-160]). My group has taken the alternative – or complementary – prodrug approach: the chemical manipulation of the "parent" molecule to optionally modify its physico-chemical properties, e.g. solubility/lipophilicity, and uptake from the gastrointestinal tract, and most importantly to insert protecting groups which prevent metabolic modifications during absorption and

distribution to the body organs, until they are eventually eliminated by unassisted or enzymatic reactions (hydrolysis), regenerating the active compound. Thus, a prodrug comprises the parent molecule (or scaffold, cargo), whose sensitive groups (hydroxyls) are linked via a labile bond to a promoiety which can impart desirable properties to the construct (fig 4). A key feature is the stability of the linker bond group under physiological conditions: it must be neither too high, because of the need to regenerate the active compound before excretion, nor, obviously, so low as to make the modification meaningless. Another point to be kept in mind is the possible bioactivity of the compounds that are generated upon shedding of the protecting groups. The prodrug approach is popular in the pharmaceutical industry, but has so far found limited application with polyphenols (for an overview see chapter 9, [161] and Biasutto & Zoratti, [162]).

In collaboration with the group of prof. Cristina Paradisi (Dept. of Chemical Sciences, University of Padua) we developed new derivatives of both, Resveratrol and Pterostilbene, bearing linker and substituent groups. The stability of each of these molecules was assessed in acid and near-neutral solution and in blood. The compounds performing satisfactorily in these assays were then assessed for absorption, distribution and regeneration of the parent compound in pharmacokinetic experiments.

Mechanisms of action:

Despite a consistent number of papers devoted to the interactions and mechanisms of action of Resveratrol and related stilbenoids, there is still a strong need for further elucidation in order to clarify how these molecules work and thus how they can be properly exploited. Furthermore Pterostilbene has gained attention only recently, thus its mechanisms of action are still poorly characterized, even though it seems logical to anticipate that they may be similar to those of Resveratrol. Recent literature suggests that Pterostilbene may be even more potent than Resveratrol, presumably due to its higher lipophilicity and built-in partial protection from metabolic modifications.

In chapters 7 and 8 I will present two investigations, still incomplete at this point, centered on the cellular mechanisms underlying the activity of Resveratrol and Pterostilbene. We adopted both *in vitro* and *in vivo* approaches to clarify - at least in part - the molecular readout. Since my research group is part of the CNR Institute of Neuroscience we are devoting attention to the activity of Pterostilbene on the Central Nervous System. Future developments will include a comparison of its efficacy and of that of its prodrugs. Given the relevance of autophagy in many biological processes, we are exploring its induction by our two stilbenoids.

Finally, in chapters 10 and 11 I include two already published articles regarding the mitochondrial targeting of resveratrol. The specific targeting of Resveratrol was a parallel activity running in my lab, carried out especially by dr. Nicola Sassi and dr. Andrea

Mattarei. I was partially involved in this project as well, performing some experiments with dr. Sassi.

References:

1. Quideau, S.; Deffieux, D.; Douat-Casassus, C.; Pouysegu, L. Plant polyphenols: chemical properties, biological activities, and synthesis. *Angewandte Chemie (International ed. in English)* **2011,** *50*, (3), 586-621.
2. Thaler, J.; Fidantsef, A.; Duffey, S.; Bostock, R. Trade-Offs in Plant Defense Against Pathogens and Herbivores: A Field Demonstration of Chemical Elicitors of Induced Resistance. *J Chem Ecol* **1999,** *25*, (7), 1597-1609.
3. Pandey, K. B.; Rizvi, S. I. Plant polyphenols as dietary antioxidants in human health and disease. *Oxidative medicine and cellular longevity* **2009,** *2*, (5), 270-8.
4. Frohnmeyer, H.; Staiger, D. Ultraviolet-B radiation-mediated responses in plants. Balancing damage and protection. *Plant physiology* **2003,** *133*, (4), 1420-8.
5. Ke, D.; Saltveit, M. E. Plant hormone interaction and phenolic metabolism in the regulation of russet spotting in iceberg lettuce. *Plant physiology* **1988,** *88*, (4), 1136-40.
6. Manach, C.; Mazur, A.; Scalbert, A. Polyphenols and prevention of cardiovascular diseases. *Current opinion in lipidology* **2005,** *16*, (1), 77-84.
7. Scalbert, A.; Johnson, I. T.; Saltmarsh, M. Polyphenols: antioxidants and beyond. *The American journal of clinical nutrition* **2005,** *81*, (1 Suppl), 215s-217s.
8. Siriwardhana, N.; Kalupahana, N. S.; Cekanova, M.; LeMieux, M.; Greer, B.; Moustaid-Moussa, N. Modulation of adipose tissue inflammation by bioactive food compounds. *The Journal of nutritional biochemistry* **2013,** *24*, (4), 613-23.
9. Li, A. N.; Li, S.; Zhang, Y. J.; Xu, X. R.; Chen, Y. M.; Li, H. B. Resources and biological activities of natural polyphenols. *Nutrients* **2014,** *6*, (12), 6020-47.
10. Malavolta, M.; Costarelli, L.; Giacconi, R.; Piacenza, F.; Basso, A.; Pierpaoli, E.; Marchegiani, F.; Cardelli, M.; Provinciali, M.; Mocchegiani, E. Modulators of cellular senescence: mechanisms, promises, and challenges from in vitro studies with dietary bioactive compounds. *Nutrition research (New York, N.Y.)* **2014,** *34*, (12), 1017-1035.
11. Barrajon-Catalan, E.; Herranz-Lopez, M.; Joven, J.; Segura-Carretero, A.; Alonso-Villaverde, C.; Menendez, J. A.; Micol, V. Molecular promiscuity of plant polyphenols in the management of age-related diseases: far beyond their antioxidant properties. *Advances in experimental medicine and biology* **2014,** *824*, 141-59.
12. Wang, S.; Moustaid-Moussa, N.; Chen, L.; Mo, H.; Shastri, A.; Su, R.; Bapat, P.; Kwun, I.; Shen, C. L. Novel insights of dietary polyphenols and obesity. *The Journal of nutritional biochemistry* **2014,** *25*, (1), 1-18.
13. Chu, A. J. Antagonism by bioactive polyphenols against inflammation: a systematic view. *Inflammation & allergy drug targets* **2014,** *13*, (1), 34-64.
14. Constant, J. Alcohol, ischemic heart disease, and the French paradox. *Coronary artery disease* **1997,** *8*, (10), 645-9.
15. Kopp, P. Resveratrol, a phytoestrogen found in red wine. A possible explanation for the conundrum of the 'French paradox'? *European journal of endocrinology / European Federation of Endocrine Societies* **1998,** *138*, (6), 619-20.
16. Baur, J. A.; Sinclair, D. A. Therapeutic potential of resveratrol: the in vivo evidence. *Nature reviews. Drug discovery* **2006,** *5*, (6), 493-506.
17. Harikumar, K. B.; Aggarwal, B. B. Resveratrol: a multitargeted agent for age-associated chronic diseases. *Cell cycle (Georgetown, Tex.)* **2008,** *7*, (8), 1020-35.
18. Pervaiz, S.; Holme, A. L. Resveratrol: its biologic targets and functional activity. *Antioxidants & redox signaling* **2009,** *11*, (11), 2851-97.
19. Shakibaei, M.; Harikumar, K. B.; Aggarwal, B. B. Resveratrol addiction: to die or not to die. *Molecular nutrition & food research* **2009,** *53*, (1), 115-28.

20. Widlund, A. L.; Baur, J. A.; Vang, O. mTOR: more targets of resveratrol? *Expert reviews in molecular medicine* **2013,** *15*, e10.
21. Temraz, S.; Mukherji, D.; Shamseddine, A. Potential targets for colorectal cancer prevention. *International journal of molecular sciences* **2013,** *14*, (9), 17279-303.
22. Bastianetto, S.; Menard, C.; Quirion, R. Neuroprotective action of resveratrol. *Biochimica et biophysica acta* **2014**.
23. Ma, T.; Tan, M.; Yu, J.; Tan, L. Resveratrol as a Therapeutic Agent for Alzheimer's Disease. *BioMed research international* **2014,** *2014*, 350516.
24. Aguirre, L.; Fernandez-Quintela, A.; Arias, N.; Portillo, M. P. Resveratrol: anti-obesity mechanisms of action. *Molecules (Basel, Switzerland)* **2014,** *19*, (11), 18632-55.
25. Paul, S.; Rimando, A. M.; Lee, H. J.; Ji, Y.; Reddy, B. S.; Suh, N. Anti-inflammatory action of pterostilbene is mediated through the p38 mitogen-activated protein kinase pathway in colon cancer cells. *Cancer prevention research (Philadelphia, Pa.)* **2009,** *2*, (7), 650-7.
26. Paul, S.; DeCastro, A. J.; Lee, H. J.; Smolarek, A. K.; So, J. Y.; Simi, B.; Wang, C. X.; Zhou, R.; Rimando, A. M.; Suh, N. Dietary intake of pterostilbene, a constituent of blueberries, inhibits the beta-catenin/p65 downstream signaling pathway and colon carcinogenesis in rats. *Carcinogenesis* **2010,** *31*, (7), 1272-8.
27. Nutakul, W.; Sobers, H. S.; Qiu, P.; Dong, P.; Decker, E. A.; McClements, D. J.; Xiao, H. Inhibitory effects of resveratrol and pterostilbene on human colon cancer cells: a side-by-side comparison. *Journal of agricultural and food chemistry* **2011,** *59*, (20), 10964-70.
28. McCormack, D.; McFadden, D. Pterostilbene and cancer: current review. *The Journal of surgical research* **2012,** *173*, (2), e53-61.
29. McCormack, D.; McFadden, D. A review of pterostilbene antioxidant activity and disease modification. *Oxidative medicine and cellular longevity* **2013,** *2013*, 575482.
30. Chang, J.; Rimando, A.; Pallas, M.; Camins, A.; Porquet, D.; Reeves, J.; Shukitt-Hale, B.; Smith, M. A.; Joseph, J. A.; Casadesus, G. Low-dose pterostilbene, but not resveratrol, is a potent neuromodulator in aging and Alzheimer's disease. *Neurobiology of aging* **2012,** *33*, (9), 2062-71.
31. Estrela, J. M.; Ortega, A.; Mena, S.; Rodriguez, M. L.; Asensi, M. Pterostilbene: Biomedical applications. *Critical reviews in clinical laboratory sciences* **2013,** *50*, (3), 65-78.
32. Yeo, S. C.; Ho, P. C.; Lin, H. S. Pharmacokinetics of pterostilbene in Sprague-Dawley rats: the impacts of aqueous solubility, fasting, dose escalation, and dosing route on bioavailability. *Molecular nutrition & food research* **2013,** *57*, (6), 1015-25.
33. Rahman, I.; Biswas, S. K.; Kirkham, P. A. Regulation of inflammation and redox signaling by dietary polyphenols. *Biochemical pharmacology* **2006,** *72*, (11), 1439-52.
34. De Marchi, U.; Biasutto, L.; Garbisa, S.; Toninello, A.; Zoratti, M. Quercetin can act either as an inhibitor or an inducer of the mitochondrial permeability transition pore: A demonstration of the ambivalent redox character of polyphenols. *Biochimica et biophysica acta* **2009,** *1787*, (12), 1425-32.
35. Cao, G.; Sofic, E.; Prior, R. L. Antioxidant and prooxidant behavior of flavonoids: structure-activity relationships. *Free radical biology & medicine* **1997,** *22*, (5), 749-60.
36. Kagan, V. E.; Tyurina, Y. Y. Recycling and redox cycling of phenolic antioxidants. *Annals of the New York Academy of Sciences* **1998,** *854*, 425-34.
37. Galati, G.; Chan, T.; Wu, B.; O'Brien, P. J. Glutathione-dependent generation of reactive oxygen species by the peroxidase-catalyzed redox cycling of flavonoids. *Chemical research in toxicology* **1999,** *12*, (6), 521-5.
38. Kessler, M.; Ubeaud, G.; Jung, L. Anti- and pro-oxidant activity of rutin and quercetin derivatives. *The Journal of pharmacy and pharmacology* **2003,** *55*, (1), 131-42.
39. Kanadzu, M.; Lu, Y.; Morimoto, K. Dual function of (--)-epigallocatechin gallate (EGCG) in healthy human lymphocytes. *Cancer letters* **2006,** *241*, (2), 250-5.
40. Bellion, P.; Olk, M.; Will, F.; Dietrich, H.; Baum, M.; Eisenbrand, G.; Janzowski, C. Formation of hydrogen peroxide in cell culture media by apple polyphenols and its effect on antioxidant biomarkers in the colon cell line HT-29. *Molecular nutrition & food research* **2009,** *53*, (10), 1226-36.

41. Long, L. H.; Hoi, A.; Halliwell, B. Instability of, and generation of hydrogen peroxide by, phenolic compounds in cell culture media. *Archives of biochemistry and biophysics* **2010,** *501*, (1), 162-9.
42. Halliwell, B. Are polyphenols antioxidants or pro-oxidants? What do we learn from cell culture and in vivo studies? *Archives of biochemistry and biophysics* **2008,** *476*, (2), 107-12.
43. Halliwell, B. Cell culture, oxidative stress, and antioxidants: avoiding pitfalls. *Biomedical journal* **2014,** *37*, (3), 99-105.
44. Murphy, M. P. How mitochondria produce reactive oxygen species. *The Biochemical journal* **2009,** *417*, (1), 1-13.
45. Lambert, A. J.; Brand, M. D. Reactive oxygen species production by mitochondria. *Methods in molecular biology (Clifton, N.J.)* **2009,** *554*, 165-81.
46. Brand, M. D. The sites and topology of mitochondrial superoxide production. *Experimental gerontology* **2010,** *45*, (7-8), 466-72.
47. Biasutto, L.; Szabo, I.; Zoratti, M. Mitochondrial effects of plant-made compounds. *Antioxidants & redox signaling* **2011,** *15*, (12), 3039-59.
48. Sena, L. A.; Chandel, N. S. Physiological roles of mitochondrial reactive oxygen species. *Molecular cell* **2012,** *48*, (2), 158-67.
49. Calabrese, E. J.; Mattson, M. P.; Calabrese, V. Resveratrol commonly displays hormesis: occurrence and biomedical significance. *Human & experimental toxicology* **2010,** *29*, (12), 980-1015.
50. Calabrese, E. J. Hormesis is central to toxicology, pharmacology and risk assessment. *Human & experimental toxicology* **2010,** *29*, (4), 249-61.
51. Ristow, M.; Zarse, K. How increased oxidative stress promotes longevity and metabolic health: The concept of mitochondrial hormesis (mitohormesis). *Experimental gerontology* **2010,** *45*, (6), 410-8.
52. Borriello, A.; Bencivenga, D.; Caldarelli, I.; Tramontano, A.; Borgia, A.; Pirozzi, A. V.; Oliva, A.; Della Ragione, F. Resveratrol and cancer treatment: is hormesis a yet unsolved matter? *Current pharmaceutical design* **2013,** *19*, (30), 5384-93.
53. Murakami, A. Dose-dependent functionality and toxicity of green tea polyphenols in experimental rodents. *Archives of biochemistry and biophysics* **2014,** *557*, 3-10.
54. Yun, J.; Finkel, T. Mitohormesis. *Cell metabolism* **2014,** *19*, (5), 757-66.
55. Ristow, M. Unraveling the truth about antioxidants: mitohormesis explains ROS-induced health benefits. *Nature medicine* **2014,** *20*, (7), 709-11.
56. Blagosklonny, M. V. Hormesis does not make sense except in the light of TOR-driven aging. *Aging* **2011,** *3*, (11), 1051-62.
57. Li, C.; Xu, X.; Tao, Z.; Wang, X. J.; Pan, Y. Resveratrol dimers, nutritional components in grape wine, are selective ROS scavengers and weak Nrf2 activators. *Food chemistry* **2015,** *173*, 218-23.
58. Soeur, J.; Eilstein, J.; Lereaux, G.; Jones, C.; Marrot, L. Skin resistance to oxidative stress induced by resveratrol: From Nrf2 activation to GSH biosynthesis. *Free radical biology & medicine* **2015,** *78*, 213-23.
59. Xia, N.; Forstermann, U.; Li, H. Resveratrol and endothelial nitric oxide. *Molecules (Basel, Switzerland)* **2014,** *19*, (10), 16102-21.
60. Singh, B.; Shoulson, R.; Chatterjee, A.; Ronghe, A.; Bhat, N. K.; Dim, D. C.; Bhat, H. K. Resveratrol inhibits estrogen-induced breast carcinogenesis through induction of NRF2-mediated protective pathways. *Carcinogenesis* **2014,** *35*, (8), 1872-80.
61. Simao, F.; Matte, A.; Pagnussat, A. S.; Netto, C. A.; Salbego, C. G. Resveratrol prevents CA1 neurons against ischemic injury by parallel modulation of both GSK-3beta and CREB through PI3-K/Akt pathways. *The European journal of neuroscience* **2012,** *36*, (7), 2899-905.
62. Liao, Z.; Liu, D.; Tang, L.; Yin, D.; Yin, S.; Lai, S.; Yao, J.; He, M. Long-term oral resveratrol intake provides nutritional preconditioning against myocardial ischemia/reperfusion injury: involvement of VDAC1 down-regulation. *Molecular nutrition & food research* **2014**.

63. Lu, Z.; Zhang, Y.; Liu, H.; Yuan, J.; Zheng, Z.; Zou, G. Transport of a cancer chemopreventive polyphenol, resveratrol: interaction with serum albumin and hemoglobin. *Journal of fluorescence* **2007,** *17*, (5), 580-7.
64. CN, N. s.-K.; St-Louis, C.; Beauregard, M.; Subirade, M.; Carpentier, R.; Hotchandani, S.; Tajmir-Riahi, H. A. Resveratrol binding to human serum albumin. *Journal of biomolecular structure & dynamics* **2006,** *24*, (3), 277-83.
65. Bourassa, P.; Kanakis, C. D.; Tarantilis, P.; Pollissiou, M. G.; Tajmir-Riahi, H. A. Resveratrol, genistein, and curcumin bind bovine serum albumin. *The journal of physical chemistry. B* **2010,** *114*, (9), 3348-54.
66. Latruffe, N.; Menzel, M.; Delmas, D.; Buchet, R.; Lancon, A. Compared binding properties between resveratrol and other polyphenols to plasmatic albumin: consequences for the health protecting effect of dietary plant microcomponents. *Molecules (Basel, Switzerland)* **2014,** *19*, (11), 17066-77.
67. Bourassa, P.; Bariyanga, J.; Tajmir-Riahi, H. A. Binding sites of resveratrol, genistein, and curcumin with milk alpha- and beta-caseins. *The journal of physical chemistry. B* **2013,** *117*, (5), 1287-95.
68. Liang, L.; Tajmir-Riahi, H. A.; Subirade, M. Interaction of beta-lactoglobulin with resveratrol and its biological implications. *Biomacromolecules* **2008,** *9*, (1), 50-6.
69. Kanakis, C. D.; Tarantilis, P. A.; Polissiou, M. G.; Tajmir-Riahi, H. A. Probing the binding sites of resveratrol, genistein, and curcumin with milk beta-lactoglobulin. *Journal of biomolecular structure & dynamics* **2013,** *31*, (12), 1455-66.
70. Hsieh, T. C.; Wang, Z.; Deng, H.; Wu, J. M. Identification of glutathione sulfotransferase-pi (GSTP1) as a new resveratrol targeting protein (RTP) and studies of resveratrol-responsive protein changes by resveratrol affinity chromatography. *Anticancer research* **2008,** *28*, (1a), 29-36.
71. Gledhill, J. R.; Montgomery, M. G.; Leslie, A. G.; Walker, J. E. Mechanism of inhibition of bovine F1-ATPase by resveratrol and related polyphenols. *Proceedings of the National Academy of Sciences of the United States of America* **2007,** *104*, (34), 13632-7.
72. Slater, S. J.; Seiz, J. L.; Cook, A. C.; Stagliano, B. A.; Buzas, C. J. Inhibition of protein kinase C by resveratrol. *Biochimica et biophysica acta* **2003,** *1637*, (1), 59-69.
73. Lin, H. Y.; Lansing, L.; Merillon, J. M.; Davis, F. B.; Tang, H. Y.; Shih, A.; Vitrac, X.; Krisa, S.; Keating, T.; Cao, H. J.; Bergh, J.; Quackenbush, S.; Davis, P. J. Integrin alphaVbeta3 contains a receptor site for resveratrol. *FASEB journal : official publication of the Federation of American Societies for Experimental Biology* **2006,** *20*, (10), 1742-4.
74. Wang, Z.; Hsieh, T. C.; Zhang, Z.; Ma, Y.; Wu, J. M. Identification and purification of resveratrol targeting proteins using immobilized resveratrol affinity chromatography. *Biochemical and biophysical research communications* **2004,** *323*, (3), 743-9.
75. Kutil, Z.; Temml, V.; Maghradze, D.; Pribylova, M.; Dvorakova, M.; Schuster, D.; Vanek, T.; Landa, P. Impact of wines and wine constituents on cyclooxygenase-1, cyclooxygenase-2, and 5-lipoxygenase catalytic activity. *Mediators of inflammation* **2014,** *2014*, 178931.
76. Park, S. J.; Ahmad, F.; Philp, A.; Baar, K.; Williams, T.; Luo, H.; Ke, H.; Rehmann, H.; Taussig, R.; Brown, A. L.; Kim, M. K.; Beaven, M. A.; Burgin, A. B.; Manganiello, V.; Chung, J. H. Resveratrol ameliorates aging-related metabolic phenotypes by inhibiting cAMP phosphodiesterases. *Cell* **2012,** *148*, (3), 421-33.
77. Zhao, P.; Chen, S. K.; Cai, Y. H.; Lu, X.; Li, Z.; Cheng, Y. K.; Zhang, C.; Hu, X.; He, X.; Luo, H. B. The molecular basis for the inhibition of phosphodiesterase-4D by three natural resveratrol analogs. Isolation, molecular docking, molecular dynamics simulations, binding free energy, and bioassay. *Biochimica et biophysica acta* **2013,** *1834*, (10), 2089-96.
78. Calleri, E.; Pochetti, G.; Dossou, K. S.; Laghezza, A.; Montanari, R.; Capelli, D.; Prada, E.; Loiodice, F.; Massolini, G.; Bernier, M.; Moaddel, R. Resveratrol and its metabolites bind to PPARs. *Chembiochem : a European journal of chemical biology* **2014,** *15*, (8), 1154-60.
79. Han, Y. S.; Bastianetto, S.; Dumont, Y.; Quirion, R. Specific plasma membrane binding sites for polyphenols, including resveratrol, in the rat brain. *The Journal of pharmacology and experimental therapeutics* **2006,** *318*, (1), 238-45.

80. Bastianetto, S.; Dumont, Y.; Han, Y.; Quirion, R. Comparative neuroprotective properties of stilbene and catechin analogs: action via a plasma membrane receptor site? *CNS neuroscience & therapeutics* **2009,** *15*, (1), 76-83.
81. Bastianetto, S.; Dumont, Y.; Duranton, A.; Vercauteren, F.; Breton, L.; Quirion, R. Protective action of resveratrol in human skin: possible involvement of specific receptor binding sites. *PloS one* **2010,** *5*, (9), e12935.
82. Tachibana, H.; Koga, K.; Fujimura, Y.; Yamada, K. A receptor for green tea polyphenol EGCG. *Nature structural & molecular biology* **2004,** *11*, (4), 380-1.
83. Umeda, D.; Yano, S.; Yamada, K.; Tachibana, H. Green tea polyphenol epigallocatechin-3-gallate signaling pathway through 67-kDa laminin receptor. *The Journal of biological chemistry* **2008,** *283*, (6), 3050-8.
84. Fujimura, Y.; Sumida, M.; Sugihara, K.; Tsukamoto, S.; Yamada, K.; Tachibana, H. Green tea polyphenol EGCG sensing motif on the 67-kDa laminin receptor. *PloS one* **2012,** *7*, (5), e37942.
85. Tsukamoto, S.; Hirotsu, K.; Kumazoe, M.; Goto, Y.; Sugihara, K.; Suda, T.; Tsurudome, Y.; Suzuki, T.; Yamashita, S.; Kim, Y.; Huang, Y.; Yamada, K.; Tachibana, H. Green tea polyphenol EGCG induces lipid-raft clustering and apoptotic cell death by activating protein kinase Cdelta and acid sphingomyelinase through a 67 kDa laminin receptor in multiple myeloma cells. *The Biochemical journal* **2012,** *443*, (2), 525-34.
86. Kumazoe, M.; Sugihara, K.; Tsukamoto, S.; Huang, Y.; Tsurudome, Y.; Suzuki, T.; Suemasu, Y.; Ueda, N.; Yamashita, S.; Kim, Y.; Yamada, K.; Tachibana, H. 67-kDa laminin receptor increases cGMP to induce cancer-selective apoptosis. *The Journal of clinical investigation* **2013,** *123*, (2), 787-99.
87. Menard, C.; Bastianetto, S.; Quirion, R. Neuroprotective effects of resveratrol and epigallocatechin gallate polyphenols are mediated by the activation of protein kinase C gamma. *Frontiers in cellular neuroscience* **2013,** *7*, 281.
88. Patel, R.; Apostolatos, A.; Carter, G.; Ajmo, J.; Gali, M.; Cooper, D. R.; You, M.; Bisht, K. S.; Patel, N. A. Protein kinase C delta (PKCdelta) splice variants modulate apoptosis pathway in 3T3L1 cells during adipogenesis: identification of PKCdeltaII inhibitor. *The Journal of biological chemistry* **2013,** *288*, (37), 26834-46.
89. Kundu, J. K.; Shin, Y. K.; Kim, S. H.; Surh, Y. J. Resveratrol inhibits phorbol ester-induced expression of COX-2 and activation of NF-kappaB in mouse skin by blocking IkappaB kinase activity. *Carcinogenesis* **2006,** *27*, (7), 1465-74.
90. Jo, J. Y.; Gonzalez de Mejia, E.; Lila, M. A. Catalytic inhibition of human DNA topoisomerase II by interactions of grape cell culture polyphenols. *Journal of agricultural and food chemistry* **2006,** *54*, (6), 2083-7.
91. Dhar, S.; Kumar, A.; Li, K.; Tzivion, G.; Levenson, A. S. Resveratrol regulates PTEN/Akt pathway through inhibition of MTA1/HDAC unit of the NuRD complex in prostate cancer. *Biochimica et biophysica acta* **2015,** *1853*, (2), 265-75.
92. Um, J. H.; Park, S. J.; Kang, H.; Yang, S.; Foretz, M.; McBurney, M. W.; Kim, M. K.; Viollet, B.; Chung, J. H. AMP-activated protein kinase-deficient mice are resistant to the metabolic effects of resveratrol. *Diabetes* **2010,** *59*, (3), 554-63.
93. Canto, C.; Jiang, L. Q.; Deshmukh, A. S.; Mataki, C.; Coste, A.; Lagouge, M.; Zierath, J. R.; Auwerx, J. Interdependence of AMPK and SIRT1 for metabolic adaptation to fasting and exercise in skeletal muscle. *Cell metabolism* **2010,** *11*, (3), 213-9.
94. Canto, C.; Gerhart-Hines, Z.; Feige, J. N.; Lagouge, M.; Noriega, L.; Milne, J. C.; Elliott, P. J.; Puigserver, P.; Auwerx, J. AMPK regulates energy expenditure by modulating NAD+ metabolism and SIRT1 activity. *Nature* **2009,** *458*, (7241), 1056-60.
95. Pacholec, M.; Bleasdale, J. E.; Chrunyk, B.; Cunningham, D.; Flynn, D.; Garofalo, R. S.; Griffith, D.; Griffor, M.; Loulakis, P.; Pabst, B.; Qiu, X.; Stockman, B.; Thanabal, V.; Varghese, A.; Ward, J.; Withka, J.; Ahn, K. SRT1720, SRT2183, SRT1460, and resveratrol are not direct activators of SIRT1. *The Journal of biological chemistry* **2010,** *285*, (11), 8340-51.
96. Lakshminarasimhan, M.; Rauh, D.; Schutkowski, M.; Steegborn, C. Sirt1 activation by resveratrol is substrate sequence-selective. *Aging* **2013,** *5*, (3), 151-4.

97. Lakshminarasimhan, M.; Curth, U.; Moniot, S.; Mosalaganti, S.; Raunser, S.; Steegborn, C. Molecular architecture of the human protein deacetylase Sirt1 and its regulation by AROS and resveratrol. *Bioscience reports* **2013,** *33*, (3).
98. Gertz, M.; Nguyen, G. T.; Fischer, F.; Suenkel, B.; Schlicker, C.; Franzel, B.; Tomaschewski, J.; Aladini, F.; Becker, C.; Wolters, D.; Steegborn, C. A molecular mechanism for direct sirtuin activation by resveratrol. *PloS one* **2012,** *7*, (11), e49761.
99. Nguyen, G. T.; Gertz, M.; Steegborn, C. Crystal structures of Sirt3 complexes with 4'-bromo-resveratrol reveal binding sites and inhibition mechanism. *Chemistry & biology* **2013,** *20*, (11), 1375-85.
100. Parihar, P.; Solanki, I.; Mansuri, M. L.; Parihar, M. S. Mitochondrial sirtuins: Emerging roles in metabolic regulations, energy homeostasis and diseases. *Experimental gerontology* **2015,** *61c*, 130-141.
101. Kiran, S.; Anwar, T.; Kiran, M.; Ramakrishna, G. Sirtuin 7 in cell proliferation, stress and disease: Rise of the Seventh Sirtuin! *Cellular signalling* **2014**.
102. Zhu, Y.; Yan, Y.; Principe, D. R.; Zou, X.; Vassilopoulos, A.; Gius, D. SIRT3 and SIRT4 are mitochondrial tumor suppressor proteins that connect mitochondrial metabolism and carcinogenesis. *Cancer & metabolism* **2014,** *2*, 15.
103. Masri, S.; Sassone-Corsi, P. Sirtuins and the circadian clock: bridging chromatin and metabolism. *Science signaling* **2014,** *7*, (342), re6.
104. Choudhary, C.; Weinert, B. T.; Nishida, Y.; Verdin, E.; Mann, M. The growing landscape of lysine acetylation links metabolism and cell signalling. *Nature reviews. Molecular cell biology* **2014,** *15*, (8), 536-50.
105. Russo, M. A.; Sansone, L.; Polletta, L.; Runci, A.; Rashid, M. M.; De Santis, E.; Vernucci, E.; Carnevale, I.; Tafani, M. Sirtuins and resveratrol-derived compounds: a model for understanding the beneficial effects of the Mediterranean diet. *Endocrine, metabolic & immune disorders drug targets* **2014,** *14*, (4), 300-8.
106. Pirola, L.; Frojdo, S. Resveratrol: one molecule, many targets. *IUBMB life* **2008,** *60*, (5), 323-32.
107. Zimmermann, G. R.; Lehar, J.; Keith, C. T. Multi-target therapeutics: when the whole is greater than the sum of the parts. *Drug discovery today* **2007,** *12*, (1-2), 34-42.
108. Wagner, H. Synergy research: approaching a new generation of phytopharmaceuticals. *Fitoterapia* **2011,** *82*, (1), 34-7.
109. Efferth, T.; Koch, E. Complex interactions between phytochemicals. The multi-target therapeutic concept of phytotherapy. *Current drug targets* **2011,** *12*, (1), 122-32.
110. Rather, M. A.; Bhat, B. A.; Qurishi, M. A. Multicomponent phytotherapeutic approach gaining momentum: Is the "one drug to fit all" model breaking down? *Phytomedicine : international journal of phytotherapy and phytopharmacology* **2013,** *21*, (1), 1-14.
111. Yang, Y.; Zhang, Z.; Li, S.; Ye, X.; Li, X.; He, K. Synergy effects of herb extracts: pharmacokinetics and pharmacodynamic basis. *Fitoterapia* **2014,** *92*, 133-47.
112. Smoliga, J. M.; Baur, J. A.; Hausenblas, H. A. Resveratrol and health--a comprehensive review of human clinical trials. *Molecular nutrition & food research* **2011,** *55*, (8), 1129-41.
113. Patel, K. R.; Scott, E.; Brown, V. A.; Gescher, A. J.; Steward, W. P.; Brown, K. Clinical trials of resveratrol. *Annals of the New York Academy of Sciences* **2011,** *1215*, 161-9.
114. Tome-Carneiro, J.; Larrosa, M.; Gonzalez-Sarrias, A.; Tomas-Barberan, F. A.; Garcia-Conesa, M. T.; Espin, J. C. Resveratrol and clinical trials: the crossroad from in vitro studies to human evidence. *Current pharmaceutical design* **2013,** *19*, (34), 6064-93.
115. Subramanian, L.; Youssef, S.; Bhattacharya, S.; Kenealey, J.; Polans, A. S.; van Ginkel, P. R. Resveratrol: challenges in translation to the clinic--a critical discussion. *Clinical cancer research : an official journal of the American Association for Cancer Research* **2010,** *16*, (24), 5942-8.
116. Planas, J. M.; Alfaras, I.; Colom, H.; Juan, M. E. The bioavailability and distribution of trans-resveratrol are constrained by ABC transporters. *Archives of biochemistry and biophysics* **2012,** *527*, (2), 67-73.

117. Neves, A. R.; Lucio, M.; Lima, J. L.; Reis, S. Resveratrol in medicinal chemistry: a critical review of its pharmacokinetics, drug-delivery, and membrane interactions. *Current medicinal chemistry* **2012,** *19*, (11), 1663-81.
118. Walle, T. Bioavailability of resveratrol. *Annals of the New York Academy of Sciences* **2011,** *1215*, 9-15.
119. Cottart, C. H.; Nivet-Antoine, V.; Laguillier-Morizot, C.; Beaudeux, J. L. Resveratrol bioavailability and toxicity in humans. *Molecular nutrition & food research* **2010,** *54*, (1), 7-16.
120. Wenzel, E.; Somoza, V. Metabolism and bioavailability of trans-resveratrol. *Molecular nutrition & food research* **2005,** *49*, (5), 472-81.
121. Azzolini, M.; La Spina, M.; Mattarei, A.; Paradisi, C.; Zoratti, M.; Biasutto, L. Pharmacokinetics and tissue distribution of pterostilbene in the rat. *Molecular nutrition & food research* **2014,** *58*, (11), 2122-32.
122. Aires, V.; Limagne, E.; Cotte, A. K.; Latruffe, N.; Ghiringhelli, F.; Delmas, D. Resveratrol metabolites inhibit human metastatic colon cancer cells progression and synergize with chemotherapeutic drugs to induce cell death. *Molecular nutrition & food research* **2013,** *57*, (7), 1170-81.
123. Derlindati, E.; Dall'Asta, M.; Ardigo, D.; Brighenti, F.; Zavaroni, I.; Crozier, A.; Del Rio, D. Quercetin-3-O-glucuronide affects the gene expression profile of M1 and M2a human macrophages exhibiting anti-inflammatory effects. *Food & function* **2012,** *3*, (11), 1144-52.
124. Ruotolo, R.; Calani, L.; Fietta, E.; Brighenti, F.; Crozier, A.; Meda, C.; Maggi, A.; Ottonello, S.; Del Rio, D. Anti-estrogenic activity of a human resveratrol metabolite. *Nutrition, metabolism, and cardiovascular diseases : NMCD* **2013,** *23*, (11), 1086-92.
125. Wu, J. M.; Hsieh, T. C.; Yang, C. J.; Olson, S. C. Resveratrol and its metabolites modulate cytokine-mediated induction of eotaxin-1 in human pulmonary artery endothelial cells. *Annals of the New York Academy of Sciences* **2013,** *1290*, 30-6.
126. Polycarpou, E.; Meira, L. B.; Carrington, S.; Tyrrell, E.; Modjtahedi, H.; Carew, M. A. Resveratrol 3-O-D-glucuronide and resveratrol 4'-O-D-glucuronide inhibit colon cancer cell growth: evidence for a role of A3 adenosine receptors, cyclin D1 depletion, and G1 cell cycle arrest. *Molecular nutrition & food research* **2013,** *57*, (10), 1708-17.
127. Ruotolo, R.; Calani, L.; Brighenti, F.; Crozier, A.; Ottonello, S.; Del Rio, D. Glucuronidation does not suppress the estrogenic activity of quercetin in yeast and human breast cancer cell model systems. *Archives of biochemistry and biophysics* **2014,** *559*, 62-7.
128. Bresciani, L.; Calani, L.; Bocchi, L.; Delucchi, F.; Savi, M.; Ray, S.; Brighenti, F.; Stilli, D.; Del Rio, D. Bioaccumulation of resveratrol metabolites in myocardial tissue is dose-time dependent and related to cardiac hemodynamics in diabetic rats. *Nutrition, metabolism, and cardiovascular diseases : NMCD* **2014,** *24*, (4), 408-15.
129. Ladurner, A.; Schachner, D.; Schueller, K.; Pignitter, M.; Heiss, E. H.; Somoza, V.; Dirsch, V. M. Impact of trans-resveratrol-sulfates and -glucuronides on endothelial nitric oxide synthase activity, nitric oxide release and intracellular reactive oxygen species. *Molecules (Basel, Switzerland)* **2014,** *19*, (10), 16724-36.
130. Maier-Salamon, A.; Bohmdorfer, M.; Riha, J.; Thalhammer, T.; Szekeres, T.; Jaeger, W. Interplay between metabolism and transport of resveratrol. *Annals of the New York Academy of Sciences* **2013,** *1290*, 98-106.
131. Andreadi, C.; Britton, R. G.; Patel, K. R.; Brown, K. Resveratrol-sulfates provide an intracellular reservoir for generation of parent resveratrol, which induces autophagy in cancer cells. *Autophagy* **2014,** *10*, (3), 524-5.
132. Scalbert, A.; Morand, C.; Manach, C.; Remesy, C. Absorption and metabolism of polyphenols in the gut and impact on health. *Biomedicine & pharmacotherapy = Biomedecine & pharmacotherapie* **2002,** *56*, (6), 276-82.
133. Scalbert, A.; Williamson, G. Dietary intake and bioavailability of polyphenols. *The Journal of nutrition* **2000,** *130*, (8S Suppl), 2073s-85s.
134. Lampe, J. W. Is equol the key to the efficacy of soy foods? *The American journal of clinical nutrition* **2009,** *89*, (5), 1664s-1667s.

135. Yuan, J. P.; Wang, J. H.; Liu, X. Metabolism of dietary soy isoflavones to equol by human intestinal microflora--implications for health. *Molecular nutrition & food research* **2007,** *51*, (7), 765-81.
136. Jackson, R. L.; Greiwe, J. S.; Schwen, R. J. Emerging evidence of the health benefits of S-equol, an estrogen receptor beta agonist. *Nutrition reviews* **2011,** *69*, (8), 432-48.
137. Shor, D.; Sathyapalan, T.; Atkin, S. L.; Thatcher, N. J. Does equol production determine soy endocrine effects? *European journal of nutrition* **2012,** *51*, (4), 389-98.
138. Williamson, G.; Clifford, M. N. Colonic metabolites of berry polyphenols: the missing link to biological activity? *The British journal of nutrition* **2010,** *104 Suppl 3*, S48-66.
139. Possemiers, S.; Bolca, S.; Verstraete, W.; Heyerick, A. The intestinal microbiome: a separate organ inside the body with the metabolic potential to influence the bioactivity of botanicals. *Fitoterapia* **2011,** *82*, (1), 53-66.
140. Calani, L.; Dall'Asta, M.; Derlindati, E.; Scazzina, F.; Bruni, R.; Del Rio, D. Colonic metabolism of polyphenols from coffee, green tea, and hazelnut skins. *Journal of clinical gastroenterology* **2012,** *46 Suppl*, S95-9.
141. Dall'Asta, M.; Calani, L.; Tedeschi, M.; Jechiu, L.; Brighenti, F.; Del Rio, D. Identification of microbial metabolites derived from in vitro fecal fermentation of different polyphenolic food sources. *Nutrition (Burbank, Los Angeles County, Calif.)* **2012,** *28*, (2), 197-203.
142. Rodriguez-Mateos, A.; Vauzour, D.; Krueger, C. G.; Shanmuganayagam, D.; Reed, J.; Calani, L.; Mena, P.; Del Rio, D.; Crozier, A. Bioavailability, bioactivity and impact on health of dietary flavonoids and related compounds: an update. *Archives of toxicology* **2014,** *88*, (10), 1803-53.
143. Forester, S. C.; Waterhouse, A. L. Metabolites are key to understanding health effects of wine polyphenolics. *The Journal of nutrition* **2009,** *139*, (9), 1824s-31s.
144. Del Rio, D.; Costa, L. G.; Lean, M. E.; Crozier, A. Polyphenols and health: what compounds are involved? *Nutrition, metabolism, and cardiovascular diseases : NMCD* **2010,** *20*, (1), 1-6.
145. Del Rio, D.; Calani, L.; Cordero, C.; Salvatore, S.; Pellegrini, N.; Brighenti, F. Bioavailability and catabolism of green tea flavan-3-ols in humans. *Nutrition (Burbank, Los Angeles County, Calif.)* **2010,** *26*, (11-12), 1110-6.
146. Del Rio, D.; Borges, G.; Crozier, A. Berry flavonoids and phenolics: bioavailability and evidence of protective effects. *The British journal of nutrition* **2010,** *104 Suppl 3*, S67-90.
147. Crozier, A.; Del Rio, D.; Clifford, M. N. Bioavailability of dietary flavonoids and phenolic compounds. *Molecular aspects of medicine* **2010,** *31*, (6), 446-67.
148. Monagas, M.; Urpi-Sarda, M.; Sanchez-Patan, F.; Llorach, R.; Garrido, I.; Gomez-Cordoves, C.; Andres-Lacueva, C.; Bartolome, B. Insights into the metabolism and microbial biotransformation of dietary flavan-3-ols and the bioactivity of their metabolites. *Food & function* **2010,** *1*, (3), 233-53.
149. Russell, W.; Duthie, G. Plant secondary metabolites and gut health: the case for phenolic acids. *The Proceedings of the Nutrition Society* **2011,** *70*, (3), 389-96.
150. Verzelloni, E.; Pellacani, C.; Tagliazucchi, D.; Tagliaferri, S.; Calani, L.; Costa, L. G.; Brighenti, F.; Borges, G.; Crozier, A.; Conte, A.; Del Rio, D. Antiglycative and neuroprotective activity of colon-derived polyphenol catabolites. *Molecular nutrition & food research* **2011,** *55 Suppl 1*, S35-43.
151. Del Rio, D.; Rodriguez-Mateos, A.; Spencer, J. P.; Tognolini, M.; Borges, G.; Crozier, A. Dietary (poly)phenolics in human health: structures, bioavailability, and evidence of protective effects against chronic diseases. *Antioxidants & redox signaling* **2013,** *18*, (14), 1818-92.
152. Clifford, M. N.; van der Hooft, J. J.; Crozier, A. Human studies on the absorption, distribution, metabolism, and excretion of tea polyphenols. *The American journal of clinical nutrition* **2013,** *98*, (6 Suppl), 1619s-1630s.
153. Fernandez-Millan, E.; Ramos, S.; Alvarez, C.; Bravo, L.; Goya, L.; Martin, M. A. Microbial phenolic metabolites improve glucose-stimulated insulin secretion and protect pancreatic beta cells against tert-butyl hydroperoxide-induced toxicity via ERKs and PKC pathways. *Food and chemical toxicology : an international journal published for the British Industrial Biological Research Association* **2014,** *66*, 245-53.

154. Pereira-Caro, G.; Borges, G.; van der Hooft, J.; Clifford, M. N.; Del Rio, D.; Lean, M. E.; Roberts, S. A.; Kellerhals, M. B.; Crozier, A. Orange juice (poly)phenols are highly bioavailable in humans. *The American journal of clinical nutrition* **2014,** *100*, (5), 1378-84.
155. Escudero-Lopez, B.; Calani, L.; Fernandez-Pachon, M. S.; Ortega, A.; Brighenti, F.; Crozier, A.; Del Rio, D. Absorption, metabolism, and excretion of fermented orange juice (poly)phenols in rats. *BioFactors (Oxford, England)* **2014,** *40*, (3), 327-35.
156. Visioli, F. The resveratrol fiasco. *Pharmacological research : the official journal of the Italian Pharmacological Society* **2014,** *90*, 87.
157. Amri, A.; Chaumeil, J. C.; Sfar, S.; Charrueau, C. Administration of resveratrol: What formulation solutions to bioavailability limitations? *Journal of controlled release : official journal of the Controlled Release Society* **2012,** *158*, (2), 182-93.
158. Smoliga, J. M.; Blanchard, O. Enhancing the delivery of resveratrol in humans: if low bioavailability is the problem, what is the solution? *Molecules (Basel, Switzerland)* **2014,** *19*, (11), 17154-72.
159. Augustin, M. A.; Sanguansri, L.; Lockett, T. Nano- and micro-encapsulated systems for enhancing the delivery of resveratrol. *Annals of the New York Academy of Sciences* **2013,** *1290*, 107-12.
160. Pangeni, R.; Sahni, J. K.; Ali, J.; Sharma, S.; Baboota, S. Resveratrol: review on therapeutic potential and recent advances in drug delivery. *Expert opinion on drug delivery* **2014,** *11*, (8), 1285-98.
161. Biasutto, L.; Mattarei, A.; Sassi, N.; Azzolini, M.; Romio, M.; Paradisi, C.; Zoratti, M. Improving the efficacy of plant polyphenols. *Anti-cancer agents in medicinal chemistry* **2014,** *14*, (10), 1332-42.
162. Biasutto, L.; Zoratti, M. Prodrugs of quercetin and resveratrol: a strategy under development. *Current drug metabolism* **2014,** *15*, (1), 77-95.

1. Acetal derivatives as prodrugs of resveratrol

molecular pharmaceutics

Article

pubs.acs.org/molecularpharmaceutics

Acetal Derivatives as Prodrugs of Resveratrol

Andrea Mattarei,[†,‡] Michele Azzolini,[§] Massimo Carraro,[‡] Nicola Sassi,[†,§] Mario Zoratti,[†,§] Cristina Paradisi,*[,‡] and Lucia Biasutto*[,†,§]

[†]CNR Institute of Neuroscience, viale G. Colombo 3, 35121 Padova, Italy

[‡]Department of Chemical Sciences, University of Padova, via F. Marzolo 1, 35131 Padova, Italy

[§]Department of Biomedical Sciences, University of Padova, viale G. Colombo 3, 35121 Padova, Italy

Supporting Information

ABSTRACT: The pharmacological exploitation of resveratrol is hindered by rapid phase-II conjugative metabolism in enterocytes and hepatocytes. One approach to the solution of this problem relies on prodrugs. We report the synthesis and characterization as well as the assessment of *in vivo* absorption and metabolism of a set of prodrugs of resveratrol in which the OH groups are engaged in the formal ($-OCH_2OR$) or the more labile acetal ($-OCH(CH_3)OR$) linkages. As carrier group (R) of the prodrug, we have used short ethyleneglycol oligomers (OEG) capped by a terminal methoxy group: $-O-(CH_2CH_2O)_n-CH_3$ (n = 0, 1, 2, 3, 4, 6). These moieties are expected to exhibit, to a degree, the favorable properties of longer polyethyleneglycol (PEG) chains, while their relatively small size makes for a more favorable drug loading capacity. After administration of formal-based prodrugs to rats by oral gavage, significant concentrations of derivatives were measured in blood samples over several hours, in all cases except for n = 0. Absorption was maximal for n = 4. Complete deprotection to give resveratrol and its metabolites was however too slow to be of practical use. Administration of the acetal prodrug carrying tetrameric OEG chains resulted instead in the protracted presence of resveratrol metabolites in blood, consistent with a progressive regeneration of the parent molecule from the prodrug after its absorption. The results suggest that prodrugs of polyphenols based on the acetal bond and short ethyleneglycol oligomers of homogeneous size may be a convenient tool for the systemic delivery of the unconjugated parent compound.

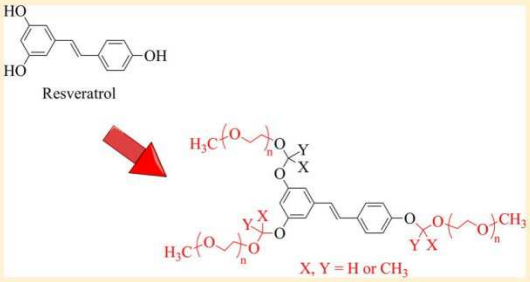

KEYWORDS: *resveratrol, oligoethyleneglycol, bioavailability, pharmacokinetic, prodrugs*

INTRODUCTION

Resveratrol (Figure 1), one of the most intensely studied plant polyphenols, exhibits a range of activities[1] of biomedical interest. It acts on several cellular signaling pathways,[2−11] overlapping to a considerable extent those mediating the effects of dietary restriction and exercise. Ensuing beneficial effects include lifespan extension in model systems,[12] improvements of functionality in aging,[2,8,10,12,13] protection of the cardiovascular system,[4,14] anti-inflammatory activity,[4] for example in arthritis,[15,16] cancer chemoprevention,[17−19] and potentiation of chemotherapy,[20,21] neuroprotection,[22,23] antagonism of the metabolic syndrome,[24,25] improvement of glucose handling in diabetes,[26] and of fat mobilization.[27,28] Despite the evidence summarized in the cited reviews, the efficacy of resveratrol administration *in vivo* remains in doubt.[29,30] Meta-reviews consider the still preliminary results of human clinical trials inconclusive.[31,32] This is because resveratrol, like other polyphenols, has a relatively poor bioavailability due to a built-in propensity to phase II metabolism, that is, "detoxification" via covalent modification of the hydroxyl groups by the sulfo- and glucuronosyl-transferases of enterocytes and hepatocytes.[33−35] These conjugates can then be re-exported from cells by MDR pumps.[36,37]

Part of the bioefficacy of resveratrol may well be due to hormesis, that is, a response to a low level of stress induced by the bioactive compound, affording protection against subsequent higher doses.[38,39] Such a model implies that even a modest, in absolute terms, increase of bioavailability may have significant consequences, if hormesis induction is achieved. A very relevant aspect currently under investigation is the bioactivity of metabolites formed by phase II "detoxification". The available results suggest that, in general, these conjugates are less bioactive than resveratrol itself,[40−44] hence the dual goal of improving its absorption and of slowing down metabolism to hopefully enhance favorable effects.

Various approaches are being tested: formulations,[45−47] nanovectors,[48,49] and prodrugs[50−53] are the major ones and could represent a useful pharmacological tool to improve the *in*

Received: April 17, 2013
Revised: June 1, 2013
Accepted: June 4, 2013
Published: June 4, 2013

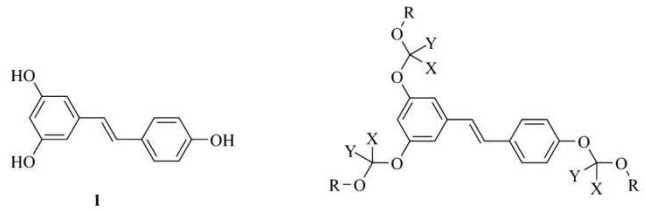

2a-g: X, Y = H;
R = CH_3 (**2a**); CH_2CH_3 (**2b**); $CH_2CH_2OCH_3$ (**2c**); $(CH_2CH_2O)_2CH_3$ (**2d**); $(CH_2CH_2O)_3CH_3$ (**2e**); $(CH_2CH_2O)_4CH_3$ (**2f**); $(CH_2CH_2O)_6CH_3$ (**2g**)
3: X, Y = CH_3; R = CH_3
4: X = H, Y = CH_3; R = $(CH_2CH_2O)_4CH_3$

Figure 1. Resveratrol (**1**) and new derivatives synthesized: formals (**2a–g**), acetals (**3**), and ketals (**4**).

vivo activity of resveratrol.[54] We report here the synthesis, properties, and pharmacokinetics in rats of a family of prodrugs of resveratrol utilizing the acetal bond system to link protective/solubilizing groups to resveratrol hydroxyls ("acetal" is used here, as is customary, as a generic label including all three bonding groups used in this work, see Figure 1). This linkage, often used for the protection of hydroxyls in synthesis procedures, offers the advantage of low polarity and steric hindrance and is therefore expected to allow passage through biomembranes. Furthermore it is acid-sensitive, a characteristic which may lead to a requirement for protection by a suitable formulation during gastric transit, but also offers in principle a tool for targeted release of the active principle in acidic environments. Its use in prodrugs has precedents,[55] and recently a variant has been used to produce derivatives of quercetin, another remarkable polyphenol, with enhanced stability and membrane permeability.[56−58] Notably, the acetal bond system links the polyphenolic scaffold to the glycosidic moiety in polyphenol glycosides, a major class of natural derivatives, and glucuronides, a major product of phase II metabolism. These natural derivatives are characterized by high hydrophilicity and solubility and poor adsorption in their native form.

Polyethyleneglycol (PEG) has been used in a number of formulations and prodrugs to increase solubility, improve absorption, and limit immune response.[59,60] PEG is known to be nontoxic, nonantigenic, and biocompatible, to be rapidly eliminated from the body, to be soluble both in water and many organic solvents, and to have pronounced solubilizing properties. Incorporation of PEG chains can increase resistance to hydrolases and stability in the gastrointestinal tract. PEG has been successfully used as a "carrier" of peptides and proteins as well as of small bioactive molecules. In this latter case however an intrinsic limitation is its low drug loading capacity, that is, the high molecular weight of prodrugs incorporating polymeric chains. We have previously reported the synthesis of a resveratrol prodrug bearing PEG chains linked via carboxyester moieties.[51] In experiments assessing transport across rat intestine, this construct succeeded in determining the translocation of unmodified resveratrol. When using resveratrol as such, practically only conjugation metabolites appeared on the basolateral side. To remedy the low loading capacity we have now used as carrier groups short polyether chains of defined size (oligoethyleneglycol: OEG) and performed a structure−function study to determine the optimal chain size for absorption in pharmacokinetics. To overcome the fragility of the carboxyester moiety[51,61] we have, as mentioned, turned to the acetal linkage.

EXPERIMENTAL SECTION

Materials and General Methods. Resveratrol was purchased from Waseta Int. Trading Co. (Shangai, P.R. China). Other starting materials and reagents were purchased from Aldrich, Fluka, Merck-Novabiochem, Riedel de Haen, J.T. Baker, Cambridge Isotope Laboratories Inc., Acros Organics, Carlo Erba and Prolabo, and were used as received. ^{1}H NMR spectra were recorded with a Bruker AC250F spectrometer operating at 250 MHz and a Bruker AVII500 spectrometer operating at 500 MHz. Chemical shifts (δ) are given in ppm relative to the signal of the solvent. HPLC-UV analyses were performed with an Agilent 1290 Infinity LC System (Agilent Technologies), equipped with binary pump and a diode array detector (190−500 nm). High-performance liquid chromatography/electrospray ionization−mass spectrometry (HPLC/ESI-MS) analyses and mass spectra were performed with a 1100 Series Agilent Technologies system, equipped with binary pump (G1312A) and MSD SL Trap mass spectrometer (G2445D SL) with an ESI source. ESI-MS positive spectra of reaction intermediates and final purified products were obtained from solutions in acetonitrile, eluting with a 1:1 water−acetonitrile mixture containing 0.1% formic acid. Thin-layer chromatographies (TLCs) were run on silica gel supported on plastic (Macherey-Nagel PolygramSIL G/UV_{254}, silica thickness 0.2 mm) or on silica gel supported on glass (Fluka) (silica thickness 0.25 mm, granulometry 60 Å, medium porosity) and visualized by UV detection. Flash chromatography was performed on silica gel (Macherey-Nagel 60, 230−400 mesh granulometry (0.063−0.040 mm)) under air pressure. The solvents were analytical or synthetic grade and were used without further purification. All experiments reported were performed in triplicate unless otherwise stated, and means ± standard deviation values are reported.

*General Procedure for the Preparation of the Formal Derivatives of Resveratrol (**2a−g**).* NaH (17.5 mmol, 4 eq 60% in mineral oil) was washed three times in 5 mL of *n*-hexane. The suspension was decanted after each wash, and hexane traces were removed under reduced pressure. A sample of 10 mL of tetrahydrofuran (THF) was then added, and the suspension was stirred for 5 min. A solution of resveratrol (**1**) (4.4 mmol, 1 equiv) in 5 mL of anhydrous THF was then added. After stirring for 30 min, a solution of the desired chloromethyl ether (24.2 mmol, 5.5 equiv) in 5 mL of anhydrous THF was added dropwise, and the mixture was

vigorously stirred for 2 min at room temperature. Dimethylformamide (DMF, 5 mL) was then added, and the reaction progress was monitored by TLC. After the disappearance of resveratrol, the reaction mixture was diluted in CH_2Cl_2 (150 mL) and washed with 0.3 N HCl (100 mL). The organic layer was dried over $MgSO_4$ and filtered. The solvent was evaporated under reduced pressure, and the residue was purified by chromatography to give the trisubstituted formal derivative of resveratrol.

*trans-3,4′,5-Tri(methoxymethoxy)stilbene (**2a**).* Purified by flash-chromatography (CH_2Cl_2/AcOEt = 95:5). Yield: 1.15 g (73% based on resveratrol) as a white powder. ESI-MS (ion trap): m/z 361 $[M + H]^+$. ^1H NMR (250 MHz, $CDCl_3$, 25 °C): δ = 3.49 (s, 3H, −O−CH_3), 3.50 (s, 6H, 2 × −O−CH_3), 5.19 (s, 6H, 3 × −O−CH_2−O−), 6.64 (t, 1H, $^4J_{H,H}$ = 2.3 Hz, H-4), 6.85 (d, 2H, $^4J_{H,H}$ = 2.0 Hz, H-2, H-6), 6.87−7.07 (m, 4H, H-2′, H-6′, H-7, H-8), 7.44 (d, 2H, $^3J_{H,H}$ = 8.8 Hz, H-3′, H-5′) ppm. ^{13}C NMR (250 MHz, $CDCl_3$, 25 °C): δ = 158.5, 156.9, 139.8, 131.0, 128.8, 127.8, 126.7, 116.4, 107.6, 104.0, 94.5, 94.4, 56.1, 56.0 ppm. Purity (HPLC-UV) ≥ 95%.

*trans-3,4′,5-Tri(ethoxymethoxy)stilbene (**2b**).* Purified by flash-chromatography (hexane/AcOEt = 50:50). Yield: 1.34 g (76%) as a yellow oil. ESI-MS (ion trap): m/z 403 $[M + H]^+$. ^1H NMR (250 MHz, $CDCl_3$, 25 °C): δ = 1.11−1.17 (m, 9H, 3 × CH_2−CH_3), 3.62−3.70 (m, 6H, 3 × −O−CH_2-), 5.24 (s, 6H, 3 × −O−CH_2−O−), 6.57 (t, 1H, $^4J_{H,H}$ = 2,0 Hz, H-4), 6.87 (d, 2H, $^4J_{H,H}$ = 2.0 Hz, H-2, H-6), 7.00−7.21 (m, 4H, H-2′, H-6′, H-7, H-8), 7.54 (d, 2H, $^3J_{H,H}$ = 8,5 Hz, H-3′, H-5′) ppm. ^{13}C NMR (250 MHz, $CDCl_3$, 25 °C): δ = 158.0, 156.6, 139.3, 130.3, 128.5, 127.8, 126.3, 116.2, 107.1, 104.5, 92.5, 92.4, 63.7, 63.6, 15.0 ppm. Purity (HPLC-UV) ≥ 95%.

*trans-3,4′,5-Tri-((2-methoxyethoxy)methoxy)stilbene (**2c**).* Purified by flash-chromatography (hexane/AcOEt = 50:50). Yield: 1.44 g (67%) as a yellow oil. ESI-MS (ion trap): m/z 493 $[M + H]^+$. ^1H NMR (250 MHz, $CDCl_3$, 25 °C): δ = 3.38 (s, 3H, −O−CH_3), 3.39 (s, 6H, 2 × −O−CH_3), 3.56−3.60 (m, 6H, 3 × −O−CH_2−), 3.82−3.86 (m, 6H, 3 × −O−CH_2−), 5.28−5.29 (m, 6H, 3 × −O−CH_2−O−), 6.64 (t, 1H, $^4J_{H,H}$ = 2,0 Hz, H-4), 6.87 (d, 2H, $^4J_{H,H}$ = 2,0 Hz, H-2, H-6), 6.93−7.06 (m, 4H, H-2′, H-6′, H-7, H-8), 7.43 (d, 2H, $^3J_{H,H}$ = 8,5 Hz, H-3′, H-5′) ppm. ^{13}C NMR (250 MHz, $CDCl_3$, 25 °C): δ = 158.3, 156.9, 139.6, 130.8, 128.7, 127.6, 126.6, 116.3, 107.5, 104.0, 93.3, 93.2, 71.5, 67.5, 58.9 ppm. Purity (HPLC-UV) ≥ 95%.

*trans-3,4′,5-Tri((2-(2-methoxyethoxy)ethoxy)methoxy)-stilbene (**2d**).* Purified by flash-chromatography (in two steps, using, respectively, CH_2Cl_2/acetone = 80:20 and hexane/AcOEt = 20:85). Yield: 1.84 g (67%) as a yellow oil. ESI-MS (ion trap): m/z 625 $[M + H]^+$. ^1H NMR (250 MHz, $CDCl_3$, 25 °C): δ = 3.33−3.34 (m, 9H, 3 × −O−CH_3), 3.48−3.52 (m, 6H, 3 × −O−CH_2−), 3.59−3.67 (m, 12H, 6 × −O−CH_2−), 3.82−3.86 (m, 6H, 3 × −O−CH_2−) 5.24−5.25 (m, 6H, 3 × −O−CH_2−O−), 6.61 (t, 1H, $^4J_{H,H}$ = 2,0 Hz, H-4), 6.83 −7.04 (m, 6H, H-2, H-6, H-2′, H-6′, H-7, H-8), 7.40 (d, 2H, $^3J_{H,H}$ = 8,5 Hz, H-3′, H-5′) ppm. ^{13}C NMR (250 MHz, $CDCl_3$, 25 °C): δ = 158.3, 156.8, 139.5, 130.8, 128.6, 127.6, 126.5, 116.3, 107.4, 103.9, 93.2, 93.2, 71.7, 70.4, 70.3, 70.2, 67.6, 58.9 ppm. Purity (HPLC-UV) ≥ 99%.

*trans-3,4′,5-Tri(2,5,8,11-tetraoxadodecyloxy)stilbene (**2e**).* Purified by flash-chromatography (hexane/AcOEt/diethyl ether/acetone = 10:30:30:30). Yield: 2.15 g (65%) as a yellow oil. ESI-MS (ion trap): m/z 757 $[M + H]^+$. ^1H NMR (250 MHz, $CDCl_3$, 25 °C): δ = 3.33−3.34 (m, 9H, 3 × −O−CH_3), 3.47−3.53 (m, 6H, 3 × −O−CH_2−), 3.57−3.66 (m, 24H, 12 × −O−CH_2−), 3.79−3.83 (m, 6H, 3 × −O−CH_2−) 5.23−5.24 (m, 6H, 3 × −O−CH_2−O−), 6.59 (t, 1H, $^4J_{H,H}$ = 2,0 Hz, H-4), 6.81 −7.03 (m, 6H, H-2, H-6, H-2′, H-6′, H-7, H-8), 7.39 (d, 2H, $^3J_{H,H}$ = 8,5 Hz, H-3′, H-5′) ppm. ^{13}C NMR (250 MHz, $CDCl_3$, 25 °C): δ = 158.3, 156.9, 139.5, 130.8, 128.6, 127.6, 126.5, 116.3, 107.4, 103.9, 93.2, 93.2, 71.7, 70.4, 70.4, 70.2, 67.6, 58.9 ppm. Purity (HPLC-UV) ≥ 99%.

*trans-3,4′,5-Tri(2,5,8,11,14-pentaoxapentadecyloxy)-stilbene (**2f**).* Purified by preparative HPLC (ACE 5 AQ column 150 × 21.2 mm i.d.). Solvents A and B were H_2O and acetonitrile each containing 0.05% TFA. The gradient for B was as follows: 37.5% for 2 min, from 37.5% to 65% in 10 min. The flow rate was 17 mL/min. The eluate was monitored at 300 nm. Yield: 2.59 g (66%) as a colorless oil. ESI-MS (ion trap): m/z 889.5 $[M + H]^+$. ^1H NMR (250 MHz, $CDCl_3$, 25 °C): δ = 3.27 (s, 9H, 3 × −O−CH_3), 3.43−3.46 (m, 6H, 3 × −O−CH_2−), 3.52−3.61 (m, 36H, 18 × −O−CH_2−), 3.74−3.77 (m, 6H, 3 × −O−CH_2−) 5.17−5.18 (m, 6H, 3 × −O−CH_2−O−), 6.54 (t, 1H, $^4J_{H,H}$ = 2,0 Hz, H-4), 6.76−6.98 (m, 6H, H-2, H-6, H-2′, H-6′, H-7, H-8), 7.34 (d, 2H, $^3J_{H,H}$ = 8,5 Hz, H-3′, H-5′) ppm. ^{13}C NMR (250 MHz, $CDCl_3$, 25 °C): δ = 158.1, 156.7, 139.3, 130.5, 128.4, 127.4, 126.3, 116.1, 107.2, 103.7, 93.0, 92.9, 71.5, 70.1, 70.0, 69.9, 67.4, 58.5 ppm. Purity (HPLC-UV) ≥ 98%.

*trans-3,4′,5-Tri(2,5,8,11,14,17,20-heptaoxahenicosyloxy)-methylenoxy)stilbene (**2g**).* Purified by preparative HPLC (ACE 5 AQ column 150 × 21.2 mm i.d.). Solvents A and B were H_2O and acetonitrile each containing 0.05% TFA. The gradient for B was as follows: from 27.5% to 65% in 13 min. The flow rate was 17 mL/min. The eluate was monitored at 300 nm. Yield: 3.25 g (64%) as a colorless oil. ESI-MS (ion trap): m/z 1153.6 $[M + H]^+$. ^1H NMR (250 MHz, $CDCl_3$, 25 °C): δ = 3.21 (s, 9H, 3 × −O−CH_3), 3.47−3.51 (m, 6H, 3 × −O−CH_2−), 3.57−3.64 (m, 60H, 30 × −O−CH_2−), 3.77−3.81 (m, 6H, 3 × −O−CH_2−) 5.22−5.23 (m, 6H, 3 × −O−CH_2−O−), 6.57 (t, 1H, $^4J_{H,H}$ = 2,0 Hz, H-4), 6.79 −7.01 (m, 6H, H-2, H-6, H-2′, H-6′, H-7, H-8), 7.38 (d, 2H, $^3J_{H,H}$ = 8,5 Hz, H-3′, H-5′) ppm. ^{13}C NMR (250 MHz, $CDCl_3$, 25 °C): δ = 158.2, 156.8, 139.5, 130.7, 128.5, 127.5, 126.5, 116.2, 107.3, 103.9, 93.2, 93.1, 71.6, 70.3, 70.3, 70.2, 70.1, 67.5, 58.8 ppm. Purity (HPLC-UV) ≥ 95%.

*trans-3,4′,5-Tri(2-methoxypropan-2-yloxy)stilbene (**3**).* 2-Methoxypropene (1.58 g, 21.9 mmol, 10.0 equiv) was added to a mixture of resveratrol (0.5 g, 2.19 mmol, 1 equiv) and pyridinium *p*-toluenesulphonate (55 mg, 0.22 mmol, 0.1 equiv) under nitrogen pressure and strictly anhydrous conditions. The neat reaction mixture was stirred at room temperature for 72 h. The excess of 2-methoxypropene was removed under reduced pressure, and the crude product was purified by flash chromatography (hexane/acetone = 98:2 + 2% of triethylamine). Yield: 0.20 g (21%) as pale yellow oil. ESI-MS (ion trap): m/z 445 $[M + H]^+$. ^1H NMR (300 MHz, acetone-d_6, 25 °C): δ = 1.45 (s, 6H, −O−C(CH_3)$_2$−O−), 1.48 (s, 12H, 2 × −O−C(CH_3)$_2$−O−), 3.38 (s, 3H, −O−CH_3), 3.40 (s, 6H, 2 × −O−CH_3), 6.91 (t, 1H, $^4J_{H,H}$ = 2.1 Hz, H-4), 6.98 (d, 2H, $^4J_{H,H}$ = 2.1 Hz, H-2, H-6), 7.01−7.16 (m, 4H, H-2′, H-6′, H-7, H-8), 7.50 (d, 2H, $^3J_{H,H}$ = 8.7 Hz, H-3′, H-5′) ppm. ^{13}C NMR (300 MHz, acetone-d_6, 25 °C): δ = 157.0, 156.0, 139.7, 132.6, 129.2, 128.2, 127.9, 121.9, 114.2, 113.8, 104.2, 49.2, 25.4, 25.1 ppm. Purity (HPLC-UV) ≥ 95%.

*trans-3,4′,5-Tri(2,5,8,11,14-pentaoxahexadecan-15-yloxy)stilbene (**4**).* Tetraethylene glycol methyl vinyl ether (0.8 g, 3.4 mmol, 6.0 equiv) was added to a mixture of resveratrol

(0.13 g, 0.57 mmol, 1 equiv) and pyridinium *p*-toluenesulphonate (50 mg, 0.19 mmol, 0.3 equiv) under nitrogen pressure and strictly anhydrous conditions. The neat reaction mixture was stirred at room temperature for 24 h. The crude product was purified by flash chromatography (hexane/acetone = 5:3 + 2% of triethylamine). Yield: 0.23 g (43%) as a pale yellow oil. ESI-MS (ion trap): m/z 932 $[M + H]^+$. ^{1}H NMR (500 MHz, acetone-d_6, 25 °C): δ = 1.45−1.47 (m, 9H, 3 × −O−CH(CH_3)−O−, 3.27 (s, 6H, 2 × −O−CH_3), 3.28 (s, 3H, −O−CH_3), 3.44−3.47 (m, 6H, 3 × −O−CH_2−), 3.51−3.62 (m, 36H, 18 × −O−CH_2−), 3.64−3.85 (m, 6H, 3 × −O−CH_2−) 5.52−5.57 (m, 3H, 3 × −O−CH(CH_3)−O−), 6.65 (t, 1H, $^4J_{H,H}$ = 2.0 Hz, H-4), 6.91 (d, 2H, $^4J_{H,H}$ = 1.7 Hz, H-2, H-6), 7.03−7.21 (m, 4H, H-2′, H-6′, H-7, H-8), 7.53 (d, 2H, $^3J_{H,H}$ = 8.6 Hz, H-3′, H-5′) ppm. ^{13}C NMR (500 MHz, acetone-d_6, 25 °C): δ = 159.3, 157.8, 140.6, 131.9, 129.5, 128.6, 127.5, 118.4, 109.6, 106.6, 100.4, 100.4, 72.6, 71.2, 71.2, 71.2, 71.0, 66.0, 66.0, 65.9, 58.8, 20.6, 20.5 ppm. Purity (HPLC-UV) ≥ 95%.

General Procedure for the Preparation of the Non-commercially Available Chloromethyl Ethers. Paraformaldehyde (10.5 mmol, 1.05 equiv) was added to a solution of the desired alcohol (10.0 mmol, 1 equiv) in trimethylsilyl chloride (5 mL), and the reaction mixture was stirred for 2.5 h at room temperature. The solvent was evaporated under reduced pressure, and the chloromethyl ether obtained was used without further purification.

HPLC-UV Analysis. Samples (2 μL) were analyzed using a reversed phase column (Zorbax RRHD Eclipse Plus C18, 1.8 μm, 50 × 2.1 mm i.d.). Solvents A and B were H_2O containing 0.1% TFA and CH_3CN, respectively. The gradient for B was as follows: 10% for 2 min, from 10% to 20% in 3 min, then from 20% to 30% in 1 min, then from 30% to 100% in 1 min; the flow rate was 0.6 mL/min. The eluate was preferentially monitored at 286, 300, and 320 nm. These analytical conditions were used to determine the purity of the synthesized compounds. Formal derivatives **2a−g** proved to be stable under these analytical conditions; on the contrary, 0.1% TFA in the eluting aqueous phase (A) caused partial hydrolysis of derivative **4**. For this reason, HPLC analysis of **4** was performed in the absence of TFA. Samples from pharmacokinetic studies of **4** were analyzed both in the absence and in the presence of TFA, to optimally quantify acetal derivatives or resveratrol and phase II metabolites, respectively. Optimal resolution for di- and monosubstituted isomers was achieved using another reversed phase column (Zorbax RRHD Eclipse Plus Phenyl-Hexyl, 1.8 μm, 50 × 2.1 mm i.d.), with a gradient for B as follows: 28% for 3 min, from 28% to 65% in 2 min, then from 65% to 100% in 0.7 min, 100% for 0.5 min.

HPLC/ESI-MS Analysis. Samples (20 μL) were analyzed using a reversed phase column (Synergi-MAX, 4 μm, 150 × 4.6 mm i.d.; Phenomenex). Solvents A and B were H_2O containing 0.1% TFA and CH_3CN, respectively. The gradient for B was as follows: 10% for 2 min, from 10% to 35% in 20 min, then from 35% to 100% in 20 min; the flow rate was 1 mL/min. The eluate was preferentially monitored at 286, 300, and 320 nm. MS analysis was performed with an ESI source operating in full-scan mode in positive ion mode.

Solubility in Water. A known amount (approximately 2 × 10^{-5} mol) of the compound was mixed with 2 mL of bidistilled water and kept under stirring in a sealed vial at 25 °C. After 24 h the solution was filtered using a 0.45 μm PTFE filter and centrifuged (10 000 *g*, 10 min, 25 °C). A small aliquot was withdrawn, diluted with acetonitrile, and analyzed by HPLC-UV. Each measurement was repeated in triplicate and also with a mixing time of 48 and 72 h to verify the constancy of the solubility values. The overall average is presented.

Octanol/Water Partition Coefficient (log P_{ow}). Octanol and bidistilled water were reciprocally saturated by shaking them together for 24 h before use. A known amount (approximately 5 × 10^{-7} mol) of the compound was dissolved in 5 mL of octanol and placed in a sealed vial at 25 °C with 5 mL of water under stirring. After 24 h the two phases were separated and centrifuged (12 000 *g*, 20 min). A small aliquot of each phase was then diluted with acetonitrile and subjected to HPLC analysis. Each measurement was repeated in triplicate and also with a mixing time of 48 and 72 h to verify the constancy of the log P_{ow} values. The overall average is presented.

Hydrolysis Reactions. The chemical stability of all new compounds was tested in aqueous media mimicking gastric (0.1 N HCl, NormaFix) and intestinal (0.1 M PBS buffer, pH 6.8) pH values. A 50 μM solution of the compound was made from a 5 mM stock solution in DMSO and incubated at 37 °C for 24 h; samples withdrawn at different times were analyzed by HPLC-UV. Hydrolysis products were identified by HPLC/ESI-MS analysis of selected samples. Nonlinear curve fitting was performed using Origin 8.0 data analysis software, using the equations described in the Supporting Information.

Stability in Blood. Rats were anesthetised and blood was withdrawn from the jugular vein, heparinised and transferred into tubes containing EDTA. Blood samples (1 mL) were spiked with 5 μM of compound (dilution from a 5 mM stock solution in DMSO) and incubated at 37 °C for 4 h (the maximum period allowed by blood stability). Aliquots were taken after 10 min, 30 min, 1 h, 2 h, and 4 h and treated as described below (blood sample treatment and analysis). Cleared blood samples were finally subjected to HPLC-UV analysis. Ad hoc tests demonstrated that compound **4** withstood the extraction procedure without undergoing detectable hydrolysis.

Blood Sample Treatment and Analysis. Before starting the treatment, 4,4′-dihydroxybiphenyl was added as internal standard to a carefully measured blood volume (25 μM final concentration). Blood was then stabilized with a freshly prepared 10 mM solution of ascorbic acid (0.1 vol) and acidified with 0.6 M acetic acid (0.1 vol); after mixing, an excess of acetone (4 vol) was added, followed by sonication (2 min) and centrifugation (12 000 *g*, 7 min, 4 °C). The supernatant was finally collected and stored at −20 °C. Before analysis, acetone was allowed to evaporate at room temperature using a Univapo 150H (UniEquip) vacuum concentrator centrifuge, and up to 40 μL of CH_3CN was added to precipitate residual proteins. After centrifugation (12 000 *g*, 5 min, 4 °C), cleared samples were directly subjected to HPLC-UV analysis. Metabolites and hydrolysis products were identified by HPLC/ESI-MS analysis and/or comparison of chromatographic retention time with true samples.

The recovery yields of resveratrol and its metabolites have been reported previously.[62,63] Internal standard recovery was 68.7 ± 6.3% (N = 7). For the new prodrugs the corresponding recoveries, expressed as the ratio to the recovery of internal standard, were as follows: **2a**: 1.19 ± 0.07; **2b**: 1.18 ± 0.08.; **2c**: 1.21 ± 0.07; **2d**: 0.62 ± 0.06; **2e**: 0.93 ± 0.04; **2f**: 0.77 ± 0.02; **2g**: 0.94 ± 0.05; **4**: 0.69 ± 0.04 (N = 5). Recoveries of partially protected (disubstituted) derivatives were assumed to be the same as those of the corresponding fully substituted prodrug.

Scheme 1. Synthesis of Formal Derivatives (2a–g) from Resveratrol (1) and Alkoxymethylene Chlorides

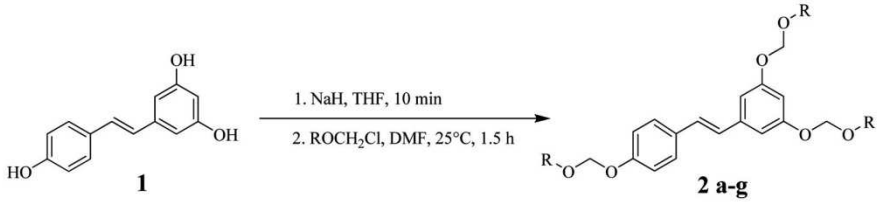

R = CH_3 (**a**), CH_2CH_3 (**b**), $CH_2CH_2OCH_3$ (**c**), $(CH_2CH_2O)_2CH_3$ (**d**), $(CH_2CH_2O)_3CH_3$ (**e**), $(CH_2CH_2O)_4CH_3$ (**f**), $(CH_2CH_2O)_6CH_3$ (**g**)

Knowledge of these ratios allowed us to determine the unknown amount of analyte in a blood sample by measuring the recovery of the internal standard.

Permeation of the Rat Intestinal Wall (Ex Vivo). Intestine was excised from 18 h fasted rats and transferred into a saline solution (154 mM NaCl in water) at 37 °C. The jejunum was cut into 1 cm long strips, opened longitudinally, rinsed free of luminal content, and mounted in Ussing-type chambers. Apical and basolateral compartments were filled with 1 mL of oxygenated HEPES buffer each (248 mM NaCl, 55.3 mM glucose, 50 mM $NaHCO_3$, 9.9 mM KCl, 1.9 mM $MgSO_4$, 40 mM HEPES, pH 6.8) and incubated in a water bath at 37 °C until all chambers (normally six per experimental run) were assembled. The buffer was then removed and substituted with 1 mL of a 20 μM solution of the compound to be tested in the same buffer on the apical side. During the experiment, oxygen was continuously bubbled in each basolateral compartment. An aliquot of the initial apical solutions was incubated separately at 37 °C for the period of the experiment, to verify the stability of each compound in the absence of jejunum. At the end of the experiment (2.5 h) 800 μL of chamber contents on both apical and basolateral sides were collected and mixed with 8 μL of 100 mM ascorbic acid in water, 8 μL of 6 M acetic acid, and 80 μL of 250 μM 4,4′-dihydroxybiphenyl (internal standard) in CH_3CN. The samples were then centrifuged (12 000 *g*, 7 min, 4 °C), and supernatants were frozen and maintained at −20 °C until HPLC-UV analysis.

Pharmacokinetics. Derivatives **2a–g** and **4** were administered to overnight-fasted male Wistar rats from the stabulary of the Department of Biomedical Sciences as a single intragastric dose (88 μmol/kg, dissolved in 250 μL DMSO). Blood samples were obtained by the tail bleeding technique: before drug administration, rats were anesthetised with isoflurane, and the tip of the tail was cut off; blood samples (80–100 μL each) were then taken from the tail tip at different time points after drug administration. Blood was collected in heparinised tubes, kept in ice, and treated as described below within 10 min. The AUC values were calculated using the trapezoidal rule. All experiments involving animals were performed with the permission and supervision of the University of Padova Ethical Committee for Experimentation on Animals (CEASA) and Central Veterinary Service, in compliance with Italian Law DL 116/92, embodying UE Directive 86/609.

Statistics. Significance in comparisons was assessed using the Wilcoxon Rank Test.

RESULTS

Synthesis. Resveratrol formal derivatives **2a–g** were synthesized via nucleophilic substitution by deprotonated resveratrol (**1**) on the appropriate alkoxymethylene chloride as sketched in Scheme 1. Alkoxymethylene chlorides are well-known and useful reagents for protection of phenolic hydroxyls with formal groups.[64] Despite its apparent simplicity the key step of coupling resveratrol with the alkoxymethylene chloride proved rather tricky. Attempts to perform the reaction in tetrahydrofuran (THF) were not successful: when sodium hydride was added to a THF resveratrol solution, a precipitate was formed, and it did not react appreciably upon addition of alkoxymethylene chloride at room temperature. The desired product was instead obtained in high yield by adding a small amount of dimethylformamide (DMF), which resulted in a very fast change of the suspension color from pale yellow to a dark orange, followed by color fading within a few minutes. It is interesting to note that, when pure DMF was used as solvent, a very fast reaction occurred leading to a complex product mixture, the precipitation of a gummy colored material, and low yields in the desired resveratrol derivative.

The alkoxymethylene chloride agents used for the synthesis of **2a–c** are commercially available, whereas those for **2d–g** had to be synthesized *in situ* from the corresponding alcohol via reaction with paraformaldehyde as shown in Scheme 2. The

Scheme 2. Synthesis of Alkoxymethylene Chloride from Alcohol and Paraformaldehyde

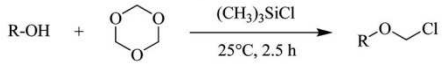

high reactivity of alkoxymethylene chlorides does not allow their purification via column chromatography on silica. Thus, after removal of excess trimethylchlorosilane under vacuum, they were used immediately in the next step without any further purification.

The reactivity of the acetal bond can be modulated by the introduction of suitable substituents onto the methylenic carbon. In particular, alkyl groups are known to favor acid-catalyzed hydrolysis.[64] To assess the stability of these bonds in the context of our compounds and conditions we therefore synthesized the ketal **3** and the acetal **4** by reaction of resveratrol with the appropriate isopropenyl and vinyl ethers, respectively, in the presence of catalytic amounts of pyridinium *p*-toluenesulfonate (Scheme 3).

Determination of Solubility and of log P_{ow}. We determined the effect of varying the length of the OEG chain on the solubility in water and on the octanol/water partition coefficient (log P_{ow}) (Table 1) of the formal derivatives. Log P_{ow} is indeed considered to be an important predictive parameter for absorption of passively absorbed drugs.[65]

Scheme 3. Synthesis of Ketal 3 and Acetal 4

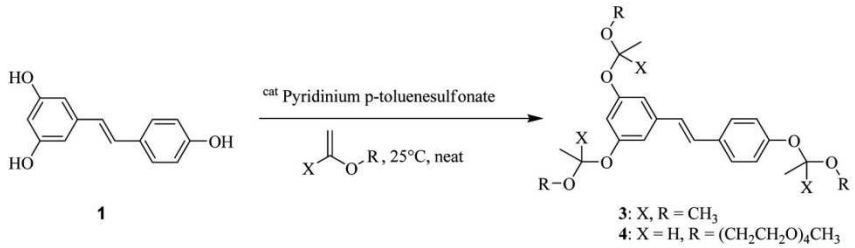

Table 1. Water Solubility and log P_{ow} of Resveratrol and of Its Formal Derivatives (N = 3)

	2a	2b	2c	2d	2e	2f	2g	1
solubility (μM)	*a*	*a*	90 ± 10	230 ± 50	>6000	>6000	>6000	170 ± 40
log P_{ow}	3.41 ± 0.03	3.88 ± 0.09	3.67 ± 0.06	2.95 ± 0.06	2.34 ± 0.01	1.70 ± 0.01	0.43 ± 0.02	2.69 ± 0.12

[a]Below detection limit.

Compounds **2a–c** are less soluble than resveratrol itself; the solubility markedly increased with the presence of additional ethoxy groups in the chain. The octanol–water partition coefficients of formal OEG derivatives show an opposite trend. Compounds **2e** and **2f** possess a remarkable solubility in water and have, at the same time, a log P_{ow} value in the optimum range for oral administration and absorption.

Stability Studies. Hydrolysis of **2a** and **2b** was not assayed due to the very low solubility of these compounds in water-based media. The other formals proved stable under near-neutral pH conditions (no reaction over 24 h at 37 °C in 0.1 M phosphate buffer, pH 6.8) as well as in blood (no reaction over 4 h). In 0.1 N HCl they all hydrolyzed at similar rates. For each derivative, suitable HPLC elution conditions were found to separate all components of the hydrolysis reaction mixture comprising, besides the reagent and the final product (resveratrol), four reaction intermediates, that is, the two isomeric disubstituted (3,4′- and 3,5-) and the two isomeric monosubstituted (3- and 4′-) derivatives. As an example, the concentration vs time profiles of all six species involved in the hydrolysis if **2f** are shown in Figure 2a. Kinetic analysis of the data was then performed by assuming that hydrolysis to resveratrol occurs via consecutive losses of the three protecting groups in pseudofirst order processes and by considering each pair of isomeric intermediates as a single species, that is, the two monosubstituted and the two disubstituted intermediates are handled as species B and C, respectively (Scheme 4).

Figure 2b shows the time course of the four species (A, B, C, and D) involved in the case of **2f** and the fit of the experimental data obtained using a set of equations analogous to those utilized by Kozerski et al.[66] and presented as Supporting Information. The excellent fit observed allows to conclude that the assumptions made are justified and that the rate of hydrolysis of each individual formal bond does not depend significantly on the position occupied on the resveratrol scaffold or on the presence of other analogous linkages in the molecule. In fact, at any given time the concentration of one disubstituted resveratrol (the 3,4′-disubstituted) was close to twice that of the other disubstituted isomer (the 3,5-disubstituted), indicating that the formal bonds at the various positions react at about the same rate both in the trisubstituted compound and in the disubstituted ones. Consistently, the amount of one monosubstituted (the 3-substituted) resveratrol was always close to twice that of the other isomer (the 4′-substituted molecule) (Figure 2a).

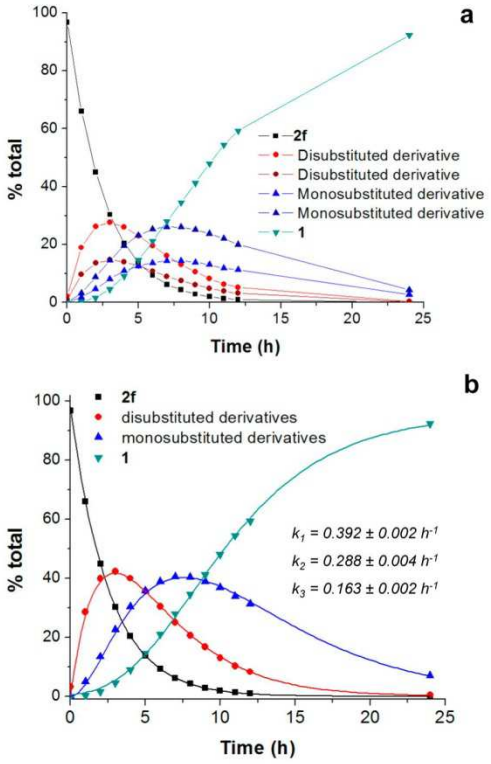

Figure 2. Kinetics of the hydrolysis of **2f** in 0.1 N HCl. Data from a single representative experiment. (a) Time profiles of reagent, product, and four reaction intermediates as obtained by HPLC analysis; (b) kinetic fit of the experimental data shown in panel a according to Scheme 4 (see text and Supporting Information).

Analogous analyses and procedures were used to obtain kinetic data for the hydrolysis of the other formal derivatives (**2c–e** and **2g**). The obtained rate constant values are reported in Table S1 (Supporting Information).

Scheme 4. Kinetic Scheme for the Hydrolysis of 2c–g

$$A \xrightarrow{k_1} B \xrightarrow{k_2} C \xrightarrow{k_3} D$$

A: trisubstituted resveratrol derivative

B: disubstituted resveratrol derivatives

C: monosubstituted resveratrol derivatives

D: resveratrol

k_1, k_2, k_3: observed pseudo-first order rate constants

The ketal derivative **3** proved too labile, with about 50% complete hydrolysis to resveratrol in 10 min at pH 7.4 and room temperature (not shown). This compound therefore was not studied further. In contrast, acetal **4** was stable at pH 6.8 and in blood but underwent hydrolysis under acidic conditions. Hydrolysis was too rapid for determination of kinetic parameters at pH 1 (HCl 0.1N). The pH of the rat stomach is however 3–4, higher than in humans.[67] We therefore determined the kinetics of hydrolysis of **4** as a function of pH in a higher pH range (20 mM acetate buffer, pH 3.6–5.6). Figure 3 presents the *k* values, determined with reference to Scheme 4 as described above, for the consecutive hydrolysis steps of **4** in the pH range 4.0–5.6 (a reliable fit could not be obtained for the reaction at pH 3.6).

The results shown in Figure 3 at any given pH value support and extend the conclusions reached for reaction of the formal

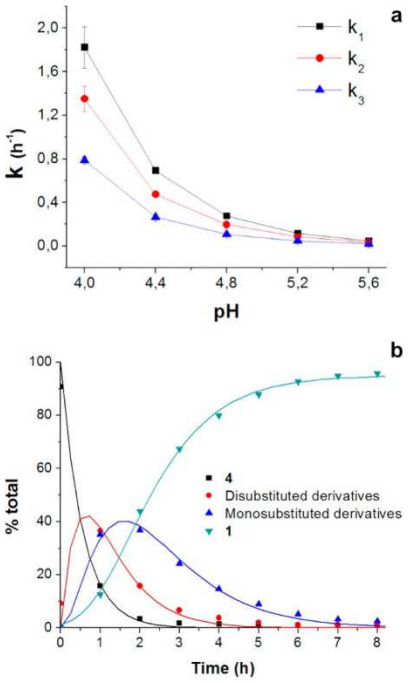

Figure 3. Kinetics of the hydrolysis of **4** at different pH values. (a) Observed rate constants (± standard error) for the hydrolysis of **4**, as a function of pH; (b) kinetic fit of the experimental data at pH 4.0, according to Scheme 4 (see text and Supporting Information).

derivatives described above. It is indeed apparent that the rate of hydrolysis of this class of protecting groups of phenolic hydroxyls is not significantly influenced by the specific site of substitution or by the presence of additional similar groups in the molecule.

Transport across Explanted Rat Intestinal Segments. Using Ussing chambers we also assayed the transport of formals **2a–g** across explanted rat jejunum segments to verify what effect the length of the OEG chain might have on this process. In these experiments, the same molar amount of resveratrol or prodrug was placed in the apical-side chamber, and the solution on the basolateral side was collected and analyzed after 2.5 h (see Materials and Methods for experimental details). Figure 4

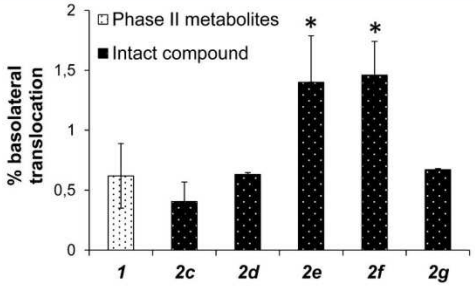

Figure 4. Transport across the explanted rat intestinal segments. Plotted is the amount found in the basolateral chamber (mean ± standard deviation; $N = 3$), expressed as percentage of the total amount of stilbenoid compounds recovered at the end of the 2.5-h incubation. See text and Materials and Methods for details. *: significantly different from basolateral translocation of **1** ($p \leq 0.1$).

summarizes the results, showing the amounts of stilbene derivatives found in the basolateral compartment at the end of the experiment expressed as percentage of the total species recovered in the apical and basolateral sides. When the compound provided was resveratrol, no resveratrol could be detected in the basolateral chamber, which contained instead metabolites adding up to 0.6 ± 0.3% of the total recovered amount. No compounds ascribable to a stilbenoid skeleton could be detected in the basolateral chamber when compounds **2a** or **2b** were loaded. The other formal derivatives appeared instead on the basolateral side without alteration. In the case of compounds **2d** and **2e** the fraction translocated exceeded that of resveratrol (metabolites) (1.4 ± 0.4% and 1.5 ± 0.3% for **2d** and **2e**, respectively; $N = 3$). A substituent chain containing 3 or 4 monomeric units seems therefore optimal for permeation of the intestinal wall.

Pharmacokinetics and Absorption. All synthesized derivatives, except **3**, were then used in pharmacokinetic tests in rats. The administration of 88 μmol/kg of compounds **2a–b** did not result in the appearance of resveratrol, derivatives, or any metabolites in blood samples. Compound **2c** was absorbed to a small extent, but circulating species were below the quantification limit (0.12 μM).[62] In contrast, compounds **2d–f** appeared in blood in unmodified form within 10 min of administration, with a concentration peak between 30 and 60 min. The products of partial hydrolysis, including disubstituted formal derivatives and coeluting trisubstituted species carrying shortened OEG chains, were also found with a similar kinetic profile but in lower concentration. As an example, the results of HPLC/ESI-MS analysis of a blood sample from a pharmaco-

kinetic experiment with **2f** are shown in Figure 5. Besides a major peak due to **2f**, a few minor and coeluting chromatographic peaks are detected which are assigned to products due to hydrolysis of one formal linkage, to give a disubstituted derivative, and to progressive loss of the terminal methyl groups ($\Delta\ m/z = -14$) and single ethyleneglycol units ($\Delta\ m/z = -44$) (Figure 5). Interestingly, this type of degradation of the substituent groups does not take place upon incubation of the original precursors (**2f** in this case) in solution. We presume these species derive from the action of bacterial enzymes in the gut. Degradation of PEGs by intestinal microbes is known to occur.[68−70] No resveratrol or resveratrol conjugates (glucuronides, sulfates) could be detected in the blood samples with any of the formal-based prodrugs.

The results of pharmacokinetic tests with compound **2f** are summarized in Figure 6, which also shows the pharmacokinetics of resveratrol when administered as such for comparison. Analogous graphs for compounds **2d**, **2e**, and **2g** are provided as Supporting Information (Figure S1).

The outcome of pharmacokinetic experiments with the acetal derivative **4** (Figure 7) was clearly different from those of the tests with the formals. The major species found in blood was resveratrol glucuronide(s) as identified in HPLC/ESI-MS analyses by comparison with an authentic sample. Its concentration peaked at approximately 8 h after administration.

The area under the curve (AUC) parameter for the formal derivatives increases with the length of the OEG chain reaching a maximum for derivative **2f** (Figure 8). Interestingly, in the case of this compound the AUC vastly exceeds that measured for resveratrol as such—and is comparable to the combined value for resveratrol and its metabolites—after administration of the same dose of resveratrol. In the case of **4** the overall AUC was somewhat lower than for **2f**, which carries the same substituent group.

■ DISCUSSION AND CONCLUSIONS

The prodrugs we synthesized and tested possess desirable properties. In the case of acetal derivatives, the protective groups are rapidly hydrolyzed in a strongly acidic environment. In contrast, acid hydrolysis of formals is sufficiently slow, even at pH ∼ 1, similar to that of the human stomach, not to constitute a deterrent: in our pharmacokinetic experiments hydrolysis of formal bond-linked protective groups was indeed very limited. A well-developed formulation technology is available in any case to permit the safe transit of acid-sensitive drugs through the gastric compartment.[71−73] Importantly, short OEG chains appear to be a good choice as carrier group in these resveratrol prodrugs: specifically, for chains comprising three or more monomeric units the derivatives are much more soluble in water than resveratrol. The method we used to determine water solubility led to an estimated value of about 170 μM for resveratrol. It is to note that accurate solubility data are notoriously hard to obtain for compounds which can form colloids, and literature values for resveratrol range from less than 1 μM[74] to about 10 μM[75] and all the way up to 300 μM.[76] Solubility is relevant: essentially water-insoluble **2a** and **2b** do not cross the intestinal wall in Ussing chamber experiments even if kept in solution by the presence of DMSO as a cosolvent and are not absorbed from the gastrointestinal tract after oral administration. OEG-decorated, more soluble derivatives can permeate explanted rat intestinal segments (Figure 4) and are absorbed after oral administration (Figures 6, 7, and 8). The AUC of stilbenoid compounds in blood was

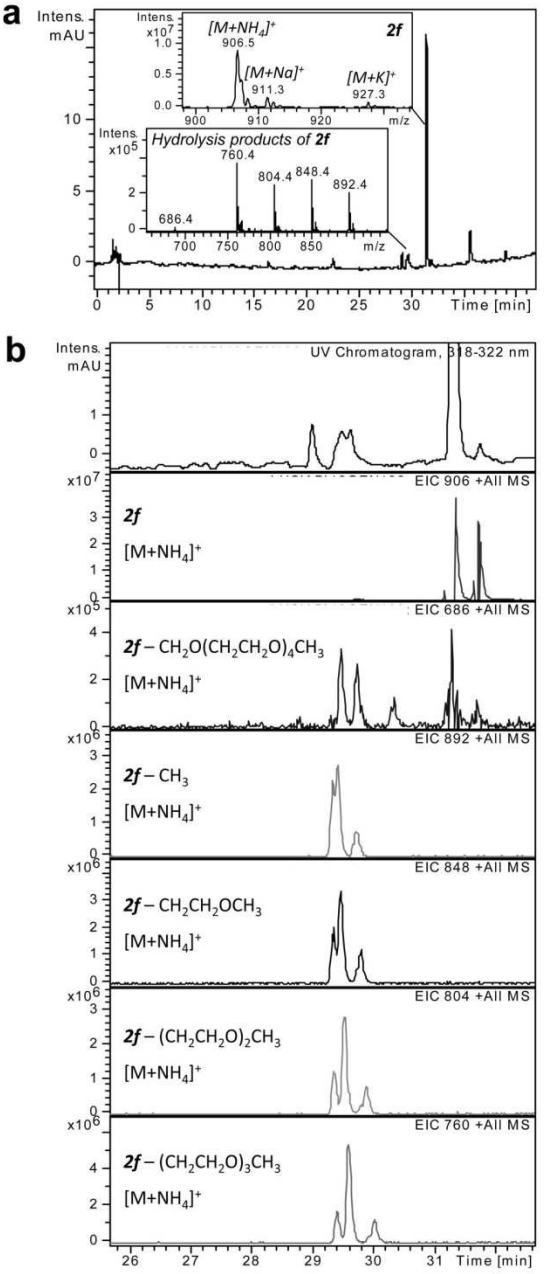

Figure 5. HPLC/ESI-MS analysis of a blood sample taken 1 h after administration of **2f** in a pharmacokinetic experiment. (a) UV chromatogram (320 nm) showing the presence of **2f** and of its partial hydrolysis products (inserts reproduce the corresponding mass spectra). Disubstituted resveratrol derivatives are not well-resolved from the products of partial loss of ethyleneglycol units. (b) Extracted ion chromatograms (EIC) for the m/z values corresponding to intact **2f** (m/z 906 $[M + NH_4]^+$), disubtituted derivatives (m/z 686 $[M + NH_4]^+$) and products of partial loss of ethyleneglycol units (m/z 892, 848, 804, 760, all due to $[M + NH_4]^+$).

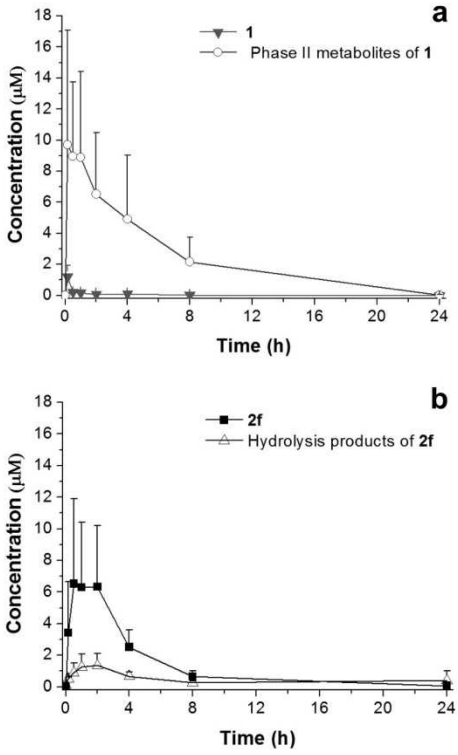

Figure 6. Pharmacokinetic profiles for: (a) resveratrol (**1**) and (b) compound **2f**. "Hydrolysis products" stands for disubstituted derivatives and coeluting species carrying shortened OEG chains as described in the text. Reported are mean values ± standard deviation (N = 5 and 4 for **1** and **2f**, respectively).

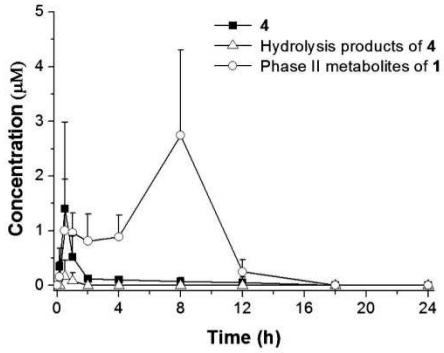

Figure 7. Pharmacokinetics of **4**. Reported are mean values ± standard deviation (N = 4).

similar after administration of resveratrol or of **2f**, the derivative with tetraethyleneglycol chains. This is remarkable when considering the much higher molecular weight and water solubility of the compound and is presumably related to a partition coefficient still favoring permeation of membranes (Table 1). This result, in keeping with the remarkable properties of PEG, offers the perspective of achieving high level systemic or targeted delivery of resveratrol-generating

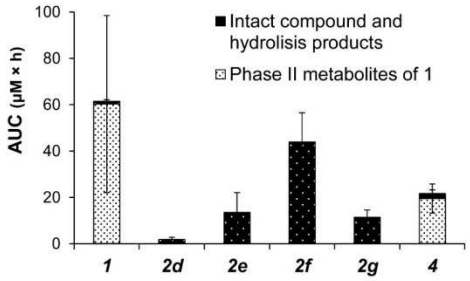

Figure 8. AUC parameter, as calculated from plots analogous to those of Figures 6 and 7. For compounds **2d–g** the values reported are the sum of the AUC parameters measured for the prodrug itself and its partial hydrolysis products, which were in all cases a minor component. Conjugation products of resveratrol were detectable only after administration of resveratrol itself (**1**) and of **4**. In these two cases AUC values are shown for both the compound as administered and for total blood stilbenoids.

molecules, bypassing the xenobiotics-inactivating defense systems of the gut and liver.

When resveratrol is administered, the vast majority of the circulating species consists of its phase II metabolites; in the case of our derivatives, still fully or partially protected molecules were found in the bloodstream. This highlights the shortcoming of the formal bond: it is probably too stable at physiological pH values to regenerate the parent compound at useful rates.

To destabilize the bond, we substituted one (**4**) or two (**3**) of the methylene hydrogens with methyl groups. These substitutions had indeed marked effects on the rate of hydrolysis. Compound **3** proved to be too reactive to be of practical use. Compound **4** was also deprotected at an appreciable rate in the pH range of the rat stomach (Figure 3), but deprotection was clearly not complete *in vivo*. The original prodrug and the species resulting from loss of one of the protecting groups were present in blood samples taken over the first hour or so after administration, along with resveratrol glucuronide (Figure 8). At later times, the glucuronide was essentially the only stilbenoid found in blood. Interestingly, its concentration profile in time was different from that observed after administration of resveratrol (Figure 6a): the peak concentration was reached at about 8 h vs about 1 h in the case of resveratrol.

The bond linkage in **4** bears a close resemblance to that present in glycoside and glucuronide derivatives of polyphenols. In the case of glycosides, studies conducted mostly with quercetin derivatives have led to a model envisioning both the cleavage of the acetal bond by lactase phlorizin hydrolase located on the luminal intestinal surface, followed by diffusion of the aglycone into enterocytes, and the transport of the glycoside by glucose transporter SGLT1 followed by deglycosylation inside the cell.[77−80] Similar mechanisms may apply to resveratrol glycosides as well.[81] Considering their log P_{ow} values and what is known about PEG chains-containing prodrugs, our OEG decorated compounds presumably can enter enterocytes and reach the blood by diffusing through biomembranes, independently of transporters. Given that it contains an acetal bond, **4** might be a substrate for lactase phloridzin hydrolase. The results of pharmacokinetics with this prodrug could therefore be explained by slow hydrolysis in the intestine generating resveratrol which would be promptly

imported by enterocytes and appear in blood as the glucuronide. This model however does not explain why the fully or partially protected species disappear from blood after about one hour: if resveratrol is produced by their hydrolysis in the intestine over the subsequent at least 7 h, they should obviously still be present and continue to transit from the intestinal lumen to blood through the intestinal wall. Of note, we were unable to detect any species containing both OEG chain(s) and glucuronide (or sulfate) moieties in blood. The hypothesis that **4** is completely hydrolyzed in the stomach to produce resveratrol which then moves to the intestine to be absorbed is also unlikely, given the different pharmacokinetics observed upon administration of resveratrol and of **4**.

An alternative model envisions the rapid absorption of the prodrug (as well as of some resveratrol formed in the stomach; Figure 3b), which then disappears from blood because it becomes associated with other, less polar, environments (tissues, membranes) due to its physicochemical properties. Slow hydrolysis, possibly mediated by ubiquitous glucuronidase/glycosylase activities, would gradually release resveratrol which would then be glucuronidated and thus converted to a hydrophilic species, returning therefore to the blood.

Whether this model is correct remains to be investigated. Regardless, this study establishes that linkage to short OEG chains may be a convenient stratagem to protect polyphenols and possibly other drugs from metabolism while still allowing sustained absorption. Coupling such a substituent to the core molecule through a chemical bond with appropriate stability characteristics in physiological environments may well result in a functional prodrug for oral delivery. The acetal bond system, adopted by nature and exploited in this study, appears to be a viable candidate.

■ ASSOCIATED CONTENT

Supporting Information

Kinetics of hydrolysis of compounds **2c–g** in 0.1 M HCl; pharmacokinetic profiles of compounds **2d**, **2e**, **2g**. This material is available free of charge via the Internet at http://pubs.acs.org.

■ AUTHOR INFORMATION

Corresponding Author

*C.P.: e-mail: cristina.paradisi@unipd.it; phone: +39 049 8275661. L.B.: e-mail: lucia.biasutto@cnr.it; phone: +39 049 8276483.

Author Contributions

A.M. and M.A. contributed equally to this work.

Notes

The authors declare no competing financial interest.

■ ACKNOWLEDGMENTS

We thank Prof. S. Garbisa for discussions and support, Dr. E. Marotta for useful discussions, Dr. E. Bradaschia for performing some of the pharmacokinetics, and Mr. M. Ghidotti for technical help. This work was supported by grants from the Fondazione Cassa di Risparmio di Padova e Rovigo (CARIPARO) ("Developing a Pharmacology of Polyphenols"), the University of Padova (postdoctoral fellowships to L.B. and N.S.), and the CNR Project of Special Interest on Aging.

■ ABBREVIATIONS

AcOEt, ethyl acetate; AUC, area under the curve; CEASA, Ethical Committee for Experimentation on Animals; EIC, extracted ion chromatograms; ESI, electrospray ionization; log P_{ow}, octanol/water partition coefficient; MDR, multi-drug resistance; OEG, oligoethyleneglycol; PBS, phosphate-buffered saline; PEG, polyethyleneglycol; PTFE, polytetrafluoroethylene; SGLT1, sodium/glucose cotransporter 1; TFA, trifluoroacetic acid; TLC, thin-layer chromatography

■ REFERENCES

(1) Chachay, V. S.; Kirkpatrick, C. M.; Hickman, I. J.; Ferguson, M.; Prins, J. B.; Martin, J. H. Resveratrol—pills to replace a healthy diet? *Br. J. Clin. Pharmacol.* **2011**, *72*, 27–38.

(2) Biasutto, L.; Szabó, I.; Zoratti, M. Mitochondrial effects of plant-made compounds. *Antioxid. Redox Signal.* **2011**, *15*, 3039–3059.

(3) Hu, Y.; Liu, J.; Wang, J.; Liu, Q. The controversial links among calorie restriction, SIRT1, and resveratrol. *Free Radical Biol. Med.* **2011**, *51*, 250–256.

(4) Csiszar, A. Anti-inflammatory effects of resveratrol: possible role in prevention of age-related cardiovascular disease. *Ann. N.Y. Acad. Sci.* **2011**, *1215*, 117–122.

(5) Lin, H. Y.; Tang, H. Y.; Davis, F. B.; Davis, P. J. Resveratrol and apoptosis. *Ann. N.Y. Acad. Sci.* **2011**, *1215*, 79–88.

(6) Athar, M.; Back, J. H.; Kopelovich, L.; Bickers, D. R.; Kim, A. L. Multiple molecular targets of resveratrol: Anti-carcinogenic mechanisms. *Arch. Biochem. Biophys.* **2009**, *486*, 95–102.

(7) Harikumar, K. B.; Aggarwal, B. B. Resveratrol: a multitargeted agent for age-associated chronic diseases. *Cell Cycle* **2008**, *7*, 1020–1035.

(8) Shukla, Y.; Singh, R. Resveratrol and cellular mechanisms of cancer prevention. *Ann. N.Y. Acad. Sci.* **2011**, *1215*, 1–8.

(9) Yu, W.; Fu, Y. C.; Wang, W. Cellular and molecular effects of resveratrol in health and disease. *J. Cell. Biochem.* **2012**, *113*, 752–759.

(10) Park, S. J.; Ahmad, F.; Philp, A.; Baar, K.; Williams, T.; Luo, H.; Ke, H.; Rehmann, H.; Taussig, R.; Brown, A. L.; Kim, M. K.; Beaven, M. A.; Burgin, A. B.; Manganiello, V.; Chung, J. H. Resveratrol ameliorates aging-related metabolic phenotypes by inhibiting cAMP phosphodiesterases. *Cell* **2012**, *148*, 421–433.

(11) Yuan, H.; Marmorstein, R. Biochemistry. Red wine, toast of the town (again). *Science* **2013**, *339*, 1156–1157.

(12) Agarwal, B.; Baur, J. A. Resveratrol and life extension. *Ann. N.Y. Acad. Sci.* **2011**, *1215*, 138–143.

(13) Foti Cuzzola, V.; Ciurleo, R.; Giacoppo, S.; Marino, S.; Bramanti, P. Role of resveratrol and its analogues in the treatment of neurodegenerative diseases: focus on recent discoveries. *CNS Neurol. Disord. Drug Targets* **2011**, *10*, 849–862.

(14) Kroon, P. A.; Iyer, A.; Chunduri, P.; Chan, V.; Brown, L. The cardiovascular nutrapharmacology of resveratrol: pharmacokinetics, molecular mechanisms and therapeutic potential. *Curr. Med. Chem.* **2010**, *17*, 2442–2455.

(15) Khanna, D.; Sethi, G.; Ahn, K. S.; Pandey, M. K.; Kunnumakkara, A. B.; Sung, B.; Aggarwal, A.; Aggarwal, B. B. Natural products as a gold mine for arthritis treatment. *Curr. Opin. Pharmacol.* **2007**, *7*, 344–351.

(16) Khalifé, S.; Zafarullah, M. Molecular targets of natural health products in arthritis. *Arthritis Res. Ther.* **2011**, *13*, 102.

(17) Aggarwal, B. B.; Bhardwaj, A.; Aggarwal, R. S.; Seeram, N. P.; Shishodia, S.; Takada, Y. Role of resveratrol in prevention and therapy of cancer: preclinical and clinical studies. *Anticancer Res.* **2004**, *24*, 2783–2840.

(18) Szekeres, T.; Saiko, P.; Fritzer-Szekeres, M.; Djavan, B.; Jäger, W. Chemopreventive effects of resveratrol and resveratrol derivatives. *Ann. N.Y. Acad. Sci.* **2011**, *1215*, 89–95.

(19) Huang, X.; Zhu, H. L. Resveratrol and Its Analogues: Promising Antitumor Agents. *Anticancer Agents Med. Chem.* **2011**, *11*, 479–490.

(20) Kaminski, B. M.; Steinhilber, D.; Stein, J. M.; Ulrich, S. Phytochemicals Resveratrol and Sulforaphane as Potential Agents for Enhancing the Anti-Tumor Activities of Conventional Cancer Therapies. *Curr. Pharm. Biotechnol.* **2012**, *13*, 137−146.
(21) Gupta, S. C.; Kannappan, R.; Reuter, S.; Kim, J. H.; Aggarwal, B. B. Chemosensitization of tumors by resveratrol. *Ann. N.Y. Acad. Sci.* **2011**, *1215*, 150−160.
(22) Huber, K.; Superti-Furga, G. After the grape rush: Sirtuins as epigenetic drug targets in neurodegenerative disorders. *Bioorg. Med. Chem.* **2011**, *19*, 3616−3124.
(23) Quincozes-Santos, A.; Gottfried, C. Resveratrol modulates astroglial functions: neuroprotective hypothesis. *Ann. N.Y. Acad. Sci.* **2011**, *1215*, 72−78.
(24) Beaudeux, J. L.; Nivet-Antoine, V.; Giral, P. Resveratrol: a relevant pharmacological approach for the treatment of metabolic syndrome? *Curr. Opin. Clin. Nutr. Metab. Care* **2010**, *13*, 729−736.
(25) Cherniack, E. P. Polyphenols: planting the seed of treatment for the metabolic syndrome. *Nutrition* **2011**, *27*, 617−623.
(26) Szkudelski, T.; Szkudelska, K. Anti-diabetic effects of resveratrol. *Ann. N.Y. Acad. Sci.* **2011**, *1215*, 34−39.
(27) Baile, C. A.; Yang, J. Y.; Rayalam, S.; Hartzell, D. L.; Lai, C. Y.; Andersen, C.; Della-Fera, M. A. Effect of resveratrol on fat mobilization. *Ann. N.Y. Acad. Sci.* **2011**, *1215*, 40−47.
(28) Rayalam, S.; Yang, J. Y.; Della-Fera, M. A.; Baile, C. A. Novel molecular targets for prevention of obesity and osteoporosis. *J. Nutr. Biochem.* **2011**, *22*, 1099−1104.
(29) Bishayee, A. Cancer prevention and treatment with resveratrol: from rodent studies to clinical trials. *Cancer Prev. Res. (Phila)* **2009**, *2*, 409−418.
(30) Subramanian, L.; Youssef, S.; Bhattacharya, S.; Kenealey, J.; Polans, A. S.; van Ginkel, P. R. Resveratrol: challenges in translation to the clinic—a critical discussion. *Clin. Cancer Res.* **2010**, *16*, 5942−5948.
(31) Smoliga, J. M.; Baur, J. A.; Hausenblas, H. A. Resveratrol and health—a comprehensive review of human clinical trials. *Mol. Nutr. Food Res.* **2011**, *55*, 1129−1141.
(32) Patel, K. R.; Scott, E.; Brown, V. A.; Gescher, A. J.; Steward, W. P.; Brown, K. Clinical trials of resveratrol. *Ann. N.Y. Acad. Sci.* **2011**, *1215*, 161−169.
(33) Walle, T. Bioavailability of resveratrol. *Ann. N.Y. Acad. Sci.* **2011**, *1215*, 9−15.
(34) Delmas, D.; Aires, V.; Limagne, E.; Dutartre, P.; Mazué, F.; Ghiringhelli, F.; Latruffe, N. Transport, stability, and biological activity of resveratrol. *Ann. N.Y. Acad. Sci.* **2011**, *1215*, 48−59.
(35) Cottart, C. H.; Nivet-Antoine, V.; Laguillier-Morizot, C.; Beaudeux, J. L. Resveratrol bioavailability and toxicity in humans. *Mol. Nutr. Food Res.* **2010**, *54*, 7−16.
(36) van de Wetering, K.; Burkon, A.; Feddema, W.; Bot, A.; de Jonge, H.; Somoza, V.; Borst, P. Intestinal breast cancer resistance protein (BCRP)/Bcrp1 and multidrug resistance protein 3 (MRP3)/Mrp3 are involved in the pharmacokinetics of resveratrol. *Mol. Pharmacol.* **2009**, *75*, 876−885.
(37) Juan, M. E.; González-Pons, E.; Planas, J. M. Multidrug resistance proteins restrain the intestinal absorption of trans-resveratrol in rats. *J. Nutr.* **2010**, *140*, 489−495.
(38) Calabrese, E. J.; Mattson, M. P.; Calabrese, V. Resveratrol commonly displays hormesis: occurrence and biomedical significance. *Hum. Exp. Toxicol.* **2010**, *9*, 980−1015.
(39) Calabrese, E. J.; Mattson, M. P.; Calabrese, V. Dose response biology: the case of resveratrol. *Hum. Exp. Toxicol.* **2010**, *29*, 1034−1037.
(40) Kenealey, J. D.; Subramanian, L.; van Ginkel, P.; Darjatmoko, S.; Lindstrom, M.; Somoza, V.; Ghosh, S.; Song, Z.; Hsung, R.; Kwon, G. S.; Eliceiri, K.; Albert, D.; Polans, A. Resveratrol metabolites do not elicit early pro-apoptotic mechanisms in neuroblastoma cells. *J. Agric. Food Chem.* **2011**, *59*, 4979−4986.
(41) Forester, S. C.; Waterhouse, A. L. Metabolites are key to understanding health effects of wine polyphenolics. *J. Nutr.* **2009**, *139*, 1824−1831.
(42) Calamini, B.; Ratia, K.; Malkowski, M. G.; Cuendet, M.; Pezzuto, J. M.; Santarsiero, B. D.; Mesecar, A. D. Pleiotropic mechanisms facilitated by resveratrol and its metabolites. *Biochem. J.* **2010**, *429*, 273−282.
(43) Hoshino, J.; Park, E. J.; Kondratyuk, T. P.; Marler, L.; Pezzuto, J. M.; van Breemen, R. B.; Mo, S.; Li, Y.; Cushman, M. Selective synthesis and biological evaluation of sulfate-conjugated resveratrol metabolites. *J. Med. Chem.* **2010**, *53*, 5033−5043.
(44) Miksits, M.; Wleck, K.; Svoboda, M.; Kunert, O.; Haslinger, E.; Thalhammer, T.; Szekeres, T.; Jäger, W. Antitumor activity of resveratrol and its sulfated metabolites against human breast cancer cells. *Planta Med.* **2009**, *75*, 1227−1230.
(45) Ansari, K. A.; Vavia, P. R.; Trotta, F.; Cavalli, R. Cyclodextrin-based nanosponges for delivery of resveratrol: in vitro characterisation, stability, cytotoxicity and permeation study. *AAPS PharmSciTech* **2011**, *12*, 279−286.
(46) Das, S.; Ng, K. Y. Colon-specific delivery of resveratrol: optimization of multi-particulate calcium-pectinate carrier. *Int. J. Pharmaceutics* **2010**, *385*, 20−28.
(47) Das, S.; Chaudhury, A.; Ng, K. Y. Polyethyleneimine-modified pectin beads for colon-specific drug delivery: In vitro and in vivo implications. *J. Microencapsul.* **2011**, *28*, 268−279.
(48) Frozza, R. L.; Bernardi, A.; Paese, K.; Hoppe, J. B.; da Silva, T.; Battastini, A. M.; Pohlmann, A. R.; Guterres, S. S.; Salbego, C. Characterization of trans-resveratrol-loaded lipid-core nanocapsules and tissue distribution studies in rats. *J. Biomed. Nanotechnol.* **2010**, *6*, 694−703.
(49) Wang, X. X.; Li, Y. B.; Yao, H. J.; Ju, R. J.; Zhang, Y.; Li, R. J.; Yu, Y.; Zhang, L.; Lu, W. L. The use of mitochondrial targeting resveratrol liposomes modified with a dequalinium polyethylene glycol-distearoylphosphatidyl ethanolamine conjugate to induce apoptosis in resistant lung cancer cells. *Biomaterials* **2011**, *32*, 5673−5687.
(50) Larrosa, M.; Tomé-Carneiro, J.; Yáñez-Gascón, M. J.; Alcántara, D.; Selma, M. V.; Beltrán, D.; García-Conesa, M. T.; Urbán, C.; Lucas, R.; Tomás-Barberán, F.; Morales, J. C.; Espín, J. C. Preventive oral treatment with resveratrol pro-prodrugs drastically reduce colon inflammation in rodents. *J. Med. Chem.* **2010**, *53*, 7365−7376.
(51) Biasutto, L.; Marotta, E.; Mattarei, A.; Beltramello, S.; Caliceti, P.; Salmaso, S.; Bernkop-Schnurch, A.; Garbisa, S.; Zoratti, M.; Paradisi, C. Absorption and metabolism of resveratrol carboxyesters and methanesulfonate by explanted rat intestinal segments. *Cell Physiol. Biochem.* **2009**, *24*, 557−566.
(52) Gupta, D.; Gupta, S. V.; Lee, K.-D.; Amidon, G. L. Chemical and enzymatic stability of amino acid prodrugs containing methoxy, ethoxy and propylene glycol linkers. *Mol. Pharmaceutics* **2009**, *6*, 1604−1611.
(53) Torres, P.; Poveda, A.; Jimenez-Barbero, J.; Ballesteros, A.; Plou, F. J. Regioselective lipase-catalyzed synthesis of 3-o-acyl derivatives of resveratrol and study of their antioxidant properties. *J. Agric. Food Chem.* **2010**, *58*, 807−813.
(54) Koide, K.; Osman, S.; Garner, A. L.; Song, F. L.; Dixon, T.; Greenberger, J. S.; Epperly, M. W. The use of 3,5,4′-tri-O-acetylresveratrol as a potential prodrug for resveratrol protects mice from γ-irradiation-induced death. *ACS Med. Chem. Lett.* **2011**, *2*, 270−274.
(55) Nomura, M.; Shuto, S.; Matsuda, A. Synthesis of the cyclic and acyclic acetal derivatives of 1-(3-C-ethynyl-beta-D-ribo-pentofuranosyl)cytosine, a potent antitumor nucleoside. Design of prodrugs to be selectively activated in tumor tissues via the bio-reduction-hydrolysis mechanism. *Bioorg. Med. Chem.* **2003**, *11*, 2453−2461.
(56) Kim, M. K.; Park, K. S.; Lee, C.; Park, H. R.; Choo, H.; Chong, Y. Enhanced stability and intracellular accumulation of quercetin by protection of the chemically or metabolically susceptible hydroxyl groups with a pivaloxymethyl (POM) promoiety. *J. Med. Chem.* **2010**, *53*, 8597−8607.

(57) Kim, M. K.; Park, K. S.; Chong, Y. Remarkable Stability and Cytostatic Effect of a Quercetin Conjugate, 3,7-Bis-O-Pivaloxymethyl (POM) Quercetin. *ChemMedChem.* **2012**, *7*, 229−232.
(58) Cho, S. Y.; Kim, M. K.; Park, K. S.; Choo, H.; Chong, Y. Quercetin-POC conjugates: Differential stability and bioactivity profiles between breast cancer (MCF-7) and colorectal carcinoma (HCT116) cell lines. *Bioorg. Med. Chem.* **2013**, *21*, 1671−1679.
(59) Harris, J. M.; Chess, R. B. Effect of pegylation on pharmaceuticals. *Nat. Rev. Drug Discovery* **2003**, *2*, 214−221.
(60) Pasut, G.; Veronese, F. M. State of the art in PEGylation: the great versatility achieved after forty years of research. *J. Controlled Release* **2012**, *161*, 461−472.
(61) Biasutto, L.; Marotta, E.; De Marchi, U.; Zoratti, M.; Paradisi, C. Ester-based precursors to increase the bioavailability of quercetin. *J. Med. Chem.* **2007**, *50*, 241−53.
(62) Biasutto, L.; Marotta, E.; Garbisa, S.; Zoratti, M.; Paradisi, C. Determination of quercetin and resveratrol in whole blood–implications for bioavailability studies. *Molecules* **2010**, *15*, 6570−6579.
(63) Biasutto, L.; Marotta, E.; Bradaschia, A.; Fallica, M.; Mattarei, A.; Garbisa, S.; Zoratti, M.; Paradisi, C. Soluble polyphenols: synthesis and bioavailability of 3,4′,5-tri(alpha-D-glucose-3-O-succinyl) resveratrol. *Bioorg. Med. Chem. Lett.* **2009**, *19*, 6721−6724.
(64) Greene, T. W.; Wuts, P. G. M. *Protective groups in organic synthesis*, 3rd ed.; John Wiley & Sons: New York, 1999; pp 257−259.
(65) Raevsky, O. A. Physicochemical descriptors in property-based drug design. *Mini Rev. Med. Chem.* **2004**, *4*, 1041−1052.
(66) Kozerski, G. E.; Gallavan, R. H.; Ziemelis, M. J. Investigation of trialkoxysilane hydrolysis kinetics using liquid chromatography with inductively coupled plasma atomic emission spectrometric detection and non-linear regression modeling. *Anal. Chim. Acta* **2003**, *489*, 103−114.
(67) McConnell, E. L.; Basit, A. W.; Murdan, S. Measurements of rat and mouse gastrointestinal pH, fluid and lymphoid tissue, and implications for in-vivo experiments. *J. Pharm. Pharmacol.* **2008**, *60*, 63−70.
(68) Dwyer, D. F.; Tiedje, J. M. Degradation of ethylene glycol and polyethylene glycols by methanogenic consortia. *Appl. Environ. Microbiol.* **1983**, *46*, 185−190.
(69) Frings, J.; Schramm, E.; Schink, B. Enzymes Involved in Anaerobic Polyethylene Glycol Degradation by Pelobacter venetianus and Bacteroides Strain PG1. *Appl. Environ. Microbiol.* **1992**, *58*, 2164−2167.
(70) Kawai, F. Microbial degradation of polyethers. *Appl. Microbiol. Biotechnol.* **2002**, *58*, 30−38.
(71) Krishnaiah, Y. S.; Khan, M. A. Strategies of targeting oral drug delivery systems to the colon and their potential use for the treatment of colorectal cancer. *Pharm. Dev. Technol.* **2012**, *17*, 521−540.
(72) Pinto, J. F. Site-specific drug delivery systems within the gastrointestinal tract: from the mouth to the colon. *Int. J. Pharmaceutics* **2010**, *395*, 44−52.
(73) McConnell, E. L.; Fadda, H. M.; Basit, A. W. Gut instincts: explorations in intestinal physiology and drug delivery. *Int. J. Pharmaceutics* **2008**, *364*, 213−226.
(74) Das, S.; Lin, H. S.; Ho, P. C.; Ng, K. Y. The impact of aqueous solubility and dose on the pharmacokinetic profiles of resveratrol. *Pharm. Res.* **2008**, *25*, 2593−2600.
(75) Bertacche, V.; Lorenzi, N.; Nava, D.; Pini, E.; Sinico, C. Host-guest interaction study of resveratrol with natural and modified cyclodextrins. *J. Incl. Phenom. Macrocycl. Chem.* **2006**, *55*, 279−287.
(76) Camont, L.; Cottart, C. H.; Rhayem, Y.; Nivet-Antoine, V.; Djelidi, R.; Collin, F.; Beaudeux, J. L.; Bonnefont-Rousselot, D. Simple spectrophotometric assessment of the trans-/cis-resveratrol ratio in aqueous solutions. *Anal. Chim. Acta* **2009**, *634*, 121−128.
(77) Gee, J. M.; DuPont, M. S.; Day, A. J.; Plumb, G. W.; Williamson, G.; Johnson, I. T. Intestinal transport of quercetin glycosides in rats involves both deglycosylation and interaction with the hexose transport pathway. *J. Nutr.* **2000**, *130*, 2765−2771.
(78) Day, A. J.; DuPont, M. S.; Ridley, S.; Rhodes, M.; Rhodes, M. J.; Morgan, M. R.; Williamson, G. Deglycosylation of flavonoid and isoflavonoid glycosides by human small intestine and liver beta-glucosidase activity. *FEBS Lett.* **1998**, *436*, 71−75.
(79) Day, A. J.; Cañada, F. J.; Díaz, J. C.; Kroon, P. A.; Mclauchlan, R.; Faulds, C. B.; Plumb, G. W.; Morgan, M. R.; Williamson, G. Dietary flavonoid and isoflavone glycosides are hydrolysed by the lactase site of lactase phlorizin hydrolase. *FEBS Lett.* **2000**, *468*, 166−170.
(80) Day, A. J.; Gee, J. M.; DuPont, M. S.; Johnson, I. T.; Williamson, G. Absorption of quercetin-3-glucoside and quercetin-4′-glucoside in the rat small intestine: the role of lactase phlorizin hydrolase and the sodium-dependent glucose transporter. *Biochem. Pharmacol.* **2003**, *65*, 1199−1206.
(81) Henry-Vitrac, C.; Desmoulière, A.; Girard, D.; Mérillon, J. M.; Krisa, S. Transport, deglycosylation, and metabolism of trans-piceid by small intestinal epithelial cells. *Eur. J. Nutr.* **2006**, *45*, 376−382.

Supporting Information

Acetal derivatives as prodrugs of resveratrol

Andrea Mattarei,[a,b,&] *Michele Azzolini,*[c,&] *Massimo Carraro,*[b] *Nicola Sassi,*[a,c] *Mario Zoratti,*[a,c] *Cristina Paradisi,*[b,*] *and Lucia Biasutto.*[a,c,*]

[a] CNR Institute of Neuroscience, viale G. Colombo 3, 35121 Padova, Italy

[b] Department of Chemical Sciences, University of Padova, via F. Marzolo 1, 35131 Padova, Italy

[c] Department of Biomedical Sciences, University of Padova, viale G. Colombo 3, 35121 Padova, Italy.

Table of contents

Kinetics of hydrolysis in acidic media

The hydrolysis resveratrol derivatives in acidic environment was studied as a series of consecutive pseudo first order reactions (consecutive loss of the three protecting groups):

$$A \xrightarrow{k_1} B \xrightarrow{k_2} C \xrightarrow{k_3} D$$

(where: A is the trisubstituted resveratrol formal derivative; B is the mix of disubstituted isomers; C is the mix of monosubstituted isomers; D is resveratrol)

The fit was obtained using a set of equations describing the temporal behaviour of the system in terms of the rate constants (k_1, k_2, k_3) and the initial amount of the intact derivative ($[A]_0$) (Kozerski et al, 2003):

$$[A] = [A]_0 \cdot e^{-k_1 t}$$

$$[B] = \left(\frac{k_1 \cdot [A]_0}{k_1 - k_2}\right) \cdot \left(e^{-k_1 t} - e^{-k_2 t}\right)$$

$$[C] = \left(\frac{k_1 \cdot k_2 \cdot [A]_0}{(k_2 - k_1) \cdot (k_3 - k_1)}\right) \cdot e^{-k_1 t} + \left(\frac{k_1 \cdot k_2 \cdot [A]_0}{(k_1 - k_2) \cdot (k_3 - k_2)}\right) \cdot e^{-k_2 t} + \left(\frac{k_1 \cdot k_2 \cdot [A]_0}{(k_1 - k_3) \cdot (k_2 - k_3)}\right) \cdot e^{-k_3 t}$$

$$[D] = [A]_0 \cdot \left(1 - \frac{k_2 \cdot k_3 \cdot e^{-k_1 t}}{(k_2 - k_1) \cdot (k_3 - k_1)} - \frac{k_1 \cdot k_3 \cdot e^{-k_2 t}}{(k_1 - k_2) \cdot (k_3 - k_2)} - \frac{k_1 \cdot k_2 \cdot e^{-k_3 t}}{(k_1 - k_3) \cdot (k_2 - k_3)}\right)$$

Table S1. *Observed pseudo first-order rate constants for the hydrolysis of resveratrol derivatives* ***2c-g*** *in 0.1N HCl, 37°C. Values ± standard error are reported as obtained from the fit of all the available data.*

	2c	**2d**	**2e**	**2f**	**2g**
$\mathbf{k_1}$ (h^{-1})	0.270 ± 0.003	0.358 ± 0.010	0.367 ± 0.011	0.323 ± 0.015	0.344 ± 0.006
$\mathbf{k_2}$ (h^{-1})	0.200 ± 0.002	0.291 ± 0.010	0.289 ± 0.008	0.269 ± 0.011	0.261 ± 0.009
$\mathbf{k_3}$ (h^{-1})	0.099 ± 0.003	0.176 ± 0.008	0.166 ± 0.007	0.149 ± 0.011	0.147 ± 0.005

Pharmacokinetic profiles

Figure S1. *Pharmacokinetic profiles for compounds* ***2d*** *(a),* ***2e*** *(b),* ***2g*** *(c).*

a)

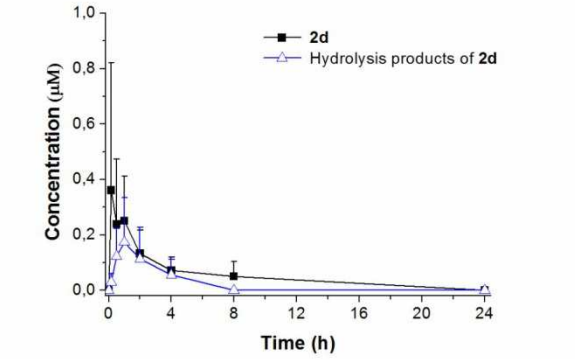

b)

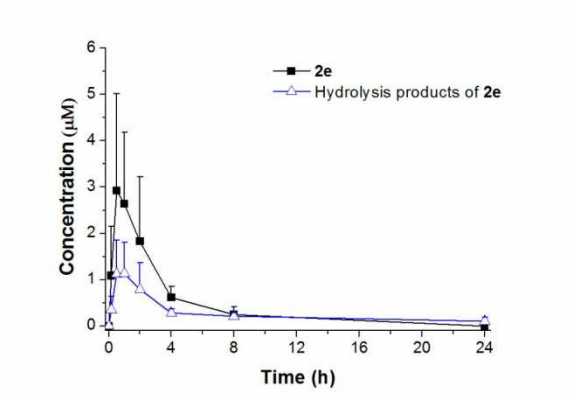

c)

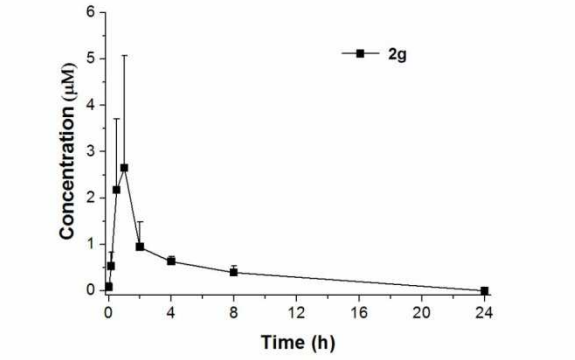

S3

2. New water-soluble carbamate ester derivatives of resveratrol

Molecules **2014**, *19*, 15900-15917; doi:10.3390/molecules191015900

OPEN ACCESS

molecules

ISSN 1420-3049

www.mdpi.com/journal/molecules

Article

New Water-Soluble Carbamate Ester Derivatives of Resveratrol

Andrea Mattarei [1], Massimo Carraro [2], Michele Azzolini [3], Cristina Paradisi [1], Mario Zoratti [3,4] and Lucia Biasutto [3,4,*]

[1] Department of Chemical Sciences, University of Padova, Via F. Marzolo 1, 35131 Padova, Italy; E-Mails: andrea.mattarei@unipd.it (A.M.); cristina.paradisi@unipd.it (C.P.)

[2] Department of Chemistry and Pharmacy, University of Sassari, Viale Vienna 2, 07100 Sassari, Italy; E-Mail: mcarraro@uniss.it (M.C.)

[3] Department of Biomedical Sciences, University of Padova, Viale G. Colombo 3, 35121 Padova, Italy; E-Mails: michele.azzolini@gmail.com (M.A.); zoratti@mail.bio.unipd.it (M.Z.)

[4] CNR Neuroscience Institute, Viale G. Colombo 3, 35121 Padova, Italy

* Author to whom correspondence should be addressed; E-Mail: lucia.biasutto@cnr.it; Tel.: +39-049-8276-483; Fax: +39-049-8276-040.

External Editor: Arthur S. Polans

Received: 27 August 2014; in revised form: 22 September 2014 / Accepted: 24 September 2014 / Published: 1 October 2014

Abstract: Low bioavailability severely hinders exploitation of the biomedical potential of resveratrol. Extensive phase-II metabolism and poor water solubility contribute to lowering the concentrations of resveratrol in the bloodstream after oral administration. Prodrugs may provide a solution—protection of the phenolic functions hinders conjugative metabolism and can be exploited to modulate the physicochemical properties of the compound. We report here the synthesis and characterization of carbamate ester derivatives of resveratrol bearing on each nitrogen atom a methyl group and either a methoxy-poly(ethylene glycol)-350 (mPEG-350) or a butyl-glucosyl promoiety conferring high water solubility. *Ex vivo* absorption studies revealed that the butyl-glucosyl conjugate, unlike the mPEG-350 one, is able to permeate the intestinal wall. *In vivo* pharmacokinetics confirmed absorption after oral administration and showed that no hydrolysis of the carbamate groups takes place. Thus, sugar groups can be attached to resveratrol to obtain soluble derivatives maintaining to some degree the ability to permeate biomembranes, perhaps by facilitated or active transport.

Keywords: resveratrol; prodrugs; carbamate esters; solubility; poly(ethylene glycol); glucose

1. Introduction

Resveratrol has the potential to prevent, alleviate or slow the progression of a wide variety of illnesses, including cardiovascular disease, metabolic syndrome, cancer, ischemic injuries, cognitive decline, inflammatory ailments. It can enhance stress resistance and extend the lifespan of some model organisms. Studies dealing with the mechanisms underlying the bioactivity of resveratrol have been summarized in many reviews (e.g., [1–8]). Activation of the AMP-regulated kinase AMPK and of the NAD-dependent deacetylase Sirt-1, and the consequent effects on gene expression, are important features of the signaling network [9–12].

Bioavailability is fundamental for the full realization of the biomedical potential of nutraceuticals; many polyphenols have pharmacokinetic/pharmacodynamic and physicochemical properties that limit their chance of being developed into pharmaceutical products. The efficacy of orally administrated resveratrol depends on its absorption, metabolism, and tissue distribution. The distribution of resveratrol and its metabolites in organs has been investigated [13–15]. Only trace amounts (below 5 ng/mL, *i.e.*, 22 nM) of unchanged resveratrol could be detected in human plasma after a 25 mg oral dose [16]. A recent study of the distribution of pterostilbene (3,5-*O*-dimethylresveratrol) and pterostilbene sulfate in the rat has however shown that blood or plasma concentrations cannot be automatically considered a reliable index of total body levels [17]. The dose escalation approach has been investigated, covering a total dose range of 25–5,000 mg [18] but even at the highest doses the concentrations of resveratrol in plasma (peak: 550 ng/mL, *i.e.*, ~2.4 μM) seemed too low to provide a plausible explanation of effects. Indeed in enterocytes resveratrol is rapidly converted by conjugating enzymes to metabolites that are re-exported, largely to the intestinal lumen, by ABC transporters [19,20]. Liver sulfotransferases (SULTs) and glucuronosyltransferases (UGTs) then intervene on the molecules that have entered the circulation. Studies on *in vivo* bioavailability and metabolism of resveratrol indicate that glucuronides, sulfates and double-bond reduction products formed by gut microflora are major metabolites [13,18,21–23]. Marked differences in the relative relevance of these conjugative processes may be observed, depending on the species and also on factors such as gender or dosage (see, e.g., [24–26]). Most studies suggest sulfation to be the major modification in rodents, while glucuronidation appears more important in humans [17], but the significance of sulfation in humans may need reconsideration [14]. Metabolites themselves may have some degree of bioactivity (e.g., [27–34]) and the relative proportions of the two major sets of metabolites—sufates *vs.* glucuronides—may be a factor in determining overall bioactivity. While the contribution of these conjugates would be expected to depend on the specific cellular or molecular process being considered, in general their increased size, polarity and hydrophilicity may be seen as an obstacle for interaction with many enzymes.

Experimental data support the idea that sulfates and glucuronides of resveratrol may act as a sort of storage device, regenerating the aglycone through the action of sulfatases and glucuronidases [35–37]. Nonetheless, devising ways to increase levels and slow metabolic transformation of resveratrol after oral administration clearly is an important endeavor [38]. Many formulation-based approaches to

overcome the solubility obstacle, improving stability and/or enhancing absorption and efficacy of resveratrol have been considered: inclusion into cyclodextrins [39,40], micro/nano emulsions [41–43], nano suspensions [44], micelles [45,46], nanostructured lipid carriers [47–49], liposomes [43,47,50], nanochannel delivery membrane systems [51], and various types of nanoparticulated carriers [48,52–61]. Another main strategy used to prevent drug metabolism and enhance bioavailability and effectiveness is based on the development of "prodrugs" [62,63]. In the case of resveratrol this would consist in protecting reactive sites (hydroxyl moieties) with removable groups (promoieties), thus opposing phase II metabolic processes. The prodrug approach is furthermore often used to introduce favorable physicochemical properties, in particular to modulate water solubility, via the promoieties. An ideal prodrug has both good absorption and bioconversion characteristics. The latter clearly depend on the type of chemical bond system used to link the promoiety to the "core" of the molecule.

Carbamate esters are one of the most popular types of prodrugs, used for example with duocarmycin [64], camptothecin [65], entacapone [66] and (−)-3-(3-hydroxyphenyl)-N-propylpiperidine [67]. We report here the synthesis and performance of *N,N*-disubstituted resveratrol carbamates. To improve solubility, butyl-glucosyl or methoxy-poly(ethylene glycol)-350 (mPEG-350; average molecular weight ~ 350 Da) groups were introduced as promoieties (Scheme 1).

Scheme 1. Chemical structures of resveratrol **1** and carbamoyl derivatives **2** and **3**.

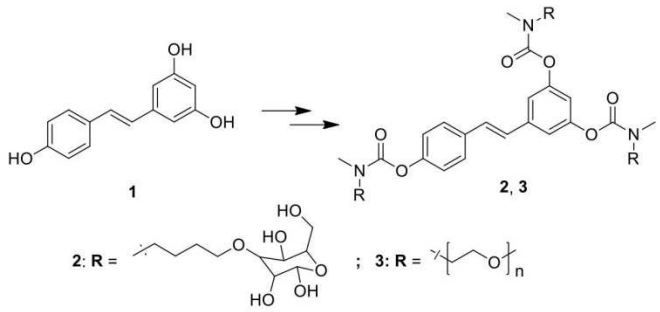

Many prodrugs designed to increase water solubility involve the addition of an ionizable promoiety to the parent molecule. Because charged molecules have great difficulty crossing biological membranes, one must balance increased water solubility against a potentially decreased permeability. Based on this consideration we chose non-ionizable solubilizing groups. Conversion of a compound into a more hydrophilic one is not necessarily going to help absorption either, since the energetic barrier opposing diffusion through the lipid core of biological membranes is expected to become more important. However both groups we used, glucose and mPEG-350, have features that may provide increased solubility without unduly compromising absorption. Increased water solubility constitutes an obvious advantage also for administration routes other than oral, such as intravenous injection or slow-release implanted capsules.

It may be possible, by incorporating glucose into the promoiety, to take advantage of the presence of glucose transporters in the absorbing epithelium. While flavonoid or resveratrol intestinal uptake may also occur by simple diffusion through the enterocyte membrane, studies have implicated intestinal transporters of the SGLT and GLUT families in the uptake of glycosylated derivatives [68,69].

Attachment of poly(ethylene glycol) (PEG) moieties to therapeutic compounds ("pegylation") may improve drug absorption and pharmacokinetics [70–74]. PEG is known to be non-toxic, non-antigenic and biocompatible and indeed the FDA has approved its use as a vehicle or base in foods, cosmetics and pharmaceuticals. In this work, mPEG-350 was chosen as a promoiety to modify resveratrol because it can increase both water and lipid solubility of a drug and we reasoned that the latter effect may facilitate the penetration of resveratrol through biological membranes.

2. Results and Discussion

2.1. Synthesis

Derivatives **2–3** (Scheme 1) were obtained through condensation of resveratrol (**1**) with the appropriate carbamoyl chloride. The synthesis of **2** is outlined in Scheme 2. The starting material for the glucosyl carbamate was commercially available 1,2:5,6-di-*O*-isopropylidene-α-D-glucofuranose (**4**) which was allowed to react with an excess of 1-bromo-4-chlorobutane in the presence of sodium hydride to give **5** in fair yield through Williamson etherification. In the second step, compound **5** was treated with methylamine under microwave irradiation to obtain the secondary amine **6** in a short reaction time. This intermediate was allowed to react with triphosgene under mild conditions to give the carbamoyl chloride (**7**) which was used without further purification in the subsequent step. Compound **7** was added in slight excess to resveratrol (**1**) in pyridine and allowed to react at reflux to obtain the carbamate derivative **8** in good yield. The last step consisted in the removal of the acetonide protecting groups from the glucofuranosyl rings, freeing the hydroxyl functions necessary to enhance the solubility in water of the final product (**2**). The reaction was performed in trifluoroacetic acid:water, 9:1, at room temperature. Under these conditions the carbamate group is stable and the desired product was obtained in excellent yield.

Scheme 2. Synthesis of compound **2**.

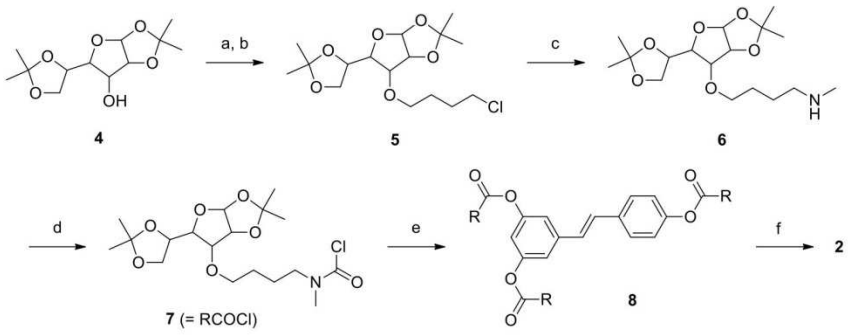

Reagents and conditions: (a) NaH, DMF, r.t., 30 min; (b) $Br(CH_2)_4Cl$, 40 °C, 24 h; (c) CH_3NH_2, EtOH, Microwave 150 °C, 30 min; (d) triphosgene, pyridine, DCM, 0 °C to r.t., 45 min; (e) DMAP, **1**, pyridine, reflux, overnight; (f) trifluoroacetic acid : water 9:1, r.t., 1 h.

The synthesis of derivative **3** (Scheme 3) was more straightforward, since there was no need to introduce a spacer or for a deprotection step. The starting material was a simple and cheap methoxy-poly(ethylene glycol) with an average molecular weight of 350 Da (**9**), possessing one free hydroxyl

group which was esterified with tosyl chloride to obtain compound **10**. The tosylate group of **10** was easily displaced in the second step by methylamine under microwave irradiation giving the secondary amine **11** in nearly quantitative yield. Finally, amine **11** was treated with triphosgene to give the carbamoyl chloride **12**, which in turn was allowed to react with resveratrol to afford the desired product **3**.

Scheme 3. Synthesis of compound **3**.

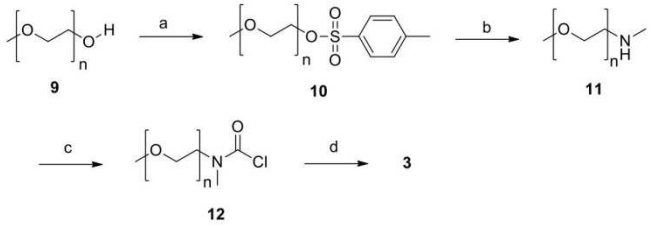

Reagents and conditions: (a) 1. NaOH, H_2O/THF, 0 °C, 2. TosCl, 5 °C, 2 h; (b) CH_3NH_2, EtOH, Microwave 150 °C, 30 min; (c) triphosgene, pyridine, DCM, 0 °C to r.t., 45 min; (d) DMAP, **1**, pyridine, reflux, overnight.

2.2. Solubility

Both derivatives displayed good water solubility (>50 mM). This represents a strong increase with respect to resveratrol, the reported solubility for which ranges from ≤1 μM to 300 μM [75–78]. As can be noticed, these data from the literature are very variable, probably because of the difficulty in determining accurate solubility data for compounds that can form colloids.

2.3. Permeation across Rat Intestine

We assayed transport of the derivatives across explanted rat jejunum segments using Ussing-type chambers. This system allows the study of transepithelial transport separately from other processes taking place in the intestinal lumen, in blood, or in the liver. In these experiments, the same amount of resveratrol or derivative was loaded on the apical side; both apical and basolateral chambers were then analyzed after 2.5 h (see Experimental Sections for details).

In agreement with our previous observations [78,79], resveratrol reached the basolateral compartment mainly (≥90%) in the form of phase II metabolites (sulfate(s) and glucuronide(s)); basolateral species collectively accounted for 0.6%–1.5% of the amount placed initially in the apical side chamber. In the same experimental setup and conditions, a similar translocation (1.7 ± 0.7%) was observed for derivative **2**; in this case, however, only the intact derivative was detected in the basolateral chamber; resveratrol and its metabolites were below the detection threshold, and no products deriving from partial deprotection of the hydroxyl groups (hydrolysis of one or two of the three carbamate groups) could be detected either. Somewhat to our surprise, no compounds with a stilbenoid structure could be detected in the basolateral chamber when derivative **3** was placed in the apical one. No further experiments were conducted with this compound.

Passage of the glucosyl-derivative **2** across the intestinal wall is remarkable, since it is too hydrophilic to undergo passive diffusion through cell membranes. A possible explanation may be the

involvement of a facilitated or active transport mechanism, possibly mediated by glucose transporters. Dietary glucose crosses the apical membrane of the enterocyte by the Na^+/glucose cotransporter (SGLT1) and exits across the basolateral membrane through the facilitative transporter GLUT2. Before a meal, the concentration of glucose in the lumen is very low. Any glucose is rapidly captured by SGLT1, which is ideal for this purpose, being a low-capacity, high-affinity transporter and the only transporter capable of moving glucose against a concentration gradient. GLUT2 is a high-capacity, low-affinity facilitative transporter that equilibrates glucose between plasma and enterocyte. We thus investigated the absorption of derivative **2** through excised rat jejunum in the presence of different concentrations and combinations of inhibitors of SGLT-1 (phlorizin) and GLUT-2 (phloretin and cythochalasin B). To minimize the possibility of competitive inhibition by medium glucose, we also decreased glucose concentration in the assay medium from ~55 to 1 mM, substituting it with mannitol, and/or increased the concentration of derivative **2** to levels close to that of glucose (0.5 *vs* 1 mM).

After a meal, there is a high effective glucose concentration at the surface of the apical membrane. The initial glucose transport across the apical membrane results in rapid insertion of GLUT2 into the apical membrane from intracellular vesicles underlying the membrane. Apical GLUT2 is now the major pathway of absorption. Then, when the glucose concentration in the lumen falls, the whole signaling system is reversed so that GLUT2 is inactivated and traffics away from the apical membrane to restore the situation before a meal [80,81]. To determine if the administration of glucose could enhance the absorption of derivative **2**, thus providing evidence for a role of GLUT2 in its transport, we performed transport experiments using the intestine from non-fasted rats, and from rats who had received glucose in their drinking water (20 g/L) in the 24 h prior to the experiment.

The extents of translocation under the various conditions mentioned above turned out not to differ significantly one from the others. Dynamic trafficking of GLUT-2 [82] may contribute to the observed variability: its levels in *ex vivo* intestinal preparations can be greatly reduced compared to the *in vivo* situation, because GLUT-2 traffic to the brush border of enterocytes is regulated by endogenous hormones through PKC βII activation, and this process is inactivated upon intestine explantation. A variable contribution by paracellular absorption may also take place; this can be altered/increased by stretching of the intestinal segment during the assembly of Ussing chambers, which in turn depends on the particular anatomical features of each explanted intestine. To gain more information on the absorption of derivative **2**, we thus performed *in vivo* pharmacokinetic experiments.

2.4. In Vivo Pharmacokinetics

Oral administration by gavage of derivative **2** to rats resulted in low concentrations of the derivative in the bloodstream during the 4 hours following administration; maximum levels were reached after about 60 min (Figure 1). This suggests that the paracellular pathway may not be involved in uptake, but the mechanism of absorption remains to be defined. Besides sugar carriers, other candidates are provided by the families of Organic Anion Transporter Polypeptides (OATPs) (e.g., [83–86]) and/or Organic Cation Transporters (OCTs) [87,88].

Neither resveratrol nor its common metabolites were present in detectable amounts either in the basolateral chamber in *ex vivo* assays or in the blood of rats after oral administration. It follows that while **2** can be transported across the intestinal wall, although with a low efficiency, it resists the

action of hydrolytic enzymes in the gut, gut wall, blood and liver. Also derivative **3** exhibited complete stability at physiological pH values and in blood; one can thus conclude that *N,N*-disubstituted carbamate derivatives are stable under the conditions of interest here. The ideal bond in prodrugs needs on the other hand to have a finite lifetime *in vivo*. The stability of the carbamate ester group can be fine-tuned by acting on the substitution pattern of the N atom: *N*-monosubstituted carbamates are known to be less stable than *N,N*-disubstituted ones [89].

Figure 1. Results of pharmacokinetic experiments in rats with derivative **2**. Blood concentration *vs* time profile. Mean values ± st. dev. (n = 5). To compare these results with the pharmacokinetic profile obtained administering resveratrol itself, please see [78].

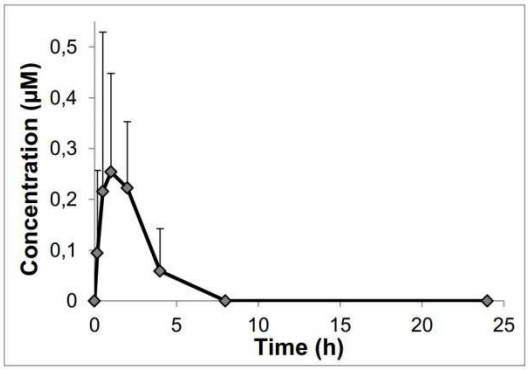

3. Experimental Section

3.1. Materials, Reagents and Standard Procedures

Resveratrol was purchased from Waseta Int. Trading Co. (Shangai, China). Other starting materials and reagents were purchased from Sigma-Aldrich, Fluka, Merck-Novabiochem, Riedel de Haen, J.T. Baker, Cambridge Isotope Laboratories Inc., Acros Organics, Carlo Erba and Prolabo, and were used as received. ^{1}H-NMR spectra were recorded with a Bruker AC250F spectrometer operating at 250 MHz. Chemical shifts (δ) are given in ppm relative to the signal of the solvent. HPLC/ESI-MS analyses and mass spectra determinations were performed with a 1100 Series Agilent Technologies system, equipped with a binary pump (G1312A) and a MSD SL Trap mass spectrometer (G2445D SL) with an ESI source. Reaction intermediates and final purified products were injected as solutions in acetonitrile; elution was carried out with a water:acetonitrile 1:1 mixture containing 0.1% formic acid. TLCs were run on silica gel supported on plastic (Macherey-Nagel Polygram®SIL G/UV$_{254}$, silica thickness 0.2 mm), or on silica gel supported on glass (Fluka) (silica thickness 0.25 mm, granulometry 60 Å, medium porosity) and visualized by UV detection or $KMnO_4$ oxidation. Flash chromatography was performed on silica gel (Macherey-Nagel 60, 230–400 mesh granulometry (0.063–0.040 mm)) under air pressure. Solvents were analytical or synthetic grade and were used without further purification. Elemental analyses were carried out using a Fisons-EA-1108 CHNS-O Element Analyzer (Thermo Scientific).

3.2. Synthesis

1,2,5,6-Di-O-isopropylidene-3-(4-chlorobutoxy)-α-D-glucofuranose (**5**): NaH (0.31 g, 7.7 mmol, 2.0 eq., 60% in mineral oil) was washed three times with 5 mL of *n*-hexane. The suspension was decanted after each wash and *n*-hexane traces were removed under reduced pressure. Anhydrous DMF (15 mL) was then added and the suspension was stirred for 5 min. A solution of 1,2,5,6-Di-*O*-isopropylidene-α-D-glucofuranose (**4**, 1.00 g, 3.8 mmol, 1.0 eq.) in anhydrous DMF (15 mL) was then added dropwise. After stirring for 30 min under nitrogen flow, a solution of 1-bromo-4-chlorobutane (2.63 g, 15.4 mmol, 4.0 eq.) in anhydrous DMF (5 mL) was added dropwise and the mixture was vigorously stirred for 24 hours at 40 °C. The reaction mixture was then diluted in CH_2Cl_2 (150 mL) and washed with 0.3 N HCl (5 × 100 mL). The organic layer was dried over $MgSO_4$ and filtered. The solvent was evaporated under reduced pressure and the residue was purified by column chromatography (CH_2Cl_2:EtOAc 9:1) to give **5** (0.81 g, 60% yield) as a pale yellow oil. ^{1}H-NMR ($CDCl_3$) δ (ppm) = 5.87 (d, *J* = 3.7 Hz, 1H, -CH-), 4.53 (d, *J* = 3.8 Hz, 1H, -CH-), 4.32–4.24 (m, 1H, -CH-), 4.12–4.06 (m, 2H, -CH_2-), 4.00–3.95 (m, 1H, -CH-), 3.86–3.44 (m, 5H, -CH-, -O-CH_2-, -CH_2-Cl), 1.84–1.60 (m, 4H, -CH_2-CH_2-), 1.49, 1.41, 1.34, 1.31 (4 s, 12H, 4 × -CH_3); ^{13}C-NMR ($CDCl_3$) δ (ppm) = 111.76, 108.98, 105.25, 83.05, 82.12, 81.21, 72.34, 69.54, 67.39, 44.76, 29.26, 26.99, 26.80, 26.77, 26.21, 25.34; ESI-MS (ion trap): *m/z* 351 $[M+H]^+$. Anal. calcd. for $C_{16}H_{27}ClO_6$: C, 54.78; H, 7.76 Found: C, 54.69; H, 7.71.

1,2,5,6-Di-O-isopropylidene-3-(4-N-methyl-N-butoxyamino)-α-D-glucofuranose (**6**): In a sealed microwave reactor **5** (1.99 g, 5.7 mmol, 1.0 eq.) was added to methylamine solution (33 wt. % in absolute EtOH, 25 mL, 198.5 mmol, 35.0 eq.). The reaction mixture was stirred for 30 min under microwave irradiation (150 °C, 150 W). The solvent was evaporated under reduced pressure and the residue was purified by column chromatography (CH_2Cl_2/MeOH 8.5:1.5) to give **6** (1.78 g, 91% yield) as a white solid. ^{1}H-NMR (DMSO-d_6) δ (ppm) = 5.83 (d, *J* = 3.7 Hz, 1H, -CH-), 4.63 (d, *J* = 3.8 Hz, 1H, -CH-), 4.27–4.20 (m, 1H, -CH-), 4.04–3.94 (m, 2H, -CH_2-), 3.84–3.74 (m, 2H, -CH_2-), 3.64–3.56 (m, 1H, -CH-), 3.46–3.32 (m, 4H, -CH-, -NH-CH_3), 2.90–2.76 (m, 2H, -NH-CH_2-), 2.43 (br, 1H, -NH-), 1.72–1.48 (m, 4 H, -CH_2-CH_2-), 1.39, 1.32, 1.27, 1.25 (4 s, 12H, 4 × -CH_3); ^{13}C-NMR (DMSO-d_6) δ (ppm) = 110.78, 107.98, 104.67, 81.56, 81.48, 80.28, 72.29, 68.72, 65.93, 47.83, 32.18, 26.65, 26.61, 26.22, 26.08, 25.32, 22.26; ESI-MS (ion trap): *m/z* 346 $[M+H]^+$. Anal. calcd. for $C_{17}H_{31}NO_6$: C, 59.11; H, 9.05; N, 4.05 Found: C, 59.15; H, 9.01; N, 4.11.

3,4',5-Tri-[1,2,5,6-Di-O-isopropylidene-α-D-glucofuranose-3-(4-N-methyl-N-butoxy)]-resveratrol carbamate (**8**): A solution of **6** (2.03 g, 5.9 mmol, 1.0 eq.) and pyridine (5.0 mL) in dry CH_2Cl_2 (20 mL) was slowly added to triphosgene (1.74 g, 5.9 mmol, 1.0 eq.) in dry CH_2Cl_2 (20 mL) at 0 °C. The mixture was stirred at room temperature for 45 min followed by addition of 0.1 N HC1 (50.0 mL). The organic layer was separated, and washed 4 × 100 mL with 0.1 N HCl and then dried over $MgS0_4$, filtered and concentrated under reduced pressure. The residue was then filtered through a short silica-gel column (CH_2Cl_2:EtOAc 8.25:1.75) and the eluate concentrated to give **7** as a pale yellow oil, which was used immediately without further purification. Compound **7** (1.70 g, 4.2 mmol, 5 eq.) was then added to a solution of resveratrol (**1**, 0.190 g, 0.8 mmol, 1 eq.) and DMAP (0.407 g, 3.3 mmol, 4 eq.) in pyridine (5 mL) and the resulting solution was vigorously stirred for 16 hours at 135 °C. The reaction

mixture was then diluted in EtOAc (150 mL) and washed with 0.5 N HCl (5 × 100 mL). The organic layer was dried over $MgSO_4$ and filtered. The solvent was evaporated under reduced pressure and the residue was purified by column chromatography (CH_2Cl_2:EtOAc 5.5:4.5) to give **8** (0.86 g, 76% yield) as a white solid. ^{1}H-NMR ($CDCl_3$) δ (ppm) = 7.46 (d, *J* = 8.6 Hz, 2H, 2 × Ar-H), 7.17–6.92 (m, 6H, 6 × Ar-H), 6.89–6.81 (m, 1H, Ar-H), 5.87 (d, *J* = 3.7 Hz, 3H, 3 × -CH-), 4.58–4.50 (m, 3H, 3 × -CH-), 4.35–4.27 (m, 3H, 3 × -CH-), 4.15–3.96 (m, 9H, 3 × -CH-, 3 × -CH_2-), 3.89–3.84 (m, 3H, 3 × -CH-), 3.72–3.52 (m, 6H, 3 × -CON(CH_3)-CH_2-), 3.48–3.32 (m, 6H, 3 × -O-CH_2-), 3.10–2.96 (2 s, 9H, 3 × -CON(CH_3)-, 1.77–1.55 (m, 12H, 3 × -CH_2-CH_2-), 1.49, 1.42, 1.35, 1.31 (4 s, 36H, 12 × -CH_3); ^{13}C-NMR ($CDCl_3$) δ (ppm) = 154.73, 154.42, 151.07, 150.78 127.61, 122.09, 116.59, 111.89, 111.81, 109.94, 109.10, 105.38, 82.57, 82.28, 81.28, 72.58, 70.18, 70.15, 67.43, 49.19, 49.09, 31.09, 26.96, 26.34, 25.57; ESI-MS (ion trap): *m/z* 1365 $[M+H]^+$. Anal. calcd. for $C_{68}H_{99}N_3O_{24}$: C, 60.84; H, 7.43; N, 3.13 Found: C, 60.77; H, 7.40; N, 3.08.

3,4',5-Tri-[α/β-D-glucopyranose-3-(4-N-methyl-N-butoxy)]-resveratrol carbamate (**2**): A solution of **8** (0.30 g, 0.2 mmol), trifluoroacetic acid (1.8 mL), and water (0.2 mL) was stirred for 1.5 hours at room temperature. The reaction mixture was then added dropwise to diethyl ether (10 mL) under stirring and the precipitate was centrifuged (1000 g, 5 min). The solvent was decanted and the precipitate was washed three times with diethyl ether (10 mL) in order to eliminate residual traces of trifluoroacetic acid. The resulting solid was dissolved in water (5 mL) and lyophilized to give **2** (0.23 g, 93% yield) as a bright white solid. ^{1}H-NMR (DMSO-d_6) δ (ppm) = 7.61 (d, *J* = 8.6 Hz, 2H, 2 × Ar-H), 7.37–6.11 (m, 6H, 6 × Ar-H), 6.89–6.81 (m, 1H, Ar-H), 4.89 (d, *J* = 3.7 Hz, 3H, 3 × -CH-), 4.28 (d, *J* = 7.0 Hz, 3H, 3 × -CH-), 3.79–2.86 (m, 36H), 1.75–1.43 (m, 12H, 3 × -CH_2-CH_2-); ^{13}C-NMR ($CDCl_3$) δ (ppm) = 153.69, 153.48, 151.82, 150.94, 138.76, 133.57, 132.62, 127.39, 126.63, 122.16, 96.84, 92.27, 85.16, 81.90, 76.64, 74.51, 72.03, 71.44, 71.43, 71.41, 71.40, 71.38, 69.85, 69.83, 69.66, 69.65, 61.00, 48.54, 34.43, 34.13, 26.99, 26.97; ESI-MS (ion trap): *m/z* 1124.5 $[M+H]^+$. Anal. calcd. for $C_{50}H_{75}N_3O_{24}$: C, 54.49; H, 6.86; N, 3.81 Found: C, 54.54; H, 6.84; N, 3.71.

(Methoxypolyethylene glycol 350)-p-toluenesulfonate (**10**): A solution of sodium hydroxide (2.29 g, 57.3 mmol, 2.0 eq.) in water (20 ml) and mPEG-350 (**9**, 10.0 g, 28.6 mmol, 1 eq.) in THF (20 mL) was cooled in an ice–water bath with stirring and tosyl chloride (10.9 g, 57.3 mmol, 2 eq.) in THF (20 ml) was added dropwise over 2 hours. The reaction mixture was stirred for an additional 2 hours at 5 °C, poured into ice–water (100 mL) and extracted with CH_2Cl_2 (3 × 100 mL). The combined organic extracts were dried over $MgSO_4$ and filtered. The solvent was evaporated under reduced pressure and the residue was purified by column chromatography ($CHCl_3$:MeOH 9.9:0.1 and increasing methanol content) to give **10** (11.03 g, 77% yield) as a colourless oil. ^{1}H-NMR ($CDCl_3$) δ (ppm) = 7.78 (d, *J* = 8.3 Hz, 2H, 2 × Ar-H), 7.33 (d, *J* = 8.3 Hz, 2H, 2 × Ar-H), 4.15 (t, *J* = 4.90 Hz, 2H, -(SO_2)O-CH_2-), 3.70–3.51 (m, 30H, 7 × -O-CH_2-CH_2-O- + -O-CH_2-), 3.37 (s, 3H, -O-CH_3), 2.44 (s, 3H, Ar-CH_3); ^{13}C-NMR ($CDCl_3$) δ (ppm) = 144.74, 132.90, 129.77, 127.93, 71.87, 70.68, 70.54, 70.50, 70.46, 69.20, 68.62, 58.98, 21.62; ESI-MS (ion trap): *m/z* 495 $[M_{(n=7)}+H]^+$.

N-methyl-N-(methoxypolyethylene glycol 350) amine (**11**): In a sealed microwave reactor **10** (5.43 g, 10.1 mmol, 1.0 eq.) was added to methylamine solution (33 wt. % in absolute ethanol, 44 mL, 353.5

mmol, 35.0 eq.). The reaction mixture was stirred for 30 min under microwave irradiation (150 °C, 150 W). After evaporation of the solvent, the residue was dissolved in 5% HCl (20 mL) and extracted with $CHCl_3$ (3 × 20 mL). The $CHCl_3$ extracts were washed separately with 5% HCl (2 × 10 mL) and all the HCl fractions were combined, 30% sodium hydroxide (15 mL) was added and the resulting solution was extracted with chloroform (3 × 25 mL). The chloroform extracts were then washed separately with water (10 mL). The organic layer was dried over $MgSO_4$ and filtered. The solvent was then evaporated under reduced pressure to give **11** as a pale yellow oil (3.60 g, 98% yield). ^{1}H-NMR ($CDCl_3$) δ (ppm) = 3.70–3.51 (m, 30H, 7 × -O-CH_2-CH_2-O- + -O-CH_2-), 3.36 (s, 3H, -O-CH_3), 2.74 (t, J = 4.90 Hz, 2H, -NH-CH_2-), 2.43 (s, 3H, -NH-CH_3), 2.16 (s, 1H, -NH-); ^{13}C-NMR ($CDCl_3$) δ (ppm) = 71.86, 70.53, 70.50, 70.42, 70.24, 70.07, 58.97, 51.11, 36.15; ESI-MS (ion trap): *m/z* 354 $[M_{(n=7)}+H]^+$.

3,4',5-Tri-[N-methyl-N-(methoxypolyethylene glycol 350)]-resveratrol carbamate (**3**): A solution of **11** (3.70 g, 10.2 mmol, 1.0 eq.) and pyridine (5.0 mL) in dry CH_2Cl_2 (20 mL) was slowly added to triphosgene (3.02 g, 10.2 mmol, 1.0 eq.) in dry CH_2Cl_2 (34 mL) at 0 °C. The mixture was stirred at room temperature for 45 min, followed by addition of 0.1 N HCl (50 mL). The organic layer was separated, washed with 0.1 N HCl (4 × 100 mL) and then dried over $MgS0_4$, filtered and concentrated under reduced pressure. The residue was then filtered through a short silica-gel column (CH_2Cl_2:MeOH 9:1) and the eluate concentrated to give **12** as a pale yellow oil, which was used immediately without further purification. **12** (1.77 g, 4.2 mmol, 5 eq.) was added to a solution of resveratrol (**1**, 0.190 g, 0.8 mmol, 1 eq.) and DMAP (0.407 g, 3.3 mmol, 4 eq.) in pyridine (5 mL) and the resulting solution was vigorously stirred for 16 hours at 135 °C. The reaction mixture was then diluted in EtOAc (150 mL) and washed with 0.5 N HCl (5 × 100 mL). The organic layer was dried over $MgSO_4$ and filtered. The solvent was evaporated under reduced pressure and the residue was purified by column chromatography (eluent: ACN) to give **3** (0.88 g, 76% yield) as a colourless oil. ^{1}H-NMR ($CDCl_3$) δ (ppm) = 7.45 (d, J = 8.6 Hz, 2H, 2 × Ar-H), 7.26-6.97 (m, 6H, 6 × Ar-H), 6.92–6.83 (m, 1H, Ar-H), 3.71-3.52 (m, 9H, 21 × -O-CH_2-CH_2-O-, 3 × -O-CH_2-, 3 × -CON(CH_3)-CH_2-), 3.37 (s, 9H, 3 × -O-CH_3), 3.15–3.07 (2 s, 9H, 3 × -NH-CH_3), 2.16 (s, 1 H, -NH-); ^{13}C-NMR ($CDCl_3$) δ (ppm) = 154.33, 154.17, 151.93, 151.07, 139.11, 133.99, 129.29, 129.23, 127.39, 127.16, 127.13, 121.94, 116.43, 116.41, 71.88, 70.53, 70.48, 69.71, 69.32, 59.03, 59.00, 49.12, 49.07, 48.98, 36.04; ESI-MS (ion trap): *m/z* 1367 $[M_{(n=7)}+H]^+$.

3.3. Permeation Studies with Rat Intestinal Segments (Ex Vivo)

All experiments involving animals were performed with the permission and supervision of the University of Padova Ethical Committee for Experimentation on Animals (CEASA) and Central Veterinary Service, in compliance with Italian Law DL 116/92, embodying UE Directive 86/609.

Intestine was excised from 18 h fasted rats and transferred into a saline solution (154 mM NaCl in water) at 37 °C. The jejunum was cut into 1 cm long strips, opened longitudinally, rinsed free of luminal content and mounted in Ussing-type chambers. Apical and basolateral compartments were filled with 1 mL each of oxygenated HEPES buffer (248 mM NaCl, 55.3 mM glucose, 50 mM $NaHCO_3$, 9.9 mM KCl, 1.9 mM $MgSO_4$, 40 mM HEPES, pH 6.8), and incubated in a water bath at 37 °C until all chambers were assembled (approximately 20 min). The buffer was then removed and substituted with

1 mL of a 20 μM solution (in the same buffer) of the compound to be tested on the apical side (dilution from a 20 mM stock solution), and with 1 mL of fresh HEPES buffer on the basolateral one. Stock solutions of the compounds were prepared in water (for the derivatives) or in DMSO (for resveratrol, due to its limited water solubility). During the experiment, oxygen was continuously bubbled in each basolateral compartment. An aliquot of the initial apical solutions was incubated separately at 37 °C for the period of the experiment, to verify the stability of each compound in the absence of jejunum. At the end of the experiment (2.5 h), 800 μL of chamber contents from apical and basolateral sides were collected and mixed with 8 μL of 100 mM ascorbic acid in water and 8 μL of 6 M acetic acid. The samples were then centrifuged (12,000× *g*, 7 min, 4 °C), and supernatants were frozen and maintained at −20 °C until HPLC-UV analysis (see below).

3.4. Pharmacokinetic Studies

Derivative **2** was administered to overnight-fasted male Wistar rats from the facility of the Department of Biomedical Sciences as a single intragastric dose (88 μmol/kg, dissolved in 250 μL water). Blood samples were obtained by the tail bleeding technique: before drug administration, rats were anesthetised with isoflurane and the tip of the tail was cut off; blood samples (80–100 μL each) were then taken from the tail tip at different time points after drug administration. Blood was collected in heparinised tubes, kept in ice and treated as described in [90] within 10 min.

3.5 HPLC-UV Analysis

Samples (2 μL) were analyzed by HPLC/UV (1290 Infinity LC System, Agilent Technologies) using a reverse phase column (Zorbax RRHD Eclipse Plus C18, 1.8 μm, 50 x 2.1 mm i.d.; Agilent Technologies) and a UV diode array detector (190-500 nm). Solvents A and B were water containing 0.1% trifluoroacetic acid (TFA) and acetonitrile, respectively. The gradient for B was as follows: 22% for 0.2 min, from 22% to 30% in 1.2 min, then from 30% to 100% in 1.2 min; the flow rate was 0.6 mL/min. The temperature of the column was kept at 35 °C.

The eluate was monitored at 300 or 320 nm, corresponding to absorbance maxima of derivatives (**2** and **3**) and resveratrol, respectively. The absorption coefficients (ε_{300}, ε_{320}) of resveratrol derivatives, resveratrol and metabolites are very similar. For quantification purposes we assumed the same absorption coefficient.

3.6 Statistics

Significance in comparisons was assessed using the Wilcoxon Rank Test.

4. Conclusions

The work presented here shows that sugar groups can be attached to resveratrol, thus making it completely soluble in water - a significant feature - while maintaining to some degree the ability to permeate biomembranes. The next goal may thus be that of producing carbamate derivatives carrying a single substituent on the nitrogen atom, designed to result in a permeant molecule with a lifetime compatible with its intended function as a prodrug.

Acknowledgments

We thank M. Ghidotti for technical help and NÓOS Srl for generous support and consultations. This work was also supported by grants from the Fondazione Cassa di Risparmio di Padova e Rovigo (CARIPARO) ("Developing a Pharmacology of Polyphenols"), from the Italian Ministry of the University and Research (PRIN n. 20107Z8XBW_004), and by the CNR Project of Special Interest on Aging.

Author Contributions

All authors contributed to the design and conduction of the work and to writing the manuscript.

Conflicts of Interest

The authors declare no conflict of interest.

References

1. Harikumar, K.B.; Aggarwal, B.B. Resveratrol: A multitargeted agent for age-associated chronic diseases. *Cell Cycle* **2008**, *7*, 1020–1035.
2. Pervaiz, S.; Holme, A.L. Resveratrol: Its biologic targets and functional activity. *Antioxid. Redox Sign.* **2009**, *11*, 2851–2897.
3. Biasutto, L.; Szabo, I.; Zoratti, M. Mitochondrial effects of plant-made compounds. *Antioxid. Redox Sign.* **2011**, *15*, 3039–3059.
4. Biasutto, L.; Mattarei, A.; Zoratti, M. Resveratrol and health: the starting point. *ChemBioChem* **2012**, *13*, 1256–1259.
5. McCalley, A.E.; Kaja, S.; Payne, A.J.; Koulen, P. Resveratrol and calcium signaling: Molecular mechanisms and clinical relevance. *Molecules* **2014**, *19*, 7327–7340.
6. Wang, S.; Moustaid-Moussa, N.; Chen, L.; Mo, H.; Shastri, A.; Su, R.; Bapat, P.; Kwun, I.; Shen, C.L. Novel insights of dietary polyphenols and obesity. *J. Nutr. Biochem.* **2014**, *25*, 1–18.
7. Pallas, M.; Porquet, D.; Vicente, A.; Sanfeliu, C. Resveratrol: New avenues for a natural compound in neuroprotection. *Curr. Pharm. Des.* **2013**, *19*, 6726–6731.
8. Widlund, A.L.; Baur, J.A.; Vang, O. mTOR: More targets of resveratrol? *Expert Rev. Mol. Med.* **2013**, *15*, doi:10.1017/erm.2013.11.
9. Park, S.J.; Ahmad, F.; Philp, A.; Baar, K.; Williams, T.; Luo, H.; Ke, H.; Rehmann, H.; Taussig, R.; Brown, A.L.; *et al.* Resveratrol ameliorates aging-related metabolic phenotypes by inhibiting cAMP phosphodiesterases. *Cell* **2012**, *148*, 421–433.
10. Wang, Y.; Li, Y.; Liu, X.; Cho, W.C. Genetic and epigenetic studies for determining molecular targets of natural product anticancer agents. *Curr. Cancer Drug Targets* **2013**, *13*, 506–518.
11. Um, J.H.; Park, S.J.; Kang, H.; Yang, S.; Foretz, M.; McBurney, M.W.; Kim, M.K.; Viollet, B.; Chung, J.H. AMP-activated protein kinase-deficient mice are resistant to the metabolic effects of resveratrol. *Diabetes* **2010**, *59*, 554–563.
12. Price, N.L.; Gomes, A.P.; Ling, A.J.; Duarte, F.V.; Martin-Montalvo, A.; North, B.J.; Agarwal, B.; Ye, L.; Ramadori, G.; Teodoro, J.S.; *et al.* SIRT1 is required for AMPK activation and the beneficial effects of resveratrol on mitochondrial function. *Cell Metab.* **2012**, *15*, 675–690.

13. Azorin-Ortuno, M.; Yanez-Gascon, M.J.; Vallejo, F.; Pallares, F.J.; Larrosa, M.; Lucas, R.; Morales, J.C.; Tomas-Barberan, F.A.; Garcia-Conesa, M.T.; Espin, J.C. Metabolites and tissue distribution of resveratrol in the pig. *Mol. Nutr. Food Res.* **2011**, *55*, 1154–1168.
14. Abd El-Mohsen, M.; Bayele, H.; Kuhnle, G.; Gibson, G.; Debnam, E.; Srai, S.K.; Rice-Evans, C.; Spencer, J.P. Distribution of [3H]*trans*-resveratrol in rat tissues following oral administration. *Br. J. Nutr.* **2006**, *96*, 62–70.
15. Juan, M.E.; Maijo, M.; Planas, J.M. Quantification of *trans*-resveratrol and its metabolites in rat plasma and tissues by HPLC. *J. Pharm. Biomed. Anal.* **2010**, *51*, 391–398.
16. Walle, T.; Hsieh, F.; DeLegge, M.H.; Oatis, J.E., Jr.; Walle, U.K. High absorption but very low bioavailability of oral resveratrol in humans. *Drug Metab. Dispos.* **2004**, *32*, 1377–1382.
17. Azzolini, M.; Spina, M.L.; Mattarei, A.; Paradisi, C.; Zoratti, M.; Biasutto, L. Pharmacokinetics and tissue distribution of pterostilbene in the rat. *Mol. Nutr. Food Res.* **2014**, doi:10.1002/mnfr.201400244.
18. Walle, T. Bioavailability of resveratrol. *Ann. N. Y. Acad. Sci.* **2011**, *1215*, 9–15.
19. Planas, J.M.; Alfaras, I.; Colom, H.; Juan, M.E. The bioavailability and distribution of *trans*-resveratrol are constrained by ABC transporters. *Arch. Biochem. Biophys.* **2012**, *527*, 67–73.
20. Kaldas, M.I.; Walle, U.K.; Walle, T. Resveratrol transport and metabolism by human intestinal Caco-2 cells. *J. Pharm. Pharmacol.* **2003**, *55*, 307–312.
21. Wenzel, E.; Somoza, V. Metabolism and bioavailability of *trans*-resveratrol. *Mol. Nutr. Food Res.* **2005**, *49*, 472–481.
22. Bode, L.M.; Bunzel, D.; Huch, M.; Cho, G.S.; Ruhland, D.; Bunzel, M.; Bub, A.; Franz, C.M.; Kulling, S.E. *In vivo* and *in vitro* metabolism of *trans*-resveratrol by human gut microbiota. *Am. J. Clin. Nutr.* **2013**, *97*, 295–309.
23. Yu, C.; Shin, Y.G.; Chow, A.; Li, Y.; Kosmeder, J.W.; Lee, Y.S.; Hirschelman, W.H.; Pezzuto, J.M.; Mehta, R.G.; van Breemen, R.B. Human, rat, and mouse metabolism of resveratrol. *Pharm. Res.* **2002**, *19*, 1907–1914.
24. Maier-Salamon, A.; Bohmdorfer, M.; Thalhammer, T.; Szekeres, T.; Jaeger, W. Hepatic glucuronidation of resveratrol: Interspecies comparison of enzyme kinetic profiles in human, mouse, rat, and dog. *Drug Metab. Pharmacokinet.* **2011**, *26*, 364–373.
25. Menet, M.C.; Marchal, J.; Dal-Pan, A.; Taghi, M.; Nivet-Antoine, V.; Dargere, D.; Laprevote, O.; Beaudeux, J.L.; Aujard, F.; Epelbaum, J.; *et al.* Resveratrol metabolism in a non-human primate, the grey mouse lemur (Microcebus murinus), using ultra-high-performance liquid chromatography-quadrupole time of flight. *PLoS One* **2014**, *9*, e91932.
26. Dellinger, R.W.; Garcia, A.M.; Meyskens, F.L., Jr. Differences in the glucuronidation of resveratrol and pterostilbene: Altered enzyme specificity and potential gender differences. *Drug Metab. Pharmacokinet.* **2014**, *29*, 112–119.
27. Miksits, M.; Wlcek, K.; Svoboda, M.; Kunert, O.; Haslinger, E.; Thalhammer, T.; Szekeres, T.; Jager, W. Antitumor activity of resveratrol and its sulfated metabolites against human breast cancer cells. *Planta Med.* **2009**, *75*, 1227–1230.
28. Calamini, B.; Ratia, K.; Malkowski, M.G.; Cuendet, M.; Pezzuto, J.M.; Santarsiero, B.D.; Mesecar, A.D. Pleiotropic mechanisms facilitated by resveratrol and its metabolites. *Biochem. J.* **2010**, *429*, 273–282.

29. Hoshino, J.; Park, E.J.; Kondratyuk, T.P.; Marler, L.; Pezzuto, J.M.; van Breemen, R.B.; Mo, S.; Li, Y.; Cushman, M. Selective synthesis and biological evaluation of sulfate-conjugated resveratrol metabolites. *J. Med. Chem.* **2010**, *53*, 5033–5043.
30. Lasa, A.; Churruca, I.; Eseberri, I.; Andres-Lacueva, C.; Portillo, M.P. Delipidating effect of resveratrol metabolites in 3T3-L1 adipocytes. *Mol. Nutr. Food Res.* **2012**, *56*, 1559–1568.
31. Ruotolo, R.; Calani, L.; Fietta, E.; Brighenti, F.; Crozier, A.; Meda, C.; Maggi, A.; Ottonello, S.; Del Rio, D. Anti-estrogenic activity of a human resveratrol metabolite. *Nutr. Metab. Cardiovasc. Dis.* **2013**, *23*, 1086–1092.
32. Aires, V.; Limagne, E.; Cotte, A.K.; Latruffe, N.; Ghiringhelli, F.; Delmas, D. Resveratrol metabolites inhibit human metastatic colon cancer cells progression and synergize with chemotherapeutic drugs to induce cell death. *Mol. Nutr. Food Res.* **2013**, *57*, 1170–1181.
33. Walker, J.; Schueller, K.; Schaefer, L.M.; Pignitter, M.; Esefelder, L.; Somoza, V. Resveratrol and its metabolites inhibit pro-inflammatory effects of lipopolysaccharides in U-937 macrophages in plasma-representative concentrations. *Food Funct.* **2014**, *5*, 74–84.
34. Bresciani, L.; Calani, L.; Bocchi, L.; Delucchi, F.; Savi, M.; Ray, S.; Brighenti, F.; Stilli, D.; Del Rio, D. Bioaccumulation of resveratrol metabolites in myocardial tissue is dose-time dependent and related to cardiac hemodynamics in diabetic rats. *Nutr. Metab. Cardiovasc. Dis.* **2014**, *24*, 408–415.
35. Sharan, S.; Iwuchukwu, O.F.; Canney, D.J.; Zimmerman, C.L.; Nagar, S. *In vivo*-formed *versus* preformed metabolite kinetics of *trans*-resveratrol-3-sulfate and *trans*-resveratrol-3-glucuronide. *Drug Metab. Dispos.* **2012**, *40*, 1993–2001.
36. Patel, K.R.; Andreadi, C.; Britton, R.G.; Horner-Glister, E.; Karmokar, A.; Sale, S.; Brown, V.A.; Brenner, D.E.; Singh, R.; Steward, W.P.; *et al.* Sulfate metabolites provide an intracellular pool for resveratrol generation and induce autophagy with senescence. *Sci. Transl. Med.* **2013**, *5*, 205ra133.
37. Andreadi, C.; Britton, R.G.; Patel, K.R.; Brown, K. Resveratrol-sulfates provide an intracellular reservoir for generation of parent resveratrol, which induces autophagy in cancer cells. *Autophagy* **2014**, *10*, 524–525.
38. Subramanian, L.; Youssef, S.; Bhattacharya, S.; Kenealey, J.; Polans, A.S.; van Ginkel, P.R. Resveratrol: Challenges in translation to the clinic—a critical discussion. *Clin. Cancer Res.* **2010**, *16*, 5942–5948.
39. Moyano-Mendez, J.R.; Fabbrocini, G.; de Stefano, D.; Mazzella, C.; Mayol, L.; Scognamiglio, I.; Carnuccio, R.; Ayala, F.; la Rotonda, M.I.; de Rosa, G. Enhanced antioxidant effect of *trans*-resveratrol: Potential of binary systems with polyethylene glycol and cyclodextrin. *Drug Dev. Ind. Pharm.* **2014**, *40*, 1300–1307.
40. Ansari, K.A.; Vavia, P.R.; Trotta, F.; Cavalli, R. Cyclodextrin-based nanosponges for delivery of resveratrol: *In vitro* characterisation, stability, cytotoxicity and permeation study. *AAPS PharmSciTech* **2011**, *12*, 279–286.
41. Lee, M.H.; Kao, L.; Lin, C.C. Comparison of the antioxidant and transmembrane permeative activities of the different Polygonum cuspidatum extracts in phospholipid-based microemulsions. *J. Agric. Food Chem.* **2011**, *59*, 9135–9141.

42. Sessa, M.; Tsao, R.; Liu, R.; Ferrari, G.; Donsi, F. Evaluation of the stability and antioxidant activity of nanoencapsulated resveratrol during *in vitro* digestion. *J. Agric. Food Chem.* **2011**, *59*, 12352–12360.
43. Hung, C.F.; Chen, J.K.; Liao, M.H.; Lo, H.M.; Fang, J.Y. Development and evaluation of emulsion-liposome blends for resveratrol delivery. *J. Nanosci. Nanotechnol.* **2006**, *6*, 2950–2958.
44. Kobierski, S.; Ofori-Kwakye, K.; Muller, R.H.; Keck, C.M. Resveratrol nanosuspensions: Interaction of preservatives with nanocrystal production. *Pharmazie* **2011**, *66*, 942–947.
45. Stammet, M.; Kwon, G.S.; Rao, D.A. Drug loading in Pluronic(R) micelles made by solvent casting and equilibrium methods using resveratrol as a model drug. *J. Control. Release* **2010**, *148*, e50–e51.
46. Lu, X.; Ji, C.; Xu, H.; Li, X.; Ding, H.; Ye, M.; Zhu, Z.; Ding, D.; Jiang, X.; Ding, X.; *et al.* Resveratrol-loaded polymeric micelles protect cells from Abeta-induced oxidative stress. *Int. J. Pharm.* **2009**, *375*, 89–96.
47. Kristl, J.; Teskac, K.; Caddeo, C.; Abramovic, Z.; Sentjurc, M. Improvements of cellular stress response on resveratrol in liposomes. *Eur. J. Pharm. Biopharm.* **2009**, *73*, 253–259.
48. Neves, A.R.; Lucio, M.; Martins, S.; Lima, J.L.; Reis, S. Novel resveratrol nanodelivery systems based on lipid nanoparticles to enhance its oral bioavailability. *Int. J. Nanomedicine* **2013**, *8*, 177–187.
49. Figueiro, F.; Bernardi, A.; Frozza, R.L.; Terroso, T.; Zanotto-Filho, A.; Jandrey, E.H.; Moreira, J.C.; Salbego, C.G.; Edelweiss, M.I.; Pohlmann, A.R.; *et al.* Resveratrol-loaded lipid-core nanocapsules treatment reduces *in vitro* and *in vivo* glioma growth. *J. Biomed. Nanotechnol.* **2013**, *9*, 516–526.
50. Cadena, P.G.; Pereira, M.A.; Cordeiro, R.B.; Cavalcanti, I.M.; Barros Neto, B.; Pimentel, M.C.C.B.; José Luiz Lima Filho; Silva, V.L.; Santos-Magalhaes, N.S. Nanoencapsulation of quercetin and resveratrol into elastic liposomes. *Biochim. Biophys. Acta* **2013**, *1828*, 309–316.
51. Sih, J.; Bansal, S.S.; Filippini, S.; Ferrati, S.; Raghuwansi, K.; Zabre, E.; Nicolov, E.; Fine, D.; Ferrari, M.; Palapattu, G.; *et al.* Characterization of nanochannel delivery membrane systems for the sustained release of resveratrol and atorvastatin: New perspectives on promoting heart health. *Anal. Bioanal. Chem.* **2013**, *405*, 1547–1557.
52. Shao, J.; Li, X.; Lu, X.; Jiang, C.; Hu, Y.; Li, Q.; You, Y.; Fu, Z. Enhanced growth inhibition effect of resveratrol incorporated into biodegradable nanoparticles against glioma cells is mediated by the induction of intracellular reactive oxygen species levels. *Colloids Surf. B Biointerfaces* **2009**, *72*, 40–47.
53. Frozza, R.L.; Bernardi, A.; Paese, K.; Hoppe, J.B.; da Silva, T.; Battastini, A.M.; Pohlmann, A.R.; Guterres, S.S.; Salbego, C. Characterization of *trans*-resveratrol-loaded lipid-core nanocapsules and tissue distribution studies in rats. *J. Biomed. Nanotechnol.* **2010**, *6*, 694–703.
54. Teskac, K.; Kristl, J. The evidence for solid lipid nanoparticles mediated cell uptake of resveratrol. *Int. J. Pharm.* **2010**, *390*, 61–69.
55. Gokce, E.H.; Korkmaz, E.; Dellera, E.; Sandri, G.; Bonferoni, M.C.; Ozer, O. Resveratrol-loaded solid lipid nanoparticles *versus* nanostructured lipid carriers: Evaluation of antioxidant potential for dermal applications. *Int. J. Nanomedicine* **2012**, *7*, 1841–1850.
56. Sanna, V.; Roggio, A.M.; Siliani, S.; Piccinini, M.; Marceddu, S.; Mariani, A.; Sechi, M. Development of novel cationic chitosan-and anionic alginate-coated poly(D,L-lactide-co-

glycolide) nanoparticles for controlled release and light protection of resveratrol. *Int. J. Nanomedicine* **2012**, *7*, 5501–5516.

57. Lu, X.; Xu, H.; Sun, B.; Zhu, Z.; Zheng, D.; Li, X. Enhanced neuroprotective effects of resveratrol delivered by nanoparticles on hydrogen peroxide-induced oxidative stress in rat cortical cell culture. *Mol. Pharm.* **2013**, *10*, 2045–2053.
58. Lee, C.W.; Yen, F.L.; Huang, H.W.; Wu, T.H.; Ko, H.H.; Tzeng, W.S.; Lin, C.C. Resveratrol nanoparticle system improves dissolution properties and enhances the hepatoprotective effect of resveratrol through antioxidant and anti-inflammatory pathways. *J. Agric. Food Chem.* **2012**, *60*, 4662–4671.
59. Tsai, C.H.; Vivero-Escoto, J.L.; Slowing, II; Fang, I.J.; Trewyn, B.G.; Lin, V.S. Surfactant-assisted controlled release of hydrophobic drugs using anionic surfactant templated mesoporous silica nanoparticles. *Biomaterials* **2011**, *32*, 6234–6244.
60. Bu, L.; Gan, L.C.; Guo, X.Q.; Chen, F.Z.; Song, Q.; Qi, Z.; Gou, X.J.; Hou, S.X.; Yao, Q. *Trans*-resveratrol loaded chitosan nanoparticles modified with biotin and avidin to target hepatic carcinoma. *Int. J. Pharm.* **2013**, *452*, 355–362.
61. Guo, L.; Peng, Y.; Yao, J.; Sui, L.; Gu, A.; Wang, J. Anticancer activity and molecular mechanism of resveratrol-bovine serum albumin nanoparticles on subcutaneously implanted human primary ovarian carcinoma cells in nude mice. *Cancer Biother. Radiopharm.* **2010**, *25*, 471–477.
62. Biasutto, L.; Zoratti, M. Prodrugs of quercetin and resveratrol: A strategy under development. *Current drug metabolism* **2014**, *15*, 77–95.
63. Biasutto, L.; Mattarei, A.; Sassi, N.; Azzolini, M.; Romio, M.; Paradisi, C.; Zoratti, M. Improving the efficacy of plant polyphenols. *Anticancer Agents Med. Chem.* **2014**, doi: 10.2174/1871520614666140627150054.
64. Nagamura, S.; Kanda, Y.; Kobayashi, E.; Gomi, K.; Saito, H. Synthesis and antitumor activity of duocarmycin derivatives. *Chem. Pharm. Bull. (Tokyo)* **1995**, *43*, 1530–1535.
65. Senter, P.D.; Beam, K.S.; Mixan, B.; Wahl, A.F. Identification and activities of human carboxylesterases for the activation of CPT-11, a clinically approved anticancer drug. *Bioconjug. Chem.* **2001**, *12*, 1074–1080.
66. Savolainen, J.; Leppanen, J.; Forsberg, M.; Taipale, H.; Nevalainen, T.; Huuskonen, J.; Gynther, J.; Mannisto, P.T.; Jarvinen, T. Synthesis and *in vitro*/*in vivo* evaluation of novel oral *N*-alkyl- and *N,N*-dialkyl-carbamate esters of entacapone. *Life Sci.* **2000**, *67*, 205–216.
67. Thorberg, S.O.; Berg, S.; Lundstrom, J.; Pettersson, B.; Wijkstrom, A.; Sanchez, D.; Lindberg, P.; Nilsson, J.L. Carbamate ester derivatives as potential prodrugs of the presynaptic dopamine autoreceptor agonist (−)-3-(3-hydroxyphenyl)-N-propylpiperidine. *J. Med. Chem.* **1987**, *30*, 2008–2012.
68. Gee, J.M.; DuPont, M.S.; Day, A.J.; Plumb, G.W.; Williamson, G.; Johnson, I.T. Intestinal transport of quercetin glycosides in rats involves both deglycosylation and interaction with the hexose transport pathway. *J. Nutr.* **2000**, *130*, 2765–2771.
69. Cermak, R.; Landgraf, S.; Wolffram, S. Quercetin glucosides inhibit glucose uptake into brush-border-membrane vesicles of porcine jejunum. *Br. J. Nutr.* **2004**, *91*, 849–855.
70. Harris, J.M.; Chess, R.B. Effect of pegylation on pharmaceuticals. *Nat. Rev. Drug Discov.* **2003**, *2*, 214–221.

71. Veronese, F.M.; Pasut, G. PEGylation, successful approach to drug delivery. *Drug Discov. Today* **2005**, *10*, 1451–1458.
72. Veronese, F.M.; Mero, A. The impact of PEGylation on biological therapies. *BioDrugs* **2008**, *22*, 315–329.
73. Ryan, S.M.; Mantovani, G.; Wang, X.; Haddleton, D.M.; Brayden, D.J. Advances in PEGylation of important biotech molecules: Delivery aspects. *Expert Opin. Drug Del.* **2008**, *5*, 371–383.
74. Hamidi, M.; Azadi, A.; Rafiei, P. Pharmacokinetic consequences of pegylation. *Drug Deliv.* **2006**, *13*, 399–409.
75. Das, S.; Lin, H.S.; Ho, P.C.; Ng, K.Y. The impact of aqueous solubility and dose on the pharmacokinetic profiles of resveratrol. *Pharm. Res.* **2008**, *25*, 2593–2600.
76. Camont, L.; Cottart, C.H.; Rhayem, Y.; Nivet-Antoine, V.; Djelidi, R.; Collin, F.; Beaudeux, J.L.; Bonnefont-Rousselot, D. Simple spectrophotometric assessment of the *trans*-/*cis*-resveratrol ratio in aqueous solutions. *Anal. Chim. Acta* **2009**, *634*, 121–128.
77. Bertacche, V.; Lorenzi, N.; Nava, D.; Pini, E.; Sinico, C. Host-Guest interaction study of resveratrol with natural and modified cyclodextrins. *J. Incl. Phenom. Macrocycl. Chem.* **2006**, *55*, 279–287.
78. Mattarei, A.; Azzolini, M.; Carraro, M.; Sassi, N.; Zoratti, M.; Paradisi, C.; Biasutto, L. Acetal derivatives as prodrugs of resveratrol. *Mol. Pharm.* **2013**, *10*, 2781–2792.
79. Biasutto, L.; Marotta, E.; Mattarei, A.; Beltramello, S.; Caliceti, P.; Salmaso, S.; Bernkop-Schnurch, A.; Garbisa, S.; Zoratti, M.; Paradisi, C. Absorption and metabolism of resveratrol carboxyesters and methanesulfonate by explanted rat intestinal segments. *Cell. Physiol. Biochem.* **2009**, *24*, 557–566.
80. Gouyon, F.; Caillaud, L.; Carriere, V.; Klein, C.; Dalet, V.; Citadelle, D.; Kellett, G.L.; Thorens, B.; Leturque, A.; Brot-Laroche, E. Simple-sugar meals target GLUT2 at enterocyte apical membranes to improve sugar absorption: A study in GLUT2-null mice. *J. Physiol.* **2003**, *552*, 823–832.
81. Kellett, G.L.; Brot-Laroche, E. Apical GLUT2: A major pathway of intestinal sugar absorption. *Diabetes* **2005**, *54*, 3056–3062.
82. Helliwell, P.A.; Richardson, M.; Affleck, J.; Kellett, G.L. Stimulation of fructose transport across the intestinal brush-border membrane by PMA is mediated by GLUT2 and dynamically regulated by protein kinase C. *Biochem. J.* **2000**, *350*, 149–154.
83. Tamai, I. Oral drug delivery utilizing intestinal OATP transporters. *Adv. Drug Deliv. Rev.* **2012**, *64*, 508–514.
84. Tamai, I.; Nakanishi, T. OATP transporter-mediated drug absorption and interaction. *Curr. Opin. Pharmacol.* **2013**, *13*, 859–863.
85. Shitara, Y.; Maeda, K.; Ikejiri, K.; Yoshida, K.; Horie, T.; Sugiyama, Y. Clinical significance of organic anion transporting polypeptides (OATPs) in drug disposition: Their roles in hepatic clearance and intestinal absorption. *Biopharm. Drug Dispos.* **2013**, *34*, 45–78.
86. Riha, J.; Brenner, S.; Bohmdorfer, M.; Giessrigl, B.; Pignitter, M.; Schueller, K.; Thalhammer, T.; Stieger, B.; Somoza, V.; Szekeres, T.; *et al.* Resveratrol and its major sulfated conjugates are substrates of organic anion transporting polypeptides (OATPs): Impact on growth of ZR-75–1 breast cancer cells. *Mol. Nutr. Food Res.* **2014**, *58*, 1830–1842.
87. Pochini, L.; Scalise, M.; Galluccio, M.; Indiveri, C. OCTN cation transporters in health and disease: Role as drug targets and assay development. *J. Biomol. Screen.* **2013**, *18*, 851–867.

88. Tamai, I. Pharmacological and pathophysiological roles of carnitine/organic cation transporters (OCTNs: SLC22A4, SLC22A5 and Slc22a21). *Biopharm. Drug Dispos.* **2013**, *34*, 29–44.
89. Vacondio, F.; Silva, C.; Mor, M.; Testa, B. Qualitative structure-metabolism relationships in the hydrolysis of carbamates. *Drug Metab. Rev.* **2010**, *42*, 551–589.
90. Biasutto, L.; Marotta, E.; Garbisa, S.; Zoratti, M.; Paradisi, C. Determination of quercetin and resveratrol in whole blood—implications for bioavailability studies. *Molecules* **2010**, *15*, 6570–6579.

Sample Availability: Samples of the compounds **2** and **3** are available from the authors.

3. N-monosubstituted carbamate ester derivatives of resveratrol

Abstract:

Resveratrol (3, 5, 4'-trihydroxy-*trans*-stilbene) has demonstrated several biological activities, but its pharmacological exploitation *in vivo* is hindered by its rapid elimination via phase II conjugative metabolism at the intestinal level and, most importantly, in the liver. One approach to bypass this problem relies on prodrugs. We report here the synthesis, characterization, stability and *in vivo* pharmacokinetic behavior of 7 prodrugs of resveratrol, in which the OH groups are engaged in an N-monosubstituted carbamate ester (-OC(O)NHR) linkage. The purpose was to modulate the physicochemical properties and promote the absorption of the parent compound. Each -NHR group derived from the corresponding amine RNH_2, selected from methoxyoligoethylene glycol amines and natural amino acids.

We report also a convenient, mild-conditions, high-yield protocol for the synthesis of 3,4',5-trisubstituted-resveratrol N-monosubstituted carbamate esters involving the synthesis and isolation of activated 4-nitrophenyl urethanes followed by transesterification with resveratrol. The N-monosubstituted carbamate ester linkage showed good stability under acidic conditions, while it underwent slow hydrolysis at physiological pH and in whole blood. After administration of carbamate ester-based prodrugs to rats by oral gavage, only the methoxyoligoethylene glycol amines- and isoleucine-containing prodrugs were absorbed, reaching the circulation as non-metabolized and partially hydrolyzed species.

The results suggest that prodrugs of resveratrol based on the carbamate ester bond have the appropriate stability profile to be a convenient tool for the systemic delivery of the unconjugated parent compound. The choice of promoiety linked to the nitrogen atom in the carbamate linkage is a key factor in modulating the properties of the prodrug (i.e., water solubility, LogP, chemical and enzymatic stability, absorbtion through biomembranes (or via transporters)). Tri-substituted derivatives of Rv may however be too bulky to be efficiently absorbed by the intestine.

Introduction:

Resveratrol (trans-3,5,4'-trihydroxystilbene), is a naturally occurring phytoalexin produced by plants in response to fungal, bacterial or viral infection or abiotic stresses, such as heavy metal ions or ultraviolet light (UV).[1]

A large number of studies have identified a range of activities of biomedical interest for this compound, including lifespan extension in model systems,[2] protection of the cardiovascular apparatus,[3-6] anti-inflammatory activity,[3] improvement of glucose handling in diabetes,[7, 8] decrease of fat and cholesterol load,[9-12] improvements of functionality in aging,[2, 13-15] neuroprotection,[16] cancer chemoprevention[17, 18] and potentiation of chemotherapy.[19, 20]
The efficacy of orally administered resveratrol depends on its absorption, metabolism, and tissue distribution. Clinical studies with humans reported mostly small effects, and sometimes controversial results.[21, 22] Beneficial effects *in vivo* are in fact limited by low bioavailability. Thus, for example, only trace amounts (below 5 ng/mL, i.e., 0.022 μM) of intact resveratrol could be detected in blood after administration of a 25 mg oral dose to human volunteers.[23] Even when a very large dose (2.5 g - 5.0 g) was administered, circulating levels of non-metabolized resveratrol were so low as to be considered insufficient for any bioactivity.[24] Resveratrol, like other polyphenols, is rapidly converted to phase II metabolites (mainly glucuronides and sulfates) during absorption and first pass through the liver. These hydrophilic metabolites are re-exported to the intestinal lumen by enterocyte ABC transporters, and/or rapidly excreted with feces and urine.[24, 25] Nonetheless, they represent the vast majority of resveratrol-derived species in the body and their bioactivities are now under investigation to verify whether they may account for resveratrol's effects. The available data suggest that a level of activity may well be maintained in specific contexts (e.g.[26-29]), but conjugation often determines at least a partial loss of bioefficacy.[30-35] Retention of bioactivity *in vivo* may be due in part to the metabolites acting as a temporary reservoir from which the more active species may be regenerated through the activity of enzymes such as glucuronidases and sulfatases.[36, 37] While investigation of these aspects continues, a reduction or delay of phase II metabolism would allow progress in the exploitation of resveratrol for biomedical purposes.

One of the strategies used to prevent drug metabolism and enhance bioavailability and effectiveness is based on prodrugs: the sites undergoing phase II conjugation (in this case the phenolic hydroxyls) are temporarily protected by removable groups during absorption, first pass through the liver and distribution. This approach is expected to increase circulating levels of non-metabolized species, with final regeneration of resveratrol, thanks to the removal of protective groups by chemical and/or enzyme-catalyzed hydrolysis.

The carbamoyl moiety provides a promising and versatile protecting group for phenols.[38, 39] It is also suitable for fine-tuning the properties of the molecule, since the nitrogen atom can carry one or two substituents which can be used to modulate the stability and physicochemical properties of the resulting prodrug. Many prodrugs have been developed to improve oral bioavailability of phenolic compounds[40-42] but surprisingly there are only few examples of carbamate ester prodrugs of polyphenols. Mulholland *et al.*[43] reported the synthesis and evaluation of a water-soluble glycine N-monosubstituted carbamate ester prodrug (QC12) of the natural occurring flavonoid quercetin. The advantage of QC12 was its high aqueous solubility compared to that of quercetin, eliminating the need for formulation in DMSO. Quercetin conjugates with amino acids, linked through the N-monosubstituted carbamate ester, were also synthesized by Kim *et al.,*[44] and showed remarkable increases in water solubility, stability, and cell permeability compared with the parent polyphenol.

We report here the synthesis of a series of resveratrol prodrugs, consisting of methoxyoligoethylene glycol amines and natural amino acids attached to the resveratrol phenolic functions via the N-monosubstituted carbamate linkage (scheme 1).

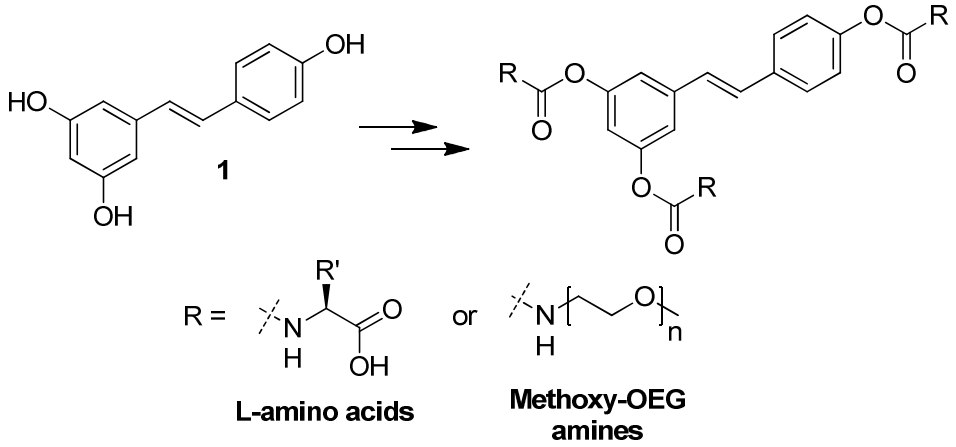

Scheme 1. Molecular structure of resveratrol (trans-3,5,4'-trihydroxy stilbene) and its carbamate esters.

Short methoxyoligoethylene glycol chains were previously shown to be very useful in modulating physicochemical and absorption properties of derivatives, maintaining many properties of longer PEG chains with a more favorable drug loading capacity.[45] Among all possible amino acid substituents, Leu, Ile and Phe were chosen because they are LAT1 substrates with affinities in the µM range; aminoacid transporters LAT1 and LAT2 have been previously exploited for the transport/absorption of drugs, and they are especially useful for the permeation of the blood brain barrier.[46-48] Threonine was used as "control".

Pharmacokinetic studies were then performed in rats, in order to evaluate *in vivo* absorption, stability and metabolism of these new prodrugs.

Experimental protocols:

Materials and instrumentation. Resveratrol was purchased from Waseta Int. Trading Co. (Shangai, P.R.China). Other starting materials and reagents were purchased from Aldrich, Fluka, Merck-Novabiochem, Riedel de Haen, J.T. Baker, Cambridge Isotope Laboratories Inc., Acros Organics, Carlo Erba and Prolabo, and were used as received. TLCs were run on silica gel supported on plastic (Macherey-Nagel Polygram® SIL G/UV_{254}, silica thickness 0.2 mm) and visualized by UV detection. Flash chromatography was performed on silica gel (Macherey-Nagel 60, 230-400 mesh granulometry (0.063-0.040 mm)) under air pressure. The solvents were analytical or synthetic grade and were used without further purification. ^{1}H NMR spectra were recorded with a Bruker AC250F spectrometer operating at 250 MHz and a Bruker AVII500 spectrometer operating at 500 MHz. Chemical shifts (δ) are given in ppm relative to the signal of the solvent. HPLC-UV analyses were performed with an Agilent 1290 Infinity LC System (Agilent Technologies), equipped with binary pump and a diode array detector (190-500 nm). HPLC/ESI-MS analyses and mass spectra were performed with a 1100 Series Agilent Technologies system, equipped with binary pump (G1312A) and MSD SL Trap mass spectrometer (G2445D SL) with ESI source. ESI-MS positive spectra of reaction intermediates and final purified products were obtained from solutions in acetonitrile, eluting with a water:acetonitrile, 1:1 mixture containing 0.1% formic acid. All experiments reported were performed in triplicate unless otherwise stated, and means ± standard deviation values are reported.

Stability assays:

Stability under physiological-like conditions. The chemical stability of all new compounds was tested in aqueous media imitating gastric (0.1 N HCl, NormaFix) and intestinal (0.1 M PBS buffer, pH 6.8) conditions. A 5 µM solution of the compound was prepared from a 5 mM stock solution in DMSO, and incubated at 37°C for 24 hours; samples withdrawn at different times were analysed by HPLC-UV. Hydrolysis products were identified by HPLC/ESI-MS analysis of selected samples. Stability of compounds **5e** and **7d** was also studied in 0.1 M PBS buffer, pH 7.4 in the absence or in the presence of 35 mg/ml HSA. Samples withdrawn at different time points (0, 10 and 30 min; 1, 2, and 4 h) were deproteinized adding 1 vol of acetone, and the supernatants obtained after centrifugation (12,000 *g*, 7 min, 4°C) were analysed by HPLC-UV.

Non-linear curve fitting was performed using Origin 8.0 data analysis software, using the equations described in [45, 49].

Stability in murine whole blood. Rats were anesthetised and blood was withdrawn from the jugular vein, heparinised and transferred into tubes containing EDTA. Blood samples (1 mL) were spiked with 5 µM compound (dilution from a 5 mM stock solution in DMSO), and incubated at 37°C for 4 hours (the maximum period allowed by blood stability). Aliquots were taken after 10 min, 30 min, 1 h, 2 h and 4 h and treated as described below

(blood sample treatment and analysis). Cleared blood samples were finally subjected to HPLC-UV analysis.

Blood sample treatment and analysis. Before starting the treatment, 4,4'-dihydroxybiphenyl was added as internal standard to a carefully measured blood volume (25 µM final concentration). Blood was then stabilized with a freshly-prepared 10 mM solution of ascorbic acid (0.1 vol) and acidified with 0.6 M acetic acid (0.1 vol); after mixing, an excess of acetone (4 vol) was added, followed by sonication (2 min) and centrifugation (12,000 g, 7 min, 4°C). The supernatant was finally collected and stored at -20°C. Before analysis, acetone was allowed to evaporate at room temperature using a Univapo 150H (UniEquip) vacuum concentrator centrifuge, and up to 40 µL of CH_3CN were added to precipitate residual proteins. After centrifugation (12,000 g, 5 min, 4°C), cleared samples were directly subjected to HPLC-UV analysis. An alternative treatment was used for the aminoacid derivatives to achieve acceptable recovery yields: 0.1 vol of 0.6 M TEA (pH 8.0) and 4 vol of methanol were added to blood samples (previously spiked with the internal standard), then sonicated (2 min) and centrifuged (12,000 g, 7 min, 4°C). The supernatant was finally collected and stored at -20°C. Before analysis, methanol was allowed to evaporate at room temperature using a Univapo 150H (UniEquip) vacuum concentrator centrifuge, and up to 40 µL of CH_3CN were added to precipitate residual proteins. After centrifugation (12,000 g, 5 min, 4°C), cleared samples were directly subjected to HPLC-UV analysis. Metabolites and hydrolysis products were identified by comparison of chromatographic retention time with true samples.

The recovery yields of resveratrol and its metabolites have been reported previously.[50, 51] Internal standard recovery from the two different treatments used to extract OEG- or AA-derivatives was 68.7 ± 6.3%[45] and 91.8 ± 10.7%, respectively. For the new prodrugs the corresponding recoveries, expressed as ratio to the recovery of internal standard, were as follows: **7d**: 0.903 ± 0.104; **8d**: 0.967 ± 0.100; **3e**: 0.633 ± 0.088. Recoveries of partially protected (disubstituted) derivatives were assumed to be the same as those of the corresponding fully substituted prodrug. Knowledge of these ratios allowed us to determine the unknown amount of analyte in a blood sample by measuring the recovery of the internal standard.[52]

Since sample treatment includes an evaporation/concentration step, and there are no interfering peaks from the tissue matrix, LOD and LOQ were determined relatively to the analytical part of the method (HPLC/UV analysis). The derivatives showed the same absorption coefficient of resveratrol itself; LOD and LOQ were thus the same of resveratrol (i.e., 0.04 and 0.12 M, respectively; [50]), and quantification of the analytes in blood samples was done using the same calibration curve of resveratrol (y = 5.3085 x), taking into account the recovery ratio of each analyte to that of the internal standard.[52]

Pharmacokinetics studies. Derivatives **2e-5e** and **6d-8d** were administered to overnight-fasted male Wistar rats from the facility of the Department of Biomedical Sciences, University of Padova, as a single intragastric dose (88 µmol/Kg, dissolved in 250 µl DMSO).

Blood samples were obtained by the tail bleeding technique: before drug administration, rats were anesthetised with isoflurane and the tip of the tail was cut off; blood samples (80-100 µL each) were then taken from the tail tip at different time points after drug administration. Blood was collected in heparinised tubes, kept in ice and treated as described above within 10 min. The AUC values were calculated using the trapezoidal rule. All experiments involving animals were performed with the permission and supervision of the University of Padova Ethical Committee for Experimentation on Animals (CEASA) and Central Veterinary Service, in compliance with Italian Law DL 116/92, embodying UE Directive 86/609.

Statistics. Significance in comparisons was assessed using the Wilcoxon Rank Test.

Results and discussion:

Chemistry (Prof. C. Paradisi's group):

Scheme 2 presents the structures of all resveratrol carbamate esters (-OC(O)NHR) synthesized in this piece of work. Different R groups were selected, with the aim of modulating and optimizing the physicochemical properties of the derivative (see below, Section 3.3). Each -NHR group derives from the corresponding methoxyoligoethylene glycol amine (RNH_2), with 3 (**6d**), 4 (**7d**) and 6 (**8d**) monomeric units or from a natural amino acid (leucine (**2e**), isoleucine (**3e**), threonine (**4e**), phenylalanine (**5e**)).

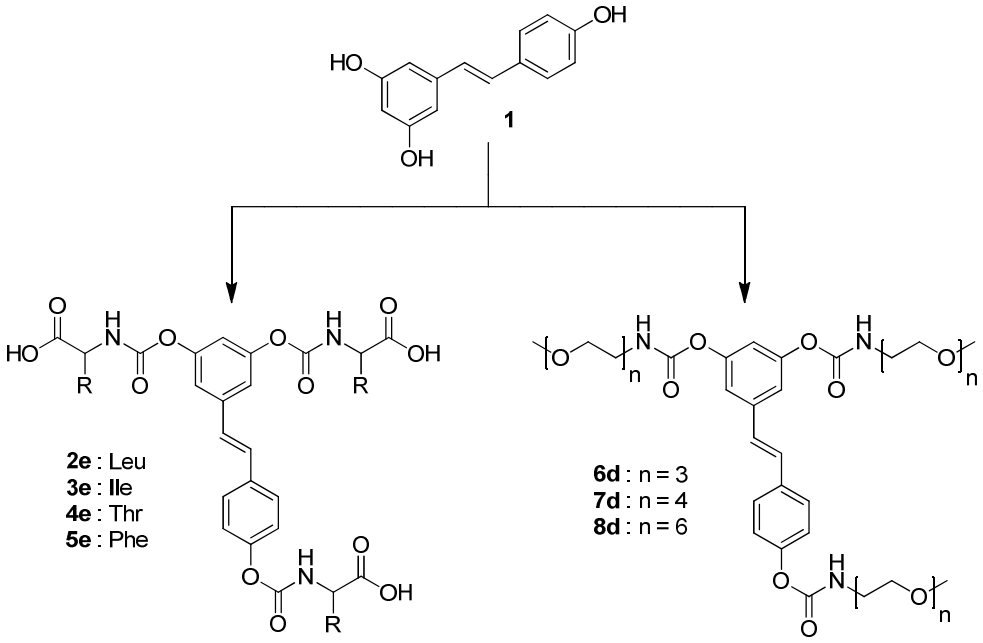

Scheme 2. Chemical structure of resveratrol and synthetic resveratrol carbamate ester prodrugs

Synthesis of N-monosubstituted carbamate esters is usually carried out in two steps: reaction of the desired primary amine with phosgene or its equivalent to give a reactive isocyanate derivative, followed by its coupling with the phenolic function.[53] These

procedures tested on resveratrol led to low yields for the trisubstituted derivatives, probably due to the high reactivity of the isocyanate group promoting side reactions of polymerization entraining the stilbene double bond function. In this study we prepared N-monosubstituted resveratrol carbamate esters through conversion of the corresponding primary amines (**2**-**8**) to the activated 4-nitrophenyl carbamates (scheme 3).

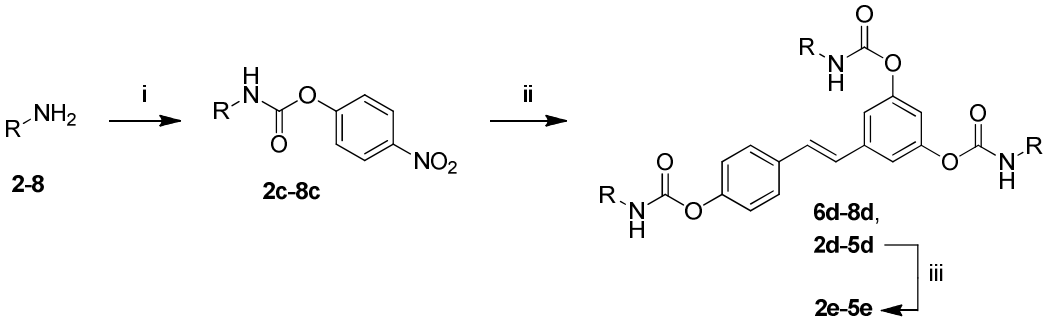

Scheme 3. Synthesis of resveratrol N-monosubstituted carbamate ester prodrugs.
Reagents and conditions: (i) bis(4-nitrophenyl) carbonate, DMAP, ACN, 50 °C, 3 h; (ii) Resveratrol, DMAP, ACN, 50 °C, 24 h; (iii) TFA, DCM, TIPS, from 0 °C to RT., overnight.

Isolation of the activated 4-nitrophenyl carbamate esters (**2c**-**8c**) followed by transesterification with resveratrol provided the desired N-methoxyoligoethylen glycol (**6d**-**8d**) derivatives as well as the t-butyl ether-protected resveratrol-amino acid carbamate ester conjugates (**2d**-**5d**) in good to excellent yields under mild conditions. Amino acids attached to the resveratrol phenolic functions via the N-monosubstituted carbamate ester linkage (**2e**-**5e**) were obtained by removal of the tert-butyl protecting group by treatment with TFA (**iii** in scheme 3).

Methoxyoligoethylene glycol amines (**6**-**8**) (reagents for the synthesis of **6d**-**8d**) were synthesized under mild conditions and with high yields by Staudinger reduction of the corresponding methoxyoligoethylene glycol azides, in turn obtained by substitution of the tosylate function with sodium azide (scheme 4).

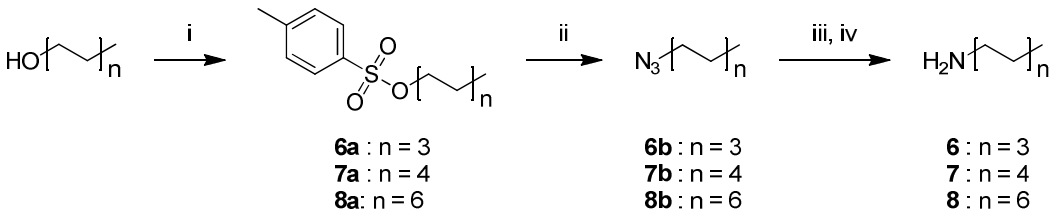

Scheme 4: Synthesis of methoxyoligoethylene glycol amines.
Reagents and conditions: (i) TsCl, Pyridine, DMAP, DCM, from 0 °C to RT., 6 h; (ii) NaN_3, water/acetone (1:3), 75 °C, overnight; (iii) PPh_3, THF, RT, 5 h; (iv) Water, 80 °C, overnight.

Hydrolysis studies:

We previously reported that N,N-disubstituted carbamoyl derivatives are too stable under physiological conditions to be used as prodrugs.[54] In this work, we thus synthesized

N-monosubstituted carbamoyl derivatives, and assessed their hydrolytic reactivity in solutions mimicking gastric and intestinal pH and in blood.

All the tested derivatives turned out to be stable at pH values close to that of the human stomach (no reaction over 24 hours at 37°C in 0.1 N HCl), but underwent hydrolysis at near-neutral pH (pH 6.8, representing intestinal pH) and in blood, with kinetics that may be suitable for use *in vivo*.

Kinetic analysis of the data was performed by assuming that hydrolysis to resveratrol occurred via consecutive loss of the three protecting groups in pseudo-first order processes and by considering each pair of isomeric intermediates (potentially) resulting from the first and second hydrolysis steps as a single species, i.e. the two monosubstituted and the two disubstituted intermediates were handled as species B and C, respectively (scheme 5).

$$A \xrightarrow{k_1} B \xrightarrow{k_2} C \xrightarrow{k_3} D$$

A: trisubstituted resveratrol derivative

B: disubstituted resveratrol derivatives

C: monosubstituted resveratrol derivatives

D: resveratrol

k_1, k_2, k_3: observed pseudo-first order rate constants

Scheme 5. Kinetic scheme for hydrolysis of **2e**-**5e** and **6d**-**8d**

Figure 1 shows, as an example, the time course of the four species (A, B, C and D) involved in the case of derivative **6d** (incorporating methoxytriethylene glycol amine) and the fit of the experimental data obtained using a set of equations analogous to those utilized by Kozerski *et al.*[49] and in our previous work.[45]

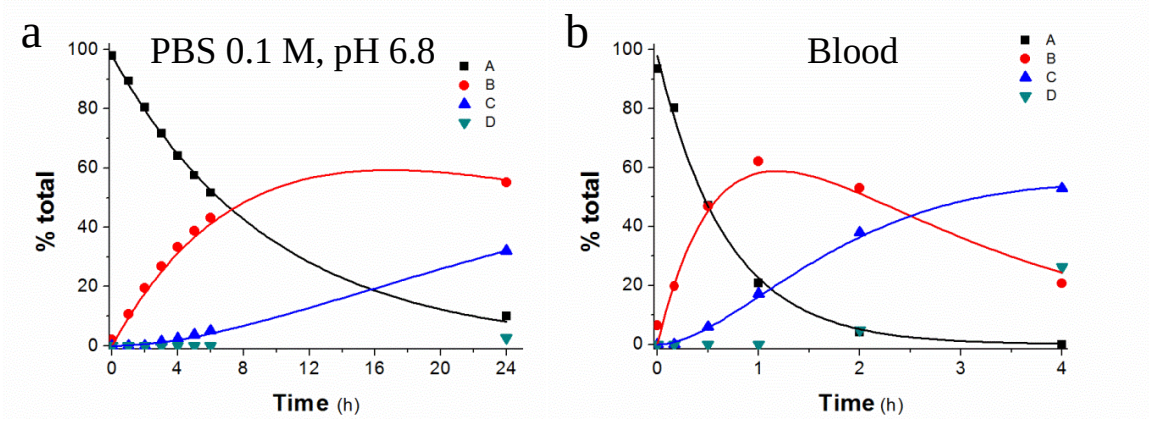

Figure 1. Kinetics of the hydrolysis of derivative **6d** in PBS 0.1 M, pH 6.8, 37°C (**a**) and in rat blood (**b**). Data from a single representative experiment. Kinetic fit of the experimental data (i.e., time profiles of derivative **6d** and its hydrolysis products), according to scheme 5.

Derivative	PBS 0.1 M, pH 6.8, 37°C				Blood			
	$t_{1/2}$ (h)	k_1 (h^{-1})	k_2 (h^{-1})	k_3 (h^{-1})	$t_{1/2}$ (h)	k_1 (h^{-1})	k_2 (h^{-1})	k_3 (h^{-1})
6d	6	0,104 ± 0,002	0,030 ± 0,002	0,005 ± 0,002	0,5	1,47 ± 0,07	0,43 ± 0,04	0,155 ± 0,009
7d	3,5	0,134 ± 0,007	0,042 ± 0,005	0,007 ± 0,003	0,3	2,0 ± 0,2	0,42 ± 0,06	0,17 ± 0,03
8d	4,5	0,158 ± 0,002	0,0510 ± 0,0006	0,0250 ± 0,0002	0,5	1,25 ± 0,08	0,48 ± 0,05	0,22 ± 0,03
5e	17	0,0425 ± 0,0002	0,0136 ± 0,0004	0,002 ± 0,001	0,3	1,86 ± 0,06	0,056 ± 0,007	0,09 ± 0,02
4e	15	0,0530 ± 0,0008	0,014 ± 0,001	0,006 ± 0,001	0,17	3,9 ± 0,2	0,057 ± 0,006	0,45 ± 0,09
3e	> 24	0,0221 ± 0,0002	0,004 ± 0,004	*	1	0,63 ± 0,04	0,12 ± 0,03	0,4 ± 0,1
2e	> 24	0,0198 ± 0,0003	0,009 ± 0,002	*	1	0,57 ± 0,06	ND[#]	ND[#]

*: k_3 not calculated; monosubstituted derivative detected only at the latest time point

[#]: k_2 and k_3 not determined because of co-elution of di- and mono-substituted derivatives with matrix background interfering peaks

Table 1. Observed pseudo first-order rate constants for the hydrolysis of resveratrol derivatives **2e-5e** and **6d-8d** in PBS 0.1M, pH 6.8, 37°C and in rat blood. Values ± standard error are reported as obtained from the fit of all the available data.

The full set of kinetic constants resulting from fits of this type is presented in table 1 and in fig 2.

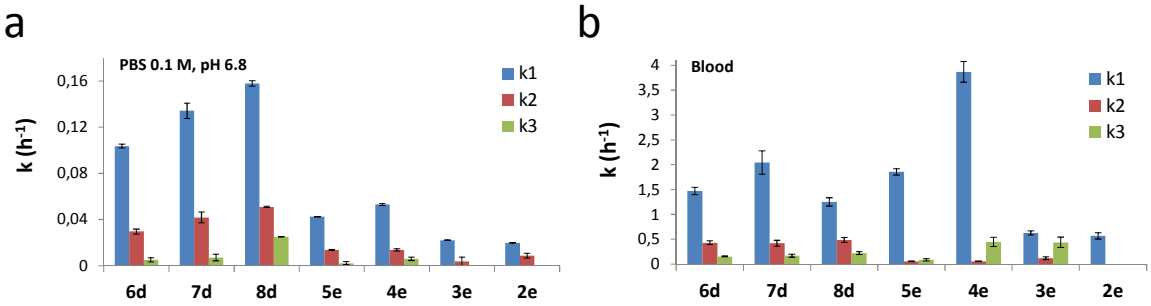

Figure 2. Observed pseudo first-order rate constants for the hydrolysis of resveratrol derivatives **2e-5e** and **6d-8d** in PBS 0.1M, pH 6.8, 37°C (**a**) and in rat blood (**b**). Values ± standard error are reported as obtained from the fit of all the available data.

Interestingly, the first hydrolysis rate constants of the methoxyoligoethylene glycol derivatives (**6d**-**8d**) in PBS were considerably higher than those of the amino acid derivatives. Within the N-Oligo Ethylene Glycol group, the rates increased slightly as the length of the chain increased.

The stability of the carbamate group in acidic solution and its reactivity at higher pH's are coherent with a mechanism of non-enzymatic hydrolysis for phenolic carbamates which envisions the deprotonation of the amidic nitrogen [R(CO)NHR'] followed by loss of the phenate anion to give an isocyanate which rapidly adds water and decomposes releasing the amine[55] (scheme 6).

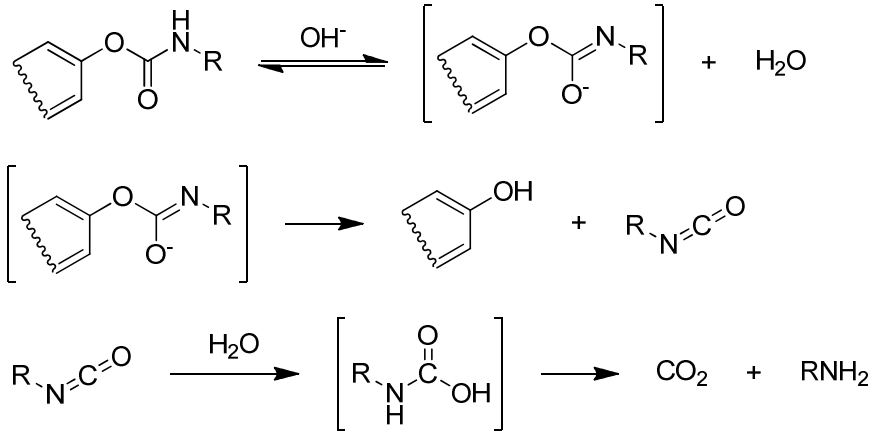

Scheme 6: Hydrolysis scheme of carbamate in alkaline solution.

This mechanism may help explain the differences in reactivity in PBS solution just mentioned: in aminoacid derivatives the presence of a (deprotonated) carboxy group in α to the amidic nitrogen would be expected to increase the pKa value of the latter, thus slowing down the reaction. The relationship between OEG chain length and rate of hydrolysis may on the other hand be tentatively attributed to an increasing destabilization of the reagent as the chain length increases due to steric crowding.

While the fits obtained in analyses such as the one exemplified in fig 1 are satisfactory, some features of the data indicate that the assumption of equal reactivity of the carbamate group in all three possible species (tri-, di- and mono-substituted resveratrol) may not be correct. If it were, one would expect a 3:2:1 proportion for the k_1:k_2:k_3 values. This is not the case. In particular, in most cases $k_1 > 1.5k_2$, suggesting that one of the carbamate groups is hydrolyzed preferentially. Indeed, further data obtained in this project and presented in chapter 4 indicate that hydrolysis of the substituent groups in positions 3,5 is favoured over hydrolysis of the third substituent, in position 4'.

Hydrolysis rates greatly increased in blood, suggesting the involvement of enzymes. This notion is reinforced by the variability of the rates from one compound to the other.

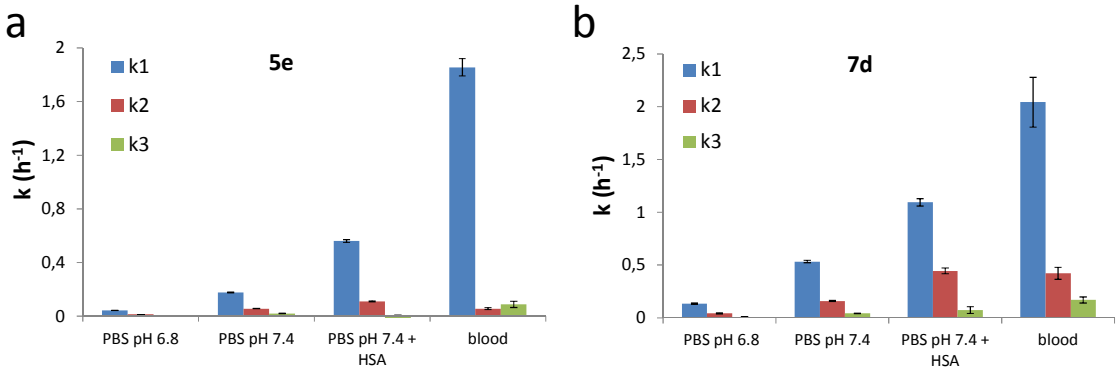

Figure 3. Observed pseudo first-order rate constants for the hydrolysis of resveratrol derivatives **5e (a)** and **7d (b)** in PBS at pH 6.8, at pH 7.4 in the absence or presence of 35 mg/mL human serum albumin, and in rat blood. Values ± standard error are reported as obtained from the fit of all the available data.

Since plasma albumin is thought to have carbamoyl esterase activity (e.g.[56, 57]) and it was reported to be the predominant component of human plasma catalyzing the hydrolysis of phenolic carbamate esters,[39] we verified its involvement performing hydrolysis studies in aqueous buffer at blood pH values (PBS 0.1M, pH 7.4), in the absence or in the presence of a physiological concentration of albumin (35 mg/mL). Two representative members of the two different families of derivatives were used for these experiments (**7d** for OEG derivatives; **5e** (Phe) for aminoacid derivatives). A slight increase in the hydrolysis rate was observed increasing pH from 6.8 to 7.4, but a considerably greater increase was indeed observed in the presence of albumin.

Rates measured in rat blood are considerably higher than achieved with 35 mg/mL of human serum albumin. There are multiple possible explanations for this observation: rat albumin may be more active than its human counterpart; it may be considerably more concentrated than 35 mg/mL; blood may contain a significant level of other carbamate esterase activities, not present in commercial albumin; a combination of the above may apply.

It is interesting that the acceleration in blood in comparison with albumin is only observed for k_1 and, to a lesser extent, k_3. k_2, the rate of loss of a second protecting group from the di-substituted hydrolysis intermediate, is similar with 35 mg/mL HSA or BSA and in rat blood. This suggests that a non-albumin hydrolase activity in rat blood may be responsible for the strong acceleration observed for k_1.

Pharmacokinetics studies:

All the N-monosubstituted carbamate ester derivatives were tested for their *in vivo* absorption and metabolism. Pharmacokinetic studies were performed with rats, and each compound was administered as a single intragastric bolus, in an equimolar dose/kg body weight (88 µmol/kg). Blood samples were taken at different time points, treated as described in the Materials and Methods section and analyzed.

Administration of compounds **6d**, **4e**, **5e** did not result in the appearance of detectable amounts of resveratrol, derivatives or any metabolites in blood samples. Measurable levels of stilbene derivatives could be found in blood samples only in the case of compounds **7d**, **8d** and **3e**. The products of partial hydrolysis of **2e** unfortunately turned out to co-migrate with background masking blood components carried over by the extraction procedure. Their presence, at low concentrations, cannot therefore be excluded.

The pharmacokinetic profiles for **7d**, **8d** and **3e** are presented in fig 4.

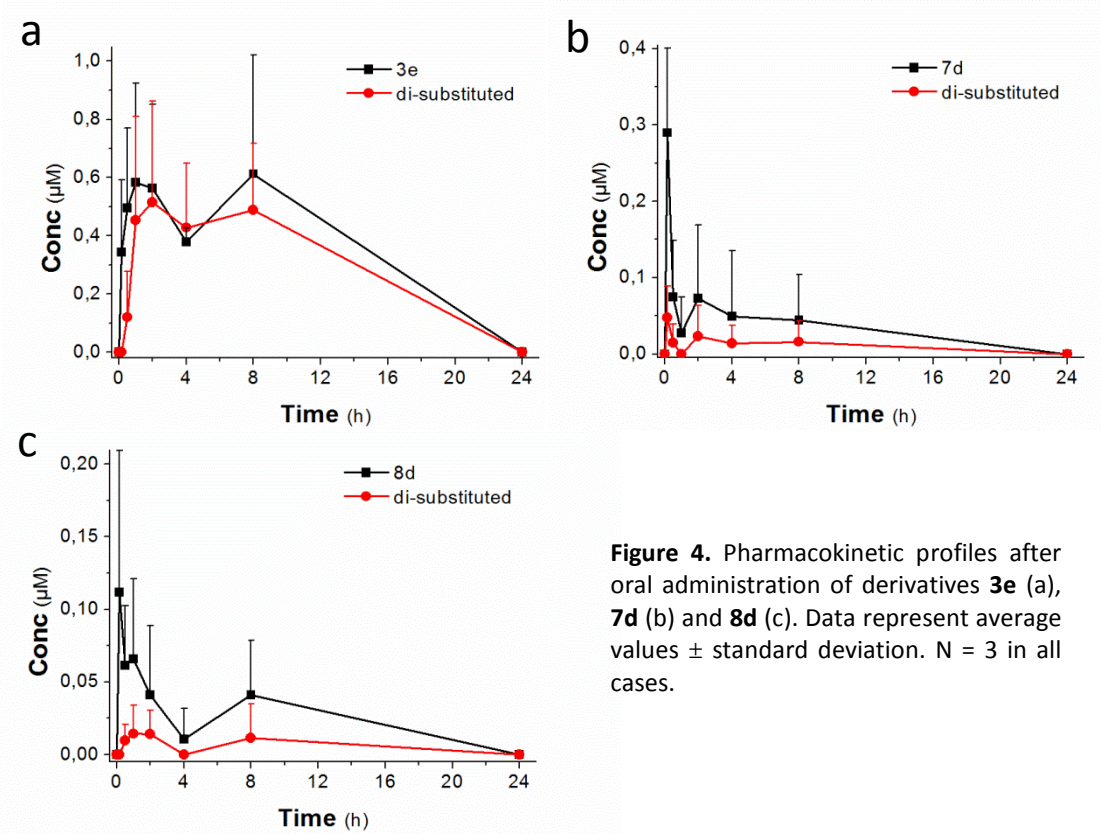

Figure 4. Pharmacokinetic profiles after oral administration of derivatives **3e** (a), **7d** (b) and **8d** (c). Data represent average values ± standard deviation. N = 3 in all cases.

Both **7d** and **8d** were rapidly, although poorly, absorbed, peaking 10min after their oral administration. In agreement with the results previously obtained with acetal prodrugs ([45], chapter 1), the derivative with four units of ethyleneglycol (**7d)** was better absorbed than its counterpart with 6 units (0.3µM vs 0.1µM). In both cases the di-substituted hydrolysis products were also present. No measurable amounts of mono-substituted derivatives or of Resveratrol could be detected.

The pharmacokinetic profile of **3e** was undoubtedly more rewarding than those of **7d** and **8d.** After the oral administration of the amino acid derivative, levels of the tri-substituted prodrug in the blood were higher than 0.5µM and, notably, remained at this level for several hours. This may indicate that the derivative is constantly absorbed from the intestinal mucosae or that it is poorly cleared from the body, so that its level in blood may be in equilibrium with its level in the various organs. Di-substituted hydrolysis products are also present, and, interestingly, their level is similar to that of the tri-substituted molecule.

Conclusions:

As hypothesized, the N-monosubstituted carbamate bond is a convenient linker for prodrugs of Resveratrol. We previously tested the N,N-disubstituited carbamate linker[54] concluding that it was too stable to regenerate Resveratrol with opportune kinetics. The N-monosubsituted version as expected is more labile and presents hydrolysis kinetics suitable for a prodrug.

The pharmacokinetic performance of the derivatives presented here is however poor. Of the whole set of molecules tested, only three derivatives could be measured in blood after their oral administration. The one incorporating isoleucine gave the best results.

While the stability of derivatives bearing the N-monosubstituted carbamate linker is satisfactory, absorption is still problematic. More work needs to be done in this sense in order to enhance intestinal absorption of carbamate ester derivatives of resveratrol.

References:

1. Jeandet, P.; Delaunois, B.; Conreux, A.; Donnez, D.; Nuzzo, V.; Cordelier, S.; Clement, C.; Courot, E. Biosynthesis, metabolism, molecular engineering, and biological functions of stilbene phytoalexins in plants. *BioFactors (Oxford, England)* **2010,** *36*, (5), 331-41.
2. Agarwal, B.; Baur, J. A. Resveratrol and life extension. *Annals of the New York Academy of Sciences* **2011,** *1215*, 138-43.
3. Csiszar, A. Anti-inflammatory effects of resveratrol: possible role in prevention of age-related cardiovascular disease. *Annals of the New York Academy of Sciences* **2011,** *1215*, 117-22.
4. Kroon, P. A.; Iyer, A.; Chunduri, P.; Chan, V.; Brown, L. The cardiovascular nutrapharmacology of resveratrol: pharmacokinetics, molecular mechanisms and therapeutic potential. *Current medicinal chemistry* **2010,** *17*, (23), 2442-55.
5. Khurana, S.; Venkataraman, K.; Hollingsworth, A.; Piche, M.; Tai, T. C. Polyphenols: benefits to the cardiovascular system in health and in aging. *Nutrients* **2013,** *5*, (10), 3779-827.
6. Raederstorff, D.; Kunz, I.; Schwager, J. Resveratrol, from experimental data to nutritional evidence: the emergence of a new food ingredient. *Annals of the New York Academy of Sciences* **2013,** *1290*, 136-41.
7. Szkudelski, T.; Szkudelska, K. Anti-diabetic effects of resveratrol. *Annals of the New York Academy of Sciences* **2011,** *1215*, 34-9.
8. Liu, K.; Zhou, R.; Wang, B.; Mi, M. T. Effect of resveratrol on glucose control and insulin sensitivity: a meta-analysis of 11 randomized controlled trials. *The American journal of clinical nutrition* **2014,** *99*, (6), 1510-1519.
9. Baile, C. A.; Yang, J. Y.; Rayalam, S.; Hartzell, D. L.; Lai, C. Y.; Andersen, C.; Della-Fera, M. A. Effect of resveratrol on fat mobilization. *Annals of the New York Academy of Sciences* **2011,** *1215*, 40-7.
10. Wang, S.; Moustaid-Moussa, N.; Chen, L.; Mo, H.; Shastri, A.; Su, R.; Bapat, P.; Kwun, I.; Shen, C. L. Novel insights of dietary polyphenols and obesity. *The Journal of nutritional biochemistry* **2014,** *25*, (1), 1-18.
11. Andrade, J. M.; Frade, A. C.; Guimaraes, J. B.; Freitas, K. M.; Lopes, M. T.; Guimaraes, A. L.; de Paula, A. M.; Coimbra, C. C.; Santos, S. H. Resveratrol increases brown adipose tissue thermogenesis markers by increasing SIRT1 and energy expenditure and decreasing fat accumulation in adipose tissue of mice fed a standard diet. *European journal of nutrition* **2014**.
12. Andrade, J. M.; Paraiso, A. F.; de Oliveira, M. V.; Martins, A. M.; Neto, J. F.; Guimaraes, A. L.; de Paula, A. M.; Qureshi, M.; Santos, S. H. Resveratrol attenuates hepatic steatosis in high-fat fed mice by decreasing lipogenesis and inflammation. *Nutrition (Burbank, Los Angeles County, Calif.)* **2014,** *30*, (7-8), 915-9.
13. Biasutto, L.; Szabo, I.; Zoratti, M. Mitochondrial effects of plant-made compounds. *Antioxidants & redox signaling* **2011,** *15*, (12), 3039-59.
14. Park, S. J.; Ahmad, F.; Philp, A.; Baar, K.; Williams, T.; Luo, H.; Ke, H.; Rehmann, H.; Taussig, R.; Brown, A. L.; Kim, M. K.; Beaven, M. A.; Burgin, A. B.; Manganiello, V.; Chung, J. H. Resveratrol ameliorates aging-related metabolic phenotypes by inhibiting cAMP phosphodiesterases. *Cell* **2012,** *148*, (3), 421-33.

15. Foti Cuzzola, V.; Ciurleo, R.; Giacoppo, S.; Marino, S.; Bramanti, P. Role of resveratrol and its analogues in the treatment of neurodegenerative diseases: focus on recent discoveries. *CNS & neurological disorders drug targets* **2011,** *10*, (7), 849-62.
16. Quincozes-Santos, A.; Gottfried, C. Resveratrol modulates astroglial functions: neuroprotective hypothesis. *Annals of the New York Academy of Sciences* **2011,** *1215*, 72-8.
17. Aggarwal, B. B.; Bhardwaj, A.; Aggarwal, R. S.; Seeram, N. P.; Shishodia, S.; Takada, Y. Role of resveratrol in prevention and therapy of cancer: preclinical and clinical studies. *Anticancer research* **2004,** *24*, (5a), 2783-840.
18. Vanden Berghe, W. Epigenetic impact of dietary polyphenols in cancer chemoprevention: lifelong remodeling of our epigenomes. *Pharmacological research : the official journal of the Italian Pharmacological Society* **2012,** *65*, (6), 565-76.
19. Kaminski, B. M.; Steinhilber, D.; Stein, J. M.; Ulrich, S. Phytochemicals resveratrol and sulforaphane as potential agents for enhancing the anti-tumor activities of conventional cancer therapies. *Current pharmaceutical biotechnology* **2012,** *13*, (1), 137-46.
20. Gupta, S. C.; Kannappan, R.; Reuter, S.; Kim, J. H.; Aggarwal, B. B. Chemosensitization of tumors by resveratrol. *Annals of the New York Academy of Sciences* **2011,** *1215*, 150-60.
21. Cottart, C. H.; Nivet-Antoine, V.; Beaudeux, J. L. Review of recent data on the metabolism, biological effects, and toxicity of resveratrol in humans. *Molecular nutrition & food research* **2014,** *58*, (1), 7-21.
22. Subramanian, L.; Youssef, S.; Bhattacharya, S.; Kenealey, J.; Polans, A. S.; van Ginkel, P. R. Resveratrol: challenges in translation to the clinic--a critical discussion. *Clinical cancer research : an official journal of the American Association for Cancer Research* **2010,** *16*, (24), 5942-8.
23. Walle, T.; Hsieh, F.; DeLegge, M. H.; Oatis, J. E., Jr.; Walle, U. K. High absorption but very low bioavailability of oral resveratrol in humans. *Drug metabolism and disposition: the biological fate of chemicals* **2004,** *32*, (12), 1377-82.
24. Walle, T. Bioavailability of resveratrol. *Annals of the New York Academy of Sciences* **2011,** *1215*, 9-15.
25. Yu, C.; Shin, Y. G.; Chow, A.; Li, Y.; Kosmeder, J. W.; Lee, Y. S.; Hirschelman, W. H.; Pezzuto, J. M.; Mehta, R. G.; van Breemen, R. B. Human, rat, and mouse metabolism of resveratrol. *Pharmaceutical research* **2002,** *19*, (12), 1907-14.
26. Bresciani, L.; Calani, L.; Bocchi, L.; Delucchi, F.; Savi, M.; Ray, S.; Brighenti, F.; Stilli, D.; Del Rio, D. Bioaccumulation of resveratrol metabolites in myocardial tissue is dose-time dependent and related to cardiac hemodynamics in diabetic rats. *Nutrition, metabolism, and cardiovascular diseases : NMCD* **2014,** *24*, (4), 408-15.
27. Walker, J.; Schueller, K.; Schaefer, L. M.; Pignitter, M.; Esefelder, L.; Somoza, V. Resveratrol and its metabolites inhibit pro-inflammatory effects of lipopolysaccharides in U-937 macrophages in plasma-representative concentrations. *Food & function* **2014,** *5*, (1), 74-84.
28. Eseberri, I.; Lasa, A.; Churruca, I.; Portillo, M. P. Resveratrol metabolites modify adipokine expression and secretion in 3T3-L1 pre-adipocytes and mature adipocytes. *PloS one* **2013,** *8*, (5), e63918.
29. Lasa, A.; Churruca, I.; Eseberri, I.; Andres-Lacueva, C.; Portillo, M. P. Delipidating effect of resveratrol metabolites in 3T3-L1 adipocytes. *Molecular nutrition & food research* **2012,** *56*, (10), 1559-68.
30. Kenealey, J. D.; Subramanian, L.; Van Ginkel, P. R.; Darjatmoko, S.; Lindstrom, M. J.; Somoza, V.; Ghosh, S. K.; Song, Z.; Hsung, R. P.; Kwon, G. S.; Eliceiri, K. W.; Albert, D. M.; Polans, A. S. Resveratrol metabolites do not elicit early pro-apoptotic mechanisms in neuroblastoma cells. *Journal of agricultural and food chemistry* **2011,** *59*, (9), 4979-86.
31. Lu, D. L.; Ding, D. J.; Yan, W. J.; Li, R. R.; Dai, F.; Wang, Q.; Yu, S. S.; Li, Y.; Jin, X. L.; Zhou, B. Influence of glucuronidation and reduction modifications of resveratrol on its biological activities. *Chembiochem : a European journal of chemical biology* **2013,** *14*, (9), 1094-104.
32. Calamini, B.; Ratia, K.; Malkowski, M. G.; Cuendet, M.; Pezzuto, J. M.; Santarsiero, B. D.; Mesecar, A. D. Pleiotropic mechanisms facilitated by resveratrol and its metabolites. *The Biochemical journal* **2010,** *429*, (2), 273-82.

33. Hoshino, J.; Park, E. J.; Kondratyuk, T. P.; Marler, L.; Pezzuto, J. M.; van Breemen, R. B.; Mo, S.; Li, Y.; Cushman, M. Selective synthesis and biological evaluation of sulfate-conjugated resveratrol metabolites. *Journal of medicinal chemistry* **2010,** *53*, (13), 5033-43.
34. Herath, W.; Khan, S. I.; Khan, I. A. Microbial metabolism. Part 14. Isolation and bioactivity evaluation of microbial metabolites of resveratrol. *Natural product research* **2013,** *27*, (16), 1437-44.
35. Ruotolo, R.; Calani, L.; Fietta, E.; Brighenti, F.; Crozier, A.; Meda, C.; Maggi, A.; Ottonello, S.; Del Rio, D. Anti-estrogenic activity of a human resveratrol metabolite. *Nutrition, metabolism, and cardiovascular diseases : NMCD* **2013,** *23*, (11), 1086-92.
36. Patel, K. R.; Andreadi, C.; Britton, R. G.; Horner-Glister, E.; Karmokar, A.; Sale, S.; Brown, V. A.; Brenner, D. E.; Singh, R.; Steward, W. P.; Gescher, A. J.; Brown, K. Sulfate metabolites provide an intracellular pool for resveratrol generation and induce autophagy with senescence. *Science translational medicine* **2013,** *5*, (205), 205ra133.
37. Andreadi, C.; Britton, R. G.; Patel, K. R.; Brown, K. Resveratrol-sulfates provide an intracellular reservoir for generation of parent resveratrol, which induces autophagy in cancer cells. *Autophagy* **2014,** *10*, (3), 524-5.
38. Ghosh, A. K.; Brindisi, M. Organic Carbamates in Drug Design and Medicinal Chemistry. *Journal of medicinal chemistry* **2015**.
39. Hansen, J.; Mørk, N.; Bundgaard, H. Phenyl carbamates of amino acids as prodrug forms for protecting phenols against first-pass metabolism. *International Journal of Pharmaceutics* **1992,** *81*, (2–3), 253-261.
40. Biasutto, L.; Zoratti, M. Prodrugs of quercetin and resveratrol: a strategy under development. *Current drug metabolism* **2014,** *15*, (1), 77-95.
41. Ferriz, J. M.; Vinsova, J. Prodrug design of phenolic drugs. *Current pharmaceutical design* **2010,** *16*, (18), 2033-52.
42. Dhareshwar, S.; Stella, V., Prodrugs of Alcohols and Phenols. In *Prodrugs*, Stella, V.; Borchardt, R.; Hageman, M.; Oliyai, R.; Maag, H.; Tilley, J., Eds. Springer New York: 2007; Vol. V, pp 731-799.
43. Mulholland, P. J.; Ferry, D. R.; Anderson, D.; Hussain, S. A.; Young, A. M.; Cook, J. E.; Hodgkin, E.; Seymour, L. W.; Kerr, D. J. Pre-clinical and clinical study of QC12, a water-soluble, pro-drug of quercetin. *Annals of oncology : official journal of the European Society for Medical Oncology / ESMO* **2001,** *12*, (2), 245-8.
44. Kim, M. K.; Park, K. S.; Yeo, W. S.; Choo, H.; Chong, Y. In vitro solubility, stability and permeability of novel quercetin-amino acid conjugates. *Bioorganic & medicinal chemistry* **2009,** *17*, (3), 1164-71.
45. Mattarei, A.; Azzolini, M.; Carraro, M.; Sassi, N.; Zoratti, M.; Paradisi, C.; Biasutto, L. Acetal derivatives as prodrugs of resveratrol. *Molecular pharmaceutics* **2013,** *10*, (7), 2781-92.
46. Gynther, M.; Laine, K.; Ropponen, J.; Leppanen, J.; Mannila, A.; Nevalainen, T.; Savolainen, J.; Jarvinen, T.; Rautio, J. Large neutral amino acid transporter enables brain drug delivery via prodrugs. *Journal of medicinal chemistry* **2008,** *51*, (4), 932-6.
47. Peura, L.; Malmioja, K.; Laine, K.; Leppanen, J.; Gynther, M.; Isotalo, A.; Rautio, J. Large amino acid transporter 1 (LAT1) prodrugs of valproic acid: new prodrug design ideas for central nervous system delivery. *Molecular pharmaceutics* **2011,** *8*, (5), 1857-66.
48. Peura, L.; Malmioja, K.; Huttunen, K.; Leppanen, J.; Hamalainen, M.; Forsberg, M. M.; Gynther, M.; Rautio, J.; Laine, K. Design, synthesis and brain uptake of LAT1-targeted amino acid prodrugs of dopamine. *Pharmaceutical research* **2013,** *30*, (10), 2523-37.
49. Kozerski, G. E.; Gallavan, R. H.; Ziemelis, M. J. Investigation of trialkoxysilane hydrolysis kinetics using liquid chromatography with inductively coupled plasma atomic emission spectrometric detection and non-linear regression modeling. *Analytica Chimica Acta* **2003,** *489*, (1), 103-114.
50. Biasutto, L.; Marotta, E.; Garbisa, S.; Zoratti, M.; Paradisi, C. Determination of quercetin and resveratrol in whole blood--implications for bioavailability studies. *Molecules (Basel, Switzerland)* **2010,** *15*, (9), 6570-9.

51. Biasutto, L.; Marotta, E.; Bradaschia, A.; Fallica, M.; Mattarei, A.; Garbisa, S.; Zoratti, M.; Paradisi, C. Soluble polyphenols: synthesis and bioavailability of 3,4',5-tri(alpha-D-glucose-3-O-succinyl) resveratrol. *Bioorganic & medicinal chemistry letters* **2009,** *19*, (23), 6721-4.
52. Azzolini, M.; La Spina, M.; Mattarei, A.; Paradisi, C.; Zoratti, M.; Biasutto, L. Pharmacokinetics and tissue distribution of pterostilbene in the rat. *Molecular nutrition & food research* **2014,** *58*, (11), 2122-32.
53. Wu, X.; Cheng, L.; Xiang, D.; Wei, Y. Syntheses of Carbamate Derivatives of Quercetin by Reaction with Amino Acid Ester Isocyanates. *Letters in Organic Chemistry* **2005,** *2*, (6), 535-538.
54. Mattarei, A.; Carraro, M.; Azzolini, M.; Paradisi, C.; Zoratti, M.; Biasutto, L. New water-soluble carbamate ester derivatives of resveratrol. *Molecules (Basel, Switzerland)* **2014,** *19*, (10), 15900-17.
55. Adams, P.; Baron, F. A. Esters of Carbamic Acid. *Chemical Reviews* **1965,** *65*, (5), 567-602.
56. Sogorb, M. A.; Alvarez-Escalante, C.; Carrera, V.; Vilanova, E. An in vitro approach for demonstrating the critical role of serum albumin in the detoxication of the carbamate carbaryl at in vivo toxicologically relevant concentrations. *Archives of toxicology* **2007,** *81*, (2), 113-9.
57. Sogorb, M. A.; Vilanova, E. Serum albumins and detoxication of anti-cholinesterase agents. *Chemico-biological interactions* **2010,** *187*, (1-3), 325-9.

Appendix:

Synthesis of derivatives 2e-8d:

Derivatives were synthesized by the group of prof. Cristina Paradisi, Department of Chemical Sciences, University of Padova.

Preparation of methoxyoligoethylene glycol-amines (**6**-**8**, Scheme 2).

General *Procedure for the preparation of methoxyoligoethylene glycol-p-toluenesulfonates* (**6a**-**8a**). Pyridine (1.09 mL, 13.5 mmol, 2.0 eq.) and DMAP (1.65 g, 13.5 mmol, 2.0 eq.) were added to a solution of methoxyoligoethylene glycol (6.75 mmol, 1.0 eq.) in DCM (10 mL), and the mixture was stirred at 0 °C for 15 min. A solution of tosyl chloride (1.93 g, 10.1 mmol, 1.5 eq.) in DCM (10 mL) was then added dropwise and the reaction mixture was stirred at room temperature for 6 hours. The resulting mixture was diluted in DCM (150 mL) and washed with 0.5 N HCl (100 mL). The aqueous layer was washed with DCM (5 × 75 mL) and all the organic fractions were collected, dried over $MgSO_4$ and filtered. The solvent was evaporated under reduced pressure and the residue was purified by flash chromatography.

2-(2-(2-methoxyethoxy)ethoxy)ethyl 4-methylbenzenesulfonate (**6a**). Purified by flash chromatography using DCM:EtOAc 8:2 as eluent. 95 % yield as a colourless oil. ^{1}H-NMR (250 MHz, $CDCl_3$) δ (ppm): 2.43 (s, 3 H, Ar-C*H*$_3$), 3.35 (s, 3 H, -O-C*H*$_3$), 3.49-3.66 (m, 10 H, 2 × -O-C*H*$_2$-C*H*$_2$-O- + -O-C*H*$_2$-), 4.14 (t, 2 H, Ts-C*H*$_2$-, $^3J_{H\text{-}H}$ = 5.75 Hz), 7.32 (d, 2 H, Ar-*H*, $^3J_{H\text{-}H}$ = 8.25 Hz), 7.77 (d, 2 H, Ar-*H*, $^3J_{H\text{-}H}$ = 8.25 Hz); ^{13}C-NMR (62.9 MHz, $CDCl_3$) δ (ppm): 144.7, 132.9, 129.7, 127.9, 71.8, 70.6, 70.5, 70.4, 69.2, 68.6, 58.9, 21.6; ESI-MS (ion trap): m/z 337 $[M+H_2O+H]^+$.

2,5,8,11-tetraoxatridecan-13-yl 4-methylbenzenesulfonate (**7a**). Purified by flash chromatography using DCM:Acetone 8:2 as eluent. 94 % yield as a colourless oil. ^{1}H-NMR (250 MHz, $CDCl_3$) δ (ppm): 2.41 (s, 3 H, Ar-C*H*$_3$), 3.33 (s, 3 H, -O-C*H*$_3$), 3.48-3.67 (m, 14 H, 3 × -O-C*H*$_2$-C*H*$_2$-O- + -O-C*H*$_2$-), 4.12 (t, 2 H, Ts-C*H*$_2$-, $^3J_{H\text{-}H}$ = 4.90 Hz), 7.30 (d, 2 H, Ar-*H*, $^3J_{H\text{-}H}$ = 8.30 Hz), 7.76 (d, 2 H, Ar-*H*, $^3J_{H\text{-}H}$ = 8.00 Hz); ^{13}C-NMR (62.9 MHz, $CDCl_3$) δ (ppm): 144.7, 132.8, 129.7, 127.8, 71.8, 70.6, 70.4, 70.4, 70.4, 70.3, 69.1, 68.5, 58.9, 21.5; ESI-MS (ion trap): m/z 381 $[M+H_2O+H]^+$.

2,5,8,11,14,17-hexaoxanonadecan-19-yl 4-methylbenzenesulfonate (**8a**). Purified by flash chromatography using DCM:Acetone 6.5:3.5 as eluent. 98 % yield as a colourless oil. ^{1}H-NMR (250 MHz, $CDCl_3$) δ (ppm): 2.35 (s, 3 H, Ar-C*H*$_3$), 3.27 (s, 3 H, -O-C*H*$_3$), 3.42-3.60 (m, 22 H, 2 × -O-C*H*$_2$-C*H*$_2$-O- + -O-C*H*$_2$-), 4.05 (t, 2 H, Ts-C*H*$_2$-, $^{3}J_{H-H}$ = 5.00 Hz), 7.25 (d, 2 H, Ar-*H*, $^{3}J_{H-H}$ = 7.93 Hz), 7.70 (d, 2 H, Ar-*H*, $^{3}J_{H-H}$ = 8.34 Hz); ^{13}C-NMR (62.9 MHz, $CDCl_3$) δ (ppm): 144.6, 132.7, 129.6, 127.7, 71.7, 70.5, 70.4, 70.4, 70.3, 70.3, 70.3, 69.1, 68.4, 58.8, 21.4; ESI-MS (ion trap): m/z 451 $[M+H]^+$.

General Procedure for the preparation of methoxyoligoethylene glycol-azides (**6b**-**8b**). Sodium azide (10.72 g, 0.165 mol, 5.0 eq.) were added to a solution of methoxyoligoethylene glycol-p-toluenesulfonate (**6a**-**8a**) (33 mmol, 1.0 eq.) in a water/acetone solution (1:3, 65 mL), and the mixture was stirred at 75 °C overnight. The mixture was then diluted in DCM (250 mL) and washed with water (250 mL). The aqueous layer was washed with DCM (5 × 100 mL) and all the organic fractions were collected, dried over $MgSO_4$ and filtered. The solvent was evaporated under reduced pressure and the residue was purified by flash chromatography.

1-azido-2-(2-(2-methoxyethoxy)ethoxy)ethane (**6b**). Purified by flash chromatography using DCM:Acetone 9:1 as eluent. 99 % yield as a colourless oil. ^{1}H-NMR (250 MHz, $CDCl_3$) δ (ppm): 3.32-3.36 (m, 5 H, -O-C*H*$_3$ + -O-CH$_2$-C*H*$_2$-N$_3$), 3.48-3.58 (m, 2 H, -O-C*H*$_2$-CH$_2$-N$_3$), 3.48-3.58 (m, 8 H, 2 × -O-C*H*$_2$-C*H*$_2$-O-); ^{13}C-NMR (62.9 MHz, $CDCl_3$) δ (ppm): 71.7, 70.5, 70.5, 70.4, 69.9, 58.8, 50.5; ESI-MS (ion trap): m/z 190 $[M+H]^+$.

13-azido-2,5,8,11-tetraoxatridecane (**7b**). Purified by flash chromatography using DCM:Acetone 85:15 as eluent. 97 % yield as a colourless oil. ^{1}H-NMR (250 MHz, $CDCl_3$) δ (ppm): 3.32-3.36 (m, 5 H, -O-C*H*$_3$ + -O-CH$_2$-C*H*$_2$-N$_3$), 3.48-3.52 (m, 2 H, -O-C*H*$_2$-CH$_2$-N$_3$), 3.58-3.65 (m, 12 H, 3 × -O-C*H*$_2$-C*H*$_2$-O-); ^{13}C-NMR (62.9 MHz, $CDCl_3$) δ (ppm): 71.8, 70.5, 70.5, 70.5, 70.4, 70.3, 69.9, 58.9, 50.5; ESI-MS (ion trap): m/z 234 $[M+H]^+$.

19-azido-2,5,8,11,14,17-hexaoxanonadecane (**8b**). Purified by flash chromatography using DCM:Acetone 8:2 as eluent. 96 % yield as a colourless oil. ^{1}H-NMR (250 MHz, $CDCl_3$) δ (ppm): 3.28-3.32 (m, 5 H, -O-C*H*$_3$ + -O-CH$_2$-C*H*$_2$-N$_3$), 3.43-3.48 (m, 2 H, -O-C*H*$_2$-CH$_2$-N$_3$), 3.53-3.61 (m, 20 H, 5 × -O-C*H*$_2$-C*H*$_2$-O-); ^{13}C-NMR (62.9 MHz, $CDCl_3$) δ (ppm): 71.6, 70.4, 70.4, 70.3, 70.3, 70.3, 70.3, 70.3, 70.2, 69.7, 58.7, 50.4; ESI-MS (ion trap): m/z 322 $[M+H]^+$.

General Procedure for the preparation of methoxyoligoethylene glycol-amines (**6**-**8**). Triphenylphosphine (10.88 g, 41.5 mmol, 1.25 eq.) in anhydrous THF (25 mL) was added dropwise to a solution of methoxyoligoethylene glycol-azide (**6b**-**8b**) (33.0 mmol, 1.0 eq.) in anhydrous THF (25 mL), and the solution was stirred at RT for 5 hours. Distilled water (20 mL) was then added and the mixture was heated under reflux (80°C) and vigorously stirred overnight. The resulting mixture was evaporated under reduced pressure and the residue was purified by flash chromatography.

2-(2-(2-methoxyethoxy)ethoxy)ethanamine (**6**). Purified by flash chromatography using DCM:MeOH = 9:1 (+ 1% Et_3N) as eluent. 97 % yield as a pale yellow oil. ^{1}H-NMR (250 MHz, $CDCl_3$) δ (ppm): 1.57 (s, 2 H, -CH$_2$-N*H*$_2$), 2.79 (t, 2 H, $^{3}J_{H-H}$ = 5.25 Hz, -CH$_2$-C*H*$_2$-NH$_2$), 3.31 (s, 3 H, -O-C*H*$_3$), 3.41-3.51 (m, 4 H, -O-CH$_2$-C*H*$_2$-O- + -O-C*H*$_2$-CH$_2$-NH$_2$), 3.52-3.63 (m, 6 H, -O-C*H*$_2$-C*H*$_2$-O- + -O-C*H*$_2$-CH$_2$-O-); ^{13}C-NMR (62.9 MHz, $CDCl_3$) δ (ppm): 73.2, 71.6, 70.3, 70.3, 70.0, 58.8, 41.5; ESI-MS (ion trap): m/z 164 $[M+H]^+$.

2,5,8,11-tetraoxatridecan-13-amine (**7**). Purified by flash chromatography using DCM:MeOH = 9:1 (+ 1% Et_3N) as eluent. 96 % yield as a pale yellow oil. ^{1}H-NMR (250 MHz, $CDCl_3$) δ (ppm): 1.54 (s, 2 H, -CH_2-N*H*$_2$), 2.71 (t, 2 H, $^3J_{H-H}$ = 5.25 Hz, -CH_2-C*H*$_2$-NH_2), 3.22 (s, 3 H, -O-C*H*$_3$), 3.34-3.41 (m, 4 H, -O-CH_2-C*H*$_2$-O- + -O-C*H*$_2$-CH_2-NH_2), 3.45-3.51 (m, 10 H, 2 × -O-C*H*$_2$-C*H*$_2$-O- + -O-C*H*$_2$-CH_2-O-); ^{13}C-NMR (62.9 MHz, $CDCl_3$) δ (ppm): 40.7, 39.3, 38.0, 37.9, 37.9, 37.9, 37.6, 26.4, 9.1; ESI-MS (ion trap): m/z 208 $[M+H]^+$.

2,5,8,11,14,17-hexaoxanonadecan-19-amine (**8**). Purified by flash chromatography using DCM:MeOH = 9:1 (+ 1% Et_3N) as eluent. 98 % yield as a pale yellow oil. ^{1}H-NMR (250 MHz, $CDCl_3$) δ (ppm): 1.78 (s, 2 H, -CH_2-N*H*$_2$), 2.76 (t, 2 H, $^3J_{H-H}$ = 5.25 Hz, -CH_2-C*H*$_2$-NH_2), 3.26 (s, 3 H, -O-C*H*$_3$), 3.39-3.46 (m, 4 H, -O-CH_2-C*H*$_2$-O- + -O-C*H*$_2$-CH_2-NH_2), 3.51-3.56 (m, 18 H, 4 × -O-C*H*$_2$-C*H*$_2$-O- + -O-C*H*$_2$-CH_2-O-); ^{13}C-NMR (62.9 MHz, $CDCl_3$) δ (ppm): 72.8, 71.6, 70.3, 70.3, 70.3, 70.2, 70.2, 70.2, 70.0, 58.7, 41.4; ESI-MS (ion trap): m/z 296 $[M+H]^+$.

General procedure for the preparation of activated 4-nitrophenyl urethanes (**2c**-**11c**, Scheme 1).

A solution of amine (**2**-**8**) (8.2 mmol, 1.0 eq.) and DMAP (2.00 g, 16.4 mmol, 2.0 eq.) in acetonitrile (15 mL) was added dropwise to a solution of bis(4-nitrophenyl) carbonate (2.74 g, 9.0 mmol, 1.1 eq.) in acetonitrile (15 mL) and the resulting solution was stirred at 50 °C for 3 hours. The reaction mixture was then diluted in DCM (150 mL) and washed with 0.5 N HCl (100 mL). The aqueous layer was washed with DCM (5 × 100 mL) and all the organic fractions were collected, dried over $MgSO_4$ and filtered. The solvent was evaporated under reduced pressure and the residue was purified by flash chromatography.

tert-butyl 4-methyl-2-(((4-nitrophenoxy)carbonyl)amino)pentanoate (**2c**). Purified by flash chromatography using DCM:Acetone:Hexane = 8:0.5:1.5 as eluent. The first two spots were collected and the solvent was evaporated under reduced pressure, then the residue was absorbed on silica and purified by flash chromatography using Hexane:Ethyl Ether = 6.5:3.5 as eluent. 65% yield as a pale yellow oil. ^{1}H-NMR (250 MHz, $CDCl_3$) δ (ppm): 0.97-1.01 (m, 6 H, 2 × -CH-C*H*$_3$), 1.49 (s, 1 H, -C*H*-CH_3), 1.52-1.85 (m, 11 H, 3 × -C-C*H*$_3$ and -CH-C*H*$_2$-), 4.27-4.36 (m, 1 H, NH-C*H*-), 5.56 (d, 1 H, -CH-N*H*-, $^3J_{H-H}$ = 8.5 Hz), 7.33 (d, 2 H, Ar-*H*, $^3J_{H-H}$ = 9.25 Hz), 8.24 (d, 2 H, Ar-*H*, $^3J_{H-H}$ = 9.25 Hz); ^{13}C-NMR (62.9 MHz, $CDCl_3$) δ (ppm): 171.7, 155.8, 152.7, 125.1, 122.0, 82.5, 53.2, 42.0, 28.0, 27.9, 24.9, 22.8, 22.0. ESI-MS (ion trap): m/z 353 $[M+H]^+$.

tert-butyl 3-methyl-2-(((4-nitrophenoxy)carbonyl)amino)pentanoate (**3c**). Purified by flash chromatography using DCM:Acetone:Hexane = 8:0.5:1.5. 93% yield as a pale yellow oil. ^{1}H-NMR (300 MHz, $CDCl_3$) δ (ppm): 0.95-1.38 (m, 5 H, -CH_2-C*H*$_3$, CH_3-C*H*$_2$-), 1.52 (s, 9 H, 3 × -C-C*H*$_3$), 1.87-2.04 (m, 1 H, -C*H*-CH_2-), 4.29 (dd, 1 H, -C*H*-NH-, $^3J_{H-H}$ = 8.7, 4.3 Hz), 5.76 (d, 1 H, -CH-N*H*-, $^3J_{H-H}$ = 8.6 Hz), 7.32-7.37 (d, 2 H, Ar-*H*, $^3J_{H-H}$ = 9.25 Hz), 8.22-8.28 (d, 2 H, Ar-*H*, $^3J_{H-H}$ = 9.25 Hz); ^{13}C-NMR (300 MHz, $CDCl_3$) δ(ppm): 172.2, 157.6, 154.6, 145.5, 126.8, 123.7, 84.3, 79.2, 78.8, 78.3, 60.5, 29.8, 26.9, 17.1, 13.4. ESI-MS (ion trap): m/z 353 $[M+H]^+$.

tert-butyl 3-(tert-butoxy)-2-(((4-nitrophenoxy)carbonyl)amino)butanoate (**4c**). Purified by flash chromatography using DCM:Acetone:Hexane = 8:0.5:1.5 as eluent. 93% yield as a pale yellow oil. ^{1}H-NMR (250 MHz, $CDCl_3$) δ (ppm): 1.19 (s, 9 H, 3 × C-C*H*$_3$), 1.28 (d, 3 H, -CH-C*H*$_3$, $^3J_{H-H}$ = 6.3 Hz), 1.49 (s, 9 H, 3 × -C-C*H*$_3$), 4.05-4.17 (m, 1 H, -O-C*H*-), 4.22-4.33 (m, 1 H, NH-C*H*-), 5.94 (d, 1 H, CH-N*H*-, $^3J_{H-H}$= 9.5 Hz), 7.35 (d, 2 H, Ar-*H*, $^3J_{H-H}$ = 9.25 Hz), 8.27 (d, 2 H, Ar-*H*, $^3J_{H-H}$ = 9.25 Hz); ^{13}C-NMR

(62.9 MHz, $CDCl_3$) δ(ppm): 169.7, 156.2, 153.8, 144.9, 125.2, 122.2, 82.5, 74.2, 67.2, 60.8, 28.9, 28.3, 21.4. ESI-MS (ion trap): m/z 397 $[M+H]^+$.

tert-butyl 2-(((4-nitrophenoxy)carbonyl)amino)-3-phenylpropanoate (**5c**). Purified by flash chromatography using DCM:Acetone = 9:1 as eluent. 81 % yield as a pale yellow oil. 1H-NMR (250 MHz, CDCl3) δ (ppm): 1.54 (s, 9 H, 3 × -C-CH_3), 3.05-3.35 (m, 2 H, 2 × C-CH_2), 4.70 (dd, 1 H, -NH-C*H*-CH_2- J = 14.7, 6.5 Hz), 6.33 (d, 1 H, -N*H*-, J = 8.3 Hz), 7.22-7.45 (m, 7 H, Ar-*H*), 8.23 (d, 2 H, Ar-*H*, $^3J_{H-H}$= 15.5 Hz); 13C-NMR (62.9 MHz, CDCl3) δ (ppm): 170.4, 155.8, 152.6, 144.6, 136.0, 129.5, 128.1, 127.5, 124.9, 121.9, 82.7, 55.6, 38.2, 27.3. ESI-MS (ion trap): m/z 387 $[M+H]^+$.

4-nitrophenyl (2-(2-(2-methoxyethoxy)ethoxy)ethyl)carbamate (**6c**). Purified by flash chromatography using DCM:Acetone = 9:1 as eluent. 87 % yield as a pale yellow oil. ^{1}H-NMR (250 MHz, $CDCl_3$) δ (ppm): 3.31 (s, 3 H, -O-C*H*$_3$), 3.37-3.43 (m, 2 H, -O-CH_2-C*H*$_2$-NH-), 3.49-3.63 (m, 10 H, 2 × -O-C*H*$_2$-C*H*$_2$-O- + -O-C*H*$_2$-CH_2-NH-), 6.06 (t, 1 H, -N*H*-, $^3J_{H-H}$ = 5 Hz), 7.25 (d, 2 H, Ar-*H*, $^3J_{H-H}$ = 9.25 Hz), 8.15 (d, 2 H, Ar-*H*, $^3J_{H-H}$ = 9.25 Hz); ^{13}C-NMR (62.9 MHz, $CDCl_3$) δ (ppm): 155.9, 153.1, 144.3, 124.8, 121.8, 71.6, 70.2, 70.2, 69.9, 69.3, 58.7, 40.8; ESI-MS (ion trap): m/z 329 $[M+H]^+$.

4-nitrophenyl 2,5,8,11-tetraoxatridecan-13-ylcarbamate (**7c**). Purified by flash chromatography using DCM:Acetone = 85:15 as eluent. 85 % yield as a pale yellow oil. ^{1}H-NMR (250 MHz, $CDCl_3$) δ (ppm): 3.17 (s, 3 H, -O-C*H*$_3$), 3.24-3.30 (m, 2 H, -O-CH_2-C*H*$_2$-NH-), 3.35-3.50 (m, 14 H, 3 × -O-C*H*$_2$-C*H*$_2$-O- + -O-C*H*$_2$-CH_2-NH-), 6.21 (t, 1 H, -N*H*-, $^3J_{H-H}$ = 5 Hz), 7.15 (d, 2 H, Ar-*H*, $^3J_{H-H}$ = 9.25 Hz), 8.03 (d, 2 H, Ar-*H*, $^3J_{H-H}$ = 9.25 Hz); ^{13}C-NMR (62.9 MHz, $CDCl_3$) δ (ppm): ^{13}C-NMR (63 MHz, $CDCl_3$) δ (ppm) 156.1, 153.2, 144.3, 124.9, 121.9, 71.7, 70.4, 70.3, 70.2, 70.1, 69.4, 58.7, 41.0; ESI-MS (ion trap): m/z 373 $[M+H]^+$.

4-nitrophenyl 2,5,8,11,14,17-hexaoxanonadecan-19-ylcarbamate (**8c**). Purified by flash chromatography using DCM:Acetone gradient from 8:2 to 6:4 as eluent. 84 % yield as a pale yellow oil. ^{1}H-NMR (250 MHz, $CDCl_3$) δ (ppm): 3.30 (s, 3 H, -O-C*H*$_3$), 3.37-3.50 (m, 4 H, -O-C*H*$_2$-C*H*$_2$-NH-), 3.55-3.61 (m, 20 H, 5 × -O-C*H*$_2$-C*H*$_2$-O-), 6.04 (t, 1 H, -N*H*-, $^3J_{H-H}$ = 5 Hz), 7.26 (d, 2 H, Ar-*H*, $^3J_{H-H}$ = 9.25 Hz), 8.17 (d, 2 H, Ar-*H* , $^3J_{H-H}$ = 9.25 Hz); ^{13}C-NMR (62.9 MHz, $CDCl_3$) δ (ppm): 125.8, 124.9, 121.8, 115.5, 71.6, 70.3, 70.3, 70.3, 70.2, 70.0, 69.3, 58.8, 40.9; ESI-MS (ion trap): m/z 461 $[M+H]^+$.

General procedure for the preparation of 3,4',5-N-monosubstituted-resveratrol carbamate esters (**2d**-**8d**). A solution of resveratrol (0.24 g, 1.1 mmol, 1.0 eq.) and DMAP (0.52 g, 4.2 mmol, 4.0 eq.) in ACN (15 mL) was added to a solution of the activated 4-nitrophenyl urethane (**2c**-**8c**) (4.8 mmol, 4.5 eq) in ACN (5 mL) and the resulting mixture was allowed to react under vigorous stirring at 50 °C for 24 h. The reaction mixture was diluted with methylene chloride (150 mL) and washed with 0.5 N HCl (100 mL). The aqueous layer was washed with DCM (5 × 75 mL) and all the organic fractions were collected, dried over $MgSO_4$ and filtered. The solvent was evaporated under reduced pressure and the residue was purified by flash chromatography.

(E)-di-tert-butyl 2,2'-((((5-(4-(((1-(tert-butoxy)-4-methyl-1-oxopentan-2-yl)carbamoyl)oxy)styryl)-1,3-phenylene)bis(oxy))bis(carbonyl))bis(azanediyl))bis(4-methylpentanoate) (**2d**). Purified by flash chromatography using $CHCl_3$ as eluent. 55% yield as a colourless oil. ^{1}H-NMR (250 MHz, $CDCl_3$) δ (ppm): 0.93 (m, 18 H, 6 × CH-C*H*$_3$), 1.44 (s, 27 H, 9 × -C-C*H*$_3$), 1.48-1.53 (m, 9 H, 3 × CH_3-C*H* and 3 × -CH-C*H*$_2$), 4.23-4.32 (m, 3 H, 3 × -NH-C*H*), 5.64 (m, 3 H, 3 × -N*H*-), 6.80-7.07 (m, 7 H, H-4, H-3', H-5', H-2, H-6, H-7, H-8), 7.47 (d, 2 H, $^3J_{H-H}$ = 8.5 Hz, H-2', H-6'); ^{13}C-NMR (62.9 MHz, $CDCl_3$) δ (ppm):

172.1, 172.3, 154.0, 153.7, 151.4, 150.5, 139.0, 134.0, 129.2, 134.0, 129.2, 127.3, 127.0, 121.7, 116.4, 114.2, 82.0, 53.1, 41.9, 27.9, 24.8, 22.8, 21.9. ESI-MS (ion trap): m/z 868 $[M+H]^+$.

(E)-di-tert-butyl 2,2'-((((5-(4-(((1-(tert-butoxy)-3-methyl-1-oxopentan-2-yl)carbamoyl)oxy)styryl)-1,3-phenylene)bis(oxy))bis(carbonyl))bis(azanediyl))bis(3-methylpentanoate) (**3d**). Purified by flash chromatography using Hexane: EtOAc = 8:2. The first spot was separated and the remaining spots were collected and the solvent was evaporated under reduced pressure, then purified by flash chromatography using DCM:Hexane:EtOAc = 7:2:1. 60 % yield as a colourless oil. ^{1}H-NMR (300 MHz, $CDCl_3$) δ (ppm): 0.87-1.05 (m, 18 H, 3 × CH_2-C*H*$_3$, 3 × CH-C*H*$_3$), 1.12-1.33 (m, 6 H, 3 × CH-C*H*$_2$-CH_3), 1.49 (s, 27 H, 9 × C-C*H*$_3$), 1.87-2.00 (m, 3 H, 3 × CH-C*H*-CH_3), 4.11 (q, 1 H, -NH-*CH*-CH-, $^3J_{H\text{-}H}$ = 7.1 Hz), 4.23-4.33 (m, 2 H, 2 × -NH-*CH*-CH-), 5.79 (d, 3 H, 3 × -N*H*-, $^3J_{H\text{-}H}$ = 8.7 Hz), 6.82-7.30 (m, 7 H, H-4, H-3', H-5', H-2, H-6, H-7, H-8), 7.43 (d, 2 H, $^3J_{H\text{-}H}$ = 8.5 Hz, H-2', H-6'); ^{13}C-NMR (300 MHz, $CDCl_3$) δ(ppm): 170.7, 170.6, 154.1, 153.7, 151.4, 150.6, 139.1, 134.0, 129.2, 127.3, 116.3, 114.2, 82.1, 58.6, 38.2, 27.9, 25.1, 15.3, 11.6. ESI-MS (ion trap): m/z 868 $[M+H]^+$.

(E)-di-tert-butyl 2,2'-((((5-(4-(((1,3-di-tert-butoxy-1-oxobutan-2-yl)carbamoyl)oxy)styryl)-1,3-phenylene)bis(oxy))bis(carbonyl))bis(azanediyl))bis(3-(tert-butoxy)butanoate) (**4d**). Purified by flash chromatography using DCM:ethyl ether = 95:5 as eluent. 58 % yield as a colourless oil. ^{1}H-NMR (250 MHz, $CDCl_3$) δ (ppm): 1.15 (s, 27 H, 9 × C-C*H*$_3$), 1.23 (d, 9 H, 3 × CH-C*H*$_3$, $^3J_{H\text{-}H}$ = 6.2 Hz), 1.45 (s, 27 H, 9 × C-C*H*$_3$), 4.04-4.25 (m, 6 H, 3 × CH_3-*CH* and 3×NH-*CH*), 5.78 (d, 3 H, 3 × -N*H*-, $^3J_{H\text{-}H}$ = 9.5 Hz), 6.85-7.30 (m, 7 H, H-4, H-3', H-5', H-2, H-6, H-7, H-8), 7.43 (d, 2 H, $^3J_{H\text{-}H}$ = 8.5 Hz, H-2', H-6'); ^{13}C-NMR (62.9 MHz, $CDCl_3$) δ (ppm): 169.6, 154.7, 154.3, 151.4, 150.5, 139.0, 133.9, 129.1, 127.3, 127.1, 121.6, 116.2, 114.1, 81.9, 81.8, 73.7, 66.9, 60.3, 28.5, 27.9, 20.8. ESI-MS (ion trap): m/z 832 $[M+H]^+$.

(E)-di-tert-butyl 2,2'-((((5-(4-(((1-(tert-butoxy)-1-oxo-3-phenylpropan-2-yl)carbamoyl)oxy)styryl)-1,3-phenylene)bis(oxy))bis(carbonyl))bis(azanediyl))bis(3-phenylpropanoate) (**5d**). Purified by flash chromatography using Hexane:Diethyl ether = 7:3 as eluent until the exit of 4-nitrophenol from the column, and Hexane:Diethyl ether:EtOAc = 5:3.5:1.5 thereafter. 57 % yield as a colourless oil. ^{1}H-NMR (250 MHz, $CDCl_3$) δ (ppm): 1.41 (s, 27 H, 3 × -C-C*H*$_3$), 3.02-3.30 (m, 6 H, 3 × Ph-C*H*$_2$), 4.16 (q, 1 H, NH-C*H*-CH_2, $^3J_{H\text{-}H}$ = 7.1 Hz), 4.64 (q, 2 H, 2 × NH-C*H*-CH_2, $^3J_{H\text{-}H}$ = 6.2 Hz), 5.79 (m, 3 H, 3 × -N*H*-), 6.81-7.56 (m, 24 H, Ar-*H*); ^{13}C-NMR (62.9 MHz, $CDCl_3$) δ (ppm): 170.6, 154.0, 153.7, 151.6, 150.8, 139.4, 136.2, 128.8, 128.7, 127.7, 127.3, 122.0, 116.7, 114.5, 82.8, 55.6, 38.6, 28.2. ESI-MS (ion trap): m/z 970 $[M+H]^+$.

(E)-5-(4-(2-(2-(2-methoxyethoxy)ethoxy)ethyl)carbamate)-1,3-phenylene bis((2-(2-(2-methoxyethoxy)ethoxy)ethyl)carbamate) (**6d**). purified by flash chromatography using DCM:Acetone = 6.5:3.5 as eluent. 75 % yield as a pale yellow oil. ^{1}H-NMR (250 MHz, $CDCl_3$) δ (ppm): 3.08 (m, 9 H, 3 × -O-C*H*$_3$), 3.39 (s, 9 H, 3 × -O-C*H*$_3$) 3.42-3.69 (m, 36 H, 6 × -O-C*H*$_2$-C*H*$_2$-O- + 3 × -O-C*H*$_2$-C*H*$_2$-NH-), 5.80 (m, 3 H, 3 × -N*H*-), 6.86 (t, 1 H, $^4J_{H,H}$ = 2.0 Hz, H-4), 6.90-7.12 (m, 6 H, H-2, H-3', H-5', H-6, H-7, H-8), 7.45 (d, 2 H, $^3J_{H,H}$ = 8.75 Hz, H-2', H-6'); ^{13}C-NMR (62.9 MHz, $CDCl_3$) δ (ppm): 154.6, 154.3, 151.6, 150.7, 139.1, 133.9, 129.2, 127.4, 127.1, 121.8, 116.3, 114.3, 71.8, 70.5, 70.2, 70.2, 69.8, 59.0, 40.9; ESI-MS (ion trap): m/z 818 $[M+Na]^+$.

(E)-5-(4-(,5,8,11-tetraoxatridecan-13-ylcarbamate)styryl)-1,3-phenylene bis(2,5,8,11-tetraoxatridecan-13-ylcarbamate) (**7d**). Purified by flash chromatography using DCM:Acetone = 5:5 as eluent. 88% yield as a colourless oil. 1H-NMR (250 MHz, CDCl3) δ (ppm): 3.35 (s, 9 H, 3 × -O-C*H*$_3$), 3.41-3.56 (m, 12 H, 3 × -O-C*H*$_2$-C*H*$_2$-NH-), 3.60-3.68 (m, 36 H, 9 × -O-C*H*$_2$-C*H*$_2$-O-), 5.81-5.88

(m, 3 H, 3 × -N*H*-), 6.80-7.14 (m, 7 H, H-2, H-4, H-3', H-5', H-6, H-7, H-8), 7.44 (d, 2 H, $^{3}J_{H,H}$ = 8.75 Hz, H-2', H-6'); 13C-NMR (62.9 MHz, CDCl3) δ (ppm): 154.5, 154.2, 151.5, 150.6, 138.9, 133.7, 129.1, 127.3, 126.9, 121.7, 116.2, 114.2, 71.7, 70.4, 70.3, 70.3, 70.1, 70.0, 69.6, 58.8, 40.8; ESI-MS (ion trap): m/z 928 $[M+H]^{+}$.

(E)-5-(4-(2,5,8,11,14,17-hexaoxanonadecan-19-ylcarbamate)styryl)-1,3-phenylene bis(2,5,8,11,14,17-hexaoxanonadecan-19-ylcarbamate) (**8d**). Purified by flash chromatography using DCM:Acetone from 4:6 to 2:8 as eluent. 76 % yield as a colourless oil. ^{1}H-NMR (250 MHz, $CDCl_3$) δ (ppm): 3.33 (s, 9 H, 3 × -O-CH_3), 3.38-3.51 (m, 12 H, 3 × -O-CH_2-CH_2-NH-), 3.57-3.68 (m, 60 H, 15 × -O-CH_2-CH_2-O-), 5.80-5.86 (m, 3 H, 3 × -N*H*-), 6.80-7.12 (m, 7 H, H-2, H-4, H-3', H-5', H-6, H-7, H-8), 7.41 (d, 2 H, $^{3}J_{H,H}$ = 8.75 Hz, H-2', H-6'); ^{13}C-NMR (62.9 MHz, $CDCl_3$) δ (ppm): 154.4, 154.1, 151.5, 150.6, 138.9, 133.8, 129.1, 127.3, 127.0, 121.7, 116.2, 114.2, 71.7, 70.4, 70.4, 70.3, 70.3, 70.3, 70.2, 69.7, 58.8, 40.9; ESI-MS (ion trap): m/z 1193 $[M+H]^{+}$.

General procedure for the tert-butyl ester deprotection in resveratrol-amino acid carbamoyl conjugates (**2e**-**5e**)

Resveratrol-amino acid carbamoyl conjugate (**2d-5d**) (1.12 mmol) was dissolved in 10 mL of dichloromethane at 0°C. 500 µL of triisopropyl silane and 10 mL of TFA were then added and the reaction mixture was stirred at room temperature under nitrogen steam overnight. The solvent and residual TFA were removed under reduced pressure. The residue was washed with toluene (3 × 5 mL), and then solvent was evaporated under reduced pressure. The product was purified by preparative reverse phase HPLC.

(E)-2,2'-((((5-(4-(((1-carboxy-3-methylbutyl)carbamoyl)oxy)styryl)-1,3-phenylene)bis(oxy))bis(carbonyl))bis(azanediyl))bis(4-methylpentanoic acid) (**2e**). Purified using a reverse-phase preparative HPLC column (ACE 5AQ 150 mm × 21.2 mm from 7.5 % to 38 % of ACN in water in 14.5 minutes). 89 % yield as a white powder after freeze-drying. ^{1}H-NMR (250 MHz, DMSO-d_6) δ (ppm): 0.89-0.94 (m, 18 H, 3 × -CH(CH_3)$_2$), 1.45-1.81 (m, 9 H, 3 × -CH-CH_2- and 3 × $(CH_3)_2$C*H*-), 3.98-4.07 (m, 3 H, -NH-C*H*-), 6.76 (t, 1 H, $^{4}J_{H\text{-}H}$ = 2 Hz, H-4), 7.10-7.38 (m, 6 H, H-3', H-5', H-2, H-6, H-7, H-8), 7.63 (d, 2 H, H-2', H-6', $^{3}J_{H\text{-}H}$ = 8.7 Hz), 8.12-8.21 (m, 3 H, 3 × -N*H*-); ^{13}C-NMR (250 MHz, DMSO-d_6) δ(ppm): 174.1, 174.0, 154.4, 154.2, 151.6, 150.7, 139.1, 133.7, 129.3, 127.6, 126.8, 121.9, 116.3, 114.4, 52.5, 39.6, 24.4, 23.0, 21.2. ESI-MS (ion trap): m/z 700 $[M+H]^{+}$.

(E)-2,2'-((((5-(4-(((1-carboxy-2-methylbutyl)carbamoyl)oxy)styryl)-1,3-phenylene)bis(oxy))bis(carbonyl))bis(azanediyl))bis(3-methylpentanoic acid) (**3e**). Purified using a reverse-phase preparative HPLC column (ACE 5AQ 150 mm × 21.2 mm from 40 % to 70 % of ACN in water in 11 minutes). 93 % yield as a white powder after freeze-drying. ^{1}H-NMR (300 MHz, DMSO) δ (ppm): 0.86-0.95 (m, 18H, 3 × -CH_2-CH_3 and 3 × -CH-CH_3), 1.21-1.55 (m, 6H, 3 × -CH-CH_2), 1.80-1.91 (m, 3 H, -CH-C*H*-CH_3), 3.89-4.13 (m, 3 H, 3 × NH-*CH*-CH), 6.77 (t, 1 H, $^{4}J_{H\text{-}H}$ = 2 Hz, H-4), 7.06-7.37 (m, 6 H, H-3', H-5', H-2, H-6, H-7, H-8), 7.63 (d, 2 H, H-2', H-6', $^{3}J_{H\text{-}H}$ = 8.7 Hz), 8.04 (d, 1 H, -N*H*-, $^{3}J_{H\text{-}H}$ = 8.4 Hz), 8.10 (d, 2 H, 2 × -N*H*-, $^{3}J_{H\text{-}H}$ = 8.4 Hz); ^{13}C-NMR (300 MHz, DMSO) δ(ppm): 175.1, 175.0, 156.7, 156.5, 153.8, 152.9, 141.3, 135.8, 131.5, 129.8, 124.1, 118.4, 97.3, 61.0, 38.3, 26.9, 17.8, 13.5. ESI-MS (ion trap): m/z 700 $[M+H]^{+}$.

(E)-2,2'-((((5-(4-(((1-carboxy-2-hydroxypropyl)carbamoyl)oxy)styryl)-1,3-phenylene)bis(oxy))bis(carbonyl))bis(azanediyl))bis(3-hydroxybutanoic acid) (**4e**). Purified using a reverse-phase preparative HPLC column (ACE 5AQ 150 mm × 21.2 mm from 7.5 % to 38 % of ACN

in water in 14.5 minutes). 91 % yield as a white powder after freeze-drying. ^{1}H-NMR (250 MHz, DMSO-d_6) δ (ppm): 1.17-1.19 (m, 9 H, 3 × -CH-C*H*$_3$), 4.00-4.23 (m, 6 H, 3 × CH_3-C*H*- and 3× NH-C*H*-), 6.80 (t, 1 H, $^{4}J_{H-H}$ = 2 Hz, H-4), 7.01-7.39 (m, 6 H, H-3', H-5', H-2, H-6, H-7, H-8), 7.61-7.72 (m, 5 H, 3 × -N*H*- and H-2', H-6'); ^{13}C-NMR (250 MHz, DMSO-d_6) δ(ppm):172.1, 172.1, 154.8, 154.6, 151.7, 150.8, 139.2, 133.8, 129.4, 127.7, 126.9, 122.0, 116.4, 114.6, 66.5, 60.4, 48.7, 20.5. ESI-MS (ion trap): m/z 664 $[M+H]^+$.

(E)-2,2'-((((5-(4-(((1-carboxy-2-phenylethyl)carbamoyl)oxy)styryl)-1,3-phenylene)bis(oxy))bis(carbonyl))bis(azanediyl))bis(3-phenylpropanoic acid) (**5e**). Purified using a reverse-phase preparative HPLC column (ACE 5AQ 150 mm × 21.2 mm from 35 % to 65 % of ACN in water in 13 minutes). 91 % yield as a white powder after freeze-drying. 1H-NMR (250 MHz, DMSO-d_6) δ (ppm): 2.86-3.19 (m, 6 H, 3 × Ph-C*H*$_2$), 4.21-4.30 (m, 3H, 3 × -NH-C*H*-CH_2), 6.47 (t, 1 H, $^{4}J_{H-H}$ = 2 Hz, H-4), 6.91-7.33 (m, 21 H, Ar-*H* and H-3', H-5', H-2, H-6, H-7, H-8), 7.58 (d, 2 H, H-2', H-6', $^{3}J_{H-H}$ = 8.7 Hz), 8.20-8.29 (m, 3H, 3 × -N*H*-); 13C-NMR (62.9 MHz, DMSO-d_6) δ (ppm): 173.0, 154.3, 154.0, 151.5, 150.7, 139.1, 137.8, 137.8, 133.6, 129.3, 128.3, 127.6, 126.6, 121.8, 116.1, 114.2, 55.8, 55.0, 36.6; ESI-MS (ion trap): m/z 802 $[M+H]^+$.

4. Synthesis and evaluation of hydrophilic carbamate ester analogs of resveratrol

Abstract:

Resveratrol (3, 5, 4'-trihydroxy-*trans*-stilbene) is an unfulfilled promise for health care: its exploitation is hindered by rapid conjugative metabolism in enterocytes and hepatocytes. Prodrug development has the potential to improve bioavailability and to advantageously modify the chemico-physical properties of the compound. We report here the synthesis of precursors in which all or part of the hydroxyl groups are linked via an N-monosubstituted carbamate ester group to promoieties derived from glycerol or galactose, conferring higher water solubility. Kinetic studies of their hydrolysis in solutions and in blood indicated that regeneration of resveratrol took place in an appropriate time frame. Hydrophilicity hindered absorption from the gastrointestinal tract, which was acceptable only for some of the compounds. In these cases the prodrug-derived species found in blood after administration of a bolus consisted mainly of partially deprotected molecules and of the products of their glucuronidation, thus providing proof-of-principle evidence of behavior as prodrugs. The soluble compounds largely reached the lower intestinal tract of rats. Upon administration of resveratrol, the major species to be found in this region is dihydroresveratrol, produced by enzymes of the intestinal flora. In experiments with a fully protected (trisubstituted) deoxygalactose-containing prodrug, the major species were the prodrug itself and partially deprotected derivatives, along with small amounts of dihydroresveratrol. We conclude that the N-monosubstituted carbamate moiety is a suitable one for the generation of prodrugs of polyphenols. The behavior of these prodrugs vis-à-vis absorption from the intestine is bound to depend on the properties of the chosen promoieties. Groups imparting a high water solubility hinder absorption and lead to accumulation of the prodrug and its derivatives in the lower part of the intestine, providing a method for the delivery of resveratrol to that organ, where it is thought to exert anti-inflammatory and anti-carcinogenic activities.

Introduction:

The scope of resveratrol's biomedical potentialities is vast. It is well known to the public as a "natural drug", potentially useful on major health battlefields: afflictions of the cardiovascular system,[2-4] neurodegeneration,[5-8] aging,[9, 10] diabetes, obesity, metabolic syndrome,[11-13] cancer.[14, 15] Reports suggest effectiveness against such conditions as, e.g., acne,[16, 17] caries,[18] H. pylori-induced pathologies,[19, 20] erectile dysfunction in diabetes,[21] osteoporosis,[22] noise-induced hearing loss,[23, 24] hypertension,[25] allergy,[26] macular degeneration of the retina,[27, 28] fatigue.[29]

This multiplicity of potential biomedical effects stems from the impact resveratrol has on the activity of apical or key proteins in interconnected cellular signaling networks. Among its major effects observed in vitro, resveratrol inhibits phosphodiesterases (in particular PDE4), leading to an increase of cellular cAMP.[30-32] Downstream events include the upregulation of AMPK, whose activation by resveratrol (and other phytochemicals)[33] is clearly supported by data from several labs.[34-42] AMPK is a key sensor and regulator of cellular energetic status with roles in many pathophysiological situations.[43, 44] After much debate, a consensus now seems to have been reached that resveratrol also induces upregulation of SIRT1, an important NAD-dependent histone deacetylase.[45, 46] SIRT1 activation has actually been reported to be upstream of AMPK activation at low resveratrol doses.[46, 47] Upregulation of AMPK activity induces mitogenesis and autophagy,[48-50] largely through inhibition of mTORC1[51-53] whose activity downregulates these processes[50] and which is also commonly upregulated in cancers.[54] The cAMP-AMPK-mTORC1 axis presumably accounts to a considerable degree for the antagonistic activity vs. neurodegeneration, metabolic syndrome[55] and cancer.[56] Activation of SIRT1 has pleiotropic epigenetic effects, reportedly culminating in life extension and health improvement in mice when elicited by novel small molecules.[57, 58] Another, interwined[44, 59, 60] major way resveratrol acts is by antagonizing inflammation.[61, 62] Resveratrol suppresses NF-kB activation,[63-65] with the attendant reduction of NO and prostaglandin production due to downregulation of iNOS and COX-2 expression. Chronic inflammation is well recognized to be a factor in carcinogenesis.[66-68] A relevant example is provided by the frequent insurgence of polyposis and colon cancer in humans[69-71] and laboratory animals[72, 73] affected by (experimental in the latter) colitis (inflammatory bowel disease). Resveratrol has been reported to be beneficial in rodent models of colitis, polyposis and colon cancer induced by sodium dextran sulfate (DSS) or azoxymethane (AOM) + DSS.[74-78]

Resveratrol is not, however, free of shortcomings. The major one is its poor bioavailability, due to the built-in propensity, common to all polyphenols, to undergo phase II metabolic conjugation to give sulfated and glucuronidated derivatives[79-86] and reduction of the double bond plus other transformations by the colonic flora.[87, 88] It has therefore often been pointed out[89] that the results of studies carried out *in vitro* with high concentrations of unmodified resveratrol may be of little pharmacological or nutritional relevance. Another unfavorable characteristic of the "aglycone" is its low

water solubility. A variety of formulations and nano-structured delivery systems are being tested with the goal of overcoming these obstacles.[90-93] Another approach relies on the construction of prodrugs, i.e. derivatives with favourable physico-chemical and absorption properties which can offer initial protection from metabolism and regenerate the active compound with appropriate kinetics.[91, 94] Indeed, in view of the many-fold activities and possible applications of resveratrol there is a need for customized delivery vehicles and/or chemical elaborations to best conform to the specific task at hand. Returning to the example of the possible use of resveratrol against colitis and associated pathologies, specific delivery to the colon has been achieved using a formulation (Ca pectinate beads)[95] and sophisticated prodrugs comprising a glucose moiety linked to resveratrol via a glycosidic bond and an hydrocarbon chain linked to the sugar ring by esterification.[96]

Here we report the synthesis and characterization of mono-, di- and tri-substituted resveratrol derivatives incorporating promoieties imparting water solubility (dihydroxypropyl and 6-deoxygalactosyl moieties) linked via N-monosubstituted carbamate ester bonds to the phenolic oxygens of resveratrol (scheme 1). The N-monosubstituted linkage undergoes hydrolysis more rapidly than N,N-disubstituted carbamates,[97] and is thus suitable for use in prodrugs. The kinetics of hydrolysis to produce progressively de-protected species have been studied, and the fate of the prodrugs after oral administration to rats has been investigated. The compounds may be useful for all applications in which water solubility and protection from metabolism and oxidation are important.

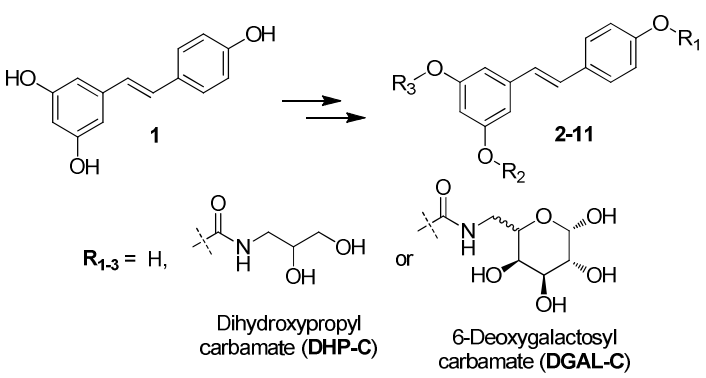

Scheme 1: Molecular structure of resveratrol (**1**, trans-3,5,4'-trihydroxy stilbene) and its carbamate esters derivatives (**2**-**11**).

	R_1	R_2	R_3
2	DHP-C	H	H
3	H	DHP-C	H
4	DHP-C	DHP-C	H
5	H	DHP-C	DHP-C
6	DHP-C	DHP-C	DHP-C
7	DGAL-C	H	H
8	H	DGAL-C	H
9	DGAL-C	DGAL-C	H
10	H	DGAL-C	DGAL-C
11	DGAL-C	DGAL-C	DGAL-C

Experimental section:

Materials and general chemistry. Resveratrol was purchased from Waseta Int. Trading Co. (Shangai, P.R.China). Other starting materials and reagents were purchased from Sigma-Aldrich, Fluka, Merck-Novabiochem, Riedel de Haen, J.T. Baker, Cambridge Isotope

Laboratories Inc., Acros Organics, Carlo Erba and Prolabo, and were used as received. ^{1}H and ^{13}C NMR spectra were recorded with a Bruker AC250F spectrometer and a Bruker Avance DMX 600. Chemical shifts (δ) are given in ppm relative to the signal of the solvent. TLCs were run on silica gel supported on plastic (Macherey-Nagel Polygram®SIL G/UV_{254}, silica thickness 0.2 mm) and visualized by UV detection, ninhydrin reaction or $KMnO_4$ oxidation. Flash chromatography was performed on silica gel (Macherey-Nagel 60, 230-400 mesh granulometry (0.063-0.040 mm)) under air pressure. The solvents were analytical or synthetic grade and were used without further purification. Preparative HPLC was performed using a Shimadzu LC-8A equipped with a UV/VIS detector SPD-20A Prominence® and a reverse phase column (ACE 5AQ (150 × 21.2 mm)).

Animals. Adult male Wistar rats (approximately 400 g body weight) from the facility of the Department of Biomedical Sciences were used for pharmacokinetic experiments. All experiments involving animals were performed after approval by the University of Padova Ethical Committee for Experimentation on Animals (CEASA) (Permit Number: 80/2011) and of the Italian Ministry of Health, and with the supervision of the Central Veterinary Service of the University of Padova, in compliance with Italian Law DL 116/92, embodying UE Directive 86/609.

LogP, Solubility and TPSA. Unless otherwise indicated, the $LogP_{ow}$ and solubility values reported are predictions obtained using the software ALOGPS 2.1 (available at Virtual Computational Chemistry Laboratory, http://www.vcclab.org). "Topological" Polar Surface Area[98] values were predicted using the Molinspiration Property Calculator (www.molinspiration.com).

HPLC-UV Analysis. Samples (2 µl) were analyzed by HPLC/UV (1290 Infinity LC System, Agilent Technologies) using a reverse phase column (Zorbax RRHD Eclipse Plus C18, 1.8 µm, 50 x 2.1 mm i.d.; Agilent Technologies) and a UV diode array detector (190-500 nm). Solvents A and B were water containing 0.1% trifluoroacetic acid (TFA) and acetonitrile, respectively. The gradient for B was as follows: 2% (0.5 min), from 2% to 10% in 0.3 min, then from 10% to 18% in 1.7 min, then from 18% to 28% in 0.5 min, 28% for 0.5 min then from 28% to100% in 1.8 min; the flow rate was 0.6 mL/min. The eluate was preferentially monitored at 286, 300 and 320 nm (corresponding to absorbance maxima of the internal standard, derivatives and resveratrol, respectively). The column compartment was thermostated at 35°C.

HPLC/ESI-MS Analysis. HPLC/ESI-MS analyses and mass spectra were performed with a 1100 Series Agilent Technologies system, equipped with binary pump (G1312A) and MSD SL Trap mass spectrometer (G2445D SL) with ESI source operating in full-scan positive or negative ion mode, with nebulizer pressure 70 psi, dry gas flow 12 L/min, dry gas temperature 350°C. ESI-MS positive mass spectra of reaction intermediates and final purified products were obtained by flow injection analysis of solutions in acetonitrile, eluting with a water:acetonitrile, 1:1 mixture containing 0.1% formic acid. HPLC/ESI-MS was also performed on selected samples from hydrolysis studies and pharmacokinetics.

Samples (20 µl) were analyzed using a reversed phase column (Synergi-MAX, 4 µm, 150 x 4.6 mm i.d.; Phenomenex, Castel Maggiore (BO), Italy). Solvents A and B were water containing 0.1% TFA or 5 mM NH_4OAc and acetonitrile, respectively. The gradient for B was as follows: 10% for 2 min, from 10% to 35% in 20 min, from 35% to 100% in 20 min, then 100% for 2 min; the flow rate was 1 mL/min. The eluate was preferentially monitored at 286, 300 and 320 nm. MS analysis was performed with an ESI source operating in full-scan positive or negative ion mode

Hydrolysis Reactions. The chemical stability of all new compounds was tested in aqueous media approximating gastric (0.1 N HCl, NormaFix) and intestinal (0.1 M PBS buffer, pH 6.8) pH values. A 5 µM solution of the compound was prepared from a 5 mM stock solution in DMSO, and incubated at 37°C for 24 hours; samples withdrawn at different times were analysed by HPLC-UV. Hydrolysis products were identified by comparison of chromatographic retention time with true samples. Non-linear curve fitting was performed using Origin 8.0 data analysis software; the hydrolysis reaction rate constants (k) of the starting compounds were calculated through interpolation of data with the equation for pseudo-first order reactions: $[C] = [C]_0 e^{-kt}$, where:

[*C*] : concentration of the compound

[*C*]$_0$: concentration of the compound at the initial time t_0

t: time.

To evaluate the long-term stability under mildly acidic conditions, we stored compound **11** dissolved in citrate buffer (5 mM) / sucrose (5 mM) solution, pH 5.0, at 4°C or R.T., following the disappearance of **11** by HPLC analysis of samples taken at intervals over a period of several months.

Hydrolysis in blood. Rats were anesthetized and blood was withdrawn from the jugular vein, heparinized and transferred into tubes containing EDTA. Blood samples (1 mL) were spiked with compound (5 µM; dilution from a 5 mM stock solution in DMSO), and incubated at 37°C for 4 hours (the maximum period allowed by blood stability). Aliquots were taken after 10 min, 30 min, 1 h, 2 h and 4 h and treated as described below. Cleared blood samples were finally subjected to HPLC-UV analysis.

Blood Sample Treatment and Analysis. Before starting the treatment, 4,4'-dihydroxybiphenyl was added as internal standard to a carefully measured blood volume (25 µM final concentration). Blood was then stabilized with a freshly-prepared 10 mM solution of ascorbic acid (0.1 vol) and acidified with 0.6 M acetic acid (0.1 vol); after mixing, an excess of acetone (4 vol) was added, followed by sonication (2 min) and centrifugation (12,000 *g*, 7 min, 4°C). The supernatant was finally collected and stored at -20°C. Before analysis, acetone was allowed to evaporate at room temperature using a Univapo 150H (UniEquip) vacuum concentrator centrifuge, and up to 40 µL of CH_3CN were added to precipitate residual proteins. After centrifugation (12,000 *g*, 5 min, 4°C), cleared samples were directly subjected to HPLC-UV analysis.

Metabolites and hydrolysis products were identified by HPLC/ESI-MS analysis and/or comparison of chromatographic retention time with true samples.

The recovery yields of resveratrol and its metabolites have been reported previously.[99, 100] For the new prodrugs the corresponding recoveries, expressed as ratio to the recovery of internal standard, were as follows: **2**: 0.751 ± 0.122, **3**: 0.752 ± 0.103, **4**: 0.985 ± 0.083, **5**: 1.022 ± 0.035, **6**: 0.855 ± 0.111; **7**: 1.358 ± 0.119, **8**: 1.097± 0.253, **9**: 0.682 ± 0.070, **10**: 0.672 ± 0.068, **11**: 0.903 ± 0.104 (N = 4 or 5 for all derivatives; mean values ± standard deviation). Recoveries ratios of glucuronides were approximated as follows: for the glucuronide of **2** (retention time 2.35 min) the ratio used was that of compound **4**, which has the same substitution pattern; for the two glucuronides of **3** (r.t. 2.38 and 3.08 min) the ratio was assumed to be close to 1.0, since the recovery ratios of both isomeric prodrugs carrying two protecting groups (**4** and **5**) were not significantly different from 1. Knowledge or assumption of these ratios allowed us to determine the unknown amount of analyte in a blood sample by quantifying the recovered internal standard.[101]

Pharmacokinetics Studies. Derivatives **2-11** were administered to overnight-fasted male rats as a single intragastric dose (88 µmol/Kg, dissolved in 250 µl DMSO). Blood samples were obtained by the tail bleeding technique: before drug administration, rats were anesthetized with isoflurane and the tip of the tail was cut off; blood samples (80-100 µL each) were then taken from the tail tip at different time points after drug administration. Blood was collected in heparinized tubes, kept in ice and treated as described below within 10 min.

Intestinal accumulation and distribution. Resveratrol or **11** were chronically administered to rats for 48 h. The beverage for the treatments was 5mM citrate buffer with sucrose (5mM), pH 5, supplemented with the compound at a concentration calculated to provide a daily intake of approximately 220µmoles/kg × day. Preliminary experiments showed that this solution was well-liked by rats, which drank an average of about 35 mL daily (hence, e.g., the concentration of resveratrol or derivative was 2.51 mM for a 400-gram rat). The slightly acidic pH insured the stability of the carbamoyl derivative (see below). In the case of resveratrol, 2-hydroxypropyl-β-cyclodextrin (HP-β-CD) was used to allow its solubilization: resveratrol and HP-β-CD were mixed in a 1:3 ratio in citrate buffer, and stirred overnight.

At the end of the treatment, the treatment solution was replaced with tap water; 1h later, animals were sacrificed, and the intestine explanted and cut into 10 cm-long segments. The luminal content of each segment was collected, 100mg were weighed, H_2O (1 vol) was added and the mixture was homogenized by vortexing (2 min). Samples were then stabilized and extracted adding 10 mM ascorbic acid (0.1 vol), 0.6 M acetic acid (0.1 vol) and acetonitrile (3 vol), vortexed (2 min), sonicated (2 min) and centrifuged (12,000 *g*, 7 min, 4°C); the supernatant was collected, concentrated, and finally analyzed via HPLC-UV and LC-ESI/MS.

Statistics. All experiments were performed at least in triplicate. Averages ± s.d. are presented. Significance in comparisons was assessed using the Wilcoxon Rank Test.

Results:

Synthesis. Syntheses were performed by Prof. C. Paradisi's group. Derivatives **2**-**11** (scheme 1) were obtained through transesterification of resveratrol (**1**) with the appropriate activated 4-nitrophenyl carbamate ester (**13**, **23**).

The synthesis of **2**-**6** is outlined in scheme 2. The starting material for the dihydroxypropyl carbamate (**DHP-C**) moiety was commercially available 2,2-Dimethyl-1,3-dioxolane-4-methanamine (**12**) which was allowed to react with bis-(4-nitrophenyl) carbonate in presence of 4-(dimethylamino)pyridine (DMAP) to give the corresponding activated urethane (**13**) in good yield. Compound **13** was added in slight excess to resveratrol (**1**) in pyridine and in presence of DMAP and allowed to react at 70°C to obtain a mixture of all the possible mono-, di- and tri- substituted resveratrol derivatives (**14**-**18**). The last step consisted in the removal of the isopropylidene protecting groups, freeing the hydroxyl functions necessary to enhance the solubility in water of the final products (**2**-**6**) which were finally isolated by preparative reverse-phase HPLC.

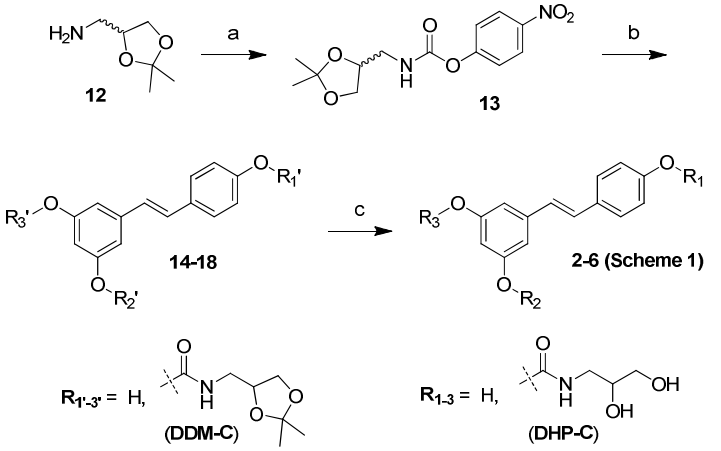

	$R_{1'}$	$R_{2'}$	$R_{3'}$
14	DDM-C	H	H
15	H	DDM-C	H
16	DDM-C	DDM-C	H
17	H	DDM-C	DDM-C
18	DDM-C	DDM-C	DDM-C

Scheme 2. Synthesis of derivatives **2**-**6** *Reagents and conditions:* (a) bis-(4-nitrophenyl) carbonate, DMAP, THF, r.t., 3 h; (b) Resveratrol (**1**), Pyridine, DMAP, 70°C, 16 h; (c) trifluoroacetic acid : water 9:1, r.t., 1.5 h.

The synthesis of derivatives **7**-**11** (scheme 3) was less straightforward, because of the need to synthesize the commercially unavailable amine (**22**). The starting material in this case was 1,2:3,4-di-*O*-isopropylidene-α-D-galactopyranose (**19**), possessing one free hydroxyl group, which was esterified with tosyl chloride to obtain compound **20**. The tosylate group of **20** was easily displaced in the second step by sodium azide giving the azide (**21**) in nearly quantitative yield. Azide **21** was then reduced to the desired primary amine (**22**) under Staudinger reaction conditions in excellent yield. The subsequent synthetic steps are equivalent to those reported above for derivatives (**2**-**6**), which consist in the production of the active urethane (**23**) followed by transesterification with resveratrol to give a mixture of all the possible mono-, di- and tri- substituted resveratrol

derivatives (**24**-**28**), and cleavage of the isopropylidene protecting groups to afford, after preparative HPLC isolation, all the desired resveratrol-6-deoxy-galactosyl carbamate ester conjugates (**7**-**11**).

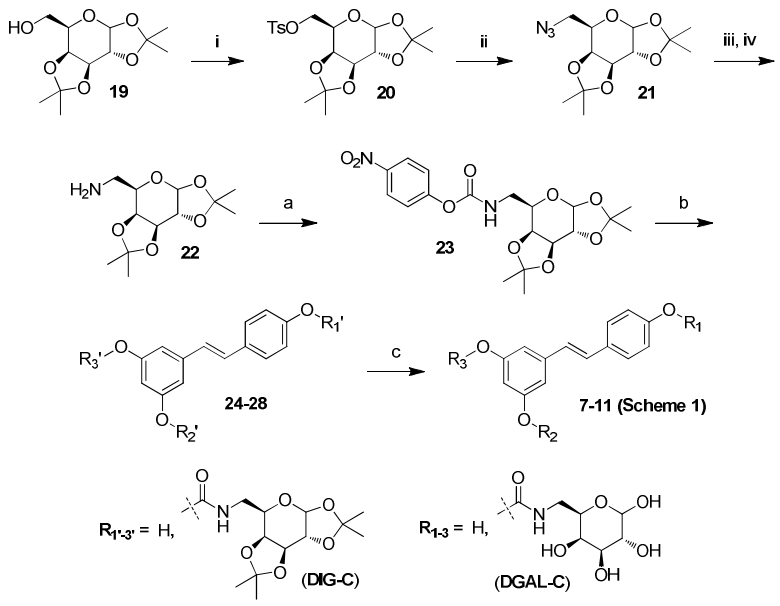

	$R_{1'}$	$R_{2'}$	$R_{3'}$
24	DIG-C	H	H
25	H	DIG-C	H
26	DIG-C	DIG-C	H
27	H	DIG-C	DIG-C
28	DIG-C	DIG-C	DIG-C

Scheme 3. Synthesis of derivatives **7-11**
Reagents and conditions: (i) Tosyl chloride, Pyridine, DMAP, from 0°C to r.t., 5 h; (ii) Sodium azide, DMSO, 160°C, 1.5 h; (iii) Triphenylphosphine, THF, r.t., 4 h; (iv) Water, reflux, 16 h; (a) bis-(4-nitrophenyl) carbonate, DMAP, THF, r.t., 3 h; (b) Resveratrol (**1**), Pyridine, DMAP, 70°C, 16 h; (c) trifluoroacetic acid : water 9:1, r.t., 1.5 h.

LogP, Solubility and TPSA. The octanol/water partition coefficient, water solubility, and the polar surface area were estimated for each compound (see Materials and Methods). The molecular polar surface area is the sum of the surfaces of polar atoms (oxygen, nitrogen) in a molecule.[98] The ability to permeate cell membranes is considered to be inversely related to this parameter, which is instead positively linked to water solubility.

Compound	Log P_{ow}	PSA (Å^2)	Solubility (g/L)
Resveratrol (**1**)	2.69 ± 0.12 [(b)]	60.68	0.039 ± 0.009 [(b)]
2	1.57	119.24	0.049
3	1.57	119.24	0.054
4	0.15	177.80	0.12
5	0.15	177.80	0.13
6	-1.27	236.36	0.20
7	0.52	168.93	1.38
8	0.52	168.93	1.51
9	-1.94	277.18	2.53
10	-1.94	277.18	2.80
11	-4.34	385.43	> 4.22 [(b)]

[(b)] Experimental value; see[1]

Table 1. $LogP_{ow}$, water solubility and topological PSA values of resveratrol and of its carbamate ester derivatives. Algorithm-predicted values unless indicated.

Hydrolysis in Acid and Near-Neutral Solution. All the compounds proved to be stable over a 24 h period in acid solution (0.1 N HCl, 37°C). On the other hand, derivatives underwent hydrolysis of the carbamoyl bond in 0.1 M PBS buffer, pH 6.8, 37°C (fig 1). Table 2 shows the pseudo 1st order hydrolysis rate costants (k) of the starting compounds, and fig 1 presents the kinetic plots and fits for the dihydroxylpropyl derivatives. Kinetics were very similar for dihydroxypropyl and 6-deoxygalactosyl carbamate ester derivatives (cf. **2** vs. **7**, **3** vs. **8**, **4** vs. **9**, **5** vs **10**, **6** vs. **11** in table 2).

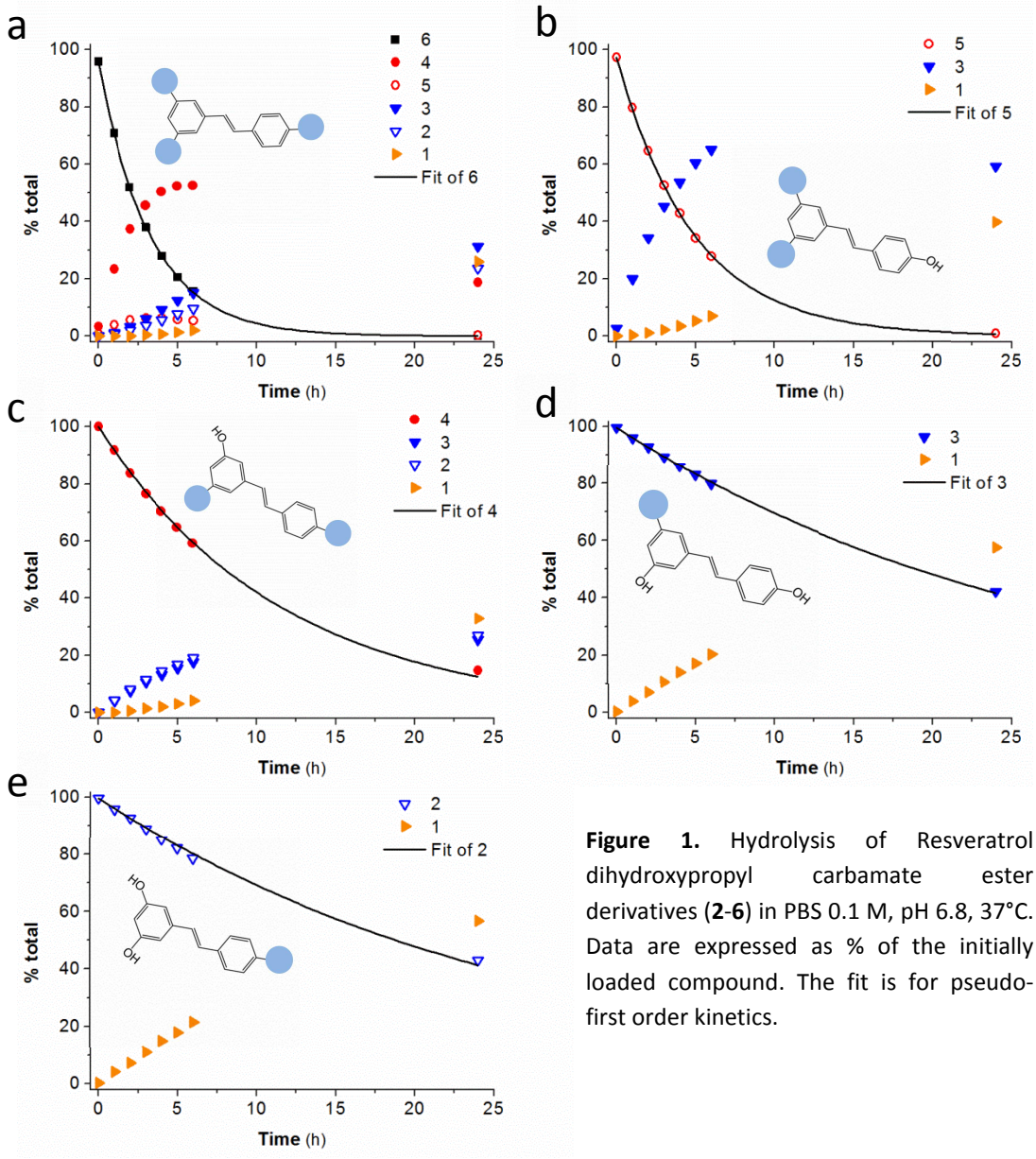

Figure 1. Hydrolysis of Resveratrol dihydroxypropyl carbamate ester derivatives (**2**-**6**) in PBS 0.1 M, pH 6.8, 37°C. Data are expressed as % of the initially loaded compound. The fit is for pseudo-first order kinetics.

The different reactivity of the two di-substituted isomers (3,4'- vs 3,5-; i.e. **4** vs. **5**, **9** vs. **10**) suggests that the simultaneous presence of two carbamoyl moieties in positions 3 and 5 accelerates the hydrolysis process at these positions. This hypothesis is supported by the hydrolysis behaviour of the tri-substituted derivatives **6** and **11**, which generate mainly the 3,4'- isomers **4** and **9**. The 3,5-disubstituted isomers **5** and **10** were detected only in very low amounts, because of the higher hydrolysis rate at position 3- in

comparison to position 4'- when all the three OH's of resveratrol are carbamoylated, and because of the higher hydrolysis rate of the 3,5-disubstituted derivatives compared to the 3,4'-disubstituted ones. When only one carbamoyl function is present in the molecule, the rate of its hydrolysis is not affected by the position occupied (similar reactivity of 4'- and 3- monosubstituted derivatives, cf. **2** vs **3**, **7** vs **8** in table 2).

	2	**3**	**4**	**5**	**6**	**7**	**8**	**9**	**10**	**11**
k (h^{-1})	**0.0366 ± 0.0008**	**0.0362 ± 0.0003**	**0.087 ± 0.001**	**0.2063 ± 0.0009**	**0.3072 ± 0.0008**	**0.0369 ± 0.0009**	**0.0315 ± 0.0003**	**0.088 ± 0.001**	**0.238 ± 0.007**	**0.329 ± 0.003**

Table 2. Hydrolysis reaction rate costants (k) in PBS 0.1M, pH 6.8, 37°C.

To verify whether these derivatives would withstand long-term storage in liquid form we followed the hydrolysis of compound **11** in citrate buffer (5 mM each) at pH 5.0 or 6.0, 4°C or R.T., over several months. The results (fig 2) indicate that indeed hydrolysis is very slow under these conditions.

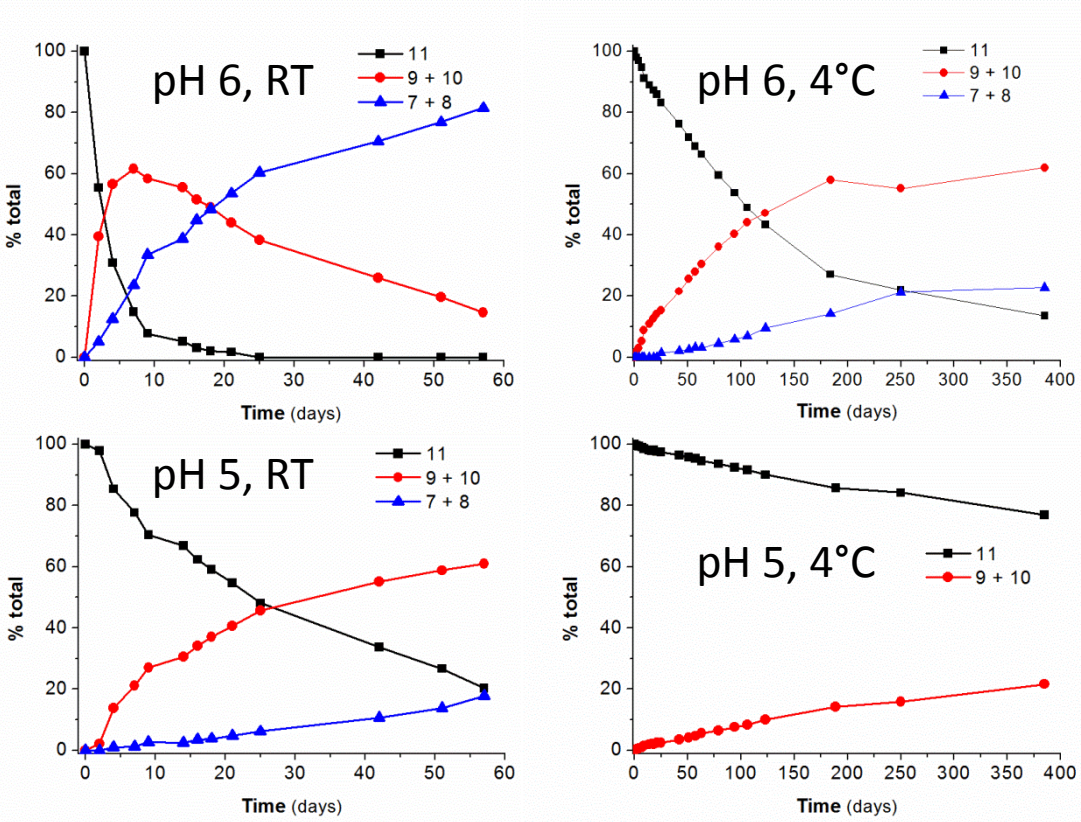

Figure 2. Kinetics of hydrolysis of **11** under the specified conditions.

Hydrolysis in Blood. Hydrolysis in blood (fig 3) was faster than in PBS pH 6.8. Reaction rates were similar for dihydroxypropyl and 6-deoxygalactosyl carbamate ester derivatives. As in PBS, hydrolysis was accelerated/promoted by the presence of two carbamoyl groups in positions 3- and 5-. When only one carbamoyl moiety was present in the molecule (i.e., with mono-substituted derivatives), the rate of hydrolysis depended on the substitution

position, with the compound substituted in 4'- reacting markedly more rapidly than the 3-substituted isomer (see fig 3 and table 3). This indicates the involvement of a regioselective (enzymatic) hydrolysis mechanism, since in PBS the kinetics are similar in the two cases. Plasma albumin has carbamoyl esterase activity[102, 103] and it has been reported to be the main component of plasma catalyzing hydrolysis of phenolic carbamate esters.[104]

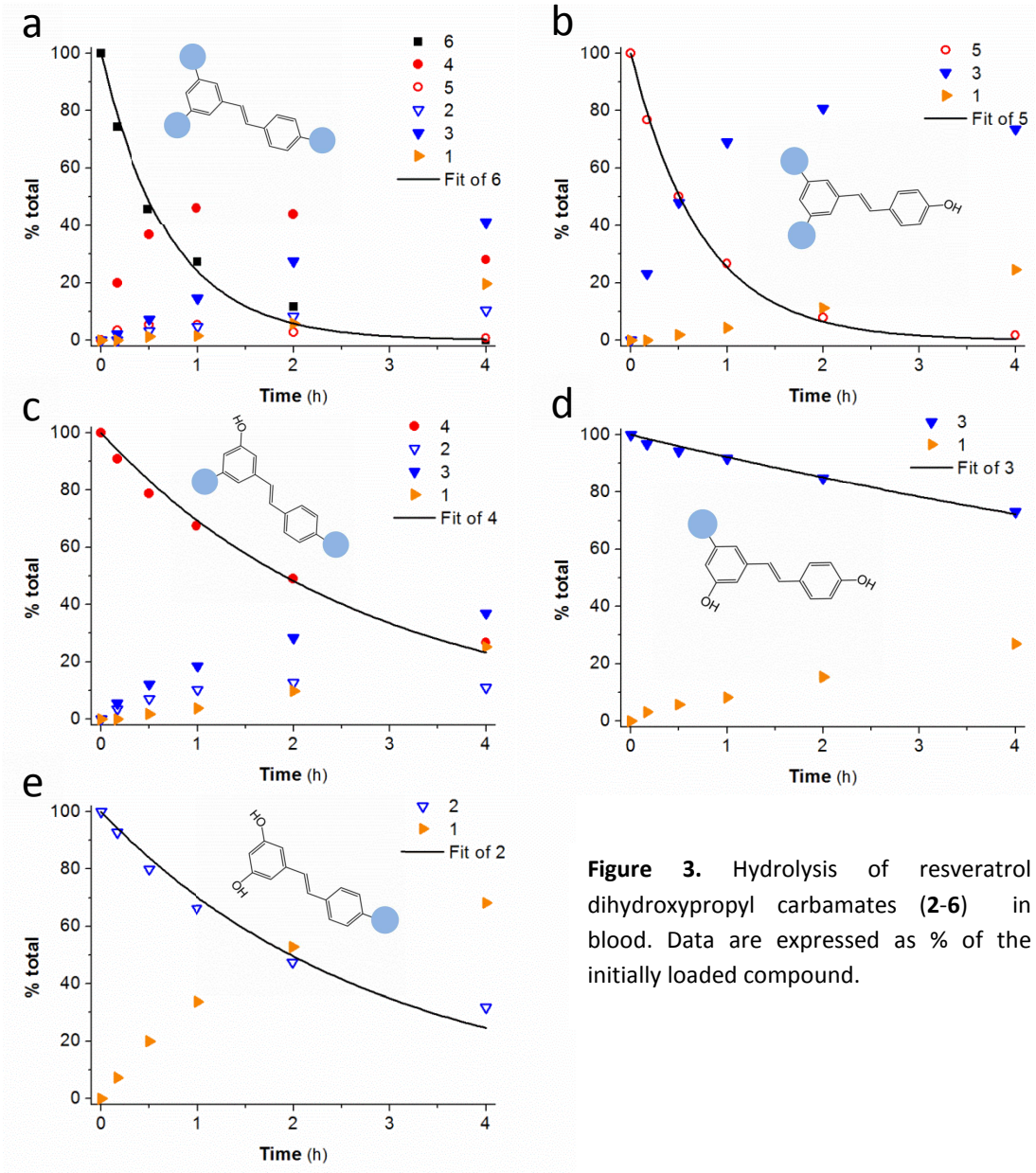

Figure 3. Hydrolysis of resveratrol dihydroxypropyl carbamates (**2**-**6**) in blood. Data are expressed as % of the initially loaded compound.

	2	3	4	5	6	7	8	9	10	11
k (h^{-1})	0.35 ± 0.03	0.081 ± 0.003	0.36 ± 0.02	1.36 ± 0.04	1.4 ± 0.1	0.70 ± 0.06	0.114 ± 0.009	0.34 ± 0.02	1.1 ± 0.2	3.9 ± 0.5

Table 3. Pseudo 1st order hydrolysis rate costants (k) in rat blood, 37°C

Pharmacokinetic Studies. *In vitro* stability studies thus indicated that the rate of hydrolysis of the carbamoyl bond in our derivatives is of the correct order of magnitude for our intended applications as prodrugs. We therefore proceeded to investigate the behaviour of our compounds in pharmacokinetics studies *in vivo*.

Dihydroxypropyl carbamate ester derivatives

Following administration of a single intragastric bolus, the mono-substituted derivatives were readily absorbed, but also extensively metabolized: low concentrations of the unmodified derivative were detected in blood, together with considerably higher amounts of metabolite(s) (fig 4). The mono-substituted derivative **3** produced two different metabolites, while the 4'-isomer **2** produced only one. Maximum concentration was reached approximately 1 hour after administration (fig 5, **d**-**e**). The two isomers differed however in their kinetic profile: both **2** and its metabolite persisted in the bloodstream for a longer time than **3** and its metabolites.

HPLC-UV-ESI/MS analysis showed that the metabolites were the products of glucuronidation of the mono-substituted derivatives, still bearing the protective carbamoyl group (fig 4 shows a representative analysis).

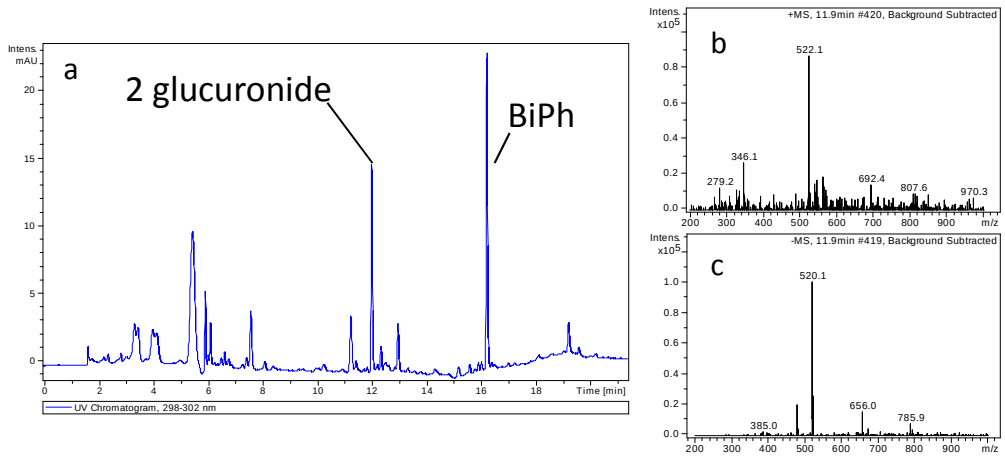

Figure 4. LC-MS analysis of a blood sample taken 2h after administration of **2**. a) UV chromatogram, 300 nm; "BiPh" is the internal standard. b, c) ESI mass spectra of the metabolite, acquired in the positive (b) and negative (c) ion current mode, respectively.

It was not possible to definitely associate each of the two peaks observed in HPLC and HPLC-MS chromatograms to one or the other of the two isomeric glucuronides formed from **3**. They are referred to below by their chromatographic retention times under our standard analysis protocol, 2.38 and 3.08 min respectively. We note however that the r.t. of 2.38 min is very similar to the r.t. of 2.35 min characteristic of the single mono-glucuronidated metabolite formed from **2**, which necessarily carries the carbamoyl promoiety in position 4' and the glucuronide group in 3. It is likely that the compound with r.t. 2.38 min, which is carbamoylated in position 3, has a similar structure, i.e., that it

carries the glucuronic acid moiety in position 4'. It follows that in the metabolite with r.t. 3.08 the two substituents probably occupy positions 3 and 5.

The tri- and di-substituted derivatives (**4**-**6**) were poorly absorbed. The relative amount of non-conjugated vs. conjugated (glucuronidated) derivatives in the bloodstream was inversely correlated to the fraction (1/3, 2/3, 3/3) of protected hydroxyls in the original prodrug.

When **6** was administered, the intact derivative rapidly reached the bloodstream, and underwent hydrolysis to the 3,4'-disubstituted derivative (**4**) (position 3/5- is more prone to hydrolysis than position 4'; see "Stability in PBS and blood"). The 3-glucuronide of **2** and the glucuronide with r.t. 3.08 of **3** were also detected, and reached maximum concentration at later times (t_{max} at 8h and 2h, respectively).

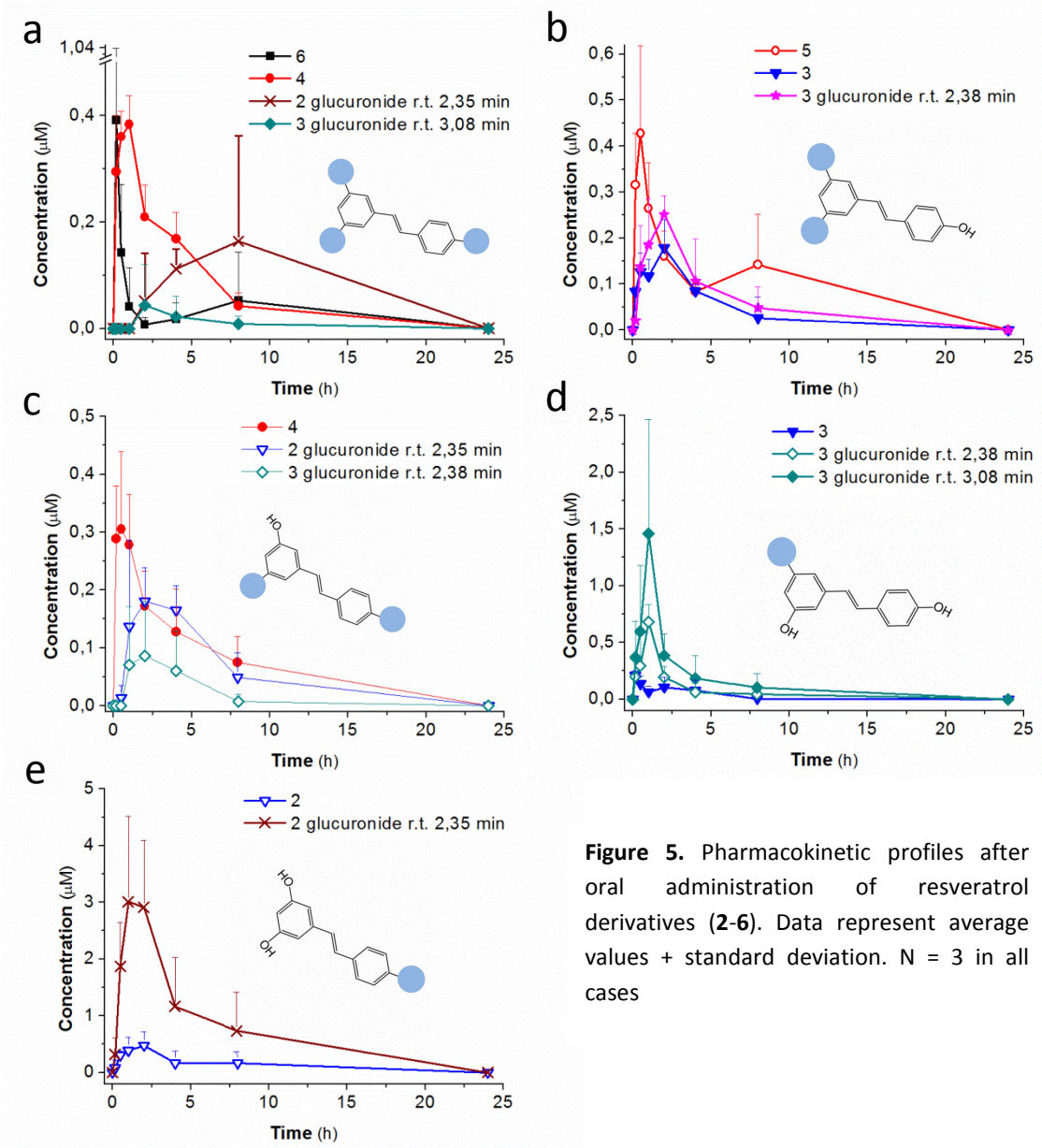

Figure 5. Pharmacokinetic profiles after oral administration of resveratrol derivatives (**2**-**6**). Data represent average values + standard deviation. N = 3 in all cases

Absorption of disubstituted derivatives was rapid, with the unmodified prodrug peaking in blood about 30 minutes after gavage. Administration of the 3,4'-(dihydroxypropyl) derivative (**4**) resulted in detectable levels of two of the possible glucuronides of **2** and **3** namely the ones with r.t. 2.35 and 2.38 min; no other intermediate products were detected. On the other hand, administration of the 3,5-(dihydroxypropyl) isomer **(5)** resulted in appearance of **3** and of its glucuronide with r.t. 2.38 min.

6-Deoxygalactosyl carbamate ester derivatives

Pharmacokinetic determinations provided no evidence of absorption for 3,4',5- and 3,5-derivatives (**11** and **10**) after oral administration.

Fig 4 shows the pharmacokinetic profiles of 3,4'-, 3- and 4'- substituted derivatives (**9**, **8** and **7** respectively). Compounds were generally poorly absorbed (fig 6**, a**). Absorption of **9** was rapid, reaching 10 minutes after administration a low peak blood concentration, which then remained approximately constant for up to 2 hours. **8** reached an early peak in blood (fig 6B), with the concentration then decaying in an approximately exponential manner, down to undetectable levels after about 4 hours. The 4'-substituted derivative (**7**) again differed significantly from its isomer: it showed a delayed absorption with the maximum concentration of total species in blood reached at approximately 2 hours after administration. Metabolites or resveratrol could not be reliably identified in any pharmacokinetic run with deoxygalactosyl carbamate ester derivatives.

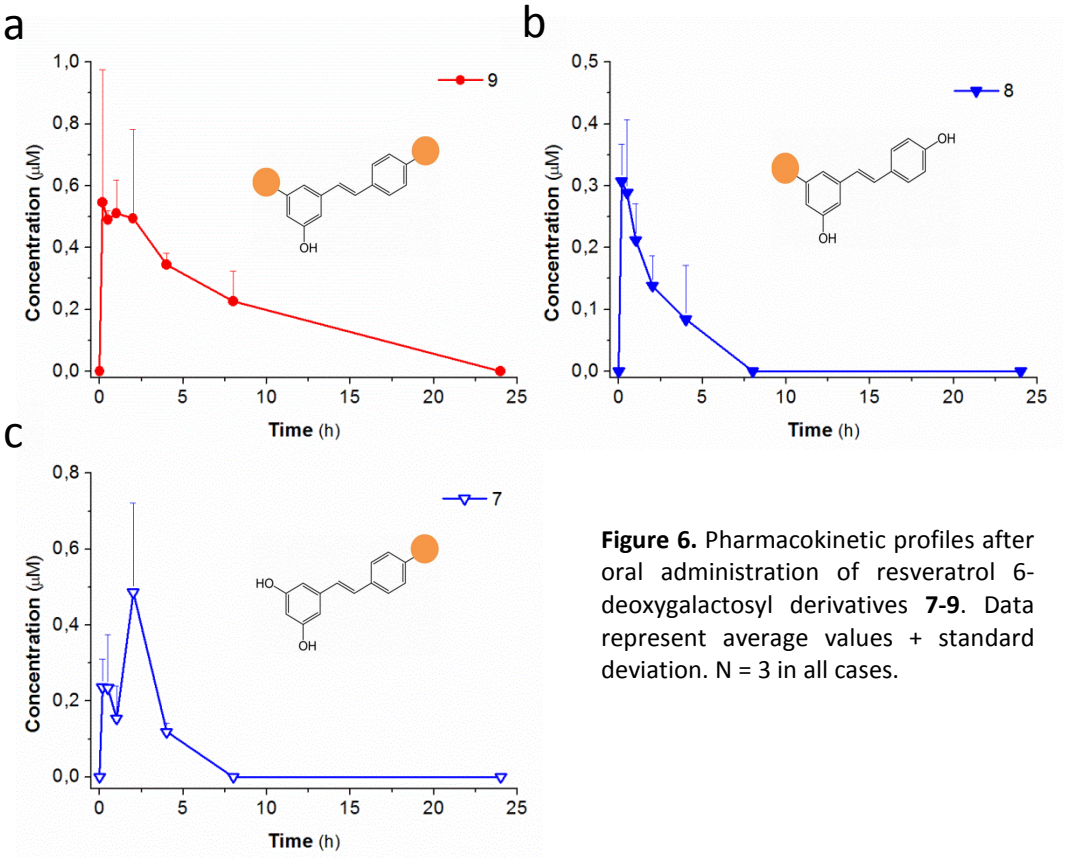

Figure 6. Pharmacokinetic profiles after oral administration of resveratrol 6-deoxygalactosyl derivatives **7-9**. Data represent average values + standard deviation. N = 3 in all cases.

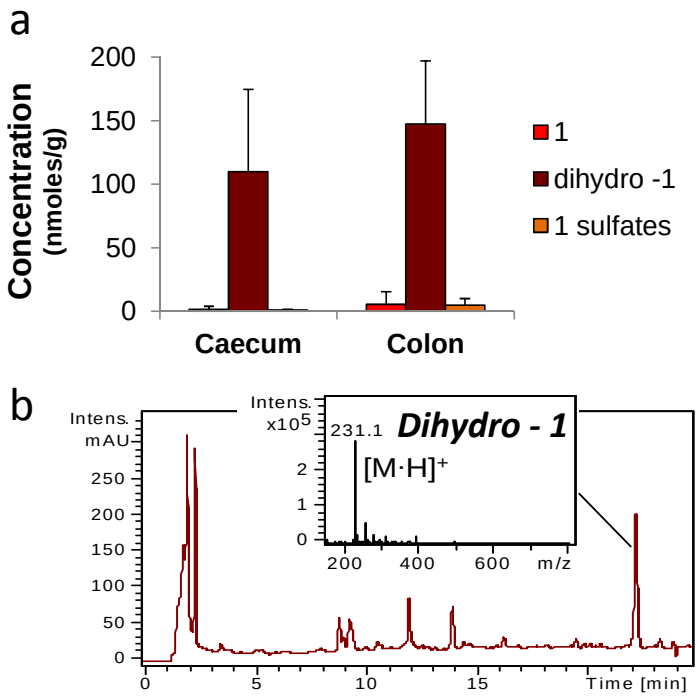

Figure 7. Resveratrol and its metabolites in the lower intestine of rats after chronic administration. a) Amounts of resveratrol dihydroresveratrol and resveratrol sulfates in caecum and colon after 48h of chronic treatment with approx. 220 µmol/kg×day of resveratrol. b) HPLC-UV chromatogram (286 nm) and ESI mass spectrum of dihydro-resveratrol (insert).

Intestinal Levels. The highly soluble derivative **11** did not enter systemic circulation after oral administration. Poor intestinal absorption may however be expected to result in high levels in the lumen of the lower intestinal tract, suggesting possible applications for the treatment of intestinal disorders.

After chronic administration, a striking difference was observed in the intestinal fate of resveratrol and **11**: in the colon and caecum the former was present mainly as its bacterial metabolite dihydroresveratrol (fig 7), while the latter was mainly present as partially hydrolyzed derivatives (fig 8). Low amounts of resveratrol and dihydroresveratrol were also detected.

Conclusions:

The new resveratrol derivatives presented here proved to have a satisfactory reactivity vs. chemical hydrolysis. In particular, they are stable in acid solution, and can therefore survive the gastric stage. In near-neutral solution and blood the rate of hydrolysis is relatively slow. *In vivo* experiments they displayed satisfactory adsorption in the case of mono-substituted dihydroxypropyl derivatives (**2**, **3**). Remarkably, sulphated metabolites were below detection limits in all cases. We were also unable to confirm formation of the products expected to arise from glucuronidation of di-protected species, while the compounds bearing only one promoiety could be acted upon by glucuronyltransferase activities *in vivo*.

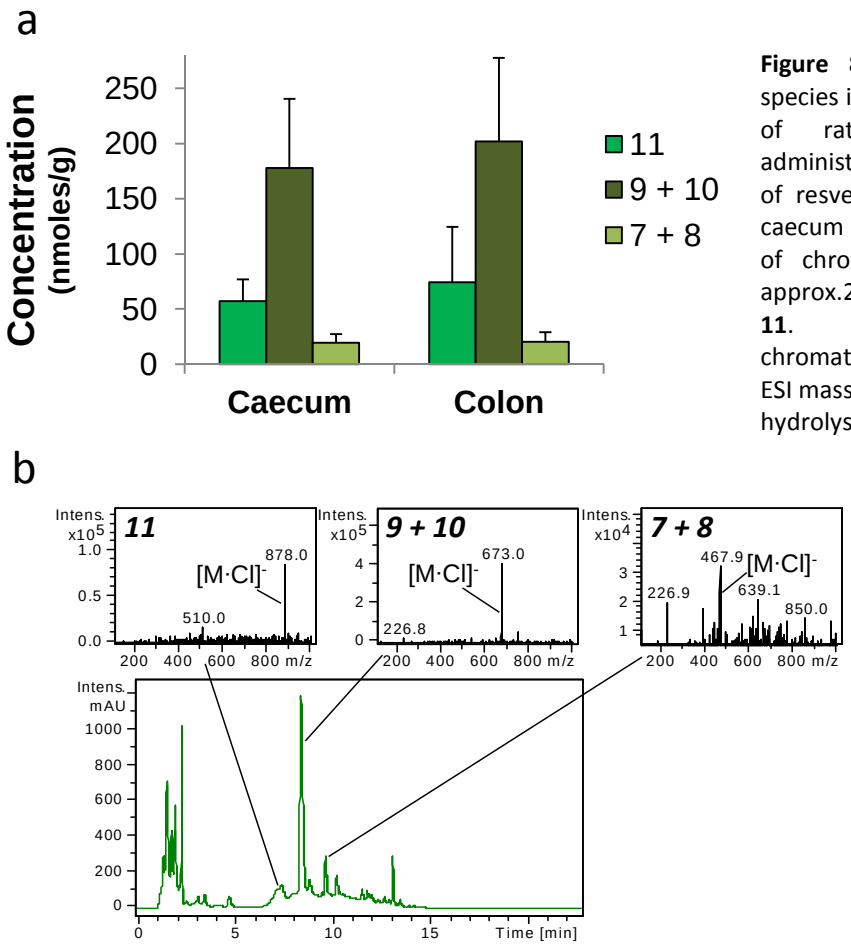

Figure 8. **11** and derived species in the lower intestine of rats after chronic administration. a) Amounts of resveratrol derivatives in caecum and colon after 48h of chronic treatment with approx.220 µmol/kg×day of **11**. b) HPLC-UV chromatogram (286 nm) and ESI mass spectra of **11** and its hydrolysis products (inserts).

Derivatives comprising the 6-deoxygalactose moiety (**7**-**11**) are more hydrophilic, and thus less permeable than derivatives **2**-**6** which incorporate the dihydroxypropyl moiety. The trisubstituted compound **11** is the most soluble, and was not absorbed in the gastrointestinal tract; however, interestingly, chronic administration of this compound resulted in its accumulation in the intestine. The presence in colon and caecum of partially hydrolyzed derivatives of **11** suggests protracted gradual release of intact resveratrol, which would be expected to be rapidly reduced to dihydroresveratrol by bacterial enzymes. These findings suggest a possible use of glycosyl-resveratrol derivatives for the treatment of colitis and prevention of colon cancer.

Acknowledgments:

We thank Mr. M. Ghidotti for technical help, Dr. Alice Bradaschia for help with some of the pharmacokinetics, and NÓOS Srl for generous support and consultations. This work was also supported by grants from the Fondazione Cassa di Risparmio di Padova e Rovigo (CARIPARO) ("Developing a Pharmacology of Polyphenols"), from the Italian Ministry of the University and Research (PRIN n. 20107Z8XBW_004), and by the CNR Project of Special Interest on Aging.

References:

1. Mattarei, A.; Azzolini, M.; Carraro, M.; Sassi, N.; Zoratti, M.; Paradisi, C.; Biasutto, L. Acetal derivatives as prodrugs of resveratrol. *Molecular pharmaceutics* **2013,** *10*, (7), 2781-92.
2. Khurana, S.; Venkataraman, K.; Hollingsworth, A.; Piche, M.; Tai, T. C. Polyphenols: benefits to the cardiovascular system in health and in aging. *Nutrients* **2013,** *5*, (10), 3779-827.
3. Mattison, J. A.; Wang, M.; Bernier, M.; Zhang, J.; Park, S. S.; Maudsley, S.; An, S. S.; Santhanam, L.; Martin, B.; Faulkner, S.; Morrell, C.; Baur, J. A.; Peshkin, L.; Sosnowska, D.; Csiszar, A.; Herbert, R. L.; Tilmont, E. M.; Ungvari, Z.; Pearson, K. J.; Lakatta, E. G.; de Cabo, R. Resveratrol prevents high fat/sucrose diet-induced central arterial wall inflammation and stiffening in nonhuman primates. *Cell Metab* **2014,** *20*, (1), 183-90.
4. Wong, R. H.; Coates, A. M.; Buckley, J. D.; Howe, P. R. Evidence for circulatory benefits of resveratrol in humans. *Ann N Y Acad Sci* **2013,** *1290*, 52-8.
5. Bigford, G. E.; Del Rossi, G. Supplemental substances derived from foods as adjunctive therapeutic agents for treatment of neurodegenerative diseases and disorders. *Adv Nutr* **2014,** *5*, (4), 394-403.
6. Li, F.; Gong, Q.; Dong, H.; Shi, J. Resveratrol, a neuroprotective supplement for Alzheimer's disease. *Curr Pharm Des* **2012,** *18*, (1), 27-33.
7. Pallas, M.; Porquet, D.; Vicente, A.; Sanfeliu, C. Resveratrol: new avenues for a natural compound in neuroprotection. *Curr Pharm Des* **2013,** *19*, (38), 6726-31.
8. Porquet, D.; Grinan-Ferre, C.; Ferrer, I.; Camins, A.; Sanfeliu, C.; Del Valle, J.; Pallas, M. Neuroprotective role of trans-resveratrol in a murine model of familial Alzheimer's disease. *J Alzheimers Dis* **2014,** *42*, (4), 1209-20.
9. Marchal, J.; Pifferi, F.; Aujard, F. Resveratrol in mammals: effects on aging biomarkers, age-related diseases, and life span. *Ann N Y Acad Sci* **2013,** *1290*, 67-73.
10. Witte, A. V.; Kerti, L.; Margulies, D. S.; Floel, A. Effects of resveratrol on memory performance, hippocampal functional connectivity, and glucose metabolism in healthy older adults. *J Neurosci* **2014,** *34*, (23), 7862-70.
11. Hausenblas, H. A.; Schoulda, J. A.; Smoliga, J. M. Resveratrol treatment as an adjunct to pharmacological management in type 2 diabetes mellitus-systematic review and meta-analysis. *Mol Nutr Food Res* **2014**.
12. Timmers, S.; Hesselink, M. K.; Schrauwen, P. Therapeutic potential of resveratrol in obesity and type 2 diabetes: new avenues for health benefits? *Ann N Y Acad Sci* **2013,** *1290*, 83-9.
13. Wang, S.; Moustaid-Moussa, N.; Chen, L.; Mo, H.; Shastri, A.; Su, R.; Bapat, P.; Kwun, I.; Shen, C. L. Novel insights of dietary polyphenols and obesity. *The Journal of nutritional biochemistry* **2014,** *25*, (1), 1-18.
14. Shukla, Y.; Singh, R. Resveratrol and cellular mechanisms of cancer prevention. *Ann N Y Acad Sci* **2011,** *1215*, 1-8.
15. Yang, X.; Li, X.; Ren, J. From French Paradox to cancer treatment: anti-cancer activities and mechanisms of resveratrol. *Anticancer Agents Med Chem* **2014,** *14*, (6), 806-25.
16. Coenye, T.; Brackman, G.; Rigole, P.; De Witte, E.; Honraet, K.; Rossel, B.; Nelis, H. J. Eradication of Propionibacterium acnes biofilms by plant extracts and putative identification of icariin, resveratrol and salidroside as active compounds. *Phytomedicine* **2012,** *19*, (5), 409-12.
17. Fabbrocini, G.; Staibano, S.; De Rosa, G.; Battimiello, V.; Fardella, N.; Ilardi, G.; La Rotonda, M. I.; Longobardi, A.; Mazzella, M.; Siano, M.; Pastore, F.; De Vita, V.; Vecchione, M. L.; Ayala, F. Resveratrol-containing gel for the treatment of acne vulgaris: a single-blind, vehicle-controlled, pilot study. *Am J Clin Dermatol* **2011,** *12*, (2), 133-41.
18. Kwon, Y. R.; Son, K. J.; Pandit, S.; Kim, J. E.; Chang, K. W.; Jeon, J. G. Bioactivity-guided separation of anti-acidogenic substances against Streptococcus mutans UA 159 from Polygonum cuspidatum. *Oral Dis* **2010,** *16*, (2), 204-9.

19. Lv, G.; Zhu, H.; Zhou, F.; Lin, Z.; Lin, G.; Li, C. AMP-activated protein kinase activation protects gastric epithelial cells from Helicobacter pylori-induced apoptosis. *Biochem Biophys Res Commun* **2014**.
20. Zaidi, S. F.; Ahmed, K.; Yamamoto, T.; Kondo, T.; Usmanghani, K.; Kadowaki, M.; Sugiyama, T. Effect of resveratrol on Helicobacter pylori-induced interleukin-8 secretion, reactive oxygen species generation and morphological changes in human gastric epithelial cells. *Biol Pharm Bull* **2009,** *32*, (11), 1931-5.
21. Yu, W.; Wan, Z.; Qiu, X. F.; Chen, Y.; Dai, Y. T. Resveratrol, an activator of SIRT1, restores erectile function in streptozotocin-induced diabetic rats. *Asian J Androl* **2013,** *15*, (5), 646-51.
22. Mobasheri, A.; Shakibaei, M. Osteogenic effects of resveratrol in vitro: potential for the prevention and treatment of osteoporosis. *Ann N Y Acad Sci* **2013,** *1290*, 59-66.
23. Rajguru, R. Military aircrew and noise-induced hearing loss: prevention and management. *Aviat Space Environ Med* **2013,** *84*, (12), 1268-76.
24. Seidman, M.; Babu, S.; Tang, W.; Naem, E.; Quirk, W. S. Effects of resveratrol on acoustic trauma. *Otolaryngol Head Neck Surg* **2003,** *129*, (5), 463-70.
25. Dolinsky, V. W.; Chakrabarti, S.; Pereira, T. J.; Oka, T.; Levasseur, J.; Beker, D.; Zordoky, B. N.; Morton, J. S.; Nagendran, J.; Lopaschuk, G. D.; Davidge, S. T.; Dyck, J. R. Resveratrol prevents hypertension and cardiac hypertrophy in hypertensive rats and mice. *Biochim Biophys Acta* **2013,** *1832*, (10), 1723-33.
26. Okada, Y.; Oh-oka, K.; Nakamura, Y.; Ishimaru, K.; Matsuoka, S.; Okumura, K.; Ogawa, H.; Hisamoto, M.; Okuda, T.; Nakao, A. Dietary resveratrol prevents the development of food allergy in mice. *PLoS One* **2012,** *7*, (9), e44338.
27. Bola, C.; Bartlett, H.; Eperjesi, F. Resveratrol and the eye: activity and molecular mechanisms. *Graefes Arch Clin Exp Ophthalmol* **2014,** *252*, (5), 699-713.
28. Nagineni, C. N.; Raju, R.; Nagineni, K. K.; Kommineni, V. K.; Cherukuri, A.; Kutty, R. K.; Hooks, J. J.; Detrick, B. Resveratrol Suppresses Expression of VEGF by Human Retinal Pigment Epithelial Cells: Potential Nutraceutical for Age-related Macular Degeneration. *Aging Dis* **2014,** *5*, (2), 88-100.
29. Wu, R. E.; Huang, W. C.; Liao, C. C.; Chang, Y. K.; Kan, N. W.; Huang, C. C. Resveratrol protects against physical fatigue and improves exercise performance in mice. *Molecules* **2013,** *18*, (4), 4689-702.
30. Biasutto, L.; Mattarei, A.; Zoratti, M. Resveratrol and health: the starting point. *Chembiochem* **2012,** *13*, (9), 1256-9.
31. Chung, J. H.; Manganiello, V.; Dyck, J. R. Resveratrol as a calorie restriction mimetic: therapeutic implications. *Trends Cell Biol* **2012,** *22*, (10), 546-54.
32. Park, S. J.; Ahmad, F.; Philp, A.; Baar, K.; Williams, T.; Luo, H.; Ke, H.; Rehmann, H.; Taussig, R.; Brown, A. L.; Kim, M. K.; Beaven, M. A.; Burgin, A. B.; Manganiello, V.; Chung, J. H. Resveratrol ameliorates aging-related metabolic phenotypes by inhibiting cAMP phosphodiesterases. *Cell* **2012,** *148*, (3), 421-33.
33. Hwang, J. T.; Kwon, D. Y.; Yoon, S. H. AMP-activated protein kinase: a potential target for the diseases prevention by natural occurring polyphenols. *N Biotechnol* **2009,** *26*, (1-2), 17-22.
34. Chan, A. Y.; Dolinsky, V. W.; Soltys, C. L.; Viollet, B.; Baksh, S.; Light, P. E.; Dyck, J. R. Resveratrol inhibits cardiac hypertrophy via AMP-activated protein kinase and Akt. *J Biol Chem* **2008,** *283*, (35), 24194-201.
35. Dasgupta, B.; Milbrandt, J. Resveratrol stimulates AMP kinase activity in neurons. *Proc Natl Acad Sci U S A* **2007,** *104*, (17), 7217-22.
36. Ding, D. F.; You, N.; Wu, X. M.; Xu, J. R.; Hu, A. P.; Ye, X. L.; Zhu, Q.; Jiang, X. Q.; Miao, H.; Liu, C.; Lu, Y. B. Resveratrol attenuates renal hypertrophy in early-stage diabetes by activating AMPK. *Am J Nephrol* **2010,** *31*, (4), 363-74.
37. Gu, X. S.; Wang, Z. B.; Ye, Z.; Lei, J. P.; Li, L.; Su, D. F.; Zheng, X. Resveratrol, an activator of SIRT1, upregulates AMPK and improves cardiac function in heart failure. *Genet Mol Res* **2014,** *13*, (1), 323-35.

38. Park, C. E.; Kim, M. J.; Lee, J. H.; Min, B. I.; Bae, H.; Choe, W.; Kim, S. S.; Ha, J. Resveratrol stimulates glucose transport in C2C12 myotubes by activating AMP-activated protein kinase. *Exp Mol Med* **2007,** *39*, (2), 222-9.
39. Puissant, A.; Robert, G.; Fenouille, N.; Luciano, F.; Cassuto, J. P.; Raynaud, S.; Auberger, P. Resveratrol promotes autophagic cell death in chronic myelogenous leukemia cells via JNK-mediated p62/SQSTM1 expression and AMPK activation. *Cancer Res* **2010,** *70*, (3), 1042-52.
40. Um, J. H.; Park, S. J.; Kang, H.; Yang, S.; Foretz, M.; McBurney, M. W.; Kim, M. K.; Viollet, B.; Chung, J. H. AMP-activated protein kinase-deficient mice are resistant to the metabolic effects of resveratrol. *Diabetes* **2010,** *59*, (3), 554-63.
41. Vingtdeux, V.; Giliberto, L.; Zhao, H.; Chandakkar, P.; Wu, Q.; Simon, J. E.; Janle, E. M.; Lobo, J.; Ferruzzi, M. G.; Davies, P.; Marambaud, P. AMP-activated protein kinase signaling activation by resveratrol modulates amyloid-beta peptide metabolism. *J Biol Chem* **2010,** *285*, (12), 9100-13.
42. Yun, H.; Park, S.; Kim, M. J.; Yang, W. K.; Im, D. U.; Yang, K. R.; Hong, J.; Choe, W.; Kang, I.; Kim, S. S.; Ha, J. AMP-activated protein kinase mediates the antioxidant effects of resveratrol through regulation of the transcription factor FoxO1. *Febs j* **2014,** *281*, (19), 4421-38.
43. Canto, C.; Auwerx, J. AMP-activated protein kinase and its downstream transcriptional pathways. *Cell Mol Life Sci* **2010,** *67*, (20), 3407-23.
44. Grahame Hardie, D. AMP-activated protein kinase: a key regulator of energy balance with many roles in human disease. *J Intern Med* **2014**.
45. Hubbard, B. P.; Sinclair, D. A. Small molecule SIRT1 activators for the treatment of aging and age-related diseases. *Trends Pharmacol Sci* **2014,** *35*, (3), 146-54.
46. Sinclair, D. A.; Guarente, L. Small-molecule allosteric activators of sirtuins. *Annu Rev Pharmacol Toxicol* **2014,** *54*, 363-80.
47. Price, N. L.; Gomes, A. P.; Ling, A. J.; Duarte, F. V.; Martin-Montalvo, A.; North, B. J.; Agarwal, B.; Ye, L.; Ramadori, G.; Teodoro, J. S.; Hubbard, B. P.; Varela, A. T.; Davis, J. G.; Varamini, B.; Hafner, A.; Moaddel, R.; Rolo, A. P.; Coppari, R.; Palmeira, C. M.; de Cabo, R.; Baur, J. A.; Sinclair, D. A. SIRT1 is required for AMPK activation and the beneficial effects of resveratrol on mitochondrial function. *Cell Metab* **2012,** *15*, (5), 675-90.
48. Biasutto, L.; Szabo, I.; Zoratti, M. Mitochondrial effects of plant-made compounds. *Antioxidants & redox signaling* **2011,** *15*, (12), 3039-59.
49. Dunlop, E. A.; Tee, A. R. The kinase triad, AMPK, mTORC1 and ULK1, maintains energy and nutrient homoeostasis. *Biochem Soc Trans* **2013,** *41*, (4), 939-43.
50. Russell, R. C.; Yuan, H. X.; Guan, K. L. Autophagy regulation by nutrient signaling. *Cell Res* **2014,** *24*, (1), 42-57.
51. Inoki, K.; Kim, J.; Guan, K. L. AMPK and mTOR in cellular energy homeostasis and drug targets. *Annu Rev Pharmacol Toxicol* **2012,** *52*, 381-400.
52. Widlund, A. L.; Baur, J. A.; Vang, O. mTOR: more targets of resveratrol? *Expert Rev Mol Med* **2013,** *15*, e10.
53. Xu, J.; Ji, J.; Yan, X. H. Cross-talk between AMPK and mTOR in regulating energy balance. *Crit Rev Food Sci Nutr* **2012,** *52*, (5), 373-81.
54. Tan, H. K.; Moad, A. I.; Tan, M. L. The mTOR signalling pathway in cancer and the potential mTOR inhibitory activities of natural phytochemicals. *Asian Pac J Cancer Prev* **2014,** *15*, (16), 6463-75.
55. Wilson, C. M.; Magnaudeix, A.; Yardin, C.; Terro, F. Autophagy dysfunction and its link to Alzheimer's disease and type II diabetes mellitus. *CNS Neurol Disord Drug Targets* **2014,** *13*, (2), 226-46.
56. Chen, S.; Zhu, X.; Lai, X.; Xiao, T.; Wen, A.; Zhang, J. Combined Cancer Therapy with Non-Conventional Drugs: All Roads Lead to AMPK. *Mini Rev Med Chem* **2014,** *14*, (8), 642-54.
57. Mercken, E. M.; Mitchell, S. J.; Martin-Montalvo, A.; Minor, R. K.; Almeida, M.; Gomes, A. P.; Scheibye-Knudsen, M.; Palacios, H. H.; Licata, J. J.; Zhang, Y.; Becker, K. G.; Khraiwesh, H.; Gonzalez-Reyes, J. A.; Villalba, J. M.; Baur, J. A.; Elliott, P.; Westphal, C.; Vlasuk, G. P.; Ellis, J. L.;

Sinclair, D. A.; Bernier, M.; de Cabo, R. SRT2104 extends survival of male mice on a standard diet and preserves bone and muscle mass. *Aging Cell* **2014,** *13*, (5), 787-96.
58. Mitchell, S. J.; Martin-Montalvo, A.; Mercken, E. M.; Palacios, H. H.; Ward, T. M.; Abulwerdi, G.; Minor, R. K.; Vlasuk, G. P.; Ellis, J. L.; Sinclair, D. A.; Dawson, J.; Allison, D. B.; Zhang, Y.; Becker, K. G.; Bernier, M.; de Cabo, R. The SIRT1 activator SRT1720 extends lifespan and improves health of mice fed a standard diet. *Cell Rep* **2014,** *6*, (5), 836-43.
59. Chen, C. C.; Lin, J. T.; Cheng, Y. F.; Kuo, C. Y.; Huang, C. F.; Kao, S. H.; Liang, Y. J.; Cheng, C. Y.; Chen, H. M. Amelioration of LPS-induced inflammation response in microglia by AMPK activation. *Biomed Res Int* **2014,** *2014*, 692061.
60. Park, D. W.; Jiang, S.; Liu, Y.; Siegal, G. P.; Inoki, K.; Abraham, E.; Zmijewski, J. W. GSK3beta-dependent inhibition of AMPK potentiates activation of neutrophils and macrophages and enhances severity of acute lung injury. *Am J Physiol Lung Cell Mol Physiol* **2014,** *307*, (10), L735-45.
61. Gupta, S. C.; Tyagi, A. K.; Deshmukh-Taskar, P.; Hinojosa, M.; Prasad, S.; Aggarwal, B. B. Downregulation of tumor necrosis factor and other proinflammatory biomarkers by polyphenols. *Arch Biochem Biophys* **2014,** *559*, 91-9.
62. Renaud, J.; Martinoli, M. G. Resveratrol as a protective molecule for neuroinflammation: a review of mechanisms. *Curr Pharm Biotechnol* **2014,** *15*, (4), 318-29.
63. Gupta, S. C.; Kim, J. H.; Kannappan, R.; Reuter, S.; Dougherty, P. M.; Aggarwal, B. B. Role of nuclear factor kappaB-mediated inflammatory pathways in cancer-related symptoms and their regulation by nutritional agents. *Exp Biol Med (Maywood)* **2011,** *236*, (6), 658-71.
64. Kundu, J. K.; Shin, Y. K.; Kim, S. H.; Surh, Y. J. Resveratrol inhibits phorbol ester-induced expression of COX-2 and activation of NF-kappaB in mouse skin by blocking IkappaB kinase activity. *Carcinogenesis* **2006,** *27*, (7), 1465-74.
65. Kundu, J. K.; Shin, Y. K.; Surh, Y. J. Resveratrol modulates phorbol ester-induced pro-inflammatory signal transduction pathways in mouse skin in vivo: NF-kappaB and AP-1 as prime targets. *Biochem Pharmacol* **2006,** *72*, (11), 1506-15.
66. Kundu, J. K.; Surh, Y. J. Inflammation: gearing the journey to cancer. *Mutat Res* **2008,** *659*, (1-2), 15-30.
67. Mariani, F.; Sena, P.; Roncucci, L. Inflammatory pathways in the early steps of colorectal cancer development. *World J Gastroenterol* **2014,** *20*, (29), 9716-31.
68. Sethi, G.; Shanmugam, M. K.; Ramachandran, L.; Kumar, A. P.; Tergaonkar, V. Multifaceted link between cancer and inflammation. *Biosci Rep* **2012,** *32*, (1), 1-15.
69. Conteduca, V.; Sansonno, D.; Russi, S.; Dammacco, F. Precancerous colorectal lesions (Review). *Int J Oncol* **2013,** *43*, (4), 973-84.
70. Janakiram, N. B.; Rao, C. V. The role of inflammation in colon cancer. *Adv Exp Med Biol* **2014,** *816*, 25-52.
71. Rasch, S.; Algul, H. A clinical perspective on the role of chronic inflammation in gastrointestinal cancer. *Clin Exp Gastroenterol* **2014,** *7*, 261-72.
72. Kanneganti, M.; Mino-Kenudson, M.; Mizoguchi, E. Animal models of colitis-associated carcinogenesis. *J Biomed Biotechnol* **2011,** *2011*, 342637.
73. Neurath, M. F. Animal models of inflammatory bowel diseases: illuminating the pathogenesis of colitis, ileitis and cancer. *Dig Dis* **2012,** *30 Suppl 1*, 91-4.
74. Cui, X.; Jin, Y.; Hofseth, A. B.; Pena, E.; Habiger, J.; Chumanevich, A.; Poudyal, D.; Nagarkatti, M.; Nagarkatti, P. S.; Singh, U. P.; Hofseth, L. J. Resveratrol suppresses colitis and colon cancer associated with colitis. *Cancer Prev Res (Phila)* **2010,** *3*, (4), 549-59.
75. Juan, M. E.; Alfaras, I.; Planas, J. M. Colorectal cancer chemoprevention by trans-resveratrol. *Pharmacol Res* **2012,** *65*, (6), 584-91.
76. Larrosa, M.; Yanez-Gascon, M. J.; Selma, M. V.; Gonzalez-Sarrias, A.; Toti, S.; Ceron, J. J.; Tomas-Barberan, F.; Dolara, P.; Espin, J. C. Effect of a low dose of dietary resveratrol on colon microbiota, inflammation and tissue damage in a DSS-induced colitis rat model. *J Agric Food Chem* **2009,** *57*, (6), 2211-20.

77. Sanchez-Fidalgo, S.; Cardeno, A.; Villegas, I.; Talero, E.; de la Lastra, C. A. Dietary supplementation of resveratrol attenuates chronic colonic inflammation in mice. *Eur J Pharmacol* **2010,** *633*, (1-3), 78-84.
78. Sharma, M.; Mohapatra, J.; Wagh, A.; Patel, H. M.; Pandey, D.; Kadam, S.; Argade, A.; Deshpande, S. S.; Shah, G. B.; Chatterjee, A.; Jain, M. R. Involvement of TACE in colon inflammation: a novel mechanism of regulation via SIRT-1 activation. *Cytokine* **2014,** *66*, (1), 30-9.
79. Cottart, C. H.; Nivet-Antoine, V.; Laguillier-Morizot, C.; Beaudeux, J. L. Resveratrol bioavailability and toxicity in humans. *Mol Nutr Food Res* **2010,** *54*, (1), 7-16.
80. Delmas, D.; Aires, V.; Limagne, E.; Dutartre, P.; Mazue, F.; Ghiringhelli, F.; Latruffe, N. Transport, stability, and biological activity of resveratrol. *Ann N Y Acad Sci* **2011,** *1215*, 48-59.
81. Muzzio, M.; Huang, Z.; Hu, S. C.; Johnson, W. D.; McCormick, D. L.; Kapetanovic, I. M. Determination of resveratrol and its sulfate and glucuronide metabolites in plasma by LC-MS/MS and their pharmacokinetics in dogs. *J Pharm Biomed Anal* **2012,** *59*, 201-8.
82. Rotches-Ribalta, M.; Andres-Lacueva, C.; Estruch, R.; Escribano, E.; Urpi-Sarda, M. Pharmacokinetics of resveratrol metabolic profile in healthy humans after moderate consumption of red wine and grape extract tablets. *Pharmacol Res* **2012,** *66*, (5), 375-82.
83. Vitaglione, P.; Sforza, S.; Galaverna, G.; Ghidini, C.; Caporaso, N.; Vescovi, P. P.; Fogliano, V.; Marchelli, R. Bioavailability of trans-resveratrol from red wine in humans. *Mol Nutr Food Res* **2005,** *49*, (5), 495-504.
84. Walle, T. Bioavailability of resveratrol. *Annals of the New York Academy of Sciences* **2011,** *1215*, 9-15.
85. Wenzel, E.; Soldo, T.; Erbersdobler, H.; Somoza, V. Bioactivity and metabolism of trans-resveratrol orally administered to Wistar rats. *Mol Nutr Food Res* **2005,** *49*, (5), 482-94.
86. Yu, C.; Shin, Y. G.; Chow, A.; Li, Y.; Kosmeder, J. W.; Lee, Y. S.; Hirschelman, W. H.; Pezzuto, J. M.; Mehta, R. G.; van Breemen, R. B. Human, rat, and mouse metabolism of resveratrol. *Pharmaceutical research* **2002,** *19*, (12), 1907-14.
87. Bode, L. M.; Bunzel, D.; Huch, M.; Cho, G. S.; Ruhland, D.; Bunzel, M.; Bub, A.; Franz, C. M.; Kulling, S. E. In vivo and in vitro metabolism of trans-resveratrol by human gut microbiota. *Am J Clin Nutr* **2013,** *97*, (2), 295-309.
88. Rotches-Ribalta, M.; Urpi-Sarda, M.; Llorach, R.; Boto-Ordonez, M.; Jauregui, O.; Chiva-Blanch, G.; Perez-Garcia, L.; Jaeger, W.; Guillen, M.; Corella, D.; Tinahones, F. J.; Estruch, R.; Andres-Lacueva, C. Gut and microbial resveratrol metabolite profiling after moderate long-term consumption of red wine versus dealcoholized red wine in humans by an optimized ultra-high-pressure liquid chromatography tandem mass spectrometry method. *J Chromatogr A* **2012,** *1265*, 105-13.
89. Visioli, F. The resveratrol fiasco. *Pharmacol Res* **2014**.
90. Amri, A.; Chaumeil, J. C.; Sfar, S.; Charrueau, C. Administration of resveratrol: What formulation solutions to bioavailability limitations? *J Control Release* **2012,** *158*, (2), 182-93.
91. Biasutto, L.; Mattarei, A.; Sassi, N.; Azzolini, M.; Romio, M.; Paradisi, C.; Zoratti, M. Improving the efficacy of plant polyphenols. *Anticancer Agents Med Chem* **2014,** *14*, (10), 1332-42.
92. Pangeni, R.; Sahni, J. K.; Ali, J.; Sharma, S.; Baboota, S. Resveratrol: review on therapeutic potential and recent advances in drug delivery. *Expert Opin Drug Deliv* **2014,** *11*, (8), 1285-98.
93. Santos, A. C.; Veiga, F.; Ribeiro, A. J. New delivery systems to improve the bioavailability of resveratrol. *Expert Opin Drug Deliv* **2011,** *8*, (8), 973-90.
94. Biasutto, L.; Zoratti, M. Prodrugs of quercetin and resveratrol: a strategy under development. *Current drug metabolism* **2014,** *15*, (1), 77-95.
95. Abdin, A. A. Targeting sphingosine kinase 1 (SphK1) and apoptosis by colon-specific delivery formula of resveratrol in treatment of experimental ulcerative colitis in rats. *Eur J Pharmacol* **2013,** *718*, (1-3), 145-53.
96. Larrosa, M.; Tome-Carneiro, J.; Yanez-Gascon, M. J.; Alcantara, D.; Selma, M. V.; Beltran, D.; Garcia-Conesa, M. T.; Urban, C.; Lucas, R.; Tomas-Barberan, F.; Morales, J. C.; Espin, J. C.

Preventive oral treatment with resveratrol pro-prodrugs drastically reduce colon inflammation in rodents. *J Med Chem* **2010,** *53*, (20), 7365-76.
97. Mattarei, A.; Carraro, M.; Azzolini, M.; Paradisi, C.; Zoratti, M.; Biasutto, L. New water-soluble carbamate ester derivatives of resveratrol. *Molecules* **2014,** *19*, (10), 15900-17.
98. Ertl, P.; Rohde, B.; Selzer, P. Fast calculation of molecular polar surface area as a sum of fragment-based contributions and its application to the prediction of drug transport properties. *J Med Chem* **2000,** *43*, (20), 3714-7.
99. Biasutto, L.; Marotta, E.; Bradaschia, A.; Fallica, M.; Mattarei, A.; Garbisa, S.; Zoratti, M.; Paradisi, C. Soluble polyphenols: synthesis and bioavailability of 3,4',5-tri(alpha-D-glucose-3-O-succinyl) resveratrol. *Bioorganic & medicinal chemistry letters* **2009,** *19*, (23), 6721-4.
100. Biasutto, L.; Marotta, E.; Garbisa, S.; Zoratti, M.; Paradisi, C. Determination of quercetin and resveratrol in whole blood--implications for bioavailability studies. *Molecules (Basel, Switzerland)* **2010,** *15*, (9), 6570-9.
101. Azzolini, M.; La Spina, M.; Mattarei, A.; Paradisi, C.; Zoratti, M.; Biasutto, L. Pharmacokinetics and tissue distribution of pterostilbene in the rat. *Molecular nutrition & food research* **2014,** *58*, (11), 2122-32.
102. Sogorb, M. A.; Alvarez-Escalante, C.; Carrera, V.; Vilanova, E. An in vitro approach for demonstrating the critical role of serum albumin in the detoxication of the carbamate carbaryl at in vivo toxicologically relevant concentrations. *Archives of toxicology* **2007,** *81*, (2), 113-9.
103. Sogorb, M. A.; Vilanova, E. Serum albumins and detoxication of anti-cholinesterase agents. *Chemico-biological interactions* **2010,** *187*, (1-3), 325-9.
104. Hansen, K. T.; Faarup, P.; Bundgaard, H. Carbamate ester prodrugs of dopaminergic compounds: synthesis, stability, and bioconversion. *J Pharm Sci* **1991,** *80*, (8), 793-8.

Appendix:

Synthesis of derivatives 2-9

Derivatives were synthesized by the group of prof. Cristina Paradisi, Department of Chemical Sciences, University of Padova.

[N-(2,2-dimethyl-1,3-dioxolane-4-methan)-carbamoyl]-4-nitrophenol (13): Bis-4-(nitrophenyl) carbonate (3.47 g, 11.4 mmol, 1 eq.) in 20 mL of anhydrous THF and DMAP (2.79 g, 22.8 mmol, 2 eq.) were mixed in a 100 mL round-bottom flask with a magnetic stirrer under N_2. 2,2-dimethyl-1,3-dioxolane-4-methanamine (**12**, 1.5 g, 11.4 mmol, 1 eq.) in THF (20 mL) was then added dropwise at RT. After three hours the mixture was taken up in EtOAc (150 mL), transferred to a 500 mL separation funnel and washed with 0.5 M HCl (3 × 150 mL). The organic phase was then dried over $MgSO_4$ and filtered. The solvent was evaporated under reduced pressure and the residue was purified by flash chromatography on silica gel (eluent: CH_2Cl_2/EtOAc, 9.5:0.5) to afford **13** (75% yield). ^{1}H-NMR (250 MHz, $CDCl_3$) δ (ppm): 1.38 (s, 3H, -C*H*$_3$), 1.48 (s, 3H, -C*H*$_3$), 3.28-3.61 (m, 2H, -NH-C*H*$_2$), 3.70-4.14 (m, 2H, -C*H*$_2$-), 4.28-4.37 (m, 1H, -C*H*-), 7.32 (d, 2H, Ar-*H*, $^3J_{H-H}$: 9.25 Hz), 8.25 (d, 2H, Ar-*H*, $^3J_{H-H}$: 9.25 Hz); ^{13}C-NMR (62.9 MHz, $CDCl_3$) δ (ppm): 155.7, 153.3, 144.7, 125.1, 121.9, 109.6, 74.2, 66.5, 43.6, 26.7, 25.0; ESI-MS (ion trap): m/z 297 $[M+H]^+$.

(4'-mono-, 3-mono-, 3,4'-di-, 3,5-di-, 3,4',5-tri-) [N-(2,2-dimethyl-1,3-dioxolane-4-methan)-carbamoyl]-resveratrol (14-18): **13** (1.24 g, 4.2 mmol, 2.6 eq.) and pyridine (10 mL) were placed in a 100 mL round-bottom flask with magnetic stirrer and under N_2. Resveratrol (**1**, 0.37 g, 1.6 mmol, 1.0 eq.) and DMAP (0.79 g, 6.4 mmol, 4.0 eq.) in pyridine (10 mL) was added and the reaction was allowed to proceed at 70°C overnight. The mixture was then taken up with 150 mL of EtOAc, transferred to a separation funnel and washed with 0.5 M HCl (5 × 150 mL). The organic phase

was then dried over $MgSO_4$ and filtered. The solvent was evaporated under reduced pressure. The resulting solid was purified by flash chromatography (eluent: CH_2Cl_2/Acetone, 7.5:2.5) to afford 0.57 g of a mixture of **14**-**18** used as such for the subsequent synthetic step. ESI-MS (ion trap): **14**, **15**: m/z 386 $[M+H]^+$; **16**, **17**: m/z 543 $[M+H]^+$; **18**: m/z 700 $[M+H]^+$.

(4'-mono-, 3-mono-, 3,4'-di-, 3,5-di-, 3,4',5-tri-)[N-(2,3-dihydroxypropyl)-carbamoyl]-resveratrol conjugates (2-6): The mixture (**14**-**18**, 0.57 g) obtained in the previous step was added to a solution of TFA/water (90:10, 5 mL). The resulting mixture was vigorously stirred for 1.5 h at RT and then dried under vacuum. The residue was then separated by preparative HPLC (from 0% to 40% ACN in 17 minutes) and lyophilized to afford derivatives: **2** (0.129 g, cumulative yield of the final two steps: 23%), **3** (0.068 g, cumulative yield of the final two steps: 12%), **4** (0.135 g, cumulative yield of the final two steps: 18%), **5** (0.038 g, cumulative yield of the final two steps: 5%) and **6** (0.085 g, cumulative yield of the final two steps: 9%).

2: ^{1}H-NMR (250 MHz, DMSO-d_6) δ (ppm): 2.95-3.25 (m, 2H, -C*H*$_2$-), 3.35 (d, 2H, $^3J_{H-H}$ = 5.25 Hz, -C*H*$_2$-), 3.51-3.66 (m, 1H, -C*H*-), 6.17 (t, 1H, $^4J_{H,H}$ = 2.0 Hz, H-4), 6.45 (d, 2H, $^4J_{H,H}$ = 2.0 Hz, H-2, H-6), 7.03-7.10 (m, 4H, H-3', H-5', H-7, H-8), 7.57 (d, 2H, $^3J_{H-H}$ = 8.5 Hz, H-2', H-6'), 7.65 (t, 1H, $^3J_{H-H}$ = 5.75 Hz, -N-*H*); ^{13}C-NMR (62.9 MHz, DMSO-d_6) δ (ppm): 158.5, 154.5, 150.5, 138.8, 133.8, 128.6, 127.2, 127.1, 121.9, 104.7, 102.3, 70.3, 63.8, 44.1; ESI-MS (ion trap): m/z 346 $[M+ H]^+$.

3: ^{1}H-NMR (250 MHz, DMSO-d_6) δ (ppm): 2.93-3.23 (m, 2H, -C*H*$_2$-), 3.34 (d, 2H, $^3J_{H-H}$ = 5.25 Hz, -C*H*$_2$-), 3.52-3.61 (m, 1H, -C*H*-), 6.38 (t, 1H, $^4J_{H,H}$ = 2.0 Hz, H-4), 6.73-6.78 (m, 4H, H-2, H-6, H-3', H-5'), 6.90 (d, 1H, $^3J_{H-H}$ = 16.5, H-7), 7.07 (d, 1H, $^3J_{H-H}$ = 16.5, H-8), 7.42 (d, 2H, $^3J_{H-H}$ = 8.75, H-2', H-6'), 7.58 (t, 2H, $^3J_{H-H}$ = 5.75 Hz, 2 × -N-*H*); ^{13}C-NMR (62.9 MHz, DMSO-d_6) δ (ppm): 158.0, 157.4, 154.5, 152.2, 139.3, 128.9, 128.0, 127.8, 124.6, 115.5, 110.0, 109.7, 107.8, 70.3, 63.8, 44.0; ESI-MS (ion trap): m/z 346 $[M+ H]^+$.

4: ^{1}H-NMR (250 MHz, DMSO-d_6) δ (ppm): ^{1}H-NMR (250 MHz, DMSO-d_6) δ (ppm): 2.95-3.25 (m, 4H, 2 × -C*H*$_2$-), 3.36 (d, 4H, $^3J_{H-H}$ = 5.25 Hz, 2 × -C*H*$_2$-), 3.53-3.62 (m, 2H, -C*H*-), 6.41-6.43 (m, 1H, H-4), 6.77-6.80 (m, 2H, H-2, H-6), 7.02-7.19 (m, 4H, H-3', H-5', H-7, H-8), 7.52-7.61 (m, 4H, 2 × -N*H*-, H-2', H-6'); ^{13}C-NMR (62.9 MHz, DMSO-d_6) δ (ppm): 158.1, 154.5, 154.4, 152.2, 150.6, 138.7, 133.6, 128.0, 127.6, 127.3, 121.9, 110.3, 110.1, 108.4, 70.2, 70.3, 63.7, 44.0; ESI-MS (ion trap): m/z 463 $[M+H]^+$.

5: ^{1}H-NMR (250 MHz, $CDCl_3$) δ (ppm): ^{1}H-NMR (250 MHz, DMSO-d_6) δ (ppm): 2.96-3.25 (m, 4H, 2 × -C*H*$_2$-), 3.36 (d, 4H, $^3J_{H-H}$ = 5.25 Hz, 2 × -C*H*$_2$-), 3.54-3.63 (m, 2H, 2 × -C*H*-), 6.64-6.80 (m, 3H, H-4, H-2, H-6), 6.97-7.24 (m, 4H, H-3', H-5', H-7, H-8), 7.40 (d, 2H, $^3J_{H-H}$ = 8.5 Hz, H-2', H-6'), 7.70 (t, 2H, $^3J_{H-H}$ = 5.75 Hz, 2 × -N-*H*); ^{13}C-NMR (62.9 MHz, DMSO-d_6) δ (ppm): 157.6, 154.3, 151.8, 139.4, 130.0, 128.2, 127.7, 123.7, 115.8, 115.6, 114.0, 70.3, 63.8, 44.2; ESI-MS (ion trap): m/z 463 $[M+H]^+$.

6: ^{1}H-NMR (250 MHz, $CDCl_3$) δ (ppm): ^{1}H-NMR (250 MHz DMSO-d_6) δ (ppm): 2.94-3.25 (m, 6H, 3 × -C*H*$_2$-), 3.35 (d, 6H, $^3J_{H-H}$ = 5.25 Hz, 3 × -C*H*$_2$-), 3.53-3.62 (m, 3H, 3 × -C*H*-), 6.78 (t, 1H, $^4J_{H,H}$ = 2.0 Hz, H-4), 7.10-7.36 (m, 6H, H-2, H-6, H-3', H-5', H-7, H-8), 7.59-7.74 (m, 5H, H-2', H-6', 3 × -N-*H*); ^{13}C-NMR (62.9 MHz, DMSO-d_6) δ (ppm): 154.4, 154.2, 151.7, 150.8, 138.8, 133.5, 129.1, 127.5, 126.7, 122.0, 116.2, 114.6, 70.3, 63.8, 44.1; ESI-MS (ion trap): m/z 580 $[M+H]^+$.

(1,2:3,4-di-*O*-isopropylidene-6-*O*-(p-toluensulfonate))-α-D-galactopiranose (20): Pyridine (3.1 mL, 38.4 mmol, 2.0 eq.) and DMAP (3.51 g, 28.7 mmol, 1.5 eq.) were added to a solution of

1,2:3,4-di-*O*-isopropylidene-α-D-galactopiranose (**19**, 5.0 g, 19.2 mmol, 1.0 eq.) in CH_2Cl_2 (20 mL), and the mixture was stirred at 0°C for 15 min. A solution of tosyl chloride (5.49 g, 28.7 mmol, 1.5 eq.) in CH_2Cl_2 (20 mL) was then added dropwise and the mixture was stirred at room temperature for 5 hours. After adding H_2O (30 mL), the mixture was diluted in CH_2Cl_2 (150 mL) and washed with 0.5 N HCl (5 × 100 mL). The organic layer was dried over $MgSO_4$ and filtered. The solvent was evaporated under reduced pressure and the residue was purified by flash chromatography (eluent: CH_2Cl_2/EtOAc, 9:1) to afford 7.33 g of **20** (92 % yield). ^{1}H-NMR (250 MHz, $CDCl_3$) δ (ppm): 1.26 (s, 3H, -C-C*H*$_3$), 1.30 (s, 3H, -C-C*H*$_3$), 1.33 (s, 3H, -C-C*H*$_3$), 1.49 (s, 3H, -C-C*H*$_3$), 2.43 (s, 3H, Ar-C*H*$_3$), 4.00-4.20 (m, 4H, H-4, H-5, H-6), 4.28 (dd, 1H, $^3J_{3\text{-}2}$ = 2.5 Hz, $^3J_{3\text{-}4}$ = 2.5 Hz, H-3), 4.57 (dd, 1H, $^3J_{2\text{-}1}$ = 2.5 Hz, H-2), 5.44 (d, 1H, $^3J_{1\text{-}2}$ = 5 Hz, H-1), 7.32 (d, 2H, Ar-*H*, $^3J_{H\text{-}H}$ = 10 Hz), 7.80 (d, 2H, $^3J_{H\text{-}H}$ = 7.5 Hz); ^{13}C-NMR (62.9 MHz, $CDCl_3$) δ (ppm): 144.7, 132.7, 129.7, 128.0, 109.5, 108.9, 96.0, 70.4, 70.3, 70.3, 68.1, 65.8, 25.9, 25.7, 24.9, 24.3, 21.6; ESI-MS (ion trap): m/z 415 $[M+H]^+$.

(1,2:3,4-di-*O*-isopropylidene-6-deoxy-azido)-α-D-galactopiranose (21): Sodium azide (5.84 g, 89.8 mmol, 5.0 eq.) was added to a solution of **20** (7.22 g, 17.4 mmol, 1.0 eq.) in DMSO (40 mL), and the mixture was stirred at 160 °C for 1.5 hours under nitrogen. The resulting mixture was poured into ice water (500 mL), and extracted with EtOAc (2 × 250 mL). The organic layer was dried over $MgSO_4$ and filtered. The solvent was evaporated under reduced pressure and the residue was purified by flash chromatography (eluent: CH_2Cl_2/EtOAc, 97:3) to afford 4.60 g of **11** (93 % yield). ^{1}H-NMR (250 MHz, $CDCl_3$) δ (ppm): 1.33 (s, 6H, 2 × -C-C*H*$_3$), 1.44 (s, 3H, -C-C*H*$_3$), 1.53 (s, 3H, -C-C*H*$_3$), 3.34 (dd, 1H, $^2J_{6^*\text{-}6}$ = 12.5 Hz, $^3J_{6^*\text{-}5}$ = 5 Hz, H-6*), 3.50 (dd, 1H, $^2J_{6\text{-}6^*}$ = 12.5 Hz, $^3J_{6\text{-}5}$ = 7.5 Hz, H-6), 3.87-3.93 (m, 1H, H-5), 4.18 (dd, 1H, $^3J_{4\text{-}3}$ = 2.5 Hz, $^3J_{4\text{-}5}$ = 7.5 Hz, H-4), 4.31 (dd, 1H, $^3J_{3\text{-}2}$ = 2.5 Hz, $^3J_{3\text{-}4}$ = 2.5 Hz, H-3), 4.61 (dd, 1H, $^3J_{2\text{-}1}$ = 7.5 Hz, $^3J_{2\text{-}3}$ = 2.5 Hz, H-2), 5.53 (d, 1H, $^3J_{1\text{-}2}$ = 5 Hz, H-1); ^{13}C-NMR (62.9 MHz, $CDCl_3$) δ (ppm): 109.5, 108.7, 96.3, 71.0, 70.7, 70.3, 66.9, 50.6, 25.9, 25.9, 24.8, 24.3; ESI-MS (ion trap): m/z 286 $[M+H]^+$.

(1,2:3,4-di-*O*-isopropylidene-6-deoxy-amino)-α-D-galactopiranose (22): A solution of triphenylphosphine (5.49 g, 20.9 mmol, 1.3 eq.) in THF (35 mL) was added dropwise to a solution of **21** (4.60 g, 16.1 mmol, 1.0 eq.) in THF (60 mL), and the mixture was stirred at RT for 4 hours under nitrogen. Distilled water (25 mL) was then added and the resulting mixture was heated to reflux and vigorously stirred for 15 hours. Solvents were removed under vacuum and the residue was purified by flash chromatography (eluent: CH_2Cl_2/MeOH, 95:5 + 1% of triethylamine) to afford 4.05 g of **22** (97 % yield). ^{1}H-NMR (250 MHz, $CDCl_3$) δ (ppm): 1.32 (s, 6H, 2 × -C-C*H*$_3$), 1.34 (s, 2H, -N*H*$_2$), 1.43 (s, 3H, -C-C*H*$_3$), 1.51 (s, 3H, -C-C*H*$_3$), 2.82 (dd, 1H, $^2J_{6^*6}$ = 15 Hz, $^3J_{6^*\text{-}5}$ = 5 Hz, H-6*), 2.95 (dd, 1H, $^2J_{6\text{-}6^*}$ = 12.5 Hz, $^3J_{6\text{-}5}$ = 7.5 Hz, H-6), 3.65-3.71 (m, 1H, H-5), 4.21 (dd, 1H, $^3J_{4\text{-}3}$ = 7.5 Hz, $^3J_{4\text{-}5}$ = 2.5 Hz, H-4), 4.30 (dd, 1H, $^3J_{3\text{-}2}$ = 5 Hz $^3J_{3\text{-}4}$ = 2.5Hz, H-3), 4.58 (dd, 1H, $^3J_{2\text{-}1}$ = 10 Hz, $^3J_{2\text{-}3}$ = 2.5 Hz, H-2), 5.53 (d, 1H, $^3J_{1\text{-}2}$ = 2.5Hz, H-1); ^{13}C-NMR (62.9 MHz, $CDCl_3$) δ (ppm): 109.1, 108.4, 96.3, 71.7, 70.7, 70.5, 69.4, 42.3, 26.0, 25.9, 24.9, 24.3; ESI-MS (ion trap): m/z 260 $[M+H]^+$.

[N-(1,2:3,4-di-*O*-isopropylidene-6-deoxy-α-D-galactopyranosyl)-carbamoyl]-4-nitrophenol (23): A solution of **22** (1.0 g, 3.9 mmol, 1.0 eq.) in THF (15 mL) was added dropwise to a solution of bis (4-nitrophenyl) carbonate (1.17 g, 3.9 mmol, 1.0 eq.) and DMAP (1.01 g, 7.8 mmol, 2.0 eq.) in THF (20 mL) and the mixture was stirred at RT for 5 hours. The resulting mixture was diluted in EtOAc (150 mL) and washed with 0.5 N HCl (3 × 100 mL). The organic layer was dried over $MgSO_4$ and filtered. The solvent was evaporated under reduced pressure and the residue was purified by flash chromatography (eluent: CH_2Cl_2/Hexane, 75:25) to afford 1.27 g of **23** (78 % yield). ^{1}H-NMR (250 MHz, $CDCl_3$) δ (ppm): 1.34 (s, 3H, -C-C*H*$_3$), 1.35 (s, 3H, -C-C*H*$_3$), 1.46 (s, 3H, -C-C*H*$_3$), 1.51 (s,

3H, -C-C*H*$_3$), 3.34-3.44 (m, 1H, H-6*), 3.55-3.65 (m, 1H, H-6), 3.95-4.01 (m, 1H, H-5), 4.23 (dd, 1H, $^3J_{4-3}$ = 10 Hz, $^3J_{4-5}$ = 2.5 Hz, H-4), 4.34 (dd, 1H, $^3J_{3-2}$ = 2.5 Hz, $^3J_{3-4}$ = 5 Hz, H-3), 4.63 (dd, 1H, $^3J_{2-1}$ = 7.5 Hz, $^3J_{2-3}$ = 2.5 Hz, H-2), 5.55 (d, 1H, $^3J_{1-2}$ = 5 Hz, H-1), 5.60 (dd, 1H, $^3J_{NH-6*}$ = 7.5 Hz, J_{NH-6} = 5 Hz, -N*H*), 7.28-7.32 (m, 2H, H-2', H-6'), 8.21-8-25 (m, 2H, H-3', H-5'); ^{13}C-NMR (250 MHz, $CDCl_3$) δ (ppm): 155.9, 153.3, 144.7, 125.0, 121.9, 109.5, 108.8, 96.3, 71.5, 70.7, 70.4, 66.0, 41.8, 26.0, 25.9, 24.9, 24.3; ESI-MS (ion trap): m/z 425 $[M+H]^+$.

(4'-mono-, 3-mono-, 3,4'-di-, 3,5-di-, 3,4',5-tri-)-[N-(1,2:3,4-di-*O*-isopropylidene-6-deoxy-α-D-galactopyranosyl)-carbamoyl]-resveratrol (24-28): A solution of resveratrol (0.15 g, 0.66 mmol, 1.0 eq.) and DMAP (0.32 g, 2.64 mmol, 4.0 eq.) in pyridine (10 mL) was added to a solution of **23** (1.13 g, 2.7 mmol, 4.0 eq.) in pyridine (10 mL) and the resulting mixture was allowed to react under vigorous stirring at 70°C for 16 hours. The reaction mixture was then diluted in EtOAc (200 mL) and washed with 0.5 N HCl (5 × 150 mL). The organic layer was dried over $MgSO_4$ and filtered. The solvent was evaporated under reduced pressure and the residue was purified by flash chromatography using EtOAc:Hexane 5.5:4.5 as eluent to afford 0.39 g of a mixture of **24**-**28** used as such for the subsequent synthetic step. ESI-MS (ion trap): **24**, **25**: m/z 514 $[M+H]^+$; **26**, **27**: m/z 799 $[M+H]^+$; **28**: m/z 1084 $[M+H]^+$.

(4'-mono-, 3-mono-, 3,4'-di-, 3,5-di-, 3,4',5-tri-)-[N-(6-deoxy-galactosyl)-carbamoyl]-resveratrol (7-11)

The mixture (**24**-**28**, 0.39 g) obtained in the previous step was added to a solution of TFA/water (90:10, 3 mL) and vigorously stirred at RT. After 1.5 hours the resulting mixture was precipitated with 40 mL of diethyl ether, the material was centrifuged and the solvent was decanted. The white powder obtained was then washed with diethyl ether three more times to eliminate traces of TFA. The residue was then dried under vacuum, separated by preparative HPLC (from 0% to 38% ACN in 17 minutes) and lyophilized to afford derivatives: **7** (0.040 g, cumulative yield of the final two steps: 14%), **8** (0.023 g, cumulative yield of the final two steps: 8%), **9** (0.093 g, cumulative yield of the final two steps: 22%), **10** (0.025 g, cumulative yield of the final two steps: 6%) and **11** (0.094 g, cumulative yield of the final two steps: 17%).

7: ^{1}H-NMR (600 MHz, DMSO-d_6) δ(ppm): 8.00 (t, 1H, J_{NH-6*}= J_{NH-6} = 6 Hz, -N*H*-), 7.56 (d, 2H, $J_{2''-3''}$ = 12 Hz, H-2'', 6''), 7.07 (d, 2H, $J_{3''-2''}$ = 6 Hz, H-3'', 5''), 7.10-7.31 (m, 2H, H-8, 9), 6.43 (s, 2H, H-2', 6'), 6.15 (s, 1H, H-4'), 4.89-5.00 (m, 1H, H-1), 4.24-3.17 (m, 12H, H-2, 3, 4, 5, 6, 6*, 6 O*H*); ^{13}C-NMR (151 MHz, DMSO-d_6) δ (ppm): 158.6, 154.5, 150.5, 138.8, 133.9, 128.7, 127.3, 127.1, 121.9, 104.7, 102.4, 97.6, 92.7, 73.3, 72.4, 71.9, 69.5, 69.2, 68.9, 68.6, 68.0, 41.8, 41.6; ESI-MS (ion trap): m/z 434 $[M+H]^+$.

8: ^{1}H-NMR (600 MHz, DMSO-d_6) δ (ppm): 7.68 (t, 1H, J_{NH-6*}= J_{NH-6} = 6 Hz, -N*H*-), 7.41 (d, 2H, $J_{2''-3''}$= 6 Hz, H-2'', 6''), 6.16-7.08 (m, 7H, H-3'',5'', 2', 4', 6', 8, 9), 3.17-4.95(m, 13H, H-1, 2, 3, 4, 5, 6, 6*,6 O*H*); ^{13}C-NMR (151 MHz, DMSO-d_6) δ (ppm): 158.5, 157.9, 154.9, 152.6, 139.8, 129.4, 128.4, 128.3, 125.0, 115.9, 115.5, 115.1, 114.8, 110.4, 110.2, 108.2, 97.9, 93.1, 73.7, 72.8, 72.3, 69.9, 69.6, 69.3, 69.0, 68.5, 42.1, 42.0; ESI-MS (ion trap): m/z 434 $[M+H]^+$.

9: ^{1}H-NMR (600 MHz, DMSO-d_6) δ (ppm): 7.71 (m, 2H, -N*H*-), 7.58 (d, 2H, $J_{2''-3''}$= 6 Hz, H-2'', 6''), 7.08-7.18 (m, 4H, H-3''5'', 8, 9), 6.81 (s, 1H, H-2'), 6.79 (s, 1H, H-4'), 6.41 (s, 1H, H-6'), 4.94-5.01 (m, 2H, 2 × H-1), 3.18-4.26 (m, 22H, 2 × H-1, 2, 3, 4, 5, 6, 6*, 8 O*H*); ^{13}C-NMR (151 MHz, DMSO-d_6) δ (ppm): 158.2, 154.5, 154.5, 152.3, 150.6, 138.9, 133.7, 128.2, 127.7, 127.4, 121.9, 110.4, 110.2,

108.4, 101.7, 97.5, 97.5, 92.7, 82.6, 82.2, 76.2, 73.3, 73.3, 72.4, 72.4, 72.0, 71.9, 69.5, 69.2, 68.9, 68.6, 68.1, 68.0, 41.7, 41.6; ESI-MS (ion trap): m/z 639 $[M+H]^+$.

10: ^{1}H-NMR (600 MHz, DMSO-d_6) δ (ppm): 7.74 (t, 2H, $J_{NH\text{-}6*}$= $J_{NH\text{-}6}$ = 6 Hz, -N*H*-), 7.42 (d, 2H, $J_{2''\text{-}3''}$= 6 Hz, H-2'', 6''), 6.97-7.18 (m, 4H, H-3''5'', 8, 9), 6.79 (s, 1H, H-2'), 6.76(s, 1H, H-4'), 3.07-4.24 (m, 23H, H-6', 2 × H-1, 2, 3, 4, 5, 6, 6*, 8 O*H*); ^{13}C-NMR (151 MHz, DMSO-d_6) δ (ppm): 157.6, 154.3, 154.2, 151.7, 151.7, 130.1, 130.0, 128.2, 127.8, 115.6, 115.3, 97.5, 97.5, 92.7, 73.3, 73.3, 72.4, 71.9, 71.9, 69.4, 69.3, 68.9, 68.8, 68.6, 68.0, 41.8, 41.7, 41.6. ESI-MS (ion trap): m/z 639 $[M+H]^+$.

11: ^{1}H-NMR (600 MHz, DMSO-d_6) δ (ppm): 7.68-7.81 (m, 3H, -N*H*-), 7.60 (d, 2H, $J_{2''\text{-}3''}$= 6 Hz, H-2'', 6''), 7.11-7.33 (m, 6H, H-3''5'', 8, 9, 2', 6'), 6.78 (s, 1H, H-4'), 2.98-4.95 (m, 33H, 3 × H-1, 2, 3, 4, 5, 6, 6*, 12 O*H*); ^{13}C-NMR (151 MHz, DMSO-d_6) δ (ppm): 154.4, 154.2, 151.7, 150.8, 138.9, 134.5, 133.5, 129.2, 127.5, 126.7, 122.0, 116.3, 101.7, 97.5, 92.7, 82.6, 82.1, 76.1, 73.3, 72.4, 71.9, 69.4, 69.2, 68.9, 68.6, 68.0, 68.0, 41.8, 41.7. ESI-MS (ion trap): m/z 845 $[M+H]^+$.

5. Pharmacokinetics and tissue distribution of pterostilbene in the rat

DOI 10.1002/mnfr.201400244 *Mol. Nutr. Food Res.* 2014, *58*, 2122–2132

RESEARCH ARTICLE

Pharmacokinetics and tissue distribution of pterostilbene in the rat

Michele Azzolini[1], Martina La Spina[1,2], Andrea Mattarei[2,3], Cristina Paradisi[3], Mario Zoratti[1,2] and Lucia Biasutto[1,2]

[1] Department of Biomedical Sciences, University of Padova, Padova, Italy
[2] CNR Neuroscience Institute, Padova, Italy
[3] Department of Chemical Sciences, University of Padova, Padova, Italy

Scope: Pterostilbene (Pt) is emerging as an important health-promoting natural compound. Pharmacokinetic studies so far have focused on plasma levels, while Pt distribution in tissues is most relevant for biological action. This study determined tissue distribution of Pt and its major metabolite, pterostilbene-4′-sulfate (Pt-S), in rats after oral administration.

Methods and results: Upon intravenous (iv) administration (88 μmol/kg), Pt was cleared from blood with a half-life of 1.8 ± 0.3 h. Oral administration (same dose) resulted in moderate Pt bioavailability (~35%) and in an increased abundance of Pt-S in blood ($AUC_{Pt}/AUC_{Pt\text{-}S}$ ~0.75 and ~0.05 after iv or oral administration, respectively). Pt-S was the major species in all organs except the brain, where intact Pt was predominant ($AUC_{Pt}/AUC_{Pt\text{-}S}$ ~5). Both Pt and Pt-S peaked in all tissues at approximately 2 h. The highest levels (~200 nmoles/g for Pt-S and 40 nmoles/g for Pt) were measured in the liver, the lowest (≤7 nmol/g) in skeletal muscles and testes.

Conclusion: AUC_{Pt} was ~2- to ~25-fold higher in tissues than in blood; this may explain its bioactivity despite barely detectable blood levels. Of particular interest is the high fraction of nonmetabolized Pt in the brain, given the reports of its activity at the level of the central nervous system.

Received: April 9, 2014
Revised: July 15, 2014
Accepted: July 17, 2014

Keywords:
Area under the curve / LC / Pharmacokinetics / Pterostilbene / Tissue distribution

Additional supporting information may be found in the online version of this article at the publisher's web-site

1 Introduction

An already substantial and rapidly growing literature describes the favorable effects of pterostilbene (*trans*-3,5-dimethoxy-4′-hydroxystilbene; Pt) on processes and conditions of physiological and medical relevance [1–3]. This phytoalexin—found in blueberries, deerberries [4, 5], grapes [6], and in plants used by ayurvedic medicine [7]—acts as an anti-inflammatory compound [8–10], with a consequent positive impact on inflammation-associated pathologies, such as cancer [11,12] and neurodegeneration [13]. Pt exhibits chemopreventive [4,11,14] and chemotherapeutic properties [15–19]; it is cardioprotective [20] and antidiabetic [21, 22]. It reportedly exerts anti-aging and neuroprotective effects, effectively reversing cognitive behavioral deficits in aging rats [23, 24], and positively modulating markers of cellular stress, inflammation, and Alzheimer's disease pathology in a mouse model of aging [13]. These effects were associated with normalized expression of peroxisome proliferator-activated receptor alpha (PPARalpha), which is downregulated in senescent mice [13]. At a molecular level, Pt was reported to activate transcription factor Nrf2 [12,25], thus promoting the downstream anti-oxidant response [26, 27]. In a mouse model of chemically induced colon carcinogenesis, Pt was shown to inhibit multiple signaling pathways: Wnt/β-catenin, Ras, PI3K/Akt, EGFR [28]. Furthermore, Pt was reported to inhibit tumor growth through metastasis-associated protein 1 (MTA1) [15], and to inhibit phosphorylation of protein kinase C-β2

Correspondence: Dr. Lucia Biasutto, CNR Neuroscience Institute, Viale G. Colombo 3, 35121 Padova, Italy
E-mail: lucia.biasutto@cnr.it
Fax: +39-0498276040

Abbreviations: **AUC**, area under the curve; **HP-β-CD**, 2-hydroxypropyl-β-cyclodextrin; **iv**, intravenous; **Pt**, pterostilbene; **Pt-S**, pterostilbene-4′-sulfate

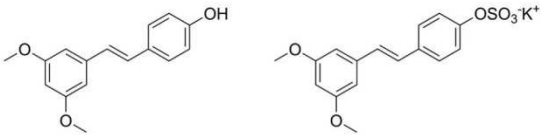

Pterostilbene (Pt) **Pterostilbene-4'-sulfate** (Pt-S)

Figure 1. Chemical structure of Pterostilbene (Pt) and Pterostilbene-4′-sulfate (Pt-S).

(PKC-β2), decreasing expression of its downstream target genes, which include proinflammatory inducible nitric oxide synthase (iNOS), cyclooxygenase-2 (COX-2), and aldose reductase (AR) [12]. Pt was also found to inhibit the catalytic activity of CYP1A1 and CYP1B1 in vitro, at sub-μM K_i values. These enzymes are inducible, extra-hepatic forms of cytochrome P450, and are responsible for converting polycyclic aromatic hydrocarbons, heterocyclic amines, and estradiol to potentially carcinogenic metabolites [29].

What makes Pt particularly interesting, compared to its nonmethylated analog resveratrol, is the ability to reach higher plasma levels after oral administration [30]. An analogous improvement is shown also by other methylated polyphenols [31]. Interestingly, methylation often does not abolish but rather even potentiates the biological activity of the compounds (e.g. [10, 31]), possibly because it increases lipophilicity. Thus methylated polyphenols are very promising pharmacological agents. Determination of levels and distribution/accumulation of Pt and its metabolites in tissues is of crucial importance to understand its therapeutic potential. However, studies on Pt absorption and metabolism were all focused only on plasma levels of Pt and its metabolites [30, 32–34]. Orally administered pterostilbene was shown to be mainly sulfated in rats; pterostilbene-4′-glucuronide can also be produced, but its abundance is very low compared to the sulfate and also to pterostilbene itself [30]. Peak plasma concentrations of both Pt and its metabolites were reached 2–4 h after oral administration. To our knowledge, no pharmacokinetic studies investigated tissue levels of Pt, with the only exception of [13] which observed its presence in the brain of mice fed for 8 weeks with 120 mg pterostilbene/kg of diet.

We thus developed a method to extract and quantify Pt and its main in vivo metabolite, pterostilbene-4′sulfate (Pt-S; [30]) (Fig. 1), from various tissues. We then applied the method in pharmacokinetic studies in the rat model, and assessed blood and tissue levels of Pt and its metabolite(s) at different time points after administration of a single intragastric dose of Pt.

The dosage we used was 88 μmoles/kg, i.e. 22.5 mg/kg of pterostilbene. This is similar to dosages used in other pharmacokinetic studies in the rat [33, 34], and is roughly equivalent to the administration of 250 mg to an average human ([33] and refs. therein). Such an amount can hardly be obtained from food; for example, pterostilbene content is estimated to be 100–520 ng/g in blueberries [5, 35], one of the richest sources of this compound. However, it may well be clinically relevant, since administering this dose daily to volunteers reportedly lowered blood pressure [36]. Furthermore, it seems safe to consider it nontoxic since consumption of 22.5 mg/kg twice daily for 30 days by rats did not cause any evident ill effects (not shown). Oral administration of 125 mg twice daily for 6–8 weeks to humans [37] and of up to 3 g/kg/day for 28 days to mice [38] was also reported to be innocuous.

2 Materials and methods

2.1 Chemicals

Pterostilbene was purchased from Wonda Science (Changzhou, Jiang, People's Republic of China, batch n. WF12062501). Other materials were purchased from Sigma/Aldrich/Fluka/Riedel de-Haen (Milan, Italy) and Merck-Novabiochem (Milan, Italy), and were used as received.

2.2 Animals

Adult male Wistar rats (approximately 400 g body weight) from the facility of the Department of Biomedical Sciences were used for the pharmacokinetic experiments. All experiments involving animals were performed after approval by the University of Padova Ethical Committee for Experimentation on Animals (CEASA) (Permit Number: 80/2011) and of the Italian Ministry of Health, and with the supervision of the Central Veterinary Service of the University of Padova, in compliance with Italian Law DL 116/92, embodying UE Directive 86/609.

2.3 Synthesis of pterostilbene-4′-sulfate

Pterostilbene-4′-sulfate is the main in vivo phase II metabolite of Pt in rats [30]. We thus chemically synthesized it as an analytical standard, adapting an existing synthetic protocol [39, 40]. The crude reaction mixture was diluted with brine and washed with methylene chloride. Combined organic fractions were then concentrated under reduced pressure (500 mbar, 40°C) and the resulting mixture was applied to a column of cation-exchange resin (Dowex 50WX8-200, K^+ form) prepared as described in [41]. Fractions containing the product were combined and concentrated. The Pt-S potassium salt was finally purified through reversed phase preparative HPLC (ACE 5 AQ, 150 × 21.2 mm, Advanced Chromatography Technologies, Aberdeen, Scotland; acetonitrile/water, from 10% to 60% acetonitrile in 20 min, 17 mL/min, 280 nm). Details about the synthetic protocols and spectroscopic data can be found in the Supporting Information.

2.4 Calibration/standard curves

Standard solutions of Pt and Pt-S in acetonitrile (in the concentration range 0.15–500 μM) were analyzed by HPLC/UV as described below; peak area at the maximum absorption wavelength (320 nm for Pt and 300 nm for Pt-S) was plotted against concentration to establish the correlation between peak area and amount analyzed.

2.5 HPLC analysis

Samples (2 μL) were analyzed by HPLC/UV (1290 Infinity LC System, Agilent Technologies) using a reverse phase column (Zorbax RRHD Eclipse Plus C18, 1.8 μm, 50 × 2.1 mm id; Agilent Technologies) and a UV diode array detector (190–500 nm). Solvents A and B were water containing 0.1% TFA and acetonitrile, respectively. The gradient for B was as follows: 10% for 0.5 min, then from 10 to 100% in 3.5 min, 100% for 1 min; the flow rate was 0.6 mL/min. The eluate was preferentially monitored at 286, 300, and 320 nm (corresponding to absorbance maxima of the internal standard, Pt-S and Pt, respectively). The temperature of the column was kept at 35°C.

2.6 HPLC/ESI-MS analysis

HPLC/ESI-MS was performed on selected samples with a 1100 Series system (Agilent Technologies). Samples (20 μL) were analyzed using a reversed phase column (Synergi-MAX, 4 μm, 150 × 4.6 mm id; Phenomenex, Castel Maggiore (BO), Italy). Solvents A and B were water containing 0.1% TFA and acetonitrile, respectively. The gradient for B was as follows: 10% for 2 min, from 10 to 100% in 20 min, then 100% for 2 min; the flow rate was 1 mL/min. The eluate was preferentially monitored at 286, 300, and 320 nm. MS analysis was performed with an ESI source operating in full-scan positive ion mode, applying the following ESI parameters: capillary 3762.30 V, skimmer 19.18 V, cap exit 50.00 V, nebulizer pressure 70 psi, dry gas flow 12 L/min, dry gas temperature 350°C.

2.7 Pharmacokinetic studies

2.7.1 Intravenous administration

Pt was injected in the tail vein of three rats as a single intravenous bolus (88 μmol/kg body weight, 22.5 mg/kg; injection volume: 200 μL). Because of the limited aqueous solubility of Pt, the dose was solubilized using 2-hydroxypropyl-β-cyclodextrin (HP-β-CD). Briefly, Pt and HP-β-CD were mixed in a 1:3 ratio in 5 mL of 9% NaCl solution; the solution was then sterile-filtered before injection. Serial blood samples were collected in heparinized tubes before and at different times after administration (5, 10, and 30 min; 1, 1.5, 2, 3, 4, 5, 6, 9, and 12 h); samples were kept in ice and treated as described below within 10 min.

2.7.2 Oral administration

Pt was administered to overnight-fasted rats as a single intragastric dose (88 μmol/kg body weight, dissolved in 250 μL DMSO). At different times after Pt administration (0.5, 2, 4, 8, 12, and 16 h), animals were anesthetized with isoflurane and sacrificed (N = 3 or 4 for each time point). Blood was collected in heparinized tubes, kept in ice and treated as described below within 10 min. Brain, lungs, heart, liver, kidneys, testes, and skeletal muscles (soleus, gastroctemius, and anterior tibialis) were explanted, weighed, and immediately frozen in liquid nitrogen; treatments were then performed as described below. The area under the curve (AUC) values were calculated using the trapezoidal rule.

2.8 Treatment of blood and tissue samples

2.8.1 Blood

Blood aliquots (100 μL) were treated as described in [42]. Briefly, after addition of the internal standard (4,4′-dihydroxybiphenyl; dilution from a 50 × stock solution in acetonitrile, 25 μM final concentration), samples were stabilized with a freshly prepared 10 mM solution of ascorbic acid (10 μL) and acidified with 0.6 M acetic acid (10 μL); after mixing, an excess of acetone (400 μL) was added, followed by sonication (2 min) and centrifugation (12 000 g, 7 min, 4°C). An accurately measured portion of the supernatant was finally collected and stored at –20°C. Before analysis, acetone was allowed to evaporate at room temperature using a Univapo 150 H (UniEquip) vacuum concentrator centrifuge, and up to 40 μL of acetone were added to precipitate residual proteins. After centrifugation (12 000 g, 5 min, 4°C), cleared samples were analyzed by HPLC/UV. The concentration of analytes in the original sample was determined as described in Supporting Information.

2.8.2 Tissues

One gram of thawed tissue was mixed with 1 mL of D-PBS (Euroclone), and homogenized with a motorized polypropylene pestel (Sigma) (for brain and testes) or with an Ultra-Turrax T25 homogenizer (Janke & Kunkel) (for all other tissues). Two hundred milligrams of tissue homogenate were transferred into a vial and spiked with the internal standard (4,4′-dihydroxybiphenyl, dilution from a 50 × stock solution in acetonitrile, 25 nmol/g tissue final concentration). Ten microliters of a freshly prepared 10 mM solution of ascorbic acid, 10 μL of 4.35 M acetic acid, and 500 μL of acetone were added. Samples were vortexed (2 min), sonicated (2 min), and then centrifuged (12 000 × *g*, 7 min, 4°C). An accurately

measured portion of the supernatant was finally collected and stored at –20°C. Further processing and analysis was carried out as described above for blood samples.

2.8.3 Recovery yields

To establish the recovery yields of Pt and Pt-S from blood and organs, the protocols for the treatment of blood or tissues were applied to samples spiked with a known amount of Pt or Pt-S.

One milliliter of blood (from an untreated animal) was spiked with 5 nmoles of Pt or Pt-S (dilution from a 1000× stock solution in DMSO). One hundred sixty microliters aliquots were then taken and processed as described above.

One gram of tissue (from an untreated animal) was mixed with 1 mL of PBS containing 5 nmoles of Pt or Pt-S (dilution from a 100 × stock solution in DMSO), and homogenized. Two hundred milligrams aliquots of the homogenate were then taken and processed as described above. Recoveries of Pt, Pt-S, and internal standard were determined as described in Supporting Information.

2.9 Pharmacokinetic analysis

Mean blood concentrations of pterostilbene were plotted versus time. Pharmacokinetic parameters were determined by noncompartmental analysis, using PKSolver 2.0 [43]. Absolute bioavailability for oral administration was calculated as F (%) = $AUC_{0\text{-}t}$(oral)/$AUC_{0\text{-}t}$(iv) × 100; since the same Pt dose was used for intravenous and oral administration, no dose correction was applied. Pt blood concentration was close to 0 at 16 h or 12 h after oral or iv administration, respectively; $AUC_{0\text{-}t}$ thus approaches $AUC_{0\text{-}\infty}$ in both cases.

3 Results

3.1 Development of protocols for blood and tissue sample analysis

The general protocol developed for blood and tissue treatment was adapted from [42]; it includes acidification of the sample, addition of an antioxidant (ascorbic acid) to preserve compound stability, and addition of organic solvent followed by sonication to ensure compound extraction and protein denaturation. The samples are then cleared of cell/tissue debris and denaturated proteins by centrifugation, and the supernatant concentrated and analyzed by HPLC/UV. Treatment of tissue homogenates required some adjustments of the original method; since samples are more dense than blood, an additional vortexing before sonication was required to ensure an efficient mixing and extraction. Furthermore, increased sample acidification was necessary to improve recovery of the analytes, allowing disruption of polyphenol–protein binding [44].

The main metabolite of Pt in the rat, pterostilbene-4′-sulfate (Pt-S), was synthesized and used as analytical standard. Recovery yields of Pt and Pt-S from organs (brain, lungs, liver, kidneys, heart, testes, skeletal muscles) and blood were evaluated treating and analyzing samples spiked with a known amount of the analyte (5 nmoles/g tissue or 5 nmoles /mL blood) and of the internal standard (4, 4′-dihydroxy biphenyl, 25 nmol/g tissue, or 25 nmol/mL blood). Pt, Pt-S, and internal standard were quantified at 320, 300, or 286 nm, respectively (corresponding to their absorbance maxima). Selectivity at these wavelengths was evaluated; HPLC/UV chromatograms show that both analytes, as well as the internal standard, are well resolved and free from interfering background peaks due to the matrix (blood or tissues) (Fig. 2). Figure 2 shows HPLC/UV chromatograms of "blank" tissue lysates of liver and kidneys (traces "a"), which are the organs with the most conspicuous background signal(s), compared to lysates spiked with Pt (traces "b") or Pt-S (traces "c").

The recovery yield ratio of Pt and Pt-S to the internal standard was satisfyingly reproducible (Table 1). Intraday precision, expressed as coefficient of variation (CV), was 10% at most in all cases, with exception of Pt in brain, where the CV was about 15%; interday precision was also within 10%, with exception of Pt in brain and liver, where the CV was about 15% (Table 1). HPLC analysis of standard solutions of Pt and Pt-S showed that these analytes (at their maximum UV absorption wavelengths, which are 320 and 300 nm, respectively) have the same calibration curve ($y = 4.96\,x$, where y is the peak area at the maximum absorption wavelength and x is the concentration in μM units). LOD and LOQ of the analytical part of the method were calculated measuring the average background response at 320 and 300 nm in 30 different HPLC runs, at the retention time of the analytes (2.93 and 2.33 min for Pt and Pt-S, respectively) and over a time lapse of 0.04 min, which is the typical peak width of the analytes at low concentrations (< 1 μM). LOD and LOQ were taken to be 3 or 10 times, respectively, the background response. Interpolating the data in the calibration curve, we obtained LOD and LOQ values of 0.05 and 0.15 μM, respectively, for both Pt and Pt-S. LOQ was confirmed analyzing three solutions at the LOQ concentration; peak area fitted well within the calibration curve.

3.2 Pharmacokinetics

The method was then applied to pharmacokinetic studies; intravenous administration of a single Pt bolus (88 μmol/kg, 22.5 mg/kg) to rats resulted in a bi-exponential decay of Pt levels in blood (i.e. a rapid distribution phase followed by a prolonged elimination phase) (Fig. 3A), in accordance with previous studies [32–34]. Pharmacokinetic parameters for Pt, obtained using noncompartmental analysis, are presented in Fig. 3B. Two-compartment analysis was also performed, but the values obtained in this case were affected by a much higher uncertainty due to the rapidity of the first

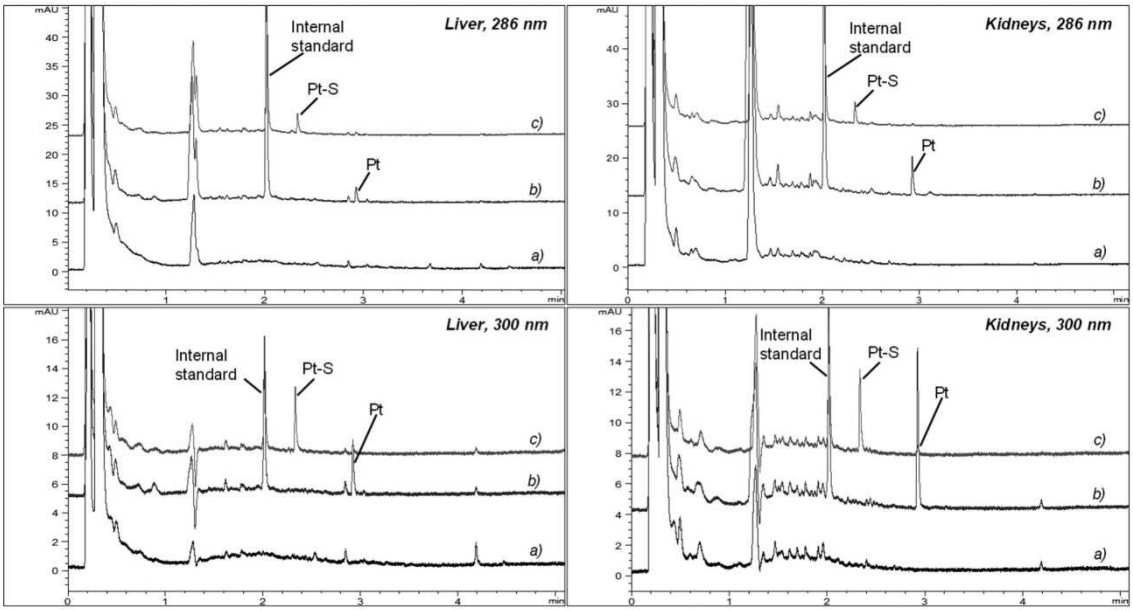

Figure 2. HPLC/UV chromatograms (286 and 300 nm) of extracts of liver and kidney lysates. (a) "blank" tissue lysate; (b) tissue lysate spiked with 5 nmol/g Pt; (c) tissue lysate spiked with 5 nmol/g Pt-S.

process. Pt-S was the only detectable metabolite in circulation; it was progressively generated, reaching the maximum concentration (11.7 ± 3.2 μM) 2 h after injection of the Pt bolus. Its $AUC_{0\text{-}12h}$ was slightly higher than that of Pt itself (52.1 ± 14.7 nmol/mL × h versus 38.8 ± 5.3 nmol/mL × h, respectively).

For the evaluation of oral bioavailability, blood samples were taken at preestablished times after administration of the same Pt dosage by oral gavage and analyzed (see Materials and methods). To study tissue distribution, rats were sacrificed, organs were explanted at different times after oral administration, and tissue levels of Pt and its metabolite(s) were determined. Measured concentrations of both Pt and Pt-S were above the LOQ in all samples in the 0.5 –12 h interval. Analytes were quantified according to their calibration curve, adjusting the result for the recovery of each analyte, determined on the basis of the recovery of the internal standard and of the known recovery ratio between analyte and internal standard (see Supporting Information for details). Figure 4 illustrates time-concentration profiles of Pt and Pt-S in blood and tissues, and Fig. 5 reports $AUC_{0\text{-}16h}$ values, C_{max} and t_{max} for both Pt and Pt-S in all analyzed tissues (N = 3 or 4 for each time point). A residual amount of blood in explanted tissues is expected if they are collected without perfusion; in rats, this amount has been estimated to account for a fraction of organ weight comprised between 1 or 2% (in muscles and brain, respectively) and 13% (in lungs and heart) [45]. The residual blood is thus not expected to significantly

Table 1. Recovery of Pt and Pt-S from blood and tissues

Tissue	Analyte/internal standard recovery ratio[a)]		Interday precision (CV)	
	Pt	Pt-S	Pt	Pt-S
Blood	0.841 ± 0.028	0.922 ± 0.056	3.3	6.1
Brain	0.732 ± 0.115	0.853 ± 0.087	15.7	10.2
Lungs	0.636 ± 0.062	0.633 ± 0.034	9.8	5.4
Heart	0.752 ± 0.085	0.497 ± 0.028	11.3	5.6
Liver	0.716 ± 0.104	0.610 ± 0.064	14.6	10.4
Kidneys	0.697 ± 0.048	0.597 ± 0.042	6.8	7.1
Testes	0.676 ± 0.064	0.720 ± 0.076	9.4	10.5
Muscles	0.708 ± 0.053	0.597 ± 0.051	7.5	8.6

a) N ≥ 4 for each condition. Mean values ± SD are shown.

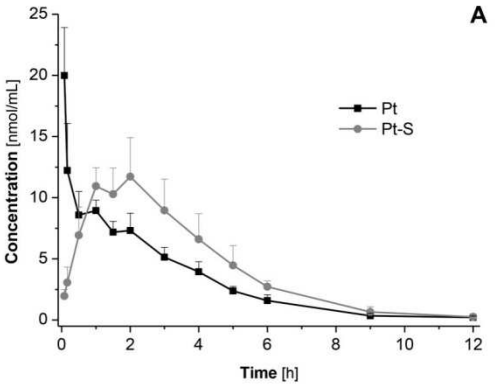

Parameter	Value	B
$AUC_{0\text{-}12h}$ [(nmol/mL)×h]	38.8 ± 5.3	
$t_{1/2}$ [h]	1.8 ± 0.3	
CL [L/h/kg]	2.3 ± 0.3	
V_{ss} [L/kg]	6.1 ± 1.0	
C_0 [nmol/mL]	35.6 ± 17.2	
λ_z [1/h]	0.39 ± 0.07	
MRT [h]	2.7 ± 0.3	

Figure 3. Pharmacokinetic profile of Pt after intravenous administration. (A) Concentration versus time profiles of Pt and Pt-S in blood. Reported are mean values ± SD (N = 3). (B) Intravenous pharmacokinetic parameters for Pt.

affect the assessment of analytes in any given tissue sample; we thus decided to collect tissues without perfusion, immediately freezing them in liquid nitrogen after explantation. Our approximation was validated a posteriori by the experimental results; in fact, the relative abundance of Pt and Pt-S in blood turned out to be very different from that found in all other tissues.

Absolute oral bioavailability for Pt, calculated as the percentage ratio between $AUC_{0\text{-}t}$(oral) and $AUC_{0\text{-}t}$(iv) in blood, was about 35%. No major differences were observed in the t_{max}; both pterostilbene and its sulfate, in all organs, reached a maximum concentration about 2 h after administration. The pharmacokinetic profile was very different in blood compared to the other tissues: Pt levels were the lowest among the tissues analyzed ($C_{max} = 1.5 \pm 1.0$ μM), and the difference between the AUCs of intact Pt versus its sulfate was the highest ($AUC_{0\text{-}16h}$ for Pt-S was about 20 times that for Pt). At all times, Pt levels were higher in any given organ than in blood, but the relative amounts of Pt and Pt-S differed depending on tissue. $AUC_{0\text{-}16h}$ for Pt-S was significantly higher than that for Pt in lungs, heart, liver, kidneys, and testes. On the contrary, brain displayed an higher $AUC_{0\text{-}16h}$ for nonmetabolized Pt compared to the sulfate, while the differences were nonsignificant in skeletal muscles. The highest amounts per gram of Pt were detected in the liver, followed by kidneys, lungs, and brain. Also Pt-S levels were highest in the liver, followed by kidneys, lungs, and blood. The other possible phase II metabolite of Pt, pterostilbene-4′-glucuronide [30], was detected only in the liver, and was present in very low amounts (at most 1% of the total amount of recovered analytes; 98% were Pt and Pt-S) (Fig. 6). Another 1% of analytes found in the liver extracts showed the characteristic absorption spectrum of stilbenes, but remained unidentified. The latter might be phase II metabolites (i.e. sulfates or glucuronides) of demethylated and/or hydroxylated pterostilbene (as reported by [46]). In all other organs however these putative metabolites were below detection limit.

4 Discussion

Our results confirm the observations by others that pterostilbene is readily transformed into phase II conjugates after oral administration [30]. This metabolism is due to enzymatic activities in hepatocytes as well as enterocytes; the relevance of the latter is made evident by the different blood $AUC_{Pt}/AUC_{Pt\text{-}S}$ ratios obtained after intravenous or oral administration (approx. 0.75 versus 0.05, respectively). In rats, the sulfate is by far the predominant metabolite, with a small amount of glucuronide being found only in liver. It should be pointed out however that there may be marked differences in the relative relevance of these conjugative processes depending on the species and also on factors such as dosage (see, e.g. in the case of resveratrol, [47, 48] and Table 1 in [49]).

It has been suggested that DMSO, used as vehicle for oral administration, may enhance absorption ([50]; but to the contrary see, e.g. [51]). However such an effect, if present, seems to have little relevance in our study since the absolute bioavailability value we calculated is intermediate between values already present in the literature and obtained administering aqueous solutions/suspensions (with HP-β-CD, carboxymethylcellulose, or methylcellulose) [30, 32, 33].

To our knowledge, this is the first extensive study of the tissue distribution of Pt and its metabolites at different times after oral administration. Pharmacokinetic data already present in the literature largely concern plasma levels [30, 32–34]. We found that Pt, as well as its main metabolite, Pt-S, is not evenly distributed in the body after oral administration. The different concentrations, as well as the different relative abundance, of Pt and Pt-S in blood versus tissues confirm the notion that analysis of blood—and even more so of plasma [42]—may not be considered as representative for the whole organism. Pt and its metabolite(s) (in this case mainly Pt-S) have different lipophilicity/hydrophilicity, and this may account for variations in their relative abundance in tissues. Soluble metabolites are expected to be enriched in aqueous environments, while the less hydrophilic parent compound may associate more readily with tissues, depending on characteristics such as lipid content and accessibility. This

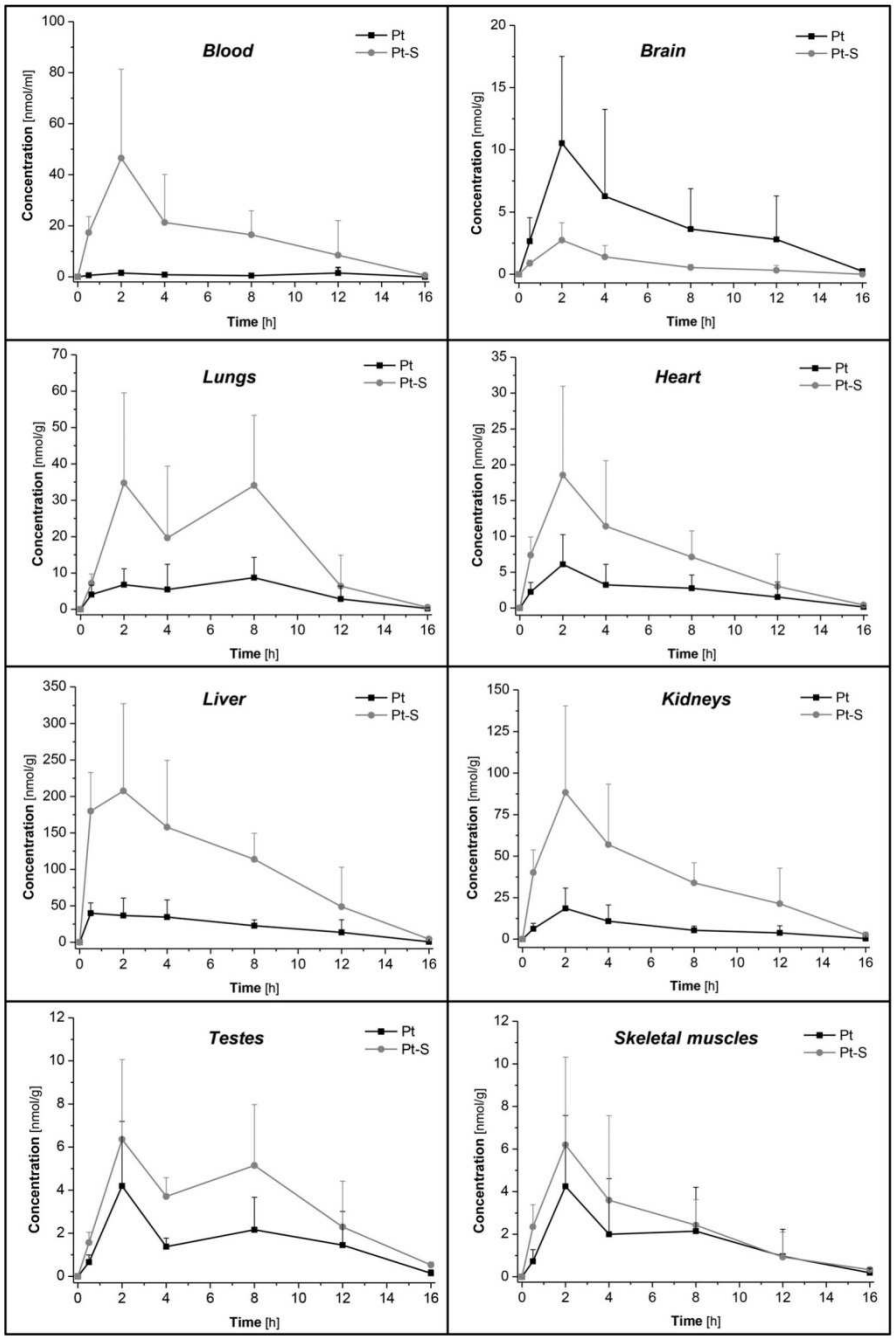

Figure 4. Concentration versus time profiles of Pt and Pt-S in blood and tissues. A single intragastric dose of pterostilbene (88 μmoles/kg body weight) was administered to rats at time 0. Reported are mean values ± SD (N = 3 or 4).

A	$AUC_{0\text{-}16h}$ [(nmol/g) x h]		C_{max} [nmol/g]		t_{max} [h]	
Tissue	Pt	Pt-S	Pt	Pt-S	Pt	Pt-S
Blood	13.7 ± 6.6	263.6 ± 76.6	1.5 ± 1.0 / 1.5 ± 2.1	46.5 ± 34.8	2	2
Brain	66.1 ± 22.4	13.2 ± 3.0	10.5 ± 7.0	2.7 ± 1.4	2	2
Lungs	79.0 ± 24.9	289.9 ± 80.5	6.8 ± 4.4 / 8.7 ± 5.5	34.7 ± 24.8 / 34.1 ± 19.3	2 / 8	2 / 8
Heart	40.0 ± 11.5	115.4 ± 30.6	6.1 ± 4.2	18.5 ± 12.4	2	2
Liver	351.6 ± 82.3	1674.2 ± 316.4	39.7 ± 14.2	207.6 ± 119.8	0.5 - 4	2
Kidneys	108.6 ± 30.3	591.6 ± 125.9	18.5 ± 12.2	88.3 ± 52.2	2	2
Testes	26.9 ± 7.3	54.1 ± 11.2	4.2 ± 3.0 / 2.2 ± 1.5	6.4 ± 3.7 / 5.1 ± 2.8	2 / 8	2 / 8
Muscles	27.0 ± 9.9	38.1 ± 11.3	4.2 ± 3.3	6.2 ± 4.1	2	2

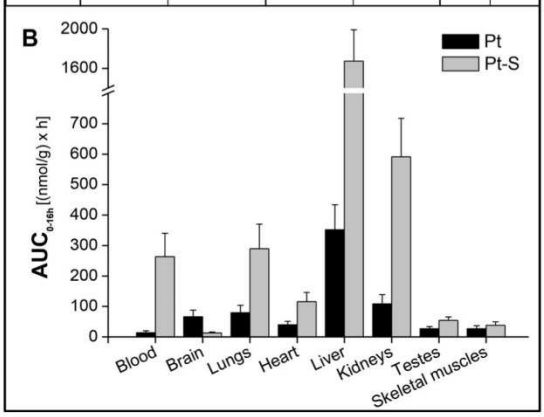

Figure 5. Pharmacokinetic parameters for Pt and Pt-S in blood and tissues. (A) AUC, C_{max}, and t_{max} values for Pt and Pt-S in blood and organs. For blood, concentrations are expressed in nmol/mL units (i.e. μM). (B) AUC values are plotted for various organs, with comparison between Pt and Pt-S.

idea is supported by the observation that blood (which has an abundant aqueous component) shows the lowest $AUC_{Pt}/AUC_{Pt\text{-}S}$ ratio (about 0.05), while the brain, which is particularly rich in lipids, is the tissue with the highest $AUC_{Pt}/AUC_{Pt\text{-}S}$ ratio (about 5). This observation has logical implications for the in vivo biological activity of pterostilbene; of particular interest is the high percentage of non-metabolized Pt in the brain, given the reports of its activity on the central nervous system [13, 24].

Since Pt-S can reach high levels in various tissues, elucidation of the activity of Pt-S would be very interesting. No studies are available at the moment on the possible biological activity of Pt-S or Pt-glucuronide, and are clearly needed. Studies of the effects of metabolites of resveratrol have indicated that conjugation with sulfate or glucuronyl groups may alter the efficacy of the natural compound, often decreasing it. For example, sulfation of resveratrol in either position 3 or 4' reduces inhibition of COX-1 and -2, as well as inhibition of Quinone Reductase 2 [41, 52]. A level of activity is nonetheless retained by metabolites. A recent study [48] for example reports that prolonged (6 weeks) administration of a relatively low (5 mg/kg × day) dose of resveratrol to diabetic rats led to the progressive appearance of approximately 0.07 nmoles/g of reveratrol sulfate and glucuronide in the heart tissue, while resveratrol itself was absent. Clear protective effects on hemodynamic function could be measured.

Another emerging aspect of relevance here is that phase II metabolites may act as a source of the natural compound, which can be regenerated from them thanks to enzymatic activities. This phenomenon is well known for flavonoids, regenerated from their glucuronides through the intervention of β-glucuronidase [53, 54]. Similar processes also take place with resveratrol glucuronides and sulfates [55, 56].

Supporting Information Table 1 summarizes pharmacokinetic data for resveratrol (from literature) and Pt (from the present work). The comparison indicates that in organs higher concentrations of the unmodified molecule can be reached in the case of pterostilbene than in the case of resveratrol.

When resveratrol was orally administered to rats at the same dose we used in this study with pterostilbene (88 μmol/kg, 20mg/kg), tissue levels of resveratrol were always below 1 nmol/g [57]. In contrast, nonmetabolized Pt found during our work was much higher: maximum concentrations ranged from 4.2 ± 3.0 nmol/g (in testes) to 39.7 ± 14.2 nmol/g (in the liver). Interestingly, t_{max} was considerably higher when Pt was administered, compared to resveratrol (2 h versus 5–15 min, respectively). Furthermore, tissue levels of resveratrol and metabolites were reported to be much lower than those of Pt and its metabolite(s), even if resveratrol was administered intravenously [44] or orally at higher dosages (219 μmol/kg [55] or 438 μmol/kg [58] instead of 88 μmol/kg). These higher levels may be attributed to a higher lipophilicity of Pt compared to resveratrol, which favours intestinal absorption and, more generally, permeation of biomembranes. Also the presence in the molecule of only one hydroxyl (instead of three, in resveratrol) gives the compound an intrinsic advantage in phase II conjugative reactions. Note however that absolute oral bioavailability, calculated as the ratio of $AUC_{0\text{-}t}$(oral) to $AUC_{0\text{-}t}$(iv) in blood, may actually be comparable or even higher for resveratrol than for Pt, because of resveratrol's low $AUC_{0\text{-}t}$(iv) values [30, 59–61].

In summary, this work shows that pterostilbene levels much higher than those found in blood are reached in some tissues and may in fact be adequate to explain effects probably mediated largely by regulation of epigenetic processes. This may help explain the apparent paradox of pterostilbene bioactivity in the face of low blood or plasma concentrations. The results of this study thus concur with those of functional and biochemical investigations to support the potential of pterostilbene for biomedical applications. It is now relevant to explore the "bioaccumulation" of pterostilbene and its metabolite(s) upon prolonged administration of relatively low levels, mimicking intake obtainable through the diet.

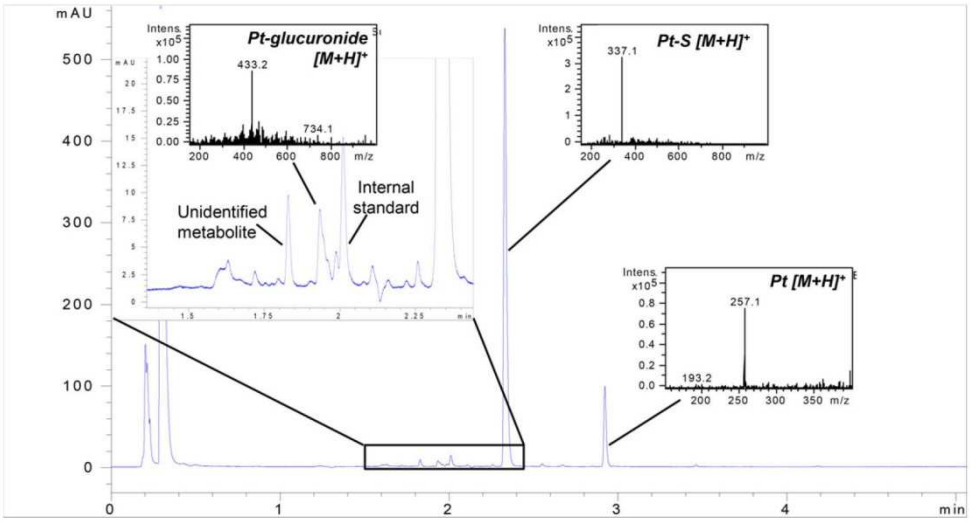

Figure 6. HPLC/UV and ESI-MS analysis of a sample from pharmacokinetic studies. A representative chromatogram (300 nm) of liver extract (2 h after Pt administration). Inserts represent an enlargement of the indicated part of the chromatogram, and ESI + mass spectra for Pt, Pt-S, and Pt-glucuronide.

We thank Mr. M. Ghidotti for technical help. This work was supported by grants from the Fondazione Cassa di Risparmio di Padova e Rovigo (CARIPARO) ("Developing a Pharmacology of Polyphenols"), from the Italian Ministry of the University and Research (PRIN n. 20107Z8XBW_004), and by the CNR Project of Special Interest on Aging.

The authors have declared no conflict of interest

5 References

[1] McCormack, D., McFadden, D., A review of pterostilbene antioxidant activity and disease modification. *Oxid. Med. Cell Longev.* 2013, *2013*, 575482.

[2] Pterostilbene. Monograph. *Altern. Med. Rev.* 2010, *15*, 159–163.

[3] Estrela, J. M., Ortega, A., Mena, S., Rodriguez, M. L. et al., Pterostilbene: Biomedical applications. *Crit. Rev. Clin. Lab. Sci.* 2013, *50*, 65–78.

[4] Paul, S., DeCastro, A. J., Lee, H. J., Smolarek, A. K. et al., Dietary intake of pterostilbene, a constituent of blueberries, inhibits the beta-catenin/p65 downstream signaling pathway and colon carcinogenesis in rats. *Carcinogenesis* 2010, *31*, 1272–1278.

[5] Rimando, A. M., Kalt, W., Magee, J. B., Dewey, J. et al., Resveratrol, pterostilbene, and piceatannol in vaccinium berries. *J. Agric. Food Chem.* 2004, *52*, 4713–4719.

[6] Schmidlin, L., Poutaraud, A., Claudel, P., Mestre, P. et al., A stress-inducible resveratrol O-methyltransferase involved in the biosynthesis of pterostilbene in grapevine. *Plant Physiol.* 2008, *148*, 1630-1639.

[7] Paul, B., Masih, I., Deopujari, J., Charpentier, C., Occurrence of resveratrol and pterostilbene in age-old darakchasava, an ayurvedic medicine from India. *J. Ethnopharmacol.* 1999, *68*, 71–76.

[8] Paul, S., Rimando, A. M., Lee, H. J., Ji, Y. et al., Anti-inflammatory action of pterostilbene is mediated through the p38 mitogen-activated protein kinase pathway in colon cancer cells. *Cancer Prev. Res. (Phila)* 2009, *2*, 650–657.

[9] McCormack, D., McDonald, D., McFadden, D., Pterostilbene ameliorates tumor necrosis factor alpha-induced pancreatitis in vitro. *J. Surg. Res.* 2012, *178*, 28–32.

[10] Cichocki, M., Paluszczak, J., Szaefer, H., Piechowiak, A. et al., Pterostilbene is equally potent as resveratrol in inhibiting 12-O-tetradecanoylphorbol-13-acetate activated NFkappaB, AP-1, COX-2, and iNOS in mouse epidermis. *Mol. Nutr. Food Res.* 2008, *52* (Suppl 1), S62–S70.

[11] Tsai, M. L., Lai, C. S., Chang, Y. H., Chen, W. J. et al., Pterostilbene, a natural analogue of resveratrol, potently inhibits 7,12-dimethylbenz[a]anthracene (DMBA)/12-O-tetradecanoylphorbol-13-acetate (TPA)-induced mouse skin carcinogenesis. *Food Funct. 2012*, *3*, 1185–1194.

[12] Chiou, Y. S., Tsai, M. L., Nagabhushanam, K., Wang, Y. J. et al., Pterostilbene is more potent than resveratrol in preventing azoxymethane (AOM)-induced colon tumorigenesis via activation of the NF-E2-related factor 2 (Nrf2)-mediated antioxidant signaling pathway. *J. Agric. Food Chem.* 2011, *59*, 2725-2733.

[13] Chang, J., Rimando, A., Pallas, M., Camins, A. et al., Low-dose pterostilbene, but not resveratrol, is a potent neuromodulator in aging and Alzheimer's disease. *Neurobiol. Aging* 2012, *33*, 2062–2071.

[14] Suh, N., Paul, S., Hao, X., Simi, B. et al., Pterostilbene, an active constituent of blueberries, suppresses aberrant crypt foci formation in the azoxymethane-induced colon carcinogenesis model in rats. *Clin. Cancer Res.* 2007, *13*, 350-355.

[15] Li, K., Dias, S. J., Rimando, A. M., Dhar, S. et al., Pterostilbene acts through metastasis-associated protein 1 to inhibit tumor growth, progression and metastasis in prostate cancer. *PLoS One* 2013, *8*, e57542.

[16] Kapoor, S., Pterostilbene and its emerging antineoplastic effects: a prospective treatment option for systemic malignancies. *Am. J. Surg.* 2013, *205*, 483.

[17] Mak, K. K., Wu, A. T., Lee, W. H., Chang, T. C. et al., Pterostilbene, a bioactive component of blueberries, suppresses the generation of breast cancer stem cells within tumor microenvironment and metastasis via modulating NF-kappaB/microRNA 448 circuit. *Mol. Nutr. Food Res.* 2013, *57*, 1123–1134.

[18] McCormack, D., McFadden, D., Pterostilbene and cancer: current review. *J. Surg. Res.* 2012, *173*, e53–e61.

[19] Mena, S., Rodriguez, M. L., Ponsoda, X., Estrela, J. M. et al., Pterostilbene-induced tumor cytotoxicity: a lysosomal membrane permeabilization-dependent mechanism. *PLoS One* 2012, *7*, e44524.

[20] Rimando, A. M., Nagmani, R., Feller, D. R., Yokoyama, W., Pterostilbene, a new agonist for the peroxisome proliferator-activated receptor alpha-isoform, lowers plasma lipoproteins and cholesterol in hypercholesterolemic hamsters. *J. Agric. Food Chem.* 2005, *53*, 3403–3407.

[21] Manickam, M., Ramanathan, M., Jahromi, M. A., Chansouria, J. P. et al., Antihyperglycemic activity of phenolics from *Pterocarpus marsupium*. *J. Nat. Prod.* 1997, *60*, 609–610.

[22] Pari, L., Satheesh, M. A., Effect of pterostilbene on hepatic key enzymes of glucose metabolism in streptozotocin- and nicotinamide-induced diabetic rats. *Life Sci.* 2006, *79*, 641-645.

[23] Joseph, J. A., Fisher, D. R., Cheng, V., Rimando, A. M. et al., Cellular and behavioral effects of stilbene resveratrol analogues: implications for reducing the deleterious effects of aging. *J. Agric. Food Chem.* 2008, *56*, 10544-10551.

[24] Cherniack, E. P., A berry thought-provoking idea: the potential role of plant polyphenols in the treatment of age-related cognitive disorders. *Br. J. Nutr.* 2012, *108*, 794–800.

[25] Ramkumar, K. M., Sekar, T. V., Foygel, K., Elango, B. et al., Reporter protein complementation imaging assay to screen and study Nrf2 activators in cells and living animals. *Anal. Chem.* 2013, *85*, 7542–7549.

[26] Kundu, J. K., Surh, Y. J., Nrf2-Keap1 signaling as a potential target for chemoprevention of inflammation-associated carcinogenesis. *Pharm. Res.* 2010, *27*, 999–1013.

[27] Copple, I. M., The Keap1-Nrf2 cell defense pathway—a promising therapeutic target? *Adv. Pharmacol.* 2012, *63*, 43–79.

[28] Chiou, Y. S., Tsai, M. L., Wang, Y. J., Cheng, A. C. et al., Pterostilbene inhibits colorectal aberrant crypt foci (ACF) and colon carcinogenesis via suppression of multiple signal transduction pathways in azoxymethane-treated mice. *J. Agric. Food Chem.* 2010, *58*, 8833–8841.

[29] Mikstacka, R., Przybylska, D., Rimando, A. M., Baer-Dubowska, W., Inhibition of human recombinant cytochromes P450 CYP1A1 and CYP1B1 by trans-resveratrol methyl ethers. *Mol. Nutr. Food. Res.* 2007, *51*, 517–524.

[30] Kapetanovic, I. M.,Muzzio, M., Huang, Z., Thompson, T. N. et al., Pharmacokinetics, oral bioavailability, and metabolic profile of resveratrol and its dimethylether analog, pterostilbene, in rats. *Cancer Chemother. Pharmacol.* 2011, *68*, 593–601.

[31] Walle, T., Methylation of dietary flavones greatly improves their hepatic metabolic stability and intestinal absorption. *Mol. Pharm.* 2007, *4*, 826–832.

[32] Lin, H. S., Yue, B. D., Ho, P. C., Determination of pterostilbene in rat plasma by a simple HPLC-UV method and its application in pre-clinical pharmacokinetic study. *Biomed. Chromatogr.* 2009, *23*, 1308–1315.

[33] Yeo, S. C., Ho, P. C., Lin, H. S., Pharmacokinetics of pterostilbene in Sprague–Dawley rats: the impacts of aqueous solubility, fasting, dose escalation, and dosing route on bioavailability. *Mol. Nutr. Food Res.* 2013, *57*, 1015–1025.

[34] Remsberg, C. M., Yanez, J. A., Ohgami, Y., Vega-Villa, K. R. et al., Pharmacometrics of pterostilbene: preclinical pharmacokinetics and metabolism, anticancer, antiinflammatory, antioxidant and analgesic activity. *Phytother. Res.* 2008, *22*, 169–179.

[35] Neto, C. C., Cranberry and blueberry: evidence for protective effects against cancer and vascular diseases. *Mol. Nutr. Food Res.* 2007, *51*, 652–664.

[36] Riche, D. M., Deschamp, D., Griswold, M. E., McEwen, C. L. et al., Impact of pterostilbene on blood pressure and other metabolic parameters in adults. *Hypertension* 2012, *60*, A617.

[37] Riche, D. M., McEwen, C. L., Riche, K. D., Sherman, J. J. et al., Analysis of safety from a human clinical trial with pterostilbene. *J. Toxicol.* 2013, *2013*, 463595.

[38] Ruiz, M. J., Fernandez, M., Pico, Y., Manes, J. et al., Dietary administration of high doses of pterostilbene and quercetin to mice is not toxic. *J. Agric. Food Chem.* 2009, *57*, 3180–3186.

[39] Gottumukkala, V. S., Hindupur, R. M., Masna, M., Novel stilbene analogs. Patent WO 2010/046926 A2. 2010.

[40] Iwuchukwu, O. F., Sharan, S., Canney, D. J., Nagar, S., Analytical method development for synthesized conjugated metabolites of trans-resveratrol, and application to pharmacokinetic studies. *J. Pharm. Biomed. Anal.* 2012, *63*, 1–8.

[41] Hoshino, J., Park, E. J., Kondratyuk, T. P., Marler, L. et al., Selective synthesis and biological evaluation of sulfate-conjugated resveratrol metabolites. *J. Med. Chem.* 2010, *53*, 5033–5043.

[42] Biasutto, L., Marotta, E., Garbisa, S., Zoratti, M. et al., Determination of quercetin and resveratrol in whole blood—implications for bioavailability studies. *Molecules* 2010, *15*, 6570–6579.

[43] Zhang, Y., Huo, M., Zhou, J., Xie, S., PKSolver: an add-in program for pharmacokinetic and pharmacodynamic data analysis in Microsoft Excel. *Comput. Methods Programs Biomed.* 2010, *99*, 306–314.

[44] Juan, M. E., Maijo, M., Planas, J. M., Quantification of trans-resveratrol and its metabolites in rat plasma and tissues by HPLC. *J. Pharm. Biomed. Anal.* 2010, *51*, 391–398.

[45] de Boer, V. C., Dihal, A. A., van der Woude, H., Arts, I. C. et al., Tissue distribution of quercetin in rats and pigs. *J. Nutr.* 2005, *135*, 1718–1725.

[46] Shao, X., Chen, X., Badmaev, V., Ho, C. T. et al., Structural identification of mouse urinary metabolites of pterostilbene using liquid chromatography/tandem mass spectrometry. *Rapid Commun. Mass. Spectrom.* 2010, *24*, 1770–1778.

[47] Dellinger, R. W., Garcia, A. M., Meyskens, F. L., Jr., Differences in the glucuronidation of resveratrol and pterostilbene: altered enzyme specificity and potential gender differences. *Drug Metab. Pharmacokinet.* 2014, *29*, 112–119.

[48] Bresciani, L., Calani, L., Bocchi, L., Delucchi, F. et al., Bioaccumulation of resveratrol metabolites in myocardial tissue is dose-time dependent and related to cardiac hemodynamics in diabetic rats. *Nutr. Metab. Cardiovasc. Dis.* 2014, *24*, 408–415.

[49] Menet, M. C., Marchal, J., Dal-Pan, A., Taghi, M. et al., Resveratrol metabolism in a non-human primate, the grey mouse lemur (*Microcebus murinus*), using ultra-high-performance liquid chromatography-quadrupole time of flight. *PLoS One* 2014, *9*, e91932.

[50] Hashimoto, H., Tokunaka, S., Sasaki, M., Nishihara, M. et al., Dimethylsulfoxide enhances the absorption of chemotherapeutic drug instilled into the bladder. *Urol. Res.* 1992, *20*, 233–236.

[51] Zhou, Y., Li, W., Chen, L., Ma, S. et al., Enhancement of intestinal absorption of akebia saponin D by borneol and probenecid in situ and in vitro. *Environ. Toxicol. Pharmacol.* 2010, *29*, 229–234.

[52] Calamini, B., Ratia, K., Malkowski, M. G., Cuendet, M. et al., Pleiotropic mechanisms facilitated by resveratrol and its metabolites. *Biochem. J.* 2010, *429*, 273–282.

[53] Menendez, C., Duenas, M., Galindo, P., Gonzalez-Manzano, S. et al., Vascular deconjugation of quercetin glucuronide: the flavonoid paradox revealed? *Mol. Nutr. Food Res.* 2011, *55*, 1780–1790.

[54] Terao, J., Murota, K., Kawai, Y., Conjugated quercetin glucuronides as bioactive metabolites and precursors of aglycone in vivo. *Food Funct.* 2011, *2*, 11–17.

[55] Abd El-Mohsen, M., Bayele, H., Kuhnle, G., Gibson, G. et al., Distribution of [3H]trans-resveratrol in rat tissues following oral administration. *Br. J. Nutr.* 2006, *96*, 62–70.

[56] Patel, K. R., Andreadi, C., Britton, R. G., Horner-Glister, E. et al., Sulfate metabolites provide an intracellular pool for resveratrol generation and induce autophagy with senescence. *Sci. Transl. Med.* 2013, *5*, 205ra133.

[57] Asensi, M., Medina, I., Ortega, A., Carretero, J. et al., Inhibition of cancer growth by resveratrol is related to its low bioavailability. *Free Radic. Biol. Med.* 2002, *33*, 387–398.

[58] Liang, L., Liu, X., Wang, Q., Cheng, S. et al., Pharmacokinetics, tissue distribution and excretion study of resveratrol and its prodrug 3,5,4′-tri-O-acetylresveratrol in rats. *Phytomedicine* 2013, *20*, 558–563.

[59] Marier, J. F., Vachon, P., Gritsas, A., Zhang, J. et al., Metabolism and disposition of resveratrol in rats: extent of absorption, glucuronidation, and enterohepatic recirculation evidenced by a linked-rat model. *J. Pharmacol. Exp. Ther.* 2002, *302*, 369–373.

[60] Colom, H., Alfaras, I., Maijo, M., Juan, M. E. et al., Population pharmacokinetic modeling of trans-resveratrol and its glucuronide and sulfate conjugates after oral and intravenous administration in rats. *Pharm. Res.* 2011, *28*, 1606–1621.

[61] Das, S., Lin, H. S., Ho, P. C., Ng, K. Y., The impact of aqueous solubility and dose on the pharmacokinetic profiles of resveratrol. *Pharm. Res.* 2008, *25*, 2593–2600.

Pharmacokinetics and tissue distribution of pterostilbene in the rat

Michele Azzolini[1], Martina La Spina[1,2], Andrea Mattarei[2,3], Cristina Paradisi[3], Mario Zoratti[1,2], Lucia Biasutto[1,2,*]

[1] Dept. Biomedical Sciences, University of Padova, Viale G. Colombo 3, 35121 Padova, Italy

[2] CNR Neuroscience Institute, Viale G. Colombo 3, 35121 Padova, Italy

[3] Dept. Chemical Sciences, Via F. Marzolo 1, 35131 Padova, Italy

Supporting Information

Synthesis of pterostilbene-4'-sulfate (Pt-S)

Chlorosulfonic acid (0.128 g, 1.10 mmol, 5.0 eq.) in acetonitrile (0.5 mL) was added dropwise to a vigorously stirred solution of pterostilbene (Pt, 0.056 g, 0.22 mmol, 1.0 eq.) and pyridine (0.5 mL) in acetonitrile (2.0 mL) in a 50 mL conical centrifugation tube (Falcon™ type) at -20 °C. The reaction mixture was allowed to warm to room temperature. After 16 h the resulting reaction mixture was concentrated to about 1.5 mL under a weak nitrogen stream and solutes were precipitated with diethyl ether (40 mL). The slurry was then centrifuged (2200 rpm, 5 minutes) and the solvent decanted. The residue (a pale yellow gel) was dissolved in the minimum amount of acetonitrile and precipitation was repeated. The resulting solid was dissolved in 2 mL of water/methanol 1:1 and applied to a column (1.5 cm × 15.0 cm) of cation-exchange resin (Dowex 50WX8, K^+ form, 10 g) and eluted with water. Fractions containing the desired product (identified by UV-detection on TLC) were combined and purified by reverse phase preparative HPLC using an ACE 5 AQ (150 mm × 21.2 mm) column and a flow rate of 17 mL/min (eluents: ACN and H_2O; from 10 to 60% ACN in 20 minutes; detection at 300 nm). Fractions containing the desired product were lyophilized to afford Pt-S as a bright white solid (0.062 g, 75%).

Purity (HPLC/UV) ≥ 99%.

^{1}H NMR (500 MHz, DMSO) δ 7.50 (d, *J* = 8.6 Hz, 2H), 7.23 (d, *J* = 16.4 Hz, 1H), 7.18 (d, *J* = 8.6 Hz, 2H), 7.06 (d, *J* = 16.4 Hz, 1H), 6.76 (d, *J* = 2.0 Hz, 2H), 6.39 (t, *J* = 2.0 Hz, 1H), 3.78 (s, 6H). ^{13}C NMR (126 MHz, DMSO) δ 161.11, 153.79, 139.79, 132.23, 129.04, 127.50, 127.47, 120.97, 104.70, 100.19, 55.65.

HRMS (ESI-): *m/z* 335.0589 $[M-H]^-$, calcd for $C_{16}H_{15}O_6S$:.335.0595.

Quantification of analytes in blood and tissue samples

The concentration of Pt or Pt-S in the original sample [A] was determined as follows:

$$\mathbf{[A]} = \frac{[A]_m}{[IS]_m} \times [IS]_{spike} \times \frac{\text{Recovery IS}}{\text{Recovery A}} =$$

$$= \frac{\text{Area}_{A,m}}{\alpha_A} \times \frac{\alpha_{IS}}{\text{Area}_{IS,m}} \times \frac{\text{Area}_{IS,spike}}{\alpha_{IS}} \times \frac{1}{R_{A/IS}} =$$

$$= \frac{\text{Area}_{A,m}}{\alpha_A} \times \frac{\text{Area}_{IS,spike}}{\text{Area}_{IS,m}} \times \frac{1}{R_{A/IS}}$$

Where:

- $[A]_m$ and $[IS]_m$ are the concentrations of analyte (A) or internal standard (IS), respectively, measured in the final/treated sample;
- $[IS]_{spike}$ is the known concentration of IS in a solution of H_2O:ACN, 1:1 spiked with the same amount of IS as in the sample before treatment;
- $\text{Area}_{A,m}$ and $\text{Area}_{IS,m}$ are the HPLC peak area of the analyte or internal standard, respectively, measured in the final/treated sample;
- $\text{Area}_{IS,spike}$ is the HPLC peak area of IS, measured in the spiked H_2O:ACN solution;
- α_A and α_{IS} are the slopes of the calibration curves for A or IS, respectively, which correlates HPLC peak area with concentrations;
- $R_{A/IS}$ is the ratio of recovery yields of A and IS, previously determined from samples spiked with known amounts of both A and IS (see below and Table 1).

We can arguably assume that 1 g of tissue corresponds to 1 mL volume, and thus the concentration of analyte per gram of tissue lysate (nmol/g) can be approximated to concentration in µM units (i.e., nomol/mL).

Recovery yields

To establish the recovery yields of Pt and Pt-S from blood and organs, the protocols for the treatment of blood or tissues were applied to samples spiked with a known amount of Pt or Pt-S.

Recoveries of Pt, Pt-S and internal standard were determined as follows:

$$\mathbf{R_{A/IS}} = \frac{\text{Recovery A}}{\text{Recovery IS}} =$$

$$= \frac{[A]_m}{[A]_{spike}} \times \frac{\text{Final volume}}{\text{Initial volume}} \Big/ \frac{[IS]_m}{[IS]_{spike}} \times \frac{\text{Final volume}}{\text{Initial volume}} =$$

$$= \frac{\text{Area}_{A,m}}{\alpha_A} \times \frac{\alpha_A}{\text{Area}_{A,spike}} \Big/ \frac{\text{Area}_{IS,m}}{\alpha_{IS}} \times \frac{\alpha_{IS}}{\text{Area}_{IS,spike}} =$$

$$= \frac{\text{Area}_{A,m}}{\text{Area}_{A,spike}} \times \frac{\text{Area}_{IS,spike}}{\text{Area}_{IS,m}}$$

Where:

- $[A]_{spike}$ is the known concentration of the analyte (A) in a solution of H_2O:ACN, 1:1 spiked with the same amount of A as in the sample before treatment;
- $\text{Area}_{A,spike}$ is HPLC peak area of A, measured in the spiked H_2O:ACN solution.

All the other abbreviations are the same as described for analyte quantification in blood and tissue samples (see above).

Supporting Information Table 1. Comparison of pharmacokinetic data for resveratrol (Resv) and pterostilbene (Pt).

					Tissue levels (nmol/g)[a]					
Compound, dose and route of administration	Ref.	Analyte	Time	Notes	Brain	Lungs	Liver	Kidneys	Testes	Heart
Resv 88 µmol/kg, oral	[57]	Resv	5-10 min	t_{max}	0.11 ± 0.05	0.81 ± 0.24	0.45 ± 0.11	0.06 ± 0.02	-	-
Resv 220 µmol/kg, oral	[55]	Resv	2 h	Sampling time; no kinetics	< 1	< 1	0	0	-	0
		Resv-metabolites (mainly glucuronide)	2 h		< 1	< 1	1 ± 0.3	4 ± 0.7	-	< 1
Resv 66 µmol/kg, i.v.	[44]	Resv	1,5 h	Sampling time; no kinetics	0.17 ± 0.04	1.13 ± 0.34	0.38 ± 0.05	1.45 ± 0.35	0.05 ± 0.01	-
		Resv- glucuronide	1,5 h		0	0.28 ± 0.02	0.58 ± 0.09	2.91 ± 0.19	0.70 ± 0.03	-
		Resv-sulfate	1,5 h		0.04 ± 0.1	0.42 ± 0.10	0.11 ± 0.02	0	0.23 ± 0.01	-
Resv 438 µmol/kg, oral	[58]	Resv	15 min	t_{max}	0.13 ± 0.02	1.66 ± 0.71	3.14 ± 0.81	2.53 ± 0.55	-	2.25 ± 0.40
Pt 88 µmol/kg, oral	This work	Pt	2 h	t_{max}	10.5 ± 7.0	6.8 ± 4.4	39.7 ± 14.2	18.5 ± 12.2	4.2 ± 3.0	6.1 ± 4.2
		Pt-S	2 h	t_{max}	2.7 ± 1.4	34.7 ± 24.8	207.6 ± 119.8	88.3 ± 52.2	6.4 ± 3.7	18.5 ± 12.4

[a] some data were deduced from published graphs.

6. Boosting pterostilbene's effects: a prodrug approach

Abstract:

Pterostilbene (trans-3,5-dimethoxy-4-hydroxystilbene, Pt) is the di-methylated analogue of Resveratrol (Rv). The methyl groups in positions 3 and 5 increase lipophilicity, bioavailability and efficacy. Pt is under investigation for its activity against metabolic disorders, neurodegenerative and cardiovascular diseases, inflammation, cancer.

The bioavailability of Pt, while higher than that of Rv, is negatively affected by the free –OH group in position 4' which is an ideal target for the conjugative enzymes of phase II metabolism. As shown in Azzolini et al.,[1] after an oral administration of Pt to fasted rats Pt sulphate was the major species in blood and organs.

We thus aimed to lessen this problem by protecting the free –OH group of Pt. Our group has developed prodrug tools to reversibly protect the free phenolic functionalities of Rv (e.g. chapters 3 and 4). Here we present a series of Pt derivatives in which the hydroxyl is protected via a carbamoyl linkage to a natural aminoacid. The carbamoyl bond presents the stability characteristics required for prodrugs, and amino acids might a priori be recognized and used by amino acid transporters, thus boosting Pt absorption.

Administration of derivatives of non-polar amino acids led to the best results. Absorption of the derivatives was high (blood concentrations in the range of 100 μM) and the release of Pt was important when isoleucine or β-alanine were used as promoiety. The Pt prodrug incorporating isoleucine was then used for further analysis, and the distribution in several organs of prodrug, Pt and Pt-sulfate was studied as a function of time after oral administration.

The results indicate that in comparison to administration of Pt as such the prodrug affords:

1. Increased absorption of the molecule
2. Considerable reduction of metabolism
3. Higher concentrations of pterostilbene, sustained for several hours, in most of the organs examined

Introduction:

Pterostilbene (trans-3,5-dimethoxy-4-hydroxystilbene, Pt) is a di-methylated form of Resveratrol (3, 5, 4'-trihydroxy-*trans*-stilbene, Rv) found in blueberries and grapes. While Rv has been intensively studied because of its potential multi-faceted usefulness in many areas of human health care, Pt has only recently emerged as a therapeutic compound. The literature suggests that, apart from the structure, Rv and Pt share also many beneficial properties. Rv was addressed to be effective against type 2 diabetes[2-5] and metabolic disease,[6-8] cardiovascular diseases,[9-11] inflammation,[12-14] neurodegenerative disorders[15-17] and cancer.[18-23] Pt now is under intensive investigation for the same targets.[24-27]

The mechanisms behind this multi-targeted activity of Pt are not fully understood, but the effects are in part ascribable to modulation of Nrf2/Keap1 signaling,[28-30] inhibition of the NF-kB pathway[31-34] and perhaps to regulation of gene expression through the MTA1/NuRD complex.[35]

Pt was found to possess a higher efficacy compared to Rv in various investigations,[36-38] a superiority possibly due to a higher bioavailability. Nutakul et al.[38] have found that, *in vitro*, intracellular levels of Pt were 2-4 fold higher than those of Rv after an equimolar dose treatment. The presence of the two methyl groups indeed renders Pt more lipophylic than Resveratrol. Its greater lipophylicity may provide the explanation for its *in vitro* potency, attributable to an efficient permeation of membranes and/or interaction with target proteins. *In vivo* data agrees with those obtained *in vitro*: Pterostilbene shows a greater bioavailability compared to Resveratrol when orally administered.[39]

However, the presence of the hydroxyl group in position 4' renders Pt a good substrate for phase II metabolism enzymes. Depending on the model used, the major phase II metabolites found after Pt oral administration are sulfates and glucuronides. In our previous work[1] we have demonstrated that, except for the brain, the main species found in major rat organs after an oral administration of Pt is the sulfate. Literature in general focuses on the activity of the aglicones, while attention for metabolites is very recent.[40] In the following chapter we show that Pt and Rv can induce autophagy. Metabolites were also investigated for their role in autophagy. While the main species found in the colon, namely dihydro-Rv and dihydro-Pt, showed high efficacy in the induction of autophagy, similar to that of the corresponding aglicones, sulfates were in general less effective. Moreover, phase II metabolites are expected to be rapidly excreted and to be confined to aqueous compartments, thus excluding themselves from important sites of action such as the brain or adipose tissue.

Prodrugs might be a convenient tool to reduce Pt phase II metabolism and slow down its clearance, thus increasing its *in vivo* efficacy. Previous work by my research group has identified the carbamoyl bond as the most convenient linkage for prodrugs of Rv (chapters 3 and 4). The carbamoyl group in fact presents an elevated stability in an acid environment similar to that of the gastric mucosae, it is fairly stable at neutral pH, similar

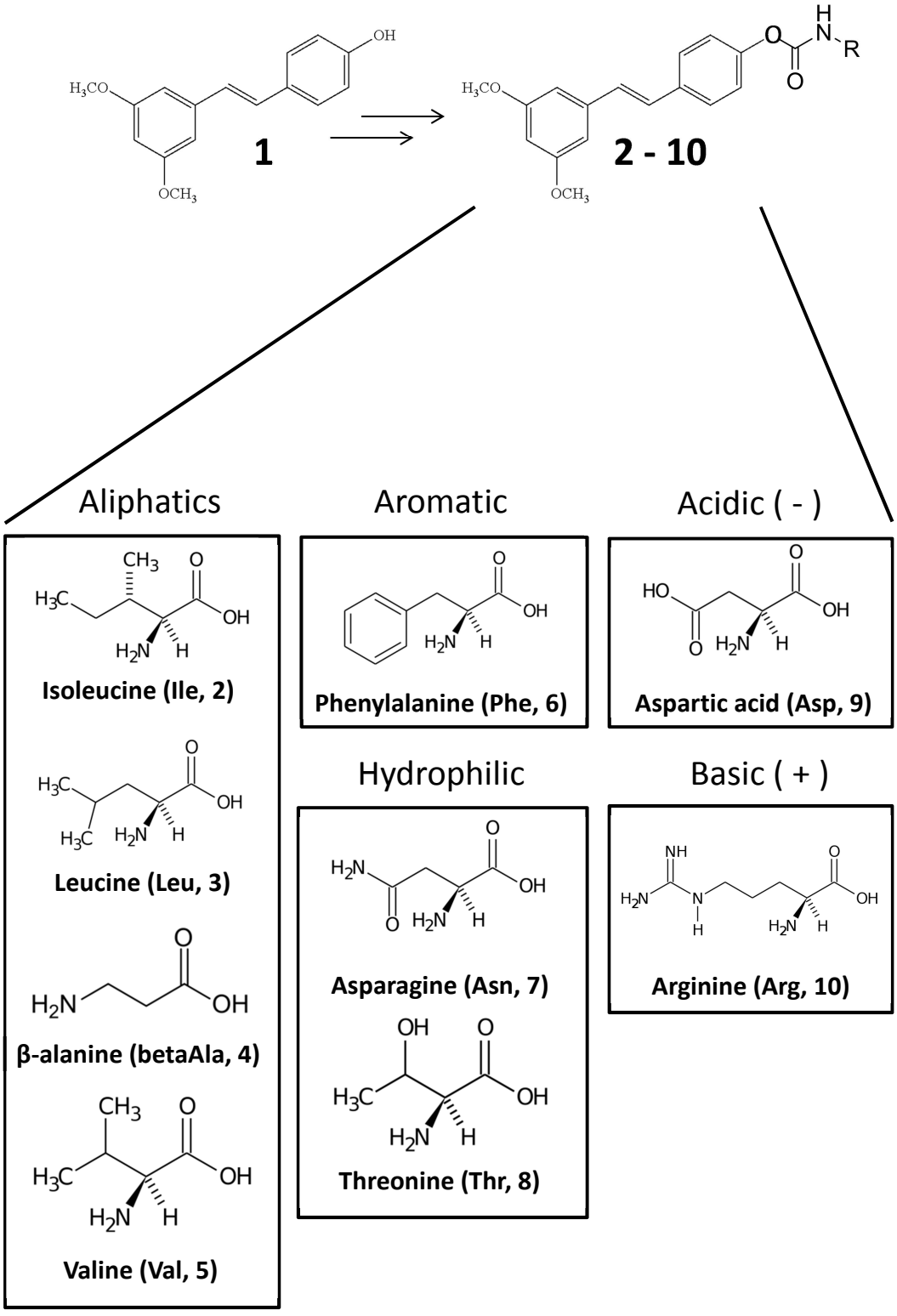

Fig 1: Pt (**1**) was protected at the hydroxyl group by chemical derivatization. The aminoacids shown were attached to the stilbenoid structure via a carbamoyl bond linking the α-amino group and the phenolic oxygen, producing the corresponding derivatives **2-10**

to that of the intestinal mucosae, and it is hydrolyzed with opportune kinetics in blood. However, we have noticed that a multiple substituent pattern may be an obstacle for the permeation of derivatives through the intestinal walls.

In chapter 4 indeed we obtained the best results (sum of prodrugs + phase II metabolites) when we administered mono-substituted derivatives. In so doing unfortunately two of the three hydroxyl's groups of Rv were exposed to phase II enzymes. Pt carries only one free hydroxyl group, so in a carbamate prodrug the obstacle to absorption should be limited. We have also previously tested several substituent groups (chapters 3 and 4). Natural amino acids can be considered the most convenient: they are indeed safe, present several transporters that might enhance the absorption of our derivatives and their structure facilitates the chemical synthesis of derivatives comprising the carbamoyl bond.

Here we present the synthesis and the characterization of a series of derivatives of Pt comprising the carbamoyl bond system and an amino acid (fig 1).

Materials and Methods:

Chemicals and general chemistry procedures. Pterostilbene was purchased from Waseta Int. Trading Co. (Shangai, P.R.China). Other starting materials and solvents were obtained from Wonda Science, Sigma Aldrich, Fluka & Riedel-de Haen, Carlo Erba Reagenti, Iris Biotech, Cambridge Isotope Laboratories Inc., Acros Organics, Prolabo, Merck-Novabiochem, J.T. Baker, and were used as received.

TLCs were run on silica gel supported on plastic (Macherey-Nagel Polygram ® SIL G/UV254, silica thickness 0.2 mm) and visualized by UV detection using a Spectroline NMS-240 lamp. Purifications were performed by flash chromatography on silica gel (Macherey-Nagel 60, 230-400 mesh granulometry 0.063-0.0040 mm) under air pressure or by the automated chromatography system BÜCHI Sepacore® flash system X10 or by preparative HPCL using a Shimadzu LC-8A with-UV-Vis spectrophotometric detection and an inverse phase column (C18-functionalized silica) ACE 5 AQ, 150x21,2 mm.

Mass spectrometry analyses were performed by Agilent Technologies MSD SL Trap with an electrospray source and ion trap analyzer. A Phenomenex® Gemini 3u 110A column was used for HPLC-ESI/MS separations.

NMR spectra were recorded with a Bruker AC 200F spectrometer operating at 200 MHz (for ^{1}H-NMR) and 50 MHz (for ^{13}C-NMR), or a Bruker AV300 FT-NMR UltraShield operating at 300 MHz (for ^{1}H-NMR) and 75 MHz (for ^{13}C-NMR), or a Bruker AVII500 UltraShield operating at 500 MHz (for ^{1}H-NMR) and 126 MHz (for ^{13}C-NMR).

Syntheses were carried out by the group of Prof. C. Paradisi (Dept. of Chemical Sciences) and are described in the Appendix.

Animals. Adult male Wistar rats (approximately 400 g body weight) from the facility of the Department of Biomedical Sciences were used for pharmacokinetic experiments. All experiments involving animals were performed after approval by the University of Padova Ethical Committee for Experimentation on Animals (CEASA) (Permit Number: 80/2011) and by the Italian Ministry of Health, and with the supervision of the Central Veterinary Service of the University of Padova, in compliance with Italian Law DL 116/92, embodying UE Directive 86/609.

HPLC-UV Analysis. Samples (2 µl) were analyzed by HPLC/UV (1290 Infinity LC System, Agilent Technologies) using a reverse phase column (Zorbax RRHD Eclipse Plus C18, 1.8 µm, 50 x 2.1 mm i.d.; Agilent Technologies) and a UV diode array detector (190-500 nm). Solvents A and B were water containing 0.1% trifluoroacetic acid (TFA) and acetonitrile, respectively. The gradient for B was as follows: 10% (0.5 min) then from 10% to 100% in 5 min; the flow rate was 0.6 mL/min. The eluate was preferentially monitored at 286, 300 and 320 nm (corresponding to absorbance maxima of the internal standard, derivatives/metabolites and pterostilbene, respectively). The column compartment was maintained at 35°C.

Hydrolysis Reactions. The chemical stability of all new compounds was tested in aqueous media approximating gastric (0.1 N HCl, NormaFix) and intestinal (0.1 M PBS buffer, pH 6.8) pH values. A 5 µM solution of the compound was prepared from a 5 mM stock solution in DMSO, and incubated at 37°C for 24 hours; samples withdrawn at different times were analyzed by HPLC-UV. Hydrolysis products were identified by comparison of chromatographic retention time with true samples. Non-linear curve fitting was performed using Origin 8.0 data analysis software; the hydrolysis reaction rate constants (k) of the starting compounds were calculated through interpolation of data with the equation for pseudo-first order reactions: $[C] = [C]_0 e^{-kt}$, where:

[*C*] : concentration of the compound

[*C*]$_0$: concentration of the compound at the initial time t$_0$

t: time.

Hydrolysis in blood. Rats were anesthetized and blood was withdrawn from the jugular vein, heparinized and transferred into tubes containing EDTA. Blood samples (1 mL) were spiked with compound (5 µM; dilution from a 5 mM stock solution in DMSO), and incubated at 37°C for 4 hours (the maximum period allowed by blood stability). Aliquots were taken after 10 min, 30 min, 1 h, 2 h and 4 h and treated as described below. Cleared blood samples were finally subjected to HPLC-UV analysis.

Blood Sample Treatment and Analysis. Before starting the treatment, 4,4'-dihydroxybiphenyl was added as internal standard to a carefully measured blood volume (25 µM final concentration). Blood was then stabilized with a freshly-prepared 10 mM solution of ascorbic acid (0.1 vol) and acidified with 0.6 M acetic acid (0.1 vol); after mixing, an excess of acetone (4 vol) was added, followed by sonication (2 min) and

centrifugation (12,000 g, 7 min, 4°C). The supernatant was finally collected and stored at -20°C. Before analysis, acetone was allowed to evaporate at room temperature using a Univapo 150H (UniEquip) vacuum concentrator centrifuge, and up to 40 µL of CH_3CN were added to precipitate residual proteins. After centrifugation (12,000 g, 5 min, 4°C), cleared samples were directly subjected to HPLC-UV analysis.

Metabolites and hydrolysis products were identified by comparison of chromatographic retention time with true samples.

The recovery yields of pterostilbene and its metabolite have been reported previously.[1] The recovery yields of the new prodrugs were obtained following the same protocol and are listed in table 1. Briefly, the recovery yield of each analyte was calculated as the ratio of the amount recovered to that of recovered internal standard. Knowledge of these ratios allowed us to determine the amount of analyte in a blood/organ sample by measuring the recovery of the internal standard (see [41]).

Pharmacokinetics Studies:

Blood. Derivatives **2-10** were administered to overnight-fasted male rats as a single intragastric dose (88 µmol/Kg, dissolved in 250 µl DMSO). Blood samples were obtained by the tail bleeding technique: before drug administration, rats were anesthetized with isoflurane and the tip of the tail was cut off; blood samples (80-100 µL each) were then taken from the tail tip at different time points after drug administration. Blood was collected in heparinized tubes, kept in ice and treated as described above (blood sample treatment and analysis) within 10 min.

Organ distribution. The organ distribution profile of derivative **2** was determined as described in Azzolini et al.[1] Briefly, after a single intragastric oral administration of the derivative (same procedure as for blood pharmacokinetic determinations) animals were anesthetized with isoflurane and sacrificed (N = 3 or 4 for each time point). Blood was collected in heparinized tubes, kept in ice and treated as described above within 10 min. Brain, lungs, heart, liver, kidneys, testes and skeletal muscles (soleus, gastroctemius and anterior tibialis) were explanted, weighed and immediately frozen in liquid nitrogen. 1 g of thawed tissue was mixed with 1 mL of D-PBS (Euroclone), and homogenized with a motorized polypropylene pestel (Sigma, for brain and testes) or with an Ultra-Turrax T25 homogenizer (Janke & Kunkel, for all other tissues). 200 mg of tissue homogenate were transferred into a vial and spiked with the internal standard (4,4'-dihydroxybiphenyl, dilution from a 50× stock solution in acetonitrile, 25 nmol/g tissue final concentration). 10 µL of a freshly-prepared 10 mM solution of ascorbic acid, 10 µL of 4.35 M acetic acid, and 500 µL of acetone were added. Samples were vortexed (2 min), sonicated (2 min) and then centrifuged (12,000 g, 7 min, 4°C). An accurately measured portion of the supernatant was finally collected and stored at -20°C. Further processing and analysis was carried out as described above for blood samples. The Area Under the Curve (AUC) values were calculated using the trapezoidal rule.

Recovery yields of **1** and **1-sulfate** from the organs are those reported in Azzolini et al.[1] The recovery yield of **2** from the organs was determined following the same procedure adopted for **1** and **1-sulfate**. Briefly, 1 g of tissue (from an untreated animal) was mixed with 1 mL of PBS containing 5 nmoles of **2** (dilution from a 100× stock solution in DMSO), and homogenized. 200 mg aliquots of the homogenate were then taken and processed as described above. Recoveries of **2** from the organs are listed in table 2.

Substituent	Recovery ratio	K (h^{-1}) in PBS pH 6,8	K (h^{-1}) in rat blood
2 Isoleucine	1.124 ± 0.088	0.00547 ± 0.00008	0.28 ± 0.01
3 Leucine	0.759 ± 0.068	0.00465 ± 0.00005	0.059 ± 0.004
4 β-alanine	0.697 ± 0.033	0.0070 ± 0.0006	0.96 ± 0.05
5 Valine	0.892 ± 0.077	0.0065 ± 0.0002	0.114 ± 0.007
6 Phenylalanine	0.854 ± 0.029	0.0050 ± 0.0004	0.025 ± 0.002
7 Asparagine	0.712 ± 0.058	0.0114 ± 0.0006	0.174 ± 0.005
8 Threonine	0.714 ± 0.063	0.01320 ± 0.00007	0.131 ± 0.005
9 Aspartic acid	0.884 ± 0.048	0.0034 ± 0.0004	0.034 ± 0.003
10 Arginine	0.778 ± 0.035	0.0099 ± 0.0002	0.31 ± 0.03

Table 1: Recovery ratios and hydrolysis constants of derivatives **2-10.** Recovery ratio (analyte/internal standard) from blood are given as mean values ± standard deviation. N ≥ 4 for each condition. Pseudo-first-order rate constant were calculated as best fit of the experimental points using the first order exponential equation: $[C] = [C_0]*\exp(-kt)$

Results:

Hydrolysis in media mimicking gastric and intestinal pH:

Apart from an easy absorption from the intestine, prodrug candidates should also regenerate the parent compound with opportune kinetics. In agreement with previous results (chapters 3 and 4) the carbamoyl bond turned out to be stable in acidic media (pH = 1; 24h, 37°C) in these compounds. At near-neutral pH (6.8), the derivatives underwent hydrolysis, whose rate depended on the substituent group (figure 1), but was generally low. Derivatives **7** and **8** hydrolyzed most rapidly, while reaction rates were slowest for derivatives **3**, **6** and **9** (see table 1).

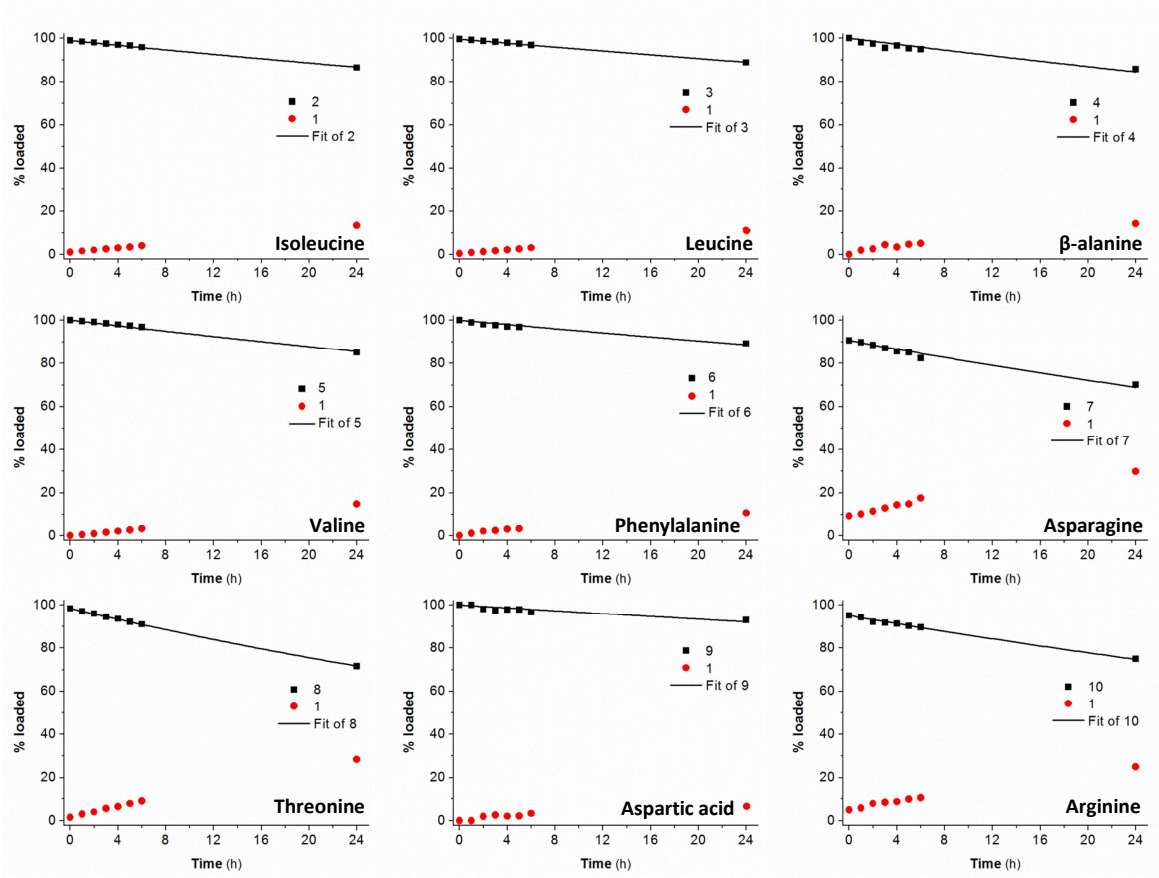

Fig 2: Hydrolysis of derivatives **2-10** in PBS 0.1M, pH 6.8, 37°C. Data are expressed as % of the initially loaded compound. The fit is for pseudo-first order kinetics.

Hydrolysis in blood:

Fresh blood from the jugular vein of a rat was thermostatically kept at 37°C and spiked with a known amount of the derivatives. Due to the limited stability of blood outside the body, the experiments were terminated after 4 hours.

The higher pH of blood in comparison to that of our PBS solution (7.4 vs. 6.8) and the presence of esterase activities in blood (for a discussion please see chapter 3) make hydrolysis in blood faster than in PBS. k values in blood are indeed in most cases higher by a factor of at least 10 compared to those obtained in PBS solution (see table 1). Derivative **4** (with β-alanine) regenerated **1** with the fastest kinetics, while derivatives **3**, **6** and **9** exhibited the lowest rates. Derivative **6** (with phenylalanine) was affected the least by the presence of an higher pH and hydrolytic enzymes (fig 3).

Blood pharmacokinetics:

In vitro (pH = 1 and pH = 6.8) and *ex vivo* (blood) stability profiles of derivatives **2-10** indicated their suitability for use as prodrugs of pterostilbene. We therefore proceeded to determine the pharmacokinetic profile of each of them.

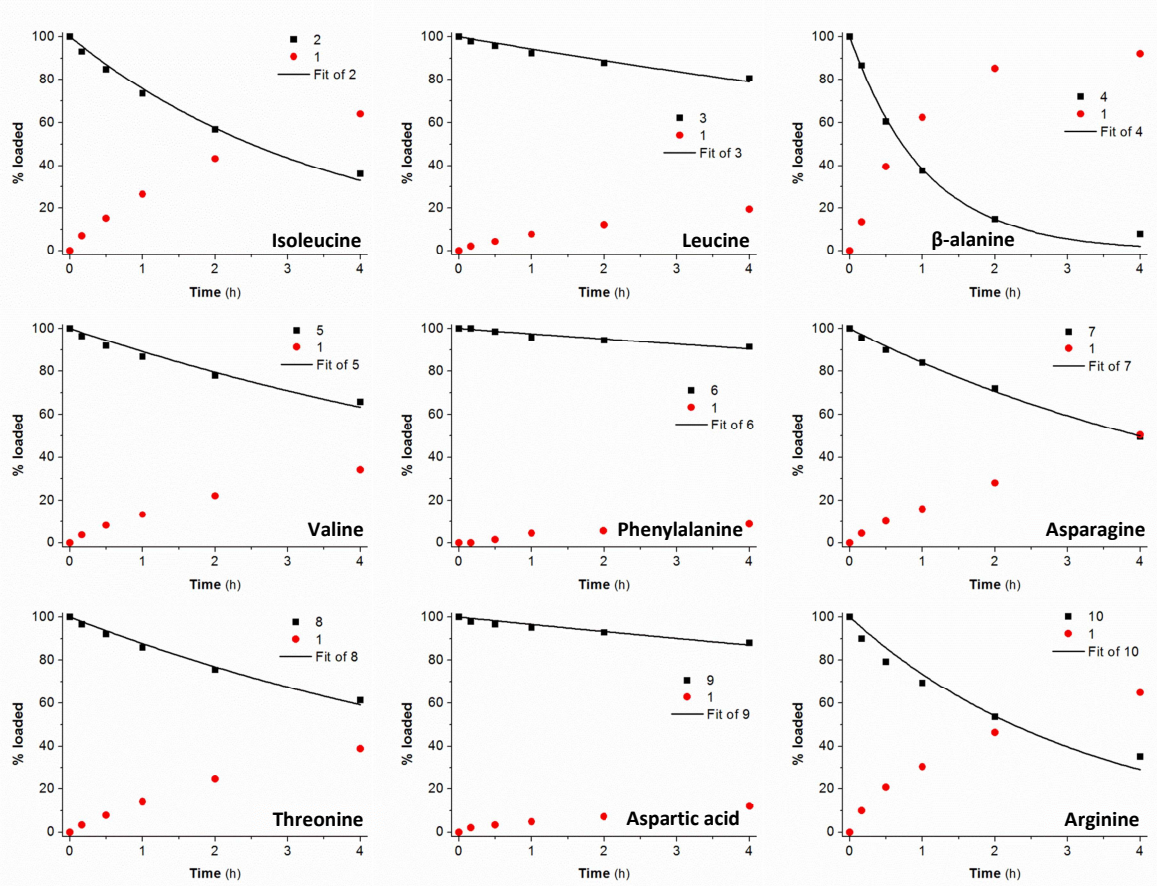

Fig 3: Hydrolysis or derivatives **2-10** in blood. Data are expressed as % of the initially loaded compound. The fit is for pseudo-first order kinetics.

	C_{max} (µM)	t_{max} (h)
2	94.07 ± 49.19	2
3	112.71 ± 85.52	2
4	49.86 ± 10.96	1/2
5	102.60 ± 36.03	4
6	40.40 ± 50.44	2
7	0.83 ± 0.32	1
8	5.74 ± 8.86	1/6
9	1.42 ± 2.02	1/6
10	0.73 ± 0.32	2

Table 2: Blood pharmacokinetics C_{max} and t_{max} parameters of derivatives **2-10.** N ≥ 3 for each condition. Mean values ± standard deviation are shown.

Here the results are presented by class of substituent group. Graphs are identified by the number of the derivative administered (see legends, black line)

*1. Derivatives with aliphatic amino acids as promoieties (**2-5**):*

Derivatives **2-5** when orally administered were rapidly and extensively absorbed by the intestine (fig 4), reaching very high concentrations in blood. As reported in table 2, compounds **2**, **3** and **5** peaked at values around 100 µM (94 ± 49 µM, 113 ± 86 µM and 202 ± 36 µM, respectively). The maximum concentration of compound **4** was also high, but less so than for the other 3 derivatives (50 ± 11 µM).

Compounds **2, 3 and 5** reached their maximum concentration in blood 2 hours after administration and their level was sustained until the 8th hour, then it slowly dropped to almost complete clearance at 24h (fig 4, **2** and **3)**. Pterostilbene (**1**), the hydrolysis product, as well as its major metabolite, **1-sulfate**, were formed in all cases. After the administration of **3** and **5** other minor metabolites were detected, but due to their low amount it was not possible to identify them.

Derivative **4** plateaued in the interval from 30 min to 2 hours after administration, then it rapidly decreased (fig 4, **4**). The high rate of hydrolysis (fig 3, **4**) and the rapid and consistent formation of **1-sulfate** suggest that this compound is also well absorbed, but it rapidly hydrolyzes to produce **1** which is subsequently sulfated. Unidentified metabolites were present also in this case (fig 4, **4**).

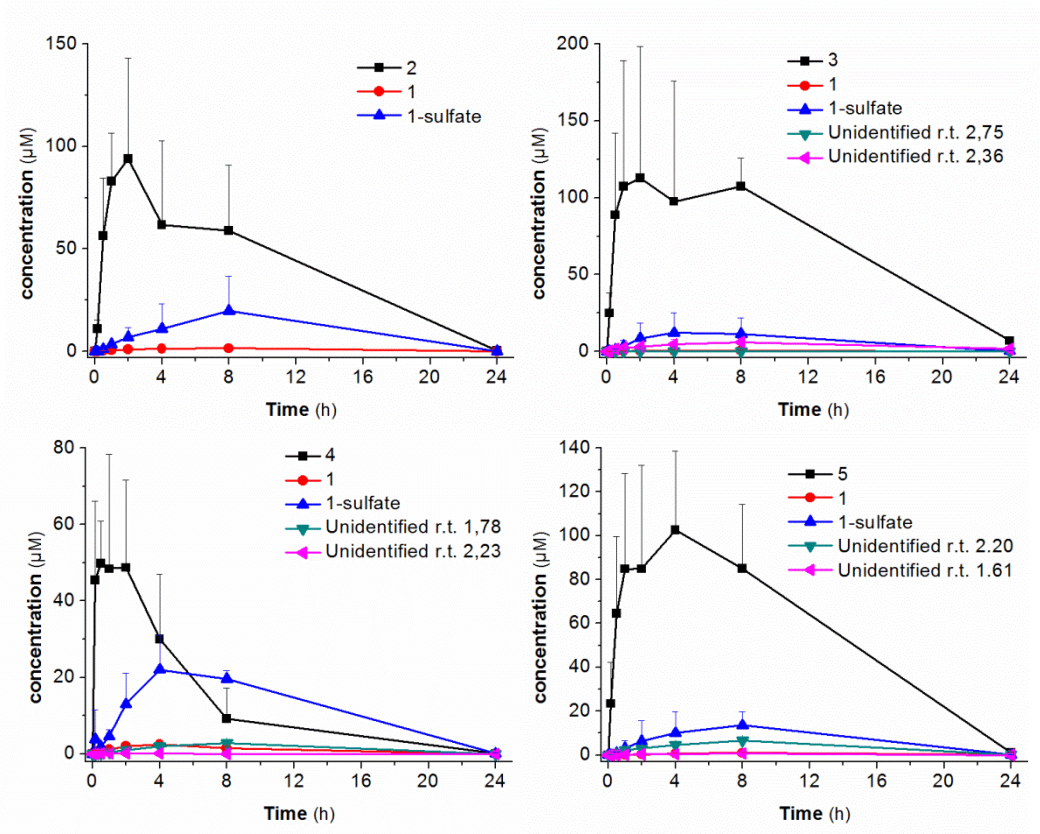

Fig 4: Pharmacokinetic profiles after oral administration of derivatives **2-5**. Data represent average values ± standard deviation. N ≥ 3 in all cases.

*2. Derivative with an aromatic amino acid promoiety (**6**):*

Derivative **6** is also lipophilic, and analogously to derivatives **2-5** it also reached an elevated concentration in blood, sustained for several hours after its oral administration (fig 5, **6**). However its high stability in blood limited the release of **1**. Levels of **1** were low, but phase II metabolite **1-sulfate** was present, indicating a certain degree of hydrolysis of the parent compound under physiological condition. **6** peaked at 2 hours and **1-sulfate** at 8 hours.

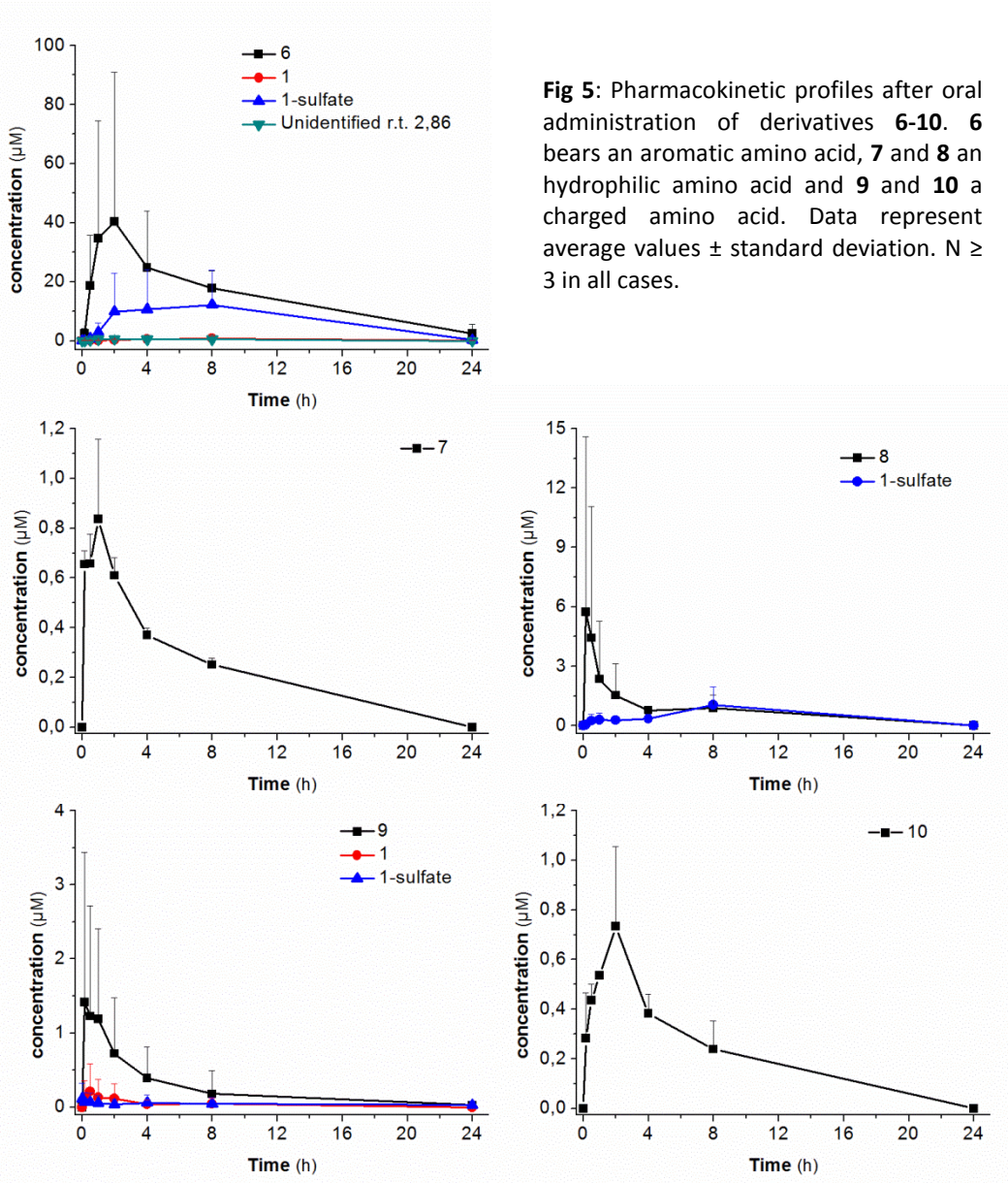

Fig 5: Pharmacokinetic profiles after oral administration of derivatives **6-10**. **6** bears an aromatic amino acid, **7** and **8** an hydrophilic amino acid and **9** and **10** a charged amino acid. Data represent average values ± standard deviation. N ≥ 3 in all cases.

*3. Derivatives with hydrophilic amino acid promoieties (**7** and **8**):*

Compared to previously discussed molecules, the concentrations attained by these two derivatives in blood were very low. **7** reached a disappointing 0.8 µM after 30 minutes, while **8** peaked at 5.7 µM after 10 minutes and then rapidly dropped. In the case of **7** no other species were detected, while **8** yielded traces of **1-sulfate.**

*4. Derivatives with charged amino acid promoieties (**9**, acidic and **10**, basic):*

Administration of **9** and **10** led to very low concentrations of the derivatives in blood (1.4 µM after 10 minutes and 0.7 µM after 2 hours, respectively, in the case of **9**). **1** and **1-sulfate** were detected only after administration of **9**, and as mere traces.

This pharmacokinetics analysis clearly indicates that compounds bearing aliphatic and aromatic amino acid promoieties (**2-6**) give the best results. We intend prodrugs as a tool to increase the levels of the parent compound in the body. Blood cannot be considered as

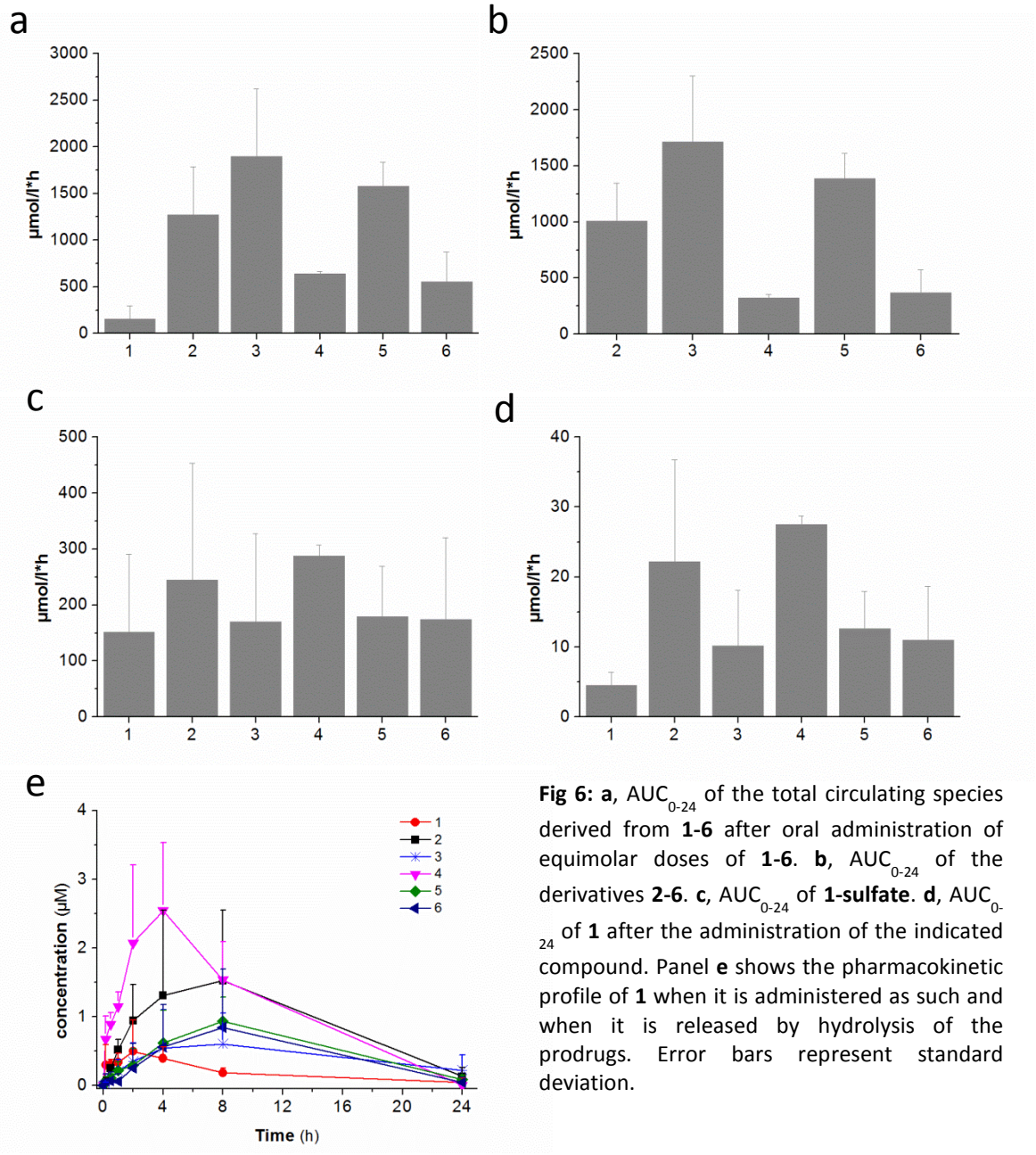

Fig 6: a, AUC_{0-24} of the total circulating species derived from **1-6** after oral administration of equimolar doses of **1-6**. **b**, AUC_{0-24} of the derivatives **2-6**. **c**, AUC_{0-24} of **1-sulfate**. **d**, AUC_{0-24} of **1** after the administration of the indicated compound. Panel **e** shows the pharmacokinetic profile of **1** when it is administered as such and when it is released by hydrolysis of the prodrugs. Error bars represent standard deviation.

fully representative of the body in terms of the levels of **1**, **1-sulfate** and of our derivatives. Its aqueous character renders the blood much more attractive for hydrophilic compounds than for lipophilic ones, as previously mentioned in Azzolini et al.[1] (chapter 5). However a complete organ distribution study of each derivative is time- and energy-expensive. Blood pharmacokinetics are therefore a useful way to separate those compounds which have no chance to function as prodrugs from those presenting desirable characteristics.

The Area Under the Curve (AUC_{0-24}) parameter gives a quantitative idea of the results obtained in blood pharmacokinetics. The AUC_{0-24} of the total amount of pterostilbene-derived species after administration of derivatives **2** to **6** was definitely higher compared to that resulting from administration of **1** as such (fig 6, **a**).

$AUC_{0\text{-}24}$ values are provided in fig 6 for the three species contributing to the total: the unchanged prodrugs (fig 6, **b**), **1-sulfate** (fig 6, **c**) and **1** (fig 6, **d**). While the $AUC_{0\text{-}24}$ of **1-sulfate** is similar in all cases (fig 6, **c**), the relative contribution of **1** and the derivatives is quite different depending on what was administered.

Derivatives **2**, **3** and **5** afforded the highest values of overall $AUC_{0\text{-}24}$. The highest $AUC_{0\text{-}24}$ for **1** was produced instead upon administration of **2** (the isoleucine derivative) and **4** (the β-alanine derivative).

The data indicate that all the derivatives when orally administered had a better $AUC_{0\text{-}24}$ compared to the oral administration of **1** as such, but at the same time they also indicate that for our purposes derivatives **3**, **5** and **6** are not convenient prodrugs of Pt. In fig 6, **d** and 6, **e** indeed it is possible to appreciate that only derivatives **2** and **4** were able to boost the $AUC_{0\text{-}24}$ of **1** to very high values.

We finally decided to proceed with a detailed analysis of the organ distribution of the compounds of interest after a single oral administration, using compound **2**.

Distribution of derivative 2 into major organs:

The recovery ratio of **2** was satisfactory for all the organs examined (see table 3). The time points at which we performed the analysis differ from those of the blood pharmacokinetics. Samplings at 10 minutes, 1 hour and 24 hours were replaced with analyses carried out at 12 and 16 hours. This was done to better cover the period in which the levels of prodrug and its derivatives in the body were high. In the blood pharmacokinetics study with **2** we detected only the prodrug itself, **1** and **1-sulfate** (fig 4, **2**). In liver and kidneys also other minor unidentified metabolites were present, which are not further mentioned here because of their low concentration.

Organs	Recovery ratio of 2
Brain	0.933 ± 0.089
Lungs	0.887 ± 0.111
Heart	0.909 ± 0.087
Liver	0.830 ± 0.063
Kidneys	0.678 ± 0.082
Testes	0.866 ± 0.091
Muscles	0.958 ± 0.064

Table 3: Recovery of **2** from tissues. N ≥ 4 for each condition. Mean values ± standard error are shown.

Blood analysis was repeated as a control for the experiment. Levels of **2**, **1** and **1-sulfate** were comparable to those observed in the blood pharmacokinetics study (fig 7, **blood**).

2 was the major species observed in most of the organs examined, exceptions being the brain and skeletal muscle. **1** and **1-sulfate** concentrations varied depending on the properties of the tissue examined.

1 was the predominant species in the brain, reaching 20 nmoles/g 8 hours after the administration of the prodrug. Notably, in brain the levels of **1** remained above 10 nmoles/g for several hours, from the 4^{th} to the 10^{th}. **1** was also

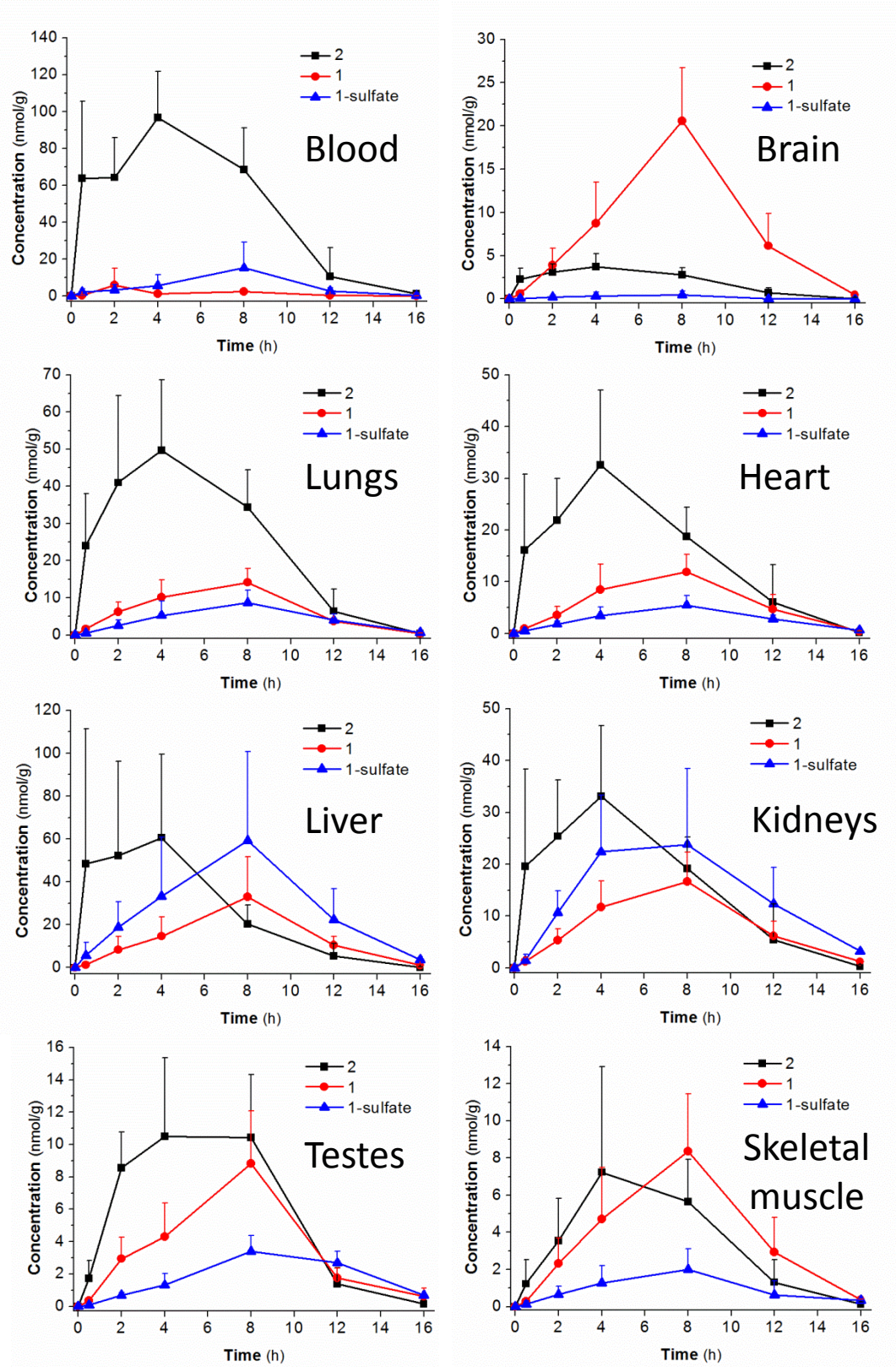

Fig 7: Concentration versus time profiles of derivative **2**, **1** and **1-sulfate** in blood and tissues. A single intragastric dose of **2** (88 µmoles/kg body weight) was administered to rats at time 0. Reported are mean values ± standard deviation. N ≥ 3.

present at appreciable levels in the other organs, with concentrations comprised between 10 and 20 nmoles/g in most of cases (except blood), peaking at the 8th hour.

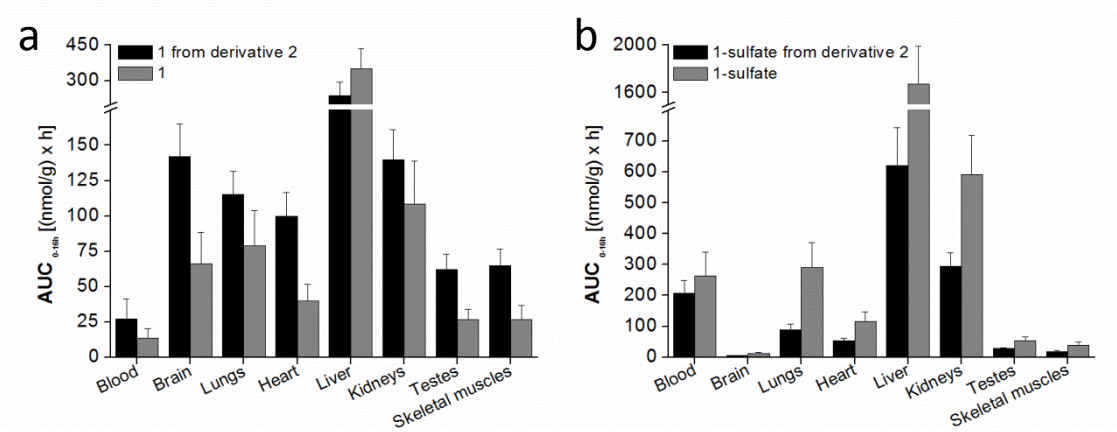

Fig 8: $AUC_{0\text{-}16h}$'s comparison between results obtained in Azzolini et al.[1] (grey bars) and those obtained in this work (black bars). **a**, $AUC_{0\text{-}16}$ of **1** after the administration of the indicated compound. **b**, $AUC_{0\text{-}16}$ of **1-sulfate** after the administration of the indicated compound. Error bars represent standard deviation.

1-sulfate was present at high levels in the liver and kidneys (C_{max} approximately 60 and 25 nmoles/g, respectively) while in the brain, testes and skeletal muscle its levels were low (C_{max} approximately 0.5, 3 and 2 nmoles/g, respectively).

Our previous article, "Pharmacokinetics and tissue distribution of pterostilbene in the rat" ([1], chapter 5) can be considered as a control for this part of the work. Figure 8 compares the AUC values for pterostilbene (**1**; panel a) and its sulfate (**1-sulfate**; panel b) obtained integrating the curves of the organ pharmacokinetics after the administration of **2** (black bars) and those from that work (grey bars). **2** was administered to fasted animals with the same molar dose used in Azzolini et al.[1] (chapter 5).

AUC comparison indicates that by administering prodrug **2** we obtained a consistent increase in the AUC of **1** in most of the organs examined. Minor differences were found in the kidneys, lungs and blood, while the AUC doubled in the brain, heart, testes and skeletal muscle. In the liver the AUC of **1** was similar in the two cases.

When orally administered, compounds are absorbed by the intestine and funneled through the systemic circulation to the liver. This might explain why administration of **2** results in a lower AUC of **1-sulfate** in the liver: while by administering **1** all the absorbed phenol is filtered in the hepatocyte network (and much remains entrapped in the tissue), by administering **2** hepatic clearance concerns to a large extent the prodrug. **1** will reach the liver only after being generated by hydrolysis of **2**, which is distributed in the body.

As previously seen (fig 6, **c**), the AUC of **1-sulfate** in blood does not differ when **1** or **2** are administered. In testes, skeletal muscle and brain its dependence on the specie administered is minor, while differences are more important in lungs, heart, liver and kidneys. In particular in the heart, skeletal muscle, testes and in the kidneys the administration of **2** reduced overall levels of **1-sulfate** by a factor of 2, while in liver and

lungs the difference was even larger. This presumably reflects the elimination of part of the prodrug as such (unaltered).

Conclusions:

Carbamoyl bond-based prodrugs of pterostilbene have been shown to be effective in increasing its bioavailability.

The stability in media mimicking gastric and intestinal pH of all the derivatives is high. At the same time derivatives **2-10** undergo hydrolysis at a moderate rate in blood. From a practical point of view this means that the derivatives, when orally administered, can pass intact through the stomach and the intestine, be distributed in the body through the blood and finally regenerate the natural compound in the organs.

All the derivatives were screened through blood pharmacokinetics. Compounds bearing aliphatic and aromatic amino acids gave the best results. Derivatives **2-6** were able to reach blood concentrations in the range of 50-100 μM. Among these derivatives, **2** and **4** afforded the highest levels of Pterostilbene.

2 was selected for further analysis. We have previously reported the distribution in major organs of pterostilbene following administration of pterostilbene itself; compound **2** was studied under the same conditions in order to compare the results obtained in the two experiments. By administering the prodrug we obtained:

1. Increased absorption of the molecule
2. Consistent reduction of metabolism
3. Higher concentrations of pterostilbene, sustained for several hours, in most of the organs examined

References:

1. Azzolini, M.; La Spina, M.; Mattarei, A.; Paradisi, C.; Zoratti, M.; Biasutto, L. Pharmacokinetics and tissue distribution of pterostilbene in the rat. *Molecular nutrition & food research* **2014,** *58*, (11), 2122-32.
2. Kitada, M.; Koya, D. Renal protective effects of resveratrol. *Oxidative medicine and cellular longevity* **2013,** *2013*, 568093.
3. Kitada, M.; Koya, D. SIRT1 in Type 2 Diabetes: Mechanisms and Therapeutic Potential. *Diabetes & metabolism journal* **2013,** *37*, (5), 315-25.
4. Szkudelski, T.; Szkudelska, K. Resveratrol and diabetes: from animal to human studies. *Biochimica et biophysica acta* **2014**.
5. Szkudelski, T.; Szkudelska, K. Anti-diabetic effects of resveratrol. *Annals of the New York Academy of Sciences* **2011,** *1215*, 34-9.
6. de Ligt, M.; Timmers, S.; Schrauwen, P. Resveratrol and obesity: Can resveratrol relieve metabolic disturbances? *Biochimica et biophysica acta* **2014**.
7. Schrauwen, P.; Timmers, S. Can resveratrol help to maintain metabolic health? *The Proceedings of the Nutrition Society* **2014,** *73*, (2), 271-7.

8. Timmers, S.; Hesselink, M. K.; Schrauwen, P. Therapeutic potential of resveratrol in obesity and type 2 diabetes: new avenues for health benefits? *Annals of the New York Academy of Sciences* **2013,** *1290*, 83-9.
9. Nabavi, S. F.; Li, H.; Daglia, M.; Nabavi, S. M. Resveratrol and stroke: from chemistry to medicine. *Current neurovascular research* **2014,** *11*, (4), 390-7.
10. Mattison, J. A.; Wang, M.; Bernier, M.; Zhang, J.; Park, S. S.; Maudsley, S.; An, S. S.; Santhanam, L.; Martin, B.; Faulkner, S.; Morrell, C.; Baur, J. A.; Peshkin, L.; Sosnowska, D.; Csiszar, A.; Herbert, R. L.; Tilmont, E. M.; Ungvari, Z.; Pearson, K. J.; Lakatta, E. G.; de Cabo, R. Resveratrol prevents high fat/sucrose diet-induced central arterial wall inflammation and stiffening in nonhuman primates. *Cell metabolism* **2014,** *20*, (1), 183-90.
11. Zordoky, B. N.; Robertson, I. M.; Dyck, J. R. Preclinical and clinical evidence for the role of resveratrol in the treatment of cardiovascular diseases. *Biochimica et biophysica acta* **2014**.
12. Koeberle, A.; Werz, O. Multi-target approach for natural products in inflammation. *Drug discovery today* **2014,** *19*, (12), 1871-1882.
13. Cardozo, L. F.; Pedruzzi, L. M.; Stenvinkel, P.; Stockler-Pinto, M. B.; Daleprane, J. B.; Leite, M., Jr.; Mafra, D. Nutritional strategies to modulate inflammation and oxidative stress pathways via activation of the master antioxidant switch Nrf2. *Biochimie* **2013,** *95*, (8), 1525-33.
14. Renaud, J.; Martinoli, M. G. Resveratrol as a protective molecule for neuroinflammation: a review of mechanisms. *Current pharmaceutical biotechnology* **2014,** *15*, (4), 318-29.
15. Granzotto, A.; Zatta, P. Resveratrol and Alzheimer's disease: message in a bottle on red wine and cognition. *Frontiers in aging neuroscience* **2014,** *6*, 95.
16. Pasinetti, G. M.; Wang, J.; Ho, L.; Zhao, W.; Dubner, L. Roles of resveratrol and other grape-derived polyphenols in Alzheimer's disease prevention and treatment. *Biochimica et biophysica acta* **2014**.
17. Rege, S. D.; Geetha, T.; Griffin, G. D.; Broderick, T. L.; Babu, J. R. Neuroprotective effects of resveratrol in Alzheimer disease pathology. *Frontiers in aging neuroscience* **2014,** *6*, 218.
18. Khan, A.; Aljarbou, A. N.; Aldebasi, Y. H.; Faisal, S. M.; Khan, M. A. Resveratrol suppresses the proliferation of breast cancer cells by inhibiting fatty acid synthase signaling pathway. *Cancer epidemiology* **2014,** *38*, (6), 765-72.
19. Dhar, S.; Kumar, A.; Li, K.; Tzivion, G.; Levenson, A. S. Resveratrol regulates PTEN/Akt pathway through inhibition of MTA1/HDAC unit of the NuRD complex in prostate cancer. *Biochimica et biophysica acta* **2014,** *1853*, (2), 265-275.
20. Singh, C. K.; Ndiaye, M. A.; Ahmad, N. Resveratrol and cancer: Challenges for clinical translation. *Biochimica et biophysica acta* **2014**.
21. Hasima, N.; Ozpolat, B. Regulation of autophagy by polyphenolic compounds as a potential therapeutic strategy for cancer. *Cell death & disease* **2014,** *5*, e1509.
22. Hu, Y.; Li, C.; Li, H.; Li, M.; Shu, X. Resveratrol-Mediated Reversal of Tumor Multi-Drug Resistance. *Current drug metabolism* **2014**.
23. Phuah, N. H.; Nagoor, N. H. Regulation of microRNAs by natural agents: new strategies in cancer therapies. *BioMed research international* **2014,** *2014*, 804510.
24. Paul, S.; Rimando, A. M.; Lee, H. J.; Ji, Y.; Reddy, B. S.; Suh, N. Anti-inflammatory action of pterostilbene is mediated through the p38 mitogen-activated protein kinase pathway in colon cancer cells. *Cancer prevention research (Philadelphia, Pa.)* **2009,** *2*, (7), 650-7.
25. Paul, S.; DeCastro, A. J.; Lee, H. J.; Smolarek, A. K.; So, J. Y.; Simi, B.; Wang, C. X.; Zhou, R.; Rimando, A. M.; Suh, N. Dietary intake of pterostilbene, a constituent of blueberries, inhibits the beta-catenin/p65 downstream signaling pathway and colon carcinogenesis in rats. *Carcinogenesis* **2010,** *31*, (7), 1272-8.
26. McCormack, D.; McFadden, D. Pterostilbene and cancer: current review. *The Journal of surgical research* **2012,** *173*, (2), e53-61.
27. McCormack, D.; McFadden, D. A review of pterostilbene antioxidant activity and disease modification. *Oxidative medicine and cellular longevity* **2013,** *2013*, 575482.

28. Zhang, B.; Wang, X. Q.; Chen, H. Y.; Liu, B. H. Involvement of the Nrf2 Pathway in the Regulation of Pterostilbene-Induced Apoptosis in HeLa Cells via ER Stress. *Journal of pharmacological sciences* **2014,** *126*, (3), 216-29.
29. Saw, C. L.; Guo, Y.; Yang, A. Y.; Paredes-Gonzalez, X.; Ramirez, C.; Pung, D.; Kong, A. N. The berry constituents quercetin, kaempferol, and pterostilbene synergistically attenuate reactive oxygen species: involvement of the Nrf2-ARE signaling pathway. *Food and chemical toxicology : an international journal published for the British Industrial Biological Research Association* **2014,** *72*, 303-11.
30. Bhakkiyalakshmi, E.; Shalini, D.; Sekar, T. V.; Rajaguru, P.; Paulmurugan, R.; Ramkumar, K. M. Therapeutic potential of pterostilbene against pancreatic beta-cell apoptosis mediated through Nrf2. *British journal of pharmacology* **2014,** *171*, (7), 1747-57.
31. Das, S.; Das, D. K. Anti-inflammatory responses of resveratrol. *Inflammation & allergy drug targets* **2007,** *6*, (3), 168-73.
32. Kumar, A.; Negi, G.; Sharma, S. S. Neuroprotection by resveratrol in diabetic neuropathy: concepts & mechanisms. *Current medicinal chemistry* **2013,** *20*, (36), 4640-5.
33. Kumar, A.; Sharma, S. S. NF-kappaB inhibitory action of resveratrol: a probable mechanism of neuroprotection in experimental diabetic neuropathy. *Biochemical and biophysical research communications* **2010,** *394*, (2), 360-5.
34. Mak, K. K.; Wu, A. T.; Lee, W. H.; Chang, T. C.; Chiou, J. F.; Wang, L. S.; Wu, C. H.; Huang, C. Y.; Shieh, Y. S.; Chao, T. Y.; Ho, C. T.; Yen, G. C.; Yeh, C. T. Pterostilbene, a bioactive component of blueberries, suppresses the generation of breast cancer stem cells within tumor microenvironment and metastasis via modulating NF-kappaB/microRNA 448 circuit. *Molecular nutrition & food research* **2013,** *57*, (7), 1123-34.
35. Li, K.; Dias, S. J.; Rimando, A. M.; Dhar, S.; Mizuno, C. S.; Penman, A. D.; Lewin, J. R.; Levenson, A. S. Pterostilbene acts through metastasis-associated protein 1 to inhibit tumor growth, progression and metastasis in prostate cancer. *PloS one* **2013,** *8*, (3), e57542.
36. Chang, J.; Rimando, A.; Pallas, M.; Camins, A.; Porquet, D.; Reeves, J.; Shukitt-Hale, B.; Smith, M. A.; Joseph, J. A.; Casadesus, G. Low-dose pterostilbene, but not resveratrol, is a potent neuromodulator in aging and Alzheimer's disease. *Neurobiology of aging* **2012,** *33*, (9), 2062-71.
37. Chiou, Y. S.; Tsai, M. L.; Nagabhushanam, K.; Wang, Y. J.; Wu, C. H.; Ho, C. T.; Pan, M. H. Pterostilbene is more potent than resveratrol in preventing azoxymethane (AOM)-induced colon tumorigenesis via activation of the NF-E2-related factor 2 (Nrf2)-mediated antioxidant signaling pathway. *Journal of agricultural and food chemistry* **2011,** *59*, (6), 2725-33.
38. Nutakul, W.; Sobers, H. S.; Qiu, P.; Dong, P.; Decker, E. A.; McClements, D. J.; Xiao, H. Inhibitory effects of resveratrol and pterostilbene on human colon cancer cells: a side-by-side comparison. *Journal of agricultural and food chemistry* **2011,** *59*, (20), 10964-70.
39. Yeo, S. C.; Ho, P. C.; Lin, H. S. Pharmacokinetics of pterostilbene in Sprague-Dawley rats: the impacts of aqueous solubility, fasting, dose escalation, and dosing route on bioavailability. *Molecular nutrition & food research* **2013,** *57*, (6), 1015-25.
40. Del Rio, D.; Costa, L. G.; Lean, M. E.; Crozier, A. Polyphenols and health: what compounds are involved? *Nutrition, metabolism, and cardiovascular diseases : NMCD* **2010,** *20*, (1), 1-6.
41. Biasutto, L.; Marotta, E.; Garbisa, S.; Zoratti, M.; Paradisi, C. Determination of quercetin and resveratrol in whole blood--implications for bioavailability studies. *Molecules (Basel, Switzerland)* **2010,** *15*, (9), 6570-9.

Appendix:

Synthesis of derivatives 2-10:

Derivatives were synthesized by the group of prof. Cristina Paradisi, Department of Chemical Sciences, University of Padova.

4'-[N-(isoleucinyl)-carbamoyl]-pterostilbene (Pt-CP-Ile, 2):

1. 4'-[N-(isoleucinyl-tert-butyl)]-pterostilbene

A solution of L-isoleucine tert butyl ester hydrochloride (0.5005 g, MW = 223.74 g/mol, n = 2.23 10^{-3} mol, 1 eq) and DMAP (1.0883 g, MW = 122.17 g/mol, 8.91 10^{-3} mol, 4 eq) in DCM dry (7 mL) was added dropwise to a solution of bis-(4-nitrophenyl) carbonate (0.7142 g, MW = 304.21 g/mol, n = 2.35 10^{-3} mol, 1.05 eq) in DCM dry (4.5 mL). The resulting mixture was stirred at 50°C for 4 hours. Then, pterostilbene (0.7523 g, MW = 256.3 g/mol, n = 2.93 10^{-3} mol, 1.3 eq) was added to the solution. The resulting mixture was stirred at 50°C overnight, and then it was diluted in DCM (100 mL) and extracted with HCl 0.5 M (2 × 100 mL). The organic layer was dried over with $MgSO_4$ and filtered. The solvent was evaporated under reduced pressure and the product was purified from PNP, and Pt by flash chromatography using petroleum ether/DCM/ethylic ether (5/4/1) as eluent, and from Ile-OtBu-PNPC by flash chromatography using petroleum ether/Et_2O (7/3) as eluent, to afford Pt-CP-Ile-OtBu as a colourless oil (0.7803 g, MW = 469.25 g/mol, n = 1.66 10^{-3} mol, 74.3 % yield).

MS-ESI (ion trap) = 470 m/z [$M+H^+$]

^{1}H NMR (200 MHz, $CDCl_3$) δ (ppm) = 7.48 (d, J = 8.4 Hz, 2H), 7.19 – 6.82 (m, 4H), 6.66 (d, J = 2.0 Hz, 2H), 6.39 (m, 1H), 5.62 (m, 1H), 4.29 (m, 1H), 3.83 (s, 6H), 1.95 (m, 1H), 1.50 (m, 11H), 0.97 (m, 6H).

^{13}C NMR (50 MHz, $CDCl_3$) δ(ppm) = 170.91, 161.20, 154.31, 150.64, 139.40, 134.54, 128.45, 127.50, 121.90, 104.66, 100.17, 82.40, 58.82, 55.49, 38.50, 28.21, 25.30, 15.54, 11.88.

2. 4'-[N-(isoleucinyl)-carbamoyl]-pterostilbene

TFA (2.5 mL, MW = 114.02 g/mol, n = 3.26 10^{-2} mol, 40.25 eq) was added to a solution of Pt-CP-Ile-OtBu (0.3798 g, MW = 469.25 g/mol, n = 8.1 10^{-4} mol, 1 eq) and TIPS (0.625 mL, 5 % v/v) in DCM dry (10 mL). The mixture was stirred at 0°C overnight. The TFA and the solvent were evaporated under reduced pressure. The product was titrated with toluene (2 × 5 mL) and purified by flash chromatography using petroleum ether/acetone (7/3) as eluent, to afford Pt-CP-Ile-OH as a white solid (0.2537 g, MW = 413.18 g/mol, n = 6.14 10^{-4} mol, 76 % yield).

MS-ESI (ion trap) = 413 m/z, 434 m/z [$M+Na]^+$

^{1}H NMR (200 MHz, $CDCl_3$) δ (ppm) = 8.06-8.03 (m, 1H) 7.49 (d, J = 8.5 Hz, 2H), 7.04 (m, 4H), 6.66 (d, J = 1.9 Hz, 2H), 6.40 (m, 1H), 4.46 (m, 1H), 3.83 (s, 6H), 1.86 (m, 1H)1.53-1.21 (m, 1H) 0.94-0.85 (m, 1H), 1.03 (m, 6H).

^{13}C NMR (50 MHz, $CDCl_3$) δ (ppm) = 176.02, 160.66, 154.11, 150.02, 138.93, 134.31, 128.42, 127.93, 127.11, 121.42, 104.27, 99.77, 58.05, 55.07, 37.53, 24.60, 15.25, 11.32.

4'-[N-(leucinyl)-carbamoyl]-pterostilbene (Pt-CP-Leu, 3)

1. [N-(tert-butyl-leucinyl)-carbamoyl]-p-nitrophenol (PNPC-Leu-OtBu).

Leucine tert butyl ester hydrocloride (1.5997 g, MW = 223.74 g/mol, n = $7.15 \cdot 10^{-3}$ mol, 1 eq) was dissolved in 35 mL of acetonitrile. DMAP (1.7590 g, MW = 122.17 g/mol, n = $1.44 \cdot 10^{-2}$ mol, 2 eq) and bis(4-nitrophenyl)carbonate (2.1766g, MW = 304.21 g, n = 7.15·10-3 mol, 1 eq) were added at the previous solution. The reaction mixture was stirred at room temperature for 3 hours and then was warmed up to 50°C and stirred for another hour. The resulting mixture was diluted in DCM (200 mL), washed with 0,5 N HCl (150 mL) and extracted with 2 × 100 mL of dichloromethane. The organic layer was dried over $MgSO_4$ and filtred. The solvent was evaporated under reduced pressure and the residue was purified by flash chromatography using Petroleum Ether:Ethyl Ether=6,5:3,5 as eluent. Solvent was evaporated under reduced pressure to afford 1.9800 g of product (78.6% yield).

^{1}H NMR ($CDCl_3$, 300 MHz) δ (ppm): 8.205 (d, 2H, aromatic meta position, $^3J_{H-H}$ = 9 Hz), 7.295 (d, 2H, aromatic ortho position, $^3J_{H-H}$ = 9 Hz), 5.735 (d, 1H, CH-N*H*, $^3J_{H-H}$ = 9 Hz), 4.26-4.34 (m, 1H, NH-C*H*), 1.52-1.83 (m, 3H, NH-CH-CH_2 and CH_3-C*H*-CH_3), 1.48 (s, 9H, 3 × C-CH_3), 0.97 (d, 6H, 2 × CH-CH_3, $^3J_{H-H}$ = 9 Hz);

^{13}C NMR ($CDCl_3$, 300 MHz) δ (ppm): 171.72, 155.76, 152.69, 144.76, 125.10, 121.96, 82.50, 53.23, 41.99, 27.98, 24.89, 22.81, 21.98.

2. [N-(tert-butyl-leucinyl)-carbamoyl]-pterostilbene (Pt-CP-Leu-OtBu).

A solution of pterostilbene (0.5015 g, MW = 256.3 g/mol, n = $1.96 \cdot 10^{-3}$ mol, 1 eq) in 20 mL of acetonitrile was prepared. PNPC-Leu-OtBu (1.3791 g, MW = 396.43 g/mol, n = $3.91 \cdot 10^{-3}$ mol, 2 eq) and DMAP (0.4723 g, MW = 122,17 g/mol, n = $3{,}86 \cdot 10^{-3}$ mol, 2 eq) were added to the previous solution. The mixture was stirred at 50°C under nitrogen stream overnight. The reaction progress was checked by TLC. The resulting mixture was diluted in DCM (100 mL), washed with 0,5 N HCl (100 mL) and extracted with 2 × 100 mL of DCM. The organic layer was collected and dried over $MgSO_4$. The solvent was evaporated under reduced pressure and the residue was purified from 4-nitrophenol by flash chromatography using Petroleum Ether:Dichloromethane:Ethyl Ether=5:4:1, and from the residual PNPC-Leu-OtBu by flash chromatography using Petroleum Ether:Ethyl Ether=7:3. The solvent was evaporated under reduced pressure to afford 0.8902 g of product (86.2% yield).

^{1}H NMR ($CDCl_3$, 500 MHz) δ (ppm): 8,01 (d, 1H, O-(C=O)-N*H*, $^3J_{H-H}$ = 10 Hz), 7.465 (d, 2H, H-2' and 6', $^3J_{H-H}$ = 5 Hz), 7.13 (d, 2H, H-3' and 5', $^3J_{H-H}$ = 10 Hz), 6.93-7.06 (d+d, 2H, H-7 and 8), 6.66 (d, 2H, H-2 and 6, $^4J_{H-H}$ = 2 Hz), 6.40 (t, 1H, H-4, $^4J_{H-H}$ = 2 Hz), 4.32-4.36 (m 1H, Leu C_α-*H*), 3.80 (s, 6H, O-CH_3), 1.75-1,83 (m, 1H, Leu C_γ-*H*), 1.55-1.70 (m, 2H, Leu C_β-H_2), 1.50 (s, 9H, (C=O)-O-C(CH_3)$_3$), 0.98-1.00 (dd, 6H, Leu C_δ-H_3 and Leu Cε-H_3).

^{13}C NMR ($CDCl_3$, 500 MHz) δ (ppm): 172.12, 160.94, 154.17, 150.47, 139.22, 134.37, 128.55, 128..22, 127.33, 121.75, 104.52, 100.00, 82.03, 55.27, 41.90, 27.97, 24.86, 22.82, 21.99.

3. [N-(leucinyl)-carbamoyl]-pterostilbene (Pt-CP-Leu-OH).

Pt-CP-Leu-OtBu (0.7958 g, MW = 469.57 g/mol, n = $1.69 \cdot 10^{-3}$ mol, 1 eq) was dissolved in 25 mL of anhydrous dichloromethane and 5 mL of TFA (MW = 114.02 g/mol, n = $6.53 \cdot 10^{-2}$ mol, 42.7 eq) were added to the solution. The mixture was stirred at room temperature for 3 hours under nitrogen stream. The reaction progress was checked by TLC. After 3 hours the solvent and the residual TFA were evaporated under reduced pressure. The residue was titrated with toluene (2 × 5 mL), and then solvent was evaporated under reduced pressure. The product was purified by automated chromatography system using Petroleum ether:Acetone=7:3. Solvent was evaporated under reduced pressure to afford 0.5103 g of product (73.0% yield).

^{1}H NMR ($CDCl_3$, 500 MHz) δ (ppm): 7.47 (d, 2H, H-2' and 6', $^{3}J_{H-H}$ = 10 Hz), 7.13 (d, 2H, H-3' and 5', $^{3}J_{H-H}$ = 10 Hz), 6.94-7.06 (d+d, 2H, H-7 and 8), 6.655 (d, 2H, H-2 and 6, $^{4}J_{H-H}$ = 2 Hz), 6.40 (t, 1H, H-4, $^{4}J_{H-H}$ = 2 Hz), 4.43-4.48 (m 1H, Leu C_{α}-*H*), 3.82 (s, 6H, O-CH_3), 1.72-1.84 (m, 2H, Leu C_{β}-H_2), 1.61-1.67 (m, 1H, Leu C_{γ}-*H*), 0.98-1.00 (dd, 6H, Leu C_{δ}-H_3 and Leu C_{ε}-H_3).

^{13}C NMR ($CDCl_3$, 300 MHz) δ (ppm): 172.12, 160.94, 154.17, 150.47, 139.22, 134.37, 128.55, 128..22, 127.33, 121.75, 104.52, 100.00, 82.03, 55.27, 41.90, 27.97, 24.86, 22.82, 21.99.

ESI-MS:825 m/z $[2(\text{Pt CP-Leu-OH})]^-$

4'-[N-(β-alanin)-carbamoyl]-pterostilbene (Pt-CP-betaAla, 4):

1. [N-(β-alanin-tert-butyl)]-p-nitro-phenylcarbamate

A solution of β-alanine-tert-butyl ester (0.5048 g, MW = 181.66 g/mol, n = 2.78 10^{-3} mol, 1 eq) and 4-(dimethylamino)pyridine (0.6828 g, MW =122.17 g/mol, n = 5.59 10^{-3} mol, 2 eq) in ACN (5 mL) was added dropwise to a solution of bis(4-nitrophenyl) carbonate (0.8253 g, MW = 304.21 g/mol, n = 2.71 10^{-3} mol, 1 eq) in ACN (20 mL). The resulting mixture was stirred at 50°C overnight. The solution was diluted in DCM (150 mL) and washed with HCl (2 × 100 mL). The organic layer was dried with $MgSO_4$ and filtered. The solvent was evaporated under reduced pressure. The product was purified by flash chromatography using $CHCl_3$/acetone (99/1) as eluent, to afford β-Ala-OtBu-PNPC as a colourless oil (0.5693 g, MW = 310.3, n = 1.83 10^{-3} mol, 65.3 % yield).

MS-ESI (ion trap) = 333 m/z $[M+Na]^+$

^{1}H NMR (300 MHz, $CDCl_3$) δ (ppm) = 8.24 (d, J = 9.1 Hz, 2H), 7.32 (d, J = 9.1 Hz, 2H), 5.81 (s, 1H), 3.52 (m, 2H), 2.54 (t, J = 5.9 Hz, 2H), 1.48 (s, 9H).

^{13}C NMR (75 MHz, $CDCl_3$) δ (ppm) = 171.97, 156.26, 153.40, 145.11, 125.46, 122.26, 81.82, 37.31, 35.41, 28.36.

2. 4'-[N-(β-alanin-tert butyl ester)-carbamoyl]-pterostilbene

A solution of DMAP (0.5482 g, MW = 122.17 g/mol, n = 4.49 10^{-3} mol, 2 eq) and pterostilbene (0.7246 g, MW = 256.3 g/mol, n = 2.83 10^{-3} mol, 1.3 eq) in DCM dry (5 mL) was added to a solution of β-Ala-OtBu-PNPC (0.6685 g, MW = 310.3 g/mol, n = 2.15 10^{-3} mol, 1 eq) in DCM dry (6 mL). The mixture was stirred at 50°C overnight. The solvent was evaporated under reduced pressure and the product was purified by flash chromatography using $CHCl_3$/Et_2O/petroleum ether (5/1.5/3.5) as eluent, to afford Pt-CP-□□-Ala-OtBu as a colourless oil(0.8322 g, MW = 427.20 g/mol, n = 1.95 10^{-3} mol, 90.4 % yield).

MS-ESI (ion trap) = 428 m/z [$M+H^+$]

^{1}H NMR (500 MHz, $CDCl_3$) δ (ppm) = 7.50 (d, J = 8.5 Hz, 2H), 7.18 – 6.94 (m, 4H), 6.69 (d, J = 2.2 Hz, 2H), 6.42 (t, J = 2.1 Hz, 1H), 3.85 (s, 6H), 3.53 (m, 2H), 2.55 (t, J = 6.0 Hz, 2H), 1.51 (s, 9H).

^{13}C NMR (126 MHz, $CDCl_3$) δ (ppm) = 171.73, 160.99, 154.46, 150.57, 139.29, 134.37, 128.59, 128.33, 127.40, 121.79, 104.55, 100.03, 81.27, 55.37, 36.92, 35.34, 28.14.

3. 4'-[N-(β-alanin)-carbamoyl]-pterostilbene

TFA (5 mL, MW = 114.02 g/mol, n = 6.53 10^{-2} mol, 33.5 eq) and TIPS (5 % v/v) were added to a solution of Pt-CP-β-Ala-OtBu (0.8322 g, MW = 427.20 g/mol, n = 1.95 10^{-3} mol, 1 eq) in DCM dry (5 mL). The mixture was stirred at 0°C overnight and then the TFA and the solvent were evaporated under reduced pressure. The product was titrated with toluene (2 × 5 mL) and purified by flash chromatography using $CHCl_3$/acetone (7/3) as eluent, to afford Pt-CP-β-Ala-OH as a white solid (0.5989 g, MW = 371.14 g/mol, n = 1.61 10^{-3} mol, 82.5 % yield).

ESI+-MS (ion trap): 371 m/z

^{1}H NMR (500 MHz, DMSO) δ (ppm) = 7.60 (d, J = 8.6 Hz, 2H), 7.20 (m, 4H), 6.79 (d, J = 2.1 Hz, 2H), 6.43 (t, J = 2.1 Hz, 1H), 3.79 (s, 6H), 3.31 (m, 2H), 2.49 (t, J = 7.0 Hz, 2H)

^{13}C-NMR (126 MHz, DMSO) δ (ppm) = 172.72, 160.70, 154.21, 150.58, 139.11, 133.83, 128.14, 127.32, 121.98, 104.47, 99.90, 55.22, 39.52, 36.73, 33.97.

4'- [N-(valinyl)-carbamoyl]-pterostilbene (Pt-CP-Val, 5)

1. 4'-[N-(tert-butyl-valinyl)-carbamoyl]-p-nitrophenol (PNPC-Val-OtBu).

Valine tert butyl ester hydrocloride (0.9967 g, MW = 209.71 g/mol, n = 4.75·10^{-3} mol, 1 eq) was dissolved in 35 mL of acetonitrile. DMAP (1.1696 g, MW = 122.17 g/mol, n = 9,57·10^{-3} mol, 2 eq) and bis(4-nitrophenyl)carbonate (1.4672 g, MW = 304.21 g, n = 4.82·10^{-3} mol, 1 eq) were added at the previous solution. The reaction mixture was stirred at room temperature for 4 hours at 50°C under nitrogen stream. The resulting mixture was diluted in DCM (200 mL), washed with 0.5 N HCl (150 mL) and extracted with 2 addition of 100 mL of dichloromethane. The organic layer was dried over $MgSO_4$ and filtred. The solvent was evaporated under reduced pressure and the residue was purified by flash chromatography using Petroleum Ether:Ethyl Ether = 7:3 as eluent. Solvent was evaporated under reduced pressure to afford the product as a yellow oil (1.2316 g, 76.6% yield).

^{1}H NMR ($CDCl_3$, 500 MHz) δ (ppm): 8.16 (d, 2H, aromatic meta position, $^3J_{H-H}$ = 10 Hz), 7.29 (d, 2H, aromatic ortho position, $^3J_{H-H}$ = 10 Hz), 6.02 (d, 1H, CH-N*H*, $^3J_{H-H}$ = 10 Hz), 4.19-4.21 (m, 1H, Val C_α-H), 2.16-2.23 (m, 1H, Val C_β-H), 1.45 (s, 9H, 3 × C-C*H*$_3$), 0.975 (d, 3H, $^3J_{H-H}$ = 5 Hz, CH-C$_\gamma$*H*$_3$), 0.91(d, 3H, $^3J_{H-H}$ = 10 Hz, CH-Cγ*H*$_3$);

^{13}C NMR ($CDCl_3$, 500 MHz) δ (ppm): 170.70, 155.88, 153.11, 144.65, 124.97, 121.90, 82.44, 59.57, 31.38, 27.94, 18.87, 17.30.

2. 4'- [N-(tert-butyl-valinyl)-carbamoyl]-pterostilbene (Pt-CP-Val-OtBu).

A solution of Pt (0.7479 g, MW = 256.3 g/mol, n = 2,92·10^{-3} mol, 1 eq) in 30 mL of acetonitrile was prepared. PNPC-Val-OtBu (1.4820 g, MW = 338.36 g/mol, n = 4.38·10^{-3} mol, 1.5 eq) and DMAP

(0.7139g, MW = 122.17 g/mol, n = $5.84 \cdot 10^{-3}$ mol, 2 eq) were added to the previous solution. The mixture was stirred at 50°C under nitrogen stream overnight. The reaction progress was checked by TLC. The resulting mixture was diluted in DCM (100 mL), washed with 0.06 N HCl (100 mL) and extracted with 2 × 100 mL of DCM. The organic layer was collected and dried with $MgSO_4$. The solvent was evaporated under reduced pressure and the residue was purified from PNPC-Val-OtBu by flash chromatography using Petroleum Ether:Acetone:Ethyl Ether = 7:1:2. The fraction collected was purified from the residual 4-nitrophenol by flash chromatography using Petroleum Ether:Dichloromethane:Acetone = 5:4:1, the solvent was evaporated under reduced pressure to afford the product as a pale yellow oil (1.0492 g , 86,2% yield).

^{1}H NMR ($CDCl_3$, 500 MHz) δ (ppm): 7.455 (d, 2H, H-2' and 6', $^3J_{H-H}$ = 9 Hz), 7.14 (d, 2H, H-3' and 5', $^3J_{H-H}$ = 10 Hz), 6.92-7.05 (dd, 2H, H-7 and 8), 6.655 (d, 2H, H-2 and 6, $^4J_{H-H}$ = 3 Hz), 6.40 (t, 1H, H-4, $^4J_{H-H}$ = 3 Hz), 5,91 (t, 1H, O-(C=O)-N*H*), 4.27-4.30 (q, 1H, Val C_α-*H*), 3.78 (s, 6H, O-CH_3), 2.20-2.06 (m, 1H, Val C_β-*H*), 1.50 (s, 9H, (C=O)-O-C(CH_3)$_3$), 1.035 (d, 3H, Val CH-C_γ-H_3), 0.965 (d, 3H, Val CH-C_γ-H_3).

^{13}C NMR ($CDCl_3$, 500 MHz) δ (ppm): 170.86, 160.85, 154.36, 150.44, 139.12, 134.23, 128.43, 128.09, 127.22, 121.64, 104.43, 99.87, 81.96, 59.41, 55.11, 31.36, 27.89, 18.85, 17.34.

3. 4'- [N-(valinyl)-carbamoyl]-pterostilbene (Pt-CP-Val-OH).

Pt-CP-Val-OtBu (0.7196g, MW = 455.54 g/mol, n = $1{,}58 \cdot 10^{-3}$ mol, 1 eq) was dissolved in 25 mL of anhydrous dichloromethane and 5 mL of TFA (MW = 114.02 g/mol, n = $6.53 \cdot 10^{-2}$ mol, 42.7 eq) were added to the solution. The mixture was stirred at room temperature for 3 hours under nitrogen stream. The reaction progress was checked by TLC. After 3 hours the solvent and the residual TFA were evaporated under reduced pressure. The residue was titrated with toluene (3 × 5 mL), and then solvent was evaporated under reduced pressure. The product was purified by automated chromatography system using Petroleum ether:Acetone = 6:4 to afford 0.4504g of product (71.5% yield).

^{1}H NMR ($CDCl_3$, 500 MHz) δ (ppm): 7.49 (d, 2H, H-2' and 6', $^3J_{H-H}$ = 10 Hz), 7.14 (d, 2H, H-3' and 5', $^3J_{H-H}$ = 10 Hz), 6.95-7.07 (dd, 2H, H-7 and 8), 6.66 (d, 2H, H-2 and 6, $^4J_{H-H}$ = 3 Hz), 6.40 (t, 1H, H-4, $^4J_{H-H}$ = 3 Hz), 5.57 (d, 1H, O-(C=O)-N*H*, $^3J_{H-H}$ = 10Hz), 4.41-4.44 (q, 1H, Val C_α-*H*), 3.83 (s, 6H, O-CH_3), 2,29-2,35 (m, 1H, Val C_β-*H*), 1.085 (d, 3H, Val CH-C_γ-H_3), 1.015 (d, 3H, Val CH-C_γ-H_3);

^{13}C NMR ($CDCl_3$, 500 MHz) δ (ppm): 176.44, 161.10, 154.82, 150.40, 139.36, 134.81, 128.91, 128.35, 127.27, 121.86, 104.72, 100.22, 59.14, 55.53, 31.23, 19.20 17.52.

ESI-MS: 797 m/z [2(Pstb CP-Val-OH)]$^-$

4'-[N-(phenylalanin)-carbamoyl]-pterostilbene (Pt-CP-Phe, 6)

1. ***4'-[N-(phenylalanin tert-butyl ester)-carbamoyl]-pterostilbene***

A solution of L-phenylalanine tert butyl ester hydrochloride (0.5062 g, MW = 257.8 g/mol, n = 1.96 10^{-3} mol, 1 eq) and DMAP (1.0417 g, MW = 122.17 g/mol, 8.53 10^{-3} mol, 4.3 eq) in DCM dry (4 mL) was added dropwise to a solution of bis-(4-nitrophenyl) carbonate (0.6333 g, MW = 304.21 g/mol, n = 2.1 10^{-3} mol, 1.06 eq) in DCM dry (5 mL). The resulting mixture was stirred at 50°C for 4 hours. Then, pterostilbene (0.6651 g, MW = 256.3 g/mol, n = 2.59 10^{-3} mol, 1.3 eq) was added to the

solution. The resulting mixture was stirred at 50°C overnight, and then it was diluted in DCM (100 mL) and extracted with HCl 0.5 M (3 × 100 mL). The organic layer was dried over $MgSO_4$ and filtered. The solvent was evaporated under reduced pressure and the product was purified by flash chromatography using $CHCl_3$/EtOAc (99.5/0.5) as eluent to afford Pt-CP-Phe-OtBu as a colourless oil (0.6350 g, MW = 503.58 g/mol, n = 1.26 10^{-3} mol, 66 % yield)

MS-ESI (ion trap): 504 m/z $[M+H]^+$

^{1}H NMR (200 MHz, CDCl3) δ (ppm) = 7.52 (d, J = 8.6 Hz, 2H), 7.33 (m, 5H), 7.09 (m, 4H), 6.70 (d, J = 2.1 Hz, 2H), 6.44 (t, J = 2.1 Hz, 1H), 5.61 (m, 1H), 4.63 (m, 1H), 3.87 (s, 6H), 3.20 (m, 2H), 1.48 (s, 9H).

^{13}C NMR (75 MHz, CDCl3) δ (ppm) = 170.46, 161.12, 153.87, 150.54, 139.39, 136.08, 134.61, 129.68, 128.78, 128.61, 128.41, 127.50, 127.21, 121.87, 104.69, 100.18, 82.71, 55.49, 38.48, 31.01, 28.05.

2. 4'-[N-(phenylalanin)-carbamoyl]-pterostilbene

TFA (4.5 mL, MW = 114.02 g/mol, n = 5.87 10^{-2} mol, 54 eq) and TIPS (0.450 mL, 5 % v/v) were added to a solution of Pt-CP-Phe-OtBu (0.6350 g, MW = 503.58 g/mol, n = 1.3 10^{-3} mol, 1 eq) in DCM dry (4.5 mL). The mixture was stirred at 0°C overnight. The TFA and the solvent were evaporated under reduced pressure. The product was titrated with toluene (2 × 5 mL) and purified by flash chromatography using DCM/acetone (97/3) + 1% AcOH as eluent. The product was dissolved in acetonitrile and water and it was lyophilized to afford Pt-CP-Phe-OH as a white solid (0.380 g, MW = 447.4 g/mol, n = 8.49 10^{-4} mol, 67.4 % yield).

MS-ESI (ion trap): 447 m/z

^{1}H NMR (500 MHz, DMSO) δ(ppm) = 8.31 (s, 1H), 8.19 (m, 1H), 7.57 (d, J = 8.6 Hz, 2H), 7.29 (m, 5H), 7.06 (m, 4H), 6.77 (d, J = 2.2 Hz, 2H), 6.41 (t, J = 2.2 Hz, 1H), 4.25 (m, 1H), 3.77 (s, 6H), 3.15 (m, 1H), 2.92 (m, 1H).

^{13}C NMR (126 MHz, DMSO) δ (ppm) = 173.42, 161.13, 154.68, 150.85, 139.52, 138.23, 134.34, 129.65, 128.72, 128.52, 127.78, 126.96, 122.19, 104.91, 100.37, 79.65, 56.16, 55.67, 36.97.

4'-[N-(asparagin)-carbamoyl]-pterostilbene (Pt-CP-Asn, 7)

1. 4'-[N-(asparagin tert-butyl ester)-carbamoyl]-pterostilbene

A solution of L-asparagine tert butyl ester hydrochloride (0.4048 g, MW = 224.68 g/mol, n = 1.8 10^{-3} mol, 1 eq) and DMAP (0.8922 g, MW = 122.17 g/mol, n = 7.3 10^{-3} mol, 4 eq) in ACN dry (6 mL) and DCM dry (7 mL) was added dropwise to a solution of bis-(4-nitrophenyl) carbonate (0.5659 g, MW = 304.21 g/mol, n = 1.86 10^{-3} mol, 1.03 eq) in ACN dry (5 mL). The resulting mixture was stirred at -15°C for 15 minutes. Then, pterostilbene (0.6019 g, MW = 256.3 g/mol, n = 2.35 10^{-3} mol, 1.3 eq) was added to the solution. The resulting mixture was stirred at -15 °C and it reached r.t. overnight. The mixture was diluted in DCM (10 mL) and extracted with HCl 0.5 M (10 mL) and DCM (3 × 10 mL). The organic layer was dried over $MgSO_4$ and filtered. The solvent was evaporated under reduced pressure and the product was purified by flash chromatography using EtOAc/petroleum ether(8/2) as eluent to afford Pt-CP-Asn-OtBu as a colourless oil (0.5824 g, MW = 470.5 g/mol, n = 1.24 10^{-3} mol, 68.7 % yield)

MS-ESI = 493 m/z $[M+Na]^+$

^{1}H NMR (300 MHz, $CDCl_3$) δ (ppm) = 7.47 (d, *J* = 8.5 Hz, 2H), 7.15 – 6.84 (m, 4H), 6.65 (d, *J* = 1.9 Hz, 2H), 6.39 (m, 2H), 5.87 (m, 2H) 4.49 (m,1H), 3.82 (s, 6H), 2.83 (m, 2H), 1.48 (s, 9H).

^{13}C NMR (75 MHz, $CDCl_3$) δ (ppm) = 172.50, 169.86, 161.10, 154.64, 150.53, 139.35, 134.65, 128.83, 128.35, 127.50, 121.92, 104.69, 100.19, 82.79, 77.16, 55.48, 51.51, 37.29, 27.99.

2. 4'-[N-(asparagin)-carbamoyl]-pterostilbene

A solution of Pt-CP-Asn-OtBu (0.7599 g, MW = 470.5 g/mol, n = 1.6154 10^{-3} mol, 1 eq) in DCM dry (6.2 mL) and TIPS (0.62 mL) (5 % v/v) was stirred at -15 °C. TFA (6.2 mL, MW = 114.02 g/mol, n = 8 10^{-2} mol, 50 eq) at -15 °C was added dropwise to the previous solution. The mixture is stirred at room temperature for 4 hours. TFA and the solvent were evaporated under reduced pressure. The product was titrated with toluene (2 × 3 mL) and purified by flash chromatography using DCM/MeOH (97.5/2.5) + 1% AcOH, to afford Pt-CP-Asn-OH as a white solid (0.5115 g, MW = 414.4 g/mol, n = 1.23 10^{-3} mol, 76.4 % yield)

MS-ESI (ion trap) = 415 m/z $[M+H]^+$

^{1}H NMR (300 MHz, DMSO) δ (ppm) = 7.98 (m, 1H), 7.60 (d, *J* = 8.5 Hz, 2H), 7.34 – 6.88 (m, 4H), 6.78 (d, *J* = 1.7 Hz, 2H), 6.42 (m, 1H), 4.40 (m, 1H), 3.78 (s, 6H), 2.75 – 2.53 (m, 2H).

^{13}C NMR (75 MHz, DMSO) δ (ppm) = 172.90, 171.16, 160.68, 153.98, 150.47, 139.08, 133.89, 128.28, 128.09, 127.34, 121.79, 104.47, 99.92, 55.21, 50.84, 39.52, 36.66.

4'-[N-(threonyl)-carbamoyl]-pterostilbene (Pt-CP-Thr, 8)

1. [N-(tert-butyl-threonyl-tert-butyl)-carbamoyl]-p-nitrophenol (PNPC-Thr(OtBu)-OtBu).

A solution of tert-butyl ester threonine tert-butyl ester (1.59 g, MW = 231.34 g/mol, n = $6.89 \cdot 10^{-3}$ mol, 1 eq) and DMAP (1.7032 g, MW = 122.17 g/mol, $1.39 \cdot 10^{-2}$ mol, 2 eq) in THF (20 mL) was added dropwise to a solution of bis (4-nitrophenyl) carbonate (2.13 g, MW = 304.21 g/mol, n = $7.00 \cdot 10^{-3}$ mol, 1 eq) in THF (15 mL), and the mixture was stirred at room temperature for 3 hours. The resulting mixture was diluted in DCM (200 mL) and washed with 0.5 N HCl (3 additions of 100 mL). The organic phase was dried over $MgSO_4$ and filtred. The solvent was evaporated under reduced pressure and the residue was purified by flash chromatography using CH_2Cl_2:Acetone:Petroleum Ether = 8:0.5:1.5 as eluent, to afford 2.4842 g of product (91.0 % yield).

^{1}H NMR ($CDCl_3$, 300 MHz) δ (ppm): 8.255 (d, 2H, aromatic meta position, $^3J_{H-H}$ = 9 Hz), 7,365 (d, 2H, aromatic ortho position, $^3J_{H-H}$ = 9 Hz), 5,895 (d, 1H, CH-N*H*, $^3J_{H-H}$ = 9 Hz), 4,24-4,31 (m, 1H, NH-C*H)*, 4.09-4.13 (m, 1H, tBuO-C*H*), 1.50 (s, 9H, 3 × C-CH_3), 1,285 (d, 3H, CH-CH_3, $^3J_{H-H}$ = 9 Hz), 1.20 (s, 9H, 3 × CH_3);

^{13}C NMR ($CDCl_3$, 300 MHz) δ (ppm): 169.45, 155.95, 153.60, 144.74, 125.04, 121.94, 82.37, 74.02, 66.96, 60.60, 28.69, 28.06, 21.18.

2. [N-(tert-butyl-threonyl-tert-butyl)-carbamoyl]-pterostilbene (Pt-CP-Thr(OtBu)-OtBu).

A solution of pterostilbene (0.5027 g, MW = 256.3 g/mol, n = $1{,}96 \cdot 10^{-3}$ mol, 1 eq) in 20 mL of acetonitrile was prepared. PNPC-Thr(OtBu)-OtBu (1.5470 g, MW = 396.43 g/mol, n = $3.92 \cdot 10^{-3}$ mol,

2 eq) and DMAP (0.4784 g, MW = 122.17 g/mol, n = $3{,}92 \cdot 10^{-3}$ mol, 2 eq) were added to the previous solution. The mixture was stirred at 50°C under nitrogen stream overnight. The reaction progress was checked by TLC. The resulting mixture was diluted in DCM (3 × 100 mL) and washed with 0.05 N HCl (100 mL). The organic layer was collected and dried over $MgSO_4$. The solvent was evaporated under reduced pressure and the residue was purified by flash chromatography using Petroleum Ether:Acetone:Ethyl Ether = 8:1:1. The solvent was evaporated under reduced pressure. The product was obtained as an oil (0.8862 g, 90.3% yield).

^{1}H NMR ($CDCl_3$, 300 MHz) δ (ppm): 7.47 (d, 2H, H-2' and 6', $^3J_{H-H}$ = 6 Hz), 7.155 (d, 2H, H-3' and 5', $^3J_{H-H}$ = 9 Hz), 6.92-7.07 (d+d, 2H, H-7 and H-8), 6.645 (d, 2H, H-2 and 6, $^4J_{H-H}$ = 3 Hz), 6.39 (t, 1H, H-4, $^4J_{H-H}$ = 3 Hz), 5,815 (d, 1H, O-(C=O)-N*H*, $^3J_{H-H}$ = 9 Hz), 4.23-4.26 (dd, 1H, Thr C_α-*H*), 4,12-4,16 (dd, 1H, Thr C_β-*H*), 3.80 (s, 6H, 2 × O-CH_3), 1.49 (s, 9H, (C=O)-O-C(CH_3)$_3$), 1.27 (d, 3H, Thr C_γ-*H*, $^3J_{H-H}$ = 6 Hz), 1.19 (s, 9H, C_β-O-C(CH_3)$_3$).

^{13}C NMR ($CDCl_3$, 300 MHz) δ (ppm): 169.85, 160.99, 154.92, 150.64, 139.27, 134.37, 128.29, 121.78, 104.55, 100.02, 82.04, 71.88, 67.17, 60.56, 55.28, 28.74, 28.08, 21.05

3. [N-(threonyl)-carbamoyl]-pterostilbene (Pt CP-Thr-OH).

Pt-CP-Thr(OtBu)-OtBu (0.8862g, MW = 499.60 g/mol, n = $1.77 \cdot 10^{-3}$ mol, 1 eq) was dissolved in 25 mL of anhydrous dichloromethane and 5 mL of TFA (MW = 114.02 g/mol, n = $6.53 \cdot 10^{-2}$ mol, 36.9 eq) were added to the solution. The mixture was stirred at room temperature for 3 hours. The reaction progress was checked by TLC. After 3 hours the solvent and the residual TFA were evaporated under reduced pressure. The residue was titrated with toluene (3 × 5 mL) , and then was evaporated under reduced pressure. The product was purified by automated chromatography system using chloroform + 1% acetic acid:methanol=9.8-9.5:0.2-0.5. Solvent was evaporated under reduced pressure. The residue was dissolved in 5 mL of dichloromethane and added to 200 mL of petroleum ether where the product was riprecipitated as a white solid. The precipitate was filtered by Büchner filter to afford 0.4736 g of product (68.9% yield).

^{1}H NMR (DMSO, 300 MHz) δ (ppm): 7.54-7.62 (m, 3H, H-2', 6' and O-(C=O)-N*H*), 7.06-7.31 (m, 4H, H-3', 5', 7 and 8), 6.78 (d, 2H, H-2 and 6, $^4J_{H-H}$ = 3 Hz), 6.42 (t, 1H, H-4, $^4J_{H-H}$ = 3 Hz), 4.12-4.19 (m, 1H, Thr C_α-*H*), 4.00-4.04 (dd, 1H, Thr C_β-*H*), 3.78 (s, 6H, 2 × O-CH_3), 1.16 (d, 3H, Thr C_γ-*H*, $^3J_{H-H}$ = 6 Hz).

^{13}C NMR (DMSO, 300 MHz) δ (ppm): 171.97, 160.67, 154.85, 150.50, 159.07, 133.93, 128.18, 127.35, 121.85, 104.47, 99.92, 66.39, 60.23, 55.21, 20.42.

ESI-MS: 801 m/z $[2(\text{Pt CP-Thr-OH})]^-$

4'-[N-(aspartic acid)-carbamoyl]-pterostilbene (Pt-CP-Asp, 9)

1. 4'-[N-(aspartic acid di-tert-butyl ester)-carbamoyl]-pterostilbene

A solution of L-aspartic acid tert butyl ester hydrochloride (0.5025 g, MW = 281.77 g/mol, n = 1.78 10^{-3} mol, 1 eq) and DMAP (0.8372 g, MW = 122.17 g/mol, 6.85 10^{-3} mol, 3.8 eq) in ACN dry (7 mL) was added dropwise to a solution of bis-(4-nitrophenyl) carbonate (0.5843 g, MW = 304.21 g/mol, n = 1.92 10^{-3} mol, 1.08 eq) in ACN dry (3 mL). The resulting mixture was stirred at 50 °C for 10 minutes. Then, pterostilbene (0.5997 g, MW = 256.3 g/mol, n = 2.34 10^{-3} mol, 1.3 eq) was added

to the solution. The resulting mixture was stirred at 50°C for 1 hour, and then it was diluted in DCM (100 mL) and extracted with HCl 0.1 M (100 mL) and DCM (3 × 100 mL). The organic layer was dried over $MgSO_4$ and filtered. The solvent was evaporated under reduced pressure and the product was purified by flash chromatography using DCM/petroleum ether/ acetone (5.5/4/0.5) as eluent to afford Pt-CP-Asp(tBu)-OtBu as a colourless oil (0.5824 g, MW = 527.61 g/mol, n = 1.104 10^{-3} mol, 62 % yield)

MS-ESI (ion trap) = 550 m/z $[M+Na]^+$

^{1}H NMR (300 MHz, $CDCl_3$) δ (ppm) = 7.48 (d, *J* = 8.7 Hz, 2H), 7.18 – 6.88 (m, 4H), 6.66 (d, *J* = 2.2 Hz, 2H), 6.39 (t, *J* = 2.2 Hz, 1H), 6.06 (m, 1H), 4.50 (m, 1H), 3.82 (s, 6H), 2.87 (m, 2H), 1.47 (s, 18H).

^{13}C NMR (75 MHz, $CDCl_3$) δ (ppm) = 171.86, 171.28, 162.72, 155.96, 152.20, 141.00, 136.21, 130.37, 130.03, 129.11, 123.50, 106.28, 101.78, 84.26, 83.46, 57.45, 57.08, 52.83, 39.41, 29.83, 29.76, 29.68, 29.61.

2. 4'-[N-(aspartic acid)-carbamoyl]-pterostilbene

A solution of Pt-CP-Asp(tBu)-OtBu (0.5824 g, MW = 527.61 g/mol, n = 1.104 10^{-3} mol, 1 eq) in 3.4 mL of DCM dry and 0.34 mL of TIPS (5 % v/v) was stirred at 0 °C. TFA (3.4 mL, MW = 114.02 g/mol, n = 4.4 10^{-2} mol, 40 eq) at -78 °C was added dropwise to the previous solution. The mixture is stirred at room temperature for 4 hours. TFA and the solvent were evaporated under reduced pressure. The product was titrated with toluene (2 × 3 mL) and purified by flash chromatography using $CHCl_3$/MeOH (95/5) + 1% AcOH, to afford Pt-CP-Asp-OH as a white solid (0.3320 g, PM = 415.4 g/mol, n = 8 10^{-4} mol, 72,4 % yield)

MS-ESI (ion trap) = 416 m/z $[M+H]^+$

^{1}H NMR (300 MHz, DMSO) δ (ppm) = 8.10 (m, 2H), 7.60 (d, *J* = 8.2 Hz, 1H), 7.36 – 6.98 (m, 4H), 6.78 (m, 2H), 6.39 (m, 1H), 4.39 (m, 1H), 3.78 (s, 6H), 2.72 (m, 2H).

^{13}C NMR (75 MHz, DMSO) δ (ppm) = 172.33, 171.61, 160.66, 154.02, 150.42, 139.05, 133.92, 128.29, 128.06, 127.33, 121.77, 104.45, 99.91, 55.19, 50.68, 39.52, 36.06.

4'-[N-(arginin)-carbamoyl]-pterostilbene (Pt-CP-Arg, 10)

1. 4'-[N-(arginin-tert butyl-ester)-carbamoyl]-pterostilbene

A solution of L-arginine tert butyl ester di-hydrochloride (0.5010 g, MW = 303.23 g/mol, n = 1.65 10^{-3} mol, 1 eq) and DMAP (0.4196 g, MW = 122.17 g/mol, n = 3.43 10^{-3} mol, 2 eq) in DCM dry (4 mL) was added dropwise to a solution of bis-(4-nitrophenyl) carbonate (0.5169 g, MW = 304.21 g/mol, n = 1.7 10^{-3} mol, 1.03 eq) in DCM dry (3 mL). The resulting mixture was stirred at -15°C for 5 hours. Then, a solution of pterostilbene (0.5498 g, MW = 256.3 g/mol, n = 2.145 10^{-3} mol, 1.3 eq) and DMAP (0.2091 g, MW = 122.17 g/mol, n = 1.71 10^{-3} mol, 1 eq) in DCM dry (2 mL) was added to the solution. The resulting mixture was stirred at -15° C for two days. The resulting mixture was diluted in EtOAc (100 mL) and extracted with HCl 0.5 M (100 mL) and EtOAc (3 × 100 mL). The organic layer was dried over $MgSO_4$ and filtered. The solvent was evaporated under reduced pressure and the product was purified by flash chromatography using DCM/MeOH (9/1) as eluent to afford Pt-CP-Arg-OtBu as a colourless oil (0.4051 g, MW = 512.6 g/mol, n = 7.9 10^{-4} mol, 48 % yield)

MS-ESI = 513 m/z $[M+H]^+$

^{1}H NMR (300 MHz, $CDCl_3$) δ = 7.43 (d, *J* = 8.2 Hz, 2H), 7.00 (m, 7H), 6.62 (m, 2H), 6.40 (m, 1H), 6.36 (m, 1H), 4.13 (m, 1H), 3.78 (s, 6H), 3.44 (s, 1H), 3.16 (m, 2H), 1.82 (m, 2H), 1.64 (m, 2H), 1.44 (s, 9H).

^{13}C NMR (75 MHz, $CDCl_3$) δ (ppm) = 171.27, 161.07, 157.50, 155.09, 150.38, 139.30, 134.74, 128.95, 128.20, 127.57, 121.99, 104.74, 100.19, 82.82, 77.16, 55.45, 54.36, 41.05, 28.18, 27.99.

2. 4'-[N-(arginin)-carbamoyl]-pterostilbene

A solution of Pt-CP-Arg-OtBu (0.4051 g, MW = 512.6 g/mol, n = 7.9 10^{-4} mol, 1 eq) in DCM dry (3 mL) and TIPS (0.3 mL) (5 % v/v) was stirred at -15 °C. TFA (3 mL, MW = 114.02 g/mol, n = 3.95 10^{-2} mol, 50 eq) at -15 °C was added dropwise to the previous solution. The mixture was stirred at -15 °C for 3 hours and then overnight at room temperature. TFA and the solvent were evaporated under reduced pressure. The product was titrated with toluene (2 × 3 mL) and purified by flash chromatography using DCM/MeOH (8/2) + 1% AcOH, to afford Pt-CP-Arg-OH as a white solid (0.2700 g, PM = 456.5 g/mol, n = 6 10^{-4} mol, 75 % yield)

MS-ESI (ion trap) = 457 m/z $[M+H]^+$

^{1}H NMR (300 MHz, DMSO) δ (ppm) = 8.11 (m, 1H), 7.89 (m, 1H), 7.60 (d, *J* = 8.5 Hz, 2H), 7.36 – 6.95 (m, 7H), 6.77 (d, *J* = 1.7 Hz, 2H), 6.41 (m, 1H), 4.02 (m, 1H), 3.78 (s, 6H), 3.15 (m, 2H), 1.81 (m, 2H), 1.62 (m, 2H).

^{13}C NMR (75 MHz, $CDCl_3$) δ 173.37, 160.69, 157.00, 154.34, 150.48, 139.07, 133.91, 128.29, 128.09, 127.38, 121.83, 104.48, 99.92, 55.22, 53.76, 39.52, 25.29.

7. Transcription factor EB is a crucial transducer of the biomedical action of pterostilbene and resveratrol: work in progress

Abstract:

Polyphenols are a large and diversified class of natural compounds produced by plants mainly in response to stressing conditions. In our laboratory, we focus our attention on stilbenoids, in particular Resveratrol (*trans 3-5-4' trihydroxystilbene,* Rv) and Pterostilbene (*trans-3,5-dimethoxy-4-hydroxystilbene*, Pt). These compounds exhibit, at least *in vitro*, a variety of activities of potential relevance for many areas of health care due to not only its redox properties but mainly to its ability to interact with various proteins. Although the beneficial effects of these two compounds are well-established, much remains to be learned about their molecular mechanisms of action.

Autophagy is a cellular catabolic process activated by cells in response to stressing conditions. It involves lysosomes whose biogenesis and function are under the control of TFEB, the transcription factor activated under nutrients deprivation conditions. The relationship between polyphenols and autophagy is well established. In particular, a pro-autophagic role is ascribed to Rv.

Thus, we wanted to verify: 1) whether not only Rv but also - and perhaps more effectively - Pt could induce TFEB translocation into the nucleus of cells and consequently autophagy; 2) the efficacy in our system of Rv and Pt metabolites, the main species present in the body after the ingestion of polyphenols; 3) in case of a positive answer to the 1st point, how these two molecules trigger TFEB traslocation.

HeLa cells overexpressing TFEB-GFP, kindly provided by Prof. Ballabio of TIGEM-Naples, were treated with different concentrations of Rv and Pt and with two types of metabolites and monitored by confocal microscopy for up to three hours. To verify the implication of AMPK and its upstream signaling, cells were treated also with a known AMPK activator (A769662). Variations of cellular cAMP levels were also measured using a FRET-based sensor (Dr. Giulietta Di Benedetto, IN-CNR).

Both Rv and Pt, in our system, induce TFEB translocation into the nucleus of HeLa cells already at low, physiologically meaningful concentrations, but to a lesser extent than nutrient deprivation. Up to now, in fact, starvation remains the most potent migratory stimulus. Moreover, while sulfated forms phase II metabolites are almost uneffective, compounds resulting from the reduction of the stilbenic double bond (formed in the lower intestinal tract by bacterial enzymes) show an activity similar to that of the parent compounds.

cAMP measurements instead show that our polyphenols induce in HeLa cells a slight increase in cAMP concentration. Addition of Forskolin or of IBMX (respectively a known potent activator of AC and a broad-spectrum inhibitor of PDE) induced in both cases a further increase of cAMP.

Finally, treatment with the AMPK activator, even though performed at the concentration known from the literature to efficiently up-regulate this kinase, shows a lower TFEB translocation into the nucleus if compared to the one induced by Rv and Pt. This leads us to speculate that our compounds might induce TFEB nuclear translocation also by modulating other signaling pathways.

Introduction:

Pterostilbene (trans-3,5-dimethoxy-4-hydroxystilbene, Pt) a close relative of storied Resveratrol (Rv), is emerging as a credible candidate for membership in plant phenolics' hall of fame.[3-5] The numerous biomedically relevant activities of Pterostilbene are broadly similar to those of Resveratrol, but the former apparently is more effective,[3, 6, 7] presumably because it is absorbed more readily[8] and in most tissues it reaches higher levels after oral administration.[9] This seems to be particularly significant in the case of the brain, and coherently pterostilbene improves intellectual performance in aged animals with greater efficacy than resveratrol.[10] The (multiple) molecular mechanisms underlying the effects of Pterostilbene have not yet been comprehensively investigated, although several recent studies have dealt with aspects of its modulation of interlinked cellular signaling pathways (e.g.: [11-28]). Given the results of these studies and the structural similarity of the two compounds, it is logical to postulate that largely the same cellular processes may account for the effects of resveratrol and pterostilbene (and other natural stilbenoids such as pinosylvin and piceatannol). The signaling cascade induced by resveratrol has been delineated in many studies (e.g., [1, 2, 25, 29, 30]). A focal point is activation of AMPK which, among various effects, potentiates mitogenesis and autophagy,[31-33] largely through inhibition of mTORC1, whose activity downregulates these cellular processes (e.g. [34-37]). The antagonistic relationship between AMPK and mTORC1 is relevant in various contexts, in particular those of obesity and metabolic syndrome (e.g. [38-40]). Stimulation of autophagy has been given at least partial merit for important activities of resveratrol, such as promotion of β-amyloid disposition in neuronal cells,[41, 42] protection against

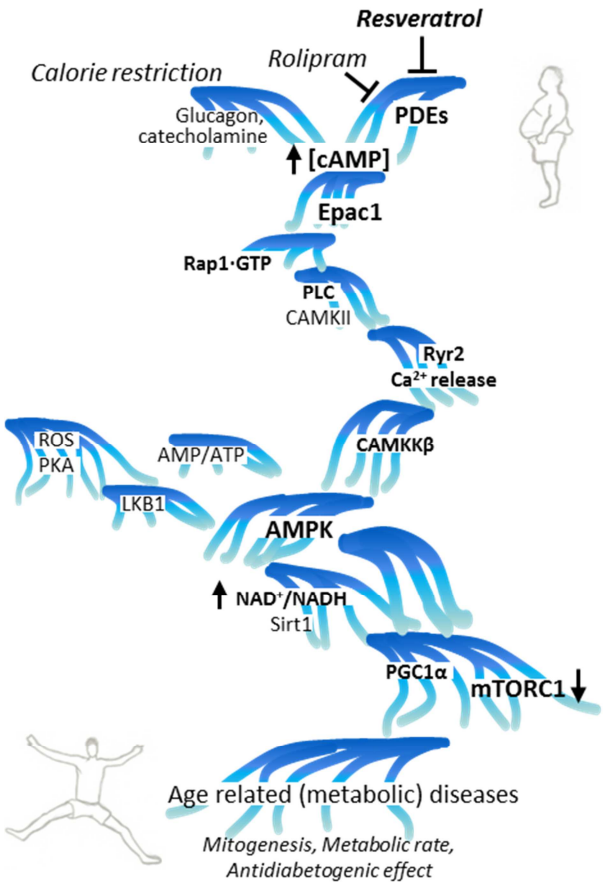

Fig1: A modified cartoon from Biasutto L et al.,[1] showing the signaling cascade identified by Park and colleagues[2] and the confluent ROS-induced signaling.

prion protein-induced neurotoxicity[43] and from oxidative damage,[44-46] cardioprotection,[47, 48] anti-inflammatory action,[49] lifespan extension in model organisms,[50-53] amelioration of age-related functional decline[54] and of neurodegeneration (e.g. [55-57]). Indeed, resveratrol has been proposed as a potential treatment for diseases such as Alzheimer's and Parkinson's (e.g. [58-60]). Pterostilbene has also been observed to stimulate autophagy.[17, 24, 61-64]

The master regulator of autophagy is Trascription Factor EB (TFEB) (revs.: [33, 65-67]). Under normal circumstances TFEBp is Ser-phosphorylated by mTORC1 (at the lysosomal surface). Phosphorylated TFEB is complexed with the 14-3-3 protein and thereby constrained to the cytosol.[68-70] Importantly, besides starvation which directly modulates the AMPK/mTOR axis, ROS are another major autophagy-stimulating factor.[71, 72] The signaling pathway involved in this case reportedly involves the assembly of complexes on the surface of peroxisomes, and also leads to the downregulation of mTORC1 activity.[73] When its phosphorylation level decreases due to downregulation of the kinase, TFEB translocates to the nucleus where it increases its own expression (a positive feedback loop) as well as that of genes involved in lysosomal autophagy, lipophagy and fatty acid β-oxidation. Thus TFEB upregulation may well help in the disposal of excess fat. A recent study has shown that hepatic overexpression of TFEB resulted in a lean phenotype, and significantly decreased both diet-induced and genetic obesity and metabolic syndrome,[66, 74] allowing hope that modulation of TFEB may permit the treatment and/ or prevention of these modern afflictions.[75] Interestingly, and coherently with the emerging picture, pterostilbene has been reported to exert anti-obesity effects[16, 76] as well as neuroprotection,[10, 77] another context where autophagy is important (e.g. [59, 78-80]).

A very recent high-profile paper[81] has reported the identification of a nutrient-sensing, autophagy-regulating axis formed by nuclear receptors FXR (farnesoid X receptor; a sensor of the nutrient-rich state) and CREB (cAMP response element binding protein). CREBp reportedly activates lipophagy and upregulates autophagy genes with the help of the co-activator CRCT2. This pleiotropic, crucial transcription factor is involved, among many other processes, in long-term memory formation, in which the cAMP-PKA-CREB-Nr4 a genes axis has a major part,[82-84] and thus its activation would help explain the cognitive effects of our compounds (chapter 8) as well.

In view of the above, we tested whether pterostilbene could cause nuclear localization of a TFEB-GFP chimera expressed by engineered HeLa cells. Since this was the case, and a point of interest in polyphenol research is the relative efficacy of a given polyphenol, its analogs and metabolites, we extended the assay to resveratrol and some metabolites of both compounds. We furthermore checked that the signaling expected to be upstream of TFEB migration is indeed taking place, verifying whether an increase of cAMP occurred.

Materials and methods:

Chemicals. Pterostilbene and Resveratrol were purchased from Waseta Int. Trading Co. (Shangai, P.R.China). Other starting materials for the synthesis of metabolites of Pt and Rv were from Wonda Science, Sigma Aldrich, Fluka & Riedel-de Haen, Carlo Erba Reagenti, Cambridge Isotope Laboratories Inc., Acros Organics, Prolabo, Merck-Novabiochem, J.T. Baker, and were used as received.

Cell culture. *in vitro* experiments were conducted with the HeLa cell line. For confocal microscopy experiments we used HeLa overexpressing a TFEB-GFP construct, from prof. Andrea Ballabio's laboratory (chimera cells were obtained as specified by Settembre C et al.[69]). Western blot and FRET experiments were performed with HeLa wild type (WT) cells, from dr. Giulietta Di Benedetto's laboratory.

HeLa WT cells were cultured in high glucose DMEM (Sigma Aldrich) supplemented with 10% FBS (fetal bovine serum, Euroclone). HeLa TFEB-GFP were cultured in high glucose DMEM supplemented with 10% FBS and G418 (Sigma Aldrich, 100µg/ml).

Confocal microscopy. A LEICA SP2 confocal microscope equipped with a Medical System Corporation thermostat was used. The light source was the emission from an Ar/HeNe laser at 488nm (25% power; gain 760, offset -0.4 for GFP fluorescence; gain 136 and offset -9.8 for bright field images). Images were taken through a 40X oil immersion objective. The thermostat was set at 37°C.

18 hours prior to the confocal microscopy experiments, 200.000 HeLa TFEB-GFP cells were seeded onto round glass coverslips (24mm diameter, BDH) placed in the wells of a 6 multiwell plate. Cells were cultured overnight in standard DMEM medium to allow adhesion. Before the experiment, the coverslip was mounted in an appropriate holder, gently rinsed with PBS (1x) and then covered with 1ml of Leibovitz's L-15 medium (Invitrogen, supplemented with 10% FBS, no phenol red).

Microscopy experiments were performed in temperature-controlled system without CO_2 superfusion. Leibovit's L-15 medium is designed for supporting cell growth in environments without CO_2 equilibration, thus it was preferred over DMEM.

Drugs, media, treatments. Controls received DMSO (Sigma Aldrich) at the final concentration associated with addition of drugs, which was in all cases 0.1% of total volume. HBSS (Sigma Aldrich), starvation medium, was used as positive control. Pterostilbene (Pt) and Resveratrol (Rv) were used at final concentrations of 25µM, 10µM, 1µM. Pterostilbene 4'-sulfate (Pt-S, 25µM), dihydro-pterostilbene (dihydro-Pt, 25µM), resveratrol 4'-sulfate (Rv-4'S, 25µM), resveratrol 3-4'-disulfate (Rv-3-4'S), dihydro-resveratrol (dihydro-Rv, 25µM) were synthesized by Dr. A Mattarei of the Dept. of Chemical Sciences of the University of Padova and were of >98% purity in all cases. Other drugs used were: A 769662 (Abcam, 25µM), Rolipram (Abcam, 100µM, 25µM), IBMX

(Abcam, 100µM), PEG-SOD and PEG-CAT (Sigma Aldrich, 40u/ml and 500u/ml, respectively).

Drugs were dissolved in a sterile solution of DMSO (Sigma Aldrich). Stock solution were prepared 1000x the desired working solution, so as to fix the final DMSO percentage at 0.1% in all cases. TFEB migration was monitored for 3 hours after the addition of the drug. Images were taken every 15 minutes.

Images were analyzed using the program ImageJ 1.48v (http://imagej.nih.gov/ij). TFEB migration was measured as a fluorescence ratio nucleus/cytosol. A few circular fields (regions of interest, ROIs) were drawn within the area of the nuclear and cytosolic cross sections of a given cell and their mean pixel intensity reading was used for fluorescence ratio determinations. For each image at least 5 cells were analyzed, and all ratios were combined to obtain a final average value of the TFEB-GFP nuclear/cytosolic concentration ratio.

cAMP-FRET based sensor. cAMP variations were measured as described by Oliveira et al.[85] Experiments were performed by dr. Giulietta Di Benedetto (CNR Institute of Neuroscience and Venetian Institute of Molecular Medicine, Padova). The EPAC1-based FRET sensor H30 described in Ponsioen B. et al.[86] was used. Briefly, HeLa WT cells were seeded onto 24-mm diameter round glass coverslips. Transfection was performed at 50-70% of confluence with the FuGENE-6 transfection reagent according to manufacturer's instructions. 1-2 µg of DNA were added to each coverslip. Imaging experiments were performed 24-48h after the transfection with H30. For imaging, cells were maintained in Hepes-buffered Ringer-modified saline (125mM NaCl, 5mM KCl, 1mM Na_3PO_4, 1mM $MgSO_4$, 5.5mM glucose, 1mM $CaCl_2$ and 20mM Hepes, pH 7.5) at room temperature. Images were taken with an inverted microscope (IX50, 60x NA 1.4 oil immersion objective, Olympus), acquired using custom-made software and processed using imageJ. FRET changes were measured as changes in the background-subtracted 480/545nm fluorescence emission intensities on excitation at 430nm and expressed as either R/R_0, where R is the ratio at time t and R_0 is the ratio at time = 0s, or $\Delta R/R_0$ where $\Delta R = R-R_0$.

Western blot. Cells were lysed in RIPA buffer supplemented with fresh phosphatase inhibitors (Sigma Aldrich, Phosphatase inhibitor cocktail 2 n° P5726 and Phosphatase inhibitor cocktail 3 n° P0044) and protease inhibitors (Sigma Aldrich, Protease inhibitor cocktail n° P2714). The RIPA lysate was kept at ice temperature for 15min, then centrifuged (14000rcf, 20min, 4°C). The supernatant was collected and stored at -80°C. Protein content was estimated with the Bradford assay. Prior to electrophoresis, the lysate was supplemented with sample buffer (1X: 62.5mM Tris-HCl pH 6.8, 2% SDS, 10% glycerol, 50mM DTT, 0.02% bromophenol blue) and heated at 95°C for 5min. From 10 to 20 micrograms of proteins per lane were loaded on 4-12% Bis-Tris gel (NUPAGE, Invitrogen). For the detection of high molecular weight proteins, 50 to 60 micrograms of proteins per lane were loaded on 3-8% Tris-Acetate gel (NUPAGE, Invitrogen). After electrophoretic separation proteins were transferred to PVDF membranes (300V-400mA-

1h at 4°C or 30V-90mA-overnight at 4°C for high molecular weight proteins). Membranes were saturated with 5% BSA (Sigma Aldrich, n° A9647) in TBS 1X at room temperature for 1h, then incubated with primary antibody (in TBS Tween 0.1%, 5% BSA) overnight at 4°C, washed with TBS Tween 0.1% and incubated with HRP-conjugated secondary antibody. Detection was performed using the ECL method (Pierce) in a ChemiDoc system (BioRad).

Antibodies against the following proteins were used: TFEB (MBS716265 - MyBiosource, polyclonal, 1:1000); H3 (#9715 - Cell Signaling, polyclonal, 1:9000); β-Tubulin (sc-9104 - Santa Cruz, polyclonal 1:1000); LC3B (#3868 - Cell Signaling, monoclonal, 1:1000); HSP90 (610419 - BD, monoclonal, 1:1000); Ph-CREB (#9198(Ser133) - Cell Signaling, monoclonal 1:1000); Ph-AKT (#4060(Ser473) - Cell Signaling, monoclonal, 1:2000 - and #13038(Thr308) – Cell Signaling, monoclonal, 1:1000); Ph-ERK (#9101(Thr202/Tyr204) - Cell Signaling, polyclonal, 1:1000); Ph-AMPKα (#2535(Thr172) - Cell Signaling, monoclonal 1:1000); Ph-ACC (#11818(Ser79) - Cell Signaling, monoclonal, 1:1000).

Nuclear/cytosolic fractionation. The protocol was adapted from Gagnon KT et al.[87] Cultured cells were lysed in a 0.5% Triton X-100 buffer (HLB) for 10 minutes at ice temperature. Buffer composition was as follows: 50mM Tris-HCl, 137.5mM NaCl, 5mM EDTA, 0,5% Triton X-100 and 10% vol/vol glycerol, freshly added phosphatase and protease inhibitors. The lysate was then vortexed (5s), then centrifuged (800rcf, 8min, 4°C). The supernatant, constituting the cytosolic fraction, was collected and stored at -80°C. The pellet, containing nuclei, was washed twice by resuspension in HLB and centrifugation (200rcf, 2min, 4°C).

Isolated nuclei were finally lysed in RIPA buffer for Western blot analysis, or preserved in ice-cold HBSS for spettrofotometric/FACS analysis.

Triton X-100 was preferred over alternative detergents such as Np-40 or Igepal CA-630 since it better preserves the endoplasmic reticulum surrounding the nucleus. TFEB is a small protein of 52-53 kDa. Nuclear pores are relatively permeable to small proteins, thus we decided to use a milder detergent and preserve as much as possible the integrity of the nuclear membranes in order to limit the loss of nuclear TFEB during the nuclei isolation procedures.

For the isolation of nuclei from liver and brain tissues the dissected organs were promptly immersed in ice-cold PBS with Ca^{2+} and Mg^{2+} (D-PBS, Sigma Aldrich), and minced with scissors. Tissues were then homogenized with a Potter device (Teflon pestle, 3-4 strokes), filtered with a cell strainer (Falcon: 352360, 100µm), centrifuged at 500rcf, 10min, 4°C. Supernatants were discarded and pellets resuspended with ice-cold HLB. Subsequent steps were as described above for the isolation of nuclei from cultured cells.

The effectiveness of the fractionation procedure was verified *a posteriori* by Western blot analysis. Histone-3 and β-tubulin were used as nuclear and cytosolic marker, respectively, to verify the purity of the two fractions.

FACS analysis of nuclei. Nuclei were obtained as described above, and kept in ice-cold HBSS. They were stained with Propidium Iodide (Sigma) at a final concentration of 1µg/ml, (incubation in darkness at 37°C, 20min). A Beckton Dickinson II flow cytometer was used. 10000 nuclei were counted for each measurement.

Synthesis of Pt and Rv metabolites. This part of the work was performed by the group of prof. Cristina Paradisi. Sulfates were synthetized as previously described in Mattarei et al.[88]

Dihydro derivatives of resveratrol and pterostilbene were prepared by hydrogenation of corresponding stilbenes following the procedure reported by D.C. Rueda et al.[89] with minor modification. Solutions of each stilbene (1.00 mmol) in absolute EtOH (15 ml) were stirred under H_2 for 6 h in the presence of 10% Pd/C. The reaction mixtures were filtered over Celite to remove the catalyst, and evaporated to dryness. The resulting residues were purified by flash column chromatography, using a hexane/EtOAc gradient, to afford target dihydro compounds dihydro-Rv (92% yield) and dihydro-Pt (95% yield). The spectroscopic data of compounds were in agreement with the literature.

Results and discussion:

Pt and Rv induce nuclear translocation of TFEB:

To test whether Pt and Rv induced TFEB translocation to the nucleus, HeLa TFEB-GFP cells in Leibovitz's L-15 medium were initially treated with 25µM Pt or Rv and TFEB migration was followed by confocal microscopy. 0.1% DMSO was added in negative controls to verify that the vehicle *per se* did not induce migration. HBSS was used as experimental

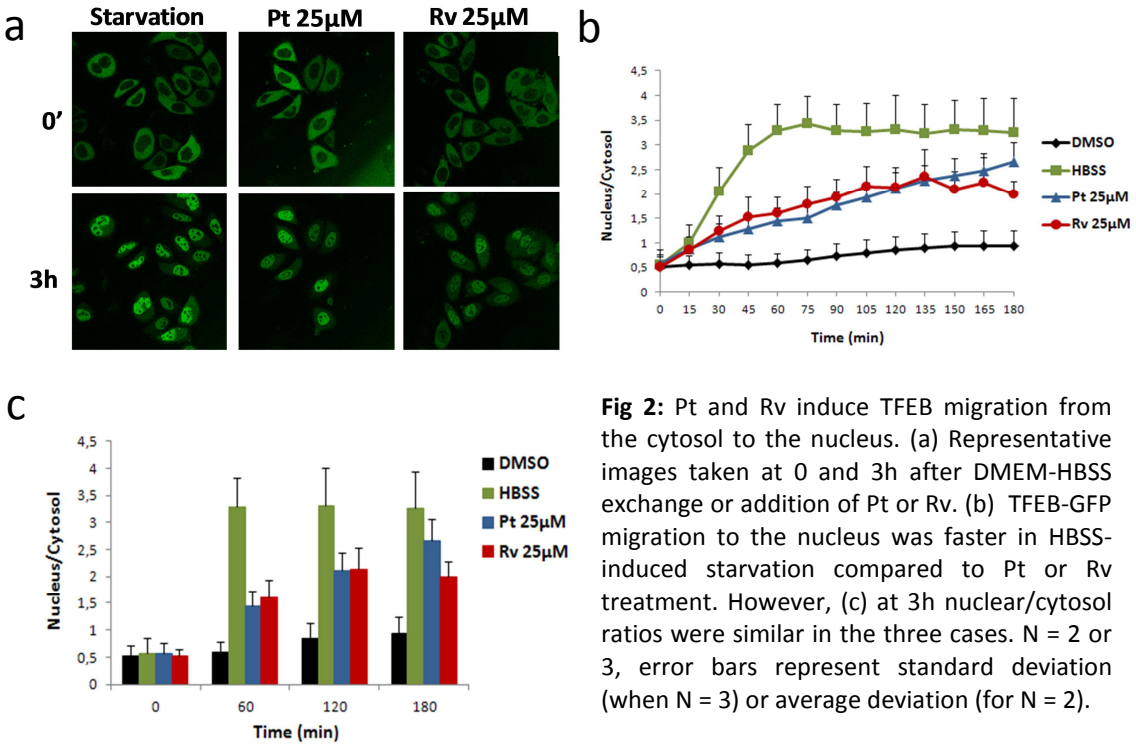

Fig 2: Pt and Rv induce TFEB migration from the cytosol to the nucleus. (a) Representative images taken at 0 and 3h after DMEM-HBSS exchange or addition of Pt or Rv. (b) TFEB-GFP migration to the nucleus was faster in HBSS-induced starvation compared to Pt or Rv treatment. However, (c) at 3h nuclear/cytosol ratios were similar in the three cases. N = 2 or 3, error bars represent standard deviation (when N = 3) or average deviation (for N = 2).

medium in order to "starve" the cells, thus providing the positive control. HBSS provides pH maintenance, osmotic balance, water and essential inorganic ions but no energy source. Energy deprivation leads to a decrease of ATP levels in the cell, while ADP and AMP levels increase, leading to the activation of AMPK.[90] mTORC1, the protein responsible for TFEB phosphorylation, and thus for its cytoplasmatic confinement, is a direct target of AMPK.[91] Phosphorylation by AMPK leads to inhibition of mTORC1 activity. The phosphorylation level of TFEB thus decreases and its migration to the nucleus is favored.[65]

As expected, the vehicle (DMSO) does not itself induce TFEB migration (fig 2, **b-c**), while HBSS-induced starvation has a strong effect (fig 2, **a-c**).

Both Pt and Rv, when supplied at 25µM in complete Leibovitz's L-15 medium, are able to induce a consistent migration of TFEB to the nucleus (fig 2, **a-c**). However, the kinetics by which starvation, Pt and Rv act are different. Starvation is the most potent stimulus: maximal nuclear translocation of TFEB is achieved in 1 hour (fig 2, **b**). The effect of Pt and Rv instead is more progressive, and migration reaches its maximum level at the end of the three-hour period (fig 2, **b-c**).

In vivo, concentrations of Pt and Rv in the 25µM range are however difficult to reach. While Pt can reach this level in organs such as liver and kidney after a moderate pharmacological dosage by oral administration,[9] for Rv it is nearly impossible to attain these levels even after administration of high doses p.o. Moreover, also for Pt, in organs such as the brain, heart, lungs and skeletal muscle the concentrations achieved are considerably lower than in liver and kidney. Given in particular the reports that Pt and Rv

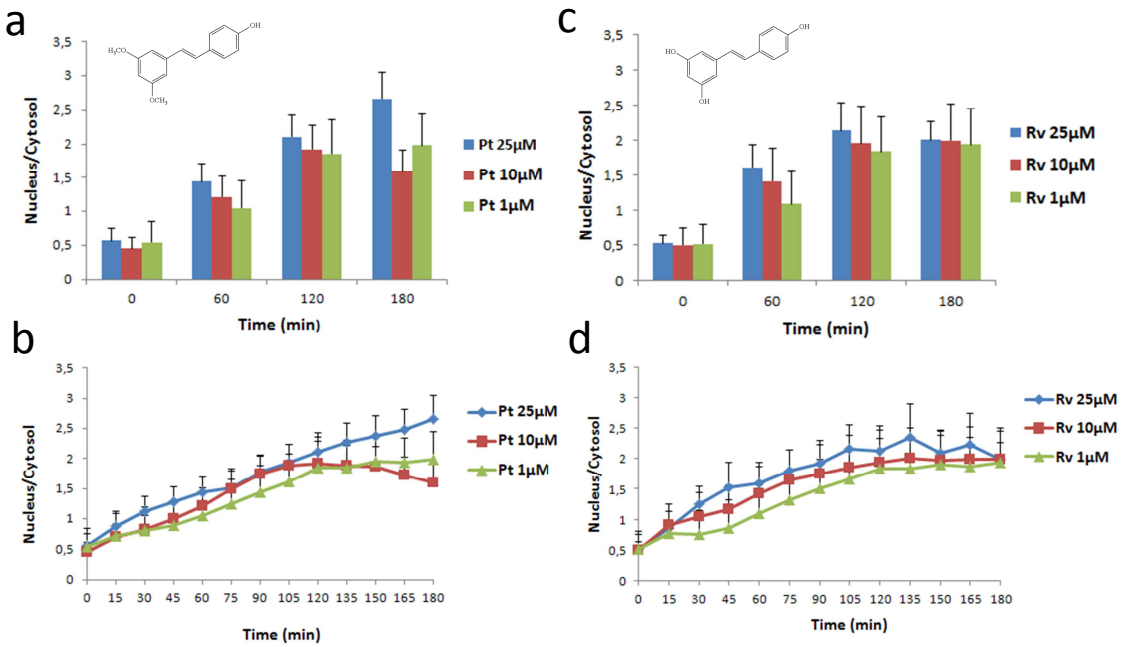

Fig 3: Low doses of Pt and Rv induce TFEB migration from the cytosol to the nucleus. 10µM and 1µM Pt (**a, b**) or Rv (**c, d**) were as effective as 25µM in inducing TFEB migration. N = 2 or 3, error bars represent standard deviation or average deviation.

exert positive effects in ameliorating brain pathologies and dysfunctions (e.g. Alzheimer's disease, Parkinson's disease, cognitive aging; see the introduction), we sought to define the effects of more physiological levels (1 and 10 µM) of both molecules on TFEB distribution.

As shown in fig 3, both concentrations, 1µM and 10µM, of both molecules, Pt and Rv, where about as effective as the higher 25µM concentration in inducing TFEB migration. While many investigations have demonstrated an activity of polyphenols at unphysiologically high concentrations (e.g. [2]), this report is one of the few showing efficacy at physiological levels.

Pt and Rv metabolites:

In vivo, Rv and Pt are mostly transformed into metabolites. Several authors therefore propose that the effects ascribed to polyphenols may instead be accounted for by their major phase II metabolites (e.g. [92, 93]). Polyphenols are also subjected to modification by the colonic flora. In another context during my thesis work (chapter 4) I administered chronically Rv to rats. In the caecum and colon I was able to quantify only dihydro-Rv, the reduced form of trans-Rv. Various authors have reported effects of Rv against colon cancer and Crohn disease.[7, 94-97] We decided therefore to also verify the effects of Pt and Rv phase II sulfates and reduced forms (synthesized by the group of prof. Cristina Paradisi) in our experimental system. Sulfates and reduced forms of Pt and Rv are present at high concentration in organs and colon, respectively, after administration p.o. of pharmacological doses. For this reason so far we have tested these compounds only at 25µM.

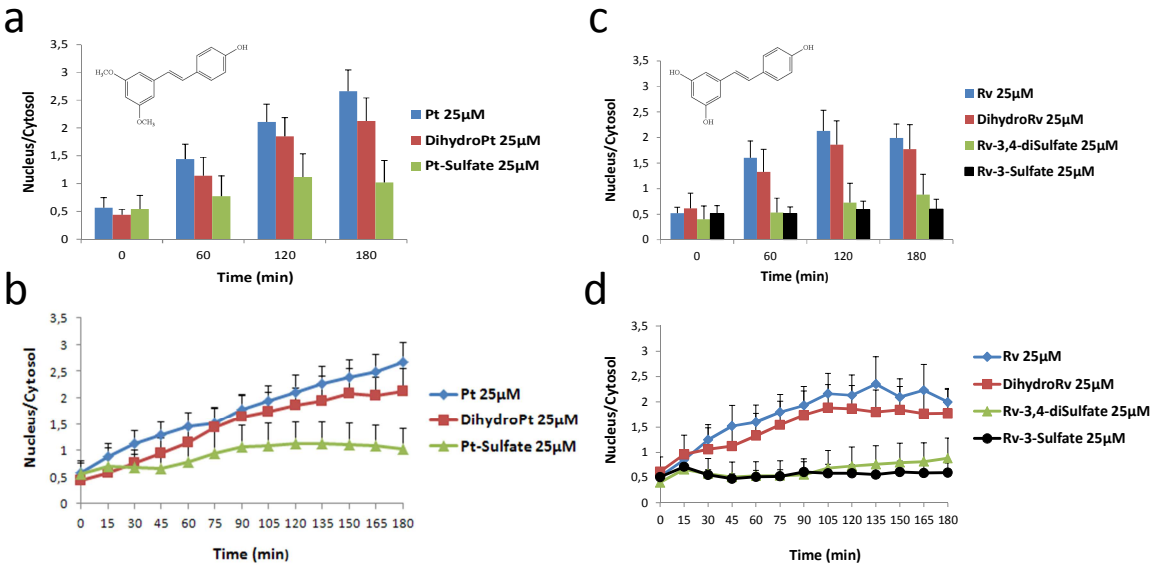

Fig 4: Reduced forms of Pt and Rv, but not sulfate metabolites, induce TFEB migration from the nucleus to the cytosol. Experiments with 25µM Pt or Rv (panels **a-d,** blue) are shown for comparison purposes. Reduced forms of Pt and Rv, namely dihydro-Pt and diydro-Rv were about as effective as Pt and Rv themselves in inducing TFEB-GFP migration to the nucleus (a-d). Sulfates of both Pt and Rv had only a small or no effect. N = 2 or 3, error bars represent standard deviation or average deviation.

TFEB distribution was perturbed by dihydro-Pt and dihydro-RV, while the sulfates were almost uneffective (fig 4, **a-d**). In fig 4 the results obtained with 25µM Rv and Pt are shown for comparison purposes. Dihydro-Pt and dihydro-Rv not only led to nuclear/cytosolic ratios for TFEB (fig 4, **a, c**) similar to those observed upon administration of the parent compounds, but did so with comparable kinetics (fig 4, **b, d**). Pt-sulfate was poorly effective, inducing only a small shift of TFEB to the nucleus, if any. Rv-3-sulfate and Rv-3,4-disulfate definitely were completely inert (fig 4, **c, d**).

One possible explanation of these results might be reconduced to the different ability of these molecules to cross the plasma membrane. While Pt and Rv, as well as the reduced forms (dihydro-Pt and dihydro-Rv) are relatively non polar, mostly neutral (at physiological pH) molecules and thus can passively diffuse through cell membranes, sulfate (and probably glucuronide) forms are bound to encounter difficulties. The negatively charged sulfate group confers an elevated hydrophilicity to the molecules, which remain confined outside of the cell.

Pt and Rv, the starting point:

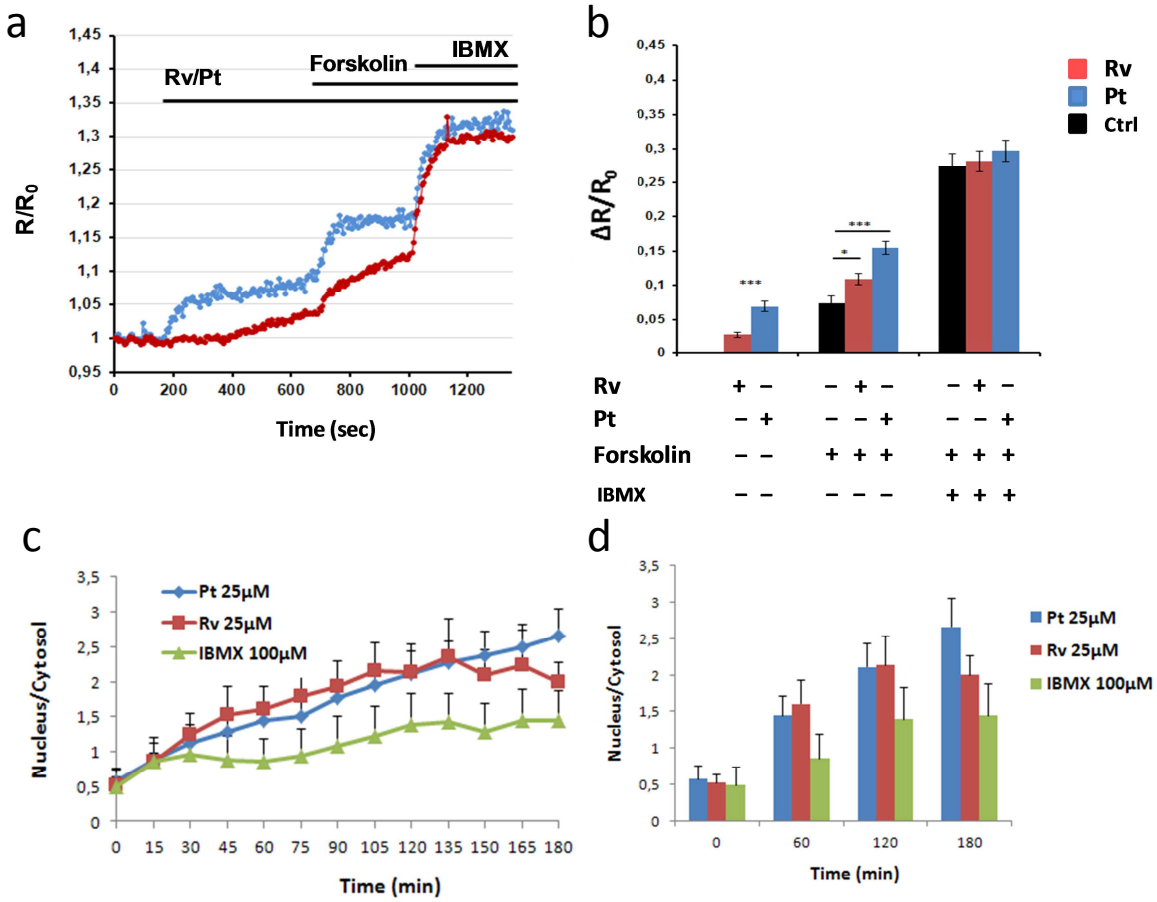

Fig 5: cAMP levels after Pt or Rv administration. Epac-based FRET sensor H30 was used. Forskolin (25µM) fully activates ACs while IBMX (100µM) inhibits PDEs. Pt and Rv induce an increase in cytosolic cAMP (a, b). The effect of Pt is more pronounced than that of Rv. Forskolin and IBMX were added after Pt or Rv, and led to a further increase in cAMP levels in the cytosol of HeLa cell. 100 µM IBMX induced TFEB-GFP migration to the nucleus, but was less effective than 25 µM Pt or Rv (c, d). N = 2 or 3, error bars represent average deviation or standard deviation.

The plethoric activity of Pt and Rv is presumably the consequence of interactions with multiple proteins. However, obviously some interactions may be more important than others for a given end-effect. In 2012, Park et al.,[2] have proposed PDE 1, 3 and 4 as a major target of Rv. In particular they discovered that Rv acts as a competitive inhibitor of cAMP on PDEs. In view of this, we decided to first, confirm their results with an alternative approach, second, to verify if Pt effects may also be part of a cAMP-dependent signaling cascade.

cAMP signaling is largely mediated by two proteins, protein kinase A (PKA) and cAMP-regulated guanine nucleotide exchange factors (Epac1 and Epac2, Oliveira R.F. et al.[85]). The binding of cAMP to PKA or Epac leads to a conformational change of these proteins. H30-FRET-based biosensors exploit the conformational change of Epac1 protein in order to measure the cAMP level in a given environment.[85] We thus measured the variation of cAMP concentration in HeLa WT cells transiently transfected with an Epac1-FRET-based biosensor (H30-FRET) after addition of Pt or Rv.

H30-FRET-based experiments were performed by dr. Giulietta Di Benedetto (CNR Institute of Neuroscience, Venetian Institute of Molecular Medicine, Padua).

Both Pt and Rv at 25µM dose induced an increase in cytosolic cAMP (fig 5, **a, b**). Pt in particular yielded the more pronounced increase. Forskolin (25µM) and IBMX (100µM) were used as controls. Forskolin potently activates Adenylate Cyclases (AC, [98]) while IBMX is a non-specific inhibitor of PDEs.[99] Both these drugs are normally used as a reference in cAMP-FRET measurements.

Administration of Forskolin and IBMX after Pt/Rv induced a further increase in cAMP levels (fig 5, **a, b**). As shown by Park et al.,[2] Rv does not increase cAMP by activating AC, but rather by inhibiting some PDE subfamilies. This can explain why by activating AC or completely inhibiting PDEs we were able to measure a further increase in cAMP levels (fig 5, **a, b**).

Notably, the increase in cAMP levels after Forskolin addition to cells previously treated with Pt or with Rv was of the same order of magnitude of that induced by the addition of Forskolin to untreated cells (fig 5, **b**). Since Rv does not act via AC, we can presume that this also applies to Pt. Otherwise, if part of the effect of Pt were mediated by AC activation, we would expect to observe a smaller change in cAMP levels when applying Forskolin to Pt-treated cells.

The addition of IBMX after forskolin instead led to a similar plateau in cAMP levels independently of whether the cells had been previously treated with Pt, Rv, or neither stilbenoid (fig 5, **a, b**). This further confirms that Rv, and probably Pt, increases intracellular cAMP levels by inhibiting certain subclasses of PDEs. When all the PDE subfamilies are inhibited by IBMX, indeed, one cannot observe a significant difference in cAMP levels related to the presence of Rv or Pt (fig 5, **b**).

However, HeLa cells treated with Pt showed an higher increase in cAMP levels than HeLa cells treated with Rv. Assuming that in both cases the mechanism involves PDEs inhibition, we can hypothesize that the superior potency of Pt might be due to:

1. Inhibition of other subclasses of PDE (besides subclasses 1, 3 and 4, as suggested by Park et al.[2])
2. A stronger inhibition of subclasses 1, 3 and 4.
3. Both of the above

We next wondered whether TFEB migration from the cytosol to the nucleus might be due to the observed increase in intracellular levels of cAMP. HeLa TFEB-GFP cells were thus treated with IBMX 100µM only. IBMX was able to induce the migration of the transcription factor to the nucleus, but to a lower extent than 25µM Pt or Rv (fig 5, **c, d**). Pt- and Rv-induced TFEB migration is thus probably in part downstream of effectors other than cAMP.

Park et al.[2] excluded PKA as a possible downstream mediator of Rv in HeLa cells, while a role of Epac was supported. The conclusion was based on specific silencing of PKA or Epac mRNAs. Briefly, Rv was able to activate AMPK when PKA was silenced, but not when Epac was silenced. Given the recent findings by Seok et al.[81] (see Introduction), I decided to also consider the possibility of a role of CREBp in autophagy. CREB is phosphorylated, and thus activated, by PKA.[100, 101] If Rv or Pt do not have PKA as a downstream effector, the phosphorylation status of CREB should be unaffected by them.

Western blot analysis is still in progress. Here I report preliminary results obtained with HeLa cells by using an extremely high concentration of Pt or Rv (100µM). This part of the work is being done in preparation for a more physiological an exhaustive investigation which is being planned (see below). HeLa WT cell were seeded in a 6 multiwell plates (200.000 cells per well, as done for the TFEB migration experiments) and treated as described in fig 6. Pt, but not Rv, induced CREB phosphorylation, at levels comparable to

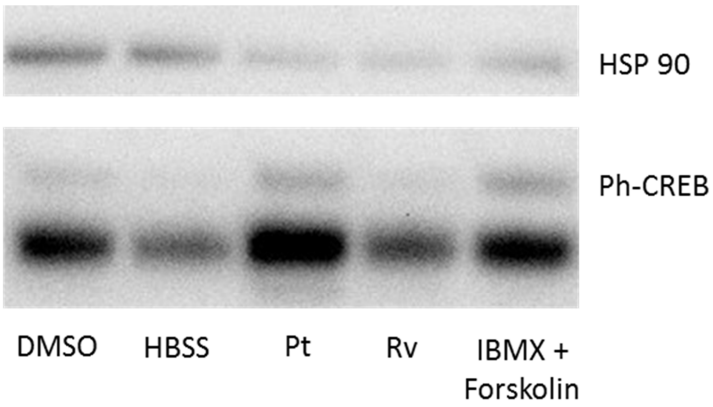

Fig 6: Western blot analysis detecting the phosphorylated forms of CREB (Ph-CREB, Ser 133) or HSP90 (housekeeping). 0.1% DMSO, starvation (HBSS), 100µM Pt or Rv and IBMX (50µM) + Forskolin (25µM) were used as treatments. Cell were lysed with RIPA buffer 90min after the beginning of the treatment.

those induced by IBMX-Forskolin treatment. This result is in agreement with the findings by Park et al.[2] Rv indeed does not induce dramatic CREB phosphorylation, thus PKA seems not to be involved in signaling downstream of Resveratrol. Conversely, Pt induces a strong phosphorylation of CREB, indicating PKA, as well as Epac, as downstream effectors of its activity.

Is AMPK involved in Pt and Rv-induced TFEB migration?

As previously shown, a rise in cAMP level is not sufficient to trigger TFEB migration in a manner similar to that of Pt and Rv (fig 5). As mentioned above, mTORC1 is a direct target of AMPK. To test and verify the hypothesis that AMPK is behind TFEB migration, we have adopted a double approach. First, we treated HeLa TFEB-GFP cell with a specific activator of AMPK, the compound A769662.[102] A769662 was used at 25µM because it affords a near-maximal activation of AMPK and still higher concentration may lead to the inhibition of mitochondrial oxygen consumption and thus to an increase in AMP:ATP ratio.[102]

As shown in fig 7, administration of A769662 to HeLa TFEB-GFP cells induced migration of TFEB to the nucleus. However the effect was relatively weak, lower than that of Rv or Pt, suggesting that AMPK may not be the only and obligatory intermediate in the signaling cascades initiated by stilbenoids.

The second approach is based on western blot analysis. As previously mentioned, this part of the work is still ongoing and data are too preliminary to be showed here.

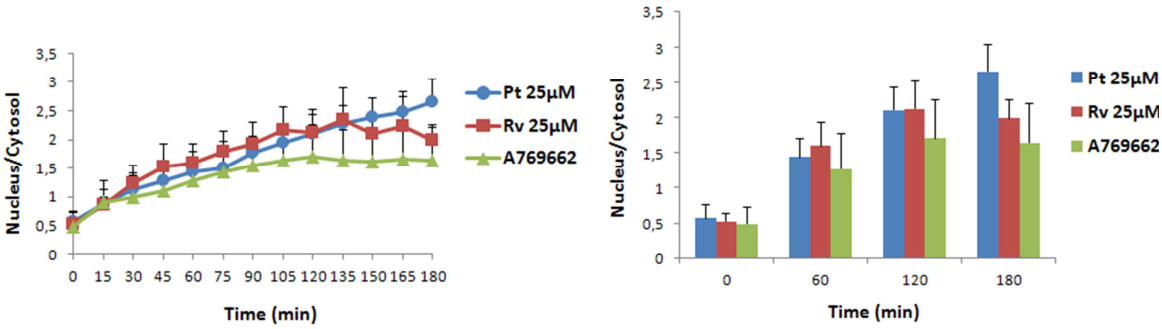

Fig 7: 25µM A769662 induces TFEB-GFP migration to the nucleus. The results obtained with 25µM Pt and Rv are shown for comparison purposes. N = 2 or 3, error bars represent average or standard deviation.

Conclusions:

As expected, given the cardinal role attributed to TFEB as a master regulator of autophagy, and the evidence that stilbenoids induce autophagy, in cultured HeLa cells Rv and Pt induce migration of a TFEB-GFP chimera to the nucleus, at concentrations as low as 1 µM.

Dihydro-Rv and dihydro-Pt, the products of bacterial hydrogenation of the carbon-carbon double bond in the stilbenoid skeleton, are about as effective as Rv and Pt themselves, a

significant finding strengthening the view that the metabolites of polyphenols may have much to do with the beneficial effects of these natural compounds. On the contrary, negatively charged, hydrophilic sulfates of Rv and Pt have no significant effect, likely because they do not enter cells.

TFEB relocation is accompanied by an increase of cAMP levels, already observed by other authors and ascribed to the primary event, inhibition of members of the PDE family. According to the mechanistic scheme developed by Park et al.[2] for resveratrol, the cAMP increase is upstream of AMPK activation and mTORC1 inhibition, i.e., autophagy induction. The signal cascade for resveratrol was found to involve the GEF Epac1, but not PKA. A recent report has furthermore implicated CREB in autophagy induction. Coherently, my preliminary results indicate that it becomes phosphorylated upon administration of Pt (but not resveratrol) to the cells (fig 6). CREB phosphorylation is executed by PKA, and thus it is also downstream of cAMP.

There appears however to be a still-to-be-investigated difference between the modes of action of Rv (which does not cause massive phosphorylation of CREB) and Pt (which does). Furthermore, my results indicate that a cAMP increase due to PDE inhibition may not be sufficient to explain the induction of TFEB translocation, since upon treatment of the cells with IBMX, a PDE pan-inhibitor, TFEB translocation was lower than that induced by Rv or Pt (fig 5).

AMPK activation also might account only partially for TFEB migration, since nearly full activation by A769662 induced nuclear translocation of the TFEB-GFP chimera to a similar or lower extent than treatment with the stilbenoids.

Perpectives:

The results obtained so far in this part of the work encourage us to concentrate our efforts on the analysis of the mechanisms of action of Rv and Pt. Having established that Pt and Rv strongly induce TFEB migration, at least in vitro, we plan to investigate downstream and especially upstream events.

Besides AMPK, mTORC1 activity can be regulated by other proteins such as AKT and ERK, the phosphorylation levels of which in the presence of stilbenoids are currently under investigation.

AMPK activation by both Pt and Rv needs to be confirmed in our experimental model.

PDEs inhibition by Rv has already been proven, but that Pt also inhibits phosphodiesterases remains an hypothesis. We plan to clarify this crucial event also for Pt.

Pt and Rv can induce an increase in ROS levels.[64, 103-105] ROS are sensed by the Nrf2/Keap1 complex, which is activated and induces the transcription of ROS scavengers. ROS are

recognized as autophagy inducers.[106] Through the use of cell permeant scavenger of ROS (namely PEG-CAT and PEG-SOD) we shall verify how important is the contribution of ROS in modulating Pt- and Rv-induced-TFEB localization.

After an in vitro detailed mechanistic investigation of Pt and Rv pro-autophagy activity, we aim to show the same effects and the involvement of the same pathways also *in vivo*. A few experiments in this direction have been already performed.

References:

1. Biasutto, L.; Mattarei, A.; Zoratti, M. Resveratrol and health: the starting point. *Chembiochem : a European journal of chemical biology* **2012,** *13*, (9), 1256-9.
2. Park, S. J.; Ahmad, F.; Philp, A.; Baar, K.; Williams, T.; Luo, H.; Ke, H.; Rehmann, H.; Taussig, R.; Brown, A. L.; Kim, M. K.; Beaven, M. A.; Burgin, A. B.; Manganiello, V.; Chung, J. H. Resveratrol ameliorates aging-related metabolic phenotypes by inhibiting cAMP phosphodiesterases. *Cell* **2012,** *148*, (3), 421-33.
3. Estrela, J. M.; Ortega, A.; Mena, S.; Rodriguez, M. L.; Asensi, M. Pterostilbene: Biomedical applications. *Critical reviews in clinical laboratory sciences* **2013,** *50*, (3), 65-78.
4. McCormack, D.; McFadden, D. A review of pterostilbene antioxidant activity and disease modification. *Oxidative medicine and cellular longevity* **2013,** *2013*, 575482.
5. McCormack, D.; McFadden, D. Pterostilbene and cancer: current review. *The Journal of surgical research* **2012,** *173*, (2), e53-61.
6. Nutakul, W.; Sobers, H. S.; Qiu, P.; Dong, P.; Decker, E. A.; McClements, D. J.; Xiao, H. Inhibitory effects of resveratrol and pterostilbene on human colon cancer cells: a side-by-side comparison. *Journal of agricultural and food chemistry* **2011,** *59*, (20), 10964-70.
7. Chiou, Y. S.; Tsai, M. L.; Nagabhushanam, K.; Wang, Y. J.; Wu, C. H.; Ho, C. T.; Pan, M. H. Pterostilbene is more potent than resveratrol in preventing azoxymethane (AOM)-induced colon tumorigenesis via activation of the NF-E2-related factor 2 (Nrf2)-mediated antioxidant signaling pathway. *Journal of agricultural and food chemistry* **2011,** *59*, (6), 2725-33.
8. Kapetanovic, I. M.; Muzzio, M.; Huang, Z.; Thompson, T. N.; McCormick, D. L. Pharmacokinetics, oral bioavailability, and metabolic profile of resveratrol and its dimethylether analog, pterostilbene, in rats. *Cancer chemotherapy and pharmacology* **2011,** *68*, (3), 593-601.
9. Azzolini, M.; La Spina, M.; Mattarei, A.; Paradisi, C.; Zoratti, M.; Biasutto, L. Pharmacokinetics and tissue distribution of pterostilbene in the rat. *Molecular nutrition & food research* **2014,** *58*, (11), 2122-32.
10. Chang, J.; Rimando, A.; Pallas, M.; Camins, A.; Porquet, D.; Reeves, J.; Shukitt-Hale, B.; Smith, M. A.; Joseph, J. A.; Casadesus, G. Low-dose pterostilbene, but not resveratrol, is a potent neuromodulator in aging and Alzheimer's disease. *Neurobiology of aging* **2012,** *33*, (9), 2062-71.
11. Paul, S.; Rimando, A. M.; Lee, H. J.; Ji, Y.; Reddy, B. S.; Suh, N. Anti-inflammatory action of pterostilbene is mediated through the p38 mitogen-activated protein kinase pathway in colon cancer cells. *Cancer prevention research (Philadelphia, Pa.)* **2009,** *2*, (7), 650-7.
12. Pan, M. H.; Chiou, Y. S.; Chen, W. J.; Wang, J. M.; Badmaev, V.; Ho, C. T. Pterostilbene inhibited tumor invasion via suppressing multiple signal transduction pathways in human hepatocellular carcinoma cells. *Carcinogenesis* **2009,** *30*, (7), 1234-42.
13. Park, E. S.; Lim, Y.; Hong, J. T.; Yoo, H. S.; Lee, C. K.; Pyo, M. Y.; Yun, Y. P. Pterostilbene, a natural dimethylated analog of resveratrol, inhibits rat aortic vascular smooth muscle cell proliferation by blocking Akt-dependent pathway. *Vascular pharmacology* **2010,** *53*, (1-2), 61-7.
14. Chiou, Y. S.; Tsai, M. L.; Wang, Y. J.; Cheng, A. C.; Lai, W. M.; Badmaev, V.; Ho, C. T.; Pan, M. H. Pterostilbene inhibits colorectal aberrant crypt foci (ACF) and colon carcinogenesis via suppression of multiple signal transduction pathways in azoxymethane-treated mice. *Journal of agricultural and food chemistry* **2010,** *58*, (15), 8833-41.

15. McCormack, D.; Schneider, J.; McDonald, D.; McFadden, D. The antiproliferative effects of pterostilbene on breast cancer in vitro are via inhibition of constitutive and leptin-induced Janus kinase/signal transducer and activator of transcription activation. *American journal of surgery* **2011,** *202*, (5), 541-4.
16. Lin, V. C.; Tsai, Y. C.; Lin, J. N.; Fan, L. L.; Pan, M. H.; Ho, C. T.; Wu, J. Y.; Way, T. D. Activation of AMPK by pterostilbene suppresses lipogenesis and cell-cycle progression in p53 positive and negative human prostate cancer cells. *Journal of agricultural and food chemistry* **2012,** *60*, (25), 6399-407.
17. Zhang, L.; Cui, L.; Zhou, G.; Jing, H.; Guo, Y.; Sun, W. Pterostilbene, a natural small-molecular compound, promotes cytoprotective macroautophagy in vascular endothelial cells. *The Journal of nutritional biochemistry* **2013,** *24*, (5), 903-11.
18. Zhao, P.; Chen, S. K.; Cai, Y. H.; Lu, X.; Li, Z.; Cheng, Y. K.; Zhang, C.; Hu, X.; He, X.; Luo, H. B. The molecular basis for the inhibition of phosphodiesterase-4D by three natural resveratrol analogs. Isolation, molecular docking, molecular dynamics simulations, binding free energy, and bioassay. *Biochimica et biophysica acta* **2013,** *1834*, (10), 2089-96.
19. Li, K.; Dias, S. J.; Rimando, A. M.; Dhar, S.; Mizuno, C. S.; Penman, A. D.; Lewin, J. R.; Levenson, A. S. Pterostilbene acts through metastasis-associated protein 1 to inhibit tumor growth, progression and metastasis in prostate cancer. *PloS one* **2013,** *8*, (3), e57542.
20. Mak, K. K.; Wu, A. T.; Lee, W. H.; Chang, T. C.; Chiou, J. F.; Wang, L. S.; Wu, C. H.; Huang, C. Y.; Shieh, Y. S.; Chao, T. Y.; Ho, C. T.; Yen, G. C.; Yeh, C. T. Pterostilbene, a bioactive component of blueberries, suppresses the generation of breast cancer stem cells within tumor microenvironment and metastasis via modulating NF-kappaB/microRNA 448 circuit. *Molecular nutrition & food research* **2013,** *57*, (7), 1123-34.
21. Yang, Y.; Yan, X.; Duan, W.; Yan, J.; Yi, W.; Liang, Z.; Wang, N.; Li, Y.; Chen, W.; Yu, S.; Jin, Z.; Yi, D. Pterostilbene exerts antitumor activity via the Notch1 signaling pathway in human lung adenocarcinoma cells. *PloS one* **2013,** *8*, (5), e62652.
22. Liu, Y.; Wang, L.; Wu, Y.; Lv, C.; Li, X.; Cao, X.; Yang, M.; Feng, D.; Luo, Z. Pterostilbene exerts antitumor activity against human osteosarcoma cells by inhibiting the JAK2/STAT3 signaling pathway. *Toxicology* **2013,** *304*, 120-31.
23. Al Rahim, M.; Rimando, A. M.; Silistreli, K.; El-Alfy, A. T. Anxiolytic action of pterostilbene: involvement of hippocampal ERK phosphorylation. *Planta medica* **2013,** *79*, (9), 723-30.
24. Siedlecka-Kroplewska, K.; Jozwik, A.; Boguslawski, W.; Wozniak, M.; Zauszkiewicz-Pawlak, A.; Spodnik, J. H.; Rychlowski, M.; Kmiec, Z. Pterostilbene induces accumulation of autophagic vacuoles followed by cell death in HL60 human leukemia cells. *Journal of physiology and pharmacology : an official journal of the Polish Physiological Society* **2013,** *64*, (5), 545-56.
25. Bhakkiyalakshmi, E.; Shalini, D.; Sekar, T. V.; Rajaguru, P.; Paulmurugan, R.; Ramkumar, K. M. Therapeutic potential of pterostilbene against pancreatic beta-cell apoptosis mediated through Nrf2. *British journal of pharmacology* **2014,** *171*, (7), 1747-57.
26. Ko, H. S.; Kim, J. S.; Cho, S. M.; Lee, H. J.; Ahn, K. S.; Kim, S. H.; Lee, E. O. Urokinase-type plasminogen activator expression and Rac1/WAVE-2/Arp2/3 pathway are blocked by pterostilbene to suppress cell migration and invasion in MDA-MB-231 cells. *Bioorganic & medicinal chemistry letters* **2014,** *24*, (4), 1176-9.
27. Saw, C. L.; Guo, Y.; Yang, A. Y.; Paredes-Gonzalez, X.; Ramirez, C.; Pung, D.; Kong, A. N. The berry constituents quercetin, kaempferol, and pterostilbene synergistically attenuate reactive oxygen species: involvement of the Nrf2-ARE signaling pathway. *Food and chemical toxicology : an international journal published for the British Industrial Biological Research Association* **2014,** *72*, 303-11.
28. Pan, C.; Hu, Y.; Li, J.; Wang, Z.; Huang, J.; Zhang, S.; Ding, L. Estrogen receptor-alpha36 is involved in pterostilbene-induced apoptosis and anti-proliferation in in vitro and in vivo breast cancer. *PloS one* **2014,** *9*, (8), e104459.
29. Dolinsky, V. W.; Dyck, J. R. Experimental studies of the molecular pathways regulated by exercise and resveratrol in heart, skeletal muscle and the vasculature. *Molecules (Basel, Switzerland)* **2014,** *19*, (9), 14919-47.

30. Zordoky, B. N.; Robertson, I. M.; Dyck, J. R. Preclinical and clinical evidence for the role of resveratrol in the treatment of cardiovascular diseases. *Biochimica et biophysica acta* **2014**.
31. Biasutto, L.; Szabo, I.; Zoratti, M. Mitochondrial effects of plant-made compounds. *Antioxidants & redox signaling* **2011,** *15*, (12), 3039-59.
32. Dunlop, E. A.; Tee, A. R. The kinase triad, AMPK, mTORC1 and ULK1, maintains energy and nutrient homoeostasis. *Biochemical Society transactions* **2013,** *41*, (4), 939-43.
33. Russell, R. C.; Yuan, H. X.; Guan, K. L. Autophagy regulation by nutrient signaling. *Cell research* **2014,** *24*, (1), 42-57.
34. Shaw, R. J. LKB1 and AMP-activated protein kinase control of mTOR signalling and growth. *Acta physiologica (Oxford, England)* **2009,** *196*, (1), 65-80.
35. Inoki, K.; Kim, J.; Guan, K. L. AMPK and mTOR in cellular energy homeostasis and drug targets. *Annual review of pharmacology and toxicology* **2012,** *52*, 381-400.
36. Xu, J.; Ji, J.; Yan, X. H. Cross-talk between AMPK and mTOR in regulating energy balance. *Critical reviews in food science and nutrition* **2012,** *52*, (5), 373-81.
37. Burgos, S. A.; Kim, J. J.; Dai, M.; Cant, J. P. Energy depletion of bovine mammary epithelial cells activates AMPK and suppresses protein synthesis through inhibition of mTORC1 signaling. *Hormone and metabolic research = Hormon- und Stoffwechselforschung = Hormones et metabolisme* **2013,** *45*, (3), 183-9.
38. Nie, J.; Han, X.; Shi, Y. SAD-A and AMPK kinases: the "yin and yang" regulators of mTORC1 signaling in pancreatic beta cells. *Cell cycle (Georgetown, Tex.)* **2013,** *12*, (21), 3366-9.
39. Stevanovic, D.; Trajkovic, V.; Muller-Luhlhoff, S.; Brandt, E.; Abplanalp, W.; Bumke-Vogt, C.; Liehl, B.; Wiedmer, P.; Janjetovic, K.; Starcevic, V.; Pfeiffer, A. F.; Al-Hasani, H.; Tschop, M. H.; Castaneda, T. R. Ghrelin-induced food intake and adiposity depend on central mTORC1/S6K1 signaling. *Molecular and cellular endocrinology* **2013,** *381*, (1-2), 280-90.
40. Martinez de Morentin, P. B.; Martinez-Sanchez, N.; Roa, J.; Ferno, J.; Nogueiras, R.; Tena-Sempere, M.; Dieguez, C.; Lopez, M. Hypothalamic mTOR: the rookie energy sensor. *Current molecular medicine* **2014,** *14*, (1), 3-21.
41. Vingtdeux, V.; Chandakkar, P.; Zhao, H.; d'Abramo, C.; Davies, P.; Marambaud, P. Novel synthetic small-molecule activators of AMPK as enhancers of autophagy and amyloid-beta peptide degradation. *FASEB journal : official publication of the Federation of American Societies for Experimental Biology* **2011,** *25*, (1), 219-31.
42. Vingtdeux, V.; Giliberto, L.; Zhao, H.; Chandakkar, P.; Wu, Q.; Simon, J. E.; Janle, E. M.; Lobo, J.; Ferruzzi, M. G.; Davies, P.; Marambaud, P. AMP-activated protein kinase signaling activation by resveratrol modulates amyloid-beta peptide metabolism. *The Journal of biological chemistry* **2010,** *285*, (12), 9100-13.
43. Jeong, J. K.; Moon, M. H.; Bae, B. C.; Lee, Y. J.; Seol, J. W.; Kang, H. S.; Kim, J. S.; Kang, S. J.; Park, S. Y. Autophagy induced by resveratrol prevents human prion protein-mediated neurotoxicity. *Neuroscience research* **2012,** *73*, (2), 99-105.
44. Guo, H.; Chen, Y.; Liao, L.; Wu, W. Resveratrol protects HUVECs from oxidized-LDL induced oxidative damage by autophagy upregulation via the AMPK/SIRT1 pathway. *Cardiovascular drugs and therapy / sponsored by the International Society of Cardiovascular Pharmacotherapy* **2013,** *27*, (3), 189-98.
45. Duan, W. J.; Liu, F. L.; He, R. R.; Yuan, W. L.; Li, Y. F.; Tsoi, B.; Su, W. W.; Yao, X. S.; Kurihara, H. Autophagy is involved in the effects of resveratrol on prevention of splenocyte apoptosis caused by oxidative stress in restrained mice. *Molecular nutrition & food research* **2013,** *57*, (7), 1145-57.
46. Lv, X. C.; Zhou, H. Y. Resveratrol protects H9c2 embryonic rat heart derived cells from oxidative stress by inducing autophagy: role of p38 mitogen-activated protein kinase. *Canadian journal of physiology and pharmacology* **2012,** *90*, (5), 655-62.
47. Gurusamy, N.; Lekli, I.; Mukherjee, S.; Ray, D.; Ahsan, M. K.; Gherghiceanu, M.; Popescu, L. M.; Das, D. K. Cardioprotection by resveratrol: a novel mechanism via autophagy involving the mTORC2 pathway. *Cardiovascular research* **2010,** *86*, (1), 103-12.

48. Wang, B.; Yang, Q.; Sun, Y. Y.; Xing, Y. F.; Wang, Y. B.; Lu, X. T.; Bai, W. W.; Liu, X. Q.; Zhao, Y. X. Resveratrol-enhanced autophagic flux ameliorates myocardial oxidative stress injury in diabetic mice. *Journal of cellular and molecular medicine* **2014,** *18*, (8), 1599-611.
49. Chen, M. L.; Yi, L.; Jin, X.; Liang, X. Y.; Zhou, Y.; Zhang, T.; Xie, Q.; Zhou, X.; Chang, H.; Fu, Y. J.; Zhu, J. D.; Zhang, Q. Y.; Mi, M. T. Resveratrol attenuates vascular endothelial inflammation by inducing autophagy through the cAMP signaling pathway. *Autophagy* **2013,** *9*, (12), 2033-45.
50. Morselli, E.; Galluzzi, L.; Kepp, O.; Criollo, A.; Maiuri, M. C.; Tavernarakis, N.; Madeo, F.; Kroemer, G. Autophagy mediates pharmacological lifespan extension by spermidine and resveratrol. *Aging* **2009,** *1*, (12), 961-70.
51. Morselli, E.; Maiuri, M. C.; Markaki, M.; Megalou, E.; Pasparaki, A.; Palikaras, K.; Criollo, A.; Galluzzi, L.; Malik, S. A.; Vitale, I.; Michaud, M.; Madeo, F.; Tavernarakis, N.; Kroemer, G. Caloric restriction and resveratrol promote longevity through the Sirtuin-1-dependent induction of autophagy. *Cell death & disease* **2010,** *1*, e10.
52. Morselli, E.; Maiuri, M. C.; Markaki, M.; Megalou, E.; Pasparaki, A.; Palikaras, K.; Criollo, A.; Galluzzi, L.; Malik, S. A.; Vitale, I.; Michaud, M.; Madeo, F.; Tavernarakis, N.; Kroemer, G. The life span-prolonging effect of sirtuin-1 is mediated by autophagy. *Autophagy* **2010,** *6*, (1), 186-8.
53. Rubinsztein, D. C.; Marino, G.; Kroemer, G. Autophagy and aging. *Cell* **2011,** *146*, (5), 682-95.
54. Pallauf, K.; Rimbach, G. Autophagy, polyphenols and healthy ageing. *Ageing research reviews* **2013,** *12*, (1), 237-52.
55. Karuppagounder, S. S.; Pinto, J. T.; Xu, H.; Chen, H. L.; Beal, M. F.; Gibson, G. E. Dietary supplementation with resveratrol reduces plaque pathology in a transgenic model of Alzheimer's disease. *Neurochemistry international* **2009,** *54*, (2), 111-8.
56. Frozza, R. L.; Bernardi, A.; Hoppe, J. B.; Meneghetti, A. B.; Matte, A.; Battastini, A. M.; Pohlmann, A. R.; Guterres, S. S.; Salbego, C. Neuroprotective effects of resveratrol against Abeta administration in rats are improved by lipid-core nanocapsules. *Molecular neurobiology* **2013,** *47*, (3), 1066-80.
57. Pallas, M.; Porquet, D.; Vicente, A.; Sanfeliu, C. Resveratrol: new avenues for a natural compound in neuroprotection. *Current pharmaceutical design* **2013,** *19*, (38), 6726-31.
58. Tan, C. C.; Yu, J. T.; Tan, M. S.; Jiang, T.; Zhu, X. C.; Tan, L. Autophagy in aging and neurodegenerative diseases: implications for pathogenesis and therapy. *Neurobiology of aging* **2014,** *35*, (5), 941-57.
59. Ghavami, S.; Shojaei, S.; Yeganeh, B.; Ande, S. R.; Jangamreddy, J. R.; Mehrpour, M.; Christoffersson, J.; Chaabane, W.; Moghadam, A. R.; Kashani, H. H.; Hashemi, M.; Owji, A. A.; Los, M. J. Autophagy and apoptosis dysfunction in neurodegenerative disorders. *Progress in neurobiology* **2014,** *112*, 24-49.
60. Ferretta, A.; Gaballo, A.; Tanzarella, P.; Piccoli, C.; Capitanio, N.; Nico, B.; Annese, T.; Di Paola, M.; Dell'aquila, C.; De Mari, M.; Ferranini, E.; Bonifati, V.; Pacelli, C.; Cocco, T. Effect of resveratrol on mitochondrial function: implications in parkin-associated familiar Parkinson's disease. *Biochimica et biophysica acta* **2014,** *1842*, (7), 902-15.
61. Chen, R. J.; Ho, C. T.; Wang, Y. J. Pterostilbene induces autophagy and apoptosis in sensitive and chemoresistant human bladder cancer cells. *Molecular nutrition & food research* **2010,** *54*, (12), 1819-32.
62. Chen, R. J.; Tsai, S. J.; Ho, C. T.; Pan, M. H.; Ho, Y. S.; Wu, C. H.; Wang, Y. J. Chemopreventive effects of pterostilbene on urethane-induced lung carcinogenesis in mice via the inhibition of EGFR-mediated pathways and the induction of apoptosis and autophagy. *Journal of agricultural and food chemistry* **2012,** *60*, (46), 11533-41.
63. Wang, Y.; Ding, L.; Wang, X.; Zhang, J.; Han, W.; Feng, L.; Sun, J.; Jin, H.; Wang, X. J. Pterostilbene simultaneously induces apoptosis, cell cycle arrest and cyto-protective autophagy in breast cancer cells. *American journal of translational research* **2012,** *4*, (1), 44-51.
64. Chakraborty, A.; Bodipati, N.; Demonacos, M. K.; Peddinti, R.; Ghosh, K.; Roy, P. Long term induction by pterostilbene results in autophagy and cellular differentiation in MCF-7 cells via ROS dependent pathway. *Molecular and cellular endocrinology* **2012,** *355*, (1), 25-40.

65. Settembre, C.; Fraldi, A.; Medina, D. L.; Ballabio, A. Signals from the lysosome: a control centre for cellular clearance and energy metabolism. *Nature reviews. Molecular cell biology* **2013,** *14*, (5), 283-96.
66. Settembre, C.; Ballabio, A. Lysosome: regulator of lipid degradation pathways. *Trends in cell biology* **2014,** *24*, (12), 743-750.
67. Shen, H. M.; Mizushima, N. At the end of the autophagic road: an emerging understanding of lysosomal functions in autophagy. *Trends in biochemical sciences* **2014,** *39*, (2), 61-71.
68. Martina, J. A.; Chen, Y.; Gucek, M.; Puertollano, R. MTORC1 functions as a transcriptional regulator of autophagy by preventing nuclear transport of TFEB. *Autophagy* **2012,** *8*, (6), 903-14.
69. Settembre, C.; Zoncu, R.; Medina, D. L.; Vetrini, F.; Erdin, S.; Erdin, S.; Huynh, T.; Ferron, M.; Karsenty, G.; Vellard, M. C.; Facchinetti, V.; Sabatini, D. M.; Ballabio, A. A lysosome-to-nucleus signalling mechanism senses and regulates the lysosome via mTOR and TFEB. *The EMBO journal* **2012,** *31*, (5), 1095-108.
70. Roczniak-Ferguson, A.; Petit, C. S.; Froehlich, F.; Qian, S.; Ky, J.; Angarola, B.; Walther, T. C.; Ferguson, S. M. The transcription factor TFEB links mTORC1 signaling to transcriptional control of lysosome homeostasis. *Science signaling* **2012,** *5*, (228), ra42.
71. Chen, Y.; Azad, M. B.; Gibson, S. B. Superoxide is the major reactive oxygen species regulating autophagy. *Cell death and differentiation* **2009,** *16*, (7), 1040-52.
72. Scherz-Shouval, R.; Elazar, Z. Regulation of autophagy by ROS: physiology and pathology. *Trends in biochemical sciences* **2011,** *36*, (1), 30-8.
73. Zhang, J.; Kim, J.; Alexander, A.; Cai, S.; Tripathi, D. N.; Dere, R.; Tee, A. R.; Tait-Mulder, J.; Di Nardo, A.; Han, J. M.; Kwiatkowski, E.; Dunlop, E. A.; Dodd, K. M.; Folkerth, R. D.; Faust, P. L.; Kastan, M. B.; Sahin, M.; Walker, C. L. A tuberous sclerosis complex signalling node at the peroxisome regulates mTORC1 and autophagy in response to ROS. *Nature cell biology* **2013,** *15*, (10), 1186-96.
74. Settembre, C.; De Cegli, R.; Mansueto, G.; Saha, P. K.; Vetrini, F.; Visvikis, O.; Huynh, T.; Carissimo, A.; Palmer, D.; Klisch, T. J.; Wollenberg, A. C.; Di Bernardo, D.; Chan, L.; Irazoqui, J. E.; Ballabio, A. TFEB controls cellular lipid metabolism through a starvation-induced autoregulatory loop. *Nature cell biology* **2013,** *15*, (6), 647-58.
75. Cuervo, A. M. Preventing lysosomal fat indigestion. *Nature cell biology* **2013,** *15*, (6), 565-7.
76. Gomez-Zorita, S.; Fernandez-Quintela, A.; Lasa, A.; Aguirre, L.; Rimando, A. M.; Portillo, M. P. Pterostilbene, a dimethyl ether derivative of resveratrol, reduces fat accumulation in rats fed an obesogenic diet. *Journal of agricultural and food chemistry* **2014,** *62*, (33), 8371-8.
77. Cherniack, E. P. A berry thought-provoking idea: the potential role of plant polyphenols in the treatment of age-related cognitive disorders. *The British journal of nutrition* **2012,** *108*, (5), 794-800.
78. Son, J. H.; Shim, J. H.; Kim, K. H.; Ha, J. Y.; Han, J. Y. Neuronal autophagy and neurodegenerative diseases. *Experimental & molecular medicine* **2012,** *44*, (2), 89-98.
79. Kesidou, E.; Lagoudaki, R.; Touloumi, O.; Poulatsidou, K. N.; Simeonidou, C. Autophagy and neurodegenerative disorders. *Neural regeneration research* **2013,** *8*, (24), 2275-83.
80. Kamat, P. K.; Kalani, A.; Kyles, P.; Tyagi, S. C.; Tyagi, N. Autophagy of mitochondria: a promising therapeutic target for neurodegenerative disease. *Cell biochemistry and biophysics* **2014,** *70*, (2), 707-19.
81. Seok, S.; Fu, T.; Choi, S. E.; Li, Y.; Zhu, R.; Kumar, S.; Sun, X.; Yoon, G.; Kang, Y.; Zhong, W.; Ma, J.; Kemper, B.; Kemper, J. K. Transcriptional regulation of autophagy by an FXR-CREB axis. *Nature* **2014,** *516*, (7529), 108-11.
82. Hawk, J. D.; Abel, T. The role of NR4A transcription factors in memory formation. *Brain research bulletin* **2011,** *85*, (1-2), 21-9.
83. Nonaka, M.; Kim, R.; Sharry, S.; Matsushima, A.; Takemoto-Kimura, S.; Bito, H. Towards a better understanding of cognitive behaviors regulated by gene expression downstream of activity-dependent transcription factors. *Neurobiology of learning and memory* **2014,** *115c*, 21-29.

84. Benito, E.; Barco, A. The Neuronal Activity-Driven Transcriptome. *Molecular neurobiology* **2014**.
85. Oliveira, R. F.; Terrin, A.; Di Benedetto, G.; Cannon, R. C.; Koh, W.; Kim, M.; Zaccolo, M.; Blackwell, K. T. The role of type 4 phosphodiesterases in generating microdomains of cAMP: large scale stochastic simulations. *PloS one* **2010,** *5*, (7), e11725.
86. Ponsioen, B.; Zhao, J.; Riedl, J.; Zwartkruis, F.; van der Krogt, G.; Zaccolo, M.; Moolenaar, W. H.; Bos, J. L.; Jalink, K. Detecting cAMP-induced Epac activation by fluorescence resonance energy transfer: Epac as a novel cAMP indicator. *EMBO reports* **2004,** *5*, (12), 1176-80.
87. Gagnon, K. T.; Li, L.; Janowski, B. A.; Corey, D. R. Analysis of nuclear RNA interference in human cells by subcellular fractionation and Argonaute loading. *Nature protocols* **2014,** *9*, (9), 2045-60.
88. Mattarei, A.; Biasutto, L.; Romio, M.; Zoratti, M.; Paradisi, C. Synthesis of resveratrol sulfates: turning a nightmare into a dream. *Tetrahedron*, (0).
89. Rueda, D. C.; Schöffmann, A.; De Mieri, M.; Raith, M.; Jähne, E. A.; Hering, S.; Hamburger, M. Identification of dihydrostilbenes in Pholidota chinensis as a new scaffold for GABAA receptor modulators. *Bioorganic & Medicinal Chemistry* **2014,** *22*, (4), 1276-1284.
90. Mihaylova, M. M.; Shaw, R. J. The AMPK signalling pathway coordinates cell growth, autophagy and metabolism. *Nature cell biology* **2011,** *13*, (9), 1016-23.
91. Hardie, D. G. AMPK-Sensing Energy while Talking to Other Signaling Pathways. *Cell metabolism* **2014,** *20*, (6), 939-952.
92. Ruotolo, R.; Calani, L.; Brighenti, F.; Crozier, A.; Ottonello, S.; Del Rio, D. Glucuronidation does not suppress the estrogenic activity of quercetin in yeast and human breast cancer cell model systems. *Archives of biochemistry and biophysics* **2014,** *559*, 62-7.
93. Bresciani, L.; Calani, L.; Bocchi, L.; Delucchi, F.; Savi, M.; Ray, S.; Brighenti, F.; Stilli, D.; Del Rio, D. Bioaccumulation of resveratrol metabolites in myocardial tissue is dose-time dependent and related to cardiac hemodynamics in diabetic rats. *Nutrition, metabolism, and cardiovascular diseases : NMCD* **2014,** *24*, (4), 408-15.
94. Rahal, K.; Schmiedlin-Ren, P.; Adler, J.; Dhanani, M.; Sultani, V.; Rittershaus, A. C.; Reingold, L.; Zhu, J.; McKenna, B. J.; Christman, G. M.; Zimmermann, E. M. Resveratrol has antiinflammatory and antifibrotic effects in the peptidoglycan-polysaccharide rat model of Crohn's disease. *Inflammatory bowel diseases* **2012,** *18*, (4), 613-23.
95. Kasdagly, M.; Radhakrishnan, S.; Reddivari, L.; Veeramachaneni, D. N.; Vanamala, J. Colon carcinogenesis: influence of Western diet-induced obesity and targeting stem cells using dietary bioactive compounds. *Nutrition (Burbank, Los Angeles County, Calif.)* **2014,** *30*, (11-12), 1242-56.
96. Liu, B.; Zhou, Z.; Zhou, W.; Liu, J.; Zhang, Q.; Xia, J.; Liu, J.; Chen, N.; Li, M.; Zhu, R. Resveratrol inhibits proliferation in human colorectal carcinoma cells by inducing G1/Sphase cell cycle arrest and apoptosis through caspase/cyclinCDK pathways. *Molecular medicine reports* **2014,** *10*, (4), 1697-702.
97. Lea, M. A.; Pourat, J.; Patel, R.; desBordes, C. Growth inhibition of colon cancer cells by compounds affecting AMPK activity. *World journal of gastrointestinal oncology* **2014,** *6*, (7), 244-52.
98. Seamon, K. B.; Padgett, W.; Daly, J. W. Forskolin: unique diterpene activator of adenylate cyclase in membranes and in intact cells. *Proceedings of the National Academy of Sciences of the United States of America* **1981,** *78*, (6), 3363-7.
99. Di Benedetto, G.; Scalzotto, E.; Mongillo, M.; Pozzan, T. Mitochondrial Ca(2)(+) uptake induces cyclic AMP generation in the matrix and modulates organelle ATP levels. *Cell metabolism* **2013,** *17*, (6), 965-75.
100. Kandel, E. R. The molecular biology of memory: cAMP, PKA, CRE, CREB-1, CREB-2, and CPEB. *Molecular brain* **2012,** *5*, 14.
101. Rosenberg, D.; Groussin, L.; Jullian, E.; Perlemoine, K.; Bertagna, X.; Bertherat, J. Role of the PKA-regulated transcription factor CREB in development and tumorigenesis of endocrine tissues. *Annals of the New York Academy of Sciences* **2002,** *968*, 65-74.

102. Guigas, B.; Sakamoto, K.; Taleux, N.; Reyna, S. M.; Musi, N.; Viollet, B.; Hue, L. Beyond AICA riboside: in search of new specific AMP-activated protein kinase activators. *IUBMB life* **2009,** *61*, (1), 18-26.
103. Tinhofer, I.; Bernhard, D.; Senfter, M.; Anether, G.; Loeffler, M.; Kroemer, G.; Kofler, R.; Csordas, A.; Greil, R. Resveratrol, a tumor-suppressive compound from grapes, induces apoptosis via a novel mitochondrial pathway controlled by Bcl-2. *FASEB journal : official publication of the Federation of American Societies for Experimental Biology* **2001,** *15*, (9), 1613-5.
104. de la Lastra, C. A.; Villegas, I. Resveratrol as an antioxidant and pro-oxidant agent: mechanisms and clinical implications. *Biochemical Society transactions* **2007,** *35*, (Pt 5), 1156-60.
105. Zheng, L. F.; Wei, Q. Y.; Cai, Y. J.; Fang, J. G.; Zhou, B.; Yang, L.; Liu, Z. L. DNA damage induced by resveratrol and its synthetic analogues in the presence of Cu (II) ions: mechanism and structure-activity relationship. *Free radical biology & medicine* **2006,** *41*, (12), 1807-16.
106. Filomeni, G.; De Zio, D.; Cecconi, F. Oxidative stress and autophagy: the clash between damage and metabolic needs. *Cell death and differentiation* **2014**.

8. Pterostilbene and cognitive performance in the aged rat model: preliminary findings

Summary:

Pterostilbene (trans-3,5-dimethoxy-4-hydroxystilbene, Pt) is a natural dietary compound and a major polyphenolic component of blueberries. This compound is emerging as potentially very beneficial for health care. Several recent papers report that it can, for example, contrast inflammation and cancer and improve cognitive performance and short-term memory impaired by old age or neurodegeneration. Pt is more bioavailable than its celebrated non-methylated analogue, Resveratrol (Rv), and, notably, it can cross the blood brain barrier. While the literature contains reports of effects of Pt in prevention/treatment of cognitive impairment in old individuals, no studies have investigated the detailed mechanisms underlying these observations.

The intent of this study is to identify the downstream effectors of Pt treatment in aged rats. At this time I have completed a preliminary feasibility study. We selected from the literature a panel of genes and proteins that potentially might be regulated by treatment with Pt. These proteins and genes are suitable markers to evaluate the impact on the general cognitive capacity of the old treated animal (BDNF and Psd95, two proteins that directly correlate with the functionality of neurons and synapses), the autophagy status (TFEB, the recently discovered master regulator of autophagy) and the modulation of protein and genes expression (RbAp48 and Rest).

The cognitive capacity of two groups of 4 aged (18 months) rats was evaluated through behavioral tests. One of the two groups then received Pt p.o. for 20 consecutive days, and the cognitive assessment was repeated. VentroMedial Prefrontal cortex (PFc), Perirhinal cortex (PRNLc), Dentate Gyrus (DG) and the rest of Hippocampus (HIP) were then collected and analyzed by RT-qPCR or western blot.

The inadequate numerosity of the experimental groups in this preliminary experiment prevents, as expected, the achievement of statistical significance of the results. Nonetheless, trends can be detected and the basis has been set for further work which is expected to lead to reliable conclusions. Data indicates that after Pt administration the treated group presented a consistent improvement in memory and learning tests administered 24 hours after the training session. Gene expression analysis indicates that in general the DG is the area most solicited by the treatment with Pt. *bdnf* gene expression seems to be unaffected by Pt treatment while *rbbp4* (the gene of RbAp48), *tfeb*, *dlg4* (the gene of Psd95) and *rest* tend to be up-regulated in the treated animal group.

Our data, although preliminary, confirm that chronic administration of pharmacological amounts of Pt has positive effects at a behavioral level in old animals. Gene and protein analysis suggests that behavioral improvement may be related to: 1. a rearrangement in the synaptic architecture (Psd95), 2. change in the acetylation level of histones (RbAp48) and 3. an increase in autophagy (TFEB).

Introduction:

A number of papers report that assuming plant-derived foods or juices rich in antioxidants enhances the intellectual performance of rodents afflicted by age or neurodegeneration.[2-14] Similar effects can be observed also in young[15] and middle-aged[16] rats and aged humans.[17-19] These foods contain a number of putative active ingredients, such as flavonoids, anthocyanins and resveratrol, which may have synergic action. While resveratrol itself has been reported to positively affect memory and cognition (e.g. [20-30]), this study focuses on pterostilbene, i.e. 3,5-dimethylresveratrol, which is emerging as a possibly more effective antagonist of age in the modulation of intellectual function[31-34] and in mice reportedly protects against inflammation-linked learning and memory impairment[35] and has anxiolytic action.[36] The question arises of the mechanisms of action of active food constituents. Considerable work to clarify these fundamental aspects has been carried out with flavonoids[37-49] and resveratrol.[50] The protective effects of the latter may be partly ascribed to its anti-inflammatory action. Neuroinflammatory processes are believed to play a crucial role in the development of neurodegenerative diseases, due in part to an increased production of reactive oxygen species (ROS) (e.g. [51-53]). Resveratrol is able to counteract ROS production by antagonizing NADPH oxidase (e.g. [54-56]) and by accelerating mitochondrial O_2^- detoxification through upregulation of SOD2 (e.g. [57, 58]). In addition resveratrol (as well as ROS and pterostilbene) can induce the expression of other antioxidant enzymes such as NAD(P)H quinone oxidoreductase 1 (NQO1), heme oxygenase 1 (HMOX1), glutamate-cysteine ligase (GCL) and glutathione S transferases (GSTs) through the upregulation of Nrf2 signaling.[59-61] The transcription factor Nrf2 is tightly bound to Keap1, which facilitates ubiquitin-mediated degradation of the transcription factor. Upon oxidative stress the Nrf2/Keap1 complex is disrupted and Nrf2 can translocate to the nucleus where it promotes the transcription of ARE-targeted genes (e.g. [62-64]). Resveratrol also contrasts inflammation through the inhibition of nuclear factor kappa B (NFkB) (e.g. [65-67]) via inhibition of upstream IKK kinase (e.g. [68-70]) and via SIRT1-mediated deacetylation of NFkB itself (e.g. [71, 72]). NFkB targets many pro-inflammatory genes, such as cytokines and chemokines (e.g. [73-78]). Resveratrol and anti-inflammatory action are recognized to have beneficial effects also on the vascular and micro-vascular system (e.g. [25, 30, 54, 79-82]). NADPH oxidases are one of the possible pharmacological targets (e.g. [83]), and resveratrol can act at this level, again through SIRT1.[54, 55] Age- or disease-related circulation deficits can contribute heavily to cognitive impairment[84-88] (see also below).

Unsurprisingly, given the structural similarity, the effects of Pt are in line with those ascribed to resveratrol,[33, 34, 89] but its efficacy seems to be higher.[31] We have determined the pharmacokinetics of Pt and its major metabolite, the sulfate, in various organs after administration of a bolus.[90] The brain differs from other organs in that Pt as such is the major specie, presumably due to its lipophilicity. The levels it reaches are considerably higher than those of resveratrol after administration of an equimolar dose; this may account, at least in part, for its greater effectiveness.

In particular, Pt improved performance in spatial learning and memory tests (radial arm, water maze),[31] implying effects on spatial memory. Thus, the hippocampus and perirhinal cortex may be affected. A question arising is therefore that of the molecular mechanisms of Pt action. Memory formation and its deterioration with aging are complex processes which are not known in full detail (rev.: [91, 92]). It is clear however that memory is linked to the strengthening, de novo formation and remodeling of connections between nervous cells, the spines, thus upregulation of proteins and activities involved in these processes may be expected.

In the early 1970's Nobel prize winner Eric Kandel and coworkers hypothesized that there may be a connection between short-memory formation and cAMP-mediated signaling.[93, 94] They observed that neurotransmitters such as serotonin and dopamine could increase levels of cAMP. This discovery was followed by the observation that long-term memory formation involved the migration of PKA and MAPK (downstream effectors of cAMP) to the nucleus, activation of the transcription factor CREB-1 (cAMP Response Element Binding Protein-1) and consequent increased expression of a set of genes leading to the growth of new synaptic connections.[95-99] Aging-related cognitive decline affects, among many other functions, long-term memory formation.[100] Given the importance of the cAMP/CREB pathway in the formation of such memory, efforts are under way to find a pharmacological approach for the modulation of memory formation.[100-102] Particularly interesting in this context is the role of Phosphodiesterases (PDEs). PDEs are a vast class of proteins (more than 100) classified in 11 groups, which can hydrolyze the phosphodiester bond of cAMP and cGMP. These protein are in some cases selective for cAMP or cGMP and they can be ubiquitously expressed or selectively expressed in certain areas. What is now clear is that their pharmacological regulation can be important for intervention on several dysfunctions. Rolipram, an inhibitor of PDE4, has already been tested for boosting long-term memory formation.[101] While Resveratrol was shown by Park et al.[103] to be an inhibitor of PDE class 1, 3 and 4, Pt activity in this respect is still not characterized. In our laboratory we have addressed the question of whether Pt can cause an increase of cellular [cAMP]. Pt turns out to be more potent than Resveratrol in this respect, thus presumably activating PKA and ultimately the CREB/CBP pathway. Part of our future efforts will aim to define the interaction of Pt with PDEs.

Epigenetic modifications of neural cells are recognized to underlie memory consolidation and learning and conversely to play a role in cognitive decline and neurodegeneration (e.g. [104-113]). Modulation of histone acetylation may be one of the mechanisms.[114-116] Epigenetic effects may well be responsible for a considerable portion of Pt action. Gene expression is strongly regulated by modifications such as DNA and histone acetylation/methylation. Activation of the cAMP/CREB/CBP pathway can be irrelevant if the target genes are not accessible to the transcription factor. Histone acetylation/deacetylation in particular leads to an alteration of the accessibility of the DNA to proteins. Histone tail acetylation causes a relaxation of the chromatin structure.

Acetyl group indeed masks the positive charge of lysine residues on the tail of histones that are important for the interaction with the negative charge of the DNA backbone.

In 2013 it was discovered that a protein, Retino Blastoma Associated Protein 48 (RbAp48), is downregulated in the dentate gyrus of senescent individuals (human and mice) and that its restoration (in a mouse model, through AAV carriers) leads to recovery of cognitive capacity in old animals.[117] This protein is part of a large complex called NuRD (Nucleosomal Remodeling and Deacetylase complex) where it directly interacts with the protein MTA-1 (among others). In general, NuRD consists of several proteins whose coordinated function is to repress gene transcription.[118-122] However, this is not the only way by which RbAp48 acts in the modulation of the gene transcriptions. Another pathway (fig 1) relies on the interaction of RbAp48 with CBP (CREB Binding Protein). CBP in particular is recruited by the phosphorylated form of CREB, which is formed downstream of an increase of intracellular cAMP levels. CBP is an acetyltransferase (HAT) which uses acetyl-coenzyme A as an acetyl group donor to transfer an acetyl group to the ε-amino group of lysine residues in the N-terminal tails of the four core histones. As previously anticipated this acetylation results in DNA relaxation, thus exposure of promoter sequences to transcription factors (e.g. [123]). Zhang and coworkers[124] demonstrated that the interaction of RbAp48 with CBP induces an increase in the acetyl-transferase activity of this protein, leading to an increase in the transcription of genes under the control of the CREB promoter.

Aging is also a matter of impaired renewal. Autophagy, in its various declinations, is the process that provides the turnover of cellular content. Dysfunctional proteins and

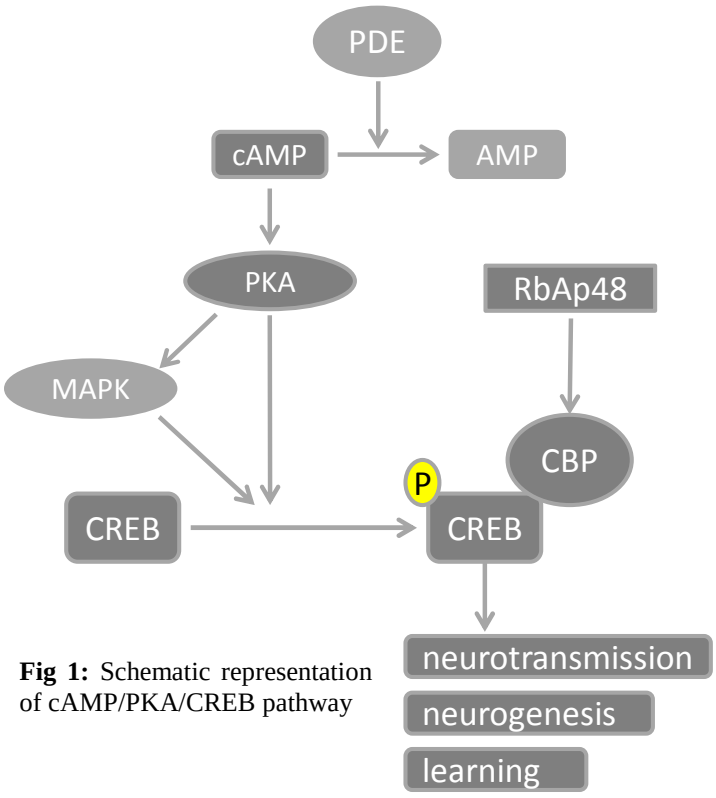

Fig 1: Schematic representation of cAMP/PKA/CREB pathway

organelles, as well as pathogens, can be recycled and constituent (mainly amino acids and lipids) reused by the cell. Recently a transcription factor (EB) has been identified as coordinator of the expression of autophagic proteins and lysosomal biogenesis.[125-129] Transcription factor EB (TFEB) under basal conditions is kept in the cytosolic compartment in a phosphorylated form. Autophagic stimuli, such as starvation, induce the translocation of this factor to the nucleus where it can bind CLEAR-box sequences (5'-GTCACGTGAC-3') inducing the transcription of the relative genes. Dysfunctional neurons often present dysfunctional organelles and stockpiles of unfolded protein.[130, 131] In chapter 7 I have reported that Pt induces the translocation of TFEB to the nucleus, thus enhancing autophagy in HeLa cells.

Given this chart of Pt's potentialities in the treatment of cognitive aging, we decided to investigate in a rat model the real effectiveness of Pt treatment and the possible involvement of autophagy (TFEB) and of the epigenetic modulator RbAp48 in its effects. For a fuller picture of Pt activity in cognitive aging we also looked at two common markers of synaptic plasticity, BDNF and Psd-95, and to another protein that is emerging as an important regulator for gene expression in old animals/humans, Rest.

The Repressor Element-1 Silencing Transcription factor (Rest) is a zinc finger repressor protein that triggers gene silencing. Rest activity is crucial during neural differentiation and in STEM cells.[132, 133] Its expression drops to very low levels after differentiation. Rest is increased again in the aged brain; its role is under investigation since recent work indicates a central role in tumorigenesis. However Rest activity is still poorly characterized and it may well be involved in cognitive aging.

The two common markers of synaptic plasticity previously mentioned are the Brain Derived Neurotropic Factor (BDNF) and the Post Synaptic Density protein-95 (Psd-95). Synaptic plasticity includes the strengthening or weakening of synaptic connections. Regulation can take place at the pre-synaptic site by modulating the release of neurotransmitter molecules or post-synaptically by changing the number, types, or properties of neurotransmitter receptor.[134] BDNF is a member of the neurotrophin (NT) family, it binds the tropomyosin-related kinase receptor B (TrkB) and their interaction leads to the activation of the Mitogen-Activated Protein Kinase (MAPK), Phospholipase Cγ (PLCγ), and Phosphatidylinositol 3-kinase (PI3K) pathways.[135-138] Psd-95 is a scaffold protein that interacts with cytoskeleton components as well as receptors, ion channels and cell adhesion molecules. Psd-95 exerts structural functions and its levels are directly correlated with synaptic plasticity.[139, 140]

Here is presented a pilot study, still incomplete at this point, whose results and perspective will be discussed in the conclusions. Part of this work is done in collaboration with the groups of prof. Nicoletta Berardi and dr. Alessandro Sale, IN-CNR of Pisa.

Materials and methods:

Animals and ethics statements. All procedures complied with Italian Ministry of Health (Law 116/92) and European Community Council (Directive 86/609/EEC) guidelines.

4 males and 4 females Sprague Dawley rats, 18 months old, were housed in an animal room with a 12h/12h light/dark cycle, with food and water available *ad libitum.* For two weeks before the experiments the rats were handled daily. All experimental procedures were carried out during the light phase.

Animals were subdivided in two groups, treated and untreated. Females and males were equally distributed among experimental groups (50%). Treated animals received twice a day (8 am – 8 pm) for 20 consecutive days a 22.5mg/kg dose of Pt (Waseta Int. Trading Co., Shangai, P.R. China) (the molar equivalent of 20 mg/kg of resveratrol) in a palatable jelly (prepared as described by Zhang Lei ([141]; materials were from commercial shops), while the untreated group received "unloaded" jelly.

Palatable jelly was preferred over incorporation in food or drinking water as a route of administration. As reported by Zhang[141], it ensures both low stress to the animal and a controlled administration of the compound. Jellies were administered as a food supplement and were prepared as follows:

- 2.8gr of dried jelly (PaneAngeli) was re-hydrated with 20ml of citrate buffer (10mM, pH 5) at room temperature for 10 minutes.
- the solution was heated at 55-60°C under stirring for 30 minutes.
- 4 drops of sweetener were added (Diete.tic, Eridania) as well as 400µl of chocolate flavoring (Estratti Bertolini). The preparate was further stirred and aliquoted into a 48 well-plate (500µl) and kept at -20°C. Pt was added to the jellies for the treated group, immediately after the sweetener and the flavoring. Each single loaded jelly contained the dose of 22.5mg/kg of Pt. During the preparation the different weight of male and female animals was considered.

To avoid initial prudence towards novel foods animals were initially trained to overcome neophobia. Training was performed as specified by Zhang[141]. All the animals were voluntary eating the jelly after the training.

As sketched in fig 2, animals were evaluated for their cognitive performances before and after the jelly administration. T maze test, object recognition test and object in context test (described below) were performed. Given the long duration of the behavioral assessment, we decided to protract the jelly administration (loaded or unloaded) during the entire period of the memory and learning evaluation post-treatment, at the end of which animals were sacrificed under deep anesthesia (Isoflurane). Brain was collected and ventromedial prefrontal cortex, perirhinal cortex, dentate gyrus and hippocampus

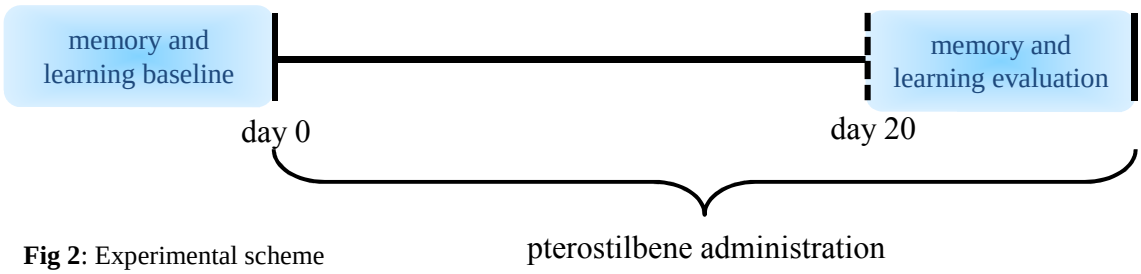

Fig 2: Experimental scheme

were dissected and rapidly frozen by immersion of a sealed vial in a bath of isopentane and dry ice. Samples were stored at -80°C until use. Lungs, heart, liver, kidneys, skeletal muscle (gastrocnemius, tibialis anterior and soleus), testes (males) and the remaining brain were also removed and frozen. Blood was collected at decapitation and immediately processed as described below.

T-maze. The T-maze protocol was adapted from Dominguez G et al.[142] Briefly, animals were placed for ten successive trails separated by 90-s inter-trial intervals at the starting point of the T-maze cage. An alternation response was considered each time the subject entered the arm opposite to the one visited on the immediately previous trial. Alternation rate was calculated taking into account the nine successive trials, and expressed as the mean of the arm alternation. To avoid olfactory cues, the apparatus was washed with water/EtOH after each trial.

Object recognition (ORT). The ORT protocol was previously described by Silingardi, et al.[143] Briefly, the apparatus consisted of a square arena constructed in PVC with black walls and white floor. The objects were three-dimensional plastic cubes (15 cm wide) made of transparent Plexiglas that differed for the visual patterns lining the walls. Box and objects were cleaned up between trials to stop the build-up of olfactory cues.[1]

The experimental protocol was modified from Ennaceur and Delacour.[144] Briefly, rats received one session of 5 min duration in the empty arena to help them habituate to the apparatus and test room (habituation phase). Twenty-four hours later, each rat was placed in the arena and exposed to two identical objects (sample phase) for 5 min and returned to its cage. After a delay of 1h or 24h, rats were placed back in the arena and exposed to a familiar object (object identical to those in sample phase) and to a novel object for 5 min (test phase). Objects were placed in the same locations as in sample phase. The time spent exploring each object was recorded for each animal and for each condition, and a discrimination index was calculated (described below in the “measurements and statistics” section).

For each retention time interval, the new object for half of the animals, treated or untreated, was the familiar object for the other half; also the position of the novel and the familiar object (left–right) was balanced. For the two test sessions, 1h or 24h, different pairs of object were used. At least 5 days separated the two tests. When different groups of animals performed the same ORT test we used the same pairs of objects.

Object in context test (OCT). The OCT protocol was previously described by De Rosa et al.[1] and adapted with minor modifications. Briefly, two open field arenas made of poly(vinyl chloride) were used. Each arena constituted a different experimental condition (A and B). In condition A, horizontal white stripes were applied on the black walls of the arena. The floor was covered with rough Plexiglas (fig. 3a). In condition B, the arena had

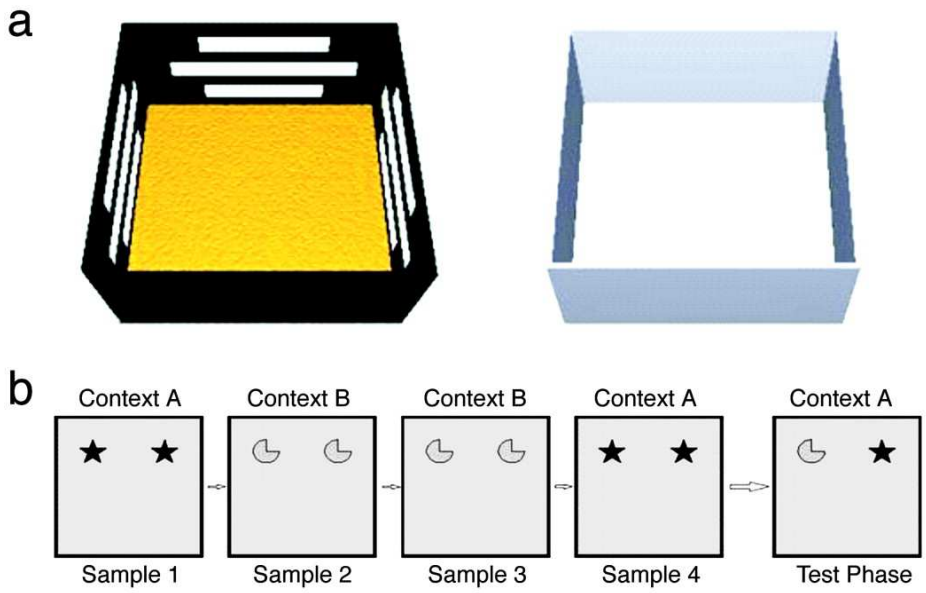

Fig 3: (a) Three-dimensional representation of conditions A (Left) and B (Right) in OCT. (b) Schematic representation of sample/test conditions in OCT. Condition A is represented by the shaded box, and condition B is shown by the plain box. Objects are represented by the symbols. Image modified from De Rosa et al.[1]

gray walls, and the floor was made of Plexiglas (fig. 3a). The particular object for a given test was randomly determined, but each object was used for only one experimental condition. The OCT was used to determine whether rats were sensitive to a change in context for a given object. Thus, previous familiarization with the two environments was fundamental. The habituation phase started 2 days before the block of tests and consisted of two sessions. In each session, treated and untreated rats were exposed to both conditions (A and B) for 5 min. The OCT was divided into four sample phases and a test phase, each lasting 3 min (fig. 3b). The retention interval within the sample phases was 3 min. There was a 5 min interval between the last sample phase and the test phase. In the sample phase, two objects were placed in adjacent corners of the arena; phases 1 and 4 comprised objects A_1 and A_2 in environment A, and phases 2 and 3 comprised

objects B_1 and B_2 in environment B (fig. 3b). The test phase was in the same environment as sample phase 4, but one of the objects (A_2) was replaced by B_2. In this way, one object was in the same environment as in the sample phase, and the other object was in a different environment from the sample phase (fig. 3b). To avoid the eventual preference for one of two environments, half of the rats began the sample phase in environment A with object A_1 and A_2 and finished with the same environment with object A_1 and B_2 and vice versa.

Measurements and Statistics. The standard measure for the statistical analysis in the ORTs was the time spent exploring the two objects. The exploration of an object was defined as directing the nose to the object at a distance of <2 cm and touching it with the nose. Turning around, climbing over, or sitting on the object were not included. In the sample phase, if the exploration time was <3 sec, the rat were discarded from the sample. Rats also were excluded from the sample if they spent <1 sec exploring both new and familiar objects in the test phase. In the sample phase, the total time spent exploring each object was recorded and compared across different treatments with Student's *t* test. For OCT, two-way ANOVA was used. In the test phase, comparisons between time spent exploring the new and old objects were performed within groups (analysis performed by using paired *t* tests). A discrimination index (DI) was calculated as the difference between the time spent exploring new and old object divided by the total time spent exploring the objects [$(n - f)/(f + n)$, where n represents new and f represents familiar]. DIs were compared across treatments with a *t* test. For the T-maze, performance in discriminating side (sx versus dx) was compared across treatments with a *t* test.

Tissue treatments and HPLC analysis. HPLC analysis, tissues and blood treatment were performed as previously described in chapter 5.[90]

Quantitative real Time-PCR (qPCR). Total RNA was obtained from dentate gyrus, hippocampus, ventromedial prefrontal cortex and perirhinal cortex of both, treated and untreated animals. RNA was extracted following TRIzol® (Invitrogen) extraction methods, according to manufacturer's instructions. RNA was eluted in RNase-free water and stored at -80°C until use. The concentration and quality of each sample were measured by NanoDrop (Thermo Scientific). 100ng of RNA were converted to cDNA using Superscript® VILO™ (Invitrogen) following the manufacturer's instructions. Reverse transcription was performed in a thermal cycler (Hybaid Touchdown Thermal Cycle): 25°C for 10 min, 42°C for 120 min, 85 °C for 5 min. All RNA samples were simultaneously converted to cDNA to minimize experimental variability. Superscript® VILO™ does not require initial denaturation of RNA, as indicated by manufacturer's instructions. Specific primers were either designed using Primer3input (http://bioinfo.ut.ee/primer3-0.4.0/primer3/) or Primer Blast NCBI (http://www.ncbi.nlm.nih.gov/tools/primer-blast/) or taken from already published sequences (for *actb*: [145]; for *gapdh* and *bdnf*: [146]). Thermodynamic specificity was determined using BLAST sequence alignment (NCBI: http://blast.ncbi.nlm.nih.gov/Blast.cgi; Integrated DNA Technologies (IDT):

http://eu.idtdna.com/calc/analyzer). All primers were purchased from Sigma Aldrich. Primer sequences were as follows:

Glyceraldehyde 3-phosphate dehydrogenase (*gapdh*): fw ATCACCATCTTCCAGGAGCG rv GATGGCATGGACTGTGGTCA

Actin beta (*actb*): fw CCGCGAGTACAACCTTCTTG rv GCAGCGATATCGTCATCCAT

Meis homeobox 1 (*meis1*): fw GCACAGGTGACGATGATGAC rv GAAGGATGGTGAGTCCCGTA

Tryptofan 2,3-dioxygenase (*tdo2*): fw AGAAAGAGGTGCTGCTCTGC rv GAGGTCAGCAACTGGAAAGG

TYRO 3 protein tyrosine kinase (*tyro3*): fw CCCTTTACTTGCTTGCTTCG rv AATGGCGTGGAAATTCTGAG

Desmoplakin (*dsp*): fw CACTCCCAGTCTTCACAGCA rv TTTCTCCAGGTCCCACAATC

Discs, large homolog 4 (*dlg4*): fw GAGTGCTTCTCAGCCATCGT rv ATGTAGGGGCCTGAGAGGTC

Retinoblastoma binding protein 4 (*rbbp4*): fw GCTCCCTAATGACGATGCTC rv ATGATGCAAGGGTTCTGAGG

RE1-silencing transcription factor (*rest*): fw AACTCACACAGGAGAACGCC rv TGTGAACCTGTCTTGCGTGT

Transcription factor EB (*tfeb*): fw GGGCTACATCAACCCCGAAA rv CCGGCTCTCAGCATCTGTTA

Brain-derived neurotrophic factor (*bdnf*): fw ATAGGAGACCCTCCGCAA rv CTGCCATGCATGAAACACTT

Quantitative PCR was performed in duplicate in a 96-well IQ5 Thermal Cycler (BioRad) using SYBR green chemistry. *gapdh* and *actb* were tested as putative reference genes. *gapdh* turned out to provide the most reproducible output, and was used to normalize cycle threshold (C_T) values. All samples were run simultaneously with RNA- and RT-negative controls. The efficiency of each run was determined by a standard curve obtained through a serial dilution of cDNAs from a pool of the analyzed sample. Normalization was performed by the ΔC_T method. Data are expressed as means ± SEM (n = 4). Comparisons were made using the t-test ($p < 0.05$).

Results:

Behavioral tests:

Before the training session animals were handled and habituated to eat jelly (vehicle only). In order to overcome the initial neophobia animals were subjected to short starving intervals (e.g. 4-6 h) during the light phase. Calorie restriction (CR) is known to attenuate age-related deficits (e.g. [147-151]). In order to exclude the possibility of a CR-induced improvement in the cognitive performance of the animals, the jelly training phase was performed one month before the beginning of the experiments. Short starving intervals were limited to the strictly necessary (2 or 3 session for each animal). The animals received vehicle jelly weekly during the baseline assessment period in order to maintain their interest for the flavor of the jelly.

Baseline evaluation of the cognitive status of the old animals indicated that the whole cohort of animals was homogeneous and presented age-related impairment in performing the tasks (data not shown).

Behavioral tests were selected to probe different areas and different functions of the brain. Aging impairs, among many other functions, memory formation and consolidation.[152] Given the nature of this pilot study, we decided to adopt a broad approach to detect any possible effect of Pt in memory.

ORT mainly reflects the activity of the perirhinal cortex. This area of the brain is heavily involved in the identification of environmental stimuli and object recognition.[143, 153-155]

OCT evaluates preferentially hippocampus activity. Hippocampus among other functions is largely responsible for processes such as consolidation of short term memory to long term memory, memory retrival and spatial navigation.[155-160] T-maze exists in many different variants developed in order to evaluate different aspect of brain function. Forced alternation and left-right discrimination tasks using the T-maze is widely used to assess working memory and reference memory in rodents, and it also depends on hippocampal function.[161, 162]

Object recognition test:

Object recognition test was performed twice, in order to evaluate the spatial memory of the animals treated and untreated 1h or 24h after the training session. Each time different objects were used avoiding reminding of the previous test.

Treated and untreated animals had a similar performance in recognizing the new object when the test was performed 1h after the training session (fig 4-a, index ctrl = 0.337 ± 0.044, index Pt = 0.215 ± 0.039). However, the treated group had a definitely improved index score in comparison with the untreated group when the test was performed 24 hours after the training session (fig 4-b, index ctrl = -0.120 ± 0.130, index Pt = 0.158 ±

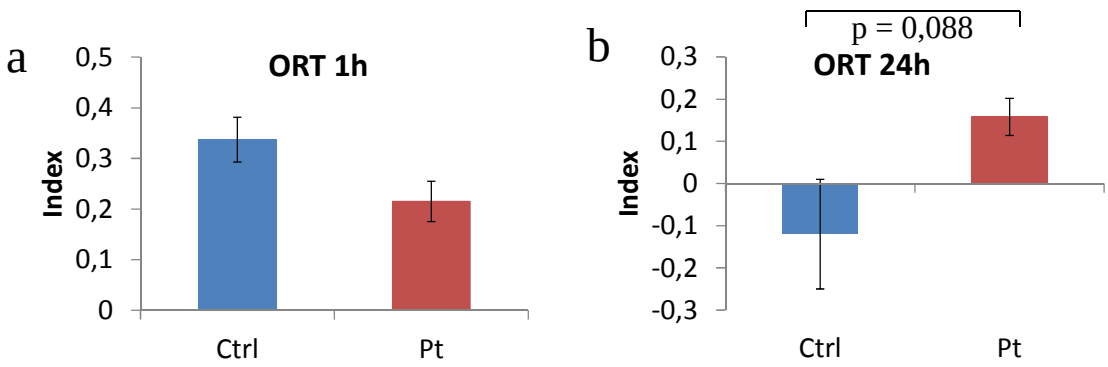

Fig 4: Object recognition memory. Tests were performed 1h (**a**) and 24h (**b**) after the training session. Discrimination index (Index) was calculated with the following formula: *(n – f)/(n + f)*, where *n* represents new and *f* represents familiar object. **a**: untreated (Ctrl) and treated (Pt) animals did not significantly differ in recognizing the new object 1h after the training phase. **b**: treated animals (Pt) tend to explore the new object more than untreated animals 24h after the training phase (*t*-test, p = 0,088). Error bars represent SEM

0.044). Even though the difference is not statistically significant (p = 0.088) due to the low numerosity, the results obtained in the 24h test suggest that Pt ameliorates the consolidation of spatial memory, while no improvement in short-term memory is suggested by the 1h test.

Object in context test:

As for ORT, object in context test was performed 1h and 24h after the training sessions. Pt treatment again was effective in the phase of memory consolidation (24h, fig 5-b), while Pt administration seemed to be ineffective when the assay was performed 1h after the training session (fig 5-a). This result confirms and supports the idea that Pt treatment positively affects memory, particularly in the phase of its consolidation.

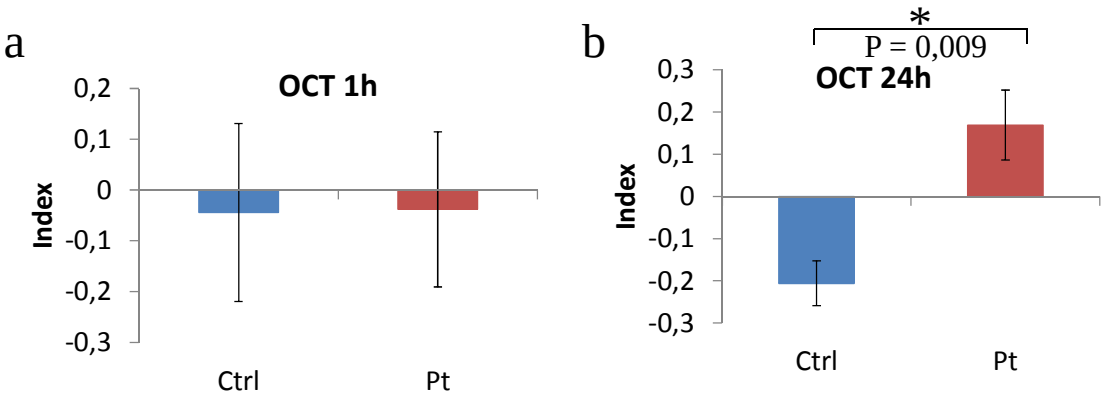

Fig 5: Object in context test. Tests were performed 1h (**a**) and 24h (**b**) after the training sessions. The discrimination index (Index) was calculated as described in fig 4. The performance of treated group (Pt) was similar to that of untreated group (ctrl) 1h after the last training session (**a**). 24h after the last training session treated animals (Pt) were significantly better than untreated animals in performing the task (**b**, p = 0,009). Error bars represent SEM

T maze:

Working memory stimulation requires the coordinated activity of many functions and areas of the brain. Sensor and motor cortex, spatial orientation and short term memory are particularly solicited. In our experiment the animals were free to choose between left and right arm, with a short latency within 10 trials. Even though differences are not significant, treated animals seem to obtain a better score than untreated animals (fig 6).

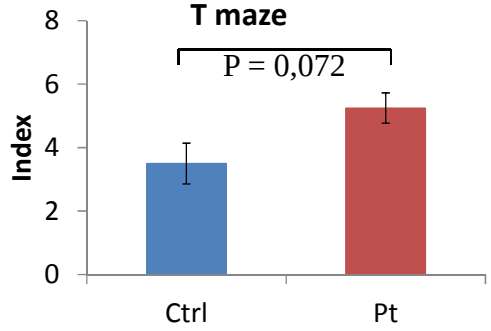

Fig 6: T maze test. The index was calculated as the mean of the arm alternation.
The working memory of the treated group seems to be more efficient than that of the untreated group (ctrl, p = 0,072). Error bars represent SEM

HPLC:

As a control for Pt administration the major organs of treated animals were analyzed by HPLC in order to verify and measure the presence of Pt and its main metabolite in rats, Pt-sulfate (Pt-S). Animals were sacrificed at different times after the last Pt administration, so absorption and clearance (in addition to the normal variability) can account in part for the variability in the concentrations of Pt and Pt-S found among the 4 treated animals.

Pt and Pt-S were present in all treated animals. Distribution in major organs of Pt and Pt-S is similar to the one previously published by our group.[90] However in this work animals were not fasted and the administration was chronic. Liver and kidney showed the highest concentration of both Pt and Pt-S; Pt was the predominant specie in the brain while the metabolite was predominant in the liver and kidneys (fig 7).

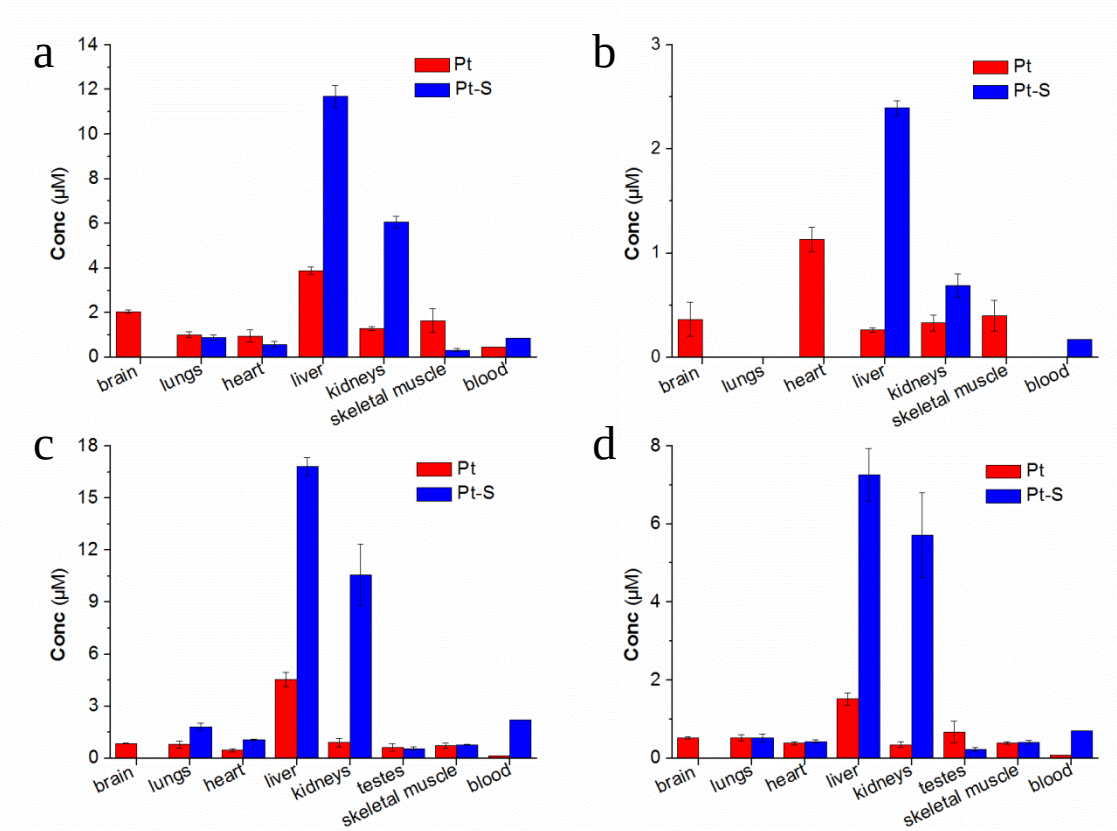

Fig 7: Levels of Pt and Pt-S in the organs of treated animals. Females (**a**, **b**) and males (**c**, **d**) have a similar amount and distribution of both species. Pt was the predominant specie in the brain (**a-d**) and in female's skeletal muscle (**a**, **b**), while Pt-S was more abundant in liver, kidneys and blood (**a-d**).

qPCR:

Kandel and coworkers[117] have identified the dentate gyrus as one of the areas most affected by age, and the area that shows decreased expression of RbAp48 upon aging.

The dentate gyrus is wrapped up by other brain structures, mostly the hippocampus. Given the difficulty of the dissection we decided to perform a molecular control for our

dentate gyrus preparation. As suggested by Hagihara[163] it is possible to verify the accuracy of the dentate gyrus dissection measuring by RT-qPCR the level of expression of certain genes that are selective for the dentate gyrus (*dsp* and *tdo2*) or for the remaining hippocampus (*meis1* and *tyro3*).

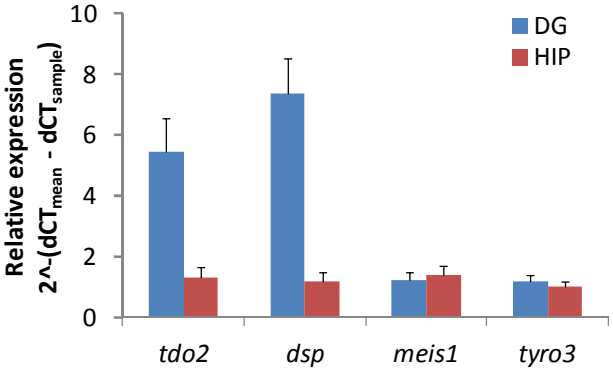

Fig 8: Gene expression in the dentate gyrus (DG) and remaining hippocampus (HIP). *gapdh* was used to normalize gene expression. Each bar represents the average of 8 animals. Error bars represent SEM.

tdo2 and *dsp* were consistently up-regulated in the whole cohort of the DG samples, indicating that the isolate contains the DG. However, *meis1* and *tyro3* expression was similar in both rest-of-hippocampus and DG preparates. This indicates that during the dissection part of the hippocampus was dissected along with the DG, and it represents a significant contamination in our samples. Since the DG was identified as DG, we decided to proceed further with the analysis even if this contamination was present (fig 8).

Markers of synaptic plasticity:

RT-qPCR analysis suggested that *bdnf* gene expression is not significantly affected by the treatment with Pt in any of the areas examined.

dlg4 (the gene of Psd-95) also seems not to be up-regulated in the treated group. However, in the DG of treated animals there might be a slight up-regulation of the gene.

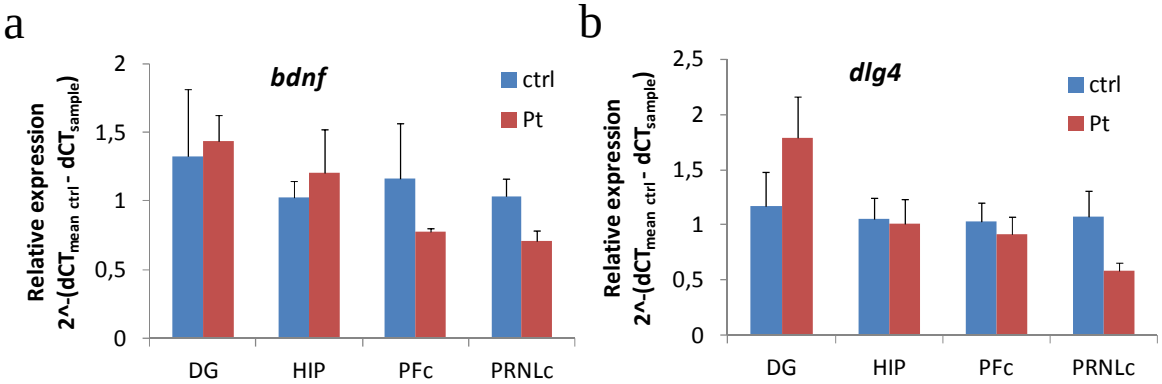

Fig 9: Quantitative PCR analysis with a *bdnf* specific probe (a) and a *dlg4* specific probe (b). Gene expression is normalized on *gapdh*. Each bar represents the average of 4 animals. Error bars represent SEM.

Both *bdnf* and *dlg4*, appeared to be negatively regulated by Pt treatment in the PRNLc. However, this result has a particularly low significance due to the small amount of PRNLc material we obtained. RNA extracted from this areas was indeed very scarce, due to the size of this portion of the cortex and due to the age of the animals. This point will be discussed in the conclusions section.

Autophagy induction:

Since it is considered the master regulator of autophagy and lysosomal biogenesis (see above), we examined TFEB as a marker of Pt autophagy induction. One of the genes controlled by TFEB is its own.[164] Its activation therefore is expected to lead to an increase of TFEB mRNA and protein levels (positive feedback loop). Hippocampus, pre-frontal cortex and perirhinal cortex TFEB levels seemed to be unaffected by Pt administration. On the other hand, the gene seems to respond in the DG. This outcome would be in agreement with the results of our previous work (chapter 7) which clearly indicates, at least *in vitro*, a correlation between Pt administration and TFEB nuclear localization.

Epigenetics and transcription silencing:

rbbp4 (gene of RbAp48 protein) and *rest* follow the same pattern seen for *dlg4* and *tfeb*. In both cases gene expression seems to be up-regulated in the DG whereas the other areas examined apparently are not influenced by Pt administration.

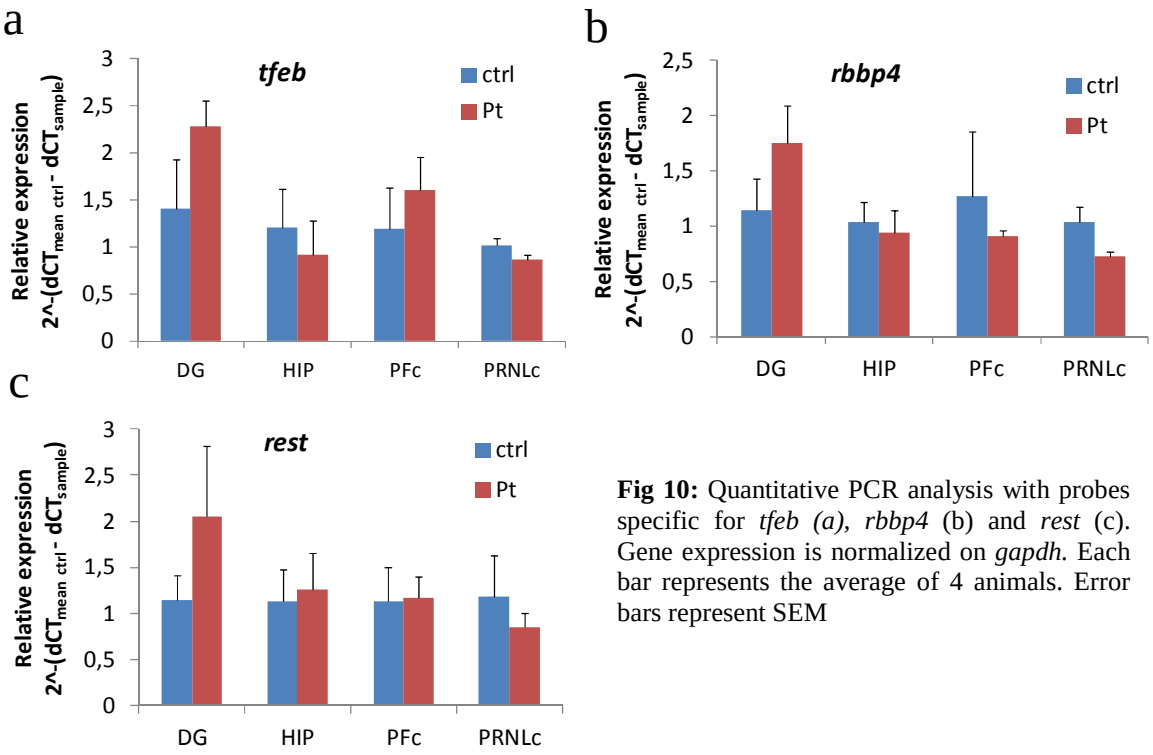

Fig 10: Quantitative PCR analysis with probes specific for *tfeb (a)*, *rbbp4* (b) and *rest* (c). Gene expression is normalized on *gapdh*. Each bar represents the average of 4 animals. Error bars represent SEM

Discussion:

Taken together our preliminary data suggests the following:

1. Behavioral results confirm that Pt ameliorates cognitive impairment in old rats, at least deficits concerning spatio-temporal memory.
2. Molecular study suggests that this effect may be due to a rearrangement in the synaptic architecture (*dlg4* increase, if any), to a change in the acetylation level of histones (*rbbp4* increase) and to an increase in autophagy level that can exert a renewal of intracellular components (*tfeb* increase).
3. Molecular differences in the treated group were primarily found in the dentate gyrus. This agrees with the fact that the DG is one of the areas most affected by the age.

However behavioral and molecular results need to be confirmed, since our sample size is too small. A similar study performed by Joseph's group[32] reports, at a behavioral level, results similar to ours. However Joseph's work used 14 animal per group (more than three times our numerosity) and a longer administration of the drug (9 weeks versus 6 weeks).

Also, dentate gyrus dissection ought to be improved. Most of the hippocampus seems to respond poorly to Pt administration: we were unable to detect any significant effect in any of the genes we monitored in this region (except of course the DG). Given the contamination of our DG isolate with part of the neighboring hippocampus tissue we can hypothesize that we are underestimating variation in the DG.

The use of old animals moreover makes the work difficult. 18 month-old rats suffer from many deficits; two of four females (the untreated animals) had a clearly formed breast cancer that was discovered at the end of the experimental protocol, while the whole cohort of animals was suffering from a mild lack of appetite that made the administration of the jelly difficult. At a molecular level we noticed a consistent reduction in the yield of the RNA extraction and protein extraction from a given weight of wet tissue.

Concluding, data are encouraging. At a behavioral level Pt treatment was effective, as previously shown in a few papers.[31, 32] Molecular data, taken with the necessary caution, are also encouraging. Except for *bdnf* expression, in the other cases there was a trend of increased gene expression in the DG. Statistics can be improved by adding more animals to the experimental set and by sharpening the DG dissection.

Interestingly, a future aspect of this work will be to find an explanation for the restricted effects of Pt treatment in the DG. The gene for phosphodiesterase-1b displays an enriched expression in the DG.[165] Resveratrol inhibits PDE 1, 3 and 4.[103] Currently there isn't any evidence that Pt acts primarily by inhibiting PDE, but we have found (chapter 7) that its administration leads to an increase in the cAMP levels in cultured cells, and many papers report similarities between the activities of Pt and Resveratrol. This suggests that

the high expression of *pde-1b* and the restricted activity of Pt in the DG might be correlated.

References:

1. De Rosa, R.; Garcia, A. A.; Braschi, C.; Capsoni, S.; Maffei, L.; Berardi, N.; Cattaneo, A. Intranasal administration of nerve growth factor (NGF) rescues recognition memory deficits in AD11 anti-NGF transgenic mice. *Proceedings of the National Academy of Sciences of the United States of America* **2005,** *102*, (10), 3811-6.
2. Willis, L. M.; Shukitt-Hale, B.; Joseph, J. A. Recent advances in berry supplementation and age-related cognitive decline. *Current opinion in clinical nutrition and metabolic care* **2009,** *12*, (1), 91-4.
3. Cantuti-Castelvetri, I.; Shukitt-Hale, B.; Joseph, J. A. Neurobehavioral aspects of antioxidants in aging. *International journal of developmental neuroscience : the official journal of the International Society for Developmental Neuroscience* **2000,** *18*, (4-5), 367-81.
4. Galli, R. L.; Shukitt-Hale, B.; Youdim, K. A.; Joseph, J. A. Fruit polyphenolics and brain aging: nutritional interventions targeting age-related neuronal and behavioral deficits. *Annals of the New York Academy of Sciences* **2002,** *959*, 128-32.
5. Bastianetto, S.; Quirion, R. Natural antioxidants and neurodegenerative diseases. *Frontiers in bioscience : a journal and virtual library* **2004,** *9*, 3447-52.
6. Lau, F. C.; Shukitt-Hale, B.; Joseph, J. A. The beneficial effects of fruit polyphenols on brain aging. *Neurobiology of aging* **2005,** *26 Suppl 1*, 128-32.
7. Joseph, J. A.; Shukitt-Hale, B.; Casadesus, G. Reversing the deleterious effects of aging on neuronal communication and behavior: beneficial properties of fruit polyphenolic compounds. *The American journal of clinical nutrition* **2005,** *81*, (1 Suppl), 313s-316s.
8. Joseph, J. A.; Shukitt-Hale, B.; Willis, L. M. Grape juice, berries, and walnuts affect brain aging and behavior. *The Journal of nutrition* **2009,** *139*, (9), 1813s-7s.
9. Shukitt-Hale, B. Blueberries and neuronal aging. *Gerontology* **2012,** *58*, (6), 518-23.
10. Shukitt-Hale, B.; Lau, F. C.; Joseph, J. A. Berry fruit supplementation and the aging brain. *Journal of agricultural and food chemistry* **2008,** *56*, (3), 636-41.
11. Papandreou, M. A.; Dimakopoulou, A.; Linardaki, Z. I.; Cordopatis, P.; Klimis-Zacas, D.; Margarity, M.; Lamari, F. N. Effect of a polyphenol-rich wild blueberry extract on cognitive performance of mice, brain antioxidant markers and acetylcholinesterase activity. *Behavioural brain research* **2009,** *198*, (2), 352-8.
12. Miller, M. G.; Shukitt-Hale, B. Berry fruit enhances beneficial signaling in the brain. *Journal of agricultural and food chemistry* **2012,** *60*, (23), 5709-15.
13. Pribis, P.; Shukitt-Hale, B. Cognition: the new frontier for nuts and berries. *The American journal of clinical nutrition* **2014,** *100*, (Supplement 1), 347s-352s.
14. Subash, S.; Essa, M. M.; Al-Adawi, S.; Memon, M. A.; Manivasagam, T.; Akbar, M. Neuroprotective effects of berry fruits on neurodegenerative diseases. *Neural regeneration research* **2014,** *9*, (16), 1557-66.
15. Rendeiro, C.; Vauzour, D.; Kean, R. J.; Butler, L. T.; Rattray, M.; Spencer, J. P.; Williams, C. M. Blueberry supplementation induces spatial memory improvements and region-specific regulation of hippocampal BDNF mRNA expression in young rats. *Psychopharmacology* **2012,** *223*, (3), 319-30.
16. Smith, J. M.; Stouffer, E. M. Concord grape juice reverses the age-related impairment in latent learning in rats. *Nutritional neuroscience* **2014,** *17*, (2), 81-7.
17. Krikorian, R.; Boespflug, E. L.; Fleck, D. E.; Stein, A. L.; Wightman, J. D.; Shidler, M. D.; Sadat-Hossieny, S. Concord grape juice supplementation and neurocognitive function in human aging. *Journal of agricultural and food chemistry* **2012,** *60*, (23), 5736-42.

18. Krikorian, R.; Nash, T. A.; Shidler, M. D.; Shukitt-Hale, B.; Joseph, J. A. Concord grape juice supplementation improves memory function in older adults with mild cognitive impairment. *The British journal of nutrition* **2010,** *103*, (5), 730-4.
19. Krikorian, R.; Shidler, M. D.; Nash, T. A.; Kalt, W.; Vinqvist-Tymchuk, M. R.; Shukitt-Hale, B.; Joseph, J. A. Blueberry supplementation improves memory in older adults. *Journal of agricultural and food chemistry* **2010,** *58*, (7), 3996-4000.
20. Dal-Pan, A.; Pifferi, F.; Marchal, J.; Picq, J. L.; Aujard, F. Cognitive performances are selectively enhanced during chronic caloric restriction or resveratrol supplementation in a primate. *PloS one* **2011,** *6*, (1), e16581.
21. Liu, G. S.; Zhang, Z. S.; Yang, B.; He, W. Resveratrol attenuates oxidative damage and ameliorates cognitive impairment in the brain of senescence-accelerated mice. *Life sciences* **2012,** *91*, (17-18), 872-7.
22. Zhao, Y. N.; Li, W. F.; Li, F.; Zhang, Z.; Dai, Y. D.; Xu, A. L.; Qi, C.; Gao, J. M.; Gao, J. Resveratrol improves learning and memory in normally aged mice through microRNA-CREB pathway. *Biochemical and biophysical research communications* **2013,** *435*, (4), 597-602.
23. Yazir, Y.; Utkan, T.; Gacar, N.; Aricioglu, F. Resveratrol exerts anti-inflammatory and neuroprotective effects to prevent memory deficits in rats exposed to chronic unpredictable mild stress. *Physiology & behavior* **2015,** *138*, 297-304.
24. Porquet, D.; Casadesus, G.; Bayod, S.; Vicente, A.; Canudas, A. M.; Vilaplana, J.; Pelegri, C.; Sanfeliu, C.; Camins, A.; Pallas, M.; del Valle, J. Dietary resveratrol prevents Alzheimer's markers and increases life span in SAMP8. *Age (Dordrecht, Netherlands)* **2013,** *35*, (5), 1851-65.
25. Ma, X.; Sun, Z.; Liu, Y.; Jia, Y.; Zhang, B.; Zhang, J. Resveratrol improves cognition and reduces oxidative stress in rats with vascular dementia. *Neural regeneration research* **2013,** *8*, (22), 2050-9.
26. Witte, A. V.; Kerti, L.; Margulies, D. S.; Floel, A. Effects of resveratrol on memory performance, hippocampal functional connectivity, and glucose metabolism in healthy older adults. *The Journal of neuroscience : the official journal of the Society for Neuroscience* **2014,** *34*, (23), 7862-70.
27. Tiwari, V.; Chopra, K. Resveratrol abrogates alcohol-induced cognitive deficits by attenuating oxidative-nitrosative stress and inflammatory cascade in the adult rat brain. *Neurochemistry international* **2013,** *62*, (6), 861-9.
28. Koz, S. T.; Etem, E. O.; Baydas, G.; Yuce, H.; Ozercan, H. I.; Kuloglu, T.; Koz, S.; Etem, A.; Demir, N. Effects of resveratrol on blood homocysteine level, on homocysteine induced oxidative stress, apoptosis and cognitive dysfunctions in rats. *Brain research* **2012,** *1484*, 29-38.
29. Harada, N.; Zhao, J.; Kurihara, H.; Nakagata, N.; Okajima, K. Resveratrol improves cognitive function in mice by increasing production of insulin-like growth factor-I in the hippocampus. *The Journal of nutritional biochemistry* **2011,** *22*, (12), 1150-9.
30. Kennedy, D. O.; Wightman, E. L.; Reay, J. L.; Lietz, G.; Okello, E. J.; Wilde, A.; Haskell, C. F. Effects of resveratrol on cerebral blood flow variables and cognitive performance in humans: a double-blind, placebo-controlled, crossover investigation. *The American journal of clinical nutrition* **2010,** *91*, (6), 1590-7.
31. Chang, J.; Rimando, A.; Pallas, M.; Camins, A.; Porquet, D.; Reeves, J.; Shukitt-Hale, B.; Smith, M. A.; Joseph, J. A.; Casadesus, G. Low-dose pterostilbene, but not resveratrol, is a potent neuromodulator in aging and Alzheimer's disease. *Neurobiology of aging* **2012,** *33*, (9), 2062-71.
32. Joseph, J. A.; Fisher, D. R.; Cheng, V.; Rimando, A. M.; Shukitt-Hale, B. Cellular and behavioral effects of stilbene resveratrol analogues: implications for reducing the deleterious effects of aging. *Journal of agricultural and food chemistry* **2008,** *56*, (22), 10544-51.
33. Estrela, J. M.; Ortega, A.; Mena, S.; Rodriguez, M. L.; Asensi, M. Pterostilbene: Biomedical applications. *Critical reviews in clinical laboratory sciences* **2013,** *50*, (3), 65-78.
34. McCormack, D.; McFadden, D. A review of pterostilbene antioxidant activity and disease modification. *Oxidative medicine and cellular longevity* **2013,** *2013*, 575482.
35. Hou, Y.; Xie, G.; Miao, F.; Ding, L.; Mou, Y.; Wang, L.; Su, G.; Chen, G.; Yang, J.; Wu, C. Pterostilbene attenuates lipopolysaccharide-induced learning and memory impairment possibly

via inhibiting microglia activation and protecting neuronal injury in mice. *Progress in neuro-psychopharmacology & biological psychiatry* **2014,** *54*, 92-102.
36. Al Rahim, M.; Rimando, A. M.; Silistreli, K.; El-Alfy, A. T. Anxiolytic action of pterostilbene: involvement of hippocampal ERK phosphorylation. *Planta medica* **2013,** *79*, (9), 723-30.
37. Spencer, J. P. The impact of fruit flavonoids on memory and cognition. *The British journal of nutrition* **2010,** *104 Suppl 3*, S40-7.
38. Spencer, J. P. Beyond antioxidants: the cellular and molecular interactions of flavonoids and how these underpin their actions on the brain. *The Proceedings of the Nutrition Society* **2010,** *69*, (2), 244-60.
39. Spencer, J. P. The impact of flavonoids on memory: physiological and molecular considerations. *Chemical Society reviews* **2009,** *38*, (4), 1152-61.
40. Spencer, J. P.; Vauzour, D.; Rendeiro, C. Flavonoids and cognition: the molecular mechanisms underlying their behavioural effects. *Archives of biochemistry and biophysics* **2009,** *492*, (1-2), 1-9.
41. Williams, R. J.; Spencer, J. P. Flavonoids, cognition, and dementia: actions, mechanisms, and potential therapeutic utility for Alzheimer disease. *Free radical biology & medicine* **2012,** *52*, (1), 35-45.
42. Rendeiro, C.; Foley, A.; Lau, V. C.; Ring, R.; Rodriguez-Mateos, A.; Vauzour, D.; Williams, C. M.; Regan, C.; Spencer, J. P. A role for hippocampal PSA-NCAM and NMDA-NR2B receptor function in flavonoid-induced spatial memory improvements in young rats. *Neuropharmacology* **2014,** *79*, 335-44.
43. Rendeiro, C.; Guerreiro, J. D.; Williams, C. M.; Spencer, J. P. Flavonoids as modulators of memory and learning: molecular interactions resulting in behavioural effects. *The Proceedings of the Nutrition Society* **2012,** *71*, (2), 246-62.
44. Rendeiro, C.; Spencer, J. P.; Vauzour, D.; Butler, L. T.; Ellis, J. A.; Williams, C. M. The impact of flavonoids on spatial memory in rodents: from behaviour to underlying hippocampal mechanisms. *Genes & nutrition* **2009,** *4*, (4), 251-70.
45. Rendeiro, C.; Vauzour, D.; Rattray, M.; Waffo-Teguo, P.; Merillon, J. M.; Butler, L. T.; Williams, C. M.; Spencer, J. P. Dietary levels of pure flavonoids improve spatial memory performance and increase hippocampal brain-derived neurotrophic factor. *PloS one* **2013,** *8*, (5), e63535.
46. Spilsbury, A.; Vauzour, D.; Spencer, J. P.; Rattray, M. Regulation of NF-kappaB activity in astrocytes: effects of flavonoids at dietary-relevant concentrations. *Biochemical and biophysical research communications* **2012,** *418*, (3), 578-83.
47. Murphy, T.; Dias, G. P.; Thuret, S. Effects of diet on brain plasticity in animal and human studies: mind the gap. *Neural plasticity* **2014,** *2014*, 563160.
48. Williams, C. M.; El Mohsen, M. A.; Vauzour, D.; Rendeiro, C.; Butler, L. T.; Ellis, J. A.; Whiteman, M.; Spencer, J. P. Blueberry-induced changes in spatial working memory correlate with changes in hippocampal CREB phosphorylation and brain-derived neurotrophic factor (BDNF) levels. *Free radical biology & medicine* **2008,** *45*, (3), 295-305.
49. Vauzour, D. Effect of flavonoids on learning, memory and neurocognitive performance: relevance and potential implications for Alzheimer's disease pathophysiology. *Journal of the science of food and agriculture* **2014,** *94*, (6), 1042-56.
50. Kulkarni, S. S.; Canto, C. The molecular targets of resveratrol. *Biochimica et biophysica acta* **2014**.
51. Thundyil, J.; Lim, K. L. DAMPs and Neurodegeneration. *Ageing research reviews* **2014**.
52. Vivekanantham, S.; Shah, S.; Dewji, R.; Dewji, A.; Khatri, C.; Ologunde, R. Neuroinflammation in Parkinson's disease: role in neurodegeneration and tissue repair. *The International journal of neuroscience* **2014**, 1-17.
53. Miller, A. A.; Spencer, S. J. Obesity and neuroinflammation: A pathway to cognitive impairment. *Brain, behavior, and immunity* **2014,** *42*, 10-21.
54. Toth, P.; Tarantini, S.; Tucsek, Z.; Ashpole, N. M.; Sosnowska, D.; Gautam, T.; Ballabh, P.; Koller, A.; Sonntag, W. E.; Csiszar, A.; Ungvari, Z. Resveratrol treatment rescues neurovascular

coupling in aged mice: role of improved cerebromicrovascular endothelial function and downregulation of NADPH oxidase. *American journal of physiology. Heart and circulatory physiology* **2014,** *306*, (3), H299-308.
55. Zarzuelo, M. J.; Lopez-Sepulveda, R.; Sanchez, M.; Romero, M.; Gomez-Guzman, M.; Ungvary, Z.; Perez-Vizcaino, F.; Jimenez, R.; Duarte, J. SIRT1 inhibits NADPH oxidase activation and protects endothelial function in the rat aorta: implications for vascular aging. *Biochemical pharmacology* **2013,** *85*, (9), 1288-96.
56. Chen, F.; Qian, L. H.; Deng, B.; Liu, Z. M.; Zhao, Y.; Le, Y. Y. Resveratrol protects vascular endothelial cells from high glucose-induced apoptosis through inhibition of NADPH oxidase activation-driven oxidative stress. *CNS neuroscience & therapeutics* **2013,** *19*, (9), 675-81.
57. Robb, E. L.; Stuart, J. A. The stilbenes resveratrol, pterostilbene and piceid affect growth and stress resistance in mammalian cells via a mechanism requiring estrogen receptor beta and the induction of Mn-superoxide dismutase. *Phytochemistry* **2014,** *98*, 164-73.
58. Robb, E. L.; Stuart, J. A. Multiple phytoestrogens inhibit cell growth and confer cytoprotection by inducing manganese superoxide dismutase expression. *Phytotherapy research : PTR* **2014,** *28*, (1), 120-31.
59. Li, H.; Horke, S.; Forstermann, U. Oxidative stress in vascular disease and its pharmacological prevention. *Trends in pharmacological sciences* **2013,** *34*, (6), 313-9.
60. Cardozo, L. F.; Pedruzzi, L. M.; Stenvinkel, P.; Stockler-Pinto, M. B.; Daleprane, J. B.; Leite, M., Jr.; Mafra, D. Nutritional strategies to modulate inflammation and oxidative stress pathways via activation of the master antioxidant switch Nrf2. *Biochimie* **2013,** *95*, (8), 1525-33.
61. Bhakkiyalakshmi, E.; Sireesh, D.; Rajaguru, P.; Paulmurugan, R.; Ramkumar, K. M. The emerging role of redox-sensitive Nrf2-Keap1 pathway in diabetes. *Pharmacological research : the official journal of the Italian Pharmacological Society* **2014**.
62. Kansanen, E.; Kuosmanen, S. M.; Leinonen, H.; Levonen, A. L. The Keap1-Nrf2 pathway: Mechanisms of activation and dysregulation in cancer. *Redox biology* **2013,** *1*, (1), 45-9.
63. Bryan, H. K.; Olayanju, A.; Goldring, C. E.; Park, B. K. The Nrf2 cell defence pathway: Keap1-dependent and -independent mechanisms of regulation. *Biochemical pharmacology* **2013,** *85*, (6), 705-17.
64. Keum, Y. S.; Choi, B. Y. Molecular and chemical regulation of the Keap1-Nrf2 signaling pathway. *Molecules (Basel, Switzerland)* **2014,** *19*, (7), 10074-89.
65. Das, S.; Das, D. K. Anti-inflammatory responses of resveratrol. *Inflammation & allergy drug targets* **2007,** *6*, (3), 168-73.
66. Kumar, A.; Negi, G.; Sharma, S. S. Neuroprotection by resveratrol in diabetic neuropathy: concepts & mechanisms. *Current medicinal chemistry* **2013,** *20*, (36), 4640-5.
67. Kumar, A.; Sharma, S. S. NF-kappaB inhibitory action of resveratrol: a probable mechanism of neuroprotection in experimental diabetic neuropathy. *Biochemical and biophysical research communications* **2010,** *394*, (2), 360-5.
68. Kundu, J. K.; Shin, Y. K.; Kim, S. H.; Surh, Y. J. Resveratrol inhibits phorbol ester-induced expression of COX-2 and activation of NF-kappaB in mouse skin by blocking IkappaB kinase activity. *Carcinogenesis* **2006,** *27*, (7), 1465-74.
69. Kundu, J. K.; Shin, Y. K.; Surh, Y. J. Resveratrol modulates phorbol ester-induced pro-inflammatory signal transduction pathways in mouse skin in vivo: NF-kappaB and AP-1 as prime targets. *Biochemical pharmacology* **2006,** *72*, (11), 1506-15.
70. Capiralla, H.; Vingtdeux, V.; Zhao, H.; Sankowski, R.; Al-Abed, Y.; Davies, P.; Marambaud, P. Resveratrol mitigates lipopolysaccharide- and Abeta-mediated microglial inflammation by inhibiting the TLR4/NF-kappaB/STAT signaling cascade. *Journal of neurochemistry* **2012,** *120*, (3), 461-72.
71. Xia, N.; Strand, S.; Schlufter, F.; Siuda, D.; Reifenberg, G.; Kleinert, H.; Forstermann, U.; Li, H. Role of SIRT1 and FOXO factors in eNOS transcriptional activation by resveratrol. *Nitric oxide : biology and chemistry / official journal of the Nitric Oxide Society* **2013,** *32*, 29-35.
72. Busch, F.; Mobasheri, A.; Shayan, P.; Lueders, C.; Stahlmann, R.; Shakibaei, M. Resveratrol modulates interleukin-1beta-induced phosphatidylinositol 3-kinase and nuclear factor kappaB

signaling pathways in human tenocytes. *The Journal of biological chemistry* **2012,** *287*, (45), 38050-63.
73. Del Prete, A.; Allavena, P.; Santoro, G.; Fumarulo, R.; Corsi, M. M.; Mantovani, A. Molecular pathways in cancer-related inflammation. *Biochemia medica* **2011,** *21*, (3), 264-75.
74. Lukiw, W. J. NF-kappaB-regulated, proinflammatory miRNAs in Alzheimer's disease. *Alzheimer's research & therapy* **2012,** *4*, (6), 47.
75. Tobon-Velasco, J. C.; Cuevas, E.; Torres-Ramos, M. A. Receptor for AGEs (RAGE) as Mediator of NF-kB Pathway Activation in Neuroinflammation and Oxidative Stress. *CNS & neurological disorders drug targets* **2014,** *13*, (9), 1615-26.
76. Ogura, H.; Arima, Y.; Kamimura, D.; Murakami, M. The gateway theory: how regional neural activation creates a gateway for immune cells via an inflammation amplifier. *Biomedical journal* **2013,** *36*, (6), 269-73.
77. Mc Guire, C.; Prinz, M.; Beyaert, R.; van Loo, G. Nuclear factor kappa B (NF-kappaB) in multiple sclerosis pathology. *Trends in molecular medicine* **2013,** *19*, (10), 604-13.
78. Murakami, M.; Harada, M.; Kamimura, D.; Ogura, H.; Okuyama, Y.; Kumai, N.; Okuyama, A.; Singh, R.; Jiang, J. J.; Atsumi, T.; Shiraya, S.; Nakatsuji, Y.; Kinoshita, M.; Kohsaka, H.; Nishida, M.; Sakoda, S.; Miyasaka, N.; Yamauchi-Takihara, K.; Hirano, T. Disease-association analysis of an inflammation-related feedback loop. *Cell reports* **2013,** *3*, (3), 946-59.
79. Wong, R. H.; Coates, A. M.; Buckley, J. D.; Howe, P. R. Evidence for circulatory benefits of resveratrol in humans. *Annals of the New York Academy of Sciences* **2013,** *1290*, 52-8.
80. Xia, N.; Forstermann, U.; Li, H. Resveratrol as a gene regulator in the vasculature. *Current pharmaceutical biotechnology* **2014,** *15*, (4), 401-8.
81. Dolinsky, V. W.; Dyck, J. R. Experimental studies of the molecular pathways regulated by exercise and resveratrol in heart, skeletal muscle and the vasculature. *Molecules (Basel, Switzerland)* **2014,** *19*, (9), 14919-47.
82. Wightman, E. L.; Reay, J. L.; Haskell, C. F.; Williamson, G.; Dew, T. P.; Kennedy, D. O. Effects of resveratrol alone or in combination with piperine on cerebral blood flow parameters and cognitive performance in human subjects: a randomised, double-blind, placebo-controlled, cross-over investigation. *The British journal of nutrition* **2014,** *112*, (2), 203-13.
83. Schramm, A.; Matusik, P.; Osmenda, G.; Guzik, T. J. Targeting NADPH oxidases in vascular pharmacology. *Vascular pharmacology* **2012,** *56*, (5-6), 216-31.
84. Kim, H. A.; Miller, A. A.; Drummond, G. R.; Thrift, A. G.; Arumugam, T. V.; Phan, T. G.; Srikanth, V. K.; Sobey, C. G. Vascular cognitive impairment and Alzheimer's disease: role of cerebral hypoperfusion and oxidative stress. *Naunyn-Schmiedeberg's archives of pharmacology* **2012,** *385*, (10), 953-9.
85. Hamel, E. The Cerebral Circulation: Function and Dysfunction in Alzheimer's disease. *Journal of cardiovascular pharmacology* **2014**.
86. Villarreal, A. E.; Barron, R.; Rao, K. S.; Britton, G. B. The effects of impaired cerebral circulation on Alzheimer's disease pathology: evidence from animal studies. *Journal of Alzheimer's disease : JAD* **2014,** *42*, (3), 707-22.
87. Dunn, K. M.; Nelson, M. T. Neurovascular signaling in the brain and the pathological consequences of hypertension. *American journal of physiology. Heart and circulatory physiology* **2014,** *306*, (1), H1-14.
88. Iadecola, C. The pathobiology of vascular dementia. *Neuron* **2013,** *80*, (4), 844-66.
89. McCormack, D.; McFadden, D. Pterostilbene and cancer: current review. *The Journal of surgical research* **2012,** *173*, (2), e53-61.
90. Azzolini, M.; La Spina, M.; Mattarei, A.; Paradisi, C.; Zoratti, M.; Biasutto, L. Pharmacokinetics and tissue distribution of pterostilbene in the rat. *Molecular nutrition & food research* **2014,** *58*, (11), 2122-32.
91. Kandel, E. R. The molecular biology of memory: cAMP, PKA, CRE, CREB-1, CREB-2, and CPEB. *Molecular brain* **2012,** *5*, 14.
92. Kandel, E. R.; Dudai, Y.; Mayford, M. R. The molecular and systems biology of memory. *Cell* **2014,** *157*, (1), 163-86.

93. Schwartz, J. H.; Castellucci, V. F.; Kandel, E. R. Functioning of identified neurons and synapses in abdominal ganglion of Aplysia in absence of protein synthesis. *Journal of neurophysiology* **1971,** *34*, (6), 939-53.
94. Cedar, H.; Kandel, E. R.; Schwartz, J. H. Cyclic adenosine monophosphate in the nervous system of Aplysia californica. I. Increased synthesis in response to synaptic stimulation. *The Journal of general physiology* **1972,** *60*, (5), 558-69.
95. Schacher, S.; Castellucci, V. F.; Kandel, E. R. cAMP evokes long-term facilitation in Aplysia sensory neurons that requires new protein synthesis. *Science (New York, N.Y.)* **1988,** *240*, (4859), 1667-9.
96. Schacher, S.; Kandel, E. R.; Montarolo, P. cAMP and arachidonic acid simulate long-term structural and functional changes produced by neurotransmitters in Aplysia sensory neurons. *Neuron* **1993,** *10*, (6), 1079-88.
97. Martin, K. C.; Michael, D.; Rose, J. C.; Barad, M.; Casadio, A.; Zhu, H.; Kandel, E. R. MAP kinase translocates into the nucleus of the presynaptic cell and is required for long-term facilitation in Aplysia. *Neuron* **1997,** *18*, (6), 899-912.
98. Bailey, C. H.; Kaang, B. K.; Chen, M.; Martin, K. C.; Lim, C. S.; Casadio, A.; Kandel, E. R. Mutation in the phosphorylation sites of MAP kinase blocks learning-related internalization of apCAM in Aplysia sensory neurons. *Neuron* **1997,** *18*, (6), 913-24.
99. Bailey, C. H.; Kandel, E. R. Structural changes accompanying memory storage. *Annual review of physiology* **1993,** *55*, 397-426.
100. Hansen, R. T., 3rd; Zhang, H. T. Senescent-induced dysregulation of cAMP/CREB signaling and correlations with cognitive decline. *Brain research* **2013,** *1516*, 93-109.
101. Barad, M.; Bourtchouladze, R.; Winder, D. G.; Golan, H.; Kandel, E. Rolipram, a type IV-specific phosphodiesterase inhibitor, facilitates the establishment of long-lasting long-term potentiation and improves memory. *Proceedings of the National Academy of Sciences of the United States of America* **1998,** *95*, (25), 15020-5.
102. Roesler, R.; Reolon, G. K.; Maurmann, N.; Schwartsmann, G.; Schroder, N.; Amaral, O. B.; Valvassori, S.; Quevedo, J. A phosphodiesterase 4-controlled switch between memory extinction and strengthening in the hippocampus. *Frontiers in behavioral neuroscience* **2014,** *8*, 91.
103. Park, S. J.; Ahmad, F.; Philp, A.; Baar, K.; Williams, T.; Luo, H.; Ke, H.; Rehmann, H.; Taussig, R.; Brown, A. L.; Kim, M. K.; Beaven, M. A.; Burgin, A. B.; Manganiello, V.; Chung, J. H. Resveratrol ameliorates aging-related metabolic phenotypes by inhibiting cAMP phosphodiesterases. *Cell* **2012,** *148*, (3), 421-33.
104. Rudenko, A.; Tsai, L. H. Epigenetic modifications in the nervous system and their impact upon cognitive impairments. *Neuropharmacology* **2014,** *80*, 70-82.
105. Rudenko, A.; Tsai, L. H. Epigenetic regulation in memory and cognitive disorders. *Neuroscience* **2014,** *264*, 51-63.
106. Saab, B. J.; Mansuy, I. M. Neuroepigenetics of memory formation and impairment: the role of microRNAs. *Neuropharmacology* **2014,** *80*, 61-9.
107. Staszewski, O.; Prinz, M. Glial epigenetics in neuroinflammation and neurodegeneration. *Cell and tissue research* **2014,** *356*, (3), 609-16.
108. Fischer, A. Targeting histone-modifications in Alzheimer's disease. What is the evidence that this is a promising therapeutic avenue? *Neuropharmacology* **2014,** *80*, 95-102.
109. Landry, C. D.; Kandel, E. R.; Rajasethupathy, P. New mechanisms in memory storage: piRNAs and epigenetics. *Trends in neurosciences* **2013,** *36*, (9), 535-42.
110. Day, J. J.; Sweatt, J. D. Epigenetic mechanisms in cognition. *Neuron* **2011,** *70*, (5), 813-29.
111. Nelson, E. D.; Monteggia, L. M. Epigenetics in the mature mammalian brain: effects on behavior and synaptic transmission. *Neurobiology of learning and memory* **2011,** *96*, (1), 53-60.
112. Lubin, F. D. Epigenetic gene regulation in the adult mammalian brain: multiple roles in memory formation. *Neurobiology of learning and memory* **2011,** *96*, (1), 68-78.
113. Puckett, R. E.; Lubin, F. D. Epigenetic mechanisms in experience-driven memory formation and behavior. *Epigenomics* **2011,** *3*, (5), 649-64.

114. Graff, J.; Tsai, L. H. Histone acetylation: molecular mnemonics on the chromatin. *Nature reviews. Neuroscience* **2013,** *14*, (2), 97-111.
115. Peixoto, L.; Abel, T. The role of histone acetylation in memory formation and cognitive impairments. *Neuropsychopharmacology : official publication of the American College of Neuropsychopharmacology* **2013,** *38*, (1), 62-76.
116. Lopez-Atalaya, J. P.; Barco, A. Can changes in histone acetylation contribute to memory formation? *Trends in genetics : TIG* **2014,** *30*, (12), 529-539.
117. Pavlopoulos, E.; Jones, S.; Kosmidis, S.; Close, M.; Kim, C.; Kovalerchik, O.; Small, S. A.; Kandel, E. R. Molecular mechanism for age-related memory loss: the histone-binding protein RbAp48. *Science translational medicine* **2013,** *5*, (200), 200ra115.
118. Basta, J.; Rauchman, M. The nucleosome remodeling and deacetylase complex in development and disease. *Translational research : the journal of laboratory and clinical medicine* **2015,** *165*, (1), 36-47.
119. Lai, A. Y.; Wade, P. A. Cancer biology and NuRD: a multifaceted chromatin remodelling complex. *Nature reviews. Cancer* **2011,** *11*, (8), 588-96.
120. Laugesen, A.; Helin, K. Chromatin repressive complexes in stem cells, development, and cancer. *Cell stem cell* **2014,** *14*, (6), 735-51.
121. Allen, H. F.; Wade, P. A.; Kutateladze, T. G. The NuRD architecture. *Cellular and molecular life sciences : CMLS* **2013,** *70*, (19), 3513-24.
122. Li, D. Q.; Pakala, S. B.; Nair, S. S.; Eswaran, J.; Kumar, R. Metastasis-associated protein 1/nucleosome remodeling and histone deacetylase complex in cancer. *Cancer research* **2012,** *72*, (2), 387-94.
123. Harrison, I. F.; Dexter, D. T. Epigenetic targeting of histone deacetylase: therapeutic potential in Parkinson's disease? *Pharmacology & therapeutics* **2013,** *140*, (1), 34-52.
124. Zhang, Q.; Vo, N.; Goodman, R. H. Histone binding protein RbAp48 interacts with a complex of CREB binding protein and phosphorylated CREB. *Molecular and cellular biology* **2000,** *20*, (14), 4970-8.
125. Settembre, C.; Ballabio, A. Lysosome: regulator of lipid degradation pathways. *Trends in cell biology* **2014,** *24*, (12), 743-750.
126. Settembre, C.; De Cegli, R.; Mansueto, G.; Saha, P. K.; Vetrini, F.; Visvikis, O.; Huynh, T.; Carissimo, A.; Palmer, D.; Klisch, T. J.; Wollenberg, A. C.; Di Bernardo, D.; Chan, L.; Irazoqui, J. E.; Ballabio, A. TFEB controls cellular lipid metabolism through a starvation-induced autoregulatory loop. *Nature cell biology* **2013,** *15*, (6), 647-58.
127. Settembre, C.; Di Malta, C.; Polito, V. A.; Garcia Arencibia, M.; Vetrini, F.; Erdin, S.; Erdin, S. U.; Huynh, T.; Medina, D.; Colella, P.; Sardiello, M.; Rubinsztein, D. C.; Ballabio, A. TFEB links autophagy to lysosomal biogenesis. *Science (New York, N.Y.)* **2011,** *332*, (6036), 1429-33.
128. Settembre, C.; Fraldi, A.; Medina, D. L.; Ballabio, A. Signals from the lysosome: a control centre for cellular clearance and energy metabolism. *Nature reviews. Molecular cell biology* **2013,** *14*, (5), 283-96.
129. Settembre, C.; Zoncu, R.; Medina, D. L.; Vetrini, F.; Erdin, S.; Erdin, S.; Huynh, T.; Ferron, M.; Karsenty, G.; Vellard, M. C.; Facchinetti, V.; Sabatini, D. M.; Ballabio, A. A lysosome-to-nucleus signalling mechanism senses and regulates the lysosome via mTOR and TFEB. *The EMBO journal* **2012,** *31*, (5), 1095-108.
130. Lauri, A.; Pompilio, G.; Capogrossi, M. C. The mitochondrial genome in aging and senescence. *Ageing research reviews* **2014,** *18c*, 1-15.
131. Leak, R. K. Heat shock proteins in neurodegenerative disorders and aging. *Journal of cell communication and signaling* **2014,** *8*, (4), 293-310.
132. Negrini, S.; Prada, I.; D'Alessandro, R.; Meldolesi, J. REST: an oncogene or a tumor suppressor? *Trends in cell biology* **2013,** *23*, (6), 289-95.
133. Bithell, A. REST: transcriptional and epigenetic regulator. *Epigenomics* **2011,** *3*, (1), 47-58.
134. Kessels, H. W.; Malinow, R. Synaptic AMPA receptor plasticity and behavior. *Neuron* **2009,** *61*, (3), 340-50.

135. Adachi, N.; Numakawa, T.; Richards, M.; Nakajima, S.; Kunugi, H. New insight in expression, transport, and secretion of brain-derived neurotrophic factor: Implications in brain-related diseases. *World journal of biological chemistry* **2014,** *5*, (4), 409-28.
136. Leal, G.; Afonso, P. M.; Salazar, I. L.; Duarte, C. B. Regulation of hippocampal synaptic plasticity by BDNF. *Brain research* **2014**.
137. Song, J. H.; Yu, J. T.; Tan, L. Brain-Derived Neurotrophic Factor in Alzheimer's Disease: Risk, Mechanisms, and Therapy. *Molecular neurobiology* **2014**.
138. Liu, D. Y.; Shen, X. M.; Yuan, F. F.; Guo, O. Y.; Zhong, Y.; Chen, J. G.; Zhu, L. Q.; Wu, J. The Physiology of BDNF and Its Relationship with ADHD. *Molecular neurobiology* **2014**.
139. Savioz, A.; Leuba, G.; Vallet, P. G. A framework to understand the variations of PSD-95 expression in brain aging and in Alzheimer's disease. *Ageing research reviews* **2014,** *18c*, 86-94.
140. Kim, E.; Sheng, M. PDZ domain proteins of synapses. *Nature reviews. Neuroscience* **2004,** *5*, (10), 771-81.
141. Zhang, L. Voluntary oral administration of drugs in mice. **2011**.
142. Dominguez, G.; Dagnas, M.; Decorte, L.; Vandesquille, M.; Belzung, C.; Beracochea, D.; Mons, N. Rescuing prefrontal cAMP-CREB pathway reverses working memory deficits during withdrawal from prolonged alcohol exposure. *Brain structure & function* **2014**.
143. Silingardi, D.; Angelucci, A.; De Pasquale, R.; Borsotti, M.; Squitieri, G.; Brambilla, R.; Putignano, E.; Pizzorusso, T.; Berardi, N. ERK pathway activation bidirectionally affects visual recognition memory and synaptic plasticity in the perirhinal cortex. *Frontiers in behavioral neuroscience* **2011,** *5*, 84.
144. Ennaceur, A.; Delacour, J. A new one-trial test for neurobiological studies of memory in rats. 1: Behavioral data. *Behavioural Brain Research* **1988,** *31*, (1), 47-59.
145. Walder, R. Y.; Wattiez, A. S.; White, S. R.; Marquez de Prado, B.; Hamity, M. V.; Hammond, D. L. Validation of four reference genes for quantitative mRNA expression studies in a rat model of inflammatory injury. *Molecular pain* **2014,** *10*, 55.
146. Hasan, M. R.; Kim, J. H.; Kim, Y. J.; Kwon, K. J.; Shin, C. Y.; Kim, H. Y.; Han, S. H.; Choi, D. H.; Lee, J. Effect of HDAC inhibitors on neuroprotection and neurite outgrowth in primary rat cortical neurons following ischemic insult. *Neurochemical research* **2013,** *38*, (9), 1921-34.
147. Mirzaei, H.; Suarez, J. A.; Longo, V. D. Protein and amino acid restriction, aging and disease: from yeast to humans. *Trends in endocrinology and metabolism: TEM* **2014,** *25*, (11), 558-566.
148. Rizza, W.; Veronese, N.; Fontana, L. What are the roles of calorie restriction and diet quality in promoting healthy longevity? *Ageing research reviews* **2014,** *13*, 38-45.
149. Duan, W. Sirtuins: from metabolic regulation to brain aging. *Frontiers in aging neuroscience* **2013,** *5*, 36.
150. Marosi, K.; Mattson, M. P. BDNF mediates adaptive brain and body responses to energetic challenges. *Trends in endocrinology and metabolism: TEM* **2014,** *25*, (2), 89-98.
151. Stranahan, A. M.; Mattson, M. P. Metabolic reserve as a determinant of cognitive aging. *Journal of Alzheimer's disease : JAD* **2012,** *30 Suppl 2*, S5-13.
152. Gkikas, I.; Petratou, D.; Tavernarakis, N. Longevity pathways and memory aging. *Frontiers in genetics* **2014,** *5*, 155.
153. Warburton, E. C.; Brown, M. W. Neural circuitry for rat recognition memory. *Behavioural brain research* **2014**.
154. Balderas, I.; Rodriguez-Ortiz, C. J.; Bermudez-Rattoni, F. Retrieval and reconsolidation of object recognition memory are independent processes in the perirhinal cortex. *Neuroscience* **2013,** *253*, 398-405.
155. Balderas, I.; Rodriguez-Ortiz, C. J.; Bermudez-Rattoni, F. Consolidation and reconsolidation of object recognition memory. *Behavioural brain research* **2014**.
156. Barco, A.; Bailey, C. H.; Kandel, E. R. Common molecular mechanisms in explicit and implicit memory. *Journal of neurochemistry* **2006,** *97*, (6), 1520-33.

157. Barker, G. R.; Warburton, E. C. When is the hippocampus involved in recognition memory? *The Journal of neuroscience : the official journal of the Society for Neuroscience* **2011,** *31*, (29), 10721-31.
158. Preston, A. R.; Eichenbaum, H. Interplay of hippocampus and prefrontal cortex in memory. *Current biology : CB* **2013,** *23*, (17), R764-73.
159. Frick, K. M. Epigenetics, oestradiol and hippocampal memory consolidation. *Journal of neuroendocrinology* **2013,** *25*, (11), 1151-62.
160. Thomas, S. A. Neuromodulatory Signaling in Hippocampus-dependent Memory Retrieval. *Hippocampus* **2014**.
161. Shoji, H.; Hagihara, H.; Takao, K.; Hattori, S.; Miyakawa, T. T-maze forced alternation and left-right discrimination tasks for assessing working and reference memory in mice. *Journal of visualized experiments : JoVE* **2012**, (60).
162. Ohira, K.; Kobayashi, K.; Toyama, K.; Nakamura, H. K.; Shoji, H.; Takao, K.; Takeuchi, R.; Yamaguchi, S.; Kataoka, M.; Otsuka, S.; Takahashi, M.; Miyakawa, T. Synaptosomal-associated protein 25 mutation induces immaturity of the dentate granule cells of adult mice. *Molecular brain* **2013,** *6*, 12.
163. Hagihara, H.; Toyama, K.; Yamasaki, N.; Miyakawa, T. Dissection of hippocampal dentate gyrus from adult mouse. *Journal of visualized experiments : JoVE* **2009**, (33).
164. Sardiello, M.; Palmieri, M.; di Ronza, A.; Medina, D. L.; Valenza, M.; Gennarino, V. A.; Di Malta, C.; Donaudy, F.; Embrione, V.; Polishchuk, R. S.; Banfi, S.; Parenti, G.; Cattaneo, E.; Ballabio, A. A gene network regulating lysosomal biogenesis and function. *Science (New York, N.Y.)* **2009,** *325*, (5939), 473-7.
165. Lein, E. S.; Zhao, X.; Gage, F. H. Defining a Molecular Atlas of the Hippocampus Using DNA Microarrays and High-Throughput In Situ Hybridization. *The Journal of Neuroscience* **2004,** *24*, (15), 3879-3889.

9. Improving the efficacy of plant polyphenols

Anti-Cancer Agents in Medicinal Chemistry, 2014, *14*, 000-000

Improving the Efficacy of Plant Polyphenols

Lucia Biasutto[1,2,*], Andrea Mattarei[1,3], Nicola Sassi[1,2], Michele Azzolini[2], Matteo Romio[3], Cristina Paradisi[3] and Mario Zoratti[1,2]

[1]*CNR Neuroscience Institute, Viale G. Colombo 3, 35121 Padova, Italy;* [2]*Dept. Biomedical Sciences, University of Padova, Viale G. Colombo 3, 35121 Padova, Italy;* [3]*Dept. Chemical Sciences, University of Padova, Via F. Marzolo 1, 35131 Padova, Italy*

Abstract: Plant polyphenols exhibit potentially useful effects in a wide variety of pathophysiological settings. They interact with proteins such as signalling kinases, transcription factors and ion channels, and modulate redox processes, such as those taking place in mitochondria. Biomedical applications of these natural compounds are however severely hindered by their low bioavailability, rapid metabolism, and often by unfavourable physico-chemical properties, e.g. a generally low water solubility. Derivatives are under development with the aim of improving their bioavailability and/or bioefficacy. Various strategies can be adopted. An increase in circulating blood levels of non-metabolized natural compound may be attainable through prodrugs. In the ideal prodrug, phenolic hydroxyls are protected by capping groups which a) help or at least do not hinder permeation of epithelia; b) prevent conjugative modifications during absorption and first-pass through the liver; c) are eliminated with opportune kinetics to regenerate the parent compound. Moreover, prodrugs may be designed with the goals of modulating physical properties of the parent compound, and/or changing its distribution in the body. A more specific action may be achieved by concentrating the compounds at specific sites of action. An example of the second approach is represented by mitochondria-targeted redox-active polyphenol derivatives, designed to intervene on radical processes in these organelles and as a tool either to protect cells from oxidative insults or to precipitate their death. Mitochondrial targeting can be achieved through conjugation with a triphenylphosphonium lipophilic cation. Quercetin and resveratrol were chosen as model polyphenols for these proof-of-concept studies. Data available at the moment show that both quercetin and resveratrol mitochondria-targeted derivatives are pro-oxidant and cytotoxic *in vitro*, selectively killing fast-growing and tumoural cells when supplied in the low μM range; the mechanism of ROS generation appears to differ between the two classes of compounds.

These approaches are emerging as promising strategies to obtain new efficient chemopreventive and/or chemotherapeutic drugs based on polyphenols derivatives.

Keywords: Bioavailability, catechins, mitochondria, polyphenols, prodrugs, quercetin, resveratrol, triphenylphosphonium.

1. BACKGROUND

An exponentially growing literature documents the potential benefits of plant polyphenols for health care. To mention just a few aspects: the three intensively studied sub-families of polyphenols we consider, namely green tea catechins [1-4], flavones [5-8] and stilbene derivatives [9-12] (Fig. **1**), can have a positive impact on neurodegenerative processes (neuroprotection) and cognitive functions. The same holds for the prevention and synergic therapy of cancer (e.g., catechins: [13-16]; flavones: [17-19]; stilbenoids: [20-23]). Epigenetic modulation is now considered to be a major mechanism accounting for the effects of these phytochemicals [24-28], along with a variety of other actions including, classically, the modulation of the redox status of cells (e.g. [29,30]) and interaction with several proteins (epigallocatechin gallate (EGCG): [31-33]; quercetin: [34-37]; resveratrol: [38,39]).

This multi-targeted mode of action has an obvious advantage in cancer therapy. In fact, tumours are characterized by a marked heterogeneity: gene expression levels, mutations and deregulated signalling pathways can differ considerably among patients affected by the same tumour type [40,41], among different regions of the tumour mass, and between primary tumour and metastasis [42-44]. Because of this heterogeneity, single-target anti-cancer therapies often fail and/or are less effective than expected. To overcome this problem and achieve an effective anticancer therapy, different approaches must be adopted. Personalized therapy [44,45], as well as multi-targeted drugs [46,47] or therapies acting on invariable targets have been proposed. These last two approaches constitute potential fields of application for the two classes of polyphenol derivatives described in this review: prodrugs and mitochondria-targeted (mitochondriotropic) compounds, respectively.

The exploitation of the favourable properties of plant polyphenols is made difficult by the generally low bioavailability of these compounds when assumed orally. Their absorption is in general expected to be low according to "Lipinki's rules" [48] due to their polarity and the presence of multiple hydrogen bond donors. Since they contain, by definition, hydroxyl groups, they are rapidly converted by sulfo-, glucuronosyl- and methyl-transferases into phase II conjugates which are rapidly eliminated (catechins: [49,50]; flavones: [51,52]; stilbenoids: [53-55]). Metabolic transformation by the intestinal flora can also be important. Thus, e.g., resveratrol can be reduced and de-hydroxylated [56], and the ring system of flavonoids can be opened (e.g., [57,58]). Furthermore, metabolites may be re-exported from enterocytes by apical MDR transporters, in particular MRP2 and BCRP (quercetin: [59-63]; resveratrol: [64-67]). These processes strongly decrease the compounds' efficacy, to the point that some studies cannot confirm it *in vivo*. Thus, for example, recent meta-analyses of trials involving administration of resveratrol [68,69] or catechins [70,71] to humans have concluded that there is still insufficient evidence of clear health benefits. It is also unclear whether the mechanisms of action identified in *in vitro* studies with cultured cells are relevant to the *in vivo* setting, given that unrealistically high concentrations of the parent compound are often used *in vitro* (e.g., catechins: [72]; quercetin: [73]; resveratrol: [74]). In fact, most of the polyphenol-protein interactions which have been characterized become significant only in the μM range. Thus, for example, resveratrol inhibits COX 1 and -2 with IC_{50}'s of 0.5-1 μM [75] and IKK at about 1 μM [39,76]. Its very interesting effects on phosphodiesterases may require concentrations in the order of at least a few μM units [77,78].

Unfortunately, the levels of "aglycone" in blood or plasma even after administration of reasonably high doses generally remain well

*Address correspondence to this author at the CNR Neuroscience Institute, Viale G. Colombo 3, 35121 Padova, Italy; Tel: +39 0498276483; Fax: +39 0498276040; E-mail: lucia.biasutto@cnr.it

1871-5206/14 $58.00+.00

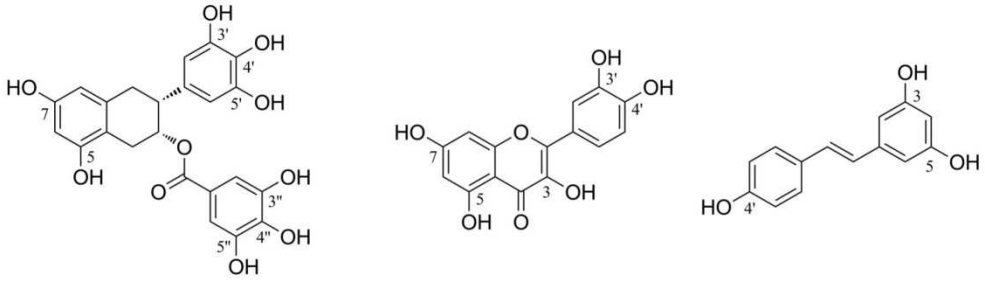

Fig. (1). Structures of the three polyphenols this review focuses on.

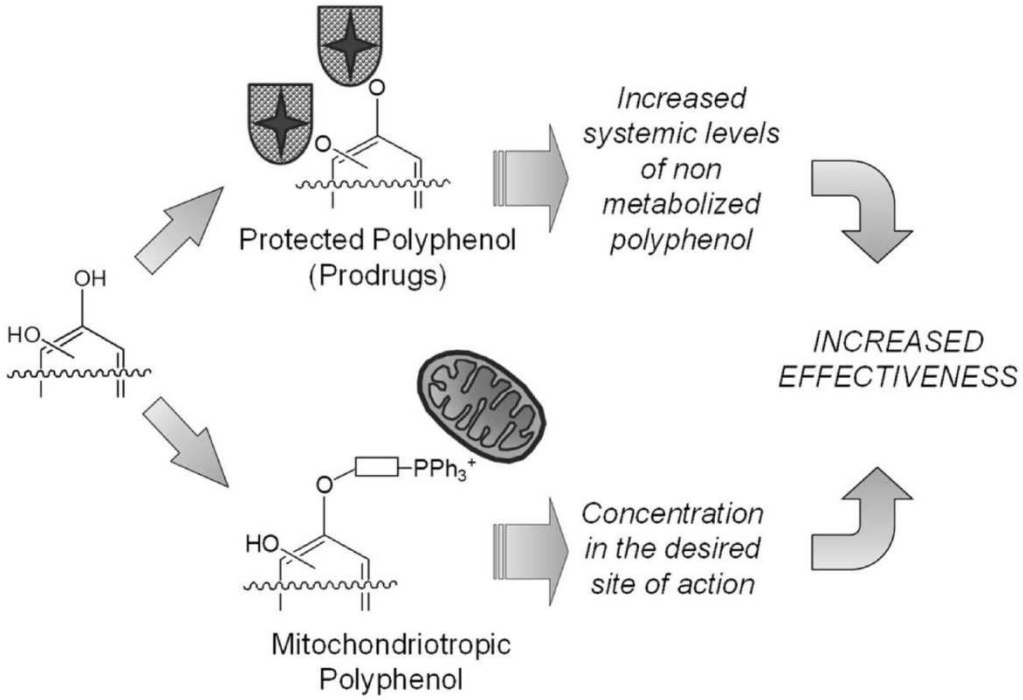

Fig. (2). Approaches to increase the effectiveness of plant polyphenols.

below 1 μM (except perhaps for transient peaks after administration) (e.g., resveratrol: [79-81]; catechins: [82-85]; quercetin: [51,86]). Increasing these levels may help put on a firm basis the assessment of the potential benefits of polyphenols, and possibly potentiate these benefits as well. We would like at any rate to emphasize that levels in blood – and even more so levels in plasma [87] – provide only a partial readout for absorption and bioavailability, since soluble metabolites will be enriched in the aqueous blood phase, while less hydrophilic ones will tend to associate more with other tissues.

2. PRODRUGS OF POLYPHENOLS

One of the strategies being explored to increase bioavailability relies on prodrugs, i.e., precursors in which the sensitive OH groups of polyphenols are protected by a reversible "cap" during absorption, and can be freed with suitable kinetics to regenerate the parent compound after they have survived the first exposure to the metabolic machinery of enterocytes and hepatocytes. This "disguising" approach is widely used in the pharmaceutical industry. As the clinical potential of polyphenols becomes more and more appreciated, it is logical to extend the same approach to these natural compounds as well. Besides offering some degree of protection against metabolic transformations, the groups temporarily attached to the active molecule may be exploited to favourably modulate the physico-chemical properties of the construct (e.g. water solubility), stability (e.g. vulnerability to oxidation) and absorption. The bond system used to link the capping group to the sensitive hydroxyl(s) must on the other hand possess the appropriate characteristics to serve in a

prodrug, i.e., it must be neither too labile nor too stable under physiologically relevant circumstances. Compounds bearing substituents linked *via* stable bonds qualify as drugs rather than prodrugs, and will not be covered here. By the same logic, we do not discuss compounds arising from permanent covalent modifications such as the introduction of atoms or groups not present in natural products.

2.1. Catechins

Much work along these lines has been carried out on green tea catechins. To our knowledge the only bioreversible bond system used has been the carboxyester moiety. Most of the work has been performed *in vitro*. We give here only a summary account given that excellent reviews of the field have been published recently [14,88,89]. The group of Q.P. Dou and co-workers focused on EGCG as an inhibitor of the proteasome and thus as an anti-cancer agent [90], and synthesized EGCG peracetate as well as a few other peracetylated analogs (lacking some of the OH groups). Peracetylation improved the stability of EGCG in solution. While the derivatives could not themselves inhibit the proteasome, they proved more efficient than the unprotected compounds in assays with cultured cells, most likely due to an increased entry into the cells followed by deacetylation [91-93]. Peracetylated EGCG also acted as a sensitizer to chemotherapy in *in vitro* assays [94]. When injected subcutaneously or intraperitoneally, it was somewhat more effective than EGCG itself in contrasting the growth of tumoural masses in nude mice [91,95]. In contrast to acylation, methylation (i.e., a permanent modification) was found to reduce anti-cancer activity, so that inhibition of catechol methyltransferase in cultured cancer cells enhanced the effects of EGCG [96,97]. This finding indicates that the improvement afforded by acylation was most likely linked to its permeation properties, and not to changes in the molecular properties. A similar approach was taken, with analogous results, by C.S. Yang, J.D. Lambert and co-workers [98]. These Authors also studied the pharmacokinetics after intragastric administration to mice, and found an approximate doubling of the AUC value compared to EGCG.

Mixtures of regioisomers of mono-acylated EGCG with various aliphatic chain lengths were synthesized by Matsumura *et al.* [99] using enzymatic catalysis. They were found to be inhibitors of cancer cell growth *in vitro* and also *in vivo* (at least in the case of the C16 acyl derivative), and to be anti-viral [100], anti-bacterial and anti-fungal agents [101]. Various partially acylated lipophilic EGCG derivatives proved to be egregious antioxidants [102], to possess anti-inflammatory properties (due to suppression of iNOS and COX-2 levels [103]) and to have anti-cancer activity in a mouse model [104,105].

In another set of studies, 3-O-acyl derivatives of epigallocatechin (EGC) bearing hydrocarbon chains of various lengths were found to inhibit the activation of the Epstein-Barr virus early antigen [106-108], with an improvement over EGCG as inhibitors of papilloma formation in a mouse skin carcinogenesis assay. Analogous compounds also showed cytotoxic effects against cultured tumoural cell lines [109,110]. 3-O-acyl epicatechins, and, more so, 3-O-acyl catechins inhibited DNA polymerase and angiogenesis more strongly than the parent compounds in *in vitro* assays [111-113]. Compounds arising from 3-O-acylation of EGC with fatty acids also proved more effective than EGCG as inhibitors of 5α-reductase [114,115]. 3-O-acyl catechins and epicatechins furthermore showed strong anti-microbial activity [116].

While the available results with acyl catechins are interesting, *in vivo* applications are so far limited to a few studies involving administration by injection. In view of the characteristics of other polyphenol acyl derivatives (see below) it can be predicted that oral administration would result in a rapid regeneration of the parent compound. Studies of the hydrolysis of acyl catechins are missing. The time seems ripe for experimenting with catechin prodrugs incorporating bonds other than carboxyester.

2.2. Quercetin

Quercetin is a paradigmatic flavonoid, widely utilized as experimental material because of its abundance in nature and foodstuffs, of its well-characterized anti- and pro-oxidant properties, and of the abundant information available about its absorption processes and metabolic transformations (for an overview, see, e.g., [81]). In this case a few different chemical functionalities have been used for the construction of prodrugs, and we organize our summary accordingly.

2.2.1. Carboxyesters

Acylation was the first type of modification to be tested, in the early 1980's, with the purpose of facilitating the entry of this "sticky" molecule into cells by decorating it with lipophilic short fatty acid chains [117]. Several variously acylated quercetin derivatives were then synthesized and tested for activity in biochemical assays. This work is only marginally relevant for the bioavailability issue, and we mention here only examples (for a more complete coverage see, e.g., [81]).

Quercetin pentacetate (QPA) turned out to be a substrate for cellular transacetylases, whose activity accounts for the observed modulation of various enzymes [118]. Analogously to acylated catechins, penta- and tetra-acetylated quercetin reduced iNOS and COX-2 expression [119,120]. QPA however was inferior to pentaether derivatives in *in vitro* assays on Epstein-Barr virus early antigen activation and of mouse skin tumour promotion [121], presumably because of hydrolytic degradation during the assay.

A set of 3-O-acyl monosubstituted quercetins was used by [122] in *in vitro* assays of skin permeability. The propionyl group turned out to be optimal for this purpose. The same Authors also studied the hydrolysis of their compounds in aqueous solution and human plasma. In the latter medium the reaction was markedly accelerated, no doubt reflecting the esterase activity of albumin. Intracellular hydrolases can also deacylate acyl quercetins, with different efficiency depending on cell line [123]. Other phenolic carboxyesters, e.g. aspirin, are more resistant. The lability of quercetin (and, in general, polyphenol) carboxyesters can be ascribed to the stability of the leaving group, the polyphenolic anion, in which the negative charge is widely delocalized. Our group has studied the hydrolysis of acylated quercetins in some detail [123,124]. The ester bond in position 7- is hydrolysed most rapidly, since the corresponding OH group is the most acidic one [125]. The two neighbouring acyl groups on the B ring are hydrolysed almost simultaneously, because of the catalytic "ortho effect" intervening as soon as one of the hydroxyls is freed. In [123], mixed derivatives were studied in which the 4'- position was esterified by an aminoacid while the other hydroxyls were acetylated. The goal was to improve water solubility and perhaps to improve absorption *via* carriers. The amino group however turned out to act as a general base, catalysing hydrolysis of the acyl groups unless blocked (by a Boc group). The N-protected derivatives permeated supported epithelial cell monolayers at a satisfactory rate maintaining at least part of the protecting groups and thus bypassing metabolism. In the same experimental conditions, quercetin itself was instead completely converted into its Phase II conjugates during translocation [123]. A set of quercetin 3-O-aminoacid esters with a Boc protection on the amino group was produced also by H. Huang *et al.* [126]. These compounds acted as inhibitors of Src kinase, but their transmembrane transport was not tested. To increase water solubility, an inositol-2-phosphate group was joined to quercetin through a succinate diester linkage [127].

Unsurprisingly, given their lability, no *in vivo* absorption/ pharmacokinetic data have been reported for carboxyester-based quercetin prodrugs. To make this type of bond useful *in vivo*, a

carefully engineered substituent moiety would have to be used, providing the necessary stability vs. hydrolysis (e.g. *via* steric hindrance) and solubility (e.g. *via* hydrophilic groups) without compromising the ability to diffuse across biomembranes.

2.2.2. Sulfonates

Peresterification with benzensulfonic acid led to compounds with high solubility in apolar solvents and methanol [128]. 90% conversion of quercetin perbenzensulfonate to quercetin required 16 hours (at pH 7.4 and 37° C). This suggests that this type of derivatives might be useful as prodrugs, but apparently this aspect was not investigated.

2.2.3. Acetals

The acetal group (Drug-O-R_1R_2C-O-R) joins the aglycone to the glycoside group in glycosides such as, e.g., quercetin 3-O-glucoside or rutin, and in quercetin glucuronides. A similar bond system, the alkylcarbonyloxymethyl group (Drug-OCH_2O(CO)-R), has been used to cap the hydroxyls in positions 3- and 7- to effectively stabilize the molecule [129,130]. The actual substituent used was pivaloxymethyl (POM), which comprises the carboxyester of pivalic acid (R = *tert*-butyl). The steric hindrance of this bulky group slows hydrolysis: once the ester is hydrolyzed, the resulting hemiacetal (Quercetin-OCH_2-OH) spontaneously decomposes to quercetin and formaldehyde. Only small amounts (with Q-7-POM) or no (with Q-3-POM) quercetin formed in the MCF-7 cell culture medium, indicating that protection was long-lasting outside cells. Q-7-POM could diffuse into HCT116 cells and regenerate quercetin inside them. On the contrary, Q-3-POM did not enter cells (and was not hydrolyzed), a difference ascribed to differences in polarity. When POM groups were attached in both 3- and 7-, the resulting prodrug could enter HCT116 cells, where only the group in 7- was eliminated. The compounds had, predictably, low solubility. In a variant on the theme, the same group produced 3-, 7- and 3,7-disubstituted quercetin derivatives carrying isopropyloxycarbonylmethoxy (POC) groups (Quercetin-OCH_2O(CO)O-iPr) [131], which behaved analogously to the POM derivatives. None of these compounds has yet been tested *in vivo*.

2.2.4. Carbamates

Carbamate esters (Drug-O-CO-NR_1R_2) are generally more resistant to hydrolysis than carboxyesters or carbonates [132] and are used in prodrugs. Mulholland and co-workers [133] (rev: [134]) used this bond system to connect glycine and quercetin (at the 4' position), thus obtaining one of the first flavonoid prodrugs, named QC12. This compound had reasonable solubility and a convenient half-life in blood, but low oral bioavailability. The same approach was used later to produce QC12 analogues comprising other aminoacids [135] as mixtures of 3'- and 4'-monosubstituted isomers. Isomeric mixtures of derivatives incorporating the dipeptides Ala-Asp (Q-AD) and Ala-Glu (Q-AE) were also produced. These prodrugs showed a much increased water solubility, were nearly stable in aqueous buffer (pH not specified) and were hydrolysed with an half-life of 0.5-3 hours range in MDCK (a canine kidney line) cell lysates. Transport across MDCK monolayers was modestly improved in comparison with quercetin, with the Q-AE derivative showing a relative increase of about 5. No *in vivo* experiments were reported.

2.3. Resveratrol

2.3.1. Carboxyesters

Carboxyester derivatives of resveratrol have stability problems similar to those of the analogous quercetin derivatives, for the same reasons. Thus, our group observed that the triacetate and the triester of carboxy-terminated mPEG were rapidly hydrolysed in blood and during transport experiments with explanted rat intestinal wall segments [136]. The total amount of material crossing the intestinal wall was slightly, but not significantly, higher than when placing resveratrol itself on the apical side. Interestingly, the amount of resveratrol reaching the basolateral side as such increased dramatically when using the PEGylated derivative. However, this also happened when using a mixture of resveratrol and PEG, suggesting that the adjuvating effect of PEG did not depend on a covalent link to the stilbenoid kernel. While others have reported that administration of resveratrol triacetate (RTA) to rats resulted in a higher plasma AUC than when resveratrol was used [137], our group found no significant difference in blood pharmacokinetic analyses following administration of RTA vs. resveratrol [81]. RTA (used in the tens-of-μM range) has been found to be as effective as resveratrol as an *in vitro* inhibitor of human colon tumor cell proliferation, inducing arrest of the cell cycle in the S phase. A marked synergism with 5-Fluoro-Uracil was noted [138,139]. Cell proliferation and colony formation by prostate [140] and breast [141] cancer cells were also suppressed.

To increase water solubility, our group coupled each hydroxyl of resveratrol to a glucose moiety *via* a succinyl linker [142]. This compound was indeed quite soluble in water, but, since it contained six carboxyester bonds, it was relatively unstable, hydrolysing to resveratrol in less than 1 hour in rat blood. Upon oral administration to rats, blood pharmacokinetics were shifted to longer times in comparison with those of resveratrol administered as such, but the AUC and the metabolite mix in blood were similar.

2.3.2. Sulfonates

In contrast with the behaviour of quercetin perbenzensulfonate (see above), permethylsulfonated resveratrol did not undergo hydrolysis in any of the conditions tested by [136] (acidic or neutral aqueous solution, blood). Permeation of the explanted rat intestinal wall was somewhat higher than for resveratrol itself, but only the unmodified compound was recovered in the basolateral chamber. Resveratrol phenylsulfonate is one of the derivatives listed in a Chinese patent [143], which provides no details about stability or membrane permeation.

2.3.3. Carbonates

Resveratrol alkyl carbonates have been patented for cosmetic and skin care applications [144]. Compared to carboxyesters, carbonates underwent a faster enzymatic hydrolysis, making them suitable for topical administration but not for oral delivery.

2.3.4. Acetals

As for flavonoids, the acetal linkage (Drug-O-R_1R_2C-O-R) is present in glycosides. Larrosa *et al*. [145] have used this design producing the four possible mono- and di-glucoside derivatives. Furthermore, five derivatives of the 4'-O-glucoside were produced carrying an acyl substituent at position 6- of the glucose moiety. These compounds were planned to have high hydrophilicity, favouring delivery to the colon rather than intestinal absorption. The compounds were tested on dextran sodium sulfate (DSS)-induced colitis. 3-O-glucoside derivatives carrying a butanoyl or an octanoyl chain on the sugar moiety effectively reduced the inflammation score.

In an attempt to improve absorbance and bioavailability our group has instead used the acetal group to link resveratrol to oligoethyleneglycol chains [79]. Compounds with $R_1 = R_2 = H$ ("formals") crossed the explanted rat intestinal wall and were absorbed after oral administration, the extent depending on the length of the oligomeric chains. Four ethyleneglycol units yielded the best performance, providing for absorption at levels similar to those of resveratrol itself. However, only the unmodified prodrug was found in blood. Thus, this type of linkage is rather too stable for use in resveratrol prodrugs. On the contrary, with $R_1 = R_2 = CH_3$ the prodrug (a "ketal") turned out to hydrolyse too rapidly. The most promising derivative turned out to be the acetal ($R_1 = H$; $R_2 = CH_3$), which was relatively well absorbed, resulting in the appearance in the rats' blood of resveratrol metabolites (predominant), the unaltered prodrug and its partial hydrolysis products. Furthermore,

the pharmacokinetic profile was shifted to longer times from administration.

3. MITOCHONDRIA-TARGETED DERIVATIVES

3.1. Mitochondria and Cancer

One of the strategies to obtain an effective anti-cancer therapy is the identification of an invariable target; this may be represented by mitochondria [146]. Cancer cells often display an altered bioenergetic and/or biosynthetic status but nonetheless mitochondrial functionality is maintained and is essential for their function [147]. Mitochondria have a wide range of tasks. In addition to ATP production, they are involved in cellular processes such as cell death [148] and Ca^{2+} homeostasis [149].

Mitochondria are also the major site of ROS generation in the cell [150]. Deregulated ROS production is known to be involved in the pathophysiology of various diseases, including cancer [151-155]. Alterations in antioxidant enzyme activities have been reported for many tumours [156,157]. Increased ROS production is important for the maintenance and evolution of the cancerous phenotype [158], and increased mitochondrial ROS have been reported to correlate with the metastatic potential of tumour cells [153,159], to activate Hif-1α [160,161] (with consequent effects on angiogenesis and metabolic adaptations affecting tumour growth), and to promote cell proliferation *via* transactivation of growth factor receptors and/or of downstream effectors such as the Akt pathway [162-165].

On the other side, ROS can also induce cell death [162,163], and thus can counteract tumor growth. For example, they can activate pro-apoptotic signalling [166], inducing cardiolipin oxidation and subsequent cytochrome c release [167], or activating pro-apoptotic kinases and transcription factors, such as those of the JNK and p38 MAPK signalling cascades [168-170]. ROS can also induce necrosis, and/or the mitochondrial permeability transition [171].

Anticancer agents acting on mitochondria and destabilizing them have been developed; they are called "mitocans", and are classified into several subfamilies depending on their specific target [151,172].

Plant polyphenols can act either as anti- or pro-oxidants. Which mode of action predominates depends on circumstances, such as the pH, the concentration of the polyphenol itself, or the presence of Cu and Fe ions [173-175]. An important contribution to the antioxidant effects attributed to many plant polyphenols may be provided by hormesis: the response to a mild pro-oxidant confers further protection against later pathological conditions in which ROS have a major role [176]. This phenomenon is largely due to activation of Nrf2 signalling, with consequent transactivation of target genes under the control of Antioxidant Response Elements (ARE) or Elecrophile Response Elements (EpRE); the final effect is protection against oxidative stress, with consequent impact on inflammatory processes and chemoprevention [177].

Redox-active compounds are thus expected to have a great potential against cancer. Both anti- or pro-oxidant behaviours may be useful to antagonize cancer; antioxidants are expected to prevent cancer development, while a pro-oxidant approach is desirable in an oncological context to (selectively) induce cancer cell death.

Concentration of redox-active compounds into the major site of ROS generation, i.e. mitochondria, represents a logical strategy to potentiate their therapeutic effect. Selectivity of mitochondria-targeted therapies towards cancer cells is an important issue to avoid/limit unwanted side effects. Since cancer cells are exposed to higher levels of oxidative stress compared to non-tumoural ones, an additional pro-oxidative stimulus may kill them more easily [154,178-180].

Mitochondrial targeting can be achieved exploiting unique properties of these organelles, such as the transmembrane voltage gradient, but also the pH gradient or mitochondria-specific enzymatic activities [151]. The latter approaches however have not been used in the case of polyphenols.

3.2. Mitochondria-Targeted Derivatives of Polyphenols

Conjugation of the compound of interest to lipophilic cations, the most commonly used of which is triphenylphosphonium (TPP), allows permeation of the construct through biological membranes (thanks to the delocalization of the positive charge) and, most importantly, its accumulation in compartments held at more negative potentials, such as the mitochondrial matrix [181-184]. This is in accordance to Nernst's law, which predicts a 10-fold accumulation of cationic compounds every -60mV of $\Delta\Psi_m$. Selectivity towards cancer cells can be achieved thanks to their higher mitochondrial transmembrane potential compared to non-tumoural cells. This is the consequence of the metabolic shift of cancer cells towards aerobic glycolysis (the so-called Warburg effect); the decreased oxidative phosphorylation activity leads to a reduced dissipation of the mitochondrial electrochemical proton gradient, with a consequent increase of transmembrane potential [185].

Mitochondria-targeted derivatives of both quercetin and resveratrol have been produced [186-189] through conjugation of the polyphenol kernel with a butyl-triphenylphosphonium lipophilic cation. To our knowledge, no catechin derivatives of such type have been developed at the moment. Different conjugation positions were tested to take into account the possible effects of the chemical modification on the properties of the parent compound [188,189]. As expected, these derivatives were shown to accumulate both into isolated rat liver mitochondria and into *in situ* mitochondria of cultured cells. Quercetin and resveratrol were reported to be cytotoxic on cultured cancer cells when used at very high concentrations (tens of μM) [190-192]. These high concentrations are not expected to be reached *in vivo,* due to the low bioavailability and rapid metabolism of the natural compounds (see above). Mitochondrial targeting of polyphenols turned out to be an effective way to reach higher local concentrations of the compounds, with a consequent potentiation of their effects. In fact, both quercetin and resveratrol derivatives were shown to be pro-oxidant and cytotoxic *in vitro*, selectively killing fast-growing and tumoural cells when supplied in the low μM range [186,187,189,193]. Importantly, the same concentrations of polyphenol plus methyl-triphenylphosphonium cation did not exhibit cytotoxicity.

For all the derivatives we tested, cytotoxicity was due to H_2O_2 produced upon their accumulation into mitochondria [189,193]. However, the mechanism of ROS generation appears to differ between quercetin and resveratrol derivatives.

In the case of quercetin-derived compounds the available evidence points to a chain "autooxidation" mechanism of action. This hypothesis was supported by the following observations: externally added membrane-permeating catalase and superoxide dismutase were both able to rescue cells from death; the presence of free phenolic hydroxyls and accumulation in mitochondria were both necessary to induce oxidative stress. According to the proposed mechanism, superoxide anion is generated by a cyclic reaction *via* transfer of an electron from the semiquinone of the quercetin derivative to oxygen, which in turn regenerates the semiquinone by oxidizing a quercetin moiety, with the concomitant production of H_2O_2. Furthermore, 7-O-(4-triphenylphosphoniumbutyl)quercetin iodide (Q-7BTPI) inhibits Glutathione Peroxidase, an effect expected to accentuate oxidative stress by interfering with the elimination of H_2O_2 [193].

In the case of resveratrol derivatives the situation is quite different; externally added superoxide dismutase in this case potentiated toxicity, and effectiveness was increased if resveratrol hydroxyls were acetylated or methylated [189]. This suggests that autooxidation of the polyphenolic nucleus is not involved. The

compounds caused also Cyclosporin A- and ROS-independent depolarization of in situ mitochondria. ROS generation is likely due to interaction of the derivatives with respiratory chain complexes (especially complex I and III) and depolarization may involve the ATP synthase [194].

In vivo studies on the chemotherapeutic potential of these derivatives are beginning. Preliminary data show an effective chemotherapeutic action, with the drawback of a relatively high systemic toxicity. New derivatives will be synthesised and tested with the goal of reducing toxicity. Molecules will be developed with the goal of regenerating the parent polyphenol after delivery to the mitochondria.

4. CONCLUSIONS AND PERSPECTIVES

The development of effective prodrugs of polyphenols is progressing, but much work still needs to be done. Capping groups imparting desirable physico-chemical properties (water solubility, membrane permeability) have been identified. Oligoethylene glycol chains are a strong candidate for the optimization of solubility and diffusive absorption. The exploitation of endogenous carriers and the behaviour of lipophilic derivatives are two attractive areas of investigation. The search for linkages providing appropriate kinetics of regeneration of the parent compound also needs to progress further. It is important to remember, in this respect, that these kinetics may depend on the characteristics of the parent compound itself (i.e., the leaving group). In much of the extant literature the prodrugs are tested in *in vitro* systems; only a minority of studies have addressed *in vivo* behaviour, which is obviously of paramount importance. Another area requiring attention is the integration of formulation and prodrug approaches. As the biomedical potential of polyphenols gains ever-increasing attention, the goal of modulating their delivery and metabolism is bound to become more and more relevant, and an expansion of the activity in this field may be expected.

The prodrug approach may be used to allow reversibility of conjugation with the triphenylphosphonium group, and thus regeneration of the parent compound after accumulation at the desired site of action. In this way, the TPP "engine" may drive accumulation of the derivative into the mitochondrial matrix, followed by regeneration of the parent compound thanks to disposal of the TPP, exploiting an enzymatic activity. The use of a chemical linkage which is selectively cleaved off by a mitochondria- specific enzymatic reaction would allow the selective regeneration of the parent compound in these organelles. This approach was used by Ripke *et al* to synthesize a TPP-linked derivative of α-lipoic acid [195]; the ester bond connecting the COOH moiety of lipoic acid with 4-triphenylphosphonium-1-hydroxybutane was shown to be selectively hydrolysed by mitochondria aldehyde dehydrogenase, while it was not rapidly cleaved by cellular esterases. Also exploitation of the mitochondrial fatty acid β-oxidation pathway was shown to be effective for delivery and activation of mitochondria-targeted prodrugs of antioxidant molecules [196-198].

The possible effects of mitochondriotropic polyphenols as protective/chemopreventive antioxidants when used at lower concentrations remains to be explored; the wider the concentration window between anti- and pro-oxidant behaviours, the higher the potential for therapeutic applications of these derivatives. This dual behaviour is expected from the dual anti-/pro-oxidant activity typical of plant polyphenols, and from data already available for other mitochondria-targeted antioxidants, such as MitoQ or SkQ1 [199,200].

CONFLICT OF INTEREST

The author(s) confirm that this article content has no conflict of interest.

ACKNOWLEDGEMENTS

The authors' work is currently supported by grants from the Fondazione Cassa di Risparmio di Padova e Rovigo (CARIPARO) ("Developing a Pharmacology of Polyphenols"), from the Italian Ministry of the University and Research (PRIN n. 20107Z8XBW_004), and by the CNR Project of Special Interest on Aging.

LIST OF ABBREVIATIONS

ARE	=	Antioxidant Response Elements
AUC	=	area under the curve
BCRP	=	Breast cancer resistance protein
Boc	=	tert-Butyloxycarbonyl
COX	=	Cyclooxygenase
ΔΨm	=	mitochondrial transmembrane potential
DSS	=	dextran sodium sulphate
EGC	=	epigallocatechin
EGCG	=	epigallocatechin gallate
EpRE	=	Elecrophile Response Elements
iNOS	=	inducible NO synthase
iPr	=	isopropyl
MDR	=	multidrug resistance
MRP2	=	multidrug resistance associated protein 2
mPEG	=	methoxy- polyethylene glycol
POC	=	isopropyloxycarbonylmethoxy
POM	=	pivaloxymethyl
Q	=	quercetin
Q-7BTPI	=	7-O-(4-triphenylphosphoniumbutyl)quercetin iodide
R	=	resveratrol
ROS	=	reactive oxygen species
RTA	=	tri-acetylated resveratrol
TPP	=	triphenylphosphonium

REFERENCES

[1] Mahler, A.; Mandel, S.; Lorenz, M.; Ruegg, U.; Wanker, E.E.; Boschmann, M.; Paul, F. Epigallocatechin-3-gallate: a useful, effective and safe clinical approach for targeted prevention and individualised treatment of neurological diseases? *Epma j.,* **2013**, *4*, 5.

[2] Mandel, S.A.; Weinreb, O.; Amit, T.; Youdim, M.B. Molecular mechanisms of the neuroprotective/neurorescue action of multi-target green tea polyphenols. *Front. Biosci. (Schol. Ed.),* **2012**, *4*, 581-598.

[3] Mandel, S.A.; Youdim, M.B. In the rush for green gold: Can green tea delay age-progressive brain neurodegeneration? *Recent Pat. CNS Drug Discov.,* **2012**, *7*, 205-217.

[4] Yang, C.S.; Hong, J. Prevention of chronic diseases by tea: possible mechanisms and human relevance. *Annu. Rev. Nutr.,* **2013**, *33*, 161-181.

[5] Spencer, J.P. The impact of fruit flavonoids on memory and cognition. *Br. J. Nutr.,* **2010**, *104 Suppl 3*, S40-47.

[6] Spencer, J.P.; Vafeiadou, K.; Williams, R.J.; Vauzour, D. Neuroinflammation: modulation by flavonoids and mechanisms of action. *Mol. Aspects Med.,* **2012**, *33*, 83-97.

[7] Rendeiro, C.; Guerreiro, J.D.; Williams, C.M.; Spencer, J.P. Flavonoids as modulators of memory and learning: molecular interactions resulting in behavioural effects. *Proc. Nutr. Soc.,* **2012**, *71*, 246-262.

[8] Williams, R.J.; Spencer, J.P. Flavonoids, cognition, and dementia: actions, mechanisms, and potential therapeutic utility for Alzheimer disease. *Free Radic. Biol. Med.,* **2012**, *52*, 35-45.

[9] Liu, G.S.; Zhang, Z.S.; Yang, B.; He, W. Resveratrol attenuates oxidative damage and ameliorates cognitive impairment in the brain of senescence-accelerated mice. *Life Sci.,* **2012**, *91*, 872-877.

[10] Pallas, M.; Porquet, D.; Vicente, A.; Sanfeliu, C. Resveratrol:new avenues for a natural compound in neuroprotection. *Curr. Pharm. Des.,* **2013**, *19*, 6726-6731.

[11] Singh, N.; Agrawal, M.; Dore, S. Neuroprotective properties and mechanisms of resveratrol in *in vitro* and *in vivo* experimental cerebral stroke models. *ACS Chem. Neurosci.,* **2013**, *4*, 1151-1162.

[12] Cherniack, E.P. A berry thought-provoking idea: the potential role of plant polyphenols in the treatment of age-related cognitive disorders. *Br. J. Nutr.,* **2012**, *108*, 794-800.

[13] Fujiki, H.; Suganuma, M. Green tea: an effective synergist with anticancer drugs for tertiary cancer prevention. *Cancer Lett.,* **2012**, *324*, 119-125.

[14] Chen, D.; Wan, S.B.; Yang, H.; Yuan, J.; Chan, T.H.; Dou, Q.P. EGCG, green tea polyphenols and their synthetic analogs and prodrugs for human cancer prevention and treatment. *Adv. Clin. Chem.,* **2011**, *53*, 155-177.

[15] Singh, B.N.; Shankar, S.; Srivastava, R.K. Green tea catechin, epigallocatechin-3-gallate (EGCG): mechanisms, perspectives and clinical applications. *Biochem. Pharmacol.,* **2011**, *82*, 1807-1821.

[16] Kanwar, J.; Taskeen, M.; Mohammad, I.; Huo, C.; Chan, T.H.; Dou, Q.P. Recent advances on tea polyphenols. *Front. Biosci. (Elite Ed.),* **2012**, *4*, 111-131.

[17] Weng, C.J.; Yen, G.C. Flavonoids, A ubiquitous dietary phenolic subclass, exert extensive *in vitro* anti-invasive and *in vivo* anti-metastatic activities. *Cancer Metastasis Rev.,* **2012**, *31*, 323-351.

[18] Gibellini, L.; Pinti, M.; Nasi, M.; Montagna, J.P.; De Biasi, S.; Roat, E.; Bertoncelli, L.; Cooper, E.L.; Cossarizza, A. Quercetin and cancer chemoprevention. *Evid. Based Complement. Alternat. Med.,* **2011**, *2011*, 591356.

[19] Mendoza, E.E.; Burd, R. Quercetin as a systemic chemopreventative agent: structural and functional mechanisms. *Mini Rev. Med. Chem.,* **2011**, *11*, 1216-1221.

[20] Shukla, Y.; Singh, R. Resveratrol and cellular mechanisms of cancer prevention. *Ann. N. Y. Acad. Sci.,* **2011**, *1215*, 1-8.

[21] Aluyen, J.K.; Ton, Q.N.; Tran, T.; Yang, A.E.; Gottlieb, H.B.; Bellanger, R.A. Resveratrol: Potential as anticancer agent. *J. Diet. Suppl.,* **2012**, *9*, 45-56.

[22] McCormack, D.; McFadden, D. Pterostilbene and cancer: Current Review. *J. Surg. Res.,* **2012**, *173*, e53-61.

[23] Borriello, A.; Bencivenga, D.; Caldarelli, I.; Tramontano, A.; Borgia, A.; Pirozzi, A.V.; Oliva, A.; Della Ragione, F. Resveratrol and cancer treatment: is hormesis a yet unsolved matter? *Curr. Pharm. Des.,* **2013**, *19*, 5384-5393.

[24] Pan, M.H.; Lai, C.S.; Wu, J.C.; Ho, C.T. Epigenetic and disease targets by polyphenols. *Curr. Pharm. Des.,* **2013**, *19*, 6156-6185.

[25] Park, L.K.; Friso, S.; Choi, S.W. Nutritional influences on epigenetics and age-related disease. *Proc. Nutr. Soc.,* **2012**, *71*, 75-83.

[26] Ong, T.P.; Moreno, F.S.; Ross, S.A. Targeting the epigenome with bioactive food components for cancer prevention. *J. Nutrigenet. Nutrigenomics,* **2011**, *4*, 275-292.

[27] Wang, Y.; Li, Y.; Liu, X.; Cho, W.C. Genetic and epigenetic studies for determining molecular targets of natural product anticancer agents. *Curr. Cancer Drug Targets,* **2013**, *13*, 506-518.

[28] Vanden Berghe, W. Epigenetic impact of dietary polyphenols in cancer chemoprevention: lifelong remodeling of our epigenomes. *Pharmacol. Res.,* **2012**, *65*, 565-576.

[29] Kelsey, N.A.; Wilkins, H.M.; Linseman, D.A. Nutraceutical antioxidants as novel neuroprotective agents. *Molecules,* **2010**, *15*, 7792-7814.

[30] Scapagnini, G.; Vasto, S.; Abraham, N.G.; Caruso, C.; Zella, D.; Fabio, G. Modulation of Nrf2/ARE pathway by food polyphenols: a nutritional neuroprotective strategy for cognitive and neurodegenerative disorders. *Mol. Neurobiol.,* **2011**, *44*, 192-201.

[31] Khan, N.; Afaq, F.; Saleem, M.; Ahmad, N.; Mukhtar, H. Targeting multiple signaling pathways by green tea polyphenol (-)-epigallocatechin-3-gallate. *Cancer Res.,* **2006**, *66*, 2500-2505.

[32] Pan, M.H.; Chiou, Y.S.; Wang, Y.J.; Ho, C.T.; Lin, J.K. Multistage carcinogenesis process as molecular targets in cancer chemoprevention by epicatechin-3-gallate. *Food Funct.,* **2011**, *2*, 101-110.

[33] Benelli, R.; Vene, R.; Bisacchi, D.; Garbisa, S.; Albini, A. Anti-invasive effects of green tea polyphenol epigallocatechin-3-gallate (EGCG), a natural inhibitor of metallo and serine proteases. *Biol. Chem.,* **2002**, *383*, 101-105.

[34] Murakami, A.; Ashida, H.; Terao, J. Multitargeted cancer prevention by quercetin. *Cancer Lett.,* **2008**, *269*, 315-325.

[35] Russo, G.L.; Russo, M.; Spagnuolo, C.; Tedesco, I.; Bilotto, S.; Iannitti, R.; Palumbo, R. Quercetin: A Pleiotropic Kinase Inhibitor Against Cancer. *Cancer Treat. Res.,* **2014**, *159*, 185-205.

[36] Hou, D.X.; Kumamoto, T. Flavonoids as protein kinase inhibitors for cancer chemoprevention: direct binding and molecular modeling. *Antioxid. Redox Signal.,* **2010**, *13*, 691-719.

[37] Sarno, S.; Moro, S.; Meggio, F.; Zagotto, G.; Dal Ben, D.; Ghisellini, P.; Battistutta, R.; Zanotti, G.; Pinna, L.A. Toward the rational design of protein kinase casein kinase-2 inhibitors. *Pharmacol. Ther.,* **2002**, *93*, 159-168.

[38] Athar, M.; Back, J.H.; Kopelovich, L.; Bickers, D.R.; Kim, A.L. Multiple molecular targets of resveratrol: Anti-carcinogenic mechanisms. *Arch. Biochem. Biophys.,* **2009**, *486*, 95-102.

[39] Kundu, J.K.; Shin, Y.K.; Kim, S.H.; Surh, Y.J. Resveratrol inhibits phorbol ester-induced expression of COX-2 and activation of NF-kappaB in mouse skin by blocking IkappaB kinase activity. *Carcinogenesis,* **2006**, *27*, 1465-1474.

[40] Parsons, D.W.; Jones, S.; Zhang, X.; Lin, J.C.; Leary, R.J.; Angenendt, P.; Mankoo, P.; Carter, H.; Siu, I.M.; Gallia, G.L.; Olivi, A.; McLendon, R.; Rasheed, B.A.; Keir, S.; Nikolskaya, T.; Nikolsky, Y.; Busam, D.A.; Tekleab, H.; Diaz, L.A., Jr.; Hartigan, J.; Smith, D.R.; Strausberg, R.L.; Marie, S.K.; Shinjo, S.M.; Yan, H.; Riggins, G.J.; Bigner, D.D.; Karchin, R.; Papadopoulos, N.; Parmigiani, G.; Vogelstein, B.; Velculescu, V.E.; Kinzler, K.W. An integrated genomic analysis of human glioblastoma multiforme. *Science,* **2008**, *321*, 1807-1812.

[41] Jones, S.; Zhang, X.; Parsons, D.W.; Lin, J.C.; Leary, R.J.; Angenendt, P.; Mankoo, P.; Carter, H.; Kamiyama, H.; Jimeno, A.; Hong, S.M.; Fu, B.; Lin, M.T.; Calhoun, E.S.; Kamiyama, M.; Walter, K.; Nikolskaya, T.; Nikolsky, Y.; Hartigan, J.; Smith, D.R.; Hidalgo, M.; Leach, S.D.; Klein, A.P.; Jaffee, E.M.; Goggins, M.; Maitra, A.; Iacobuzio-Donahue, C.; Eshleman, J.R.; Kern, S.E.; Hruban, R.H.; Karchin, R.; Papadopoulos, N.; Parmigiani, G.; Vogelstein, B.; Velculescu, V.E.; Kinzler, K.W. Core signaling pathways in human pancreatic cancers revealed by global genomic analyses. *Science,* **2008**, *321*, 1801-1806.

[42] Gerlinger, M.; Rowan, A.J.; Horswell, S.; Larkin, J.; Endesfelder, D.; Gronroos, E.; Martinez, P.; Matthews, N.; Stewart, A.; Tarpey, P.; Varela, I.; Phillimore, B.; Begum, S.; McDonald, N.Q.; Butler, A.; Jones, D.; Raine, K.; Latimer, C.; Santos, C.R.; Nohadani, M.; Eklund, A.C.; Spencer-Dene, B.; Clark, G.; Pickering, L.; Stamp, G.; Gore, M.; Szallasi, Z.; Downward, J.; Futreal, P.A.; Swanton, C. Intratumor heterogeneity and branched evolution revealed by multiregion sequencing. *N. Engl. J. Med.,* **2012**, *366*, 883-892.

[43] Yap, T.A.; Gerlinger, M.; Futreal, P.A.; Pusztai, L.; Swanton, C. Intratumor heterogeneity: Seeing the wood for the trees. *Sci. Transl. Med.,* **2012**, *4*, 127ps110.

[44] Silvestri, A.; Calvert, V.; Belluco, C.; Lipsky, M.; De Maria, R.; Deng, J.; Colombatti, A.; De Marchi, F.; Nitti, D.; Mammano, E.; Liotta, L.; Petricoin, E.; Pierobon, M. Protein pathway activation mapping of colorectal metastatic progression reveals metastasis-specific network alterations. *Clin. Exp. Metastasis,* **2013**, *30*, 309-316.

[45] Ciriello, G.; Miller, M.L.; Aksoy, B.A.; Senbabaoglu, Y.; Schultz, N.; Sander, C. Emerging landscape of oncogenic signatures across human cancers. *Nat. Genet.,* **2013**, *45*, 1127-1133.

[46] Gossage, L.; Eisen, T. Targeting multiple kinase pathways: a change in paradigm. *Clin. Cancer Res.,* **2010**, *16*, 1973-1978.

[47] Aggarwal, B.B.; Sethi, G.; Baladandayuthapani, V.; Krishnan, S.; Shishodia, S. Targeting cell signaling pathways for drug discovery: An old lock needs a new key. *J. Cell. Biochem.,* **2007**, *102*, 580-592.

[48] Lipinski, C.A.; Lombardo, F.; Dominy, B.W.; Feeney, P.J. Experimental and computational approaches to estimate solubility and permeability in drug discovery and development settings. *Adv. Drug Deliv. Rev.,* **2001**, *46*, 3-26.

[49] Lambert, J.D.; Sang, S.; Yang, C.S. Biotransformation of green tea polyphenols and the biological activities of those metabolites. *Mol. Pharm.,* **2007**, *4*, 819-825.

[50] Sang, S.; Lambert, J.D.; Ho, C.T.; Yang, C.S. The chemistry and biotransformation of tea constituents. *Pharmacol. Res.,* **2011**, *64*, 87-99.

[51] Chen, X.; Yin, O.Q.; Zuo, Z.; Chow, M.S. Pharmacokinetics and modeling of quercetin and metabolites. *Pharm. Res.,* **2005**, *22*, 892-901.

[52] Manach, C.; Williamson, G.; Morand, C.; Scalbert, A.; Remesy, C. Bioavailability and bioefficacy of polyphenols in humans. I. Review of 97 bioavailability studies. *Am. J. Clin. Nutr.,* **2005**, *81*, 230s-242s.

[53] Vitaglione, P.; Sforza, S.; Galaverna, G.; Ghidini, C.; Caporaso, N.; Vescovi, P.P.; Fogliano, V.; Marchelli, R. Bioavailability of trans-resveratrol from red wine in humans. *Mol. Nutr. Food Res.,* **2005**, *49*, 495-504.

[54] Walle, T. Bioavailability of resveratrol. *Ann. N. Y. Acad. Sci.,* **2011**, *1215*, 9-15.

[55] Wenzel, E.; Somoza, V. Metabolism and bioavailability of trans-resveratrol. *Mol. Nutr. Food Res.,* **2005**, *49*, 472-481.

[56] Bode, L.M.; Bunzel, D.; Huch, M.; Cho, G.S.; Ruhland, D.; Bunzel, M.; Bub, A.; Franz, C.M.; Kulling, S.E. *In vivo* and *in vitro* metabolism of trans-resveratrol by human gut microbiota. *Am. J. Clin. Nutr.,* **2013**, *97*, 295-309.

[57] Schoefer, L.; Mohan, R.; Schwiertz, A.; Braune, A.; Blaut, M. Anaerobic degradation of flavonoids by Clostridium orbiscindens. *App.l Environ. Microbiol,* **2003**, *69*, 5849-5854.

[58] Blaut, M.; Schoefer, L.; Braune, A. Transformation of flavonoids by intestinal microorganisms. *Int. J .Vitam Nutr Res.,* **2003**, *73*, 79-87.

[59] Walgren, R.A.; Lin, J.T.; Kinne, R.K.; Walle, T. Cellular uptake of dietary flavonoid quercetin 4'-beta-glucoside by sodium-dependent glucose transporter SGLT1. *J. Pharmacol. Exp. Ther.,* **2000**, *294*, 837-843.

[60] Williamson, G.; Aeberli, I.; Miguet, L.; Zhang, Z.; Sanchez, M.B.; Crespy, V.; Barron, D.; Needs, P.; Kroon, P.A.; Glavinas, H.; Krajcsi, P.; Grigorov, M. Interaction of positional isomers of quercetin glucuronides with the transporter ABCC2 (cMOAT, MRP2). *Drug Metab. Dispos.,* **2007**, *35*, 1262-1268.

[61] O'Leary, K.A.; Day, A.J.; Needs, P.W.; Mellon, F.A.; O'Brien, N.M.; Williamson, G. Metabolism of quercetin-7- and quercetin-3-glucuronides by an *in vitro* hepatic model: the role of human beta-glucuronidase, sulfotransferase, catechol-O-methyltransferase and multi-resistant protein 2 (MRP2) in flavonoid metabolism. *Biochem. Pharmacol.,* **2003**, *65*, 479-491.

[62] Sesink, A.L.; Arts, I.C.; de Boer, V.C.; Breedveld, P.; Schellens, J.H.; Hollman, P.C.; Russel, F.G. Breast cancer resistance protein (Bcrp1/Abcg2) limits net intestinal uptake of quercetin in rats by facilitating apical efflux of glucuronides. *Mol. Pharmacol.,* **2005**, *67*, 1999-2006.

[63] Nait Chabane, M.; Al Ahmad, A.; Peluso, J.; Muller, C.D.; Ubeaud, G. Quercetin and naringenin transport across human intestinal Caco-2 cells. *J. Pharm. Pharmacol.,* **2009**, *61*, 1473-1483.

[64] Kaldas, M.I.; Walle, U.K.; Walle, T. Resveratrol transport and metabolism by human intestinal Caco-2 cells. *J Pharm Pharmacol,* **2003**, *55*, 307-312.

[65] Maier-Salamon, A.; Hagenauer, B.; Reznicek, G.; Szekeres, T.; Thalhammer, T.; Jager, W. Metabolism and disposition of resveratrol in the isolated perfused rat liver: role of Mrp2 in the biliary excretion of glucuronides. *J. Pharm. Sci.,* **2008**, *97*, 1615-1628.

[66] Juan, M.E.; Gonzalez-Pons, E.; Planas, J.M. Multidrug resistance proteins restrain the intestinal absorption of trans-resveratrol in rats. *J. Nutr.,* **2010**, *140*, 489-495.

[67] Planas, J.M.; Alfaras, I.; Colom, H.; Juan, M.E. The bioavailability and distribution of trans-resveratrol are constrained by ABC transporters. *Arch. Biochem. Biophys.,* **2012**, *527*, 67-73.

[68] Patel, K.R.; Scott, E.; Brown, V.A.; Gescher, A.J.; Steward, W.P.; Brown, K. Clinical trials of resveratrol. *Ann N Y Acad Sci,* **2011**, *1215*, 161-169.

[69] Smoliga, J.M.; Vang, O.; Baur, J.A. Challenges of translating basic research into therapeutics: resveratrol as an example. *J. Gerontol. A Biol. Sci. Med. Sci.,* **2012**, *67*, 158-167.

[70] Ellinger, S.; Muller, N.; Stehle, P.; Ulrich-Merzenich, G. Consumption of green tea or green tea products: is there an evidence for antioxidant effects from controlled interventional studies? *Phytomedicine,* **2011**, *18*, 903-915.

[71] Johnson, R.; Bryant, S.; Huntley, A.L. Green tea and green tea catechin extracts: An overview of the clinical evidence. *Maturitas,* **2012**, *73*, 280-287.

[72] Yiannakopoulou, E.C. Effect of green tea catechins on breast carcinogenesis: A systematic review of in-vitro and in-vivo experimental studies. *Eur. J. Cancer Prev.,* **2014**, *23*, 84-89.

[73] Dajas, F. Life or death: Neuroprotective and anticancer effects of quercetin. *J. Ethnopharmacol.,* **2012**, *143*, 383-396.

[74] Poulsen, M.M.; Jorgensen, J.O.; Jessen, N.; Richelsen, B.; Pedersen, S.B. Resveratrol in metabolic health: an overview of the current evidence and perspectives. *Ann. N. Y. Acad. Sci.,* **2013**, *1290*, 74-82.

[75] Murias, M.; Handler, N.; Erker, T.; Pleban, K.; Ecker, G.; Saiko, P.; Szekeres, T.; Jager, W. Resveratrol analogues as selective cyclooxygenase-2 inhibitors: Synthesis and structure-activity relationship. *Bioorg. Med. Chem.,* **2004**, *12*, 5571-5578.

[76] Kundu, J.K.; Shin, Y.K.; Surh, Y.J. Resveratrol modulates phorbol ester-induced pro-inflammatory signal transduction pathways in mouse skin *in vivo*: NF-kappaB and AP-1 as prime targets. *Biochem. Pharmacol.,* **2006**, *72*, 1506-1515.

[77] Park, S.J.; Ahmad, F.; Philp, A.; Baar, K.; Williams, T.; Luo, H.; Ke, H.; Rehmann, H.; Taussig, R.; Brown, A.L.; Kim, M.K.; Beaven, M.A.; Burgin, A.B.; Manganiello, V.; Chung, J.H. Resveratrol ameliorates aging-related metabolic phenotypes by inhibiting cAMP phosphodiesterases. *Cell,* **2012**, *148*, 421-433.

[78] Biasutto, L.; Mattarei, A.; Zoratti, M. Resveratrol and health: the starting point. *ChemBioChem,* **2012**, *13*, 1256-1259.

[79] Mattarei, A.; Azzolini, M.; Carraro, M.; Sassi, N.; Zoratti, M.; Paradisi, C.; Biasutto, L. Acetal Derivatives as Prodrugs of Resveratrol. *Mol. Pharm.,* **2013**, *10*, 2781-2792.

[80] Meng, X.; Maliakal, P.; Lu, H.; Lee, M.J.; Yang, C.S. Urinary and plasma levels of resveratrol and quercetin in humans, mice, and rats after ingestion of pure compounds and grape juice. *J. Agric. Food Chem.,* **2004**, *52*, 935-942.

[81] Biasutto, L.; Zoratti, M. Prodrugs of Quercetin and Resveratrol: A Strategy under Development. *Curr. Drug Metab.,* **2014**, *15*, 77-95.

[82] Mata-Bilbao Mde, L.; Andres-Lacueva, C.; Roura, E.; Jauregui, O.; Escribano, E.; Torre, C.; Lamuela-Raventos, R.M. Absorption and pharmacokinetics of green tea catechins in beagles. *Br. J. Nutr.,* **2008**, *100*, 496-502.

[83] Lin, L.C.; Wang, M.N.; Tseng, T.Y.; Sung, J.S.; Tsai, T.H. Pharmacokinetics of (-)-epigallocatechin-3-gallate in conscious and freely moving rats and its brain regional distribution. *J. Agric. Food Chem.,* **2007**, *55*, 1517-1524.

[84] Lambert, J.D.; Lee, M.J.; Diamond, L.; Ju, J.; Hong, J.; Bose, M.; Newmark, H.L.; Yang, C.S. Dose-dependent levels of epigallocatechin-3-gallate in human colon cancer cells and mouse plasma and tissues. *Drug Metab. Dispos.,* **2006**, *34*, 8-11.

[85] Lambert, J.D.; Lee, M.J.; Lu, H.; Meng, X.; Hong, J.J.; Seril, D.N.; Sturgill, M.G.; Yang, C.S. Epigallocatechin-3-gallate is absorbed but extensively glucuronidated following oral administration to mice. *J. Nutr.,* **2003**, *133*, 4172-4177.

[86] Moon, Y.J.; Wang, L.; DiCenzo, R.; Morris, M.E. Quercetin pharmacokinetics in humans. *Biopharm. Drug Dispos.,* **2008**, *29*, 205-217.

[87] Biasutto, L.; Marotta, E.; Garbisa, S.; Zoratti, M.; Paradisi, C. Determination of quercetin and resveratrol in whole blood--implications for bioavailability studies. *Molecules,* **2010**, *15*, 6570-6579.

[88] Landis-Piwowar, K.; Chen, D.; Foldes, R.; Chan, T.H.; Dou, Q.P. Novel epigallocatechin gallate analogs as potential anticancer agents: a patent review (2009 - present). *Expert Opin. Ther. Pat.,* **2013**, *23*, 189-202.

[89] Bansal, S.; Vyas, S.; Bhattacharya, S.; Sharma, M. Catechin prodrugs and analogs: A new array of chemical entities with improved pharmacological and pharmacokinetic properties. *Nat. Prod. Rep.,* **2013**, *30*, 1438-1454.

[90] Nam, S.; Smith, D.M.; Dou, Q.P. Ester bond-containing tea polyphenols potently inhibit proteasome activity *in vitro* and *in vivo*. *J. Biol. Chem.,* **2001**, *276*, 13322-13330.

[91] Landis-Piwowar, K.R.; Huo, C.; Chen, D.; Milacic, V.; Shi, G.; Chan, T.H.; Dou, Q.P. A novel prodrug of the green tea polyphenol

(-)-epigallocatechin-3-gallate as a potential anticancer agent. *Cancer Res.,* **2007**, *67*, 4303-4310.

[92] Huo, C.; Wan, S.B.; Lam, W.H.; Li, L.; Wang, Z.; Landis-Piwowar, K.R.; Chen, D.; Dou, Q.P.; Chan, T.H. The challenge of developing green tea polyphenols as therapeutic agents. *Inflammopharmacology,* **2008**, *16*, 248-252.

[93] Dou, Q.P. Molecular mechanisms of green tea polyphenols. *Nutr. Cancer,* **2009**, *61*, 827-835.

[94] Davenport, A.; Frezza, M.; Shen, M.; Ge, Y.; Huo, C.; Chan, T.H.; Dou, Q.P. Celastrol and an EGCG pro-drug exhibit potent chemosensitizing activity in human leukemia cells. *Int. J. Mol. Med.,* **2010**, *25*, 465-470.

[95] Lee, S.C.; Chan, W.K.; Lee, T.W.; Lam, W.H.; Wang, X.; Chan, T.H.; Wong, Y.C. Effect of a prodrug of the green tea polyphenol (-)-epigallocatechin-3-gallate on the growth of androgen-independent prostate cancer *in vivo*. *Nutr. Cancer,* **2008**, *60*, 483-491.

[96] Landis-Piwowar, K.; Chen, D.; Chan, T.H.; Dou, Q.P. Inhibition of catechol-Omicron-methyltransferase activity in human breast cancer cells enhances the biological effect of the green tea polyphenol (-)-EGCG. *Oncol. Rep.,* **2010**, *24*, 563-569.

[97] Landis-Piwowar, K.R.; Wan, S.B.; Wiegand, R.A.; Kuhn, D.J.; Chan, T.H.; Dou, Q.P. Methylation suppresses the proteasome-inhibitory function of green tea polyphenols. *J. Cell Physiol.,* **2007**, *213*, 252-260.

[98] Lambert, J.D.; Sang, S.; Hong, J.; Kwon, S.J.; Lee, M.J.; Ho, C.T.; Yang, C.S. Peracetylation as a means of enhancing *in vitro* bioactivity and bioavailability of epigallocatechin-3-gallate. *Drug Metab. Dispos.,* **2006**, *34*, 2111-2116.

[99] Matsumura, K.; Kaihatsu, K.; Mori, S.; Cho, H.H.; Kato, N.; Hyon, S.H. Enhanced antitumor activities of (-)-epigallocatechin-3-O-gallate fatty acid monoester derivatives *in vitro* and *in vivo*. *Biochem. Biophys. Res. Commun.,* **2008**, *377*, 1118-1122.

[100] Mori, S.; Miyake, S.; Kobe, T.; Nakaya, T.; Fuller, S.D.; Kato, N.; Kaihatsu, K. Enhanced anti-influenza A virus activity of (-)-epigallocatechin-3-O-gallate fatty acid monoester derivatives: effect of alkyl chain length. *Bioorg. Med. Chem. Lett.,* **2008**, *18*, 4249-4252.

[101] Matsumoto, Y.; Kaihatsu, K.; Nishino, K.; Ogawa, M.; Kato, N.; Yamaguchi, A. Antibacterial and antifungal activities of new acylated derivatives of epigallocatechin gallate. *Front. Microbiol.,* **2012**, *3*, 53.

[102] Zhong, Y.; Shahidi, F. Lipophilized epigallocatechin gallate (EGCG) derivatives as novel antioxidants. *J. Agric. Food Chem.,* **2011**, *59*, 6526-6533.

[103] Zhong, Y.; Chiou, Y.S.; Pan, M.H.; Shahidi, F. Anti-inflammatory activity of lipophilic epigallocatechin gallate (EGCG) derivatives in LPS-stimulated murine macrophages. *Food Chem.,* **2012**, *134*, 742-748.

[104] Vyas, S.; Manon, B.; Vir Singh, T.; Dev Sharma, P.; Sharma, M. Potential O-acyl-substituted (-)-Epicatechin gallate prodrugs as inhibitors of DMBA/TPA-induced squamous cell carcinoma of skin in Swiss albino mice. *Chem. Biodivers.,* **2011**, *8*, 599-613.

[105] Vyas, S.; Sharma, M.; Sharma, P.D.; Singh, T.V. Design, semisynthesis, and evaluation of O-acyl derivatives of (-)-epigallocatechin-3-gallate as antitumor agents. *J. Agric. Food Chem.,* **2007**, *55*, 6319-6324.

[106] Uesato, S.; Kitagawa, Y.; Hara, Y.; Tokuda, H.; Okuda, M.; Mou, X.Y.; Mukainaka, T.; Nishino, H. Antitumor promoting activities of 3-O-acyl-(-)epigallocatechins. *Bioorg. Med. Chem. Lett.,* **2000**, *10*, 1673-1675.

[107] Uesato, S.; Taniuchi, K.; Kumagai, A.; Nagaoka, Y.; Seto, R.; Hara, Y.; Tokuda, H.; Nishino, H. Inhibitory effects of 3-O-acyl-(+)-catechins on Epstein-Barr virus activation. *Chem. Pharm. Bull. (Tokyo),* **2003**, *51*, 1448-1450.

[108] Kumagai, A.; Nagaoka, Y.; Obayashi, T.; Terashima, Y.; Tokuda, H.; Hara, Y.; Mukainaka, T.; Nishino, H.; Kuwajima, H.; Uesato, S. Tumor chemopreventive activity of 3-O-acylated (-)-epigallocatechins. *Bioorg. Med. Chem.,* **2003**, *11*, 5143-5148.

[109] Park, K.D.; Lee, S.G.; Kim, S.U.; Kim, S.H.; Sun, W.S.; Cho, S.J.; Jeong, D.H. Anticancer activity of 3-O-acyl and alkyl-(-)-epicatechin derivatives. *Bioorg. Med. Chem. Lett.,* **2004**, *14*, 5189-5192.

[110] Ahmed, K.; Wei, Z.L.; Zhao, Q.L.; Nakajima, N.; Matsunaga, T.; Ogasawara, M.; Kondo, T. Role of fatty acid chain length on the induction of apoptosis by newly synthesized catechin derivatives. *Chem. Biol. Interact.,* **2010**, *185*, 182-188.

[111] Matsubara, K.; Saito, A.; Tanaka, A.; Nakajima, N.; Akagi, R.; Mori, M.; Mizushina, Y. Catechin conjugated with fatty acid inhibits DNA polymerase and angiogenesis. *DNA Cell Biol.,* **2006**, *25*, 95-103.

[112] Matsubara, K.; Saito, A.; Tanaka, A.; Nakajima, N.; Akagi, R.; Mori, M.; Mizushina, Y. Epicatechin conjugated with fatty acid is a potent inhibitor of DNA polymerase and angiogenesis. *Life Sci.,* **2007**, *80*, 1578-1585.

[113] Mizushina, Y.; Saito, A.; Horikawa, K.; Nakajima, N.; Tanaka, A.; Yoshida, H.; Matsubara, K. Acylated catechin derivatives: inhibitors of DNA polymerase and angiogenesis. *Front. Biosci. (Elite Ed.),* **2011**, *3*, 1337-1348.

[114] Hiipakka, R.A.; Zhang, H.Z.; Dai, W.; Dai, Q.; Liao, S. Structure-activity relationships for inhibition of human 5alpha-reductases by polyphenols. *Biochem. Pharmacol.,* **2002**, *63*, 1165-1176.

[115] Lin, S.F.; Lin, Y.H.; Lin, M.; Kao, Y.F.; Wang, R.W.; Teng, L.W.; Chuang, S.H.; Chang, J.M.; Yuan, T.T.; Fu, K.C.; Huang, K.P.; Lee, Y.S.; Chiang, C.C.; Yang, S.C.; Lai, C.L.; Liao, C.B.; Chen, P.; Lin, Y.S.; Lai, K.T.; Huang, H.J.; Yang, J.Y.; Liu, C.W.; Wei, W.Y.; Chen, C.K.; Hiipakka, R.A.; Liao, S.; Huang, J.J. Synthesis and structure-activity relationship of 3-O-acylated (-)-epigallocatechins as 5alpha-reductase inhibitors. *Eur. J. Med. Chem.,* **2010**, *45*, 6068-6076.

[116] Park, K.D.; Park, Y.S.; Cho, S.J.; Sun, W.S.; Kim, S.H.; Jung, D.H.; Kim, J.H. Antimicrobial activity of 3-O-acyl-(-)-epicatechin and 3-O-acyl-(+)-catechin derivatives. *Planta Med.,* **2004**, *70*, 272-276.

[117] Picq, M.; Prigent, A.F.; Nemoz, G.; Pacheco, H. Selective inhibition of separated forms of cyclic nucleotide phosphodiesterase from rat heart by some pentasubstituted quercetin analogs. *Biochem. Pharmacol.,* **1982**, *31*, 2777-2782.

[118] Kohli, E.; Raj, H.G.; Kumari, R.; Rohil, V.; Kaushik, N.K.; Prasad, A.K.; Parmar, V.S. Comparison of the prevention of aflatoxin b(1)-induced genotoxicity by quercetin and quercetin pentaacetate. *Bioorg. Med. Chem. Lett.,* **2002**, *12*, 2579-2582.

[119] Chen, Y.C.; Shen, S.C.; Lee, W.R.; Hou, W.C.; Yang, L.L.; Lee, T.J. Inhibition of nitric oxide synthase inhibitors and lipopolysaccharide induced inducible NOS and cyclooxygenase-2 gene expressions by rutin, quercetin, and quercetin pentaacetate in RAW 264.7 macrophages. *J. Cell. Biochem.,* **2001**, *82*, 537-548.

[120] Ortega, M.G.; Saragusti, A.C.; Cabrera, J.L.; Chiabrando, G.A. Quercetin tetraacetyl derivative inhibits LPS-induced nitric oxide synthase (iNOS) expression in J774A.1 cells. *Arch. Biochem. Biophys.,* **2010**, *498*, 105-110.

[121] Iwase, Y.; Takemura, Y.; Ju-ichi, M.; Mukainaka, T.; Ichiishi, E.; Ito, C.; Furukawa, H.; Yano, M.; Tokuda, H.; Nishino, H. Inhibitory effect of flavonoid derivatives on Epstein-Barr virus activation and two-stage carcinogenesis of skin tumors. *Cancer Lett.,* **2001**, *173*, 105-109.

[122] Montenegro, L.; Carbone, C.; Maniscalco, C.; Lambusta, D.; Nicolosi, G.; Ventura, C.A.; Puglisi, G. *In vitro* evaluation of quercetin-3-O-acyl esters as topical prodrugs. *Int. J. Pharm.,* **2007**, *336*, 257-262.

[123] Biasutto, L.; Marotta, E.; De Marchi, U.; Zoratti, M.; Paradisi, C. Ester-based precursors to increase the bioavailability of quercetin. *J. Med. Chem.,* **2007**, *50*, 241-253.

[124] Mattarei, A.; Biasutto, L.; Rastrelli, F.; Garbisa, S.; Marotta, E.; Zoratti, M.; Paradisi, C. Regioselective O-derivatization of quercetin *via* ester intermediates. An improved synthesis of rhamnetin and development of a new mitochondriotropic derivative. *Molecules,* **2010**, *15*, 4722-4736.

[125] Musialik, M.; Kuzmicz, R.; Pawlowski, T.S.; Litwinienko, G. Acidity of hydroxyl groups: an overlooked influence on antiradical properties of flavonoids. *J. Org. Chem.,* **2009**, *74*, 2699-2709.

[126] Huang, H.; Jia, Q.; Ma, J.; Qin, G.; Chen, Y.; Xi, Y.; Lin, L.; Zhu, W.; Ding, J.; Jiang, H.; Liu, H. Discovering novel quercetin-3-O-amino acid-esters as a new class of Src tyrosine kinase inhibitors. *Eur. J. Med. Chem.,* **2009**, *44*, 1982-1988.

[127] Calias, P.; Galanopoulos, T.; Maxwell, M.; Khayat, A.; Graves, D.; Antoniades, H.N.; d'Alarcao, M. Synthesis of inositol 2-phosphate-quercetin conjugates. *Carbohydr. Res.,* **1996**, *292*, 83-90.

[128] Peng, Y.; Deng, Z.; Wang, C. Preparation and prodrug studies of quercetin pentabenzensulfonate. *Yakugaku Zasshi,* **2008**, *128*, 1845-1849.

[129] Kim, M.K.; Park, K.S.; Lee, C.; Park, H.R.; Choo, H.; Chong, Y. Enhanced stability and intracellular accumulation of quercetin by protection of the chemically or metabolically susceptible hydroxyl groups with a pivaloxymethyl (POM) promoiety. *J. Med. Chem.,* **2010**, *53*, 8597-8607.

[130] Kim, M.K.; Park, K.S.; Chong, Y. Remarkable stability and cytostatic effect of a quercetin conjugate, 3,7-bis-O-pivaloxymethyl (POM) quercetin. *Chem.Med.Chem.,* **2012**, *7*, 229-232.

[131] Cho, S.Y.; Kim, M.K.; Park, K.S.; Choo, H.; Chong, Y. Quercetin-POC conjugates: Differential stability and bioactivity profiles between breast cancer (MCF-7) and colorectal carcinoma (HCT116) cell lines. *Bioorg. Med. Chem.,* **2013**, *21*, 1671-1679.

[132] Vacondio, F.; Silva, C.; Mor, M.; Testa, B. Qualitative structure-metabolism relationships in the hydrolysis of carbamates. *Drug Metab. Rev.,* **2010**, *42*, 551-589.

[133] Mulholland, P.J.; Ferry, D.R.; Anderson, D.; Hussain, S.A.; Young, A.M.; Cook, J.E.; Hodgkin, E.; Seymour, L.W.; Kerr, D.J. Pre-clinical and clinical study of QC12, a water-soluble, pro-drug of quercetin. *Ann. Oncol.,* **2001**, *12*, 245-248.

[134] Hirpara, K.V.; Aggarwal, P.; Mukherjee, A.J.; Joshi, N.; Burman, A.C. Quercetin and its derivatives: Synthesis, pharmacological uses with special emphasis on anti-tumor properties and prodrug with enhanced bio-availability. *Anticancer Agents Med. Chem.,* **2009**, *9*, 138-161.

[135] Kim, M.K.; Park, K.S.; Yeo, W.S.; Choo, H.; Chong, Y. *In vitro* solubility, stability and permeability of novel quercetin-amino acid conjugates. *Bioorg. Med. Chem.,* **2009**, *17*, 1164-1171.

[136] Biasutto, L.; Marotta, E.; Mattarei, A.; Beltramello, S.; Caliceti, P.; Salmaso, S.; Bernkop-Schnurch, A.; Garbisa, S.; Zoratti, M.; Paradisi, C. Absorption and metabolism of resveratrol carboxyesters and methanesulfonate by explanted rat intestinal segments. *Cell. Physiol. Biochem.,* **2009**, *24*, 557-566.

[137] Liang, L.; Liu, X.; Wang, Q.; Cheng, S.; Zhang, S.; Zhang, M. Pharmacokinetics, tissue distribution and excretion study of resveratrol and its prodrug 3,5,4'-tri-O-acetylresveratrol in rats. *Phytomedicine,* **2013**, *20*, 558-563.

[138] Marel, A.K.; Lizard, G.; Izard, J.C.; Latruffe, N.; Delmas, D. Inhibitory effects of trans-resveratrol analogs molecules on the proliferation and the cell cycle progression of human colon tumoral cells. *Mol. Nutr. Food Res.,* **2008**, *52*, 538-548.

[139] Colin, D.; Gimazane, A.; Lizard, G.; Izard, J.C.; Solary, E.; Latruffe, N.; Delmas, D. Effects of resveratrol analogs on cell cycle progression, cell cycle associated proteins and 5fluoro-uracil sensitivity in human derived colon cancer cells. *Int. J. Cancer,* **2009**, *124*, 2780-2788.

[140] Hsieh, T.C.; Huang, Y.C.; Wu, J.M. Control of prostate cell growth, DNA damage and repair and gene expression by resveratrol analogues, *in vitro*. *Carcinogenesis,* **2011**, *32*, 93-101.

[141] Hsieh, T.C.; Wong, C.; John Bennett, D.; Wu, J.M. Regulation of p53 and cell proliferation by resveratrol and its derivatives in breast cancer cells: an in silico and biochemical approach targeting integrin alphavbeta3. *Int. J. Cancer,* **2011**, *129*, 2732-2743.

[142] Biasutto, L.; Marotta, E.; Bradaschia, A.; Fallica, M.; Mattarei, A.; Garbisa, S.; Zoratti, M.; Paradisi, C. Soluble polyphenols: synthesis and bioavailability of 3,4',5-tri(alpha-D-glucose-3-O-succinyl) resveratrol. *Bioorg. Med. Chem. Lett.,* **2009**, *19*, 6721-6724.

[143] Lu, Y.; Yu, B.; Dong, H.; Hong, T. Resveratrol derivatives as antitumor agents and their preparation, pharmaceutical compositions and use in the treatment of cancer. Patent CN 102126993, July 20, 2011.

[144] Boaz, N.V. Carbonate derivatives as skin care. U.S. Patent 2012/0059056 A1, March 8, 2012.

[145] Larrosa, M.; Tome-Carneiro, J.; Yanez-Gascon, M.J.; Alcantara, D.; Selma, M.V.; Beltran, D.; Garcia-Conesa, M.T.; Urban, C.; Lucas, R.; Tomas-Barberan, F.; Morales, J.C.; Espin, J.C. Preventive oral treatment with resveratrol pro-prodrugs drastically reduce colon inflammation in rodents. *J. Med. Chem.,* **2010**, *53*, 7365-7376.

[146] Ralph, S.J.; Neuzil, J. Mitochondria as targets for cancer therapy. *Mol. Nutr. Food. Res.,* **2009**, *53*, 9-28.

[147] Wallace, D.C. Mitochondria and cancer. *Nat. Rev. Cancer,* **2012**, *12*, 685-698.

[148] Nunnari, J.; Suomalainen, A. Mitochondria: in sickness and in health. *Cell,* **2012**, *148*, 1145-1159.

[149] Cali, T.; Ottolini, D.; Brini, M. Mitochondrial Ca(2+) as a key regulator of mitochondrial activities. *Adv. Exp. Med. Biol.,* **2012**, *942*, 53-73.

[150] Murphy, M.P. How mitochondria produce reactive oxygen species. *Biochem. J.,* **2009**, *417*, 1-13.

[151] Biasutto, L.; Dong, L.F.; Zoratti, M.; Neuzil, J. Mitochondrially targeted anti-cancer agents. *Mitochondrion,* **2010**, *10*, 670-681.

[152] Gius, D.; Spitz, D.R. Redox signaling in cancer biology. *Antioxid. Redox Signal.,* **2006**, *8*, 1249-1252.

[153] Pani, G.; Giannoni, E.; Galeotti, T.; Chiarugi, P. Redox-based escape mechanism from death: the cancer lesson. *Antioxid. Redox Signal.,* **2009**, *11*, 2791-2806.

[154] Ralph, S.J.; Rodriguez-Enriquez, S.; Neuzil, J.; Saavedra, E.; Moreno-Sanchez, R. The causes of cancer revisited: "mitochondrial malignancy" and ROS-induced oncogenic transformation - why mitochondria are targets for cancer therapy. *Mol. Aspects Med.,* **2010**, *31*, 145-170.

[155] Ziech, D.; Franco, R.; Pappa, A.; Panayiotidis, M.I. Reactive oxygen species (ROS)-induced genetic and epigenetic alterations in human carcinogenesis. *Mutat. Res.,* **2011**, *711*, 167-173.

[156] Policastro, L.; Molinari, B.; Larcher, F.; Blanco, P.; Podhajcer, O.L.; Costa, C.S.; Rojas, P.; Duran, H. Imbalance of antioxidant enzymes in tumor cells and inhibition of proliferation and malignant features by scavenging hydrogen peroxide. *Mol. Carcinog.,* **2004**, *39*, 103-113.

[157] Gokul, S.; Patil, V.S.; Jailkhani, R.; Hallikeri, K.; Kattappagari, K.K. Oxidant-antioxidant status in blood and tumor tissue of oral squamous cell carcinoma patients. *Oral Dis.,* **2010**, *16*, 29-33.

[158] Fiaschi, T.; Chiarugi, P. Oxidative stress, tumor microenvironment, and metabolic reprogramming: a diabolic liaison. *Int. J. Cell Biol.,* **2012**, *2012*, 762825.

[159] Ishikawa, K.; Takenaga, K.; Akimoto, M.; Koshikawa, N.; Yamaguchi, A.; Imanishi, H.; Nakada, K.; Honma, Y.; Hayashi, J. ROS-generating mitochondrial DNA mutations can regulate tumor cell metastasis. *Science,* **2008**, *320*, 661-664.

[160] Patten, D.A.; Lafleur, V.N.; Robitaille, G.A.; Chan, D.A.; Giaccia, A.J.; Richard, D.E. Hypoxia-inducible factor-1 activation in nonhypoxic conditions: the essential role of mitochondrial-derived reactive oxygen species. *Mol. Biol. Cell,* **2010**, *21*, 3247-3257.

[161] Tormos, K.V.; Chandel, N.S. Inter-connection between mitochondria and HIFs. *J. Cell. Mol. Med.,* **2010**, *14*, 795-804.

[162] Schumacker, P.T. Reactive oxygen species in cancer cells: Live by the sword, die by the sword. *Cancer Cell,* **2006**, *10*, 175-176.

[163] Gupta, S.C.; Hevia, D.; Patchva, S.; Park, B.; Koh, W.; Aggarwal, B.B. Upsides and downsides of reactive oxygen species for cancer: the roles of reactive oxygen species in tumorigenesis, prevention, and therapy. *Antioxid. Redox Signal.,* **2012**, *16*, 1295-1322.

[164] Groeger, G.; Quiney, C.; Cotter, T.G. Hydrogen peroxide as a cell-survival signaling molecule. *Antioxid. Redox Signal.,* **2009**, *11*, 2655-2671.

[165] Verschoor, M.L.; Wilson, L.A.; Singh, G. Mechanisms associated with mitochondrial-generated reactive oxygen species in cancer. *Can. J. Physiol. Pharmacol.,* **2010**, *88*, 204-219.

[166] Circu, M.L.; Aw, T.Y. Reactive oxygen species, cellular redox systems, and apoptosis. *Free Radic. Biol. Med.,* **2010**, *48*, 749-762.

[167] Orrenius, S.; Zhivotovsky, B. Cardiolipin oxidation sets cytochrome c free. *Nat. Chem. Biol.,* **2005**, *1*, 188-189.

[168] Biasutto, L.; Sassi, N.; Mattarei, A.; Marotta, E.; Cattelan, P.; Toninello, A.; Garbisa, S.; Zoratti, M.; Paradisi, C. Impact of mitochondriotropic quercetin derivatives on mitochondria. *Biochim. Biophys. Acta,* **2010**, *1797*, 189-196.

[169] Ueda, S.; Masutani, H.; Nakamura, H.; Tanaka, T.; Ueno, M.; Yodoi, J. Redox control of cell death. *Antioxid. Redox Signal.,* **2002**, *4*, 405-414.

[170] Takeda, K.; Naguro, I.; Nishitoh, H.; Matsuzawa, A.; Ichijo, H. Apoptosis signaling kinases: from stress response to health outcomes. *Antioxid. Redox Signal.,* **2011**, *15*, 719-761.

[171] Rasola, A.; Bernardi, P. Mitochondrial permeability transition in Ca(2+)-dependent apoptosis and necrosis. *Cell Calcium,* **2011**, *50*, 222-233.
[172] Neuzil, J.; Dong, L.F.; Rohlena, J.; Truksa, J.; Ralph, S.J. Classification of mitocans, anti-cancer drugs acting on mitochondria. *Mitochondrion,* **2013**, *13*, 199-208.
[173] Halliwell, B. Are polyphenols antioxidants or pro-oxidants? What do we learn from cell culture and *in vivo* studies? *Arch. Biochem. Biophys.,* **2008**, *476*, 107-112.
[174] Perron, N.R.; Brumaghim, J.L. A review of the antioxidant mechanisms of polyphenol compounds related to iron binding. *Cell Biochem. Biophys.,* **2009**, *53*, 75-100.
[175] De Marchi, U.; Biasutto, L.; Garbisa, S.; Toninello, A.; Zoratti, M. Quercetin can act either as an inhibitor or an inducer of the mitochondrial permeability transition pore: A demonstration of the ambivalent redox character of polyphenols. *Biochim. Biophys. Acta,* **2009**, *1787*, 1425-1432.
[176] Calabrese, V.; Cornelius, C.; Trovato, A.; Cavallaro, M.; Mancuso, C.; Di Rienzo, L.; Condorelli, D.; De Lorenzo, A.; Calabrese, E.J. The hormetic role of dietary antioxidants in free radical-related diseases. *Curr. Pharm. Des.,* **2010**, *16*, 877-883.
[177] Kundu, J.K.; Surh, Y.J. Nrf2-Keap1 signaling as a potential target for chemoprevention of inflammation-associated carcinogenesis. *Pharm. Res.,* **2010**, *27*, 999-1013.
[178] Leanza, L.; Trentin, L.; Becker, K.A.; Frezzato, F.; Zoratti, M.; Semenzato, G.; Gulbins, E.; Szabo, I. Clofazimine, Psora-4 and PAP-1, inhibitors of the potassium channel Kv1.3, as a new and selective therapeutic strategy in chronic lymphocytic leukemia. *Leukemia,* **2013**, *27*, 1782-1785.
[179] Ralph, S.J.; Rodriguez-Enriquez, S.; Neuzil, J.; Moreno-Sanchez, R. Bioenergetic pathways in tumor mitochondria as targets for cancer therapy and the importance of the ROS-induced apoptotic trigger. *Mol. Aspects Med.,* **2010**, *31*, 29-59.
[180] Trachootham, D.; Alexandre, J.; Huang, P. Targeting cancer cells by ROS-mediated mechanisms: a radical therapeutic approach? *Nat. Rev. Drug Discov.,* **2009**, *8*, 579-591.
[181] Murphy, M.P. Targeting lipophilic cations to mitochondria. *Biochim. Biophys. Acta,* **2008**, *1777*, 1028-1031.
[182] Murphy, M.P.; Smith, R.A. Targeting antioxidants to mitochondria by conjugation to lipophilic cations. *Annu. Rev. Pharmacol. Toxicol.,* **2007**, *47*, 629-656.
[183] Smith, R.A.; Hartley, R.C.; Cocheme, H.M.; Murphy, M.P. Mitochondrial pharmacology. *Trends Pharmacol. Sci.,* **2012**, *33*, 341-352.
[184] Hoye, A.T.; Davoren, J.E.; Wipf, P.; Fink, M.P.; Kagan, V.E. Targeting mitochondria. *Acc. Chem. Res.,* **2008**, *41*, 87-97.
[185] Modica-Napolitano, J.S.; Aprille, J.R. Delocalized lipophilic cations selectively target the mitochondria of carcinoma cells. *Adv. Drug Deliv. Rev.,* **2001**, *49*, 63-70.
[186] Biasutto, L.; Mattarei, A.; Marotta, E.; Bradaschia, A.; Sassi, N.; Garbisa, S.; Zoratti, M.; Paradisi, C. Development of mitochondria-targeted derivatives of resveratrol. *Bioorg. Med. Chem. Lett.,* **2008**, *18*, 5594-5597.

Received: April 09, 2014 **Revised: May 05, 2014** **Accepted: June 25, 2014**

[187] Mattarei, A.; Biasutto, L.; Marotta, E.; De Marchi, U.; Sassi, N.; Garbisa, S.; Zoratti, M.; Paradisi, C. A mitochondriotropic derivative of quercetin: a strategy to increase the effectiveness of polyphenols. *ChemBioChem,* **2008**, *9*, 2633-2642.
[188] Mattarei, A.; Sassi, N.; Durante, C.; Biasutto, L.; Sandonà, G.; Marotta, E.; Garbisa, S.; Gennaro, A.; Paradisi, C.; Zoratti, M. Redox properties and cytotoxicity of synthetic isomeric mitochondriotropic derivatives of the natural polyphenol quercetin. *Eur. J. Org. Chem.,* **2011**, *2011*, 5577-5586.
[189] Sassi, N.; Mattarei, A.; Azzolini, M.; Bernardi, P.; Szabo, I.; Paradisi, C.; Zoratti, M.; Biasutto, L. Mitochondria-targeted resveratrol derivatives act as cytotoxic pro-oxidants. *Curr. Pharm. Des.,* **2014**, *20*, 172-179.
[190] Lin, X.; Wu, G.; Huo, W.Q.; Zhang, Y.; Jin, F.S. Resveratrol induces apoptosis associated with mitochondrial dysfunction in bladder carcinoma cells. *Int. J. Urol.,* **2012**, *19*, 757-764.
[191] Delmas, D.; Solary, E.; Latruffe, N. Resveratrol, a phytochemical inducer of multiple cell death pathways: apoptosis, autophagy and mitotic catastrophe. *Curr. Med. Chem.,* **2011**, *18*, 1100-1121.
[192] Liu, K.C.; Yen, C.Y.; Wu, R.S.; Yang, J.S.; Lu, H.F.; Lu, K.W.; Lo, C.; Chen, H.Y.; Tang, N.Y.; Wu, C.C.; Chung, J.G. The roles of endoplasmic reticulum stress and mitochondrial apoptotic signaling pathway in quercetin-mediated cell death of human prostate cancer PC-3 cells. *Environ. Toxicol.,* **2014**, *29*, 428-439.
[193] Sassi, N.; Biasutto, L.; Mattarei, A.; Carraro, M.; Giorgio, V.; Citta, A.; Bernardi, P.; Garbisa, S.; Szabo, I.; Paradisi, C.; Zoratti, M. Cytotoxicity of a mitochondriotropic quercetin derivative: mechanisms. *Biochim. Biophys. Acta,* **2012**, *1817*, 1095-1106.
[194] Sassi, N.; Mattarei, A.; Azzolini, M.; Szabo', I.; Paradisi, C.; Zoratti, M.; Biasutto, L. Cytotoxicity of mitochondria-targeted resveratrol derivatives: Interactions with respiratory chain complexes and ATP synthase. *Biochim. Biophys. Acta*, **2014**, in press. doi: 10.1016/j.bbabio.2014.06.010.
[195] Ripcke, J.; Zarse, K.; Ristow, M.; Birringer, M. Small-molecule targeting of the mitochondrial compartment with an endogenously cleaved reversible tag. *ChemBioChem,* **2009**, *10*, 1689-1696.
[196] Anders, M.W. Putting bioactivation reactions to work: Targeting antioxidants to mitochondria. *Chem. Biol. Interact.,* **2011**, *192*, 8-13.
[197] Anders, M.W. Exploiting endobiotic metabolic pathways to target xenobiotic antioxidants to mitochondria. *Mitochondrion,* **2013**, *13*, 454-463.
[198] Roser, K.S.; Brookes, P.S.; Wojtovich, A.P.; Olson, L.P.; Shojaie, J.; Parton, R.L.; Anders, M.W. Mitochondrial biotransformation of omega-(phenoxy)alkanoic acids, 3-(phenoxy)acrylic acids, and omega-(1-methyl-1H-imidazol-2-ylthio)alkanoic acids: a prodrug strategy for targeting cytoprotective antioxidants to mitochondria. *Bioorg. Med. Chem.,* **2010**, *18*, 1441-1448.
[199] Smith, R.A.; Murphy, M.P. Animal and human studies with the mitochondria-targeted antioxidant MitoQ. *Ann. N. Y. Acad. Sci.,* **2010**, *1201*, 96-103.
[200] Skulachev, V.P. A biochemical approach to the problem of aging: "megaproject" on membrane-penetrating ions. The first results and prospects. *Biochemistry (Mosc.),* **2007**, *72*, 1385-1396.

10. Mitochondria-targeted resveratrol derivatives act as cytotoxic pro-oxidants

172 *Current Pharmaceutical Design*, 2014, *20*, 172-179

Mitochondria-targeted Resveratrol Derivatives Act as Cytotoxic Pro-oxidants

Nicola Sassi[a], Andrea Mattarei[b,c], Michele Azzolini[a], Paolo Bernardi[a,b], Ildiko' Szabo'[d], Cristina Paradisi[c], Mario Zoratti[a,b] and Lucia Biasutto[a,b,*]

[a]*Dept. of Biomedical Sciences, University of Padova;* [b]*CNR Institute of Neuroscience, Padova;* [c]*Dept. of Chemical Sciences, University of Padova;* [d]*Dept. of Biology, University of Padova*

Abstract: Resveratrol derivatives bearing an O-linked mitochondria-targeting 4-triphenylphosphoniumbutyl group at either position 3 or position 4' are prooxidant and cytotoxic for cultured cells, selectively killing fast-growing cells when supplied in the low μM range. Resveratrol is essentially without effect under these experimental conditions, while the cytotoxicity of the mitochondriotropic derivatives increases if they are methylated on the remaining hydroxyls. Experiments with $Bax^{-/-}/Bak^{-/-}$ cells and a pan-caspase inhibitor show that cell death is mostly of the necrotic type. Cytotoxicity is due to ROS produced upon accumulation of the compounds into mitochondria, and specifically to H_2O_2, since externally added membrane-permeant catalase largely prevents cell death while superoxide dismutase potentiates toxicity. The mitochondriotropic compounds cause ROS-independent depolarization of *in situ* mitochondria. Effectiveness is increased if resveratrol hydroxyls are acetylated or methylated; this excludes the involvement of autooxidation of the polyphenolic nucleus and a protonophoric cycle as the causes of ROS generation and of depolarization, respectively. Resveratrol-triphenylphosphonium conjugates may thus represent a new class of chemotherapeutic agents, redox-active "mitocans", whose mechanisms of action and *in vivo* activity are worthy of further investigation.

Keywords: Resveratrol, mitochondria, mitocans, cancer, reactive oxygen species.

INTRODUCTION

Modulating mitochondrial redox processes is an attractive challenge. These organelles are deeply involved in key cellular functions, such as ATP production, Ca^{2+} homeostasis [1] and cell death [2, 3], and are the subcellular compartment in which most Reactive Oxygen Species (ROS) are produced [4]. Enhanced ROS production is the common theme in the pathophysiology of many diseases, including cancer, I/R damage, diabetes, aging, and neurodegeneration [5]. ROS are believed to be a factor in carcinogenesis [6, 7]. The metastatic potential of cell lines is correlated to the level of ROS production by mitochondria [8]. Mitochondrial ROS are involved in the activation of Hypoxia Inducible Factor (HIF) [9], which influences angiogenesis and other aspects of tumor growth [10]. On the other hand, oxidative stress can activate pro-apoptotic signalling involving kinases (i.e., ASK1, JNK, p38, MAPK), transcription factors (i.e., p53, c-Jun) and members of the Bcl-2 family [5, 11, 12]. Oxidation of cardiolipin is needed for the release of cytochrome c [13]. Furthermore, ROS are known to induce the Mitochondrial Permeability Transition (MPT) [14]; MPT is now believed to have a fundamental role in necrotic death, such as occurs, e.g., upon reoxygenation following ischemia [15, 16]. Hindering ROS production may thus limit damage due to ischemia, neurodegeneration or aging, and oppose cancer metastasis, while targeted ROS enhancement may provide a way to eliminate cancer cells.

This has led to the birth of a new sector of pharmacology, which targets mitochondria to prevent or to induce, as the case may be, cell death [17, 18]. The most versatile strategy to target compounds to mitochondria involves coupling to a membrane-permeable lipophilic cation such as triphenylphosphonium which will drive accumulation in compartments held at negative relative voltage, such as the mitochondrial matrix, according to Nernst's law [19].

*Address correspondence to this author at the CNR Institute of Neuroscience, c/o Dept. of Biomedical Sciences, Viale Giuseppe Colombo 3, 35121 Padova, Italy; Tel: +39 049 8276483; Fax: +39 049 8276049;
E-mail: lucia.biasutto@unipd.it

These agents may exhibit selectivity towards tumor cells because of the higher mitochondrial potential ($\Delta\Psi_m$) of the latter compared to their non-tumoral counterpart [20, 21]. Cancer cells produce their ATP mostly by glycolysis (the Warburg effect), exhibiting reduced oxidative phosphorylation activity; the mitochondrial electrochemical proton gradient is thus dissipated less efficiently, and the transmembrane potential is increased [22]. Moreover, mitochondrial membrane potential seems to be correlated to tumor aggressiveness. Cells with higher $\Delta\Psi_m$ have higher levels of Vascular Endothelial Growth Factor (VEGF) and matrix metalloproteinase 7 (MMP7), and increased invasive behavior compared to cancer cells with lower $\Delta\Psi_m$ [23].

Polyphenols are plant-derived redox-active compounds with potentially useful biological properties, including the modulation of mitochondrial biogenesis and functionality via AMPK [5]. They can interact with mitochondrial components and modulate redox processes. To enhance their therapeutic potential, we are developing derivatives targeted to mitochondria by conjugation with triphenylphosphonium [24, 25]. Quercetin and resveratrol were chosen as model compounds. This study utilizes derivatives of resveratrol.

Several publications have reported that resveratrol at high dosages (e.g. 100 μM) can be cytotoxic for cancer cells (e.g.: [26]; rev.: [27]). "Intrinsic" apoptosis is generally reported to occur (e.g. [28]). Mitochondrial depolarization (e.g. [26, 28, 29]) and ROS production (e.g. [26, 29]) are observed. Cytotoxicity appears to be a dose-dependent effect; at lower concentrations, resveratrol may instead have a protective action on mitochondria (revs.: [5, 30]). These results and considerations suggest that targeting resveratrol to mitochondria and increasing its concentration in the organelles may enhance its cytotoxic activity and may possibly lead to oncological applications. In fact, mitochondria-targeted liposomes containing resveratrol have provided encouraging results [31].

We previously showed that a mitochondriotropic derivative of quercetin, 7-O-(4-triphenylphosphoniumbutyl)quercetin iodide (Q-7BTPI), in the low-μM range, displays selective cytotoxicity vs. cancerous and fast-growing cells *in vitro*. Cytotoxicity is due to hydrogen peroxide (H_2O_2) produced upon its accumulation into

1873-4286/14 $58.00+.00

mitochondria [32]. The mechanism of ROS generation appears to be a chain "autooxidation" mechanism, which requires that at least part of the hydroxyl groups in the molecule should be free. Preliminary work showed that also two mitochondriotropic derivatives of resveratrol - 4'-O-(4- triphenylphosphoniumbutyl) resveratrol iodide (R-4'BTPI) and its diacetylated analog 3,5-diacetyl-4'-O-(4-triphenylphosphoniumbutyl) resveratrol iodide (RDA-4'BTPI) - are selectively cytotoxic at low μM concentrations [25]. We report here a study of structure-activity on mitochondriotropic resveratrol derivatives, as well as on the basic mechanisms underlying their cytotoxic behavior.

MATERIALS AND METHODS

Experiments were performed at least in triplicate, and averages ± s.d are reported.

Materials. Resveratrol was purchased from Waseta Int. Trading Co (Shangai, P.R.China). Other chemicals were purchased from Sigma-Aldrich (Milan) unless otherwise specified. All chemicals for buffer preparation were of laboratory grade, obtained from Merck, J.T. Baker or Sigma.

O-(4-chlorobutyl) resveratrol was the starting reagent for the synthesis of all mitochondriotropic derivatives described in this work. The alkylation reaction was performed as described in [25], and yielded a mixture of 4'- and 3- O-substitution products which were separated by flash column chromatography (see Supplementary material for details). Triphenylphosphonium ($P^+Ph_3\Gamma$) was introduced through two consecutive nucleophilic substitution steps: –Cl → –I → – $P^+Ph_3\Gamma$. The procedures described in [25] were used to obtain 4'-O-(4- triphenylphosphoniumbutyl) resveratrol iodide (R-4'BTPI), 3-O-(4- triphenylphosphoniumbutyl) resveratrol iodide (R-3BTPI), and their acetylated analogs 3,5-diacetyl-4'-O-(4-triphenylphosphoniumbutyl) resveratrol iodide (RDA-4'BTPI) and 4',5-diacetyl-3-O-(4- triphenylphosphoniumbutyl) resveratrol iodide (RDA-3BTPI). 3,5-dimethyl-4'-O-(4- triphenylphosphoniumbutyl) resveratrol iodide (RDM-4'BTPI) and 4',5-dimethyl-3-O-(4-triphenylphosphoniumbutyl) resveratrol iodide (RDM-3BTPI) were obtained via a dimethyl-(4-iodobutyl) intermediate (RDM-4'BI or RDM-3BI). Details of the synthetic protocols and spectral data for the four novel compounds are reported in the Supplementary material.

Cells and mitochondria. Fast- (doubling time 16 hours) and slow- (doubling time 3 days) growing SV-40 immortalized Mouse Embryo Fibroblast (MEF) cells and mouse colon cancer CT-26 cells (doubling time 24 hours) were grown in Dulbecco's Modified Eagle Medium (DMEM)-supplemented with 10 mM HEPES buffer (pH 7.4), 10% (v/v) fetal bovine serum (FBS, Invitrogen), 100 U/mL penicillin G, 0.1 mg/mL streptomycin, 2 mM glutamine (GIBCO) and 1% nonessential amino acids (100× solution; GIBCO), in a humidified atmosphere of 5% CO_2 at 37°C. Jurkat T lymphocytes (doubling time 24 hours) were grown in RPMI-1640 supplemented as above.

Cell growth/viability (MTT) assays. CT-26 or MEF cells were seeded in standard 96-well plates and allowed to grow overnight in DMEM + 10% FBS (200 μL) to insure attachment. Initial densities were 3000 (for CT-26), 1000 (for fast-growing MEF) and 2500 (for slow-growing MEF) cells/well. After cell attachment, the growth medium was replaced with DMEM + 10% FBS containing the desired compounds at different concentrations. Final DMSO concentration was 0.1% in all cases (including controls). Four wells were used for each condition. Cells were incubated with the compounds for 72 hours; every 24 hours the medium was substituted by a fresh aliquot (with compounds). At the end of the incubation period the medium was removed and 100 μL of PBS containing 10% CellTiter 96® AQUEOUS One solution (Promega) were added into each well. After 1 h of color development at 37°C, absorbance at 490 nm was measured using a Packard Spectra Count 96-well plate reader. All measurements were performed in quadruplicate in each experiment.

Superoxide production assays. Superoxide generation in cells (*in situ* mitochondria) was measured in FACS (Fluorescence-Activated Cell Scanning) experiments using the mitochondriotropic probe MitoSOX™ Red (Invitrogen/Molecular Probes), as described in [32]. Briefly, Jurkat lymphocytes were washed and resuspended in Hank's Balanced Salt Solution (HBSS) at a density of $1{,}5 \times 10^6$ cells/mL and loaded with 1 μM MitoSOX™ Red in the presence of Cyclosporin A (CsA; 5μM) (37°C, 20 min). After loading, cells were diluted 1:5 in HBSS (plus CsA) and divided into identical aliquots. At time zero the various compounds were added and data were collected after the desired incubation times (10000 cells were counted for each measurement). A Beckton Dickinson Canto II flow cytometer was used. Excitation was at 488 nm and fluorescence was collected in the 542-585 nm interval. Data were analyzed using the BD VISTA software. Averages ± s.d. of the medians of cells fluorescence distribution histograms are plotted, normalized to the value measured immediately after addition of the compounds (time = 0).

Mitochondrial potential assays. Tetramethylrhodamine methyl ester (TMRM; Invitrogen/Molecular Probes) staining was used to monitor mitochondrial transmembrane potential of Jurkat lymphocytes by FACS. Cells were loaded with 20 nM TMRM for 20 min, in the presence of CsA. Procedures were then the same as described above for superoxide production assays.

Annexin/PI labelling assays. For the evaluation of cell death, Jurkat cells were labelled with Annexin V-FLUOS (Roche) and Propidium Iodide (PI), and analyzed by FACS. Briefly, cells were washed, resuspended in HBSS at a density of 3×10^5 cells/mL, and subsequently treated with compounds for 3 hours at 37°C, 5% CO_2. A 200 μl aliquot of each sample was then incubated with PI (final concentration 1 μg/mL) and Annexin V-FLUOS (1 μL/sample) in the dark at 37°C, 15 min. Samples were finally analyzed by FACS (5000 cells for each measurement). Results are presented either as percentage of cells labelled by either Annexin V-FLUOS, PI, or both (Fig. **2**), or alternatively as percentage of cell not labelled by either reagent (Fig. **4**). In this latter case the percentage of unlabelled cells in the control sample of each experiment is set as 100%.

Stability. To assess the stability of the derivatives under the conditions used in FACS experiments, Jurkat cells were washed and resuspended in HBSS at a density of 3×10^5 cells/mL. 1 mL aliquots were transferred to a 24-well plate, and incubated with the various mitochondriotropic resveratrol derivatives (5 μM, 0.1% final DMSO) for 0.5, 1, 2 and 3 hours. At the end of the experiment, cells and medium were collected together for each experimental condition; 10 μl Acetic acid (6 M), 10 μl Ascorbic acid (100 mM) and 1 mL acetone were added. The mixture was sonicated 2 min, and then centrifuged 8 min, 10000*g*; supernatant was collected and stored at -20°C. Samples (2 μl) were analyzed by HPLC (Agilent 1290 Infinity LC System) using a reversed phase column (Zorbax Extend C18, 3.5 μm, 50 × 2.1 mm i.d.) and a UV diode array detector. Solvents A and B were water containing 0.1% trifluoroacetic acid (TFA) and acetonitrile, respectively. The gradient for B was as follows: 30% for 1 min, from 30% to 65% in 3 min, then from 65% to 100% in 1 min; the flow rate was 0.8 mL/min. The eluate was preferentially monitored at 300 and 320 nm.

Fluorescence microscopy. The weak intrinsic fluorescence emission (exciting at 300-340 nm) of the derivatives was exploited to follow their localization in cultured cells. Slow-growing MEF cells were seeded (75000 cells/well) onto 24-mm coverslips in 6-well plates and grown for about two days in DMEM + 10%FBS. Coverslips were then mounted onto holders, washed twice with HBSS, and covered with 1 ml of DMEM without FBS and Phenol Red and supplemented with 2 μM CsA. An Olympus Biosystems

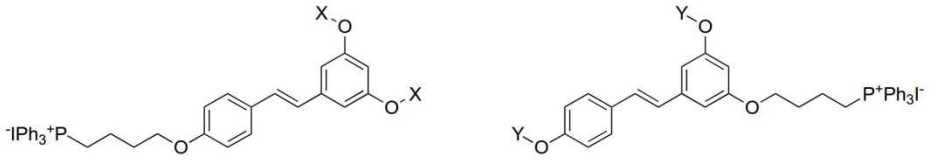

R-4'BTPI: X = H
RDA-4'BTPI: X = -C(=O)CH_3
RDM-4'BTPI: X = -CH_3

R-3BTPI: Y = H
RDA-3BTPI: Y = -C(=O)CH_3
RDM-3BTPI: Y = -CH_3

Scheme 1. Mitochondriotropic resveratrol derivatives studied in this work.

apparatus comprising an Olympus IX71 microscope and MT20 light source was used; images were acquired automatically at 1-min intervals and processed with CellR® software. Excitation was at 340 ± 15 nm and fluorescence was collected at λ > 400 nm. Additions were performed by withdrawing 0.5 ml of incubation medium, and adding back the solution into the chamber at a peripheral point. All images are presented using the same display parameters, and thus fluorescence intensities can be compared.

RESULTS

The redox properties of a polyphenol may be altered by the introduction of a substituent, and they may depend on the position occupied [33]. We thus synthesized and tested both mitochondriotropic resveratrol isomers, bearing the 4-triphenylphosphoniumbutyl (BTPI) group at either position -3 or -4'. To study the role of free hydroxyls, which were proven to be essential for the effectiveness of the quercetin mitochondriotropic derivative Q-7BTPI [32], we also synthesized their analogs with the remaining hydroxyls blocked by acetyl or methyl groups, respectively (Scheme **1**). While the acetylated compounds can undergo hydrolysis with regeneration of the free hydroxyls (see below), the methyl ether bond is stable under all our experimental conditions.

The six compounds were tested for their cytotoxic/cytostatic action on three cultured cell lines: CT-26 (a murine colon cancer cell line), and fast- or slow-growing MEFs (non-tumoral cell lines). The tetrazolium salt reduction (MTT) assay was used to quantify cell growth and viability. Figure **1** illustrates the results. Confirming the observations by [25], the mitochondriotropic resveratrol derivatives with free or acetylated hydroxyls turned out to be cytotoxic for tumoral (CT-26; Fig. **1A**) and fast-growing MEF cells (Fig. **1B**), with a much milder effect on slow-growing MEF cells (Fig. **1C**). The effect was dose-dependent.

Methylated mitochondriotropic derivatives proved to be more toxic than the others, giving similar experimental readouts at a 5-fold lower concentration (1 μM vs. 5 μM, respectively). All compounds displayed selectivity, killing cancerous CT-26 and fast-growing MEFs more efficiently than slow-growing MEFs. The isomeric structure of the compounds did not make a major difference. Furthermore, the effects of the acetylated derivatives were similar to those of R-3BTPI and R-4'BTPI. This latter observation may be considered to reflect the experimental conditions of these assays, which include a 72 h incubation period and the necessary use of FBS-supplemented culture medium. Serum albumin is known to have an intrinsic esterase activity [34], and the incubation of RDA-BTPIs with cells in the presence of FBS led to complete hydrolysis to R-BTPIs within 2 h (not shown), so that the effects observed are essentially those of R-3BTPI and R-4'BTPI. These experiments therefore did not actually allow a comparison of the effects of non-acetylated and acetylated derivatives. Resveratrol and a methyl-triphenylphosphonium (TPMP) salt at the same concentrations did not have any impact on the cells.

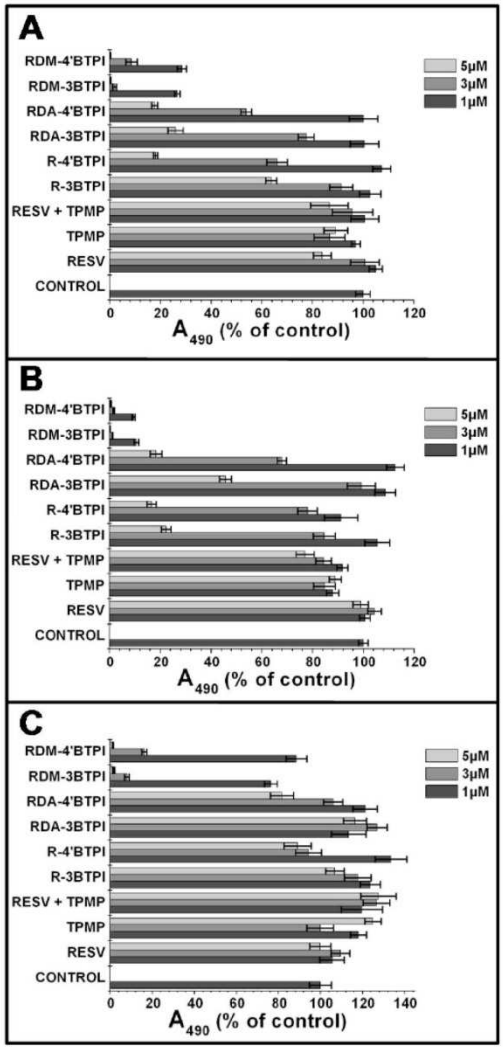

Fig. (1). Effects of resveratrol derivatives on the readout of MTT assays. Cells were allowed to grow for 3 days in the presence of the specified compounds (see Materials and Methods for details). **A**) CT-26 mouse colon tumor cells; **B**) Fast-growing Mouse Embrionic Fibroblasts (MEF); **C**) Slow-growing MEF. RESV= Resveratrol.

We studied cell death also in FACS experiments, staining with Annexin V-FLUOS and PI after a 3h incubation with the compounds. We used Jurkat lymphocytes because these cells grow in suspension, and thus possible side effects of traumatic detachment were avoided. Also using this experimental approach all six compounds proved to be cytotoxic, the methylated ones being the most effective (Fig. **2**): in these experiments the RDM-BTPIs were used at 1 μM, while R-BTPIs and RDA-BTPIs were used at 5 μM. These concentrations are high enough to have clear cytotoxic effects in MTT and Annexin/PI labelling assays, but do not cause major changes in forward- and side-scatter parameters during the course of the FACS experiment.

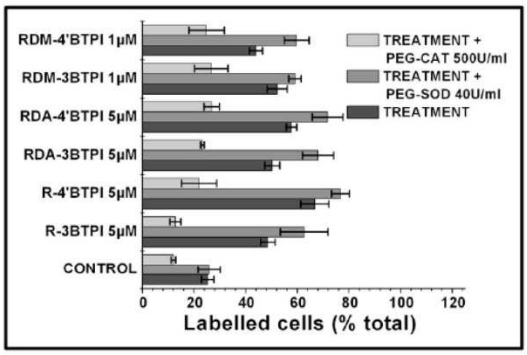

Fig. (2). Effects of resveratrol derivatives on Jurkat cells, 3h. FACS experiments measuring Annexin and/or PI labelling of Jurkat cells incubated with the indicated compounds in HBSS, in the absence or presence of PEG-SOD or PEG-CAT. When PEG-SOD (40 U/ml) or PEG-CAT (500 U/ml) were present, cells were incubated with the enzyme for 30 min before addition of the derivatives, as well as throughout the experiment.

We verified whether oxidative stress and autooxidation might be the cause of the cytotoxicity of mitochondriotropic resveratrol derivatives, as is the case for Q-7BTPI [32]. Mitochondrial superoxide production was monitored in FACS experiments with Jurkat cells, using the mitochondria-targeted fluorescent indicator MitoSOX^{TM} Red. The selectivity of MitoSOX^{TM} Red for superoxide was confirmed using PEG-SOD (40 U/ml), a membrane-permeant form of SuperOxide Dismutase, which markedly suppressed the fluorescence increase (not shown). Cyclosporine A (CsA) was routinely provided with MitoSOX^{TM} Red to block MDR pumps, thus increasing dye load. Its replacement by CsH, which inhibits MDR pumps but not the MPT, had no influence on the MitoSOX^{TM} Red response (not shown). To exclude possible contributions of processes associated with cell death to ROS production, only vital cells were selected for analysis on the basis of forward- and side-scatter parameters. The results are presented in (Fig. **3**). All compounds induced superoxide generation, RDA-4'BTPI and methylated derivatives being the most effective. Acetyl groups were only partially hydrolyzed under the conditions of FACS experiments in the presence of cells (Supplementary Fig. **1**; about 10 or 40% of RDA-3BTPI or RDA-4'BTPI was completely hydrolyzed to R-3BTPI or R-4'BTPI, respectively, over 2h). Methylated derivatives were completely stable in the same experimental conditions. Resveratrol, a TPMP salt or a combination of them did not affect the MitoSOX^{TM} Red response (Supplementary Fig. **2**).

We verified whether ROS generation was the cause of cell death. In FACS experiments with Annexin/PI staining of Jurkat cells, PEG-SOD did not have any protective effect, but actually increased staining, while PEG-CAT was able to rescue cells from death (Fig. **2**). We can thus conclude that hydrogen peroxide is the toxic specie.

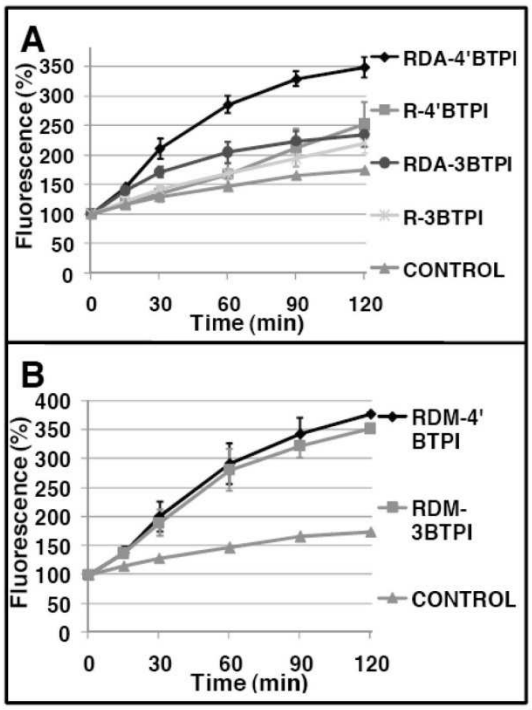

Fig. (3). Resveratrol derivatives elicit production of superoxide anion in the mitochondria of Jurkat cells. Cells were incubated with: **A**) 5 μM acetylated or non acetylated derivatives, or **B**) 1 μM methylated derivatives. MitoSOX^{TM} Red fluorescence was monitored by FACS.

ROS can induce both necrotic or apoptotic cell death; quantitative aspects and concurrent cellular signalling are very relevant for the outcome. MTT assays with double knock-out cells lacking both key pro-apoptotic proteins Bax and Bak, and FACS experiments in the presence of the pan-caspase inhibitor z-VAD-fmk showed that the derivatives bearing the mitochondria-targeting group at position 3 and RDM-4'BTPI mainly caused necrotic cell death, since the lack of Bax and Bak or the presence of z-VAD-fmk had little effect on the readout. By the same criteria, R-4'BTPI and RDA-4'BTPI additionally induced apoptosis in a fraction of the cells (Fig. **4**).

Resveratrol at high (e.g. 100 μM) concentrations has been reported to induce mitochondrial depolarization [26, 28, 29]. Mitochondrial potential was therefore monitored in FACS experiments with Jurkat cells labelled with TMRM. TMRM fluorescence decrease was in fact observed. RDM-BTPIs and RDA-BTPIs were more effective (Fig. **5B**, **C**) than their counterparts with free hydroxyls (Fig. **5A**).

Mitochondriotropic quercetin derivatives cause a loss of TMRM fluorescence by competing for the binding sites of the dye on membranes, independently of effects on the transmembrane potential [32]. This complication can be eliminated by performing the measurements in the presence of tetramethyl-7-O-(4-triphenylphosphoniumbutyl) quercetin iodide (QTM-7BTPI), which is inert and at 20 μM saturates the binding sites involved [32]. When we included QTM-7BTPI in the assays with the resveratrol derivatives, loss of TMRM fluorescence in excess of that determined by QTM-7BTPI was still evident (particularly in the case of the acetylated and methylated compounds), confirming that in this case loss

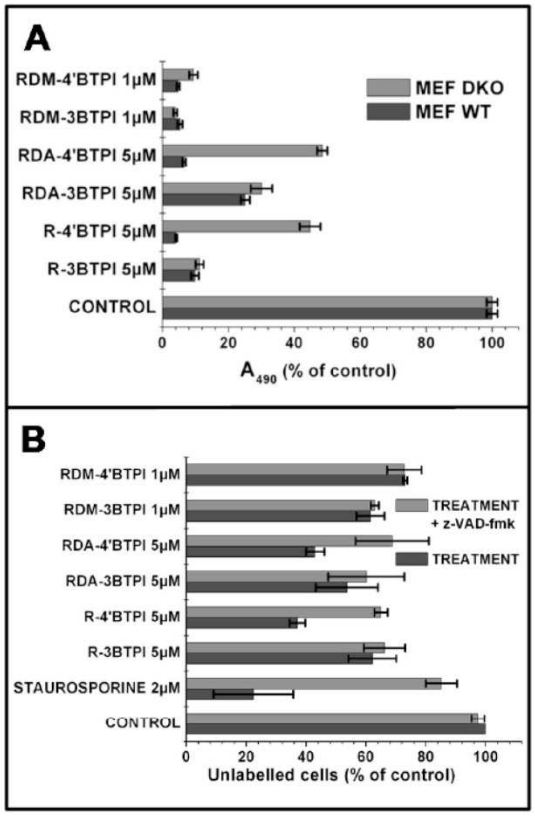

Fig. (4). Cell death is mainly necrotic. **A**) Cytotoxic effect (MTT assay readout) of mitochondriotropic resveratrol derivatives on cells expressing or not the pro-apoptotic proteins Bax and Bak. Wild type or $Bax^{-/-}/Bak^{-/-}$ (DKO) MEF cells were treated with the indicated derivatives for 72 h (see Materials and methods for details). **B**) Effects of the pan-caspase inhibitor z-VAD-fmk 100 µM on Annexin/PI labelling of Jurkat cells treated for 3h with the indicated compounds. Staurosporine is used as a positive control for apoptosis. For coherence with panel A, the percentage of cells not labelled by either Annexin or PI is shown, with the percentage of unlabelled cells in the control sample of each experiment set as 100%.

of transmembrane potential is in fact taking place (Supplementary Fig. **3**). Depolarization was also observed exploiting the intrinsic fluorescence of our derivatives (especially RDM-BTPIs) upon excitation at 340 nm. As can be seen in (Fig. **6**), addition of 1 µM RDM-4'BTPI to cultured cells caused a progressive increase of fluorescence in intracellular structures (compare panel B to panel A), which corresponds to a voltage-dependent accumulation of the compound into mitochondria, since addition of a transmembrane potential-dissipating protonophore (carbonyl cyanide p-trifluoromethoxyphenylhydrazone (FCCP)) causes a rapid redistribution of fluorescence due to efflux of the derivative (not shown). Even if no uncoupler was added, a spontaneous loss of fluorescence from the mitochondria developed after several minutes (compare panels B and C), with little visible effect by a subsequent addition of FCCP (compare panels C and D).

The demonstration that resveratrol derivatives induce mitochondrial depolarization has implications for the quantitative evaluation of superoxide production, since MitoSOX^{TM} Red is a mitochondriotropic probe; fluorescence increase upon superoxide generation may be underestimated when mitochondria are uncoupled, since MitoSOX^{TM} Red is expected to be released from the matrix.

To evaluate if the depolarization might be induced by H_2O_2, we compared the results in the presence or in the absence of a high concentration of PEG-CAT, and found that the enzyme did not affect the TMRM fluorescence decrease (Fig. **5**). CsA, which decreases the probability of MPT pore opening, was also without a clear effect on TMRM fluorescence redistribution.

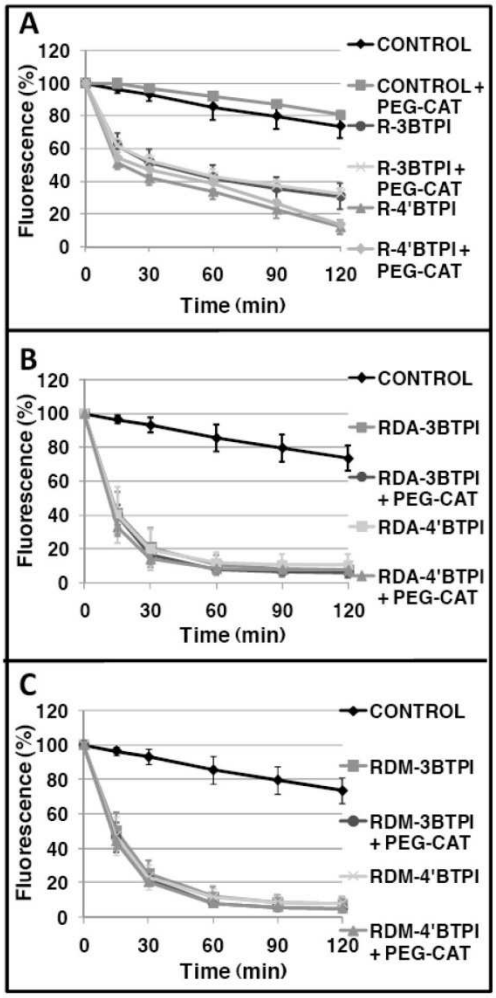

Fig. (5). Mitochondriotropic resveratrol derivatives cause a decrease of fluorescence of TMRM-labelled cells, which is not due to hydrogen peroxide. TMRM fluorescence was measured in FACS experiments using Jurkat cells treated with: **A**) 5 µM non-acetylated, or **B**) 5 µM acetylated, or **C**) 1 µM methylated mitochondriotropic derivatives. Treatments were performed in the absence or presence of PEG-CAT (500 U/ml).

DISCUSSION

The mitochondriotropic resveratrol derivatives we have studied are cytotoxic *in vitro* when used in the low µM range, showing a vast increase in effectiveness over unmodified resveratrol, presumably reflecting their electrophoretic accumulation. They are

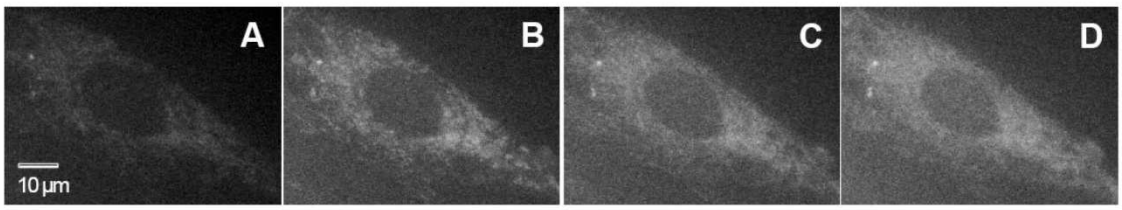

Fig. (6). RDM-4'BTPI induces mitochondrial depolarization. Representative fluorescence microscope images of cultured slow-growing MEF cells **A**) just before addition of 1 µM RDM-4'BTPI; **B**) 15 min and **C**) 25 min after addition of RDM-4'BTPI; **D**) 2 min after addition of 2 µM FCCP. Fluorescence is rendered on the greyscale for clarity.

furthermore selective, affecting preferentially cancerous and fast-growing cells. Death induction is observed both in long-term (three days) MTT viability assays (Fig. **1**) and in short-term Annexin/PI labelling experiments (Fig. **2**). Our data indicate that cytotoxicity and the upstream effects (ROS generation, depolarization) are specific of the molecules formed by the covalent linkage of the resveratrol moiety and of the mitochondria-targeting triphenylphosphonium cation, since a 1:1 mixture of the two has little effect at the concentrations used (Fig. **1**). Concentrations required for resveratrol-induced toxicity (50-100 µM; [26-29]) can hardly be reached or maintained *in vivo*, due to the poor bioavailability of this natural compound [35,36]. Mitochondria targeting allows high local concentrations of the derivatives to be reached, and thus may represent a strategy to exploit the toxic/chemotherapeutic properties of resveratrol. *In vivo* behavior of these new candidate chemotherapeutic agents remains to be explored.

It is furthermore clear that the cytotoxic agent is H_2O_2 produced by dismutation of superoxide, since the presence of PEG-CAT rescues the cells (Fig. **2**). This prooxidant and cytotoxic effect is observed *in vitro* with the mitochondriotropic derivatives used in the low µM range. Concentrations in this range favor prooxidant behavior also for mitochondria-targeted quinones such as MitoQ or SkQ1 which act as antioxidants at lower levels [37, 38]. While the possibility that mitochondriotropic polyphenols may act as protective antioxidants when used at very low concentrations remains to be explored, these compounds join the ranks of redox-active "mitocans", compounds which cause the death of cancer cells via oxidative stress at the mitochondrial level. The most promising current example of this class of potential chemotherapeutic agents is α-TOS and, especially, its mitochondriotropic derivative mitoVES (mitochondriotropic Vitamin E Succinate) [18, 39, 40].

At variance with what we observed using mitochondriotropic quercetin derivatives [32], with the resveratrol derivatives permeant SOD does not have any protective effect, and instead accentuates toxicity (Fig. **2**). This is logical, since SOD generates H_2O_2. Thus, a relevant difference must exist between the mechanisms underlying ROS production by quercetin- and resveratrol-based mitochondriotropic compounds. This can also be deduced from the fact that R-3BTPI and R-4'BTPI stimulate ROS production by about the same extent, while one would expect R-3BTPI to oxidize more readily due to the presence of a free hydroxyl group in the 4' position, from which an unpaired electron would delocalize by resonance over the whole molecule much more effectively than from the 3/5 position. Cyclic voltammetry experiments showed that resveratrol and its mitochondriotropic derivatives are not readily oxidizable at physiologically relevant voltages (Mattarei A *et al*., unpublished results), at variance from quercetin and Q-7BTPI [33]. The experiments with MitoSOX^{TM} Red (Fig. **3**) show that the methylated derivatives (at 1 µM) and RDA-4'BTPI (5 µM) are more effective inducers of ROS production than their counterparts bearing free hydroxyls or RDA-3BTPI (5 µM), confirming that oxidation of the resveratrol "nucleus" is not the source of superoxide.

α-TOS and mitoVES induce the generation of ROS via interaction with succinate dehydrogenase, suggesting that our compounds may also act as inducers of an "electron leak" from the respiratory chain. Resveratrol has been reported to inhibit respiratory chain complexes I and III [41]. Our mitochondriotropic derivatives may be expected to interact with these complexes as well, and the interaction might well lead to excess ROS generation, since complexes I and III represent the two major sites of superoxide production in mitochondria (e.g. [4]).

The conclusion that mitochondrial-level oxidative stress determines cell death provides a tentative explanation – in addition to that involving the mitochondrial transmembrane potential, mentioned in the introduction - for the selectivity of death induction in certain cell types. ROS, in particular H_2O_2, act as intracellular messengers, with effects that depend on the cellular context and on the quantitative and temporal aspects of their production (e.g. [42-44]). They are a recognized mitogenic factor: rapidly proliferating cells have higher levels than quiescent ones [10, 45] and cancerous cells in particular are characterized by an altered redox homeostasis and by an accentuated oxidative stress (e.g.: [46-50]). On the other hand a vast consensus exists that ROS can induce apoptosis [51] and, at higher levels, necrosis [52, 53]. Activation of phosphorylation cascades is the key feature of apoptotic induction by ROS [12]. Necrosis is now understood to comprise a set of interacting signaling cascades and biochemical phenomena forming a continuum with other forms of cell death like apoptosis or autophagic death and comprising a variety of subtypes such as, e.g., "necroptosis", "parthanatos", "autoschizis", etc. [54]. ROS, along with Ca^{2+} dysregulation, are a key factor in inducing the mitochondrial permeability transition and/or lysosomal rupture, characteristic features of necrotic death. Thus, despite their enhanced redox defences, an additional oxidative stress may push cancerous cells over the brink of death more easily than normal cells (e.g. [47-49, 55]). In this context, it is not surprising that cell death, mostly of a necrotic character under our conditions, may also include an apoptotic component in some cases (Fig. **4**).

Besides oxidative stress, our derivatives also cause loss of TMRM fluorescence from (the mitochondria of) treated cells (Fig. **5**). Since it is unaffected by PEG-SOD (not shown) or PEG-CAT (Fig. **5**) this uncoupling is not downstream of ROS. It cannot be attributed to protonophoric cycling of the compounds between the cytoplasm and the mitochondrial matrix [56], since the acetylated and methylated derivatives, which have no protons to carry, are much more effective than their analogs R-3BTPI and R-4'BTPI. Resveratrol's phenolic hydroxyls, furthermore, would be only slightly deprotonated at physiological pH values (pKa_1: 8.8; [57]). Even though depolarization was found to be CsA-insensitive, an involvement of the MPT cannot be ruled out. Permeabilization of the inner membrane may be the common outcome of distinct processes, regulation of this phenomenon is complex, and CsA is far from being a fail-safe inhibitor [58]. For example, its effects have been found to depend on Pi [59]. Cyclophilin D-dependent and –

independent mechanisms of pore activation may exist [60], and expression levels of Cyp D may vary depending on cell type, reflecting on the sensitivity of the MPT to CsA [61].

A fuller understanding of cytotoxicity thus requires an understanding of the mechanisms underlying ROS production and depolarization. An investigation of these aspects is under way. *In vivo* studies on mice tumor models will determine if these resveratrol mitochondriotropic derivatives may indeed qualify as candidates for a new class of chemotherapeutic agents.

CONFLICT OF INTEREST

The authors confirm that this article content has no conflicts of interest.

ACKNOWLEDGEMENTS

We thank M. Carraro, E. Marotta, S. Garbisa and J. Neuzil for useful discussions. This work was supported by grants from the Fondazione Cassa di Risparmio di Padova e Rovigo (Fondazione CARIPARO) (Excellence grant "Developing a pharmacology of polyphenols" to M.Z.), and from the Italian Association for Cancer Research (AIRC) (n. 5118 to I.S.). N.S. was the beneficiary of a University of Padova post-doctoral fellowship.

REFERENCES

[1] Calì T, Ottolini D, Brini M. Mitochondrial Ca(2+) as a key regulator of mitochondrial activities. Adv Exp Med Biol 2012; 942: 53-73.

[2] Orrenius S. Reactive oxygen species in mitochondria-mediated cell death. Drug Metab Rev 2007; 39: 443-55.

[3] Nunnari J, Suomalainen A. Mitochondria: in sickness and in health. Cell 2012; 148: 1145-59.

[4] Murphy MP. How mitochondria produce reactive oxygen species. Biochem J 2009; 417: 1-13.

[5] Biasutto L, Szabo' I, Zoratti M. Mitochondrial effects of plant-made compounds. Antioxid Redox Signal 2011; 15: 3039-59.

[6] Ziech D, Franco R, Pappa A, Panayiotidis MI. Reactive oxygen species (ROS)--induced genetic and epigenetic alterations in human carcinogenesis. Mutat Res 2011; 711: 167-73.

[7] Pani G, Giannoni E, Galeotti T, Chiarugi P. Redox-based escape mechanism from death: the cancer lesson. Antioxid Redox Signal 2009; 11: 2791-806.

[8] Ishikawa K, Takenaga K, Akimoto M, *et al*. ROS-generating mitochondrial DNA mutations can regulate tumor cell metastasis. Science 2008; 320: 661-4.

[9] Patten DA, Lafleur VN, Robitaille GA, Chan DA, Giaccia AJ, Richard DE. Hypoxia-inducible factor-1 activation in nonhypoxic conditions: the essential role of mitochondrial-derived reactive oxygen species. Mol Biol Cell 2010; 21: 3247-57.

[10] Verschoor ML, Wilson LA, Singh G. Mechanisms associated with mitochondrial-generated reactive oxygen species in cancer. Can J Physiol Pharmacol 2010; 88: 204-19.

[11] Ueda S, Masutani H, Nakamura H, Tanaka T, Ueno M, Yodoi J. Redox control of cell death. Antioxid Redox Signal 2002; 4: 405-14.

[12] Takeda K, Naguro I, Nishitoh H, Matsuzawa A, Ichijo H. Apoptosis signaling kinases: from stress response to health outcomes. Antioxid Redox Signal 2011; 15: 719-61.

[13] Orrenius S, Zhivotovsky B. Cardiolipin oxidation sets cytochrome c free. Nat Chem Biol 2005; 1: 188-9.

[14] Rasola A, Bernardi P. Mitochondrial permeability transition in Ca(2+)-dependent apoptosis and necrosis. Cell Calcium 2011; 50: 222-33.

[15] Halestrap AP. Mitochondria and reperfusion injury of the heart--a holey death but not beyond salvation. J Bioenerg Biomembr 2009; 41: 113-21.

[16] Di Lisa F, Bernardi P. Mitochondria and ischemia-reperfusion injury of the heart: fixing a hole. Cardiovasc Res 2006; 70: 191-9.

[17] Smith RA, Hartley RC, Cochemé HM, Murphy MP. Mitochondrial pharmacology. Trends Pharmacol Sci 2012; 33: 341-52.

[18] Biasutto L, Dong LF, Zoratti M, Neuzil J. Mitochondrially targeted anti-cancer agents. Mitochondrion 2010; 10: 670-81. Erratum in: Mitochondrion 2011;11: 996.

[19] Murphy MP. Targeting lipophilic cations to mitochondria. Biochim Biophys Acta 2008; 1777: 1028-31.

[20] Chen LB. Mitochondrial membrane potential in living cells. Annu Rev Cell Biol 1988; 4: 155-81.

[21] Bonnet S, Archer SL, Allalunis-Turner J, *et al*. A mitochondria-K+ channel axis is suppressed in cancer and its normalization promotes apoptosis and inhibits cancer growth. Cancer Cell 2007; 11: 37-51.

[22] Modica-Napolitano JS, Aprille JR. Delocalized lipophilic cations selectively target the mitochondria of carcinoma cells. Adv Drug Deliv Rev 2001; 49: 63-70.

[23] Heerdt BG, Houston MA, Augenlicht LH. The intrinsic mitochondrial membrane potential of colonic carcinoma cells is linked to the probability of tumor progression. Cancer Res 2005; 65: 9861-7.

[24] Mattarei A, Biasutto L, Marotta E, *et al*. A mitochondriotropic derivative of quercetin: a strategy to increase the effectiveness of polyphenols. Chembiochem 2008; 9: 2633-42.

[25] Biasutto L, Mattarei A, Marotta E, *et al*. Development of mitochondria-targeted derivatives of resveratrol. Bioorg Med Chem Lett 2008; 18: 5594-7.

[26] Lin X, Wu G, Huo WQ, Zhang Y, Jin FS. Resveratrol induces apoptosis associated with mitochondrial dysfunction in bladder carcinoma cells. Int J Urol 2012; 19: 757-64.

[27] Delmas D, Solary E, Latruffe N. Resveratrol, a phytochemical inducer of multiple cell death pathways: apoptosis, autophagy and mitotic catastrophe. Curr Med Chem 2011; 18: 1100-21.

[28] Zhang W, Wang X, Chen T. Resveratrol induces mitochondria-mediated AIF and to a lesser extent caspase-9-dependent apoptosis in human lung adenocarcinoma ASTC-a-1 cells. Mol Cell Biochem 2011; 354: 29-37.

[29] Low IC, Chen ZX, Pervaiz S. Bcl-2 modulates resveratrol-induced ROS production by regulating mitochondrial respiration in tumor cells. Antioxid Redox Signal 2010; 13: 807-19.

[30] Ungvari Z, Sonntag WE, de Cabo R, Baur JA, Csiszar A. Mitochondrial protection by resveratrol. Exerc Sport Sci Rev 2011; 39: 128-32.

[31] Wang XX, Li YB, Yao HJ, *et al*. The use of mitochondrial targeting resveratrol liposomes modified with a dequalinium polyethylene glycol-distearoylphosphatidyl ethanolamine conjugate to induce apoptosis in resistant lung cancer cells. Biomaterials 2011; 32: 5673-87.

[32] Sassi N, Biasutto L, Mattarei A, *et al*. Cytotoxicity of a mitochondriotropic quercetin derivative: Mechanisms. Biochim Biophys Acta 2012; 1817: 1095-106.

[33] Mattarei A, Sassi N, Durante C, *et al*. Redox properties and cytotoxicity of synthetic isomeric mitochondriotropic derivatives of the natural polyphenol quercetin. Eu J Organic Chem 2011; 28: 5577-86.

[34] Salvi A, Carrupt PA, Mayer JM, Testa B. Esterase-like activity of human serum albumin toward prodrug esters of nicotinic acid. Drug Metab Dispos 1997; 25: 395-8.

[35] Walle T. Bioavailability of resveratrol. Ann N Y Acad Sci 2011; 1215: 9-15.

[36] Wenzel E, Somoza V. Metabolism and bioavailability of trans-resveratrol. Mol Nutr Food Res 2005; 49: 472-81.

[37] Doughan AK, Dikalov SI. Mitochondrial redox cycling of mitoquinone leads to superoxide production and cellular apoptosis. Antioxid Redox Signal 2007; 9: 1825-36.

[38] Antonenko YN, Avetisyan AV, Bakeeva LE, *et al*. Mitochondria-targeted plastoquinone derivatives as tools to interrupt execution of the aging program. 1. Cationic plastoquinone derivatives: synthesis and *in vitro* studies. Biochemistry (Mosc) 2008; 73: 1273-87.

[39] Dong LF, Jameson VJ, Tilly D, *et al*. Mitochondrial targeting of vitamin E succinate enhances its pro-apoptotic and anti-cancer activity via mitochondrial complex II. J Biol Chem 2011; 286: 3717-28.

[40] Neuzil J, Dong LF, Rohlena J, Truksa J, Ralph SJ. Classification of mitocans, anti-cancer drugs acting on mitochondria. Mitochondrion 2012; in press. DOI: 10.1016/j.mito.2012.07.112.

[41] Zini R, Morin C, Bertelli A, Bertelli AA, Tillement JP. Effects of resveratrol on the rat brain respiratory chain. Drugs Exp Clin Res 1999; 25: 87-97.

[42] D'Autréaux B, Toledano MB. ROS as signalling molecules: mechanisms that generate specificity in ROS homeostasis. Nature Rev Mol Cell Biol 2007; 8: 813-24.

[43] Gough DR, Cotter TG. Hydrogen peroxide: a Jekyll and Hyde signalling molecule. Cell Death Dis 2011; 2:e213.

[44] Rigoulet M, Yoboue ED, Devin A. Mitochondrial ROS generation and its regulation: mechanisms involved in H(2)O(2) signaling. Antioxid Redox Signal 2011; 14: 459-68.
[45] Groeger G, Quiney C, Cotter TG. Hydrogen peroxide as a cell-survival signaling molecule. Antioxid Redox Signal 2009; 11: 2655-71.
[46] Gius D, Spitz DR. Redox signaling in cancer biology. Antioxid Redox Signal 2006; 8: 1249-52.
[47] Trachootham D, Alexandre J, Huang P. Targeting cancer cells by ROS-mediated mechanisms: a radical therapeutic approach? Nat Rev Drug Discov 2009; 8: 579-91.
[48] Ralph SJ, Rodríguez-Enríquez S, Neuzil J, Saavedra E, Moreno-Sánchez R. The causes of cancer revisited: "mitochondrial malignancy" and ROS-induced oncogenic transformation - why mitochondria are targets for cancer therapy. Mol Aspects Med 2010; 31: 145-70.
[49] Ralph SJ, Rodríguez-Enríquez S, Neuzil J, Moreno-Sánchez R. Bioenergetic pathways in tumor mitochondria as targets for cancer therapy and the importance of the ROS-induced apoptotic trigger. Mol Aspects Med 2010; 31: 29-59.
[50] Shi X, Zhang Y, Zheng J, Pan J. Reactive oxygen species in cancer stem cells. Antioxid Redox Signal 2012; 16: 1215-28.
[51] Circu ML, Aw TY. Reactive oxygen species, cellular redox systems, and apoptosis. Free Radic Biol Med 2010; 48: 749-62.
[52] Festjens N, Vanden Berghe T, Vandenabeele P. Necrosis, a well-orchestrated form of cell demise: signalling cascades, important mediators and concomitant immune response. Biochim Biophys Acta 2006; 1757: 1371-87.
[53] Vanlangenakker N, Vanden Berghe T, Krysko DV, Festjens N, Vandenabeele P. Molecular mechanisms and pathophysiology of necrotic cell death. Curr Mol Med 2008; 8: 207-20.
[54] Galluzzi L, Vitale I, Abrams JM, *et al*. Molecular definitions of cell death subroutines: recommendations of the Nomenclature Committee on Cell Death 2012. Cell Death Differ 2012; 19: 107-20.
[55] Wondrak GT. Redox-directed cancer therapeutics: molecular mechanisms and opportunities. Antioxid Redox Signal 2009; 11: 3013-69.
[56] Biasutto L, Sassi N, Mattarei A, *et al*. Impact of mitochondriotropic quercetin derivatives on mitochondria. Biochim Biophys Acta 2010; 1797: 189-96.
[57] López-Nicolás JM, García-Carmona F. Aggregation state and pKa values of (E)-resveratrol as determined by fluorescence spectroscopy and UV-visible absorption. J Agric Food Chem 2008; 56: 7600-5.
[58] Zoratti M, Szabò I, De Marchi U. Mitochondrial permeability transitions: how many doors to the house? Biochim Biophys Acta 2005; 1706: 40-52.
[59] Basso E, Petronilli V, Forte MA, Bernardi P. Phosphate is essential for inhibition of the mitochondrial permeability transition pore by cyclosporin A and by cyclophilin D ablation. J Biol Chem 2008; 283: 26307-11.
[60] Scorrano L, Nicolli A, Basso E, Petronilli V, Bernardi P. Two modes of activation of the permeability transition pore: the role of mitochondrial cyclophilin. Mol Cell Biochem 1997; 174: 181-4.
[61] Li B, Chauvin C, De Paulis D, *et al*. Inhibition of complex I regulates the mitochondrial permeability transition through a phosphate-sensitive inhibitory site masked by cyclophilin D. Biochim Biophys Acta 2012; 1817: 1628-34.

Received: March 11, 2013 **Accepted: May 15, 2013**

11. Cytotoxicity of mitochondria-targeted resveratrol derivatives: interactions with respiratory chain complexes and ATP synthase

Biochimica et Biophysica Acta 1837 (2014) 1781–1789

Contents lists available at ScienceDirect

Biochimica et Biophysica Acta

journal homepage: www.elsevier.com/locate/bbabio

Cytotoxicity of mitochondria-targeted resveratrol derivatives: Interactions with respiratory chain complexes and ATP synthase

Nicola Sassi [a,b], Andrea Mattarei [b,c], Michele Azzolini [a], Ildiko' Szabo' [d], Cristina Paradisi [c], Mario Zoratti [a,b], Lucia Biasutto [a,b,*]

[a] Department of Biomedical Sciences, Viale G. Colombo 3, 35121 Padova, Italy
[b] CNR Neuroscience Institute, Viale G. Colombo 3, 35121 Padova, Italy
[c] Department of Chemical Sciences, Via F. Marzolo 1, 35131 Padova, Italy
[d] Department of Biology, Viale G. Colombo 3, 35121 Padova, Italy

ARTICLE INFO

Article history:
Received 28 December 2013
Received in revised form 13 June 2014
Accepted 27 June 2014
Available online 2 July 2014

Keywords:
Resveratrol
Triphenylphosphonium
ROS
Mitochondria
Respiratory chain
ATP synthase

ABSTRACT

We recently reported that mitochondria-targeted derivatives of resveratrol are cytotoxic in vitro, selectively inducing mostly necrotic death of fast-growing and tumoral cells when supplied in the low μM range (N. Sassi et al., Curr. Pharm. Des. 2014). Cytotoxicity is due to H_2O_2 produced upon accumulation of the compounds into mitochondria. We investigate here the mechanisms underlying ROS generation and mitochondrial depolarization caused by these agents. We find that they interact with the respiratory chain, especially complexes I and III, causing superoxide production. "Capping" free hydroxyls with acetyl or methyl groups increases their effectiveness as respiratory chain inhibitors, promoters of ROS generation and cytotoxic agents. Exposure to the compounds also induces an increase in the occurrence of short transient [Ca^{2+}] "spikes" in the cells. This increase is unrelated to ROS production, and it is not the cause of cell death. These molecules furthermore inhibit the F_0F_1 ATPase. When added to oligomycin-treated cells, the acetylated/methylated ones cause a recovery of the cellular oxygen consumption rates depressed by oligomycin. Since a protonophoric futile cycle which might account for the uncoupling effect is impossible, we speculate that the compounds may cause the transformation of the ATP synthase and/or respiratory chain complex(es) into a conduit for uncoupled proton translocation. Only in the presence of excess oligomycin the most effective derivatives appear to induce the mitochondrial permeability transition (MPT) within the cells. This may be considered to provide circumstantial support for the idea that the ATP synthase is the molecular substrate for the MPT pore.

1. Introduction

Cancer cells have an altered redox homeostasis [1–5] and hyperpolarized mitochondria [6–9]. This latter characteristic is a consequence of the shift from mitochondrial respiration to aerobic glycolytic ATP synthesis (the so-called Warburg effect), which leads to reduced oxidative phosphorylation activity, less efficient dissipation of the mitochondrial electrochemical proton gradient, and thus to an increased transmembrane potential [6,8]. ROS-generating agents targeted to mitochondria thanks to conjugation with lipophilic cations (which accumulate in the mitochondrial matrix according to the Nerst's law) have thus been developed, and are emerging as a promising class of mitocans, i.e., anticancer agents acting on mitochondria and destabilizing them [10,11]. Mitochondrial hyperpolarization leads to preferential accumulation of the pro-oxidant agents in cancer cells. Furthermore, the additional oxidative stress they cause may push cancerous cells over the brink of death more easily than normal cells [2–5]. A recent paper has indeed shown that healthy primary B cells can be sensitized to certain pro-apoptotic drugs by induction of a mild mitochondrial oxidative stress with a mitochondriotropic quercetin derivative. Conversely, cancerous

Abbreviations: B-CLL, B-cell chronic lymphocytic leukemia; BSA, bovine serum albumin; BTPI, 4-triphenylphosphoniumbutyl; CoQ, coenzyme Q; CsA, cyclosporin A; DCPI, 2,6-dichlorophenolindophenol; $\Delta\psi_m$, mitochondrial membrane potential; DMEM, Dulbecco's Modified Eagle Medium; $\Delta\tilde{\mu}_H$, proton electrochemical gradient; ECAR, extracellular acidification rate; FACS, fluorescence-activated cell scanner; FBS, fetal bovine serum; FCCP, carbonyl cyanide p-trifluoromethoxy-phenylhydrazone; HBSS, Hank's Balanced Salt Solution; H_2DCF-DA, 2′,7′-dichlorodihydrofluorescein-diacetate; IMM, inner mitochondrial membrane; LDH, lactate dehydrogenase; MPT, mitochondrial permeability transition; OCR, oxygen consumption rate; OL, oligomycin; PEG-SOD, polyethyleneglycol-superoxide dismutase; PEG-CAT, polyethyleneglycol-catalase; PEP, phosphoenolpyruvate; PK, pyruvate kinase; R-4′BTPI, 4′-(4-triphenylphosphoniumbutyl) resveratrol iodide; R-3BTPI, 3-(4-triphenylphosphoniumbutyl) resveratrol iodide; RDA-4′BTPI, 3,5-diacetyl-4′-(4-triphenylphosphoniumbutyl) resveratrol iodide; RDA-3BTPI, 4′,5-diacetyl-3-(4-triphenylphosphoniumbutyl) resveratrol iodide; RDM-4′BTPI, 3,5-dimethyl-4′-(4-triphenylphosphoniumbutyl) resveratrol iodide; RDM-3BTPI, 4′,5-dimethyl-3-(4-triphenylphosphoniumbutyl) resveratrol iodide; RLM, rat liver mitochondria; ROI, regions of interest; ROS, reactive oxygen species; MTT, 3-(4,5-dimethylthiazol-2-yl)-2,5-diphenyltetrazolium bromide

* Corresponding author at: CNR Neuroscience Institute, Viale G. Colombo 3, 35121 Padova, Italy. Tel.: +39 049 8276483; fax: +39 049 8276040.
E-mail address: lucia.biasutto@cnr.it (L. Biasutto).

http://dx.doi.org/10.1016/j.bbabio.2014.06.010
0005-2728/

B-CLL cells lose their peculiar sensitivity to the same drugs if treated with permeant ROS scavengers PEG-SOD and PEG-CAT [5].

We previously reported the synthesis and *in vitro* activity of a group of resveratrol derivatives targeted to mitochondria via a 4-triphenylphosphoniumbutyl (BTPI) group O-linked at either position -3 or -4′ [12,13]. These derivatives, in the low-μM range, induced necrotic cell death, selectively killing cancerous and fast-growing cells *in vitro* [13]. Resveratrol itself has previously been shown to be cytotoxic, but only at much higher doses (tens of μM) [14]. Mitochondrial targeting thus appears to enhance the cytotoxicity exhibited by resveratrol itself. Cytotoxicity was found to be due to H_2O_2 produced upon accumulation of the derivatives into mitochondria; ROS-independent mitochondrial depolarization was also induced. We investigate here the mechanisms underlying these effects.

Since effectiveness increased if the two free hydroxyls of the derivatives were acetylated or methylated [13], autooxidation of the polyphenolic nucleus, which depends on the presence of free hydroxyls and is favored by their ionization [15], could be excluded. Oxidation of the resveratrol "kernel" could be ruled out as the source of superoxide also because cyclic voltammetry experiments showed that resveratrol and its mitochondriotropic derivatives are not readily oxidizable at physiologically relevant voltages (Mattarei, A. et al., unpublished results). A protonophoric cycle, such as that envisioned for mitochondriotropic quercetin derivatives [16], can be dismissed as the cause of depolarization because of the lack of proton-carrying groups in the most effective, methylated, molecules. Thus we thought that ROS were likely to be generated downstream of the interaction of our molecules with redox-active proteins. The most likely candidates were components of the respiratory chain. Indeed some evidence for a modulation of respiratory chain complexes by resveratrol has already been presented [17,18].

Ca^{2+} is a major second messenger modulating many cellular physiological functions. Calcium and ROS are linked by a reciprocal interaction: Ca^{2+} overload may cause ROS generation [19], and in turn ROS may have an impact on Ca^{2+} homeostasis. Acute as well as chronic oxidative stress can result in inhibition/downregulation/modulation of the plasma membrane Ca^{2+} ATPase, reticular Ca^{2+} ATPase, Na^+/Ca^{2+} exchanger, and other components of the Ca^{2+} homeostasis machinery [20]. Depending on ROS levels, these effects may be mediated by the action of redox-sensitive kinases, by direct modification of the "pumps" and transporters, or both [21].

Resveratrol is furthermore known to bind to the F_1 portion of the mitochondrial ATP synthase inhibiting the enzyme [22–24]. We therefore focused on Ca^{2+} levels and on ATPase functionality as well as on respiration and ROS production.

2. Materials and methods

Experiments were repeated at least three times. Averages ± s.d. are reported.

2.1. Materials

Resveratrol was purchased from Waseta Int. Trading Co. (Shanghai, P.R. China). R-4′BTPI, R-3BTPI, RDA-4′BTPI, RDA-3BTPI, RDM-4′BTPI and RDM-3BTPI were synthesized as described in [12,13]. Other chemicals were purchased from Sigma-Aldrich (Milan) unless otherwise specified. All chemicals for buffer preparation were of laboratory grade, obtained from Merck, J.T. Baker or Sigma.

2.2. Cells and mitochondria

Mouse colon cancer CT-26 cells (doubling time 24 h) were grown in high glucose (4.5 g/L) Dulbecco's Modified Eagle Medium (DMEM) supplemented with 10% (v/v) fetal bovine serum (FBS, Invitrogen), 10 mM HEPES buffer (pH 7.4), 1 mM sodium pyruvate, 100 U/mL penicillin G, 0.1 mg/mL streptomycin, 2 mM glutamine (GIBCO) and 1% nonessential amino acids (100× solution; GIBCO), in a humidified atmosphere of 5% CO_2 at 37 °C.

Rat liver mitochondria (RLM) were isolated by conventional differential centrifugation procedures [25]. The standard isolation medium was: 250 mM sucrose, 5 mM HEPES, 1 mM EGTA (pH 7.4). Protein content was quantified with a BCA Protein Assay Kit (Thermo Scientific) using an albumin calibration curve.

2.3. Fluorescence microscopy

An Olympus Biosystems apparatus comprising an Olympus IX71 microscope and MT20 light source was used; images were acquired automatically at 1-min intervals for 70 min, and processed with CellR® software. CT-26 cells were seeded on a XF24-well microplate at a density of 5×10^4 cells/well in DMEM + FBS 10% (200 μL) and incubated overnight in a humidified atmosphere with 5% CO_2 at 37 °C. Cells were then washed with HBSS (in mM units: NaCl 136.9, KCl 5.36, $CaCl_2$ 1.26, $MgSO_4$ 0.81, KH_2PO_4 0.44, Na_2HPO_4 0.34, glucose 5.55, pH 7.4 with NaOH) and loaded with dye. All experiments were performed in DMEM without Phenol red and FBS, at room temperature.

2.3.1. Intracellular Ca^{2+} levels

The non-ratiometric dye Fluo-4 was used to follow $[Ca^{2+}]$ changes in cultured cells under the same experimental conditions used in oxygen consumption assays. Cells were loaded with 20 nM Fluo-4 methyl ester, in the presence of 0.04% Pluronic acid, 100 μM Probenecid and 2 μM CsA, at 37 °C for 30 min. The medium was then replaced with 670 μL of pre-warmed (37 °C) DMEM supplemented with 0.04% Pluronic acid, 100 μM Probenecid and 2 μM CsA; cells were then incubated for 30 min at 37 °C to allow complete hydrolysis of Fluo-4 ester bonds. Excitation wavelength was 480–500 nm and fluorescence was collected at $\lambda > 510$ nm. Additions were performed by withdrawing 0.5 mL of incubation medium, adding to this aliquot the desired compound as a solution in 70 μL of DMEM and adding back the solution into the chamber at a peripheral point.

2.3.2. $O_2^{-\bullet}$ generation

$O_2^{-\bullet}$ generation in cells was followed using MitoSOX Red™ (Life Technologies). CT-26 cells were loaded with 1 μM MitoSOX Red™, in the presence of 2 μM CsA, at 37 °C for 30 min. The medium was then replaced with 670 μL of pre-warmed (37 °C) DMEM containing 2 μM CsA. Excitation was at 500–520 nm, and fluorescence was collected at $\lambda > 570$ nm. Additions were performed as described above.

2.4. Oxygen consumption assay by CT-26 cells

Respiration by adherent cells was measured using a Seahorse XF24 (Seahorse Bioscience) which measures the oxygen consumption rate (OCR) in the medium immediately surrounding adherent cells cultured in an XF24-well microplate. Adherent CT-26 cells were seeded at a density of 5×10^4 cells/well in DMEM + FBS 10% (200 μL) and incubated overnight in a humidified atmosphere with 5% CO_2 at 37 °C. The medium was then replaced with 670 μL of pre-warmed (37 °C) high-glucose DMEM supplemented with 1 mM sodium pyruvate, 4 mM L-glutamine, and without FBS. Microplates were incubated at 37 °C for 30 min to allow temperature and pH to stabilize before the measurements. OCR was measured at preset time intervals while the instrument automatically carried out the pre-programmed additions of the various compounds (final concentrations unless otherwise specified: oligomycin A 1 μg/mL, FCCP 0.2 μM, antimycin A 1 μM), added as a solution in 70 μL of DMEM. All measurements were carried out in quadruplicate (4 wells per condition). For presentation purposes the data were normalized to the initial OCR baseline measurement for each set of wells and are presented as % changes with respect to that level. ECAR (extracellular acidification rate) was also automatically measured during the same experiments.

2.5. Activity of mitochondrial respiratory chain complexes

Complex activity was extrapolated from the slope of absorbance decrease; data are expressed as % of the control (i.e., the activity without any addition of the derivative).

2.5.1. Complex I activity

To assay NADH-CoQ oxidoreductase (complex I) activity, RLM (50 μg prot./mL) were incubated with 10 μM alamethicin, 3 mg/mL bovine serum albumin (BSA), 10 mM Tris–HCl (pH 8.0), 2.5 mM NaN_3 and 65 μM coenzyme Q_1 (CoQ_1). The reaction was started with the addition of 100 μM NADH. Changes in absorbance (340 nm) were monitored at 37 °C using an Agilent Technologies Cary 100 UV–Vis spectrophotometer. After 6 min, 2 μM rotenone was added to assess the rotenone- (and thus complex I-) independent activity to be subtracted.

2.5.2. Complex II activity

To measure succinate CoQ oxidoreductase (complex II) activity, RLM (5 μg prot./mL) were incubated in the assay medium (potassium phosphate 25 mM, pH 7.5, supplemented with 5 mM $MgCl_2$, 20 mM succinate and 10 μM alamethicin) at 30 °C for 10 min. 3 mg/mL BSA, 2.5 mM NaN_3, 2 μg/mL antimycin A, 2 μM rotenone, and 125 μM 2,6-dichlorophenolindophenol (DCPI) were then added and absorbance changes were monitored at 600 nm.

2.5.3. Complex III activity

To assay CoQ cytochrome *c* oxidoreductase (complex III) activity, RLM (10 μg prot./mL) were added to a cuvette containing 50 mM potassium phosphate buffer, pH 7.5, supplemented with 10 μM alamethicin, 3 mg/mL BSA, 2.5 mM NaN_3, 2 μM rotenone, 0,025% TWEEN, and 75 μM oxidized cytochrome *c*. The reaction was started adding 75 μM of reduced decylubiquinol (produced by reduction of decylubiquinone in ethanol with $NaBH_4$ shortly before use); changes in absorbance were monitored at 550 nm, 37 °C. After 6 min, 2 μg/mL antimycin was added for assessment of the antimycin-dependent complex III enzyme activity.

2.6. F_0F_1 ATPase activity

Mitochondrial F_0F_1 ATPase activity was measured by coupling the production of ADP to the oxidation of NADH via the pyruvate kinase and lactate dehydrogenase reaction (coupled assay), as described in [26]. The reaction mixture (pH 7.6) contained 250 mM sucrose, 10 mM Tris–HCl, 200 μM EGTA–Tris, 1 mM NaH_2PO_4, 6 mM $MgCl_2$, 2 μM rotenone, 10 μM alamethicin, 3 mg/mL BSA, 1 mM phosphoenolpyruvate (PEP), 0.1 mM NADH, pyruvate kinase (PK; 20 units/mL), lactate dehydrogenase (LDH; 50 units/mL), and RLM (20 μg prot./mL). Absorbance was measured at 340 nm, 25 °C. The reaction was started by the addition of 500 μM ATP; after 6 min, 1 μg/mL oligomycin A was added to evaluate F_0F_1-ATPase-independent ATP hydrolysis.

3. Results

Since H_2O_2 is responsible for cell death induction by mitochondriotropic resveratrol derivatives [13], the mechanisms underlying ROS generation were investigated using cultured cells and isolated rat liver mitochondria. All tested compounds are illustrated in Fig. 1; both isomers were used, bearing the 4-triphenylphosphoniumbutyl (BTPI) group at either position -3 or -4′.

3.1. Effects on intracellular Ca^{2+} levels. Ca^{2+} signalling does not have a role in cytotoxicity

Since ROS and Ca^{2+} signalling can be linked [19–21], we evaluated the effects of treatment with the most cytotoxic compounds, RDM-3BTPI and RDM-4′BTPI (5 μM), on CT-26 cellular Ca^{2+} levels. The two isomers had very similar effects; observations obtained with RDM4′-BTPI are illustrated in Fig. 2A–C. The Ca^{2+} probe Fluo-4 was used in fluorescence microscopy experiments conducted under the same conditions used in the experiments on cellular respiration (SeaHorse; see Section 3.3). Ionomycin was used as a control to make sure that the Fluo-4 probe was responding adequately to Ca^{2+}, and to determine the maximum Fluo-4 fluorescence response. In control experiments (i.e., untreated cells), less than 1% of the cell population displayed sporadic (generally one or two per cell) brief (≤1 min) increases of intracellular [Ca^{2+}] during the one-hour monitoring period. The effect of the resveratrol derivatives was to increase from <1% to ~5% the fraction of cells displaying these [Ca^{2+}] "spikes". These occurred randomly, but with a preference for late times after addition of the derivative (>40 min). They did not impair the ability of the cell to take up Ca^{2+} upon the introduction of ionomycin at the end of the experiment.

Occurrence of the [Ca^{2+}] transients was not downstream of ROS production, since the presence of PEG-SOD and PEG-CAT had no effect on their prevalence, intensity or multiplicity (Fig. 2C). PEG-SOD and PEG-CAT were proven, however, to efficiently reduce ROS generation under these same experimental conditions (Fig. 2F).

Superoxide production was observed in fluorescence microscopy experiments using the MitoSOX™ probe (Fig. 2D–F). Under the same experimental conditions as in Fig. 2A–C, superoxide generation increased in all cells (Supplementary Fig. 1), beginning shortly after the addition of the mitochondriotropic derivatives (Fig. 2D). On the other hand, brief calcium spikes occurred only in a small fraction of cells, and with a random delay after compound addition (Fig. 2B and C). The comparison of the time course and prevalence of the two phenomena allows one to conclude that ROS production was not downstream of the modest Ca^{2+} signals. Note that the response elicited by antimycin A (Fig. 2E) was similar to that caused by RDM-4′BTPI (Fig. 2D), and that the two were not additive (Fig. 2D). The presence of cell-permeant PEG-SOD and PEG-CAT eliminated the MitoSOX™ fluorescence increase elicited by RDM-4′BTPI (Fig. 2F), confirming on one side that it is due to mitochondrial ROS, and on the other that the enzymes added effectively scavenge $O_2^{\bullet-}/H_2O_2$. The behavior shown in Fig. 2F is completely analogous to that exhibited by MitoSOX™-loaded but otherwise untreated (control) cells (not shown).

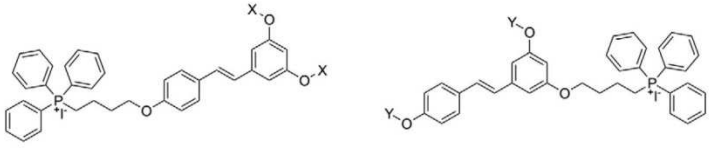

R-4′BTPI: X = H
RDA-4′BTPI: X = -C(=O)CH_3
RDM-4′BTPI: X = -CH_3

R-3BTPI: Y = H
RDA-3BTPI: Y = -C(=O)CH_3
RDM-3BTPI: Y = -CH_3

Fig. 1. Mitochondriotropic resveratrol derivatives studied.

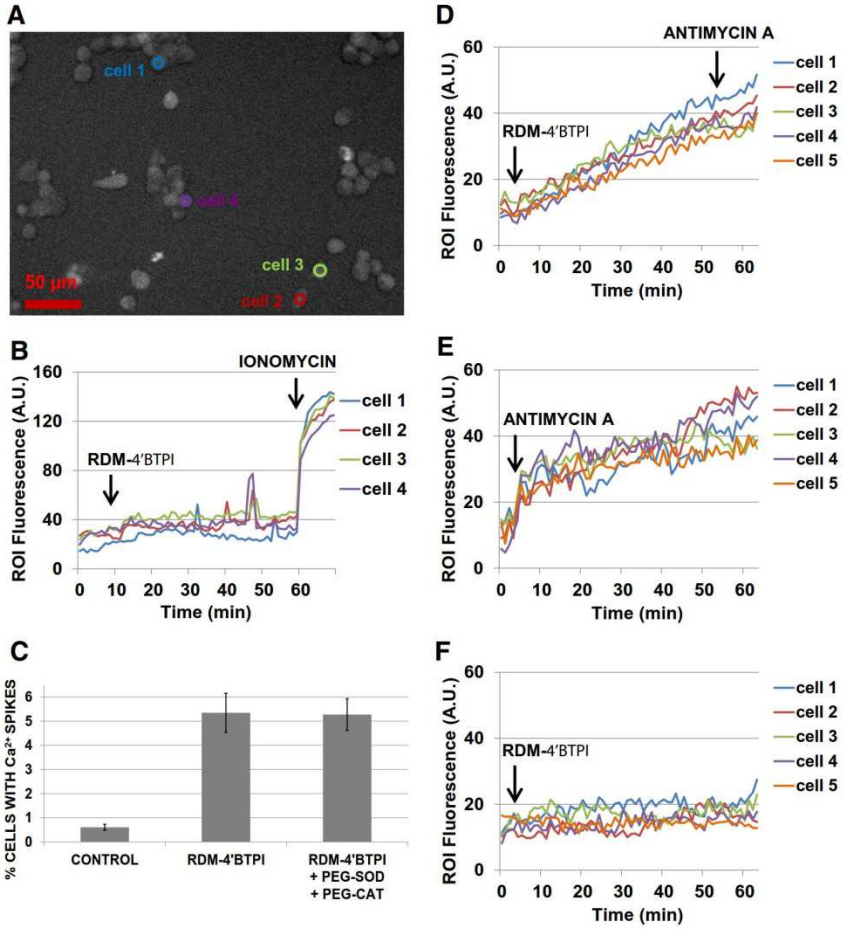

Fig. 2. Effects of RDM-4′BTPI on intracellular Ca^{2+} levels (A–C) and $O_2^{\cdot-}$ generation (D–F). A–C: Fluorescence microscopy experiments with Fluo-4 loaded CT-26 cells. A: an image (λ_{exc}: 492 nm; $\lambda_{em} > 510$ nm) acquired 30 min after addition of 5 μM RDM-4′BTPI; B: computer-generated plots of the fluorescence emitted by the regions of interest (ROI) identified in panel A, with background subtraction. The behavior of 4 cells displaying Ca^{2+} spikes is reported. 5 μM RDM-4′BTPI and 2.5 μM ionomycin were added when indicated. C: Overall extent of the phenomenon, expressed as % of cells exhibiting $[Ca^{2+}]$ spikes within 1 h, out of the total cell population. Averages ± s.d. are reported. D–F: Fluorescence microscopy experiments with MitoSOX™-loaded CT-26 cells. Computer-generated plots of the fluorescence emitted by some regions of interest (ROI); each ROI was selected to enclose one cell. The behavior of 5 representative cells is reported. 5 μM RDM-4′BTPI and/or 1 μg/mL antimycin A were added when indicated. F: PEG-SOD (40 U/mL) and PEG-CAT (500 U/mL) were present from the beginning.

3.2. Interactions with the respiratory chain

A possible rationalization of superoxide generation by our derivatives is that they may interfere with respiration, diverting part of the electron flow to superoxide production. We verified their effect on the rate of fully uncoupled (by FCCP) respiration by CT-26 cells; a high concentration (50 μM) was used, to roughly compensate for the lack of accumulation due to the dissipation of the transmembrane potential by FCCP. The compounds did decrease the rate of oxygen consumption (Fig. 3); this indicates that they can interact with respiratory chain components. This interaction seems to be favored by "masking" of the free hydroxyls with methyl or acetyl groups. Resveratrol itself caused only a modest inhibition, while rotenone and antimycin produced the expected drastic respiratory decrease, similar in extent to that observed with RDM-BTPIs (Supplementary Fig. 2).

To confirm respiratory chain inhibition and ROS generation by mitochondria we performed measurements of oxygen consumption and ROS generation with isolated rat liver mitochondria (RLM). The experiments confirmed the inhibitory effect on respiration driven by complex I (glutamate/malate) or complex II (succinate/rotenone) substrates. FACS analysis of isolated rat liver mitochondria loaded with H_2DCF-DA confirmed that our compounds cause ROS production by mitochondria energized either via complex I or complex II (Supplementary Fig. 3).

We thus verified the effect of our derivatives on the activity of the individual complexes, using alamethicin-permeabilized RLM. Also in this case, to roughly simulate the concentration of mitochondriotropic derivatives in the presence of a $\Delta\psi_m$ (which in these experiments was dissipated by permeabilization), the compounds were also used at 50 μM (Fig. 4B). Under these latter conditions inhibition of respiratory chain complexes was found to be significant in most cases, as assessed by the Mann–Whitney test. The observed effects however differed considerably in magnitude; we focus here only on the most significant ones (i.e. those inducing at least 30% activity inhibition). Complexes I and III were particularly inhibited, and methylated derivatives were the most

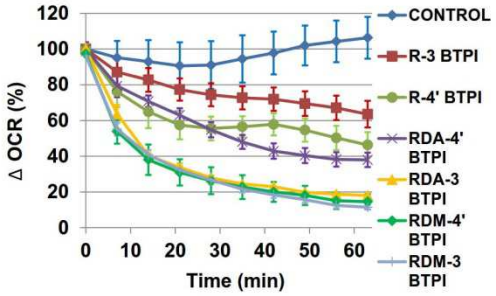

Fig. 3. Effect of mitochondriotropic resveratrol derivatives on the rate of respiration fully stimulated by FCCP. Rates of respiration by CT-26 cells were determined using a Seahorse XF24. Representative experiments are shown. Derivatives (50 μM) were added to cells after 0.2 μM FCCP. Data were normalized to the initial FCCP-elicited OCR for each set of wells and are presented as % changes with respect to that level.

effective (Fig. 4). They partially inhibited complex I (RDM-4′BTPI only) and complex III (both isomers) even at 5 μM (Fig. 4A). Resveratrol itself was shown to significantly inhibit only complex I, and only when used at 50 μM. This effect is much weaker compared to the inhibitory effects obtained with acetylated or methylated mitochondriotropic derivatives at the same concentration (about 20% inhibition vs 60–90% inhibition).

3.3. Effects on cellular oxygen consumption

5 μM R-3BTPI or R-4′BTPI had little effect on the rate of oxygen consumption by otherwise untreated CT-26 cells in experiments with Seahorse XF24 (Fig. 5A). Under the same experimental conditions, only RDM-4′BTPI reduced respiration (Fig. 5C), while RDA-3BTPI, RDA-4′BTPI and RDM-3BTPI induced relatively minor perturbations (Fig. 5B, C). However, all these four compounds drastically reduced the respiratory response to the subsequent addition of oligomycin and FCCP (Fig. 5A–C). A massive loss of cells due to death and detachment was excluded by direct microscopic observation of the cells at the end of the experiments. On the other hand, if the respiration rate was first reduced using the ATP synthase inhibitor oligomycin A, the subsequent addition of RDA-3BTPI, RDA-4′BTPI, RDM-3BTPI or RDM-4′BTPI induced an increase in oxygen consumption (respiratory "recovery"), which could hardly be further increased by the uncoupler FCCP, but was sensitive to antimycin A, an inhibitor of the mitochondrial respiratory chain (complex III) (Fig. 5E, F), thus confirming that the increase was due to respiration. R-3BTPI and R-4′BTPI had little effect in this experimental setup as well (Fig. 5D). Respiration rates in the presence of both the mitochondriotropic derivative and oligomycin were, as may be expected, similar irrespective of the order of addition.

Given the presence of oligomycin and the known interaction of resveratrol with the mitochondrial F_0F_1 ATP synthase [24,27], we initially hypothesized that the synthase may have a role in the respiratory recovery, and verified whether the compounds might be competing with oligomycin, displacing it and re-activating the enzyme. However, increasing oligomycin dosages did not prevent or markedly reduce the extent of the recovery; rather, with high oligomycin (3 or 10 μg/mL) there was a subsequent decline of the rate of respiration (Fig. 6 and Supplementary Fig. 4), which could not be rescued by FCCP, while antimycin A inhibited what respiration was left. The higher the dose of oligomycin, the more pronounced this second-stage respiratory decline, which was furthermore not affected by elimination of H_2O_2 with PEG-CAT (Supplementary Fig. 4). High concentrations of oligomycin alone caused the expected decrease of cellular respiration, which remained depressed indefinitely, without any recovery resembling that observed upon the further addition of an acylated or methylated mitochondriotropic resveratrol derivative.

The behaviour elicited by RDM-4′BTPI was again, to an extent, discrepant. With this compound the respiratory recovery in the presence of oligomycin was less pronounced than with the other compounds (Fig. 5F), and oxygen consumption after the recovery in the presence of high oligomycin declined less markedly (Fig. 6). RDM-4′BTPI is the most powerful inhibitor of complex I (Fig. 4) and the only compound which decreased OCR by untreated cells at the 5 μM level (Fig. 5C). The lower extent of respiratory recovery might thus be due to a more pronounced inhibition of the respiratory chain.

The secondary decrease of oxygen consumption at high oligomycin dosages is reminescent of an analogous phenomenon which often follows induction of the mitochondrial permeability transition (MPT), and is attributed to loss of respiratory intermediates via the MPT pore. We thus performed the same experiments in the presence of CsA, and found that the oxygen consumption rate was partially rescued by CsA when high oligomycin concentrations were used, indicating that the MPT may indeed be taking place and may at least partially account for the observations (Fig. 6). The effect is particularly evident in the case of derivatives bearing the -BTPI at position -3 of the stilbene skeleton (RDA-3BTPI and RDM-3BTPI) (Fig. 6A and C). On the other hand, we confirmed that MPT was not involved in cell death induced by our compounds alone, since CsA had no impact on the readout of MTT assays (Supplementary Fig. 5).

3.4. Interactions with the F_0F_1 ATP synthase

The effect of high oligomycin suggests an involvement of the F_0F_1 ATP synthase. Indeed, resveratrol itself is known to bind to the F_1 portion of this multimeric enzyme complex [24]. We checked the effect of the resveratrol derivatives on the hydrolytic activity of the RLM ATP synthase. Experiments were performed using isolated RLM in the

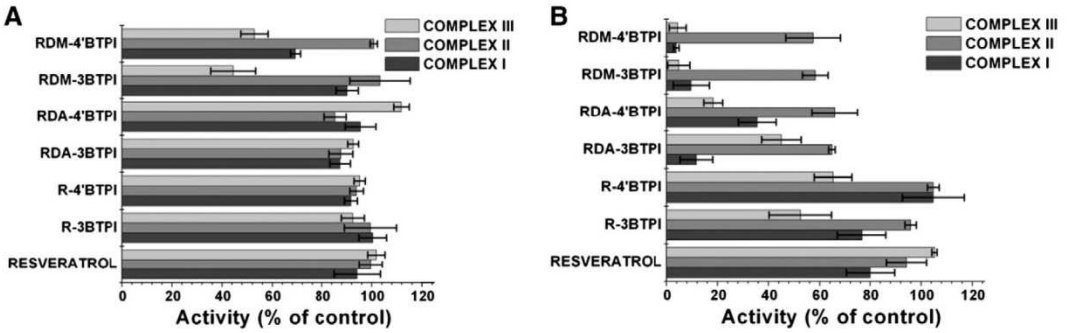

Fig. 4. Effects of resveratrol and its mitochondriotropic derivatives on the activity of the indicated respiratory chain complexes, in permeabilized RLM. Averages ± s.d. are reported (N = 3). Concentration of the derivatives was 5 μM (A) or 50 μM (B).

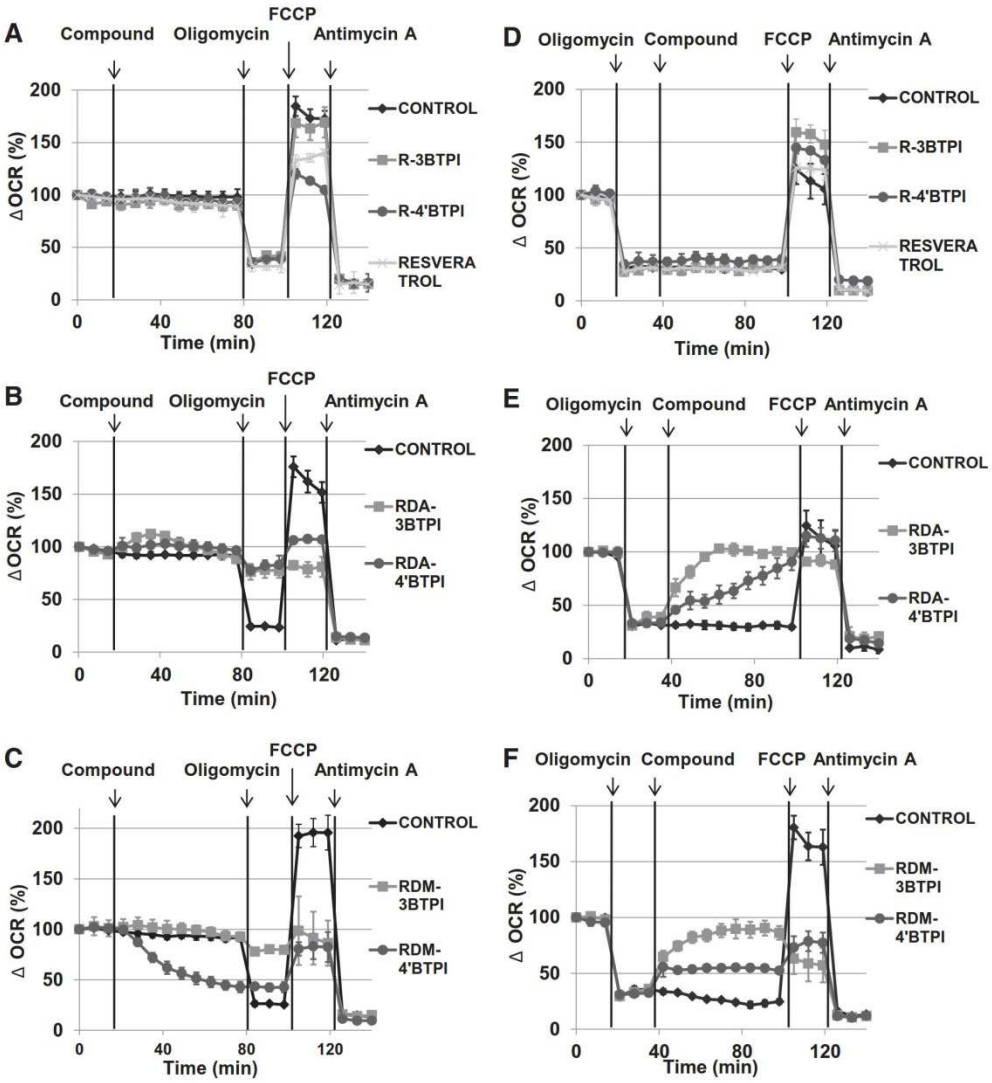

Fig. 5. Effects of mitochondriotropic resveratrol derivatives on the respiration of cultured cells. Rate of respiration by CT-26 cells as determined using Seahorse XF24. Representative experiments are shown. 5 μM of the indicated compounds was added to cells before (A, B, C) or after (D, E, F) the addition of 1 μg/mL oligomycin. A, D: resveratrol and non-acetylated/methylated derivatives; B, E: acetylated derivatives; C, F: methylated derivatives.

presence of alamethicin, which completely permeabilizes membranes to externally added reagents and also causes complete depolarization. Acetylated and methylated derivatives, as well as resveratrol, turned out to be inhibitors of the ATPase at 50 μM, while R-3BTPI and R-4′BTPI did not (Fig. 7).

ATPase inhibition by RDA-BTPIs and RDM-BTPIs was associated with an increase in the glycolytic activity of the cells, as shown by increased extracellular acidification rate (ECAR) after addition of RDA- or RDM-BTPIs (Supplementary Fig. 6).

4. Discussion

In our previous work with mitochondriotropic resveratrol derivatives [13] we had established that cell death is caused by H_2O_2, generated following accumulation of the compounds in mitochondria. Data presented above confirm this, indicating that cell death is not a consequence of Ca^{2+} dysregulation (Fig. 2) or of MPT occurrence (Supplementary Fig. 5). The compounds did increase the (low) probability of observing transient [Ca^{2+}] "spikes" in treated cells, but a relationship between this increase and the induction of cell death can be excluded because the [Ca^{2+}] spikes remained anyhow rare and were observed only in a small percentage of cells, and because death-abolishing membrane-permeant radical scavangers PEG-SOD + PEG-CAT had no effect on the [Ca^{2+}] transients. Our previous observations [13] had furthermore suggested that superoxide anion, the precursor of H_2O_2, might be formed by "slipping" complexes of the respiratory chain, which would transfer single electrons to oxygen molecules upon interaction with the compounds. This model is supported by the observation that RDA-BTPIs and RDM-BTPIs inhibit FCCP-uncoupled respiration of CT-26 cells (Fig. 3). More specifically, experiments with RLM indicate that

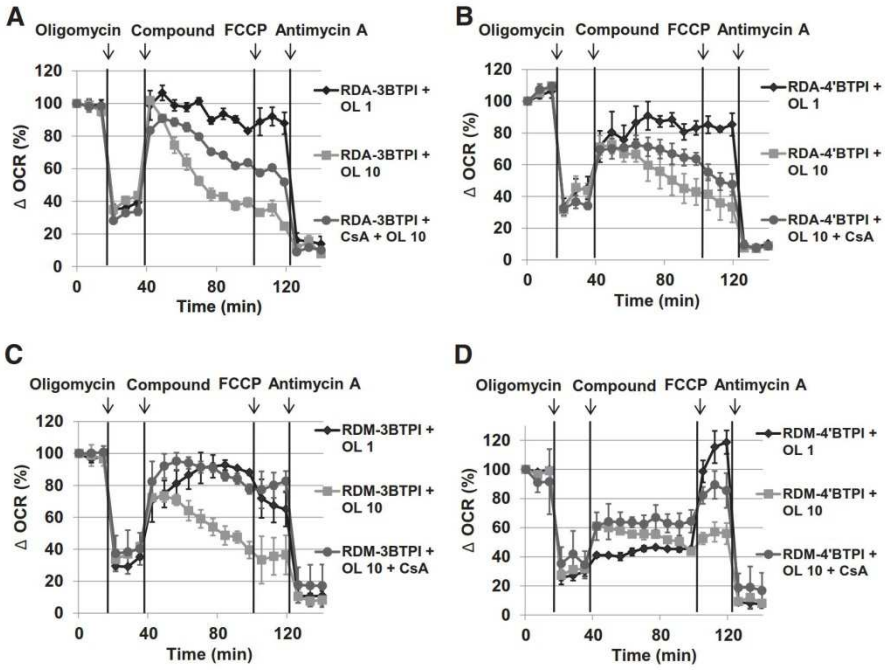

Fig. 6. Acetylated and methylated mitochondriotropic resveratrol derivatives affect respiration in an oligomycin-dependent manner. Rate of respiration by CT-26 cells as determined using Seahorse XF24. Representative experiments are shown. 5 μM of the indicated derivative was added to cells after inhibition of ATP synthase activity with oligomycin 1 μg/mL (OL 1) or 10 μg/mL (OL 10). The effect on respiration of the presence of CsA (2 μM) from the beginning of the experiment is also shown.

complexes I and III are considerably inhibited (Fig. 4). RDM-3BTPI and RDM-4′BTPI are the most powerful inhibitors; they are about equally effective on complex III, while RDM-4′BTPI appears to act more strongly than its isomer on complex I. These two complexes are known to be the major source of ROS in normal respiring mitochondria, and it is plausible that the mitochondriotropic compounds may elicit an increase of this side reaction, analogously to what happens in the case of complex II and vitamin E analogs [28]. The methylated derivatives are also, along with RDA-3BTPI, the most powerful inducers of superoxide production [13]. This correlation between inhibition of respiratory chain complexes and production of superoxide supports the notion that ROS production is a consequence of the interaction of the compounds with the complexes.

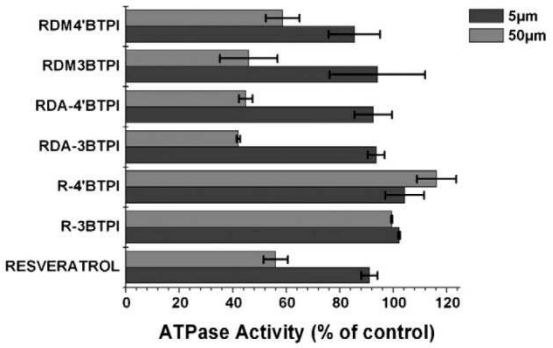

Fig. 7. Effects of resveratrol and its mitochondriotropic derivatives on the rate of ATP hydrolysis by permeabilized RLM. Averages ± s.d. are reported (N = 3).

In the same concentration range, the RLM F_0F_1 ATPase is also inhibited (Fig. 7). The four compounds with all hydroxyls capped by a substituent appear to be about equally effective. Resveratrol and other stilbene derivatives are known to interact with the F_1 portion, binding in a pocket formed by the γ and β_{TP} subunit and thereby blocking rotation ([27] and refs therein).

The higher efficiency of acetylated and methylated compounds as inhibitors and as inducers of ROS production may reflect a better partition into membranes and/or a higher affinity for the enzymes involved (see [29]). Please note that acetylated derivatives may undergo hydrolysis with rates dependent on conditions, regenerating R-3BTPI and R-4′BTPI [13].

These inhibitory properties largely account for the observations with cultured cells. In this system at least three counteracting effects of our compounds are expected to modulate oxygen consumption: inhibition of the respiratory chain and of the F_0F_1 ATP synthase (which when in operation stimulates respiratory activity via its effects on $\Delta\tilde{\mu}_H$) will tend to lower respiration while dissipation of $\Delta\tilde{\mu}_H$ [13] will tend to increase it. That ATP synthesis is hardly contributing to respiration after a one-hour exposure to 5 μM RDA- and RDM-derivatives is shown by the smallness of the effect of oligomycin (Fig. 5). That respiration is close to having exhausted its "reserve capacity" (e.g. [30]) is indicated by the lack, or near-lack of effect by FCCP (Fig. 5B–C). RDM-4′BTPI is the only compound causing a pronounced decrease of respiration by otherwise untreated CT-26 cells (Fig. 5C). This might in principle be due to a better inhibition of the ATP synthase or to a less pronounced $\Delta\psi_m$ dissipation. The data however rule these hypotheses out (Fig. 7 and [13]), leaving its greater effectiveness as an inhibitor of complex I as the plausible reason.

Measurements of respiratory rates in the presence of variable concentrations of oligomycin A, a polyketide inhibitor of the mitochondrial F_0F_1 ATP synthase acting at the interface between the c-ring and subunit

a [27], point to a further mode of action of the acetylated and in particular of the methylated compounds. If cellular respiration has previously been depressed by oligomycin, their addition induces a recovery of the respiratory rate (Fig. 5E, F). This may be simply a reflection of the loss of $\Delta\psi_m$ induced by them, the mechanism of which remains to be elucidated. By the tenets of the chemiosmotic model, depolarization with associated respiratory stimulation is likely to reflect the appearance of a $\Delta\psi_m$-dissipating proton leak. Since our derivatives interact with respiratory chain complexes and with the ATP synthase, it seems logical to propose that this proton leak may result from a functional uncoupling of the former or, more likely, the latter. In other words, we suggest that binding to complex V our compounds may not only inhibit ATP hydrolysis (and presumably synthesis), but also transform the ATP synthase into a conduit for a proton flux not associated with ATP synthesis/hydrolysis ("intrinsic uncoupling" or "proton slip"). Indeed the ATP synthase has been proposed to be able to conduct a "proton slip", a process possibly induced by isoflurane [31] or 17 β-estradiol [32] and modulated by Bcl-xL [33].

In this context it is of interest that at high oligomycin doses the respiratory recovery is followed by a CsA-sensitive decline (Fig. 6), which suggests the onset, in a stilbenoid-induced and oligomycin-sensitive process, of the permeability transition. By itself, oligomycin decreases cellular respiration due to ATP synthase inhibition, but has no further effects in the concentration range used in this work. In the literature on the MPT oligomycin is considered to be, if anything, a protective agent [34]. It follows that in our experimental system MPT pore opening can be mediated by membrane component(s) sensitive to the presence of both our mitochondriotropic derivatives and oligomycin. It seems logical to think of the ATP synthase. In the presence of excess oligomycin, the putative uncoupling ATP synthase-mediated "proton slip" may become a canonical, CsA-sensitive MPT. That development of the MPT pore may be preceded by a "small pore" phase, in which the membrane is permeable only to small ions, has been proposed in a number of papers [34–38]. It has been recently argued on the basis of electrophysiological and biochemical evidence that the ATP synthase dimer may be responsible for the generation of the MPT pore [39,40]. One point in favor of this model is the fact that the MPT pore has long been proposed to have a dimeric structure on the basis of patch-clamp recordings [34,41,42]. Our observations are therefore coherent with the emerging molecular model of the pore and reinforce it. Fig. 8 presents our working model of the cytotoxic action of mitochondriotropic resveratrol derivatives on cells. Again, while uncoupling and inhibition of the ATP synthase may well be expected to eventually lead to cell death, the most rapidly acting agent is the H_2O_2 produced. We would also like to emphasize that the onset of the MPT is only inferred to take place in our system when excess oligomycin is also provided. Judging from the lack of sensitivity of cell death to CsA (Supplementary Fig. 5), the MPT appears not to be the proximal cause of cell death induction by our mitochondriotropic resveratrol derivatives alone. The latter take in any case a front-line position in the ranks of redox-active potential "mitocans".

Acknowledgments

We thank Prof. P. Bernardi for useful discussions and access to equipment, and Mr. M. Simonetti for help with the artwork. This work was supported by grants from the Fondazione Cassa di Risparmio di Padova e Rovigo (CARIPARO) ("Developing a Pharmacology of Polyphenols"), from the Italian Ministry of the University and Research (PRIN no. 20107Z8XBW_004), and from the CNR Project of Special Interest on Aging.

Appendix A. Supplementary data

Supplementary data to this article can be found online at http://dx.doi.org/10.1016/j.bbabio.2014.06.010.

References

[1] D. Gius, D.R. Spitz, Redox signaling in cancer biology, Antioxid. Redox Signal. 8 (2006) 1249–1252.
[2] D. Trachootham, J. Alexandre, P. Huang, Targeting cancer cells by ROS-mediated mechanisms: a radical therapeutic approach? Nat. Rev. Drug Discov. 8 (2009) 579–591.

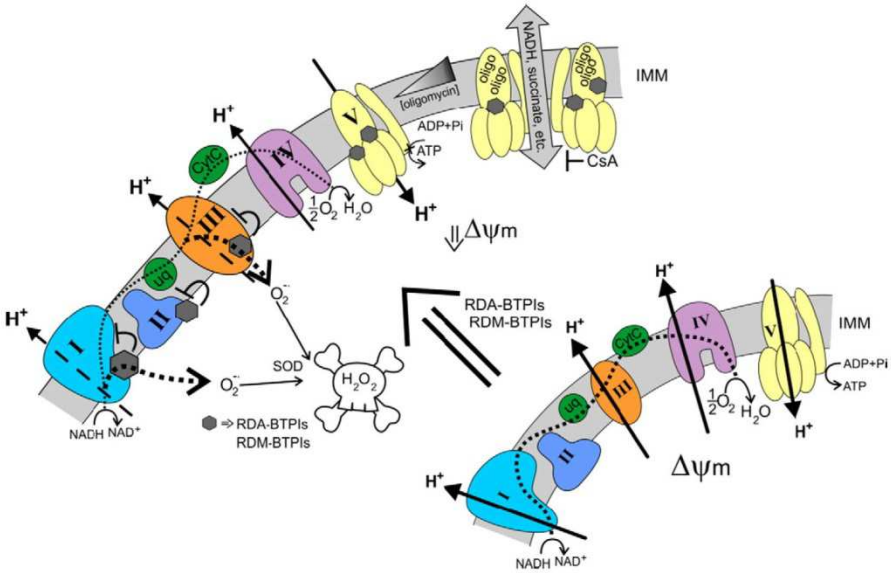

Fig. 8. Proposed mechanisms of cytotoxic action of mitochondriotropic resveratrol derivatives emerging from this work.

[3] S.J. Ralph, S. Rodriguez-Enriquez, J. Neuzil, R. Moreno-Sanchez, Bioenergetic pathways in tumor mitochondria as targets for cancer therapy and the importance of the ROS-induced apoptotic trigger, Mol. Asp. Med. 31 (2010) 29–59.
[4] S.J. Ralph, S. Rodriguez-Enriquez, J. Neuzil, E. Saavedra, R. Moreno-Sanchez, The causes of cancer revisited: "mitochondrial malignancy" and ROS-induced oncogenic transformation — why mitochondria are targets for cancer therapy, Mol. Asp. Med. 31 (2010) 145–170.
[5] L. Leanza, L. Trentin, K.A. Becker, F. Frezzato, M. Zoratti, G. Semenzato, E. Gulbins, I. Szabo, Clofazimine, Psora-4 and PAP-1, inhibitors of the potassium channel Kv1.3, as a new and selective therapeutic strategy in chronic lymphocytic leukemia, Leukemia 27 (2013) 1782–1785.
[6] J.S. Modica-Napolitano, J.R. Aprille, Delocalized lipophilic cations selectively target the mitochondria of carcinoma cells, Adv. Drug Deliv. Rev. 49 (2001) 63–70.
[7] V.R. Fantin, M.J. Berardi, L. Scorrano, S.J. Korsmeyer, P. Leder, A novel mitochondriotoxic small molecule that selectively inhibits tumor cell growth, Cancer Cell 2 (2002) 29–42.
[8] S. Bonnet, S.L. Archer, J. Allalunis-Turner, A. Haromy, C. Beaulieu, R. Thompson, C.T. Lee, G.D. Lopaschuk, L. Puttagunta, S. Bonnet, G. Harry, K. Hashimoto, C.J. Porter, M.A. Andrade, B. Thebaud, E.D. Michelakis, A mitochondria-K + channel axis is suppressed in cancer and its normalization promotes apoptosis and inhibits cancer growth, Cancer Cell 11 (2007) 37–51.
[9] S.H. Dairkee, A.J. Hackett, Differential retention of rhodamine 123 by breast carcinoma and normal human mammary tissue, Breast Cancer Res. Treat. 18 (1991) 57–61.
[10] J. Neuzil, L.F. Dong, J. Rohlena, J. Truksa, S.J. Ralph, Classification of mitocans, anti-cancer drugs acting on mitochondria, Mitochondrion 13 (2013) 199–208.
[11] L. Biasutto, L.F. Dong, M. Zoratti, J. Neuzil, Mitochondrially targeted anti-cancer agents, Mitochondrion 10 (2010) 670–681.
[12] L. Biasutto, A. Mattarei, E. Marotta, A. Bradaschia, N. Sassi, S. Garbisa, M. Zoratti, C. Paradisi, Development of mitochondria-targeted derivatives of resveratrol, Bioorg. Med. Chem. Lett. 18 (2008) 5594–5597.
[13] N. Sassi, A. Mattarei, M. Azzolini, P. Bernardi, I. Szabo, C. Paradisi, M. Zoratti, L. Biasutto, Mitochondria-targeted resveratrol derivatives act as cytotoxic pro-oxidants, Curr. Pharm. Des. 20 (2014) 172–179.
[14] D. Delmas, E. Solary, N. Latruffe, Resveratrol, a phytochemical inducer of multiple cell death pathways: apoptosis, autophagy and mitotic catastrophe, Curr. Med. Chem. 18 (2011) 1100–1121.
[15] G. Cao, E. Sofic, R.L. Prior, Antioxidant and prooxidant behavior of flavonoids: structure–activity relationships, Free Radic. Biol. Med. 22 (1997) 749–760.
[16] L. Biasutto, N. Sassi, A. Mattarei, E. Marotta, P. Cattelan, A. Toninello, S. Garbisa, M. Zoratti, C. Paradisi, Impact of mitochondriotropic quercetin derivatives on mitochondria, Biochim. Biophys. Acta 1797 (2010) 189–196.
[17] V. Desquiret-Dumas, N. Gueguen, G. Leman, S. Baron, V. Nivet-Antoine, S. Chupin, A. Chevrollier, E. Vessieres, A. Ayer, M. Ferre, D. Bonneau, D. Henrion, P. Reynier, V. Procaccio, Resveratrol induces a mitochondrial complex I-dependent increase in NADH oxidation responsible for sirtuin activation in liver cells, J. Biol. Chem. 288 (2013) 36662–36675.
[18] R. Zini, C. Morin, A. Bertelli, A.A. Bertelli, J.P. Tillement, Effects of resveratrol on the rat brain respiratory chain, Drugs Exp. Clin. Res. 25 (1999) 87–97.
[19] T.I. Peng, M.J. Jou, Oxidative stress caused by mitochondrial calcium overload, Ann. N. Y. Acad. Sci. 1201 (2010) 183–188.
[20] A.V. Zima, L.A. Blatter, Redox regulation of cardiac calcium channels and transporters, Cardiovasc. Res. 71 (2006) 310–321.
[21] S. Wagner, A.G. Rokita, M.E. Anderson, L.S. Maier, Redox regulation of sodium and calcium handling, Antioxid. Redox Signal. 18 (2013) 1063–1077.
[22] J. Zheng, V.D. Ramirez, Inhibition of mitochondrial proton F0F1-ATPase/ATP synthase by polyphenolic phytochemicals, Br. J. Pharmacol. 130 (2000) 1115–1123.
[23] J.R. Gledhill, J.E. Walker, Inhibition sites in F1-ATPase from bovine heart mitochondria, Biochem. J. 386 (2005) 591–598.
[24] J.R. Gledhill, M.G. Montgomery, A.G. Leslie, J.E. Walker, Mechanism of inhibition of bovine F1-ATPase by resveratrol and related polyphenols, Proc. Natl. Acad. Sci. U. S. A. 104 (2007) 13632–13637.
[25] C. Frezza, S. Cipolat, L. Scorrano, Organelle isolation: functional mitochondria from mouse liver, muscle and cultured fibroblasts, Nat. Protoc. 2 (2007) 287–295.
[26] A. Mattarei, L. Biasutto, E. Marotta, U. De Marchi, N. Sassi, S. Garbisa, M. Zoratti, C. Paradisi, A mitochondriotropic derivative of quercetin: a strategy to increase the effectiveness of polyphenols, Chembiochem 9 (2008) 2633–2642.
[27] S. Hong, P.L. Pedersen, ATP synthase and the actions of inhibitors utilized to study its roles in human health, disease, and other scientific areas, Microbiol. Mol. Biol. Rev. 72 (2008) 590–641 (Table of Contents).
[28] S.J. Ralph, R. Moreno-Sanchez, J. Neuzil, S. Rodriguez-Enriquez, Inhibitors of succinate: quinone reductase/complex II regulate production of mitochondrial reactive oxygen species and protect normal cells from ischemic damage but induce specific cancer cell death, Pharm. Res. 28 (2011) 2695–2730.
[29] J. Xiao, G. Kai, A review of dietary polyphenol–plasma protein interactions: characterization, influence on the bioactivity, and structure–affinity relationship, Crit. Rev. Food Sci. Nutr. 52 (2012) 85–101.
[30] B.E. Sansbury, S.P. Jones, D.W. Riggs, V.M. Darley-Usmar, B.G. Hill, Bioenergetic function in cardiovascular cells: the importance of the reserve capacity and its biological regulation, Chem. Biol. Interact. 191 (2011) 288–295.
[31] D. Pravdic, N. Hirata, L. Barber, F. Sedlic, Z.J. Bosnjak, M. Bienengraeber, Complex I and ATP synthase mediate membrane depolarization and matrix acidification by isoflurane in mitochondria, Eur. J. Pharmacol. 690 (2012) 149–157.
[32] A.J. Moreno, P.I. Moreira, J.B. Custodio, M.S. Santos, Mechanism of inhibition of mitochondrial ATP synthase by 17beta-estradiol, J. Bioenerg. Biomembr. 45 (2013) 261–270.
[33] K.N. Alavian, H. Li, L. Collis, L. Bonanni, L. Zeng, S. Sacchetti, E. Lazrove, P. Nabili, B. Flaherty, M. Graham, Y. Chen, S.M. Messerli, M.A. Mariggio, C. Rahner, E. McNay, G.C. Shore, P.J. Smith, J.M. Hardwick, E.A. Jonas, Bcl-xL regulates metabolic efficiency of neurons through interaction with the mitochondrial F_1F_O ATP synthase, Nat. Cell Biol. 13 (2011) 1224–1233.
[34] M. Zoratti, I. Szabo, The mitochondrial permeability transition, Biochim. Biophys. Acta 1241 (1995) 139–176.
[35] S.A. Novgorodov, T.I. Gudz, Permeability transition pore of the inner mitochondrial membrane can operate in two open states with different selectivities, J. Bioenerg. Biomembr. 28 (1996) 139–146.
[36] F. Ichas, J.P. Mazat, From calcium signaling to cell death: two conformations for the mitochondrial permeability transition pore Switching from low- to high-conductance state, Biochim. Biophys. Acta 1366 (1998) 33–50.
[37] Y.E. Kushnareva, P.M. Sokolove, Prooxidants open both the mitochondrial permeability transition pore and a low-conductance channel in the inner mitochondrial membrane, Arch. Biochem. Biophys. 376 (2000) 377–388.
[38] A. Toninello, M. Salvi, M. Schweizer, C. Richter, Menadione induces a low conductance state of the mitochondrial inner membrane sensitive to bongkrekic acid, Free Radic. Biol. Med. 37 (2004) 1073–1080.
[39] V. Giorgio, S. von Stockum, M. Antoniel, A. Fabbro, F. Fogolari, M. Forte, G.D. Glick, V. Petronilli, M. Zoratti, I. Szabo, G. Lippe, P. Bernardi, Dimers of mitochondrial ATP synthase form the permeability transition pore, Proc. Natl. Acad. Sci. U. S. A. 110 (2013) 5887–5892.
[40] P. Bernardi, The mitochondrial permeability transition pore: a mystery solved? Front. Physiol. 4 (2013) 95.
[41] I. Szabo, M. Zoratti, The mitochondrial permeability transition pore may comprise VDAC molecules. I. Binary structure and voltage dependence of the pore, FEBS Lett. 330 (1993) 201–205.
[42] U. De Marchi, I. Szabo, G.M. Cereghetti, P. Hoxha, W.J. Craigen, M. Zoratti, A maxi-chloride channel in the inner membrane of mammalian mitochondria, Biochim. Biophys. Acta 1777 (2008) 1438–1448.

Cytotoxicity of mitochondria-targeted resveratrol derivatives: interactions with respiratory chain complexes and ATP synthase

Nicola Sassi [a,b], Andrea Mattarei [b,c], Michele Azzolini [a], Ildiko' Szabo' [d], Cristina Paradisi [c], Mario Zoratti [a,b], Lucia Biasutto [a,b,*]

[a]Department of Biomedical Sciences, Viale G. Colombo 3, 35121 Padova, Italy
[b]CNR Neuroscience Institute, Viale G. Colombo 3, 35121 Padova, Italy
[c]Department of Chemical Sciences, Via F. Marzolo 1, 35131 Padova, Italy
[d]Department of Biology, Viale G. Colombo 3, 35121 Padova, Italy

SUPPLEMENTARY DATA

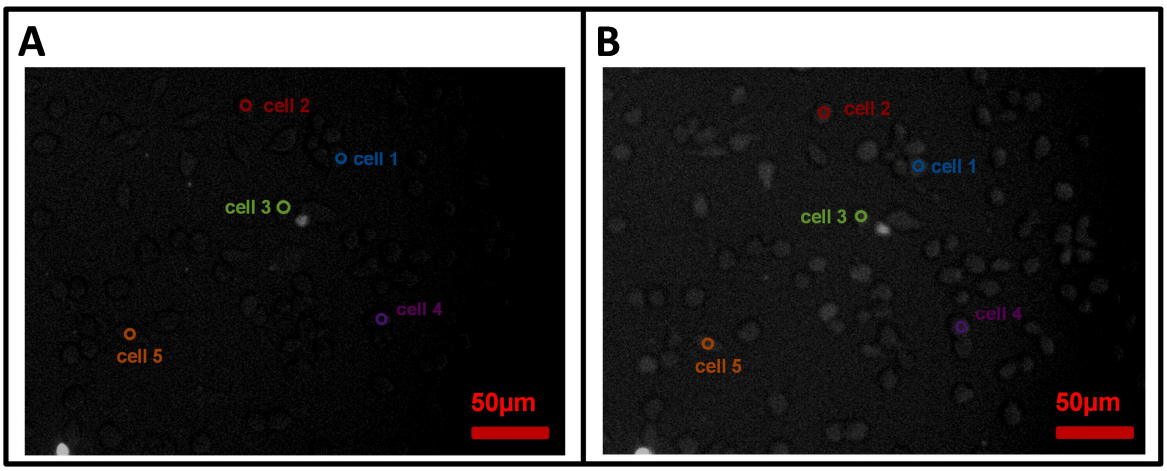

Supplementary Figure 1. *Effects of RDM-4'BTPI on intracellular $O2^{-\cdot}$ generation. Fluorescence microscopy experiment with MitoSOX^{TM}-loaded CT-26 cells. Representative images (λ_{exc}: 500-520 nm; λ_{em}>570 nm) acquired 1 minute before (A) and 30 minutes after (B) addition of 5 µM RDM-4'BTPI. The Regions of Interest (ROI) identified in panels A and B are those used to generate the fluorescence plots shown in Fig. 2D.*

The MitoSOX^{TM} fluorescence increase was homogenous and took place in all cells, at variance with the behavior reported by the Ca^{2+} probe Fluo-4 (Fig. 2A-C).

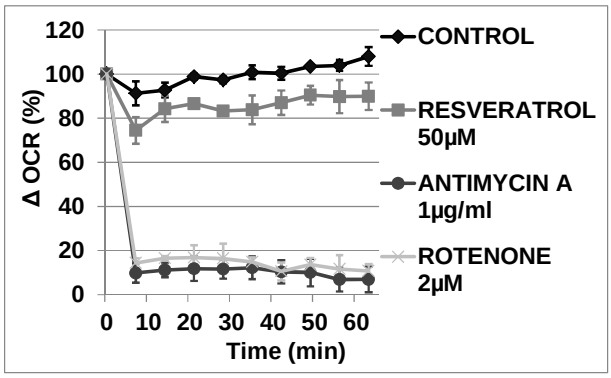

Supplementary Figure 2. *Effect of Resveratrol and known respiratory chain inhibitors on respiration fully stimulated by FCCP. Rates of respiration by CT-26 cells were determined using a Seahorse XF24. A representative experiment is shown. Compounds were added at the indicated concentration to cells previously treated with 0.2µM FCCP. Data were normalized to the initial FCCP-elicited OCR for each set of wells and are presented as % changes with respect to that level.*

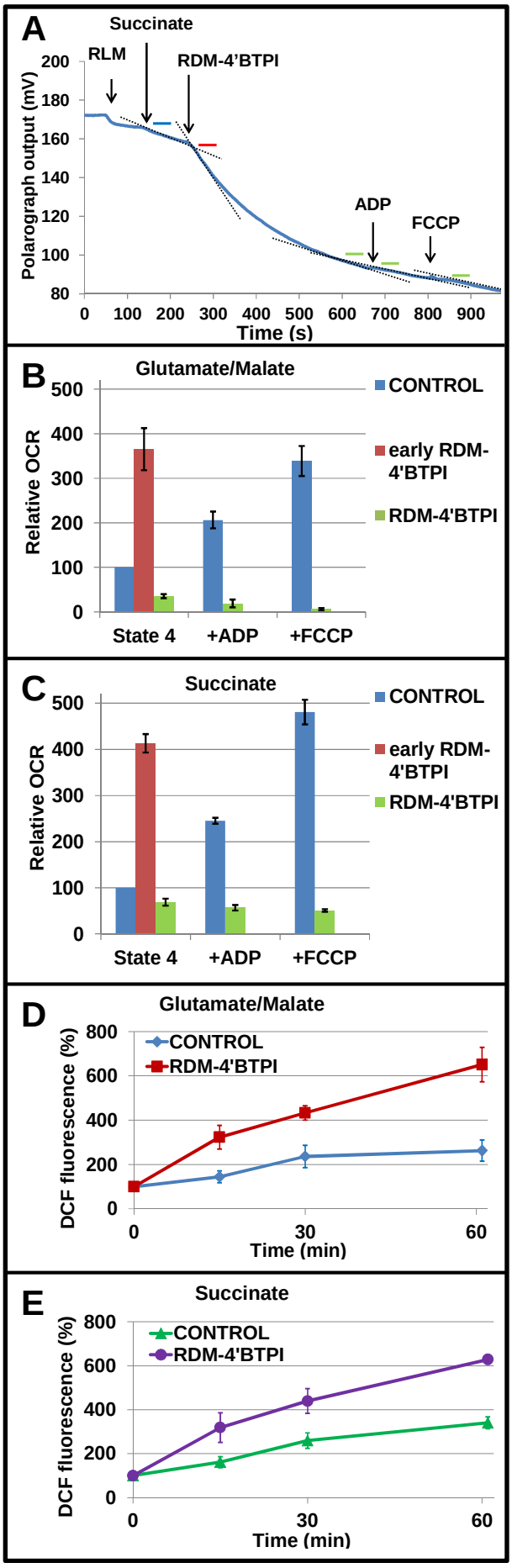
A
Succinate
RLM
RDM-4'BTPI
ADP
FCCP
Polarograph output (mV)
200
180
160
140
120
100
80
0
100
200
300
400
500
600
700
800
900
Time (s)
B
Glutamate/Malate
Relative OCR
500
400
300
200
100
0
State 4
+ADP
+FCCP
CONTROL
early RDM-4'BTPI
RDM-4'BTPI
C
Succinate
Relative OCR
500
400
300
200
100
0
State 4
+ADP
+FCCP
CONTROL
early RDM-4'BTPI
RDM-4'BTPI
D
Glutamate/Malate
DCF fluorescence (%)
800
600
400
200
0
CONTROL
RDM-4'BTPI
0
30
60
Time (min)
E
Succinate
DCF fluorescence (%)
800
600
400
200
0
CONTROL
RDM-4'BTPI
0
30
60
Time (min)

Supplementary Figure 3. *Effects of RDM-4'BTPI on the oxygen consumption rate and ROS generation by isolated rat liver mitochondria. A) An exemplary polarographic trace illustrating the experimental protocol. In this example 5 mM succinate was the respiratory substrate and 2 µM rotenone was present. The bars above the trace indicate what segments of the trace itself were used to calculate (by linear interpolation) the slope coefficients shown in panels B and C. RLM: 0.5 mg.prot./mL; RDM-4'BTPI: 50 µM; ADP: 100µM; FCCP: 100nM. See below for other details. B) and C) Plot of the average values ± s.d. of the relative slope measured in repeat experiments (N = 3) analogous to the one in panel A. Blue columns: no RDM-4'BTPI addition. Red or green columns: after RDM-4'BTPI addition. Slope values are normalized setting the slope of the state 4 (no addition except respiratory substrate) segment = 100. D) and E) Effects of RDM-4'BTPI on ROS generation by RLM. Flow cytometry experiments with H_2DCF-DA -loaded RLM.*
Respiratory substrate was glutamate/malate (5mM and 2.5mM respectively; panels B and D) or succinate (5 mM) in the presence of 2µM rotenone (panels C and E).

Rate of respiration by isolated RLM. The rate of respiration by RLM was measured in polarographic assays using a Clark electrode inserted in a thermostatted (25 °C) and stirred enclosed chamber with an airtight injection port. The electrode was controlled by an HansaTech CB1D control box and interfaced with a personal computer by a Microlink 751 digitizer. The standard medium contained 250 mM sucrose, 20 mM 3-[N-morpholino]butanesulfonic acid (MOPS), 10 mM Tris-Base, 1 mM Pi/K^+, 0.5 mM Mg^{2+}, pH 7.0. RLM were used at a concentration of 0.5 mg prot./mL. The relative rate of oxygen consumption under the various conditions was obtained as the slope of the interpolation (best linear fit) of the relevant segment of the polarograph output (dimensions: mV/min) divided by the slope of the best linear fit of the output in the presence of mitochondria and respiratory substrate only.

Flow cytometry with RLM. ROS generation in isolated RLM was measured in flow cytometry experiments using the fluorescent probe dichlorofluorescein (DCF), as described in [38]. Briefly, RLM were resuspended in the assay buffer (250 mM sucrose, 20 mM 3-[N-morpholino]butanesulfonic acid (MOPS), 10 mM Tris-Base, 1 mM Pi/K^+, 0.5 mM Mg^{2+}, pH 7.0) at a concentration of 0.5 mg prot./mL, and loaded with 2',7'-dichlorodihydrofluorescein-diacetate (H_2DCF-DA, 10 µM) in the presence of Cyclosporin A (CsA; 1 µM) (25°C, 10 min). 5 mM glutamate plus 2.5 mM malate or 5 mM succinate

plus 2 µM rotenone were added to allow respiration via complex I or complex II, respectively. After loading, RLM were divided into identical aliquots. At time zero the various compounds were added and data were collected after the desired incubation times (50,000 counts for each measurement). A Beckton Dickinson Canto II flow cytometer was used. Excitation was at 488 nm and fluorescence was collected in the 506-540 nm interval. To exclude debris and aggregates, samples were gated based on light-scattering properties in the side scatter and forward scatter modes, as determined in preliminary experiments with RLM stained with NAO or TMRM. Data were analyzed using the BD VISTA software. Averages ± s.d. of the medians of RLM fluorescence distribution histograms are plotted, normalized to the value measured immediately after addition of the compounds (time = 0).

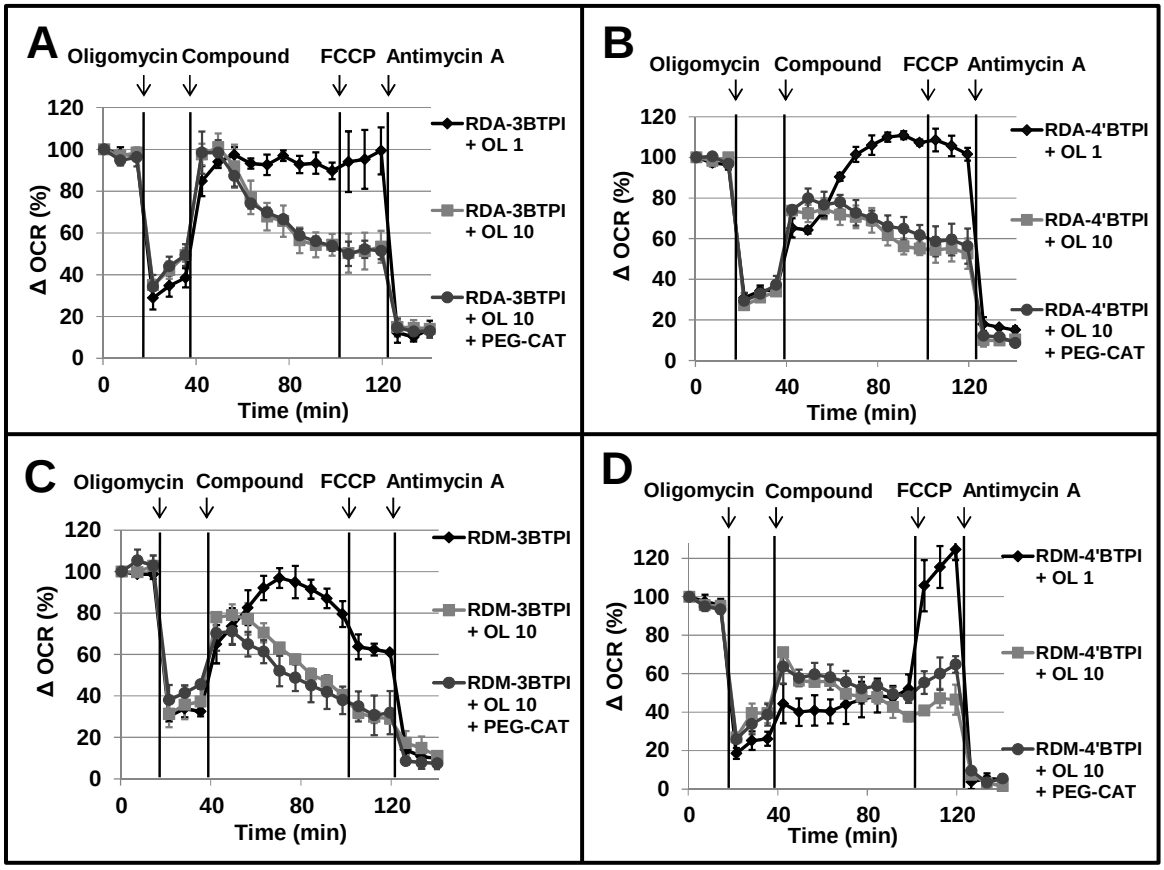

Supplementary Figure 4. *The decline of "recovered" respiration at high concentrations of oligomycin is not significantly affected by permeant Catalase (PEG-CAT) at concentrations (500 U/ml) shown to strongly reduce cell death (Sassi N., et al. Curr Pharm Des 2014). The plots show rates of respiration by CT-26 cells as determined using Seahorse XF24. Representative experiments are shown. 5 µM (final concentration) of the indicated derivative was added to cells after inhibition of ATP synthase activity with oligomycin 1 µg/mL (OL 1) or 10 µg/mL (OL 10).*

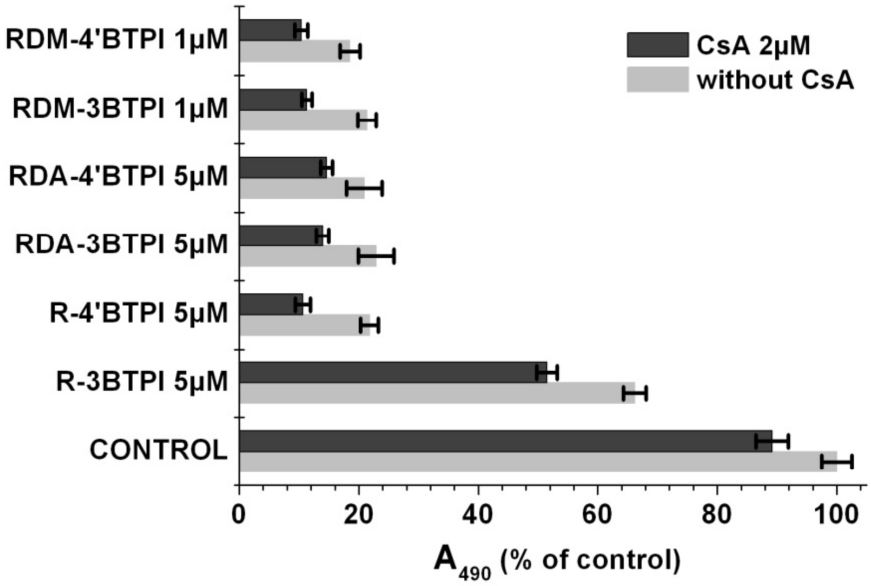

Supplementary Figure 5. *Impact of CsA on cytotoxicity induced by mitochondriotropic resveratrol derivatives. MTT assay readout. CT-26 cells were grown for 3 days in the presence of the specified compounds. Experiments were performed as described below.*

Cell growth/viability (MTT) assays. CT-26 cells were seeded in standard 96-well plates and allowed to grow overnight in DMEM + 10% FBS (200 µL) to insure their attachment. Initial density was 3000 cells/well. After cell attachment, the growth medium was replaced with DMEM + 10% FBS containing the desired compounds. Final DMSO concentration was 0.1% in all cases (including controls). Cells were incubated with the compounds for 72 h; every 24 h the medium was substituted by a fresh aliquot (with compounds). At the end of the incubation period the medium was removed and 100 µL of PBS containing 10% CellTiter 96® AQUEOUS One solution (Promega) were added into each well. After 1 h of color development at 37°C, absorbance at 490 nm was measured using a Packard Spectra Count 96-well plate reader. All measurements were performed in quadruplicate in each experiment.

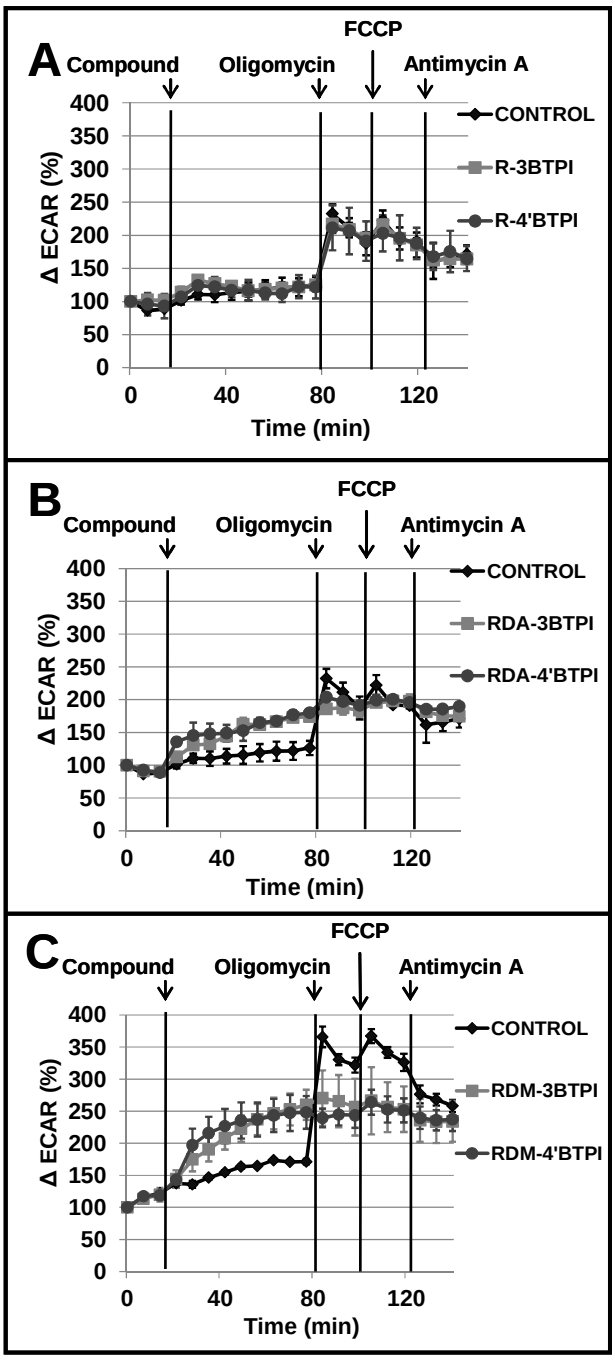

Supplementary Figure 6*. Effects of acetylated and methylated resveratrol derivatives on the extracellular acidification rate (ECAR). ECAR was determined using Seahorse XF24. Representative experiments are shown. 5 µM R-BTPIs (A), RDA-BTPIs (B) or RDM-BTPIs (C) were added to CT-26 cells when indicated.*

Abbreviations:

AC: adenylate cyclase

ACN: acetonitrile (CH_3CN)

AMP: 5'-adenosine monophosphate

AMPK: 5'-adenosine monophosphate (AMP)-activated protein kinase

AOM: azoxymethane

ARE: antioxidant response element

AUC: area under the curve

BDNF: brain-derived neurotrophic factor

BSA: bovine serum albumin

cAMP: cyclic AMP

CBP: CREB binding protein (also called CREBBP)

CREB: cAMP response element-binding protein

C_{max}: maximal concentration

COX: cyclooxygenase

D-PBS: Dulbecco's phosphate buffered saline

DG: dentate gyrus

DHP-C: dihydroxypropyl carbamate

DI: discrimination index

DMAP: 4-(dimethylamino)pyridine

DMSO: dimethyl sulfoxide

DSS: sodium dextran sulfate

EDTA: ethylenediaminetetraacetic acid

ECL: enhanced chemiluminescence

EGCG: epigallocatechin gallate

EPAC: exchange protein activated by cAMP

ER-β: estrogen receptor beta

EtOAc: ethyl acetate

EtOH: ethanol

GCL: glutamate-cysteine ligase

GSTP1: glutathione sulfotransferase-π 1

GSTs: glutathione S transferases

H30-FRET: epac-H30 Fluorescence Resonance Energy Transfer

HAT: acetyltransferase

HBSS: Hank's balanced salt solution

HIP: hippocampus

HLP: hypotonic lysis buffer

HMOX1: heme oxygenase 1

HP-β-CD: 2-hydroxypropyl-β-cyclodextrin

HPLC-ESI/MS: high performance liquid chromatography-electrospray ionization/mass spectrometry

HPLC-UV: high performance liquid chromatography-UV

HRP: horseradish peroxidase

IBMX: 3-isobutyl-1-methylxanthine

IkB: inhibitor of kappa B

IKK: IκB kinase

LAT: L-type aminoacids transporter

LOD: limit of detection

LOQ: limit of quantification

MAPK: mitogen-activated protein kinases

MTA1: metastasis associated protein 1

mTORC1: mammalian target of rapamycin complex 1

NADP: nicotinamide adenine dinucleotide phosphate

NF-kB: nuclear factor kappaB

NLB: nuclear lysis buffer

NMR: nuclear magnetic resonance

NQO2: dihydronicotinamide riboside quinone reductase 2

Nrf2/Keap1: nuclear factor erythroid 2 [NF-E2]-related factor 2/Kelch-like erythroid cell-derived protein with CNC homology [ECH]-associated protein 1

NuRD: nucleosome remodeling deacetylase complex

OCT: object in context test

OEG: oligo ethyleneglycol

ORT: object recognition test

Pd/C: palladium/carbon

PDE: phosphodiesterase

PFc: prefrontal cortex

PLCγ: phospholipase C γ

PI3K: phosphatidylinositol 3-kinase

PKA: protein kinase A

PKC: protein kinase C

PRNLc: perirhinal cortex

PSD95: postsynaptic density protein 95 (the corresponding gene is named *dlg4*)

PPAR: peroxisome proliferator-activated receptor

Pt: pterostilbene

Pt-S: pterostilbene 4'-Sulfate

RIPA: radio immune assay (buffer)

RbAp48: retinoblastoma associated protein 48 (also called RBBP4, retinoblastoma binding protein 4, the corresponding gene is named *rbbp4*)

REST: RE1-silencing transcription factor (also called neuron-restrictive silencer factor, NRSF)

ROS: reactive oxygen species

RT-qPCR: quantitative reverse transcription PCR

Rv: resveratrol

Rv-3-sulfate: resveratrol-3-Sulfate

Rv-3,4'-disulfate: resveratrol-3,4'-diSulfate

SIRT: sirtuin

SOD: superoxide dismutase

TBS: tris-buffered saline

TEA: triethylamine

TFA: trifluoroacetic acid

TFEB: transcription factor EB

T_{max}: time to maximal concentration

TrkB: tropomyosin-related kinase receptor B

Participation to congresses:

Oral communications:

- Michele Azzolini, Martina La Spina, Andrea Mattarei, Cristina Paradisi, Lucia Biasutto. *Following dietary poliphenols' fate after oral administration; a map of distribution of Pterostilbene and one of its prodrugs in major organs of rat.* 62nd International Congress and Annual Meeting of the society for Medicinal Plant and Natural Product Research – GA2014. 31 August – September 4 2014. Guimarães, Portugal.
- Michele Azzolini, Andrea Mattarei, Massimo Carraro, Nicola Sassi, Mario Zoratti, Cristina Paradisi, Lucia Biasutto. *Acetal prodrugs of polyphenols.* Resveratrol and other anti-inflammatory compounds in human health, PhD Course. 28-29 August 2012., Roskilde, Denmark.
- Andrea Mattarei, Michele Azzolini, Lucia Biasutto, Matteo Romio, Mario Zoratti, Cristina Paradisi. *Synthesis and Characterization of New Derivatives of Natural Bioactive Polyphenols to Improve Oral Bioavailability*. XXXV Convegno della Divisione di Chimica Organica della Società Chimica Italiana. Sept. 9-13, 2013. Sassari, Italy.
- Matteo Romio, Andrea Mattarei, Michele Azzolini, Lucia Biasutto, Mario Zoratti, Cristina Paradisi. *Synthesis of new derivatives to improve the bioactivity of natural polyphenols*. XXXV Convegno della Divisione di Chimica Organica della Società Chimica Italiana. Sept. 9-13, 2013. Sassari, Italy.
- Lucia Biasutto, Nicola Sassi, Andrea Mattarei, Michele Azzolini, Matteo Romio, Cristina Paradisi, Mario Zoratti. *Cytotoxicity of mitochondriotropic quercetin and resveratrol derivatives.* International PSE Symposium on Natural Products in Cancer Therapy. June 25-28, 2013. Naples, Italy.
- Nicola Sassi, Andrea Mattarei, Michele Azzolini, Cristina Paradisi, Mario Zoratti, Lucia Biasutto. *Mitochondria-targeted Resveratrol derivatives act as cytotoxic pro-oxidants*. Annual Meeting of the Italian Group of Biomembranes and Bioenergetics (GIBB). 20-22 June 2013. Padova, Italy.
- Lucia Biasutto, Nicola Sassi, Andrea Mattarei, Michele Azzolini, Paolo Bernardi, Ildiko Szabo, Cristina Paradisi, Mario Zoratti. *Cytotoxicity of mitochondria-targeted Resveratrol derivatives: interactions with respiratory chain complexes and ATP synthase*. Annual Meeting of the Italian Group of Biomembranes and Bioenergetics (GIBB). 20-22 June 2013. Padova, Italy.

Poster:

- Michele Azzolini, Martina La Spina, Andrea Mattarei, Cristina Paradisi, Mario Zoratti, Lucia Biasutto. *Soluble prodrugs for efficient intestinal delivery of resveratrol*. 62nd International Congress and Annual Meeting of the society for Medicinal Plant and Natural Product Research – GA2014. 31 August – September 4 2014. Guimarães, Portugal.
- Andrea Mattarei, Michele Azzolini, Martina La Spina, Cristina Paradisi, Mario Zoratti, Lucia Biasutto. *Amino acid carbamate ester prodrugs of pterostilbene. Synthesis, evaluation and map of distribution in major organs of rat compared with pterostilbene.* 7th International Conference and Exhibition on Nutraceuticals and Functional Foods. October 14-17, 2014. Istanbul, Turkey.

- Michele Azzolini, Martina La Spina, Andrea Mattarei, Cristina Paradisi, Lucia Biasutto, Mario Zoratti. *Sugar-decorated prodrugs for intestinal delivery of resveratrol.* 7th International Conference and Exhibition on Nutraceuticals and Functional Foods. October 14-17, 2014. Istanbul, Turkey.
- Andrea Mattarei, Michele Azzolini, Lucia Biasutto, Matteo Romio, Mario Zoratti, Cristina Paradisi. *Improving the properties of plant polyphenols.* 6th International Conference on Polyphenols and Health. October 16-20, 2013. Buenos Aires, Argentina.
- Andrea Mattarei, Michele Azzolini, Lucia Biasutto, Matteo Romio, Cristina Paradisi, Mario Zoratti. *Synthesis and evaluation of new derivatives of natural polyphenols to improve oral bioavailability*. Annual meeting of the CNR Institute of Neuroscience. Sept. 18-20, 2013. Cagliari, Italy.
- Nicola Sassi, Lucia Biasutto, Andrea Mattarei, Michele Azzolini, Matteo Romio, Cristina Paradisi, Mario Zoratti. Cytotoxicity of mitochondriotropic quercetin and resveratrol derivatives: mechanisms. Annual meeting of the CNR Institute of Neuroscience. Sept. 18-20, 2013. Cagliari, Italy.
- Lucia Biasutto, Nicola Sassi, Andrea Mattarei, Michele Azzolini, Matteo Romio, Cristina Paradisi, Mario Zoratti. *Improving the properties of plant polyphenols.* 5e Symposium International "Nutrition, Biologie de L'Oxygène et Médecine". 5-7 Juin 2013. Paris, France.
- Lucia Biasutto, Andrea Mattarei, Michele Azzolini, Alice Bradaschia, Massimo Carraro, Ester Marotta, Spiridione Garbisa, Cristina Paradisi, Mario Zoratti. *Acetal prodrugs of resveratrol*". Resveratrol 2012 - 2nd international conference of resveratrol and health. Dec. 5-7, 2012. Leicester, UK.
- Massimo Carraro, Andrea Mattarei, Michele Azzolini, Lucia Biasutto, Mario Zoratti, Cristina Paradisi. *Nanocapsules with core-shell structure for delivery of polyphenols*. XXXIV National Meeting of the Organic Chemistry Division of the Italian Chemical Society. Sept. 10-14, 2012. Pavia, Italy.
- Andrea Mattarei, Alice Bradaschia, Lucia Biasutto, Michele Azzolini, Massimo Carraro, Ester Marotta, Spiridione Garbisa, Cristina Paradisi, Mario Zoratti: "*Synthesis of acetal derivatives of resveratrol: a method to improve the oral bioavailability of polyphenols*". XXXIV National Meeting of the Organic Chemistry Division of the Italian Chemical Society. Sept. 10-14, 2012. Pavia, Italy.
- Andrea Mattarei, Lucia Biasutto, Alice Bradaschia, Michele Azzolini, Massimo Carraro, E. G. Rodríguez Velo, Ester Marotta, Spiridione Garbisa, Cristina Paradisi, Mario Zoratti. *Acetal prodrugs of polyphenols*. Annual meeting of the CNR Institute of Neuroscience. Feb. 29-March 3, 2012. Bressanone/Brixen, Italy.

Ringraziamenti:

Desidero infine ringraziare tutti i componenti del mio gruppo di ricerca, primi fra tutti il dott. Mario Zoratti e la dott.ssa Lucia Biasutto per avermi guidato con professionalità e pazienza. Ringrazio Martina La Spina, Nicola Sassi, Alice Bradaschia ed Almudena Ubieta per aver reso un po' più leggere le interminabili ore di laboratorio.

Un ringraziamento alla prof.ssa Cristina Paradisi, ai dott. Andrea Mattarei e Matteo Romio per il loro fondamentale contributo nei miei progetti di ricerca, ed a tutto il loro gruppo di lavoro: Ester Marotta, Massimo Carraro, Viviana Russo, Michele Fanin, Stefano Pluda, Veronica Bombardelli, Ennio Lavagnini e Giacomo Chiodarelli.

Un ringraziamento ai nostri collaboratori, senza i quali molte nostre idee non sarebbero state sviluppate. Grazie alla prof.ssa Nicoletta Berardi, ai dott. Alessandro Sale, Laura Baroncelli e Silvia Morea per il supporto nel progetto invecchiamento. Grazie al prof. Andrea Ballabio e alla dott.ssa Giulietta di Benedetto per il loro contributo nel progetto autofagia.

Grazie al dott. Carlo Zatti, a Mauro Ghidotti ed alla dott.ssa Sandra Furlan per avermi istruito ed affiancato nella gestione ed esecuzione di cruciali esperimenti.

Grazie a tutti i colleghi del II piano nord del Dipartimento di Scienze Biomediche, Vallisneri, per lo scambio di informazioni, idee, ma soprattutto per le serate trascorse insieme.

Desidero infine ringraziare NÓOS Srl, in particolar modo il dott. Giancarlo Moretti e la dott.ssa Rossella Restignoli, per il sostegno finanziario durante il mio dottorato, la Fondazione Cassa di Risparmio di Padova e Rovigo (Progetti d'Eccellenza), il Ministero dell' Istruzione, Università e Ricerca (grants PRIN) e il Consiglio Nazionale delle Ricerche (Progetto d'Interesse Invecchiamento) per aver supportato le nostre attività di ricerca.